WATERPOWER

DISTRIBUTION STATEMENT A
Approved for public release;
Distribution Unlimited

WATERPOWER '93

PROCEEDINGS OF THE INTERNATIONAL CONFERENCE ON HYDROPOWER

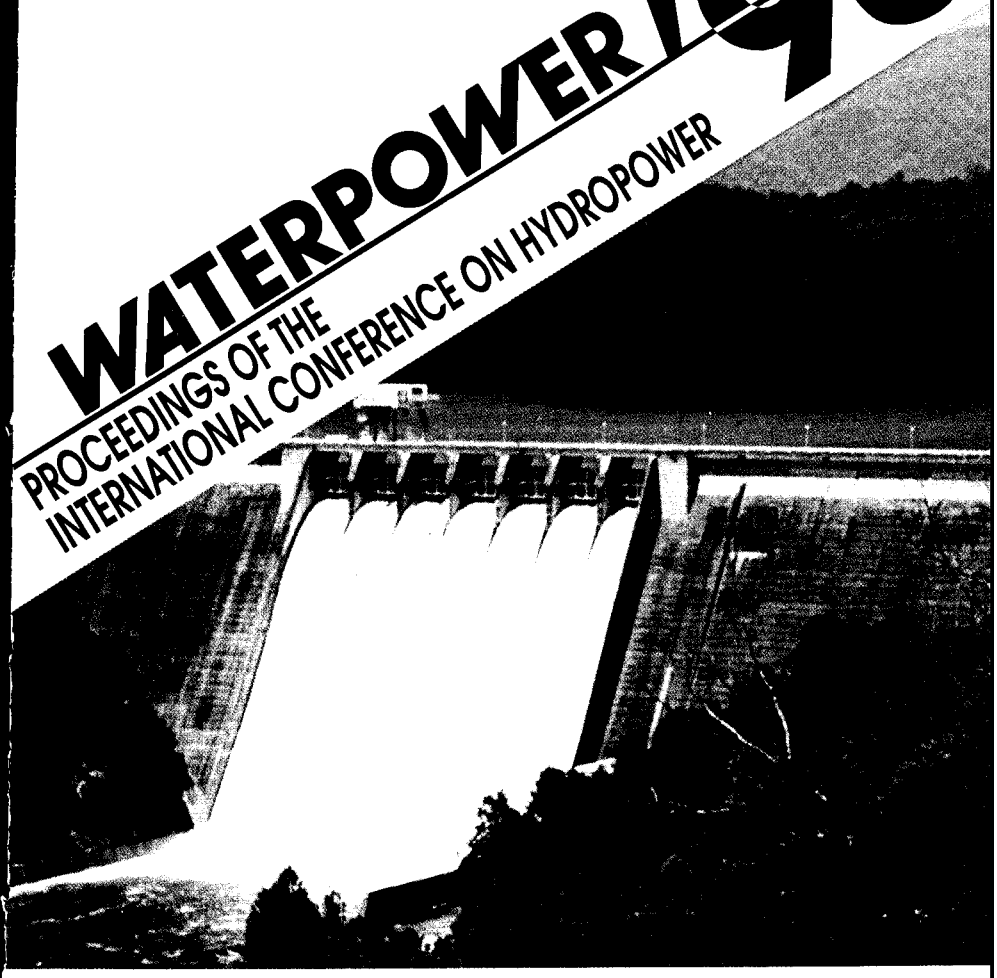

VOLUME 2

Edited by W. David Hall

WATERPOWER '93

PROCEEDINGS OF THE INTERNATIONAL CONFERENCE ON HYDROPOWER

Nashville, Tennessee
August 10-13, 1993

Edited by W. David Hall

Published by the
American Society of Civil Engineers
345 East 47th Street
New York, New York 10017-2398

19960221 073

DTIC QUALITY INSPECTED 1

Volume II

Reservoir/System Regulation
Dam Safety
Research and Development
Hydrology
Computer Applications
Civil Works
Geotechnical Aspects
Hydraulics
Mechanical Systems

ABSTRACT

This proceedings contains the papers presented at the Waterpower '93 conference held in Nashville, Tennessee, August 10-13, 1993. The conference brought together owners, planners, engineers, regulators, manufacturers, and others to share vital information surrounding the conference theme, Hydropower - Its Role in World Energy. This eighth edition of the conference series which began in 1979 was hosted by the Tennessee Valley Authority and the U.S. Army Corps of Engineers, Nashville District. Subject areas include: 1) environmental issues; 2) legal factors; 3) planning; 4) hydraulics; 5) hydrology; 6) operation and maintenance; 7) rehabilitation; 8) research and development; 9) computer applications; 10) geotechnical, mechanical, and electrical systems; 11) reservoir system operation; and case works.

The Society is not responsible for any statements made or opinions expressed in its publications.

Photocopies. Authorization to photocopy material for internal or personal use under circumstances not falling within the fair use provisions of the Copyright Act is granted by ASCE to libraries and other users registered with the Copyright Clearance Center (CCC) Transactional Reporting Service, provided that the base fee of $2.00 per article plus $.25 per page copied is paid directly to CCC, 27 Congress Street, Salem, MA 01970. The identification for ASCE Books is 0-87262-923-6/93 $2.00 + $.25. Requests for special permission or bulk copying should be addressed to Permissions & Copyright Dept., ASCE.

Copyright © 1993 by the American Society of Civil Engineers,
All Rights Reserved.
ISBN 0-87262-923-6
ISSN 1057-1841
Manufactured in the United States of America.

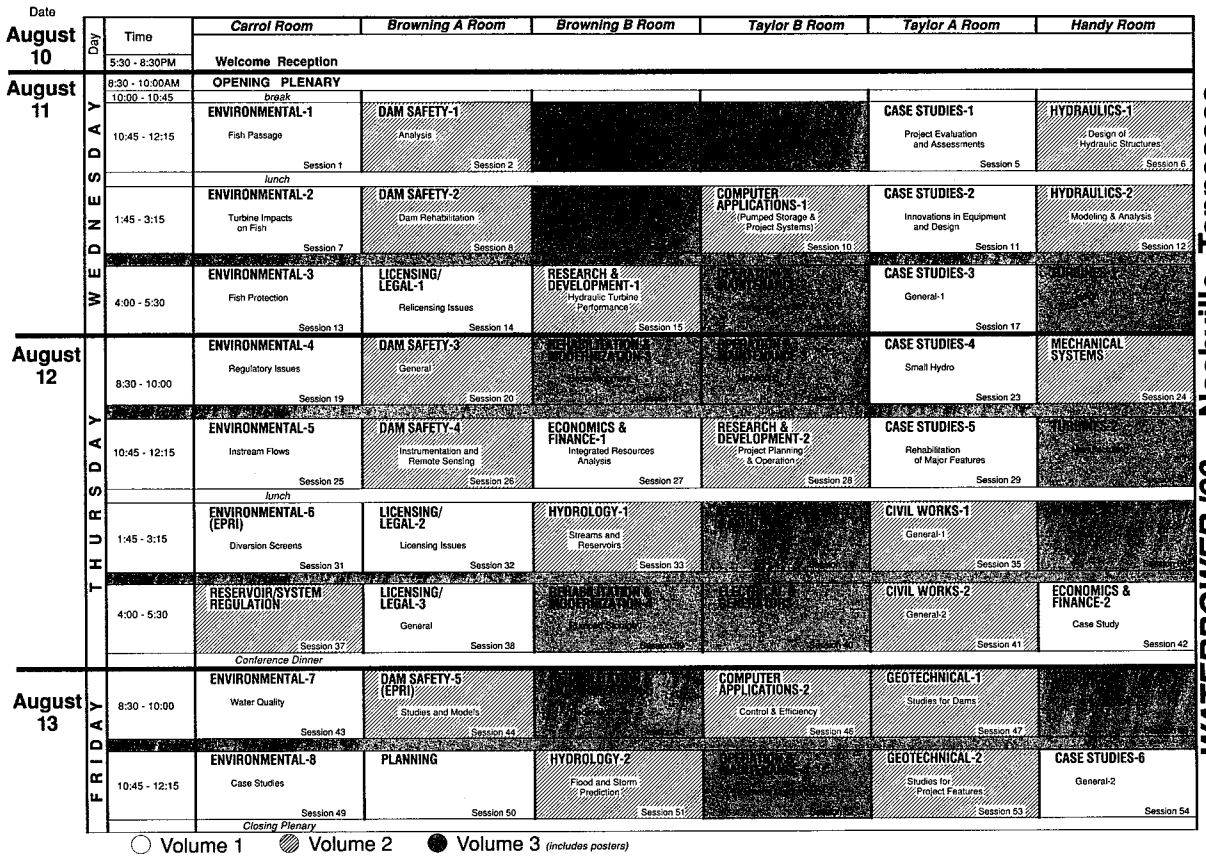

WATERPOWER '93 Nashville, Tennessee

TECHNICAL PROGRAM – OVERVIEW

CONTENTS

VOLUME I

Preface iii
Acknowledgements v
Introduction vii
Program viii

Economics & Finance 1
Planning 80
Environmental 110
Licensing/Legal 428
Case Studies 534

Economics & Finance-1: Integrated Resources Analysis
Chair: Denise Mershon, Western Area Power Admn., Phoenix, AZ
Session 27

Hydro-'Rest Of System' Integration Modeling For Analyzing Relicensing & Redevelopment Options
Mark I. Henwood, David K. Hoffman and Roger L. Raeburn 1
Hydropeaking Versus Recreation And Environment - The Power Economic Impacts Of The Glen Canyon Trade-off
Leslie Buttorff, Michael Roluti and Edmund Barbour 11
Wind/Pumped-Hydro Integration And Test
Warren S. Bollmeier II, Ning Huang and Andrew R. Trenka 24
Methods For Appraising International Projects
George K. Lagassa 29

Economics & Finance-2: Case Study
Chair: Clayton S. Palmer, Western Area Power Admn., Salt Lake City, UT
Session 42

US Army Corps Of Engineers Major Rehabilitation Program, An Overview
Craig L. Chapman 39
Reliability Analysis Of Hydropower Equipment
James A. Norlin 47
Evaluating Power Benefits For Powerhouse Rehabilitation Studies
Richard L. Mittelstadt 57

Use Of Event Trees And Economic Models In Evaluating Hydroelectric Rehabilitation Projects
Patricia Obradovich 70

Planning
Chair: Richard L. Mittelstadt, US Army Corps Of Engineers, Portland, OR
Session 50

The Corps Of Engineers In Hydropower Development
Bradford S. Price 80
Lake Elsinore Pumped Storage Project
S.T. Su 89
Environmental Impacts Of Hydropower Projects
Rameshwar D. Verma 99
Calibration Of Hydrologic And Energy Production Models For High-Head Low-Flow Hydroelectric Plants
Jeffrey E. Twitchell 766A

Environmental-1: Fish Passage
Chair: James E. Crews; HQ, US Army Corps Of Engineers; Washington, DC
Session 1

Grizzly Powerhouse's Environmental Intake
Blake D. Rothfuss and William E. Zemke 110
Cost-Effective Solutions To Fishway Design
Peter J. Christensen 120
Fish Passage/Protection Costs At Hydroelectric Projects
J.E. Francfort, B.N. Rinehart and G.L. Sommers 129
Benefits Of Fish Passage And Protection Measures At Hydroelectric Projects
Glenn F. Cada and Donald W. Jones 139

Environmental-2: Turbine Impacts On Fish
Chair: Rudd Turner, CENPE Environmental Resources Division, Portland, OR
Session 7

A Program To Improve Fish Survival Through Turbines
John W. Ferguson 149
Turbine Passage Survival At Low-Head Hydro Projects
John A. Matousek, Alan W. Wells, Kevin G. Whalen, Jack H. Hecht and Susan G. Metzger 159
Survival Of Warm-Water Fishes In Turbine Passage At A Low-Head Hydroelectric Project
Dilip Mathur, Paul G. Heisey and Douglas D. Royer 169
Hydroelectric Licensing: Toward A New Federalism
Peter W. Brown and Daniel W. Allegretti 179

Environmental-3: Fish Protection
Chair: Richard Armstrong; HQ, US Army Corps Of Engineers
Session 13

Development Of A Mathematical Model For Prediction Of Shad Population Growth On The Susquehanna River
Michael F. Dumont and Peter S. Foote 186
The Role Of Hydroelectric Project Owners In The Restoration Of American Shad To The Susquehanna River
Peter S. Foote, Michael F. Dumont and Robert B. Domermuth 197
Fisheries Studies In The Vicinity Of The Proposed Harrisburg Hydroelectric Project
Lawrence M. Miller, Peter S. Foote, Harold M. Brundage III, Thomas R. Payne and Daniel R. Lispi 208
Long Term Hydroacoustic Evaluations Of A Fixed In-Turbine Fish Diversion Screen At Rocky Reach Dam On The Columbia River, Washington
Tracey W. Steig and Bruce H. Ransom 219

Environmental-4: Regulatory Issues
Chair: Richard McDonald, CEWRC-WLRC, Portland, OR
Session 19

Case Study – 401 Permit And Discharge Aeration
Bryan R. Maurer, Daniel J. Barton and Paul C. Rizzo 229
NEPA And License Renewal: A Case Study Of The EIS Process For Projects In Relicensing
Gary D. Bachman and Mary Jane Graham 239
Snake Reservoir Drawdown A Progress Report
John J. Pizzimenti, Kevin Malone, Paul Tappel and Brian Sadden 249
Considerations In Upstream Fish Passage
R.A. Alevras and K.G. Whalen 258

Environmental-5: Instream Flows
Chair: Art Denys, US Army Corps Of Engineers, Dallas, TX
Session 25

Pool Dispersion Flow Net (PLDFLONT)
David N. Raffel and Issam M. Belmona 269
Standardizing Instream Flow Requirements At Hydropower Projects In The Cascade Mountains, Washington
Ian M. Smith and Michael J. Sale 286
FISHN – Minimum Flow Selection Made Easy
Gary M. Franc 296
Comparison Of Hydroacoustic And Net Catch Estimates Of Fish Entrainment At Tower And Kleber Dams, Black River, Michigan
Samuel V. Johnston, Bruce H. Ransom and Joseph R. Bohr 308

Environmental-6 (EPRI): Diversion Screens
Chair: Charles Sullivan, Electric Power Research Institute, Palo Alto, CA
Session 31

Hydraulics Of A New Modular Fish Diversion Screen
T.C. Cook, E.P. Taft, G.E. Hecker and C.W. Sullivan 318
Biological Evaluation Of A Modular Fish Screen
Fred Winchell, Steve Amaral, Ned Taft and Charles W. Sullivan 328
Review Of Fish Entrainment And Mortality Studies
Ned Taft, Fred Winchell, John Downing, Jack Mattice and Charles Sullivan 338
Research Update On The Eicher Screen At Elwha Dam
Fred Winchell, Ned Taft, Tom Cook and Charles Sullivan 344

Environmental-7: Water Quality
Chair: Ralph Brooks, TVA Water Resources Division, Knoxville, TN
Session 43

Limnological Considerations For Aeration At Mainstem Projects
Richard J. Ruane, Charles E. Bohac and David J. Bruggink 354
Dissolved Oxygen Analysis For Hydropower Additions On The Illinois River
Steven A. Elver and Mark J. Sundquist 363
Hydro Turbine Aeration
Brian S. Greenplate and Joseph M. Cybularz 371
A Process For Selecting Options To Improve Water Quality Below TVA Hydro Projects
J. Stephens Adams and W. Gary Brock 381

Environmental-8: Case Studies
Chair: James R. Hanchey, US Army Corps Of Engineers, Vicksburg, MS
Session 49

Zebra Mussel Control At Hydropower Facilities
Elba A. Dardeau, Jr. and Tony Bivens 391
Erosion And Sediment Control Plans For Hydropower Projects
Kathleen Sherman 400
Bank Erosion Resulting From Hydroelectric Operations
Michael J. Vecchio, Alan W. Wells, Thomas L. Englert and David S. Battige 410
The Endangered Species Act: Unlawful Takings And An Incidental Take Permit
Sam Kalen 420

Licensing/Legal-1: Relicensing Issues
Chair: Louis Rosenman, Attorney At Law, Washington, DC
Session 14

Relicensing The Ozark Beach Hydroelectric Project
Robert D. Wood and William C. Howell 428

Learning From Relicensing: Lessons For The Hydro Industry
Marla Barnes and Tom DeWitt 437
Study Requests For The Class Of '93 Hydropower Projects
Lee Emery 443
The Demise Of 'Equal Consideration'; Otherwise Known As Section 7 Consultation
Gary D. Bachman and Cheryl M. Feik 454

Licensing/Legal-2: Licensing Issues
Chair: Fred E. Springer, Federal Energy Regulatory Comm., Washington, DC
Session 32

The Battle Of Appomattox: Federal/State Conflicts In Retrofitting State And Municipal Water Impoundments
M. Curtis Whittaker and Mark J. Sundquist 464
Overcoming Permitting And Licensing Inconsistencies While Developing And Operating Projects In Different Western States
Jeffrey E. Twitchell 476
The Curse Of Sisyphus: Using License Reopeners To Impose Additional Environmental Conditions On FERC Licensed Projects
Michael A. Swiger and Miriam S. Aronoff 486
Development Options And Opportunities
Peter C. Kissel 524

Licensing/Legal-3: General
Chair: Thomas Russo, Federal Energy Regulatory Commission, Washington, DC
Session 38

In Search Of Navigable Waters
Henry G. Ecton 766F
An Overview Of The Federal Headwater Benefits Program
Charles K. Cover 494
The Results Are In: Auditing Hydropower License Compliance
Gail Ann Greely and Katherine E. Reed 504
Negotiating The Maze: Hydroelectric Development And Relicensing On Federal Lands
Michael A. Swiger and Daniel J. Whittle 514

Case Studies-1: Project Evaluation And Assessments
Chair: Edward F. Carter, Harza Engineering Co., Chicago, IL
Session 5

Hydropower Studies In The Genesee River Basin, NY
Bradford S. Price 534
Deciding Competing Resource Use Issues At FERC – From Theory To Practice
James M. Fargo 545

The Stone Creek Hydro Project – A Case Study; Building A Small Hydro Project On Public Property
Kenneth C. Fonnesbeck 556
Ruedi Hydropower – An Economic And Environmental Success
F. Robert McGregor, John Musick, Mark Fuller, Wayne Chapman, John R. Sheaffer 562

Case Studies-2: Innovations in Equipment and Design
Chair: Arvids Zagars, Harza Engineering Co., Chicago, IL
Session 11

Modern Control Systems For High Head Power Plants
Halvard Luraas 571
The Svartisen High Head Project, Turbine Design And Manufacturing
K. Bratsberg 581
Engineering Mt. Hope – A State Of The Art Pumped Storage Plant
Paul F. Shiers and Frank S. Fisher 591

Case Studies-3: General-1
Chair: Foster Pelton, Acres International Corp., Amherst, NY
Session 17

Wanapum Spillway Gate Hoist Failure
Raymond O. Ellis and Richard V. Dulin 603
Structural and Hydrologic Considerations For The Flooding Reservoir Operations Of Jiguey Dam, Dominican Republic
Guy S. Lund and Ed A. Toms 612
A Seven-Year Review Of Bath County Power Tunnel Performance
K.L. Wong, A.M. Wood and D.E. Kleiner 622
Thornapple Hydro Underseepage Correction
Richard M. Rudolph and John E. Quist 633

Case Studies-4: Small Hydro
Chair: Ashok K. Rajpal, Mead & Hunt, Inc., Madison, WI
Session 23

Deer Island Project: An Effluent Driven Hydroplant
Allen G. Corwin and Robert Getter 642
Water Treatment Plant No. 2 Power Facility Project Development
William H. Blair and Paul R. Kneitz 652
125KW Small Hydro Power Plant For Escuela El Sembrador, Catacamas, Honduras, C.A.
Edward D. Campbell, William D. Wright and Hugh G. McKay III 661
Computer Aided Design (CAD) For Small Hydroelectric Projects
Norman A. Bishop 671

Case Studies-5: Rehabilitation Of Major Features
Chair: Richard D. Stutsman, Pacific Gas & Electric Co., San Francisco, CA
Session 29

Victoria Dam Rehabilitation
Robert D. Reynolds, Robert A. Joyet and Max O. Curtis 688
Case History Of Sherman Island Hydro Buttress Dam
Jacob S. Niziol and Edward M. Paolini 698
Dodge Falls Hydro – New Technology For An Old Site
Kenneth A. Oriole, A. Sinan Koseatac and Mario Finis 710
Turbine Improvements At The Ford Hydroelectric Project
John Rohlf and George Waldow 720

Case Studies-6: General-2
Chair: Edgar T. Moore, Consulting Civil Engineer, Naperville, IL
Session 54

Conceptual Design & Physical Model Testing Of The White River Diversion Dam
Al Babb, Michael Blanchette and Robert King 747
The Eagle Mountain Pumped Storage Hydroelectric Project
Malcolm S. Jones, Jr. and Patrick E. Slattery 757
An Experimental Investigation On The Cavitation Pressure Pulsation In The Draft Tube Of A Turbine
Chen Dexin, Bai jia cong., Wang cheng xi 738
Cabinet Gorge Arch Dam Finite Element Analysis
Marc Van Patten, Mike Pavone and Steve Benson 728
Subject Index 766p
Author Index 766u

VOLUME II

Program iii

Reservoir/System Regulation 767
Dam Safety 811
Research and Development 984
Hydrology 1070
Computer Applications 1148
Civil Works 1208
Geotechnical Aspects 1291
Hydraulics 1368
Mechanical Systems 1448

Reservoir/System Regulation
Chair: Ron Yates, US Army Corps Of Engineers, Cincinnati, OH
Session 37

Modeling And Evaluation Of Alternative Operating Strategies For The Columbia River System
James D. Barton 767
The Role Of The Enhanced Version Of HEC5 In Hydropower Planning And Licensing
Wendy C. Bley, Deborah Boomhower, L. Greg Bove, Matthew P. Dillis, Bill S. Eichert, Alan B. Livingstone, Stephen D. Padula, Matthew J. Putnam, Thomas J. Sullivan, Mark J. Wamser 777
Using Pumped Storage For System Regulation – A Transatlantic Perspective
Fred R. Harty, Jr. and Jeff A. Scott 787
Two Reservoir Regulation Model For Small Hydro Developments
P.C. Helwig and T.P. Tung 796

Dam Safety-1: Analysis
Chair: Joseph L. Ehasz, Ebasco Services Inc., New York, NY
Session 2

Soda Dam: Benefits In Performing A Three Dimensional Analysis Of A Concrete Gravity Dam
Guy S. Lund, Mark Linnebur and Howard Boggs 811
FERC's Evolving Policy On Three Dimensional Stability Analysis Of Concrete Gravity Dams
Bruce Brand 821
Computer Aided Design Of Drainage Systems For Dams
Tissa H. Illangasekare, Bernard Amadei, Rodney Lyons, C. Chinnaswamy and Doug Morris 831
A Case History Of The Cabinet Gorge Dam Analysis
John Z. Gibson 805

Dam Safety-2: Dam Rehabilitation
Chair: Alton P. Davis, GEI Consultants Inc., Winchester, MA
Session 8

Modification Of Beech Dam For Seepage Control And Upgrade For The Maximum Credible Earthquake
Vann A. Newell, Harry A. Manson and Charles D. Wagner 841
Modification At Hiwassee Dam Due To Concrete Growth Problems
Vann A. Newell, David T. Tanner, Charles D. Wagner 860
Guidelines For Evaluating Aging Penstocks
Charles S. Ahlgren 870
Structural Integrity Of Fontana Emergency Spillway
C. Wagner, J. Niznik, M. Kaltsouni, V. J. Zipparro, C. H. Yeh 851

Dam Safety-3: General
Chair: Jerrold W. Gotzmer, Federal Energy Regulatory Comm., Washington, DC
Session 20

Hydro Public Safety Awareness: One Utility's Approach
Lisa Hildebrand 878
Dam Safety Inspection Of Spillway & Sluice Gate Operating Machinery At TVA Dams
Tommy McEntyre, Darle Parker and David Hegseth 885
Dam Safety Of Hydroelectric Projects In Thailand
Yin Au-Yeung and Taweesak Mahasandana 894
Soda Dam: Influence Of Reservoir Silt Deposits On The Uplift Load
Guy S. Lund, Howard Boggs and Dave Daley 903

Dam Safety-4: Instrumentation And Remote Sensing
Chair: Daniel J. Mahoney, Federal Energy Regulatory Comm., Washington, DC
Session 26

The Automated Instrumentation Monitoring System At The Bad Creek Pumped Storage Project
Edwin C. Luttrell 913
Automating Instrumentation At Navajo Dam
Stan B. Mattingly 923
The Design And Installation Of Dam Failure Monitoring Equipment For The Southern California Edison Company System Of Dams
C. Michael Knarr, Thomas J. Barker and Stephen F. McKenery 930
Use Of Advanced Technologies In Michigamme River Basin PMF Analyses
Mark S. Woodbury, Douglas T. Eberlein and Nicholas Pansic 940

Dam Safety-5 (EPRI): Studies And Models
Chair: Douglas I. Morris, Electric Power Research Institute, Palo Alto, CA
Session 44

A Guideline For The Determination Of Probable Maximum Flood For Civil Works
John J. Cassidy, Samuel L. Hui, Gerrold W. Gotzmer and Douglas I. Morris 946
Extreme Rainfall Probabilities
George A. Harper, Thomas F. O'Hara and Douglas I. Morris 955
Probable Maximum Precipitation Study For Michigan And Wisconsin: Procedures And Results
Edward M. Tomlinson and Douglas I. Morris 965
CG-Dams Software: Dam Stability Case Studies
Peter R. Barrett, H. Foadian, L. Zhang, Y.R. Rashid and Douglas I. Morris 975

Research And Development-1: Hydraulic Turbine Performance
Chair: John J. Cassidy, Bechtel Corp., San Francisco, CA
Session 15

Hydro-Electric Machine Condition Monitoring – A Technical Proposal And Business Argument
D.E. Franklin, B.C. Pollock and J. Laakso 984
Grinding Manipulator For Cavitation Repair
Randy Wallman and Gary Gusberti 994
Design Criteria And Quality Requirements For Large Turbines
Hermod Brekke 1014
Advances In Hydraulic Design Of Turbines And Pumps Using The Numerical Test Rig
M. Eichenberger, A. Sebestyen 1004

Research And Development-2: Project Planning And Operation
Chair: Frederick A. Locher, Bechtel Corp., San Francisco, CA
Session 28

A Revisit To Data Problems And Databases
Shou-shan Fan 1025
Research And Development Projects To Evaluate Non-chemical Methods For Control Of The Zebra Mussel (Dreissena Polymorpha)
A. Garry Smythe and Cameron L. Lange 1031
Prioritizing PG&E's Environmental Research For Hydropower
Steven F. Railsback, Ellen H. Yeoman and Thomas R. Lambert 1040
Oxygen Transfer Similitude For The Auto-Venting Turbine
Eric J. Thompson and John S. Gulliver 1050

Hydrology-1: Streams And Reservoirs
Chair: Andar Lin, New York Power Authority, White Plains, NY
Session 33

Sensitivity Analysis Of Design And Operational Characteristics Of Reservoirs
M.A. Mimikou, P.S. Hadjissavva, Y.S. Kouvopoulos and H. Afrateos .. 1070
Real-Time Flow Forecasting On The Saluda River Watershed
George Kanakis, Jr. and Robert A. Laura 1079
Monte Carlo Simulation Techniques For Predicting Hydropower Performance
John P. Cross 1083
Niagara River Flow Forecasting System
Ken Lacivita, Ion Corbu, Francis Kwan, Randy D. Crissman 1060

Hydrology-2: Flood And Storm Prediction
Chair: Catalino Cecilio, Consulting Engineer, San Francisco, CA
Session 51

Applications And Limitations Of The USBR 'Method Of Successive Subtraction Of Subbasin PMP Volumes' For Critical Storm Development For Dam Safety Hydrologic Assessments
Ed A. Toms 1091
Flood Frequency Analysis With FOS Distributions
S. Rocky Durrans 1100
Runoff Modeling On A Baseflow-Dominated Watershed
Ellen B. Faulkner, Gary M. Schimek and David S. McGraw 1110
Use Of A NETWORK Flood Routing Model To Reduce PMF's At LCRA Dams
John Lee Rutledge, Richard K. Frithiof and Kathryn M. Ozment 1120

Computer Applications-1: Pumped Storage And Project Systems
Chair: John Bessaw, HDR Engineering, Boise, ID
Session 10

Three-Dimensional Numerical Analysis Of Head Loss In A Bifurcation Pipe Flow
Charles C. S. Song, Jianming He and Xiang Ying Chen 1140
Development Of An Integrated Hydraulic – Electrical System Model For Hydropower Plant
Angus Simpson, Michael Gibbard and John McPheat 1150
Use Of Mainstream Computing Platforms For Power Plant Control
Robert J. Hughes 1130
Upgraded Control System For Vianden Hydro Plant
Ralf Brosowski, Karl-Ludwig Holder, Mathias Krecke and Wolfgang Butz 1160

Computer Applications-2: Control & Efficiency
Chair: Jose Tello, Pacific Gas & Electric Co., San Ramon, CA
Session 46

Improving Performance With A Hydro Control System
James Cook, James T. Walsh and Jamie Veitch 1170
Recent Developments Of Turbine Governors And Controls
J. Perry Bevivino 1180
On-line Optimal Unit Load Allocation At Nedre Vinstra
R. Nylund, O. Wangensten and M. Browne 1189
Optimal Unit Dispatch For Hydro Powerplants
Mark A. Severin and Lee L. Wang 1198

Civil Works-1: General-1
Chair: Hugh G. McKay, Duke Power Company, Charlotte, NC
Session 35

Canadian Inflatable Dam – A Unique Application
Richard Slopek, Lloyd Courage and Brian Pelz 1208
Creative Crest Control
Thomas L. Kahl and Stephen T. Ruell 1218
Bottom-Hinged Wood Flashboards
Steven A. Elver 1228
Big Chute Generating Station Redevelopment
I. Lauchlan, W. W. Hall, N. A. Bishop 1238

Civil Works-2: General-2
Chair: David Burgoine, Acres International Corp., Amherst, NY
Session 41

Design Criteria For The Kents Falls Penstock
Harbinder S. Gill, Chris W. May and Rex C. Powell 1247
Timber-Crib Dam Rehabilitation
Alan Bondarenko, Paul Martinchich, Daniel Barton and Paul C. Rizzo .. 1257
Replacement Of Deerfield No. 5 Dam
Michael E. Rook and William S. Rothgeb 1269
Some Problems Encountered In The Design And Construction Of Hydroelectric Projects
Edgar T. Moore 1279

Geotechnical-1: Studies For Dams
Chair: David E. Kleiner, Harza Engineering Co., Chicago, IL
Session 47

Geotechnical Engineering At Cowlitz Falls Project
John P. Sollo and Agerico A. Cadiz 1291
Seismic Hazard Analysis For Dams In The Southeastern United States
William J. Johnson and John P. Osterle 1301
Synthetic Geogrid Reinforces Existing Earth Dam Embankments
Frederick Lux III, James R. Bakken and Dean S. Steines 1315

Geotechnical-2: Studies For Project Features
Chair: J. Lawrence Von Thun, US Bureau Of Reclamation, Denver, CO
Session 53

Geologic Aspects of the Mt. Hope Pumped Storage Project, Dover, NJ
C.A. Foster, J. L. Rosenblad, R. Venkatakrishnan and J.F. Wearing ... 1326
Piping Security Of Glacial Till-Structure Interfaces
R. Craig Findlay 1339
Design And Performance Of Power Canal Lining
A. V. Sundaram 1349

Drawdown Stability Of A Compacted Shale Rockfill
Carlos A. Jaramillo, David E. Kleiner, Philippe P. Martin, Aniruddha Sengupta and Archivok V. Sundaram 1358

Hydraulics-1: Design Of Hydraulic Structures
Chair: George E. Hecker, Alden Research Laboratories, Holden, MA
Session 6

Design Criteria For Water Power Intakes
D. G. Murray 1368
Energy Dissipation In Stepped Spillway
Hsien-Ter Chou 1378
Hydraulic Design Of A Low Submergence Siphon Intake
David E. Hibbs, Richard L. Voigt, Mark J. Sundquist, John S. Gulliver and Norm Scott 1387
Design Methodology Of Labyrinth Weirs
Frederick Lux III 1397

Hydraulics-2: Modeling And Analysis
Chair: Robert W. Kwiatkowski, Parsons Main, Inc., Boston, MA
Session 12

Modeling Of River Ice Processes For Hydropower Facilities In Cold Regions
Randy D. Crissman 1408
Pulsation Problems In Hydroelectric Powerplants (Some Case Studies)
Anders Wedmark 1418
An Improved Fish Sampler At Cabot Station
John R. Whitfield, George E. Hecker and Thang D. Nguyen 1428
Debris Removal From A Low Velocity, Inclined Fish Screen
F.A. Locher, P.J. Ryan, V.C. Bird and P. Steiner 1438

Mechanical Systems
Chair: Divu Narayan, New York Power Authority, White Plains, NY
Session 24

Load Test Of Traveling Fish Screens At McNary Dam
Richard Vaughn 1448
Hydraulic vs. Mechanical Drives For Steel Structure
Parveen Gupta 1457
Key Technical Features Of Hydraulic Cylinders
J.A.C. Wels 1465
Lubrication Systems For Speed Increasers Used In Hydrogenerating Applications
R.S. Pelczar 1483

VOLUME III

Program iii

Rehabilitation & Modernization 1497
Operations & Maintenance 1694
Electrical Systems & Controls 1841
Electrical & Generators 1879
Turbines 1913
Poster Forum 2060

Rehabilitation & Modernization-1: General-1
Chair: Thomas W. Plunkett, US Army Corps Of Engineers, Dallas, TX
Session 3

Concrete Penstock Leakage – Investigation Of Causes And Rehabilitation Options
Param D. Bhat 1497
Fort Peck Project – Power Plant No. 1 Penstock Replacement
Ronald W. Bockerman and Donald F. Miller 1507
Elimination Of Surge Tanks At Saluda Hydroelectric Plant
Patrick Ward, Timothy Lynch, Fred Harty, Kristina Massey, Hal Riddle 1517
Modernization Of Pelton Turbine Pressure Regulators
Louis G. Silva and Difa Shveyd 1527

Rehabilitation & Modernization-2: General-2
Chair: Doug Filer, US Army Corps Of Engineers, Portland, OR
Session 9

Replacement Of Great Falls Units 1 & 2 Hydro Turbines
Timothy A. Jablonski 1537
Upgrade Of The Chippewa Falls Hydroelectric Turbines
Mark Holmberg, Bill Zawacki, Donald R. Froehlich, and Jim Singleton 1545
Three Case Studies Of Modifications To Washington Water Power Dams
John Gibson, John Hamill, Ed Schlect, Thomas Haag 1554
Synchronizing Upgrade For Hydroelectric Plants
James H. Harlow 1564

Rehabilitation & Modernization-3: Redevelopment-1
Chair: Dick Hunt, Richard Hunt Assoc., Annapolis, MD
Session 21

Replacement Of The Wood Stave Penstock And Turbine Runners At Tuxedo Hydro Plant
William A. Maynard 1574
Re-Powering Nine Mile Hydroelectric Project
Joseph A. Kurrus, Rick Zilar, Edward Schlect, Reynold A. Hokenson and Jim H. Rutherford 1584

Unit 1 And 2 Rehabilitation At Crescent And Vischer Ferry
Mohammed I. Choudhry, Michael F. Nash, William Stoiber and Andrew C. Sumer 1594
Rehabilitation Of Unit #2 At Bennetts Bridge
Paul A. Bernhardt 1607

Rehabilitation & Modernization-4: Pumped Storage
Chair: Bob Kohne, Pacific Gas & Electric Co., San Francisco, CA
Session 39

Seneca Pump Turbine Rehabilitation
Clayton C. Purdy and Curtis D. Waters 1619
Seneca P/T Rehab. Field Tests And Economic Payback
Ronald E. Deitz and James L. Kepler 1639
Ludington #5 Site Overhaul Of A Large Pump/Turbine
Peter E. Papaioannou and Stephen D. Rinehart 1629
Yards Creek Pump/Turbine Upgrade, Part 1 – Structural Redesign And Analysis
J.R. Degnan and J.J. Geuther 1649

Rehabilitation & Modernization-5: Redevelopment-2
Chair: Duke Loney, US Army Corps Of Engineers, Portland, OR
Session 45

Upgrading Of AEP's Twin Branch Hydroelectric Plant
Robert E. Dool and Stefan M. Abelin 1659
Hydro Task Force Evaluations – Northern States Power Company
Roger B. Anderson, Richard Rudolph, John Larson and John E. Quist .. 1664
Puget Power Hydro Modernization Project, A Diversified Approach
Michael J. Haynes, David F. Webber and John B. Yale 1671
The Monroe Street Hydroelectric Project Redevelopment: A Legacy Of Power 1889 – 1992
Michael J. Finn and Steven G. Silkworth 1681

Operations & Maintenance-1: General Maintenance-1
Chair: Ron Loose, Us Department Of Energy, Washington, DC
Session 4

Hydroelectric Plant Inspection And Maintenance Requirements
Stanley J. Hayes and David M. Clemen 1694
Use Of Hazard Analysis In Maintenance
Walter O. Wunderlich 1703
Cavitation Repair By Welding Without Gouging
Avaral S. Rao and Ken S. Hawthorne 1713
Repair Of Cracking In High Head (2,378') Penstock
Patrick J. Regan 1723

Operation & Maintenance-2: General Operations
Chair: Fred Munsell, Southwestern Power Administration, Tulsa, OK
Session 16

'Turn Key' Construction To Operations And Maintenance, A Transitional Program
Bob Barksdale, Mike Lewis and Russ Pytko 1733
Sediment Transport Assessment In The Old River Control Area Of The Lower Mississippi River (USA)
Sultan Alam, Cecil W. Soileau and Ralph L. Laukhuff 1756
Talking Trash: Debris Removal At Hydropower Plants
James F. Sadler 1741
Estimating The Quantities Of Organic Debris Entering Reservoirs In British Columbia, Canada
Ken Rood, Niels Nielsen and Brian Hughes 1746

Operation & Maintenance-3: Monitoring
Chair: Henry Martinez, Tennessee Valley Authority, Chattanooga, TN
Session 22

Hydro-Electric Generator Ozone Monitoring
D.E. Franklin, B.C. Pollock and J. Laakso 1767
Submerged Trash Survey At TVA Dams
F.W. Edwards, D.G. Hegseth and F.R. Swearingen 1777
Shaft Vibration Monitoring On Vertical Units
Rein Husebo 1786
Vibration Frequency Spectrum Analysis
C.F. Malm and Jim Wallace 1795

Operation & Maintenance-4: General Maintenance-2
Chair: Andrew C. Sumner, New York Power Authority, Half Moon, NY
Session 52

Considerations For Dewatering Hydro Units And Gates
Richard M. Rudolph and John R. Kries 1812
Protective Coatings To Resist Cavitation Erosion In Concrete Hydraulic Structures
Joe Wong and Dick Brighton 1822
New Low Cost Surface Preparation Process For Relining Existing Penstocks
Richard D. Stutsman 1831

Electrical Systems & Controls
Chair: Richard Coleman, Prudential Center, Boston, MA
Session 34

Automation Of The Osage Hydroelectric Plant
Steve L. Duxbury and Robert W. Ferguson 1841

Switchgear Fault, Damage Control, Recovery, And Redesign At The John Day Powerhouse
Bob Luck and Chuck Rinck 1850
Variable Speed In Hydro Power Generation Utilizing Static Frequency Converters
L. Terens and R. Schafer 1860
Summit Pumped Storage Project – Distributed Control System
Oistein Andresen and Tore Jensen 1870

Electrical & Generators
Chair: Ron Domer, Consulting Engineer, San Francisco, CA
Session 40

Spring-Type Thrust Bearings Can Be Monitored
Michael E. Coates 1879
Governor For Stand Alone Induction Generator
Dan Levy 1889
Hydro Generator Winding Specification Trends
D.G. McLaren, W. Newman and R.H. Rehder 1899
Replacement Arc Chutes For Generator Air Circuit Breakers
Charles Rinck 1907

Turbines-1: Design
Chair: Jody Key, Bonneville Power Administration, Portland, OR
Session 18

Double Runner Francis Turbines For Applications With Wide Flow Variations
D. Robert and J. Nesvadba 1913
Sizing Turbines To Use Municipal Water Supply Flow
E. June Busse, Jerry R. Waugh and R. Joseph Bergquist 1923
Yacyreta – Western World's Largest Kaplan Turbines
Randy V. Seifarth 1931
Variable Speed Power Conversion Technology
H. Meyer, Aleksander S. Roudnev 1941

Turbines-2: Manufacturing
Chair: Allen Lewey, US Army Corps Of Engineers, Portland, OR
Session 30

Aluminum Bronze – Method Of Manufacture Can Effect Performance
David F. Medley 1951
Balancing Techniques – Runner Impeller Replacements
K. David Bahn and Jeffrey L. Kepler 1959
Recovering Techniques And Possible Use Of The Geometry Of Old Runners
Andre Coutu and Stuart T. Coulson 1966

Putting Your Reputation On The Slant
Russell L. Katherman 1976

Turbines-3: Testing
Chair: Rodney Whittinger, US Army Corps Of Engineers, Portland, OR
Session 36

Modernizing A Double Francis Turbine – Flow Analysis And Hydraulic Model Testing Enhances Turbine Performance
Peter F. Magauer 1986
Turbine Performance Tests At The Robert Moses Niagara Power Plant
Robert J. Knowlton, Peter W. Ludewig, Jack C. Howe and John H. Phillips 1996
Turbine Uprating And Incremental Gains Made With Each Change
Steven C. Onken 2006
Comparison Of Maximum Efficiencies In A Cross-Flow Turbine
V.R. Desai and N.M. Aziz 2012

Turbines-4: Pump Storage
Chair: Rochell Bates, Bonneville Power Administration, Portland, OR
Session 48

Mingtan – High Head Reversible Pump/Turbine
Robert D. Steele 2022
Bad Creek & Mingtan – Pump/Turbine Commissioning Experience
Laurence F. Henry 2030
Yards Creek Pump/Turbine Upgrade, Part 2: Hydraulic Redesign
S. Chacour, W. Colwill, J. Geuther and F. Harty 2040
Yards Creek Pump/Turbine Upgrade Part 3 – Runner Manufacturing And Field Modifications
J.R. Nolt, Jr., R.B. Corbit and A. Caploon 2050

Poster Forum
Chair: Arlo Allen, US Bureau Of Reclamation, Salt Lake City, UT
Session 55

Central Valley Project Energy Efficiency Study
Martin Bauer and Guy Nelson 2060
Strategic, Operating And Economic Benefits Of Modular Pumped Storage
Rick S. Koebbe 2065
Use Of Weirs For Tailwater Improvements Downstream From Tva Hydropower Dams
Gary E. Hauser, William D. Proctor and Tony A. Rizk 2075
Transient Pulses Of Chemical Oxygen Demand In Douglas Reservoir
Richard J. Ruane 2080
Determining The Number Of Transects In IFIM Studies
Alan W. Wells, M. Elizabeth Conners, Susan G. Metzger and John Homa, Jr. 2089

Spatial Simulation Of Smallmouth Bass In Streams
H.I. Jager, M.J. Sale, W. Van Winkle, D.L. DeAngelis, D.D. Schmoyer and M.J. Sabo 2095
Flow Computation And Energy Performance Analysis For Hydropower Components
Charles C.S. Song, Xiang Ying Chen and Jianming He 2105
Hydropower Operations And Maintenance Management Innovations
Craig L. Chapman 2108
History Of Water Power On The Kansas River
David Readio and Von Rothenberger 2197
Dam Modification For Recreational Boating
Richard E. McLaughlin 2114
Plant And System Benefits Associated With Adjustable Speed Hydro
Peter Donalek 2120
Investigation On Low-cost Flowthrough Rockfill Dams And Spillways – A Summary
T.P. Tung, V. K. Garga and D. Hansen 2124
Raw Water Systems Evaluation For Zebra Mussel Control
K. Young, K. Chen, C. Lange and T. Short 2131
Hydropower Development In China
Zhang Boting 2134
Monthly Waterpower Dependability
Colby V. Ardis and Aaron Jennings 2144
Hydropower In Brazil: Past View And Future Directions
Paulo Sergio Franco Barbosa 2151
The Demolition Of Mussers Dam
Gerald L. Cross 2160
Water Leakage Through Cracks In Reinforced Concrete
Donald O. Dusenberry and Steven J. DelloRusso 2167
Hydraulic Machinery Model Testing I M H E F Test Facilities
P. Henry and H.P. Mombelli 2177
Acoustic Flow Measurements At Rocky Reach Dam
Rick Birch and David Lemon 2187
Subject Index 2203
Author Index 2209

Modeling and Evaluation of Alternative Operating Strategies for the Columbia River System

James D. Barton, P.E.[1]

Abstract

In the Columbia River Basin there are currently several major studies underway to evaluate alternative strategies for operating the river system. The need for these studies is driven by the fact that increasing demands are being placed on the limited water resources available in the basin and the current strategies for operating the system are rapidly becoming inadequate. These increasing demands are primarily in the areas of fish and wildlife and hydropower. Several species of salmon have recently been listed as endangered or threatened under the Endangered Species Act by the National Marine Fisheries Service (NMFS), and this has further increased the importance of providing water necessary for the protection and recovery of these fish. At the same time, hydroelectric power is no longer a surplus commodity in the region and population growth continues to increase demands for electric energy. In this environment of change and increased demand on the system, modeling and evaluation of alternative system operating strategies is a critical aspect of these studies which will shape the future operating strategy of the reservoir system.

There are currently three major studies which are being conducted to evaluate alternative operating strategies. The first is the System Operation Review (SOR), which is focused on developing an overall operational strategy for the system which recognizes and attempts to respond to all the water resource needs in the basin in a fair and equitable manner. It is a comprehensive study which will consider non-structural modifications to system operation and will require several years for completion. A related

[1]Hydraulic Engineer, Western Division, Corps of Engineers, P.O. Box 2870, Portland, OR 97208-2870

study is the System Configuration Study (SCS), which differs from the SOR study in that it will include analysis of structural changes to the configuration of the system such as modification of existing dams and other structures and possible addition of new dams. The other study which is currently being conducted is the Interim Columbia and Snake River Flow Improvement Measures for Salmon Supplemental Environmental Impact Statement (SEIS). The purpose of this study is to analyze short-term strategies which can be implemented to improve salmon migration conditions in the Columbia River and its tributaries prior to the completion of the long-term studies mentioned previously.

In order to effectively complete all of these studies and develop new operating strategies, it is essential to have hydroregulation models which allow realistic simulation of the river system operation under varying water conditions and operating strategies. It is also important to have good methods of evaluating the impacts of these different operating strategies for various users of the system such as fish and wildlife, hydropower, flood control, recreation, and others. In the course of completing the studies described above, over 100 different operating strategies have been modeled and evaluated using hydroregulation models and other techniques. This paper describes the operating strategies considered in these studies, how they were modeled using hydroregulation models, and how the results were evaluated and strategies compared.

Introduction

The Columbia River begins at Columbia Lake in British Columbia and extends 1,214 miles and drains portions of seven states before flowing into the Pacific Ocean near Astoria, Oregon. Its drainage area is 219,000 square miles, and with an average annual runoff of 198 million acre feet, it ranks second only to the Missouri-Mississippi River system in the United States in runoff. It supplies over 75 percent of the region's electrical generation and is operated for a wide range of other uses such as flood control, navigation, irrigation, recreation, fish and wildlife, and others.

The Columbia River System is operated as a coordinated system in an effort to combine the multiple uses on the system and increase the benefits to the people of the western U.S. and Canada. Three federal agencies, the U.S. Army Corps of Engineers (Corps), the U.S. Bureau of Reclamation (BOR), and the Bonneville Power Administration (BPA), play crucial roles in managing the

planning and operation of the coordinated system in the U.S.. In addition, there is involvement by the British Columbia Hydro and Power Authority in Canada, electric utilities in the region, fishery agencies, and numerous other entities.

Planning and operations on the Columbia River System are based on a complex and interrelated set of laws, treaties, agreements, and guidelines. The following six are particularly important in understanding the coordinated system and the necessity for the studies to be described: (1) Columbia River Treaty; (2) Canadian Entitlement Allocation Agreements; (3) Pacific Northwest Coordination Agreement; (4) Pacific Northwest Electric Power Planning and Conservation Act of 1980; (5) National Environmental Policy Act; and (6) Endangered Species Act.

The Columbia River Treaty, established in 1964, provided for construction of reservoirs in Canada that provide over half the available storage on the system. It also divided the downstream power benefits between Canada and the U.S.. It has no expiration date, but either nation can terminate the treaty after 60 years, in 2024. The Canadian Entitlement Allocation Agreements (CEAA) are five contracts that divide the Columbia River Treaty's power benefits and obligations among non-Federal beneficiaries in the U.S.. These agreements begin to expire in 1998 and are being renegotiated to establish future obligations regarding the Treaty Power benefits.

The Pacific Northwest Coordination Agreement (PNCA) is a formal agreement signed in 1964 and expiring in 2003 which prescribes planning and operating rules for coordinating operations among Federal project operators and power generating utilities of the Pacific Northwest. It is based on the "single utility concept", in which the system is operated as if by one utility to maximize efficiency. The Pacific Northwest Electric Power Planning and Conservation Act of 1980 created the Northwest Power Planning Council which was charged with developing a Fish and Wildlife Program for the Columbia River Basin and preparing a Regional Electric Power Conservation Plan. The Fish and Wildlife Program established a number of goals for restoring and protecting fish populations in the basin.

The National Environmental Policy Act of 1969 (NEPA) requires an environmental assessment or environmental impact statement (EIS) be prepared, and public hearings be held, for any proposed Federal action that might affect the environment. Renewal of the expiring power agreements described above and significant modification

of existing operations fall under the provisions of NEPA. The Endangered Species Act is also applicable to these studies because of the listing by NMFS of several species of salmon as endangered or threatened.

Current Studies

Of the three major studies currently underway to evaluate alternate methods of operating the Columbia River System, the SOR was the first to be initiated in 1990. The SOR is the environmental analysis that is required to consider major changes in system operations for the Columbia River. These changes include modification of the current multiple-use operating strategy for the river system, and renegotiation and renewal of the PNCA and CEAA agreements related to the Columbia River Treaty between the U.S. and Canada. The scope of this study is limited to 14 major Federal hydro projects in the system.

The SCS is another study being conducted by the Corps, and it will evaluate structural modifications to Federal dams and reservoirs to improve passage for anadromous fish. It is being conducted partly in response to the Northwest Power Planning Council's "Amendments to the Columbia River Basin Fish and Wildlife Program" dated December 11, 1991. It involves physical measures which directly improve passage or enable changes in river operations to improve passage. The modifications considered in this study primarily involve projects in the Snake River System, a major tributary to the Columbia. Alternatives considered under this study include: (1) reservoir drawdown to increase flow velocity, (2) new upstream storage for augmenting flows, (3) upstream fish collection and conveyance facilities, and (4) modifications and improvements to existing facilities.

The Columbia and Snake River Flow Improvement Measures for Salmon Options Analysis (OA)/Environmental Impact Statement (EIS) completed in 1992 and Supplemental EIS being completed in 1993 are the third major series of studies being conducted to evaluate alternate river operation strategies to improve migration conditions for salmon. These studies are being conducted in response to the listing by NMFS of the Snake River sockeye salmon as an endangered species under the Endangered Species Act in December of 1991, and the Snake River fall and spring/summer chinook salmon as threatened species effective in May of 1992. The SEIS addresses more immediate water management activities to be implemented in 1993 and planned for future years until the plan of action can be modified as a result of long-term studies

underway such as the SOR and SCS discussed previously. The OA/EIS was used to describe and develop an operation plan for 1992, and the SEIS is to provide similar information for operations in 1993 and beyond.

The primary difference between the OA/EIS and SEIS studies compared to the SOR and SCS studies is that the OA/EIS and SEIS studies are short-term studies completed under a very limited time frame, whereas the SOR and SCS studies are designed to provide a long-term solution and operating plan for the Columbia River System. Completion of the SOR and SCS studies and accompanying EIS's will hopefully eliminate the need to prepare EIS's such as the OA/EIS and SEIS on a yearly basis for short-term operations.

In all of the studies discussed in this paper, the Corps is using the computer hydroregulation model "Hydro System Seasonal Regulation (HYSSR)" to simulate river operations over a 50-year period of record, from 1928 through 1978. This model routes flows using a monthly time step through over 150 projects in the river system and provides output such as end-of-month reservoir elevations, monthly average flows, monthly average spill, power generation, and other data. It simulates how each project in this system will react to changes in operations and to a wide range of runoff conditions which occurred over the 50-year period of record. The output from this model is then analyzed using spreadsheets and other computer models and techniques to determine the impacts on the various river uses. In addition to HYSSR, other hydroregulation models such as BPA's HYDROSIM and SAM are used to assist in the analysis.

SOR Study Methodology

The first phase of the SOR study was a screening process in which 90 alternatives for system operation were modeled by the Corps, BOR, and BPA. Using the output from the hydroregulation simulations of these alternatives, such as reservoir elevations, releases, power generation, and other information, representatives of ten different technical work groups evaluated the impacts of these alternatives in specific areas of river use such as water quality, anadromous fish, power, flood control, and others. The 90 alternatives can be categorized as follows:

Category	Number Identified
Base Case	3
Flow Augmentation	46
Drawdown	16

Stable Pools	21
Power	4

The Base Case strategy was to operate the system essentially the same way it had been operated during the previous five years, prior to the most recent series of modifications for fish and wildlife needs. All other alternatives were compared against these studies to determine the effect of different operating strategies on users of the system. The alternatives under the Flow Augmentation category involved operating the system to meet different types of flow targets determined by anadromous fish experts. Since improvement of conditions for anadromous fish is one of the primary objectives of these studies, the majority of alternatives fell into this category. Drawdown alternatives were designed to draw down certain reservoirs to lower levels to increase flow velocities in the river for anadromous fish. Stable pool alternatives attempted to maintain storage reservoirs at target elevations devised to benefit resident fish, recreation, and wildlife. Finally, power alternatives were developed to model system operation for the primary purpose of power production, with no special operations for fish and wildlife. It took the staff of the Corps, BOR, and BPA approximately one year to process these 90 alternatives through hydroregulation and work group models.

The ten SOR interagency technical work groups were crucial in the development and analysis of alternatives. Their two primary tasks were to develop alternatives for the screening process that would optimize operation for their river use and to evaluate the impacts of all alternatives proposed on their river use. Besides providing alternatives that were optimum for their river use, work groups were asked to describe additional alternatives that may not be ideal, but would be acceptable for their river use. The work groups and optimum conditions specified by each are listed below:

Work Group	Optimum Condition
Power	Eliminate or reduce non-power operating constraints on the system
Recreation	Full reservoirs for summer recreation season (May-Oct)
Resident Fish	Stable reservoirs year around, with natural river flows
Wildlife	Draw down and stabilize reservoirs

	year around to expose maximum acreage for long-term habitat recovery
Irrigation	Full reservoirs April through October (growing season)
Anadromous Fish	Streamflows as close to "natural" river as possible, near spillway levels
Flood Control	Reservoirs drafted in early spring to capture snowmelt inflows
Navigation	No drawdowns below minimum operating pool at navigation projects
Cultural Resources	Stable reservoir elevations year around
Water Quality	Natural river flows with minimum spill

To evaluate the different alternatives, work groups defined "value measures" to serve as indicators of key resources in their river use area. These value measures were not intended to capture the full range of possible effects but provide a way to measure key impacts and compare them across alternatives. Examples of value measures used by the Wildlife Work Group were habitat quality and evidence of indicator species such as number of Canada Goose nests. The number of value measures for each work group ranged from two to as many as eleven for the Wildlife Work Group. Using the output from the hydroregulation models, such as average monthly flows and reservoir elevations, work groups used spreadsheets and other computer programs to evaluate and rank each alternative against the Base Case. In order to make the evaluation process more manageable, work groups were provided with hydroregulation results for only five of the 50 water years processed. These five years were selected to span a representative range from low to high water conditions.

The results of this analysis varied significantly from one work group to another. For example, nearly all alternatives analyzed in screening resulted in increased power system costs and most increased flood damages over the baseline operation. In contrast, many of these same alternatives resulted in improved anadromous fish survival as was expected, since this was the objective of many alternatives.

Following the completion of screening analysis, 14 public meetings were held to brief the public on the results of the studies and to obtain comments and recommendations. Based on this process, the 90 screening alternatives have been narrowed down to approximately six strategies to be studied in more detail during the final "full-scale" analysis. These final alternatives represent combinations of elements found in the 90 alternatives evaluated in screening. Full-scale analysis will consist of running hydroregulation models again, followed by a much more rigorous analysis by each work group than was used in screening to determine impacts to their particular river use. It is currently projected that the full-scale study phase and a draft EIS will be completed by late 1993.

SCS Study Methodology

The SCS study is similar to the SOR study in that both consider changes to operating strategies or facilities in the Columbia River System to improve anadromous fish passage over the long-term. It was also initiated with a screening process in which various alternatives were considered for further study. There were initially about 30 alternatives identified but after further review many alternatives were eliminated due to technical or environmental concerns. As presently envisioned, approximately 20 alternatives for reservoir drawdown will be modeled for this study. These involve drawdown of the four run-of-river projects on the lower Snake River to elevations ranging from 30 feet to 100 feet below normal operating pool levels. In the 100-foot drawdown alternative, the goal is to model the river system as it would operate under natural conditions without the dams in place. Depending on the alternative, in order to implement these types of operating strategies, it would be necessary to either modify the existing spillway, build a new low level spillway, or build a river bypass structure and river channel around each of the dams. As part of these studies, there are also minor drawdowns being considered at other reservoirs. Other potential alternatives will be considered for future hydroregulation modeling in this study. These would simulate operation of new upstream storage reservoirs to provide additional storage to be used for flow augmentation or refilling existing reservoirs following drawdowns.

The output of the HYSSR computer hydroregulation model in the form of reservoir elevations, flows and other data is used in evaluating the effectiveness of each alternative in improving anadromous fish passage efficiency. To the

extent possible, the ten SOR work groups will be used to analyze hydroregulation results. However, it is expected that much of the analyses will be completed primarily by the Corps, with the assistance of a Technical Advisory Group (TAG) to provide oversight. This group is comprised of representatives from Federal and State agencies, Indian Tribes, and various interest groups.

Evaluation of impacts to anadromous fish is the key variable being analyzed in these studies. This is being accomplished using three different sets of computer models to estimate survival of juvenile fish during passage through the Columbia and Snake River dams as well as the number of returning adult fish. Computer models, spreadsheets, and other techniques are also being used to evaluate impacts in other areas such as resident fish, water quality, wildlife, and others. Since similar analysis techniques are being used in the SOR study described previously, extensive coordination is being done between the SCS and SOR study team to minimize duplication and ensure consistency between the two studies. However, the SCS is the primary study in which detailed evaluation of reservoir drawdown and associated structural modifications will be evaluated.

OA/EIS and SEIS Study Methodology

The OA/EIS and SEIS were conducted and prepared by the Corps in cooperation with other Federal agencies such as the BPA, BOR, and NMFS. The primary objective of the river operation alternatives evaluated in these studies is to improve migration conditions and thereby help to reverse the population decline and contribute to the recovery of threatened and endangered salmon stocks during the interim period until the SOR and SCS studies are completed. These studies were conducted in a similar manner to that used in SOR and SCS studies, with the hydroregulation studies being run using the Corps HYSSR computer model to provide simulated river conditions for different operating scenarios. These results were then evaluated by the staff of many agencies in different technical areas such as anadromous fish, wildlife, water quality, and others. Because the OA/EIS was the predecessor to the SEIS, it considered and screened out a much wider range of alternatives than the SEIS. Approximately 20 different alternatives were considered in the OA/EIS, whereas only five alternatives were considered in the SEIS. The alternatives considered in the OA/EIS and SEIS fit into categories similar to those in the SOR study: (1) no action, (2) reservoir drawdown, (3) flow augmentation, and (4) combinations of flow augmentation and reservoir drawdown.

Following the completion of hydroregulation studies to develop simulated project operation data, evaluation was done to determine which of the alternatives should be selected as the preferred alternative. The primary criteria for evaluating the alternatives analyzed in these studies were: (1) juvenile salmon survival rate, (2) cost-effectiveness, and (3) environmental effects. Juvenile fish passage and salmon life-cycle computer models were used to estimate the effects of alternatives including consideration of ongoing and future actions on Snake River Basin salmon stocks. Cost-effectiveness was analyzed in terms of relative costs to achieve improved juvenile salmon survival. Environmental effects were analyzed in terms of a wide range of categories including water quality, anadromous and resident fish, power, and others. Computer models, spreadsheets and other techniques were used where available to evaluate impacts to different areas of river use. This information was supplemented with actual physical tests such as a two-reservoir drawdown test conducted in March, 1992. This test provided information unattainable through laboratory tests such as data on turbine operation, dissolved gas saturation levels, water velocity, and other data. This data is also being used to help validate ongoing modeling efforts and projections. Based on all of the analysis and tests which have been completed, a preferred operating plan has been developed which represents a combination of elements from many individual strategies such as flow augmentation, reservoir drawdown, and others.

Conclusion

The studies completed to develop new long and short-term operating strategies on the Columbia River System have provided a wealth of information and new techniques for understanding how changes in project operations can improve conditions for anadromous fish such as salmon and other users of the river system. In the process, a vehicle is being developed for adjusting future system operations as demands on the system continue to change. More importantly, through these interagency studies new relationships have been forged between different users of the river and a new spirit of understanding and cooperation have emerged. These relationships and cooperation will be very valuable as future studies are completed and new operating strategies are eventually implemented. Actual implementation and operation of the river system according to these new plans will require continued coordination and cooperation, both of which have been vastly improved through this process.

The Role of the Enhanced Version of HEC5 in Hydropower Planning and Licensing

Wendy C. Bley, Deborah D. Boomhower, L. Greg Bove, Matthew P. Dillis, Bill S. Eichert, P.E., Alan B. Livingstone, P.E., Stephen D. Padula, Matthew J. Putnam, P.E., Thomas J. Sullivan[1], P.E., Mark J. Wamser, P.E.

Abstract

This paper describes the development and use of models that simulate the operation of three river basins that are regulated by hydropower projects operated by the Central Maine Power Company (CMP) and associated companies. Specifically, the paper describes: a) the results of a literature search used to select the appropriate program for this application; b) the factors that led to the selection of the U.S. Army Corps of Engineers HEC-5 - Simulation of Flood Control and Conservation Systems program; c) the development of algorithms, program modifications, and companion programs to enhance HEC-5's ability to model small scale hydropower projects and provide information useful in an Application for License before the Federal Energy Regulatory Commission (FERC); d) the development and calibration of river-basin specific models; e) the development of a "baseline" operations scenario and the judicious selection of "production runs" simulating various licensing scenarios; f) the analysis of results in terms of the economics of lost energy and capacity as well as the effects on hydrologic and habitat time series of various licensing scenarios; g) the use of the model in evaluating alternatives to either enhance production or reduce capital, operations, and maintenance costs.

---

[1]Lead Editor and Contact Point: c/o Gomez and Sullivan Engineers, P.C., 144 Pine Hill Road, Weare, NH 03281, (603) 529-3570

Introduction

CMP owns and operates 30 FERC licensed hydroelectric powerplants with a total installed capacity of 368 MW. In addition, CMP participates in the operation of several headwater storage reservoirs. CMP's hydroelectric generation and storage facilities are primarily located in the Saco, Androscoggin and Kennebec River basins in Maine.

Hydroelectric development on the Saco River consists of 6 hydroelectric generating facilities which are owned and operated by CMP. Two of these facilities are daily cycle peaking projects, while the rest operate as run-of-river projects.

The Androscoggin River has 23 hydroelectric stations at 22 dams along its mainstem. In addition, there are 5 storage reservoirs located in the basin headwaters which provide flow regulation. CMP owns and operates the three largest hydroelectric generating stations in the system in addition to a number of smaller generating stations. Flows from the storage reservoirs are regulated by the Union Water Power Company (UWP) and the Androscoggin River Company (ARC). CMP is the sole owner of UWP and a 25 percent owner of ARC.

On the mainstem of the Kennebec River, there are a total of 10 generating facilities, 5 of which are owned by CMP with a sixth station partially owned and operated by CMP. In addition, there are 4 headwater storage reservoirs that are owned and operated by the Kennebec Water Power Company (KWP). KWP is comprised of the owners of each of the hydroelectric generating stations on the mainstem, including CMP.

Of the total of 15 FERC licensed hydroelectric generating stations owned by CMP on the mainstem in these three river basins, 5 have FERC licenses expiring on December 31, 1993. The total capacity and energy associated with these 5 projects is 155.6 MW and 733,750 MWH/yr, respectively. In addition, 2 of the storage reservoirs in the Kennebec system have licenses expiring in 1993, while 3 of the storage reservoirs in the Androscoggin system are the subject of a FERC jurisdictional investigation.

FERC licensing of the generation and storage facilities in these three basins necessitated that CMP undertake a review of the existing and potential power and non-power benefits associated with its river management. CMP initiated this review in 1986 by discussing information needs with the various resource agencies

involved and subsequently conducting numerous environmental and water use studies. Although this process will be on-going until FERC issues new licenses for several of the projects in late 1993 (or later) a significant milestone in the process was planned for and executed in December 1991 when CMP filed its Application for License for each project with FERC.

CMP undertook a rigorous approach to the process of soliciting and sorting agency requests. In the period from 1986 through 1989, CMP completed numerous baseline environmental studies such as instream flow studies, water quality monitoring and modeling, and impoundment management studies for aquatic and terrestrial habitat. As CMP scrutinized the results of these studies, it became apparent that in order to evaluate the cost and long term benefit of various combinations of the enhancements suggested by study results some type of comprehensive energy simulation model would need to be developed.

The only inhouse tools CMP had available in 1989 capable of evaluating combinations of potential operating restrictions (i.e. headwater elevations, minimum and maximum flows, etc.) were manual methods and spreadsheet models that were both time consuming and approximate at best. It was decided to assign inhouse personnel to evaluate alternative means of conducting these analyses. The System Performance Group was assigned this task and the method they ultimately selected was development of river basin specific models.

One mission of CMP's System Performance Group is to continuously monitor the performance of CMP's hydroelectric, and fossil generating facilities in order to identify potential problems early and prescribe preventative measures. This group was a logical choice for the operations modeling assignment as it had the most intimate knowledge of hydroelectric performance within the service groups at CMP and was the repository of a good deal of data on each station. In mid-1989, this group initiated an overview of available literature and vendor information on operations models. This overview involved contacting a number of vendors, including Harza Engineering Company and its wholly-owned subsidiary, Stetson-Harza, to discuss modeling alternatives.

As a result of these discussions, CMP was able to develop a very detailed specification for operations models for the lower Androscoggin River (from Gulf Island to Brunswick) and the Saco River.

CMP's requirements for the operations model, as

stated in its Request for Quotation (RFQ), are listed in Table 1.

Table 1
CMP's Model Requirements

1	Model operation was to be on an hourly time step for wet, dry, and median hydrologic conditions.
2	Models had to be calibrated to historic data.
3	If a simulation program was used (as opposed to an optimization program), it had to have the ability to maximize both on-peak energy and energy value.
4	The model had to take into account the effects of travel time and flashboard operation.
5	The program had to have the ability to match flow data with Instream Flow Incremental Methodology (IFIM) results such that habitat time series and habitat duration curves could be developed.
6	After development and calibration, the model and source program were to be installed on CMP's inhouse computer system and CMP's personnel trained in its use.
7	The model was to be configured such that it could eventually be converted to either a real time dispatch model or a short-term dispatch planning model.

As part of the proposal preparation process, the Harza Companies initiated a rigorous review of available literature on river/reservoir operations programs as well as an internal review of the available inhouse programs. In general, the available programs could be divided into either optimization or simulation approaches. The optimization programs typically were used to model an existing system with known physical and environmental limitations and optimize system operation for a single objective function such as power production. The goal of any energy or hydrologic modeling exercise in FERC licensing is to illustrate "typical" river conditions based on historic operating practices. Given this, it was decided to develop a simulation model for the project with an optional and separate extension that would maximize power production.

The Harza Companies had several options available to them for simulation programs. In the proposal phase of the project, each of these programs was evaluated in light of CMP's goals.

The choices available to the Harza Companies included several inhouse programs that had been written by staff members as well as several public domain programs. All of the choices available required some level of program modification in order to meet CMP's specification. Based on the criteria listed above, Stetson-Harza elected to use an enhanced version (from Eichert Engineering) of the U.S. Army Corps of Engineers

(COE) HEC-5 Simulation of Flood Control and Conservation Systems program for this application. The factors that weighed heavily in the decision to use HEC-5 included: a) the model's ability to make powerplant release decisions based on reservoir drawdown as well as minimum and maximum flow constraints; b) its compatibility with inhouse programs that use flow data (i.e. flow duration curves, habitat time series analysis, etc.); c) consistency with other FERC licensing projects that FERC would review in the Class of 1993 for which Stetson-Harza had done work; and d) the availability of Bill S. Eichert, to work full time on the program modifications.

The HEC5 model was written by Mr. Eichert when he worked for the COE's Hydrologic Engineering Center (HEC). The initial version of HEC5 was tailored to flood control operations and was released in 1973. Several upgrades to the hydropower and water supply routines were added to the HEC5 program in the mid-1970's and the program was matched with a water quality program (HEC5Q) in the 1980's. The HEC5 model currently has the ability to model conventional and pumped-storage hydroelectric projects. The modes of operation that can be modeled include run-of-river, daily peaking, weekly peaking, and seasonal drawdown.

Within HEC-5, reservoirs are operated to satisfy constraints at the individual reservoir, to maintain specified flows at downstream control points, and to keep the system in balance. The model operates on the basis of levels, which are user-specified target storages for a reservoir. Typically, five levels are set for a reservoir as indicated below and shown in Figure 1.

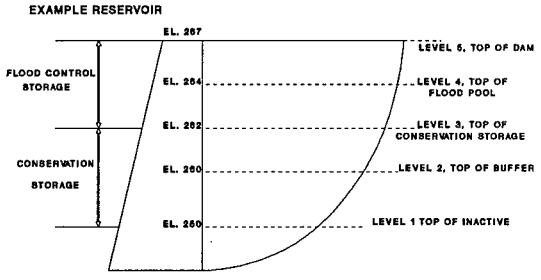

FIGURE 1: RESERVOIR INDEX LEVELS

Of these five, Level 3 is the most significant in the operation of the model. Level 3 represents the target rule curve or the ideal storage which operators

try to maintain over the period of operation. In the absence of other constraints, such as minimum flows for protection of aquatic life, peak electrical demand periods, or whitewater rafting releases, the model will maintain Level 3 given the data input for the stage/storage relationship, outlet capacity of the dam, and channel capacity below the dam. These levels can be changed seasonally, monthly, weekly, daily, or even hourly.

Some of the more important non flood control release criteria for reservoirs are listed in Table 2.

Table 2
HEC5 Flow Release Criteria

1	When the reservoir level is between the top of Conservation Pool (Level 3) and the top of the Flood Pool (Level 4), releases are made to draw the reservoir to Level 3 without exceeding the user-specified channel capacity downstream of the dam. Above Level 4, releases are made up to the outlet capacity of the dam.
2	Releases are made equal to or greater than the user-specified minimum desired flow when the reservoir level is greater than Level 2, and equal to the minimum required flow when the reservoir is between Level 2 and Level 1. Releases needed to meet power requirements will override minimum desired flows if these generation flows are greater than the minimum flows.
3	No releases are made when the reservoir level is at or below Level 1.

Within HEC-5, reservoirs can be operated to meet their own flow and drawdown constraints and/or to operate for other downstream locations. In operating a system of reservoirs, the model works to keep all reservoirs "in balance" or at the same level. In balancing levels among reservoirs for conservation operations, releases are governed by levels, such that all reservoirs will be drawn to the same level if possible.

As with storage reservoirs, hydroelectric stations operate on the basis of levels. In addition to flow requirements for the protection of aquatic resources and recreational uses, releases are made to meet energy requirements for the station. The typical procedure is to use water stored between Levels 2 and 3 for power generation. The capability of HEC-5 to use rule curves which vary over time is especially important for realistic modeling of hydroelectric stations. For example, a seasonally varying rule curve can be input to model station operations with and without flashboards. A daily varying rule curve which limits drawdown across a week can be used to model the operation of a weekly cycle plant. An hourly varying rule curve which limits drawdown across a day can be used to model a daily cycle station.

In response to the specification issued by CMP, Stetson-Harza scrutinized the version of the HEC5 program

that existed in 1989. This review of the model revealed the limitations listed in Table 3 in applying the model to FERC licensing studies for hydroelectric power projects in the northeast.

Table 3
Limitations of the 1989 Version of HEC5

1	No minimum turbine operating flow can be stipulated.
2	No mechanism is available to model weekly cycle rule curves.
3	Powerplant efficiency cannot be described as a function of reservoir outflow.
4	Only one spillway rating curve can be used to describe an entire year's operation (i.e. seasonally varying flashboard conditions could not be described).
5	Limited capabilities to describe station energy demands.
6	No internal habitat or flow duration analysis capabilities.

In order to overcome these limitations, Stetson-Harza contracted Mr. Eichert to make program modifications. Under this arrangement, Stetson-Harza, with input from CMP, developed specifications from which Mr. Eichert modified the HEC5 source code. Testing for each of the modifications was carried out in a joint effort between Mr. Eichert and Stetson-Harza. The specific enhancements made to the program are listed in Table 4.

Table 4
Enhancements Made to the 1989 Version of HEC5

1	A minimum turbine operation flow can be stipulated.
2	Powerplant efficiency can be stipulated as a function of turbine outflow.
3	Reservoir discharge curves can vary seasonally to model flashboard up/down conditions.
4	Energy and Revenue Demand Patterns can be stipulated to allow for monthly varying peak day, week day, and weekend day powerplant demand and revenue.
5	Weighted Usable Area (WUA) vs flow relationships from fisheries habitat studies using IFIM (USFWS, 1982) can be input and habitat time series files developed.
6	Duration analysis for various months can be undertaken for any HEC5 output variable including flow and WUA.
7	Minimum flows can be modeled on the basis of a stipulated flow or inflow, whichever is less. This is typically how minimum flows are stipulated by FERC. The model also has the ability to meet minimum flows from storage.
8	Enhanced reservoir operations to allow a combination of reservoirs to provide flows downstream of other reservoirs with storage.
9	Capability to make release decisions on more than one time step in a single model run. This is particularly useful in basins with storage reservoirs where release decisions are made on a weekly or daily basis and peaking powerplants where release decisions are made on an hourly basis.
10	Daily and weekly rule curves can be stipulated that allow for reservoir drawdown gradually over the powerplant cycle period.

In a parallel timeframe to the HEC5 program modifications, Stetson-Harza began development of the input for the wet, median, and dry year calibration models for each of the basins. This process started with a site inspection and the compilation of engineering, flow, demand and energy value data.

As a result of CMP's Turbine Index Testing Program, the level of engineering data available for the Kennebec, Saco, and Androscoggin River models was higher than for any comparable HEC5 project that Stetson-Harza has worked on. This was particularly true in the areas of tailwater rating curves, efficiency (index) curves, and headloss information. Where possible, all engineering data furnished by CMP was verified by Stetson-Harza and the few data gaps that existed were filled in by engineering computations based on the layouts of each powerplant.

The compilation of flow data was initiated by the selection of wet, median and dry years. This was accomplished by comparing annual flow duration curves at U.S. Geological Survey (USGS) gages within the basin to the long term period of USGS record flow duration curve. The year within the period of available CMP powerhouse records whose annual flow duration curve most closely matched the period of USGS record annual flow duration curve was selected as the median year. The wettest and driest years within the period of available CMP records were similarly delineated.

The period of available CMP powerplant records was important as the data from these records was used to calculate reservoir inflow based on plant records of outflow and change in storage. Regulated inflow from upstream projects was subtracted from the computed total inflow to make a first estimate of unregulated inflow to each project. Where these records were not available, the first estimate of inflow was calculated based on synthetic hydrology and the use of USGS gage records from similar unregulated drainage areas. Unregulated inflow hydrographs were then incorporated within the HEC5 input.

Once the data development phases of the project were completed for both river systems, the three target years were calibrated to total monthly energy production at each station. In general, the predicted monthly energy was calibrated to within 10 to 15 percent of the known monthly energy at each station, and within 5 percent of the known annual energy. The calibration procedure required for each target year and river system were typically the same. In order to calibrate the model, adjustments were made to the computed unregulated inflow or to operations criteria (drawdown, flow range of

units). In general, there was very little adjustment of engineering data during the calibration process.

Once calibration was achieved for a given target year, the engineering and unregulated inflow data were, in general, held constant and "baseline" models were developed. The baseline models typically reflect existing FERC license operating conditions relative to impoundment drawdown levels and minimum flows. The exception to holding the engineering data from the calibration models constant was if some type of unit upgrade had occurred between the target calibration year and the 1990/1991 (years of final model development) period. The reason for this is that by definition, the baseline model is to reflect existing conditions at the time of the FERC license application.

The energy, revenue, hydrologic, and habitat results from the baseline model became the standard against which alternative operating scenarios were compared. These alternative operating scenarios or "production runs" typically involved combinations of various impoundment drawdown conditions, minimum continuous flow requirements downstream of storage reservoirs or peaking power projects, and minimum continuous flows in project bypasses.

Due to the fact that these river basin models can generate large amounts of information for each run, the judicious selection of production runs was important in order to develop a data base of alternative operations that provided a useful amount of manageable information. Based on the results of its environmental specialty studies and agency consultations, CMP developed an initial list of production runs that bracketed the range of license conditions that it thought would be encountered.

For each river basin model, Stetson-Harza made the baseline run and the first five production runs. The HEC5 program and basin specific models were then installed on CMP's in-house computer system and Stetson-Harza trained CMP System Performance, Engineering, and Environmental Science personnel in model use. Due to the timing of the operations modeling project relative to the December 1991 FERC filing deadline, CMP's ability to accomplish production runs in-house was critical. This ability allowed the staff of both CMP (Saco and lower Androscoggin models) and Stetson-Harza (Kennebec model) to work in parallel during the relicensing "crunch time" from July - December 1991.

Since the filing of the license applications, FERC

has had several Additional Information Requests (AIR's) that have required the use of the operations models. In particular, FERC has asked for habitat time series analysis of downstream fisheries habitat at several projects. This analysis typically involves the development of a habitat duration curve using flow time series data and WUA vs flow curves derived from IFIM studies. A schematic of the algorithm used in HEC5 to produce habitat duration curves is included as Figure 2. Having this capability in the model has allowed CMP to easily generate these curves for a variety of operation alternatives and target species.

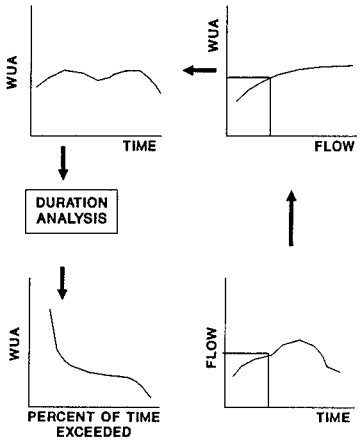

FIGURE 2: HABITAT TIME SERIES LOGIC CHART

The operations modeling project has accomplished all of the FERC licensing goals originally established by the project team. In addition, the model has been used by CMP to evaluate: powerhouse capacity upgrades to adjust operation of a 22.6 MW plant to better use water within its existing physical and environmental constraints; to evaluate the benefits associated with rubber dam replacement of wooden flashboards; and to evaluate operational alternatives to building fish ladders.

On a broader perspective the enhanced version of HEC5 has become of a standard in FERC licensing in the northeast and is recognized and accepted by the resource agencies. Models have been completed by Stetson-Harza for FERC relicensing projects for the New England Power Company, Green Mountain Power Corporation, Citizens Utilities Company, and Niagara Mohawk Power Corporation. In each case, the model has had an incalculable benefit as an overall tool for evaluating various water management plans.

USING PUMPED STORAGE FOR SYSTEM REGULATION --A TRANSATLANTIC PERSPECTIVE--

Fred R. Harty, Jr.[1] and Jeff A. Scott[2]

Abstract

Worldwide experience with the use of pumped storage has demonstrated the value of this extremely flexible load management tool such that pumped storage is being considered for several new applications throughout the United States. The authors draw on their separate experiences with pumped storage practices in the United Kingdom and the United States to describe the system regulation benefits that can be applied to U.S. power dispatching pools. The paper also emphasizes that the potential system regulation benefits -- and the associated design and cost implications -- must be acknowledged in the initial planning of a new plant.

The paper describes the use of the Dinorwig and Ffestiniog pumped storage stations in Wales to provide the National Grid Company's Pumped Storage Business with marketable system regulation products on a system of interconnected utilities. The paper also describes the development of pumped storage practices in the United States and the progression from pure energy storage to the dynamic system regulation plants being developed for specific applications today. The conclusion notes that European and U.S. pumped storage experience is being combined to provide even greater enhancement of resource utilization in the U.S. utility markets today.

---

[1] Senior Principal Civil Engineer, Stone & Webster Engineering Corporation, 245 Summer Street, Boston, MA 02210 - USA

[2] Business Development Manager, The National Grid Company plc, Deeside, Clwyd, U.K.

Introduction

The pumped storage concept began in the 19th century as a means of storing available excess energy for use at a later time. Now, as we approach the 21st century, pumped storage has evolved into a far more comprehensive integrated resource management device -- a dynamic and powerful system management tool which enables utilities to provide the high quality of electricity service demanded by a modern, developed society.

The development of pumped storage has been a worldwide phenomenon characterized by a continual exchange of ideas on the world marketplace. The earliest use of the pumped storage concept is believed to have occurred in 1879 at a project located near Zurich, Switzerland. (Ref. 1) Switzerland also contributed the first documented use of pumped storage for electric power supply when the Ruppoldingen station was constructed on the Aare River in 1904. (Ref. 2).

Pumped storage stations are now in use all over the world and there remains a continuous development of the industry facilitated by the exchange of ideas across international boundaries and supported by specialist trade associations and international conferences.

The evolution of pumped storage from pure energy storage to dynamic system regulation tool is illustrated by the sequential developments that have crossed back and forth between the United States and the United Kingdom. This transatlantic perspective has been selected to describe the authors' independent, but related experiences in the industry.

In some respects, the developments in pumped storage have been conceptual and cultural as much as technological. The relative isolation of the U.K. system from neighboring interconnections dictated the need for fast response and frequent mode change capability to maintain system frequency. The strategic value of pumped storage in providing this capability was accorded such significance that the two stations, Ffestiniog and Dinorwig, were vested in The National Grid Company during the recent privatization of the electricity industry in England and Wales.

The situation in the United States has developed differently for a number of reasons. In the U.S., frequency stability is treated over a longer time frame than in the U.K. because of the extensive interconnections between neighboring systems. The need for prompt corrective action does, however, remain and, as in the U.K., the system regulation capability has taken on greater significance with the recent passage of legislation promoting open access to transmission facilities. Thus technical needs

have given rise to technical solutions which have subsequently led to unexpected applications for dealing with cultural changes in the economy. The evolution of the pumped storage industry in the U.S. and the U.K. illustrates this interplay between applications stimulating technical developments and technical developments stimulating applications.

Technical Developments in the United States and the United Kingdom

The first pumped storage project in the U.S. was the Rocky River plant which went into service in 1929 and is still being operated by the Connecticut Light and Power Company (Ref. 3). Rocky River has one conventional 25 MW generating unit and two 3.5 MW pumping units which have been converted to reversible operation for use as pump-turbines. The plant is used for seasonal storage and release of water at an off-steam reservoir.

The modern pumped storage era in the U.S. began over 30 years later with the commissioning of reversible pump-turbine units having capacities of over 100 MW. Large capacity pumped storage stations commissioned in the early to mid-1960s included Taum Sauk, Yards Creek, Muddy Run, and Cabin Creek. These stations were intended primarily to provide for the storage of off-peak energy and return of blocks of peaking power. Once in use, however, some of these stations were operated at varying load to provide spinning reserve and load following capabilities.

These early large capacity pumped storage projects were not provided with what would now be considered as rapid start and multiple load change capabilities. Time from standstill to on-line was typically on the order of 5 minutes. A typical mode change pattern involved only one pumping session and two generating sessions per day on each unit. While, this is very severe duty compared to a conventional hydroelectric turbine, it is light duty compared to some of the more recent pumped storage stations. This more frequent mode changing has, however, taken its toll. For example, large stress changes and associated fatigue have presented considerable difficulty on the Yards Creek pump-turbines, which are presently being upgraded for continued service. Performance is expected to increase after the upgrade, but the mode changing capability will be essentially the same because of other existing limitations. The upgrade is discussed in other papers being presented at this conference but it is important to note here that the large capacity pump-turbines of the Yards Creek era were not intended for the frequent mode changes that can be accommodated by the more advanced technology of today. Even, with their limitations, these pioneers of the modern pumped storage age offered new dimensions for managing modern electricity systems. They excited the interest of utility planners and stimulated the imagination of system dispatches and designers

and plant designers and operators.

Similar developments with a slightly different emphasis were taking place in the U.K. around the same time, as illustrated by the pumped storage stations at Ffestiniog in North Wales and Cruachan in Scotland. Ffestiniog was commissioned in 1963, Cruachan in 1966. Ffestiniog, which uses separate pumps and turbines, has four units with a total installed capacity of 360 MW. Ffestiniog is capable of synchronizing from standstill within 5 minutes and has a ramping rate of around 90 MW per minute. Cruachan has a total installed capacity of 400 MW using four reversible pump-turbine units. With a head of 1200 ft, the Cruachan units were the highest head reversible pump-turbines in the world until the commissioning of Cabin Creek, back in the U.S., a year later.

The design of Cruachan also included features for more dynamic services than had previously been experienced with pumped storage -- features which would be followed with great interest elsewhere. A surge tank on the low pressure side of the system provides for a relatively short active water column which combines with the high head to provide fast starting times. A further feature which figured at Ffestiniog, and was consolidated at Cruachan, was the ability to provide a quick transition to generation from a dynamic standby mode in which the turbines are spinning in air, while synchronized to the grid system. Cruachan can achieve full load within 2 minutes from standstill and within 1 minute from the spinning in air mode.

Progress at Cruachan was closely followed by the designers and managers of the Northfield Mountain station being developed by Northeast Utilities in western Massachusetts in the U.S. Personal communication was established between the Northfield design team and the Cruachan Station personnel to share test results and other developments as they occurred at Cruachan.

Northfield Mountain has a total installed capacity of 1080 MW from four reversible pump-turbine units operating at a maximum head of around 830 ft and was commissioned in 1973. For the design of Northfield Mountain, Northeast Utilities required that significant additional steps be taken toward the achievement of a dynamically responsive station. Northfield was therefore designed with a number of features to provide quick response, including:

- a short high-pressure water conduit coupled with a surge tank on the low pressure side to provide fast water starting time for the available head;

- pumped oil lubrication to the pump-turbine guide bearing and generator-motor thrust bearing to provide immediate lubrication for quick starting;

- inlet spherical valves with water operated seals and 15 second plug opening times to permit early opening of the wicket gates (guide vanes);

- wicket gate (guide vane) total effective operating time of 8 to 15 seconds to permit rapid load pickup and changes.

Employing these features, a unit at Northfield Mountain can be brought on-line in about 1 ½ minutes from shutdown. The fast wicket gate (guide vane) timing also provides for a ramping rate comfortably exceeding design requirements and previous operating experience. Transition from spinning in air to full-load generation was included in the design but, thus far, has not been implemented. Rather, the plant is routinely dispatched to provide load regulation and spinning reserve at part load. Overall, Northfield Mountain represented a significant further step forward towards fast acting pumped storage technology.

The next link in the chain of transatlantic developments was, in many ways, a step change in the development of dynamic capability with the addition of frequent mode change operation to an even faster response characteristic in the design of the Dinorwig pumped storage station in North Wales. Dinorwig was being planned at about the same time as the last of the four Northfield Mountain units was being commissioned in 1973. In planning to meet the future demands of the electricity system in England and Wales, the designers of the Dinorwig plant advanced the pumped storage concept into a new era -an era in which pumped storage manifests itself as the generation industry's most dynamic and flexible tool available for the management of a modern electricity system, particularly a system in which open access transmission considerations can be accommodated.

The capabilities of the Dinorwig plant are impressive, practical, feasible, and dispatchable. They include:

- four-second spherical valve opening to permit early opening of the wicket gates (guide vanes) during starting or during loading from spinning in air;

- the ability to produce full output from the spinning-in-air mode within 16 seconds;

- the capability to synchronize to the line from shutdown within 1 minute;
- a maximum ramping rate up to 50 MW per second per unit;
- the capability of rapid pump deloading to the spinning in air condition and;
- the designed-in capability to operate routinely up to 40 mode changes per unit per day.

This last feature allows continual switching back and forth between operating modes (shutdown, spinning-in-air-generating, generating, pumping and spinning-in-air-pumping). This presents the system operators and dispatchers with a highly flexible tool for management of the power system.

Technical and Commercial Comparison of the U.S. and U.K. Electricity Systems

The differences and similarities between the U.S. and U.K. electricity system requirements -- and changes in requirements -- provide insight to the respective technical adaptations in the two countries.

The electricity system in England and Wales operates essentially as an independent network with relatively few interconnections. The system is linked to Scotland via direct ac grid connections of just 1000 MW capacity while the only other tie, to France, is via a dc link offering limited dynamic support. This relative isolation has imposed special requirements upon the dynamic response characteristics of system reserve to ensure the restoration of frequency following system incidents.

A typical winter day plateau on the England and Wales system consists of a total system demand equal to about 40,000 MW. The frequency characteristic for a sudden loss of 1,000 MW under these conditions requires the injection of 800 MW in 10 seconds to arrest the fall and restore frequency to within statutory limits (49.5 to 50.5 Hz). This "Primary Response" capability is drawn from the inherent thermal inertia of steam plant on the system but, due to the rapid decay of this flash steam reserve, there is an immediate need for a sustained power input over the following "Secondary Response" time scale of 10 to 30 seconds. Providing such Secondary Response from steam is inefficient and expensive since an excessive amount of thermal plant part loading, often with an unpredictable response characteristic, is needed to provide the rapid 800 MW infeed. The advent of Dinorwig provided the system operator with a generation and system management facility to schedule Secondary Response using pumped

storage spinning in air, resulting in both significant economies and increased system reliability.

The transmission interconnections in North America provide much stiffer systems than that of England and Wales. The sudden loss of a large block of generation does not generally cause a sustained decay of frequency because the load flow over the inter-ties acts to retards such decay. The resulting load flows do, however, cause distress to the adjoining interconnected utilities. Therefore, the utility or pool experiencing the incident is required to restore its system bias error to zero within 10 minutes. While this is not as severe a standard as that prevailing in England and Wales, the need for prompt corrective action remains and the flexibility of pumped storage remains a boon to system operators in such circumstances.

On the commercial side, the recent structural changes in the England and Wales system, resulting from the privatization of the U.K. electricity industry, has given rise to a need to separately evaluate and account for the system support services (termed Ancillary Services). These services include voltage control/reactive power, frequency control/regulation, and the system black start capability. The Pumped Storage Business is a significant provider of these Ancillary Services. This supports the reasoning behind vesting the pumped storage plants in the National Grid Company as part of the privatization process, and emphasizes the strategic value of pumped storage to the system in England and Wales -- a system which, since privatization, has witnessed full implementation of open access transmission concepts.

A similar challenge is presenting itself in the United States where dynamic response will take on an added significance in the coming years. The U.S. is not yet experiencing the same economic and political incentives for carrying out the identification and discrete evaluation of system services. U.S. utilities could however, benefit from such a pricing study, particularly with increasing restrictions on system flexibility resulting from the presence of must-run non-utility generation and the movement towards open access in transmission. Therefore, utility planners must appraise the full range of options for mitigation of these constraints including the options provided by state of the art pumped storage technology.

New Developments in the United States

The baton of pumped storage development is now being passed back across the Atlantic, with even more sophisticated advancements in technology appearing in a number of new projects here in the U.S. With these new developments, it is incumbent upon system planners and

designers to seek full recognition, in project evaluation and integrated resource planning assessment, of the intrinsic value of the flexibility provided by this technology.

An example of the new U.S. developments, which draw upon the experience of Dinorwig, Northfield Mountain and their distinguished predecessors, is the Mt. Hope Waterpower Project which is currently under development in New Jersey. This project will draw on the Norwegian pump-turbine supplier's design of the Dinorwig pump-turbines, The National Grid Company's experience with operating this plant and the American engineering firm's experience with U.S. pumped storage developments.

Mt. Hope promises several enhancements of the Dinorwig precedent and now permits technology to govern over topography. The project will include excavation of an upper reservoir at ground level and a lower reservoir at a selectable depth well below the surface. The available head can therefore be matched to the pump-turbine technology rather than to the available topography. Furthermore, the project could be sited near major load centers rather than at a remote distance as would normally be dictated by topographical considerations.

The Mt. Hope Waterpower Project is described in more detail in other papers being presented at this conference; the main point of emphasis here is that Mt. Hope and future pumped storage project will all draw upon and advance the wealth of industry experience worldwide. For Mt. Hope in particular, the progressive and diverse applications on opposite sides of the Atlantic provide a special opportunity for the confluence of Norwegian, British and American pumped storage skills and experience.

Expectations for the Future

Each of the existing projects described in this paper was developed to satisfy a need identified and defined at the time of its conception. Upon completion, each project proceeded to demonstrate a potential for applications and operating regimes which were previously beyond the realms of consideration. The capabilities of Dinorwig, for example, were specifically tailored to meet the requirements for fast acting reserve to restore and regulate frequency on the U.K. system, particularly in the event of a loss of generation elsewhere. The design criteria called for the ability to pick up 1320 MW in 11 seconds from the spinning in air condition. Since being commissioned in 1983, the flexibility afforded by Dinorwig to the system operators has resulted in the plant being employed in a variety of reserve and operating regimes, many of which were not envisaged at the time of the original conceptual design. This "added value" phenomenon, which hindsight shows to have been a regular feature of advancements in

pumped storage technology, is a reflection of the difficulty in assigning the full value of the outturn benefit of a project at the development stage. The potential has, however, fueled the ongoing development of pumped storage technology and the interchange and co-operation between projects world wide.

New projects, like Mt. Hope, are continuing this evolutionary development of pumped storage technology by providing for applications which today are not as yet fully evaluated, but they are definitely being used and will become more crucial as we approach the 21st century.

References

1. Civil Engineering Guidelines for Planning and Designing Hydroelectric Developments. American Society of Civil Engineers. 1989.

2. Emil Mosonyi. Water Power Development. Budapest: Publishing House of the Hungarian Academy of Sciences. 1965.

3. Personal communication with Dr. Antonio Ferreira, Project Manager for the Planning and Engineering of Northeast Utilities' Northfield Mountain Pumped Storage Plant.

Two Reservoir Regulation Model for Small Hydro Developments

P.C. Helwig[1] and T.P. Tung[2]

Abstract

At many small hydro sites in Eastern Canada there are attractive opportunities for developing upstream storage reservoirs, generally by construction of a low dam at the outlet of a natural lake and raising the water level by one or two meters above the original level.

In order to assess the advantages of such upstream storage sites a regulation study is required. Although a variety of versatile, but complicated models exist no "user friendly" system is available in the market place. TRESMOD (Two Reservoir Model) was developed to fill this need and to provide a convenient and efficient means of assessing the benefits of upstream storage associated with small hydro developments.

TRESMOD simulates, on a daily basis, the operation of a two reservoir system comprising a single power plant, a forebay reservoir and an upstream reservoir. The program accounts for inflows, outflows, flow diversions, riparian flow releases and variations in reservoir storages and determines energy production in accordance with a "rule curve" operating procedure. Variations in plant headwater levels, tailwater levels, including the effects of spillway flows, are taken into account in computing energy production.

[1]Technology Officer and [2]Manager, Hydraulic Energy Program, Efficiency and Alternative Energy Technology Branch, CANMET, Department of Energy, Mines and Resources, 580 Booth Street, Ottawa, Ontario Canada K1A 0E4, telephone (613) 996-6119 or fax (613) 996-9416.

Initial development of TRESMOD was carried out under Mr. Helwig's direction while he was an employee of ShawMont Newfoundland Limited, P.O. Box 9600, St. John's, Nfld, Canada, A1A 3C1.

Introduction

The topography of many areas in Eastern Canada is favourable to the development of storage reservoirs, generally by the construction of a low dam at the outlet of a lake and raising the water level by one or two meters above the natural level (ShawMont, 1986 and 1988). Such reservoirs significantly enhance the benefits of a downstream hydro development and can often be built at low cost and without causing unacceptable environmental impacts.

In order to assess the benefits of upstream storage sites a regulation study is required. Although a variety of versatile, but complicated reservoir regulation models exist, no "user friendly" system is available on the market. TRESMOD (Two Reservoir Model) was developed to fill this void and to provide a convenient and efficient means of assessing the benefits of upstream storage development. It was envisaged that this program would be used by engineers working in the small hydro field.

TRESMOD is the culmination of a series of site specific reservoir regulation models developed by ShawMont Newfoundland Limited to analyze small and medium sized developments in the Province of Newfoundland, Canada. Most of these studies involved medium and high head developments, where the simplifying assumptions of constant plant head, constant efficiency, monthly flows and fixed plant flow capacity were sufficiently accurate for determination of plant energy benefits. The development of TRESMOD was based upon the procedures and experience gained with these earlier models. The main enhancements incorporated in TRESMOD are a realistic representation of power plant and spillway operations, and simulation of system operation on a daily basis. With these improvements, TRESMOD becomes a more general program - equally suitable for low, medium and high head sites. TRESMOD was implemented in a menu-driven environment and is therefore very "user friendly".

The initial phase of the development of TRESMOD was carried out by ShawMont Newfoundland Ltd. in 1988-89 under a contract with the Dept. of Energy, Mines and Resources, Ottawa. At the time of writing (January, 1993) work was underway to implement further enhancements - primarily the improvement from monthly to daily simulation.

The monthly version of TRESMOD has been applied on studies in Newfoundland, Canada and in Nepal.

Description of Model

Figure 1 shows the configuration of the hydraulic system assumed in TRESMOD and defines the main variable names; while, the calculation process follows the flow chart given in Figure 2 (both figures are at end of paper). The main elements of the program were developed as eight modules,

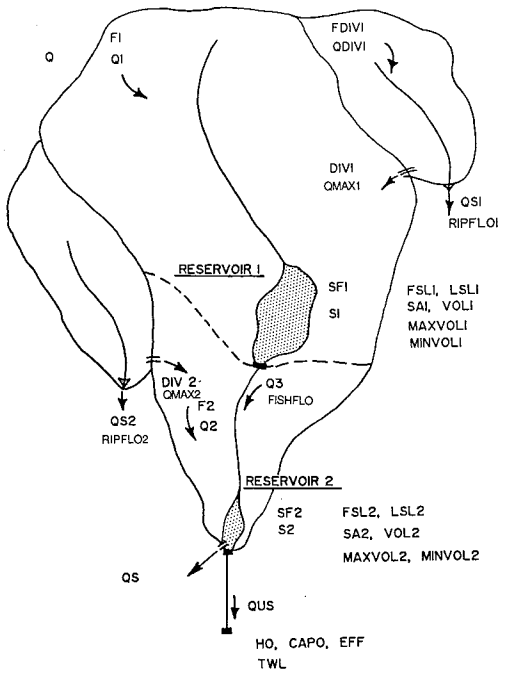

DESCRIPTION OF INPUT/OUTPUT DATA

Q	= PROJECT FLOW
F1, F2, FD1V1, FD1V2	= FLOW FACTORS
Q1, Q2, QD1V1, QD1V2	= SUB-BASIN FLOWS
QD	= POWER DEMAND FLOW
QMAX1, QMAX2	= DIVERSION CANAL CAPACITIES
QS, QS1, QS2	= SPILLAGE
DIV1, DIV2	= DIVERTED FLOWS
Q3	= RELEASE FROM RESERVOIR 1
QUS	= FLOW USED TO PRODUCE ENERGY
RIPFLO1, RIPFLO2, FISHFLOW	= RIPARIAN FLOW RELEASES
FSL1, FSL2	= RESERVOIR FULL SUPPLY LEVELS
LSL1, LSL2	= RESERVOIR LOW SUPPLY LEVELS
SA1, SA2	= RESERVOIR SURFACE AREAS
VOL1, VOL2	= RESERVOIR VOLUMES
MAXVOL1, MAXVOL2	= VOLUME AT FSL
MINVOL1, MINVOL2	= VOLUME AT LSL
SF1, SF2	= LIVE STORAGE AT FSL IN FLOW UNITS
S1, S2	= AVAILABLE LIVE STORAGE AT END OF ANY DAY, IN FLOW UNITS.
HO, CAPO, EFF, E	= MEAN (RATED) NET HEAD, RATED CAPACITY, OVERALL EFFECIENCY, DAILY ENERGY OUTPUT.
TWL	= TAILWATER LEVEL

FIGURE 1: TWO RESERVOIR MODEL WITH DIVERSIONS

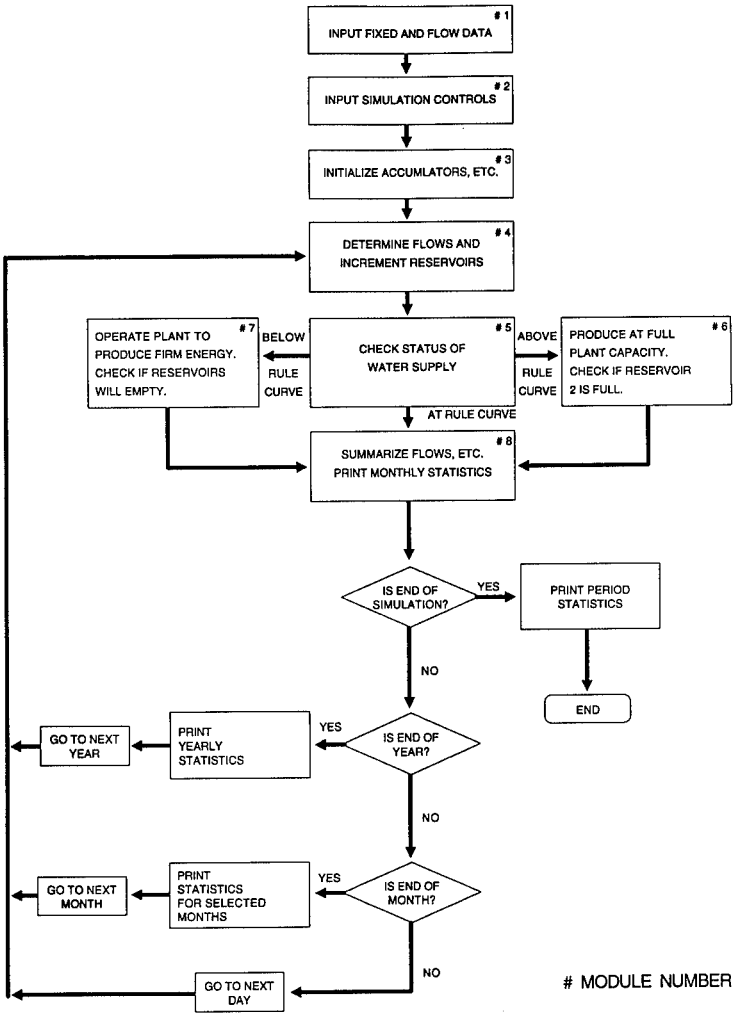

FIGURE 2: PROGRAM LOGIC

mainly for the convenience of program development and debugging. The function of each of these modules is outlined below:

a) Module 1A - Input Fixed Data

This module reads fixed data defining the characteristics of the basin, the reservoirs, the spillway, the power plant and the tail race. Data for the reservoirs is requested in the form of elevation-surface area tables. The corresponding reservoir volume tables are calculated by the computer using the conical formula.

b) Module 1B - Flow Data

Flow data is read in from Water Survey of Canada data files on floppy disk and stored in a program work file. The data will be displayed or printed out in yearly calendar tables to facilitate review by the user. The user will be required to fill in data voids or correct data to his or her satisfaction. This can be done directly from the computer keyboard.

c) Module #2 - Simulation Controls

Data for control of each simulation are read in this module. These data define the simulation period, rule curve volumes and initial reservoir contents.

d) Module #3 - Initialize

Accumulators are set to zero and the values of selected parameter limits are calculated in this module. Also in Module #3, the initial year of flow data will be read into RAM memory from the flow work file created in Module #1B.

e) Module #4 - Determine Flows and Increment Reservoirs

Module #4 is the first step in the simulation process itself. In this module a daily flow is read from the flow work file and sub-basin flows computed for each sub-basin. The computer then determines the "uncontrolled flow". This is the net power flow after inflows to the reservoirs have been stored and reservoirs out flows adjusted for the required minimum water releases. This computation step is purely for the convenience of subsequent computations, since any further adjustments will be additional releases from the reservoirs to provide the required demand flow.

f) Module #5 - Check Status of Water Supply

Water supply status is checked with reference to a rule curve of day's end reservoir contents. This comparison is done by

determining the energy production that would be obtained by adjusting the day's end reservoir contents to the rule curve value. If the "rule curve" energy production thus obtained is less than the firm energy value then the "below rule" curve condition would be indicated. If, on the other hand, the "rule curve" energy was found to be greater than the maximum plant energy capability, then the "above rule" curve condition would be indicated. A valid rule curve solution would be an energy production intermediate between the above two extremes. Based on the above determination, the appropriate computation path is selected.

- to Module #6 for "above rule curve"
- to Module #7 for "below rule curve"
- to Module #8 to output results

g) Module #6 - Above Rule Curve

The "above rule curve" condition indicates there is a potential water surplus and the optimum strategy would be produce energy at the maximum rate, so as to minimize spillage. Four possible solutions may exist in this solution domain. These solutions are:

- general solution, no spillage
- spilling, all day
- spilling at start, but not at end of day
- spilling at end, but not at start of day

Module #6 identifies the correct computation path and determines the maximum possible energy output.

h) Module #7 - Below Rule Curve

The "below rule curve" condition indicates there is a potential water deficit and the optimum strategy is to conserve water by limiting energy production to the firm energy level. In this solution domain there are two possible solutions.

- general solution, firm energy produced without emptying both reservoirs

- reservoirs are both emptied, unable to produce firm energy

Module #7 identifies the correct computation path and determines daily energy output.

i) Module #8 - Output Management

Module #8 checks the simulation status, to determine whether the computations have completed a month, or year or reached the end of

the simulation period. Depending on this status determination, Module #8 will prepare, monthly, yearly or period reports and re-initialize the next simulation cycle, if required.

Module #8 will initially read all results into an output file on disk. The simulation reports will then be prepared from this file at the end of the simulation process. This approach will permit some re-ordering of the data to prepare reports in a convenient layout. The file layout is also designed to facilitate post processing of the results by the user if he or she so desires.

The possible solutions applied in TRESMOD are summarized in Table 1 below:

Table 1 Possible Solutions List

	Status	Solution Type	Energy Output	Computation Path
1.	At rule curve	At rule curve	$Em>E>E_f$	Solution in Module 5
2.	Above rule curve	General solution, no spilling	$E = Em$	Solution in Module 6
3.	Above rule curve	Spilling all day	$E = Em$	Solution in Module 6
4.	Above rule curve	Spilling at start of day	$E = Em$	Solution in Module 6
5.	Above rule curve	Spilling at end of day	$E = Em$	Solution in Module 6
6.	Above rule curve	General solution	$E = Ef$	Solution in Module 7
7.	Above rule curve	Both reservoirs empty	$E<Ef$	Solution in Module 7

Options

Three options are provided, as below

- metric or imperial units
- overflow weir or gated spillway
- daily peaking operation

Discussions

The effort required for development of TRESMOD was evenly split between development of the data handling modules and the analysis modules. The main difficulties in design of the analysis modules concerned the development of solutions for the "above rule curve" condition. Starting with a known water level at the start of a day the solution seeks the day's end water levels, power production and flows. In this compulation the maximum plant energy and plant flow are scaled from the rating conditions and a solution found where conservation of flow is preserved. The governing equations are:

- let $\overline{H} = (\text{LASTHWL} + \text{HWL})/2$
- then $Em = Eo\left(\frac{\overline{H}}{H_0}\right)^{1.5}$

$Qus = Qo\left(\frac{\overline{H}}{H_0}\right)^{0.5}$

- where Ho, Eo, Qo = rated values
- also $Em = \text{EFF.M.}[\overline{H} - \text{TWL} - \text{HL}]$
- where $\text{TWL} = f(Q_{TOT})$

$Q_{TOT} = Qs + Qus$

$Qs = \int_{\text{LASTHWL}}^{\text{HWL}} \text{SPF.}\ (\text{HWL-CREST})^{1.5}.dH$

$HL = K.Qus^2$

- and $Q_D = Qus + Qs \pm \Delta S_2$

$M = 9.81$ (metric) or 0.0846 (imperial)

This procedure makes repeated use of a subroutine MAX which calculates the maximum output and power flow for any head water level.

A similar procedure is used for the "below rule curve condition, except that energy output is fixed at the firm value. The solution approach in the "below rule" curve condition uses another subroutine MIN which computes the plant operation parameters for any water level when firm energy, Ef, is being produced. Both procedures involve iterative solutions that are relatively slow. At the time of writing (January 1993) the possibility of implementing an alternative solution procedure was under study. In this procedure initial curves of Emax and Qus versus HWL and Ef and Qus versus HWL would be initially established in Module #3 and subsequent solutions obtained by interpolation within the results table.

As presently designed the reservoir priority is fixed with water being released preferentially from Reservoir 1 (upstream). The use of a proportionate

water release allocation procedure would allow greater flexibility in the use of the model. This modification will be considered for a future update.

TRESMOD was written in Basic-Version 3.2 for an IBM XT or AT personal computer or compatible.

Conclusion

TRESMOD has been developed stepwise from more approximate models to provide a means of assessing energy output on small hydroplants where an accurate representation of plant operating characteristics is required. The monthly version has been applied on several studies. Work to implement further enhancements is underway to produce a model with daily simulation steps.

References

ShawMont Newfoundland Limited (1986)
"An Inventory of Small Hydro Sites for Energy Supply to the Island Grid" (Volumes 1&2) for Newfoundland and Labrador Hydro, St. John's (Nfld).

ShawMont Newfoundland Limited (1989)
"Remote Hydro Study" for Energy, Mines and Resources Canada and Newfoundland and Labrador Hydro, St. John's (Nfld).

A CASE HISTORY OF THE CABINET GORGE DAM ANALYSIS

John Z. Gibson, P.E.[1]

Abstract

After a 1987 inspection of the Cabinet Gorge Dam, Part 12 consultants contracted by Washington Water Power (a private utility based in Spokane, Washington) made several recommendations in their inspection report. In response to these recommendations, three stability analyses and several monitoring and investigation programs were implemented to determine the stability of Cabinet Gorge Dam. Five years after the 1987 inspection, Washington Water Power (WWP) reviewed the stability analyses and resulting recommendations in order to evaluate how future stability analyses should be administered.

Introduction

The Cabinet Gorge Dam, operated by WWP is located in northern Idaho on the Clark Fork River approximately one mile west of the Montana border. The dam consists of a double curvature concrete arch dam with a 120.4 m long crest length with a maximum height of 63.4 m and a maximum thickness at the base of 13.7 m. The arch is abutted by two concrete gravity thrust blocks (the left and right abutments).

The Cabinet Gorge dam was licensed by WWP in 1952. WWP is required to adhere to the "Code of Federal Regulations" Part 12 (Safety of Water Power Projects and Project Works) Subpart D (Inspection by Independent Consultant). The regulations require that a independent inspection be performed and that a report be submitted once every five years. If recommendations are made in the Part 12 Inspection Report, WWP is required to submit a plan, and schedule to implement the consultants recommendations.

This paper summarizes past Part 12 Inspection Reports, analytical recommendations made in the report and the FERC review comments on Cabinet Gorge Dam. These steps are reviewed to evaluate whether appropriate recommendations were made to determine if the dam is stable. Finally, an alternative is provided to administering future analyses which focus initially on the question, "What parameter most predominantly influences stability" then addresses the question, "Is the dam stable?".

1987 Part 12 Inspection

In 1987, a consultant was retained to conduct a 5 year project safety review of the Cabinet Gorge Hydroelectric Project. The project was inspected in accordance with the

[1] Washington Water Power Company, P.O. Box 3727, Spokane, WA 99220

code of Federal Regulations, Chapter 1, Part 12, Subpart D. The project inspection report was submitted at the completion of the inspection, which summarized past design documents and provided recommendations.

EBASCO designed the Cabinet Gorge Arch Dam in 1952 utilizing the Professor William Caine "theory of Independent Arches". This theory is conservative for overstressing in the arch, but does not consider the three dimensional properties of the abutments and foundations interface. In addition, the original design did not consider the hydraulic loading corresponding to a probable maximum flood (PMF) condition. In response to these limitations, the Part 12 consultant made the following recommendations:

> **A modern state of the art structural analysis is recommended utilizing rock properties based on appropriate tests, to determine factors of safety for the dam and its support system against overstressing, overturning and sliding when subjected to appropriate combinations of loadings as designated in FERC evaluation guidelines.**
>
> **Installation of piezometers is recommended in the rock of the left abutment adjacent to its contact with the concrete gravity sections.**

A geotechnical engineering firm was retained - prior to any modeling effort - to investigate and characterize the concrete and rock mass at the Cabinet Gorge site.

Material Values

This firm investigated the site by drilling five diamond core borings through the concrete abutments and foundation. The drilling program obtained five cores which were tested: one, on the right abutment and the others on or near the left abutment. Once the cores were removed, piezometers were installed to measure the insitu uplift pressure. An engineering consultant contracted to numerically model the Cabinet Gorge site reviewed the material data, testing procedures, and utilized the following properties in their model.

Concrete	
Young's Modules E, sustained	24,449,670.0 kn/m^2
Poisson's Ratio	.2
Unit weight	23,250.8 n/m^3
Compressive Strength f_c	67,708.9 kn/m^2
Foundation	
Young's Modules E, sustained	9,515,100.0 kn/m^2
Poisson's Ratio	.2

Finite Element Model

The engineering consultant utilized SAP IV, a finite element program to determine the stress state in the arch and the resultant thrust vector in the abutments. The analysis was conducted using five load cases which adhere to FERC engineering guidelines for the evaluation of hydropower projects. The input data was obtained from as-built drawings, on-site investigations, regulatory requirements and the analysts

assumptions. Once the analysis was completed, the output data was reviewed and evaluated. The load cases, assumptions, and recommendations resulting from the analysis are summarized below.

Five load cases were used in the analysis: three normal loading combinations (Load Cases 1, 2, and 3) and two unusual loading combinations (Load Case 4 and 5). The three normal load combinations consisted of normal forebay and tailwater loadings with three seasonal temperature loadings: summer, winter and fall. The two unusual load combinations applied probable maximum flood forebay and tailwater loadings. The extreme load case (earthquake loading) was not considered, since the project is located in seismic zone 1.

Assumptions

Because of limited resources, assumptions were necessary to determine if the dam is stable. Some assumptions are mandated by FERC regulatory guidelines. For example, FERC requires the initial assumption of uplift to be linear between the forebay and tailwater elevations. In addition, the initial analysis used a linear model which was the standard in 1987. Today, nonlinear capabilities are becoming the standard for the industry. Although assumptions are inherent in any numerical analysis, the relative influence of these assumptions on the results should not be over-looked in the haste of completing the stability analysis.

The initial finite element analysis assumptions are listed below:

The closure temperature for the thermal analysis was assumed to be the average annual air temperature of 7.8° C.

Forebay and tailwater seasonal water temperature were assumed.

Uplift for all load cases was assumed to vary linearly from forebay to tailwater.

Non-linear behavior was not modeled.

The interface between the left thrust block and its foundation is horizontal.

Results

Once the initial model was constructed, two modes of failure were analyzed; overstressing in the arch and sliding of the right and left thrust blocks. The analysis concluded for all five load cases, the maximum arch and cantilever stress did not exceed the allowable concrete compressive and tensile stress. In addition, the left and right abutment obtained adequate factors of safety for sliding for all load cases, except the left thrust block for load case 3 (load case 3 - normal forebay and tailwater elevations and summer thermal load case). The engineering consultant focused his attention on reducing the driving forces since the left thrust block was not stable for load case 3.

Recommendations

The engineering consultant identified two driving forces which influence the stability of the left thrust block: 1) Uplift and 2) Forebay and tailwater temperatures (thermal loading). A preliminary review concluded that the reduction of uplift with an assumed

drainage system improved the stability of the left thrust block. Forebay and tailwater temperature values assumed in the initial analysis also influenced the stability of the left thrust block. As a result, additional analysis and monitoring programs were recommended and are stated below:

A program of headwater and tailwater temperature measurements combined with air temperature, headwater level, and tailwater level measurements should be implemented.

A study to determine the feasibility of providing a positive foundation drainage system for the left thrust block should be carried out.

Twelve months of headwater and tailwater temperature and piezometer readings were collected at the Cabinet Gorge Dam site in response to the recommendations. Once the data was collected, the University of Colorado was retained to analyze the influence of a left thrust block drainage system on factors of safety for sliding. The University of Colorado was selected to undertake this study because of its research efforts in conjunction with Electric Power Research Institute (EPRI) in the area of seepage modeling.

University of Colorado Model

The University of Colorado enhanced the initial model by making the following improvements: 1) Using field collected forebay and tailrace water temperatures.
2) Incorporation of a drainage system in the left thrust block. The University evaluated these two parameters influence on stability of the left thrust block. The University model contained all other assumptions and limitations from the initial model.

Seepage Model

A seepage model is required to model a drainage systems capacity to reduce uplift. The University of Colorado previously developed a seepage program titled SEEP3D. This program determines uplift pressures for a variety of boundary conditions and was coupled with the mechanical finite element model (SAP90). Once SEEP3D was calibrated using collected field data, five drain configurations were modeled to determine the influence of a drainage system on stability.

Results of Drainage Analysis

The results of the analysis did show some sensitivity to reduction of uplift. However, it was not significant enough to increase the factor of safety values greater than 3. For example, one drain configuration considered 100% drain efficiency (purely theoretical since this drain efficiency is not possible in the field) and obtained a factor of safety for sliding of 2.97.

The University of Colorado, observed that a drainage system did not obtain adequate factors of safety for sliding, therefore two other parameters were reviewed: 1) The slope of the left thrust block interface and 2) The closure temperature. As mentioned earlier, the initial analysis assumed a horizontal interface and a closure temperature equivalent to the average annual ambient temperature. A sensitivity analysis conducted on these two parameters revealed that these two assumptions influence stability more predominantly than a drainage system.

The Federal Energy Regulatory Commission

On April 10, 1992, FERC submitted a letter to WWP, approximately 2.5 years after the initial stability analysis submittal, with review comments regarding the initial analysis and geotechnical investigation. FERC's review comments are as follows:

> **The assumed Young's modulus and tensile strength for concrete are based on an unusually high concrete compressive strength f'c =67,708.9 kn/m^2, which is the average value obtained from laboratory testing of eleven cores taken from the left thrust block and wing dam.**
>
> **The relative difference between the assumed values for E concrete and E rock is very high and needs some justification.**
>
> **In addition, any stability analysis done must be done on failure surfaces that are physically possible.**

In 1992, a new Part 12 consultant was retained to conduct an inspection of the Cabinet Gorge Dam. In addition to the inspection, the consultant was required to review the past stability analysis and FERC's review comments. After completing the review, the consultant recommended additional modeling of the Cabinet Gorge site for the following reasons: 1) The sensitivities of closure temperature and the slope of the left thrust block interface should be incorporated in the new model, 2) The material values used in the initial model should be revised in response to FERC's comments, 3) A nonlinear model should be used to more closely represent the interaction of the arch, abutments and foundation.

ANSYS Model

WWP agreed that a more sophisticated model should be conducted of the Cabinet Gorge site. The Part 12 consultant utilized ANSYS 5.0, a nonlinear finite element program. In addition, the actual closure temperature and material values were determined by reviewing the construction records. Finally, a plausible failure plane was evaluated by plotting the resultant load vector on the left thrust block.

Improvements

The Cabinet Gorge construction records were reviewed to determine the date when individual concrete blocks were poured. A heat of hydration analysis was conducted to determine the temperature of the concrete blocks on the date they were grouted (the closure temperature). The construction records revealed two grouting stages, therefore, two closure temperatures were calculated for the Cabinet Gorge Dam. The closure temperature was determined to be 12.8° C for the first grouting stage and 18.3 C for the second grouting stage. The assumption of 7.8° C closure temperature used in the initial analysis is significantly less than what was determined from the construction records.

The material testing during construction was reviewed in response to FERC comments. The concrete compressive strength used in the analysis was determined to be 29.648.5 kn/m^2 rather than 67,708.9 kn/m^2 The foundation modulus used in the analysis was significantly less than the geotechnical investigation testing results.

Conclusion

WWP's review of past analysis of Cabinet Gorge Dam resulted in the following observations. First, an expensive material investigation and monitoring program were implemented prior to any numerical modeling effort. In other words, data was being collected at the site with no appreciation of its impact on stability. Secondly, recommendations were made to investigation parameters whose influence on stability were relatively small when compared to assumptions made. Thirdly, FERC's comments, although very helpful, were provided 2.5 years after the completion of the initial analysis and the recommendations were already completed. Finally, what obligation does a licensee have on continually updating their analysis since numerical programs are advancing so rapidly.

Alternative

An alternative focusing initially on the question "What parameter most predominantly influences stability?" then addressing the question "Is the dam stable?" is provided in the flowchart below. Here the initial emphasis is placed on a planning (parametric) model before any monitoring programs are implemented. Therefore, the planner (analysts) can prioritize the type of investigation and monitoring programs to be implemented by the results of the planning model. These programs will receive priority relative to the parameters influence on stability. Secondly, the planner can determine the modeling sophistication required to support this effort. For example, the planner can evaluate whether a linear versus a nonlinear or a seepage model is required to determine if the dam is stable. Once the data has been collected, a more sophisticated model can be developed if necessary.

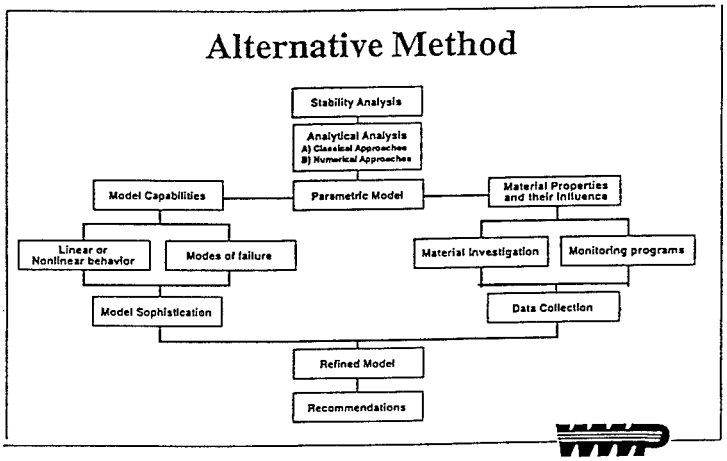

Soda Dam: Benefits in Performing Three-dimensional Analysis of a Concrete Gravity Dam

Guy S. Lund M.ASCE[1], Mark Linnebur M.ASCE[2], & Howard Boggs M.ASCE[3]

Abstract

Performing a sophisticated three-dimensional analysis more accurately models the behavior of a straight concrete gravity dam compared to results using the more traditional two-dimensional analysis. A more accurate analysis has resulted in significant cost savings for required rehabilitation.

Previous two-dimensional gravity method of analysis of Soda Dam showed the dam unstable for the Probable Maximum Flood (PMF) and Maximum Credible Earthquake (MCE) loadings. A three-dimensional finite element analysis (FEA) was completed and the results used to determine moment equilibrium and sliding stability*(ECI, 1992)*. The FEA verified that the dam behaves three-dimensionally and showed that less stable monoliths gain stability from more stable monoliths. The results of this study show that the dam is stable for all assumed loading combinations due to three-dimensional interaction. The outcome of the study, which has been approved by the FERC, will save PacifiCorp the expense of unneeded repairs suggested by the more conventional two-dimensional analysis.

Project Description

Soda Dam is located on the Bear River adjacent to U.S. Highway 30 in southern Idaho about 5 miles west of Soda Springs. Construction of the concrete gravity dam was completed in 1925. The dam was built in a narrow canyon with a steep left abutment, flat center section and moderately sloped right abutment.

Soda Dam is a concrete gravity structure 433 feet long with a maximum structural height of 103 feet. The concrete dam consists of a 210-foot-long non-overflow gravity section, a 109-foot-long integral powerhouse section, and a 114-foot-long gated overflow spillway section. The typical non-overflow gravity section has a crest thickness of 10 feet, a vertical upstream face, and a downstream face that is vertical extending 10 feet down from the dam crest then slopes at 0.53 horizontal to 1.0 vertical. The dam was constructed in monoliths,

[1] Project Manager, ECI, 5660 Greenwood Plaza Blvd., Suite 500 Englewood, Colorado, 80111 (303) 773-3788

[2] Civil Engineer, ECI

[3] Consulting Engineer, P.O.Box 338, Arvada, Colorado, 80001

each interlocked to the adjacent monolith with grouted vertical keys in the contraction joints.

Soda Dam is founded on a layered volcanic basalt which varies in thickness from more than 300 feet at the right abutment to about 80 feet at the left abutment. Three main joint sets are evident from examination of the rock outcrops at the damsite. These include a major sub-vertical joint set that strikes parallel to the river valley; randomly oriented vertical columnar cooling joints in the basalt, and discontinuous, quasi-horizontal undulatory partings between successive basalt flows.

Basis for Investigations

Previous stability studies of the dam used the two-dimensional gravity method of analysis *(HARZA, 1987, 1990)*. These studies were conservative in that they assumed that the abutments or adjacent monoliths would not contribute to the stability. The results of these analyses showed that the dam did not meet acceptable stability criteria and required post-tensioned anchors for stabilization.

Conventional gravity dams are usually constructed as vertical cantilevers (monoliths) from abutment to abutment. If the canyon is narrow, with steep sloping sidewalls, monoliths near the center of the dam will be taller than monoliths on the abutments. Consequently, the shorter cantilevers will deflect less due to the waterload than the taller cantilevers. If the transverse contraction joints in the dam are keyed and grouted, deflection of the taller cantilevers will be restrained by the shorter cantilevers. This interaction between cantilevers changes the way the dam behaves structurally and the conventional gravity method of analysis is no longer appropriate. Soda Dam falls into this category of a three-dimensional structure. First, the canyon is narrow with sloping abutments which forms adjacent cantilevers of different heights. Second, the vertical contraction joints between concrete monoliths contain massive vertical keys. Therefore, the three-dimensional FEA is the most appropriate method for performing a stability analysis.

Present Criteria

Presently there are many different criteria regarding the safety of concrete dams. These analyses followed the Federal Energy Regulatory Commission (FERC) *(FERC, 1991)* and United States Bureau of Reclamation (USBR) *(USBR, 1977)* criteria to define loads, load combinations, material properties, and safety criteria. The minimum required sliding factors of safety are summarized in Table 1.

TABLE 1
Sliding Stability Minimum Required Factors of Safety

Description	Factors of Safety
Usual Load Combination	2.0
Unusual Load Combination	1.5
Extreme Load Combination	$\geq$ 1.0

Stress Analysis

A general linear elastic finite element program was used to determine the stresses and deflections of the dam for the usual, unusual, and extreme load combinations. The dam was modeled using 426, variable noded, isoparametric thick shell elements with four elements

through the thickness. A significant portion of the foundation was modeled using 466 eight noded, isoparametric thick shell elements with eight elements through the thickness from upstream to downstream edge. The foundation extended at least one dam height upstream, downstream, and into the abutment and foundation.

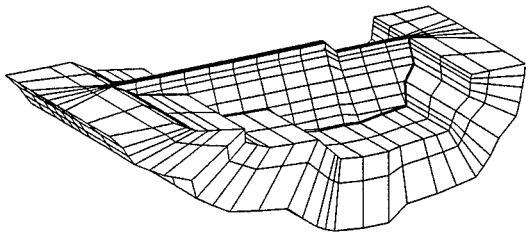

Figure 1 Finite Element Model of Soda Dam

Material Properties

The material properties for the concrete in Soda Dam were based on data collected during previous investigations. In 1989, a core drilling and testing program was completed to determine the material properties of the concrete in Soda Dam *(HARZA, 1989)*. Eleven cores were extracted from the dam and tested to determine the compressive and tensile strengths and unit weight. No test data were available for Poisson's ratio or coefficient of thermal expansion. These additional property values were based on published data by the USBR *(USBR, 1981) (USBR, 1977)*. The instantaneous concrete modulus of elasticity was computed in accordance with the American Concrete Institute (ACI) *(ACI, 1989)* based on the average compressive strength. The sustained modulus of elasticity of the concrete was assumed to be two-thirds of the instantaneous modulus of elasticity. The material properties assumed for Soda Dam are summarized in Table 2.

TABLE 2
Material Properties

Properties	Values		
Compressive Strength	3,875	lb/in^2	(26.7 MPa)
Tensile Strength	484	lb/in^2	(3.3 MPa)
Modulus of Elasticity			
Sustained	2,400,000	lb/in^2	(16.5 GPa)
Dynamic	3,590,000	lb/in^2	(24.8 GPa)
Poisson's Ratio	0.20		
Density	145	lb/ft^3	(2322.7 kg/m^3)
Coef. of Thermal Expansion	0.000,005	in/in/°F	
Reservoir Unit Weight	62.5	lb/ft^3	(1001.2 kg/m^3)
Silt Horizontal Unit Weight	85.0	lb/ft^3	(1361.6 kg/m^3)

In 1989 cores were extracted from the foundation and selected rock core samples were tested to determine the compressive strength of the rock *(HARZA, 1989)*. Data available for foundation rock similar to that at Soda Dam was used to estimate a deformation modulus *(USBR, 1974) (Hueze, 1980)*. In 1991 tests were conducted on selected rock samples to provide representative values for the foundation cohesion and internal angle of friction *(HARZA, 1991)*. The results of these tests were used to develop the foundation material properties and are summarized in Table 3.

TABLE 3
Foundation Properties

Properties	Values		
Compressive Strength	5,260	lb/in^2	(36.3 MPa)
Modulus of Deformation	2,400,000	lb/in^2	(16.5 GPa)
Poisson's Ratio	0.20		
Internal Angle of Friction	54.5	Degrees	
Cohesion	53	lb/in^2	(3.7 kgf/cm^2)

Loads

The FEA can be used to investigate numerous loads acting on the dam. In this study, each load was applied independently to the model to study its effect on the structure. Studying each load separately provides a method for checking the combined load and for determining the loads that contribute the majority of stress and deflection to each load combination. The loads included in the load combinations are summarized in Table 4.

TABLE 4
Individual Loads

Load	Description
Gravity	Dead weight of dam.
Temperature	Loads due to the volumetric changes in the concrete due to variations in reservoir and air temperatures.
Reservoir	Hydrostatic water pressure applied to the upstream face of dam and to the foundation surface upstream of the dam.
Tailwater	Hydrostatic water pressure applied to the downstream face of dam and to the foundation surface downstream of the dam.
Silt	Hydrostatic pressure applied to the upstream face of dam.
Uplift	Internal hydrostatic water pressure applied along the dam/foundation contact.
MCE	Ground accelerations due to the Maximum Credible Earthquake.

The uplift load was applied along the dam/foundation contact in accordance to the appropriate guidelines *(FERC, 1991)*. For the uncracked base analysis, the uplift load was bi-linear, varying linearly from full reservoir head at the upstream heel of the dam to a reduced head at the drain location and varying linearly from the reduced head at the drains to the tailwater head at the downstream toe of the dam. The reduced head at the drains, due to drain efficiency, was obtained from drain pressure readings.

For a cracked base analysis where the crack does not extend past the drain location, the uplift load was assumed uniform equal to full reservoir head from the upstream heel of the dam to the crack tip, vary linearly from full reservoir head at the crack tip to the reduced head at the drain location, and a vary linearly from the reduced head at the drain to tailwater pressure at the downstream toe. For a cracked base analyses where the crack extends past the drain location, the uplift load was assumed uniform equal to full reservoir head from the

upstream heel of the dam to the drain location, uniform equal to the reduced head at the drains from the drains to the crack tip, and a vary linearly from the reduced drain head at the crack tip to the tailwater head at the downstream toe of the dam.

Load Combinations

Preliminary studies were conducted for Soda Dam using the three-dimensional FEA to investigate a number of conditions, ranging from uncracked base to various lengths of cracked base, for unusual loads. Preliminary results for an uncracked base showed tensile stresses on the upstream face of the dam near the dam/foundation contact, which indicated that the dam stability relies heavily on the monolith cantilever action to support the loads. These tensile stresses are primarily produced by the hydrostatic water pressure on the upstream face of the dam and are the result of the linear elastic material property assumptions used for the concrete and foundation element in the model. These properties assume that the elements in the model can develop tension or compression. The guidelines *(FERC, 1991)* however, state that the dam/foundation contact cannot develop tensile stresses, as predicted by the model, and would be expected to separate (crack). Therefore, the finite element model was modified to simulate a cracked base and an increase in uplift pressure.

The crack length was determined by examining the normal tensile stresses distribution along the dam/ foundation contact. Tension areas were assumed to crack. The modulus of elasticity of selected elements, located along the contact within tension areas, was reduced to 10 lb/in^2 (70 KPa) to simulate a crack. The uplift load was increased based on the crack length, in accordance with the FERC guidelines.

The results of these preliminary analyses indicated that the following load combinations were the most severe.

Usual Load Combination:

USLC **Gravity, temperature** corresponding to winter conditions, NWS **reservoir** water surface elevation 5720.0, **tailwater** elevation 5641.0, **Silt, Ice,** and **Uplift** pressure for cracked base.

Unusual Load Combination:

UNLC **Gravity, temperature** load corresponding to spring/fall conditions, PMF **reservoir** water surface elevation 5735.0, **tailwater** elevation 5665.0, **Silt,** and **Uplift** pressure for cracked base.

Extreme Load Combinations:

EXLC **Gravity, temperature** corresponding to winter conditions, NWS **reservoir** water surface elevation 5720.0, **tailwater** elevation 5641.0, **Silt, Ice, Uplift** pressure for uncracked base, and effects due to the MCE..

Stress Analysis Results

Load combination USLC and UNLC analyzed the dam for a cracked base. The maximum stresses produced by the finite element model within the concrete are all less than the allowable limits. Minor horizontal tensions occur in the model on the downstream face. The vertical contraction joints in the dam, however, are unable to develop tension and would partially open to eliminate the tensile stresses from developing in the concrete dam. Evaluation of the horizontal compression stresses within the dam across the vertical

contraction joints indicate that three-dimensional monolith interaction will be maintained and transfer part of the load to the upper abutments. The interaction will result in the shorter monoliths restraining the deflection of the taller monoliths, as shown in Figure 2 which compares two-dimensional and three-dimensional crest deflection for load combination USLC.

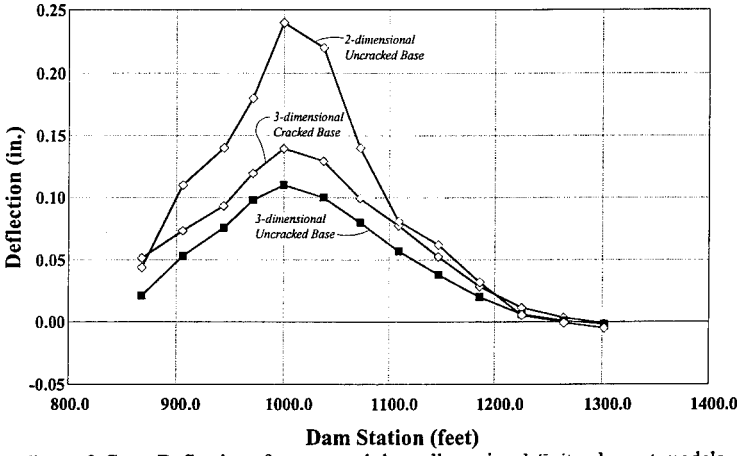

Figure 2 Crest Deflections for two- and three-dimensional finite element models.

Load combination EXLC analyzed the dam for an uncracked base. The maximum stresses in the concrete are less than allowable limits, however, tensile stresses along the dam/foundation contact are greater than allowable and indicate that cracking may occur at the base. The post earthquake loading, however, would include a cracked base nearly equal to load combination USLC. The results from USLC, therefore, can be used to determine the post-earthquake behavior of the dam.

Stability Analysis

The global stresses obtained from the three-dimensional FEA were resolved into stresses normal to the axis of overturning for each monolith. The monolith axis of overturning is defined as the average cross-canyon slope (angle) of the dam/foundation contact. To satisfy the moment equilibrium criteria the results from the FEA must show that the dam/foundation contact will not continue to crack resulting in an increase in the uplift load.

The normal stress distribution along the dam/foundation contact was integrated over the dam/foundation contact area to obtain normal tensile and compressive forces. The total moment about the toe is equal to the product of normal forces along the contact and their distance to the toe. The location of the resultant force for each monolith was determined by dividing the total moment about the toe by the total normal force. If the resultant force falls within the middle-third of the uncracked base, then the entire base is in compression and moment equilibrium is maintained.

If the location of the resultant force indicates that an individual monolith would be unstable, the three-dimensional action of the dam was analyzed to determine if monolith interaction would offer additional overturning stability. Monolith interaction is available if the resisting forces acting over the vertical contraction joint area are of sufficient magnitude to prevent differential joint movement between adjacent monoliths. The resisting force is equal to the sum of sliding friction, due to horizontal compressive stresses acting across the joint, and shear strength of the vertical keys.

A progressive sliding stability analysis was performed for each individual monolith and the entire dam. The uncracked area along the dam/foundation contact and the forces normal to the contact were used to compute the sliding resistance at the base of the dam from the following equation *(FERC, 1991)*:

$$R_{dam} = A_1 \times c + N_1 \times Tan(\Phi) \qquad (1)$$

where:

- R_{dam} Resisting force due to friction and cohesion between the dam and foundation.
- N_1 Summation of forces normal to the dam/foundation contact.
- A_1 Area in contact underneath the dam.
- c Dam/foundation cohesion.
- ϕ Dam/foundation internal angle of friction.

The dam is also keyed into the foundation. An additional resistance was computed due the foundation key *(Underweight, et al, 1977)*.

If the sliding factor of safety for a monolith was found less than the allowable criteria, three-dimensional action in the dam was evaluated to determine if additional sliding resistance could be obtained from adjacent monoliths. If sufficient monolith interaction was available to prevent differential movement, then the adjacent monoliths were analyzed for sliding stability as a single unit.

Stability Analysis Results

Moment Equilibrium. The moment equilibrium analysis for usual load combination USLC, with a cracked base, is summarized in Table 5. A positive normal force indicates compression across the dam/foundation contact. A negative moment indicates the moment about the toe is acting into the reservoir.

The results show that the resultant force for monolith 3 is outside the middle third of the base, which indicates that moment equilibrium is not satisfied. The results from the three-dimensional FEA, however, indicate that monolith 2 through 6 have sufficient cross-canyon compression to interact with each other and prevent differential joint movement. Monolith 3, therefore, will gain additional stability from adjacent monoliths. The resultant force for monolith 2 through 4, and the entire dam, is within the middle-third, which satisfies moment equilibrium.

Table 5
Usual Load Combination USLC Moment Equilibrium Analysis

	Monoliths						
	1	2	3	4	5	6	Total
Normal Force (kips)	2809	9286	7758	36,510	21,186	9258	86,908
Moment @ Toe (k-ft)	-66009	-96,513	-68,543	-565,427	-452,892	-120,418	-1,310,401
Avg. Uncracked Length (ft)	7.1	27.2	30.0	39.2	51.5	23.7	29.8
Resultant Location (distance from dam toe % of uncracked base)	33.0 %	37.8 %	29.5 %	38.5 %	41.5 %	54.9 %	50.6 %
C.J. Shear Resistance (kips)	58	1348	1330	4364	2295		
C.J. Moment Resistance (k-ft)	687	34,664	147842	158,396	58,308		

The moment equilibrium for unusual load combination UNLC, with a cracked base, is summarized in Table 6.

Table 6
Unusual Load Combination UNLC Moment Equilibrium Analysis

	Monoliths						
	1	2	3	4	5	6	Total
Normal Force (kips)	1840	8979	7081	30,888	18,182	14,030	80,999
Moment @ Toe (k-ft)	-4304	-40,078	-35,413	-216,984	-197,861	-93,722	-988,362
Avg. Uncracked Length (ft)	3.6	14.9	10.0	16.2	43.2	18.5	17.7
Resultant Location (distance from dam toe % of uncracked base)	65.6 %	30.0 %	50.0 %	43.4 %	25.2 %	36.0 %	41.0 %
C.J. Shear Resistance (kips)	550	1973	8946	13,269	7895		
C.J. Moment Resistance (k-ft)	5792	33,322	218,232	473,324	200,791		

The results for unusual load combination UNLC show that the resultant force for monolith 2 and 5 falls outside the middle third of the uncracked base. The three-dimensional FEA, similar to usual load USLC, indicates that the dam has sufficient cross-canyon interaction to cause the monoliths to interact with each other and prevent differential joint movement. This results in the dam behaving as a single unit, and the resultant force for the dam falls within the middle-third of the uncracked base satisfying moment equilibrium.

Sliding Stability. The results of the sliding stability analysis for usual load USLC are summarized in Table 7.

The results show that monolith 6 has a factor of safety less than the required minimum. The three-dimensional analysis, however, shows that monolith 6 has sufficient monolith interaction with monolith 5 to prevent differential joint movement. This results in monolith no. 6 gaining additional strength from monolith no. 5. The sliding factor of safety for monolith 5 and 6 acting as a single unit is greater than the minimum allowable criteria. The results indicate that the dam is safe against sliding for the assumed loading condition.

Table 7
Usual Load Combination USLC Sliding Analysis

	Monoliths						
	1	2	3	4	5	6	Total
Normal Force (kips)	2809	9386	7758	36,510	21,186	92,580	86,908
Shear Force (kips)	2347	6914	6654	30,792	16,964	16,019	79,687
Uncracked Area (ft^2)	920	2230	1146	5085	2949	3855	16,185
Foundation Key (kips)	2387	1014	835	3435	2751	5052	15,472
Factor of Safety	3.6	3.1	2.4	2.5	2.6	1.6	2.4

The results of the sliding stability analysis for unusual load combination UNLC are summarized in Table 8. The results show that all monoliths, and the entire dam, have factors of safety against sliding greater than the minimum allowable criteria.

Table 8
Unusual Load Combination UNLC Sliding Analysis

	Monoliths						
	1	2	3	4	5	6	Total
Normal Force (kips)	1840	8979	7081	30,888	18,182	14,030	80,999
Shear Force (kips)	3067	8686	9627	31,778	20,578	20,226	93,957
Uncracked Area (ft^2)	461	1115	3826	1781	1984	2720	8442
Foundation Key (kips)	2387	1014	835	3435	2751	5052	15,472
Factor of Safety	2.0	2.2	1.5	2.0	1.9	1.7	1.9

Evaluation of forces at different times during the MCE indicated that the most critical time for sliding stability of the dam occurs at 7.825 seconds. The results of the sliding stability analysis for the extreme load combination, at time 7.825 seconds are summarized in Table 9. The results indicate that the dam has acceptable factors of safety against sliding for the extreme load combination.

Table 9
Extreme Load Combination EXLC Sliding Analysis

	Monoliths						
	1	2	3	4	5	6	Total
Normal Force (kips)	2792	9499	10,025	38,346	26,326	10,951	97,939
Shear Force (kips)	2338	9071	9800	52,624	24,311	25,026	123,169
Uncracked Area (ft^2)	1838	2969	1528	7049	3904	6254	23,542
Foundation Key (kips)	2387	1014	835	3435	2751	5052	15,472
Factor of Safety	3.8	2.4	2.1	1.5	2.3	1.2	1.8

Conclusions

The stress analysis of Soda Dam was performed using a three-dimensional finite element model to study the behavior of the dam for usual, unusual, and extreme loading conditions. The results indicate that horizontal stresses develop in the cross-canyon direction of sufficient magnitude to cause the dam to behave three-dimensionally. The monolith interaction is sufficient to prevent differential joint movement between adjacent monoliths. This results in the shorter monoliths providing additional restraint to the taller monoliths.

Conventional two-dimensional stability analysis, which does not account for monolith interaction, indicated that the dam would not meet safety criteria for the PMF and MCE loading conditions. The results from the three-dimensional stress analysis showed that the dam benefits from cross-canyon monolith interaction. The results from the stability analyses, which accounts for the interaction, demonstrated that the dam maintains moment equilibrium and satisfies the required sliding stability criteria. The less stable monoliths gain additional stability from the more stable monoliths due to the monolith interaction. Thus, the dam is safe for all assumed loading conditions.

List of References

American Concrete Institute, "Building Code Requirements for Reinforced Concrete (ACI 318-89), Michigan, 1989.

ATC Engineering Consultants, Inc., "Report on Soda Dam Structural Stability Analysis", Denver, October 1992.

FERC Guidelines. Federal Energy Regulatory Commission, Office of Hydropower Licensing, "Engineering Guidelines for the Evaluation of Hydropower Projects", Washington, D.C., April 1991

Harza Engineering Company, "FERC Inspection and Safety Report, Oneida Dam, FERC Licensed Project No. 472-Idaho', Chicago, May 1987.

Harza Engineering Company, "Evaluation of Test Results for Soda Dam", Chicago, June 6, 1991.

Harza Engineering Company, "Supporting Design Report - Stability Improvement Project for Oneida, Dam", Chicago, April 1990.

Heuze, F.E., "Scale Effects in the Determination of Rock Mass Strength and Deformability", Rock Mechanics, Volume 12, 1980.

U.S. Department of the Interior, Bureau of Reclamation, Engineering Monograph No. 19, Design Criteria for Concrete Arch and Gravity Dams. Denver: GPO, 1977, pp29.

U.S. Department of the Interior, Bureau of Reclamation, Engineering Monograph No. 34, Control of Cracking in Mass Concrete Structures, Denver, GPO, 1981.

U.S. Department of the Interior, Bureau of Reclamation, 1974, REC-ERC-74-10, Rock Mechanics Properties of Typical Foundation Rock Types.

Underweight, Lad B., and Norman A. Dixom, "Dams on Rock Foundation", in Rock Engineering for Foundation and Slopes, American Society of Civil Engineers (ASCE), New York, 1977, pp125-146.

FERC'S EVOLVING POLICY ON THREE DIMENSIONAL STABILITY ANALYSIS OF CONCRETE GRAVITY DAMS

Bruce Brand[1]

Abstract

This paper discusses three dimensional stability analysis of concrete gravity dams from the FERC perspective. Licensee's are beginning to use three dimensional analysis in the stability evaluation of gravity dams. This paper presents three particular FERC concerns and some general insight into three dimensional behavior.

Introduction

The structural stability of concrete gravity dams is typically evaluated under the simplifying assumption of two dimensional plane strain. This simplification can result in the neglect of significant stabilizing effects afforded by the cross valley dimension. While chapter three of FERC's "Engineering Guidelines" advise that "All Straight gravity dams having keyed transverse contraction joints should be treated as three dimensional structures...", the guidance that is given is more directed to two dimensional analysis. This is because most gravity dams have been analyzed in two dimensions.

Recently, dam owners under FERC license have done three dimensional finite element analyses on gravity dams in an attempt to prove their stability. FERC welcomes this trend; however, as this paper will show, three dimensional analysis will not always provide a higher factor of safety.

From FERC's point of view, consideration of the

[1] Structural Engineer, Federal Energy Regulatory Commission, 810 1st St. N.E., Washington, DC 20426

cross valley dimension in no way alters the stability criteria that must be met. Three things must be assured:

1) Global force and moment equilibrium must be achieved within the limits of the shear strength of the foundation contact, or any other critical failure surface.

2) Uplift at the foundation contact must be properly considered.

3) The transmission of forces in the cross valley direction required for three dimensional action must be possible.

No matter what analysis technique is used, these three items must be addressed.

Global Force and Moment Equilibrium

In order to determine if global force and moment equilibrium are satisfied, the stresses at the dam/foundation contact must be integrated over the surfaces they are acting upon. When these stresses are integrated, they should exactly cancel the sum of loads applied to the dam. **If they do not, the analysis is not valid.**

The factor of safety for sliding can be expressed in terms of the interface stress state as follows:

$$F.S.S. = \frac{\int (\sigma_n * \tan(\phi) + C)\, dA}{\int \tau\, dA} \qquad EQ.\ 1$$

Where:

σ_n=*Normal stress at foundation contact*
τ=*Shear stress in the direction of impending motion*
ϕ=*Friction angle of the foundation contact*
C=*Contact cohesion*

These integrals must be evaluated only over the region of the foundation that is in compression. In three dimensional analysis as in two, the tensile strength of the concrete/foundation contact is assumed to be zero and the contact must be considered cracked if not in compression. If the finite element method is used, this means that elements at the foundation contact that show tension normal to the contact must be removed from the stiffness matrix by some means. This may be accomplished by deleting them from the model, or

assigning them an extremely low modulus of elasticity.

In addition to satisfying the "no tension across the contact" criteria, it must be shown that everywhere on the contact:

$$\tau \leq (\sigma_n * \tan(\phi) + C) \qquad EQ.2$$

Local shear stress must be within the failure envelope at all points. When the finite element method is used, several iterations are often required to bring all the element stresses on the foundation within the limits of the failure envelope.

Consideration of Uplift at the Contact

When three dimensional analysis is done, three dimensional uplift pressure distributions should be used. The procedure for consideration of uplift at the dam/foundation contact in three dimensional models is similar in concept to the two dimensional examples shown in the FERC "Engineering Guidelines". For a given monolith, uplift head must be assumed equal to full reservoir head upstream, and tailwater or foundation elevation downstream, which ever is higher. These are no different than the uplift assumptions made in two dimensional analysis, however the pressure distribution resulting from these assumptions is complicated when the plane of foundation contact is sloping with respect to the cross valley dimension and the width of the foundation is not constant.

The three dimensional effects of drains should be considered. Often drains are not continuous along the axis of the dam, but rather consist of holes spaced at some finite interval along the length of a drainage gallery. In these cases, the effect of a given drain can be expected to decrease with respect to the radial distance. This results in an uplift pressure distribution similar to the cone of depression described by the Dupuit solution for a confined aquifer. CRFLOOD, a program developed for EPRI by the University of Colorado may be helpful in determining drained contact pressure distributions.

The effect of a foundation crack is also complicated by a three dimensional analysis since the line defining the crack tip will be irregular. Figure 1 shows a half plan view of a dam/foundation contact. Note that the crack tip may pass upstream of some drains and downstream of others, causing some drains to be drowned out and

others to be functional.

As in two dimensional analysis, full reservoir uplift should be applied to the cracked portion of the foundation contact. Uplift can be assumed to decay linearly from full uplift at the crack tip, to the greater of tailwater or foundation contact elevation at the toe of the dam. When the crack tip advances beyond a drain, the drain should be considered ineffective unless piezometer readings taken in the cracked region demonstrate that uplift reduction is happening.

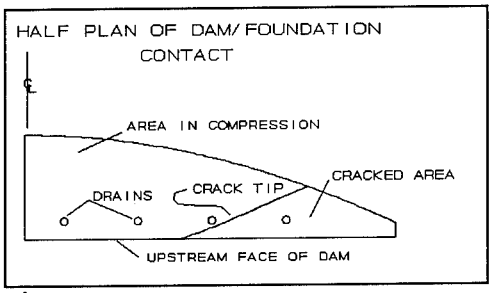

Figure 1

Application of uplift to the foundation contact using the finite element method has been the subject of much discussion. Many licensee's have modeled the foundation contact with a thin layer of solid elements. The uplift pressure can be applied to the top and bottom surfaces of the layer, correctly modeling the effective stress state on the contact. Cracked base analysis is done by relaxing or deleting elements that show tension normal to the contact. This technique is logical, straight forward, and can be performed with almost any general purpose finite element code.

Cross Valley Transmission of Forces

There are dam or valley geometries that make the failure mechanisms assumed in two dimensional analyses physically impossible. In cases where simple downstream sliding or co-axial overturning is possible, stability may be enhanced by the shearing forces mobilized at the valley sides and by the arching action which develops in a "deep beam".

When performing three dimensional stability analysis, it must be demonstrated that the shears and torsions required between monoliths can actually be transmitted across construction joints. Joint stress must be everywhere within the failure envelope of the joint (See Equation 2), just as in the case of the

foundation contact. Evidence to this effect may include the following:

- Construction photographs or as built drawings showing keys

- Joint grouting records

- Physical testing of joints

Dams are not constructed instantaneously, and therefore modeling the effect of the dam's self weight on the foundation by simply applying gravity load to the completed structure is almost always incorrect. This is because the foundation under the deeper sections of the dam will deflect downward, redistributing dead load to the valley sides. In reality, most dams are constructed monolith by monolith in such a way that the little or no cross valley transfer of force can occur until the dam is completed. Even in the case of RCC construction which is often continuous, dead loads can not be transferred through lifts that are yet to be placed.

When using the finite element method, this problem can be overcome by calculating the dead load effects using a two step process. In the first step the dam is divided into vertical sections and every other section is deleted. Gravity load is then applied. In the second step the deleted sections from the first step are analyzed under gravity load with the analyzed sections from the first step deleted. The results are then superimposed.

The resulting initial dead load case can then be combined with other load cases in which the dam acts integrally.

The Effect of the Third Dimension

Three dimensional stability analyses are more complex and usually more expensive than a two dimensional stability analysis of the same structure. For this reason it would be nice to gain some insight into whether a three dimensional analysis is going to yield significantly different results than a two dimensional analysis for a given dam. To this end, the results of a simple parametric study are presented. The author has developed a simple three dimensional generalization of the stability analysis technique presented in FERC's "Engineering Guidelines".

The following assumptions were made:

1) The dam is considered to be a rigid body for all applied forces.

2) The effective stress on the dam base is assumed to vary linearly from the heal to the toe of the dam.

3) Initially, the entire self weight for each section of the dam is supported by its own strip of foundation.

4) At every section, uplift varies linearly from heal (or crack tip), to the toe.

5) If a section is partially cracked, full reservoir uplift is applied to the cracked portion.

6) The valley is symmetrical about the dam centerline so that only half of the dam need be considered.

7) There are no stress resultants at the foundation contact in the cross valley direction. This is analogous to saying that the contact is a series of differential steps and that stresses are present only on the horizontal planes defining the steps.

For this parametric study, sliding factors of safety are compared with respect to several different valley shapes. The dam geometry and valley shape were described as shown in figure 2.

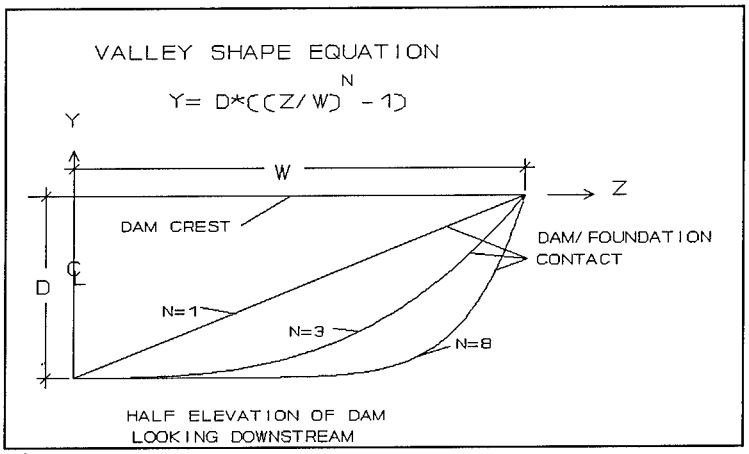

Figure 2

Valley shapes can vary between sharp "V" shapes to broad "U" shapes. In the valley equation in figure 2, the exponent N is a measure of the valley's "U" ness. Broad "U" shaped valleys are represented by large values of N. When N=1.0, the valley side slope is constant with a sharp point at the valley bottom.

Since sliding can only occur along a kinematically admissible surface, the parametric study assumed that the valley shape does not vary with respect to the upstream/downstream direction.

Figure 3 shows how valley shape and reservoir elevation effect the three dimensional sliding safety factor. F3/F2 is the ratio of the factor of safety computed in three dimensions to the factor of safety computed in two. As can be seen in figure 3, when the valley becomes more "U" shaped, the effect of the third dimension diminishes. The F3/F2 ratio approaches 1.0 as N--> ∞ and this is as one would expect.

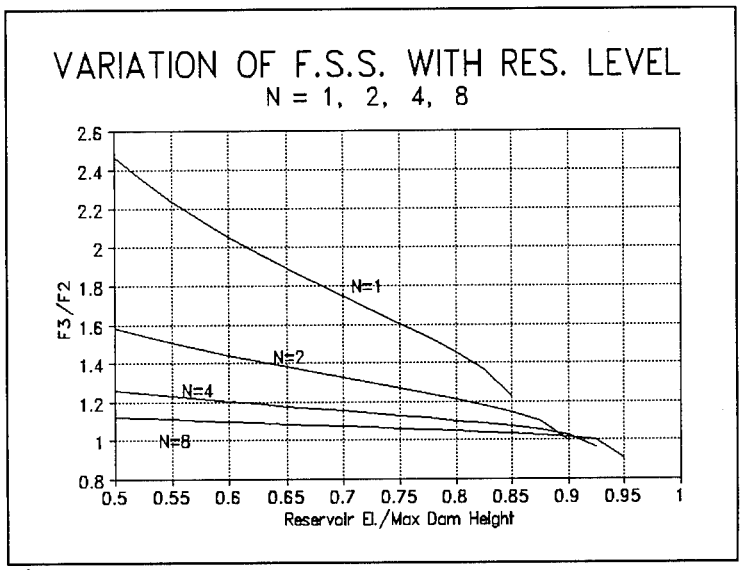

Figure 3

Also, as the reservoir level increases, the difference between the two methods decreases. This is because when the reservoir is not up to the full height of the dam, the end portions of the dam are completely

out of the water. The are subject to neither driving force or uplift, yet they help resist the loads applied to other sections.

The study also shows that while sliding stability was enhanced by consideration of the third dimension, foundation cracking began earlier, indicating that two dimensional analyses may actually over estimate overturning stability in some cases. For example, the curve for N=1 in figure 3 stops when reservoir level reaches 85% of dam height. This is because a three dimensional analysis shows that the dam overturns at higher reservoir levels.

This variation in cracking pattern with respect to valley geometry, (N) can be seen in figure 4, which shows the crack pattern on a half plan view of the dam/foundation contact. Note how the percentage of base in compression increases with increasing N. For N=2, only 59% of the base remains in compression even though 100% of the base is in compression when analyzed in two dimensions.

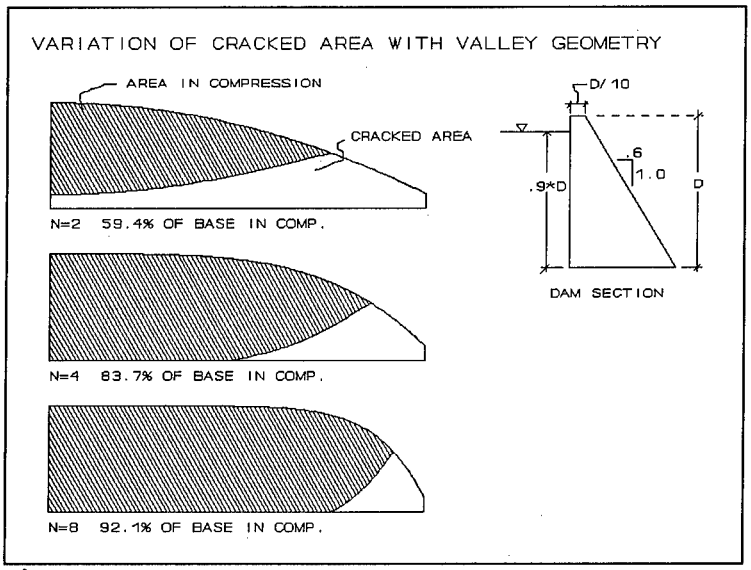

Figure 4

Figure 5 shows how the cracked area of the base grows as the reservoir level is increased. Note that

the cracking begins at the abutments where there is little dead load stress on the dam/foundation contact. Uplift and rigid body rotation of the dam will lift off the sections close to the ends first. This is because of the small amount of initial dead load compression under the short end sections of the dam, and because more of the contact for these sections is upstream of the foundation centroid.

During the initial phases of cracking, the crack propagates from the ends of the dam toward the center. The centerline of the dam is the last area to crack, even though it is subject to the largest uplift and driving pressures.

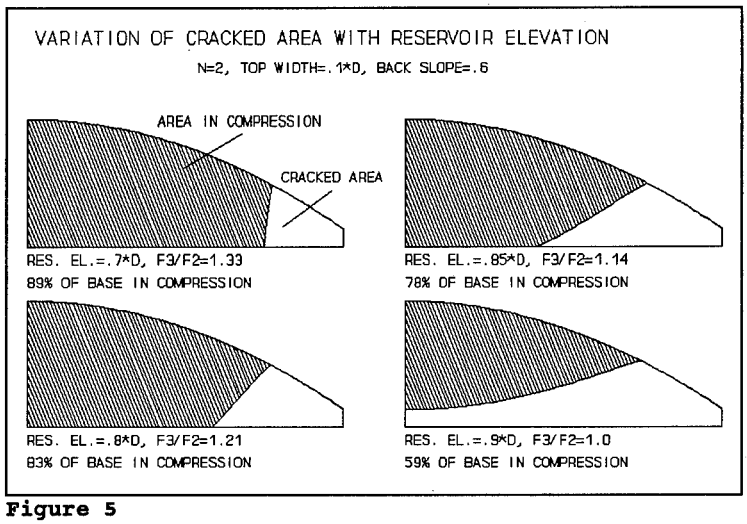

Figure 5

New Insights

The parametric study provided the author with a new insight. When a dam's resistance to sliding is strictly from friction, the ratio of valley width to depth is irrelevant. Three dimensional effects are strictly a function of the "U" ness of the valley. When a significant portion of the dam's sliding resistance is due to cohesion however, the valley width to depth ratio is a factor.

This parametric study is not intended as a

substitute for rigorous analysis which considers foundation and dam deformation. However it is hoped that the consideration of basic static equilibrium will be helpful in developing some insight into general three dimensional behavior. When performing three dimensional stability analysis, ignoring dam and foundation deformations is not recommended.

Conclusion

1) Three dimensional stability analysis is called for when dam or valley geometries are irregular, or when the valley is "V" shaped.

2) Neglecting three dimensional effects is not always conservative. Consideration of the third dimension will not always indicate that a dam is more stable than indicated by two dimensional analysis. For this reason it is important to include three dimensional effects when they are present.

3) Three dimensional behavior is determined by valley shape, ("U" ness). When resistance to sliding is due to friction only, the width to depth ratio of the dam is not a factor.

Computer Aided Design of Drainage Systems for Dams

Tissa H. Illangasekare[1], Member
Bernard Amadei[2], Associate Member
Rodney Lyons[3]
C. Chinnaswamy[4]
Doug Morris[5]

Abstract

Uplift in cracks and in foundation interfaces plays a crucial role in dam stability analysis. Drains can be designed to intersect these cracks to reduce uplift. A finite element model was developed to simulate both steady and transient flow in cracks. The capability of this model as a design and evaluation tool is demonstrated.

Introduction

In gravity dams cracks may develop in weakened zones in the concrete such as along lift lines, cold joints, or at the dam/foundation contact plane. When the entrances to these cracks are exposed to the reservoir, water enters the crack and the hydrostatic pressure in the reservoir gets transmitted to the internal structure of the dam. A knowledge of the magnitude and distribution of uplift pressure is needed when assessing the stability of dams and in the design of schemes to make the structure safe.

A remediation measure which could be implemented

---

[1]Professor, [2]Associate Professor and [4]Research Associate, respectively. Dept. of Civil and Envir. Eng., University of Colorado, Boulder, CO 80309-0428.

[3]Senior Programmer, Power Computing, Dallas, Texas.

[5]Program Manager, Storage Systems, Electric Power Research Institute, Palo Alto, California.

to reduce uplift is to use drains to intercept the flow in the crack. The effectiveness of the drains is determined by comparing the reduction of uplift with the undrained total uplift.

The flow in a crack remains steady only when the reservoir water level remains constant. In the case of a flood reaching the dam, the reservoir level changes with time creating transient flow conditions. The drain effectiveness will change as the transient flow in the crack alters the uplift. In evaluating the stability of a dam, a critical situation for which the drain effectiveness has to be assessed is when a large flood such as the probable maximum flood (PMF) reaches the reservoir.

The magnitude of the water velocity determines whether the flow is laminar or turbulent in the crack. The flow velocity depends on the physical characteristics of the crack and the head gradient. In a crack with a drain, the highest head gradients are created around the drain. When the reservoir head changes, the head gradients changes and the flow may change from laminar to turbulent in some parts of the crack. These mixed flow conditions change the uplift pressure distribution and thus affect the drain effectiveness. A drainage system which is designed to function under normal reservoir levels when the flow is laminar may change its effectiveness when subjected to higher reservoir heads during which the flow becomes turbulent.

A numerical model, CRFLOOD, was developed to estimate uplift in drained and undrained cracks under steady and transient (flood) conditions (Illangasekare et al., 1992). This model was validated using both laboratory and field data. The model was then used to conduct sensitivity analysis to evaluate the importance of some of the factors that control drain effectiveness (Illangasekare et al, 1991). A user friendly pre- and post- processor allows for the convenient use of the model for the analysis of complex problems involving flow in cracks. In this paper, the capability of this model as a computer assisted tool for the design and evaluation of drainage systems is demonstrated.

Hydraulics of flow in cracks

The flow in a crack is modelled by treating the crack as the space between two parallel plates. The flow is controlled by the head gradient, crack aperture and the crack wall roughness.

Crack flow can be categorized under four hydraulic zones based on the relative roughness and the Reynold's number (Louis, 1969). The relative roughness is defined as the ratio between the asperity height and the

hydraulic diameter of the crack.

Flow through a crack can be considered parallel for values of relative roughness less than 0.033 and non-parallel if it is greater than 0.033. It has been shown experimentally that for hydraulically smooth parallel flow (relative roughness less than 0.033), the transition from laminar to turbulent flow occurs when the Reynold's number is approximately 2300. In a rough crack with non-parallel flow (relative roughness greater than 0.033), this transition occurs at much lower Reynold's numbers.

For all four hydraulic zones, the velocity and the gradient of the total head can be related by the general expression,

$$v=-KJ^{\alpha} \qquad (1)$$

where, K is the hydraulic conductivity of the crack, v is the velocity, J is the gradient of total head along the flow direction and α a constant which depends on the hydraulic zone.

The expressions for K and values of α vary for each hydraulic zone. In the flow regions where the flow is laminar and hydraulically smooth, the exponent becomes unity, making the flow relation linear. In all other zones where the flow is turbulent the exponent is less than unity resulting in non linear flow laws.

Combining mass conservation and the flow law for saturated flow in a crack, the governing equation for two-dimensional transient flow becomes,

$$\frac{\partial}{\partial x}\left(bK\frac{\partial H}{\partial x}\right)+\frac{\partial}{\partial y}\left(bK\frac{\partial H}{\partial y}\right)=S\frac{\partial H}{\partial t} \qquad (2)$$

where H is the hydraulic (or potential) head, K is the hydraulic conductivity for laminar flow and S is the storativity of the crack. The storativity depends on the stiffness of crack wall material, compressibility of water and the crack aperture.

In addition to the governing equation, the complete formulation of the flow problem requires the specification of flow or head conditions at the boundaries of the crack and at the crack-drain intersection.

Features of CRFLOOD

The primary function of the CRFLOOD code is the solution of Eqs. 2, with its associated boundary and initial conditions. Existing analytical solutions are limited to simple crack plane geometries, constant or linearly varying apertures, and more restrictively laminar flow conditions. To handle more general

conditions of irregular crack geometries, variable apertures and roughness, the finite element method was used.

The program is designed to estimate uplift in any tensile cracks in the concrete structure, openings in the contact plane between the dam at its foundation and lift lines. The flow within a crack with any irregular geometry could be simulated. In general, crack plane is non-planar, that is the elevation of the crack can vary in space. The model allows for the variation of both aperture and roughness over the crack plane.

The model allows for the inclusion of a maximum of ten circular drains intersecting the crack plane. A box drain could be represented with a line of closely spaced drains.

Boundary conditions representing both constant and transient reservoir heads can be incorporated. Depending on the boundary conditions, the flow in the crack can be fully laminar, turbulent or mixed.

Demonstration of CRFLOOD

Three hypothetical examples are presented to demonstrate the capabilities of CRFLOOD as a computer assisted design tool.

Determination of Crack Parameters: Figure 1 shows the plan view of a suspected crack at the base of a dam. Four piezometers were installed to measure the water pressure in the crack.

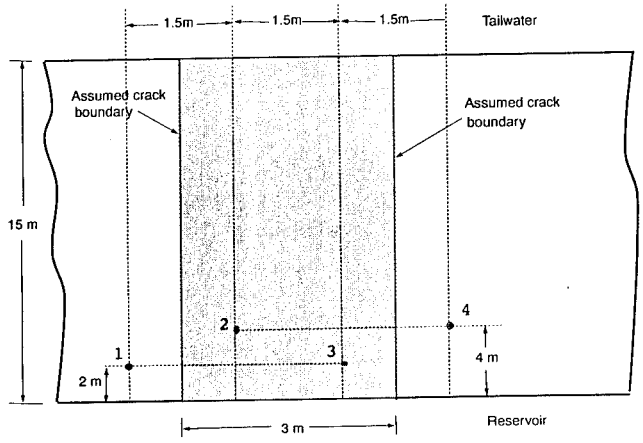

Figure 1: Plan view of crack and piezometer locations.

The pressure heads measured using the piezometers corresponding to two reservoir heads are given in Table I. If the flow through the crack is 3.67 m^3/d when the reservoir head is 17 m, use CRFLOOD to determine the extent of the crack and crack parameters.

Reservoir Head (m)	Tailwater Head (m)	Piezometer Head (m) 1	2	3	4
17	1.5	0	12.9	11.3	0
15	1.0	0	14.9	13.1	0

Table I: Observed Piezometric Head

As the piezometers 1 and 4 remain dry, the crack is considered to be only intersected by piezometers 2 and 3. If the crack is not connected to the tail water, the piezometric head in 2 and 3 should be exactly equal to the water level in the reservoir. As the piezometric heads in 2 and 3 are not constant it can be deduced that the crack is in hydraulic connection with the tail-water. To simulate the flow, the crack is assumed to be rectangular and the length and depth to be 15 m and 3 m, respectively. As no data on the crack roughness and aperture distribution are given, it is assumed that the crack is smooth and the aperture is uniform. With these assumptions, CRFLOOD will be used to estimate the effective crack aperture.

A trial and error procedure is used to calibrate the effective crack aperture. First, CRFLOOD is used to simulate the flow in the crack using an assumed value of crack aperture. Figure 2 gives a plot of the assumed effective crack aperture vs. the discharge through the crack as computed using CRFLOOD. This graph is used to estimate the effective crack aperture of 0.25mm corresponding to the discharge of 3.67 m^3/day.

Drainage System Design: Figure 3 shows the plan view of a horizontal crack at the base of a concrete dam. It is known that the crack is not hydraulically connected to the tail-water. The spatial distributions of the crack aperture and roughness are known. Under normal operating conditions the reservoir water elevation is 30.5 m. The drainage gallery is 10.7 m above the crack. It is required to design a drainage system using vertical drains drilled through the gallery floor to reduce the

total uplift by 50%. That is, the effectiveness of the drains should be 50%. Three points as shown on Fig. 3 have been identified as the possible locations for the drains. In the design, drain diameters of 5.05 cm (2 ins), 7.62 cm (3 ins) and 12.70 cm (5 ins) are to be considered.

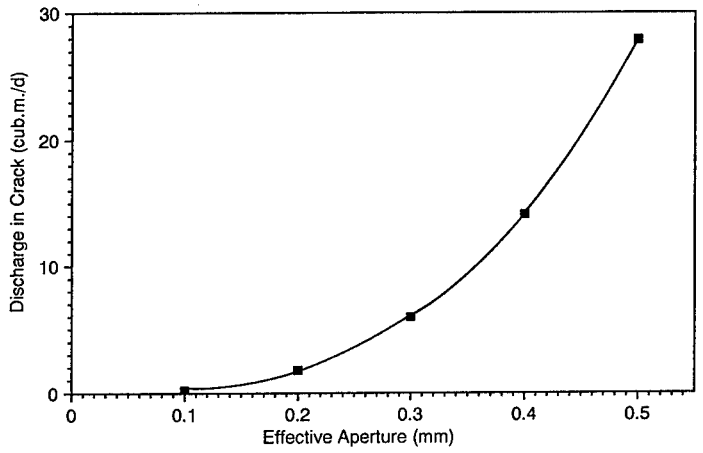

Figure 2: Effective aperture vs. computed discharge in crack.

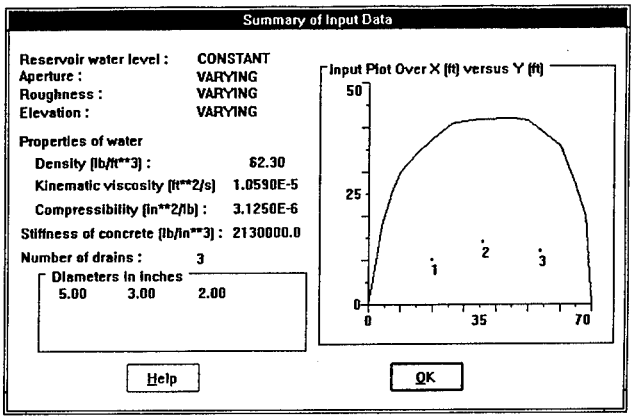

Figure 3: Crack shape and possible drain locations.

Program CRFLOOD was used to conduct a number of simulations for various combinations of drain locations and diameters. The head in all the drains was defined as the elevation of the gallery floor. Table II summarizes the results of the simulations showing the computed drain effectiveness for various drain configurations which were considered in the design.

The simulation results suggest that the drain configurations 3, 6 and 9 satisfied the 50% drain effectiveness requirement. In all these cases the simulations show that a small zone around the three drains produced turbulent flow. Figure 4 shows the uplift pressure distribution over the crack plane for drain configuration 9. Figure 5 shows the distribution of the Reynold's number over the crack plane for the same drain configuration.

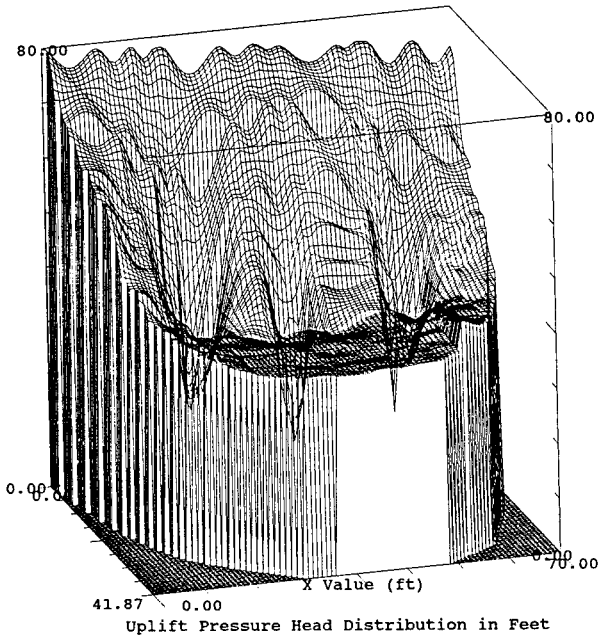

Figure 4: Uplift pressure head distribution over the crack plane.

Table II: Drain effectiveness for various drain configurations.

Drain Config.	Drain diamtere in cm at location 1	2	3	Computed Effect. %
1		5.1		35.2
2	5.1	5.1		42.2
3	5.1	5.1	5.1	50.3
4		7.6		36.8
5	7.6	7.6		45.0
6	7.6	7.6	7.6	54.0
7		12.7		37.6
8	12.7	12.7		45.8
9	12.7	12.7	12.7	55.1

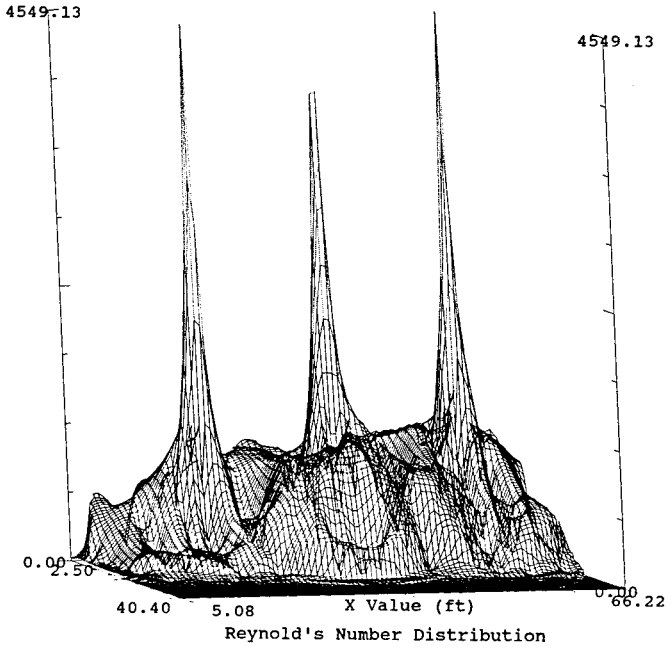

Figure 5: Distribution of Reynold's numbe over crack plane.

Evaluation of Drainage System Under High Heads: In this example, the effectiveness of the drainage system under high reservoir heads is evaluated. As shown in Table II, three drain configurations, namely, 3,6 and 9 satisfied the design requirement of maintaining a drain effectiveness higher than 50%. CRFLOOD was used to simulate the uplift for these three configurations for the two situations when the reservoir water levels changed by a factor of 2 and 3, respectively. This corresponds to crack entrance heads of 61 m and 91 m, respectively. Table III summarizes the results of these simulations, showing the drain effectiveness under normal conditions and under high heads.

Table III: Drain effectiveness under high reservoir heads.

Drain Config.	Reservoir Head (meters)		
	30.5	61.0	91.4
3	50.2	48.2	47.7
6	54.0	53.0	52.8
9	55.1	54.3	54.2

The results show that the drain effectiveness falls below the design value of 50% for configuration 3 where 5.1 cm diameter drains were used. Figure 6 shows the zones of laminar and turbulent flow in the crack for configuration 9 with a high head of 91.4 m. Even though a much larger zone of turbulence occurred in this case compared to the case when the reservoir level was normal, the drain effectiveness did not change significantly. However, configuration 3, which was an acceptable design under normal heads, failed under higher heads.

Conclusions

The capability of a computer model as tool for the design and evaluation of drainage systems was demonstrated. The model can be used to calibrate the effective crack aperture. A drainage system designed for normal operating conditions may reduce its effectiveness under conditions of high reservoir heads.

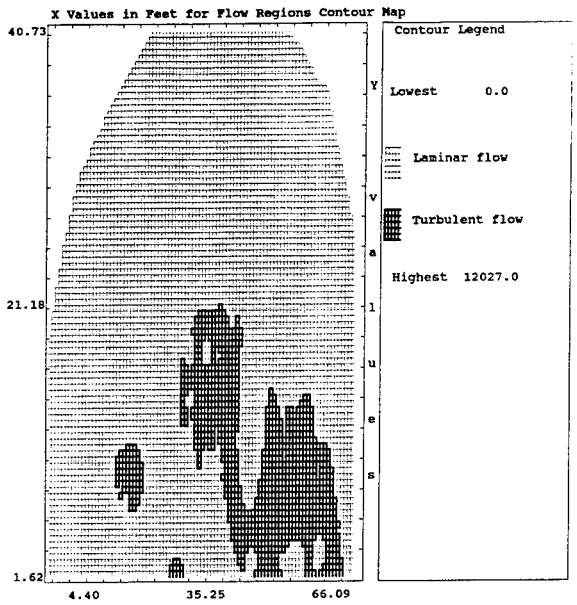

Figure 6: Zones of laminar and turbulent flow under high heads.

Acknowledgement: The work presented in this paper is supported by the Electric Power Research Institute under dam safety contract RP 2917-07.

References

1. Illangasekare, T.H., Amadei, B. and Chinnaswamy, . (1992). "CRFLOOD: A numerical model to estimate uplift in gravity dams." EPRI Final Report, Vol. 4.

2. Illangasekare, T.H., Amadei, B. and Chinnswamy, C. (1991). "Uplift Pressure reduction using drains." Proc. of ASCE Conference Waterpower 91, Denver, Colorado.

3. Louis, C., 1969, A study of groundwater flow in jointed rock and influence on the stability of rock masses, Rock Mechanics Research Report, No. 10, Imperial College, London.

MODIFICATION OF BEECH DAM FOR SEEPAGE CONTROL AND UPGRADE FOR THE MAXIMUM CREDIBLE EARTHQUAKE

by
Vann A. Newell[1], Harry A. Manson[2], Charles D. Wagner[3]

INTRODUCTION

Safety of its dams has always been of great concern to the Tennessee Valley Authority (TVA). The agency throughcut its history has enforced conservative designs, good construction practices and good operating procedures, including routine inspections. Beginning in the middle 1960's, TVA began an intensified reevaluation of the safety of its dams, especially in regard to older dams built by private power companies and obtained by TVA in the late 1930's. Special emphasis was placed on spillway capacity since hydrologic data and flood criteria have been refined in recent times. After the failure of several dams in the United States, a Federal directive on Dam Safety Guidelines was published in 1979.

TVA initiated a program to review its existing dams for conformance to present-day criteria. Beech Dam was considered a low-hazard structure when it was originally designed and constructed. Subsequent development downstream has warranted the dam to be changed to a high-hazard structure requiring design for the Probable Maximum Flood (PMF) and Maximum Credible Earthquake (MCE).

PROJECT DESCRIPTION

Beech Dam is located on the Beech River inside the city limits of Lexington in Henderson County, Tennessee. It is approximately 35.0 river miles upstream of the Tennessee River.

Original construction of Beech Dam began October 26,

---

1 Civil Engineer, BSCE, MSCE, Member ASCE
2 Civil Engineer, BSCE, Member ASCE
3 Manager of Civil Engineering, BSCE, PE, Member ASCE
Tennessee Valley Authority, 3S Signal Place
1101 Market Street, Chattanooga, TN. 37402

1962 and dam closure was made October 15, 1963. The dam consists of the main embankment, which is 39 feet high and 1,240 feet long and is constructed of impervious rolled earthfill. There is a concrete intake tower for the 42-inch inside diameter (ID) main spillway/sluiceway that passes under the dam and empties into a ripraped plunge pool, an emergency spillway with a 250 foot crest length, two earth saddle dams and the water supply intake tower for the City of Lexington. The dam impounds a reservoir volume of 11,070 acre-feet at elevation 459.9 and provides 4430 acre-feet of flood control storage capacity when headwater is between elevation 459.9 and 464.5.

HYDROLOGIC AND SEISMIC EVALUATION

Present-day criteria for high hazard dams is to design for the PMF and the MCE. Hydrologic studies indicated that the dam as originally designed and constructed would safely pass approximately 53 percent of the PMF. In larger floods up to and including the PMF, overtopping would be of sufficient depth and duration to breach and fail the earth embankment. To safely pass the PMF, the main dam and saddle dams were raised 4.5 feet, from EL 471 to EL 475.5. To control erosion at the juncture of the main embankment and the grassed emergency spillway during extreme flooding, a subsurface sheet-pile erosion barrier wall was installed into an earthfill dike. These modifications were completed in 1989.

The Beech River Dam is located approximately 75 miles from the epicentral location of the New Madrid earthquakes of 1811-1812. The peak ground acceleration of 0.25g was used in the seismic analysis for the Beech Dam. Subsurface investigations of the area revealed silty sand and sand layers below elevation 415 under the downstream valley floor and the embankment of the main dam which accounts for the high piezometric levels and artesian pressures recorded in these areas. The foundations at the abutments are composed of mostly sand which allows water from the reservoir to migrate through causing seeps, wet spots and wetlands at both of the abutment toes. The piezometric levels in the abutment areas were found not to be artesian. Beech Dam, because of its subsurface soil conditions, has had a history of seepage problems.

Slope stability, liquefaction analysis and deformation studies were made using the subsurface soil information and the peak ground acceleration for two cases. Case one was for the existing dam and case two was for the existing dam with a downstream berm. The analysis showed that without a downstream berm, the base of the dam would deform 1.2 to 2.9 feet and cause a loss of freeboard of 1.0 to 2.3 feet. The analysis with a berm added to the dam showed that it would prevent any

measurable deformation at the downstream toe.

STRUCTURAL STABILITY OF THE INTAKE TOWER (Figure 1)

The intake structure is a vertical reinforced concrete riser with a drop inlet consisting of a high level ungated weir opening with a top slab for vortex suppression, low-level 42-inch diameter gated opening and a supplemental high level 14-inch square gated opening. The structure is located at the upstream toe of the dam at station 11+20, it is 33.5 feet in height and its base is 18 feet in width by 16 feet in length by 4.5 feet in height. Two analysis cases were studied: CASE I: Stability of the tower in the direction parallel to the baseline of the dam. CASE II: Stability of the tower in the upstream/downstream direction. Both cases were analyzed for the MCE and found to be capable of withstanding overturning. The analysis showed that sliding would be a problem in the upstream direction and could cause separation between the intake structure and the main spillway/sluiceway. To prevent this separation, a stainless steel liner 4.5 feet in length was installed inside and between the intake structure and main spillway/sluiceway.

SELECTED MODIFICATION

The selected modification included construction of a berm to control seepage and to add weight to the downstream toe of the embankment for seismic loading, relocation and repair of the existing channel and its banks, extending the existing drainage system and modification of all instrumentation. The existing plunge pool was removed and the spillway/sluiceway pipe was extended to the new concrete plunge pool. Also, downstream of the right abutment of the dam, the Lexington water plant has filter drains and holding ponds. The water discharge and seepage coming from these areas had to be addressed.

CONSTRUCTION ACTIVITIES

Construction of the Beech Dam safety modification was started on August 5, 1991 and was completed on September 25, 1992.

BERM (Figure 2 and 3)

The seepage berm starts at elevation 449 on the downstream face of the main embankment and runs about 200+ feet sloping downstream for positive drainage until the berm reaches the existing ground elevation or the abutments. On the left and right abutments, the seepage berm starts at elevation 443 and runs about 100 to 150 feet sloping downstream for positive drainage until the berm reaches the existing ground elevation. Before fill for the berm could be placed, about 2.5 acres had to be

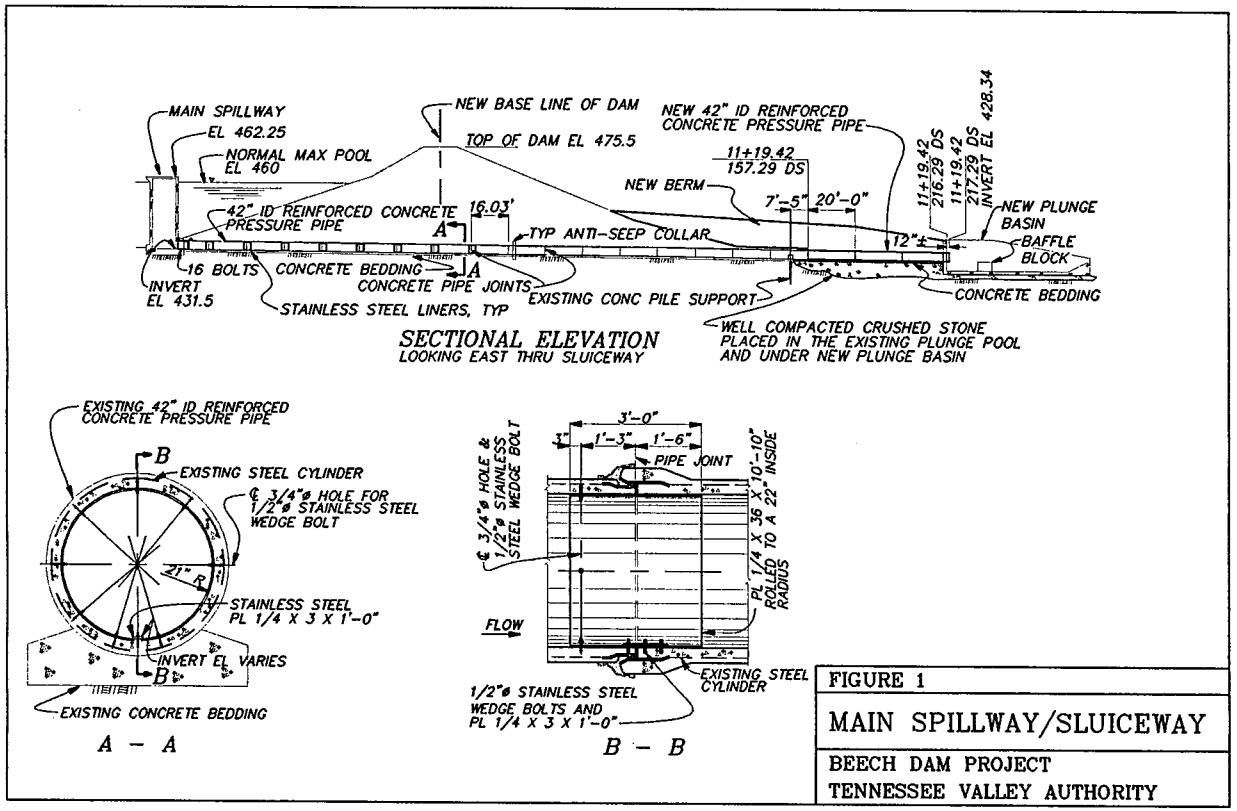

FIGURE 1

MAIN SPILLWAY/SLUICEWAY

BEECH DAM PROJECT
TENNESSEE VALLEY AUTHORITY

cleared and wet areas had to be stabilized using stone and riprap. The low areas were filled with earth and graded to have a positive slope downstream. The drainage blanket was then placed on top of the leveling fill. The drainage blanket consists of two layers of filter cloth that encases 18 inches of crushed stone and 4-inch diameter perforated pvc drainage pipes. The drainage pipes run transverse to the berm at angles between 60 and 75 degrees and tie into 12-inch diameter pvc collector pipes. The 12-inch collector pipes run either to the plunge pool, river channel or the drainage channel that is located at the toe of the left abutment. Earth fill was placed on top of the drainage blanket to the desired elevation. The berm was then sodded to prevent soil erosion. Approximately 60,000 cu. yds. of fill was used in the construction of the berm.

EXTENDING THE EXISTING DRAINAGE SYSTEM

On the left abutment, French drains were used to drain the seepage flowing from the existing ditches to the drainage channel. A concrete gutter had to be added at the end of the left abutment to facilitate rain runoff.

Three existing French drains were extended, the first was extended to the relocated channel, the second to the new plunge pool and the third to the drainage channel at the toe of the left abutment. The toe drains of the dam were extended from the old to the new plunge pool by using a French drain.

On the right abutment, the Lexington Water Treatment Plant had 5 drain lines that had to be dealt with. The first was a 6-inch diameter intake drain line that was extended to the new plunge pool. The second and third lines were 7-inch diameter concrete pipes that were extended into the drainage blanket. The fourth line was an 8-inch plastic pipe that was extended to the relocated channel. The fifth line was a 24-inch diameter cast iron pipe that was extended to a new concrete gutter that ties into the old concrete gutter that had to be removed and then replaced after the berm's construction. This new concrete gutter runs to the relocated channel.

SPILLWAY/SLUICEWAY (Figure 1)

The main spillway/sluiceway is composed of 42-inch ID reinforced concrete pressure pipe with 16 pieces at 16.03 feet and 1 piece at 10.03 feet that rests on a concrete bedding. Due to the addition of the downstream berm, the spillway/sluiceway had to be extended an additional 60 feet by adding 3 pieces of 42-inch ID reinforced concrete pressure pipe at 20 feet each. This additional pipe made the total length of the spillway/sluiceway 326.5 feet. Stainless steel liners

were also installed at the first eight joints of the reinforced concrete pressure pipe downstream of the intake structure. These liners will limit potential piping in the event of displacements and settlements at the upstream base of the dam during a seismic event.

PLUNGE POOL

The existing concrete-choked riprap plunge pool was removed and a new concrete plunge pool was constructed about 75 feet downstream from the old plunge pool. The 42-inch diameter concrete spillway/sluiceway pipe was extended to the new plunge pool. The new plunge pool consists of 18-inch thick reinforced concrete with the top of the base slab at elevation 425.78, winged retaining walls with top elevation 439.28 that taper down to elevation 431.78 at the concrete sill. During excavation of the plunge pool base, the bottom of the slab had to be raised about 2.5 feet because water was boiling up through a sand layer at elevation 424.28. Excavation was stopped and filter fabric was placed in the bottom and on the sides of the excavated area, then crushed stone was placed for the base and plastic sheets were placed on top of the stone. The base slab contains 29 3-inch diameter uplift drain holes that were opened after construction of the plunge pool was completed. Testing of the plunge pool under full flow, 330 cfs, showed that the water would jet out of the pool and cause erosion of the new river channel downstream of the sill. This effect was due to the raising of the bottom of the plunge pool. A scale model of the 43-foot wide and 63-foot long plunge pool was constructed and tested. From the model testing it was determined that a baffle block 9 feet from the spillway/sluiceway outlet would dissipate the energy. A baffle block 5 feet, 4 inches long, 5 feet wide and 3 feet in height with a triangular front was constructed in the pool and tested under full flow. The baffle block dissipated the energy and eliminated the erosion problem. The model was constructed and tested at TVA'S Engineering Laboratory in Norris, Tennessee.

RIVER CHANNEL

About 250 feet of the existing channel had to be relocated. The relocated channel extends from the new plunge pool and ties back into the existing channel about 250 feet downstream. The new and existing sides of the channel were sloped 1 vertical on 2 horizontal with filter cloth placed on the sides and bottom. Then the filter cloth was covered with a 6-inch layer of crushed stone and a 2-foot thick layer of riprap. The riprap was placed 2 feet higher than the normal high water elevation in the channel. Beyond the riprap, the sides were sloped at 1 on 6 up to the existing ground line, then seeded and mulched, except at the lower end of the channel in the area of the water treatment plant

settling ponds. Due to seepage from these ponds, the riprap was carried up to the existing ground line.

INSTRUMENTATION MODIFICATION

A total of 26 piezometers have been installed at Beech Dam over the years to monitor the high water table that exists in the sand layers under the dam and the artesian pressures. In the areas being affected by construction, 13 of the existing piezometers had to be raised to the desired elevations above the berm fill. This was accomplished by extending the piezometer's pvc pipe in sections, then placing a section of 24-inch diameter corrugated metal pipe around the piezometer and filling it with concrete. This process was repeated as the earth fill was placed for the berm. After the piezometers were raised, a galvanized well cover 6-inches by 6-inches by 5-feet was placed over the exposed pvc pipes and concrete was placed at the base of the well covers.

Three stainless steel weir boxes were fabricated and installed on the plunge pool walls so it would be possible to measure the flows from the two toe drains and the French drain that empty into the plunge pool.

ENVIRONMENTAL MITIGATIONS

The project was coordinated with the U.S. Army Corps of Engineers through the Section 404 permitting process and with the State of Tennessee through the Section 401 permitting process.

Mitigations include the planting of approximately 400 mast producing trees in the 2.75 acre area downstream of the berm and along the existing channel for the loss of existing trees. The new and existing channels assimilate the "pool and riffle" effect by the use of five double wing deflector dams that were constructed of riprap and logs and spaced approximately 100 feet apart. Public access launching ramps were extended to allow for boat access to the lake during drawdowns. A 1-mile asphaltic concrete public walking/jogging trail was constructed on top of the dam and in the flood plain below the dam. The earth berm was sodded instead of seeded to prevent soil erosion and runoff problems.

COST OF THE MODIFICATION

The cost to modify Beech Dam for the MCE, seepage control and for environmental mitigation was $1.4 million.

Engineering costs	:	$ 193,502
Construction costs	:	$ 1,107,781
Environmental mitigation:		$ 94,000
Total Cost		$ 1,395,283

Photo 1 - Downstream Berm and Drainage System

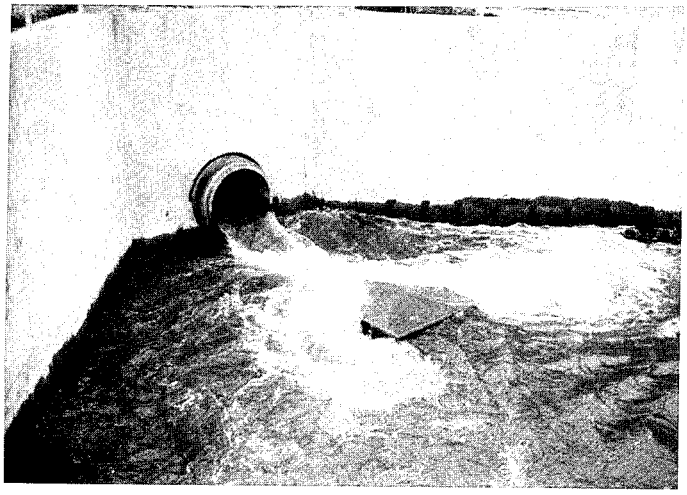

Photo 2 - Concrete Plunge Pool and Baffle Block

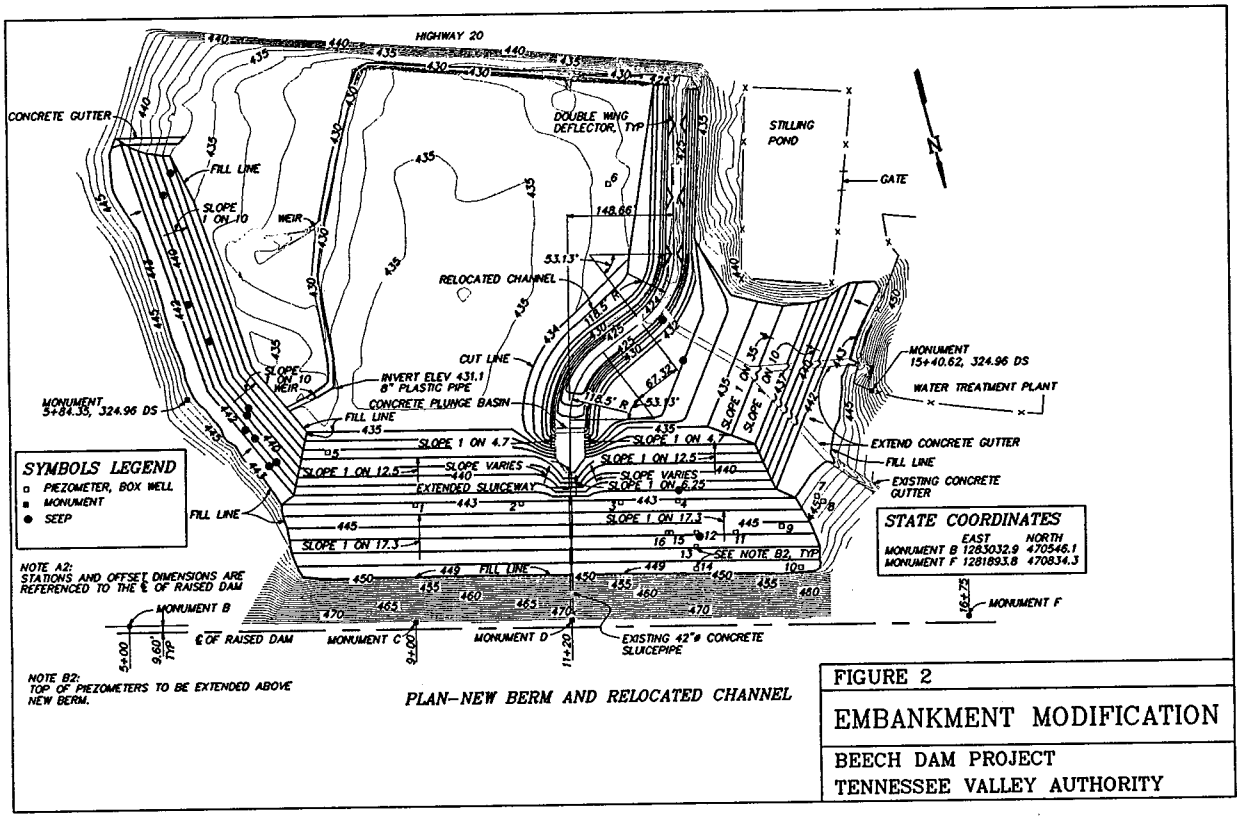

FIGURE 2

EMBANKMENT MODIFICATION

BEECH DAM PROJECT
TENNESSEE VALLEY AUTHORITY

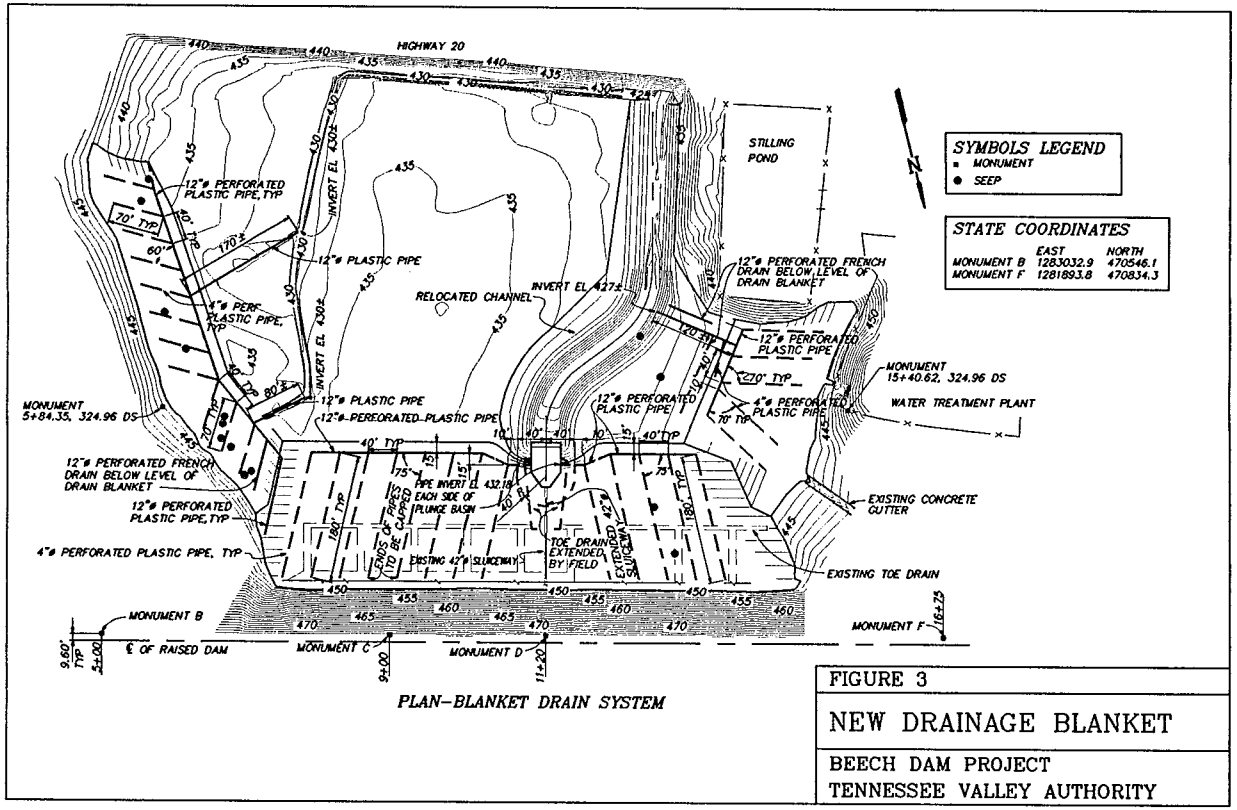

PLAN–BLANKET DRAIN SYSTEM

FIGURE 3

NEW DRAINAGE BLANKET

BEECH DAM PROJECT
TENNESSEE VALLEY AUTHORITY

STRUCTURAL INTEGRITY OF FONTANA EMERGENCY SPILLWAY

C. Wagner[1], Member ASCE, J. Niznik[1], M. Kaltsouni[2], Associate Member ASCE, V. J. Zipparro[2], Fellow ASCE, C. H. Yeh[2]

Abstract

The Fontana Emergency Spillway experienced movement in the upstream direction over the years caused by the phenomenon of concrete growth due to alkali-aggregate reaction. This resulted in considerable opening of the vertical contraction joints between the arch blocks. The purpose of this study is to evaluate the safety of the structure under hydrostatic and gravity loads when the contraction joints are open and to determine the critical length of the opening beyond which grouting of the joints becomes necessary.

Introduction

The Fontana Emergency Spillway is part of the Fontana project and is located on the Little Tennessee River in North Carolina. The spillway was constructed in the 1940s and is an unreinforced concrete circular single curvature arch dam having a radius of 26.8 m to its vertical upstream face (Fig. 1). The arch is 16.7 m high varying in thickness from 4.2 m at the base to 0.71 m near the crest. The crest is about 55 m long making a central angle of 120°. Concrete abutment blocks are interposed between

[1]Tennessee Valley Authority, 37 E Signal Place, Chattanooga, Tennessee 37402

[2]Harza Engineering Company, 233 South Wacker Drive, Chicago, Illinois 60606

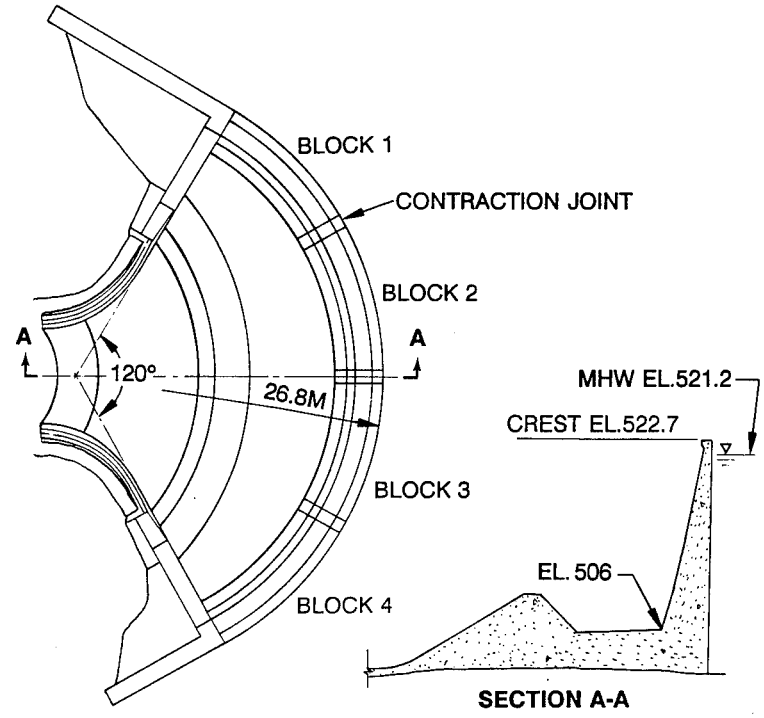

Figure 1. Plan and Section of Fontana Dam Emergency Spillway.

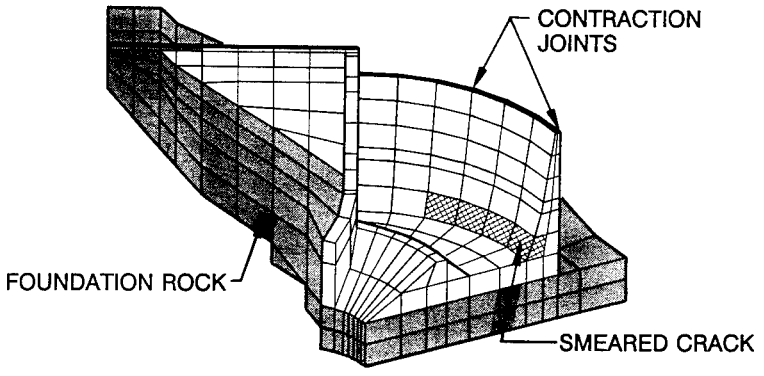

Figure 2. Finite Element Model.

the arch and the sloping rock abutments. The base of the arch dam rests on the concrete slab floor of the plunge pool.

The arch was constructed in four sections about 12.2 m long each with contraction/closure slots 1.2 m wide between them. Continuous vertical keys up to 0.15 m below the crest were constructed on both faces of contraction slots and copper seals were placed near the upstream face. Horizontal construction joints were spaced every 1.52 m.

A surveying benchmark was placed at the mid point of the arch crest in order to monitor the deformation of the structure. A substantial horizontal movement of the spillway in the upstream direction was observed over the years. The horizontal movement initially was minor, but it began to accelerate gradually and after 1970 the deformation rate was substantial. This resulted in considerable vertical cracking in the arch blocks and opening of the vertical joints in the upper portion of the arch.

By 1988 the center of the arch crest had moved 370 mm in the upstream direction. Laboratory tests revealed that the displacement was caused by the phenomenon of concrete growth due to alkali-aggregate reaction (Ref. 1, 2, 4).

The opening of the contraction joints prompted concerns about the safety of the structure due to the loss of arch action. After several cycles of grouting and reopening of the joints, it was decided that the stability of the structure should be re-evaluated analytically. A mathematical model of the structure was developed and the finite element method was employed for the structural analysis. The objective was to simulate the actual movement of the structure and to investigate its stability. The simulation process and the calibration of the finite element model of the spillway was described in a paper presented in the "International Workshop on Dam Safety Evaluation" in Switzerland on April 1993 (Ref. 5).

This paper discusses the evaluation of the safety of the structure under the effect of gravity and hydrostatic loads with open contraction joints and the determination of the critical length of the opening beyond which grouting of contraction joints is necessary.

The Structural Model

A three-dimensional finite element model was developed, using 8-node solid elements based on the as-built drawing of the emergency spillway. The model included the arch structure, the abutment, the foundation concrete slab and part of the foundation rock (Fig. 2). The symmetry of the structure about the central axis allowed modeling only half of the spillway.

The opening of the contraction joints due to the upstream movement of the structure was simulated in the finite element analysis. This was achieved by expanding the structure with an artificial temperature field (Ref. 5).

Crack size and location survey of the upstream and downstream faces of the arch revealed considerable horizontal cracking near the base of the downstream face. This was attributed to the development of tensile stresses in the cantilever direction. Preliminary finite element analysis indicated that tension in this area could cause tension. As a result, the capacity of the structure to withstand tensile stresses in the cantilever direction near the base of the downstream face was diminished. This condition was simulated by introducing a smeared crack into the finite element model at the downstream face of the arch (Fig. 2).

Loading and Analysis Procedure

Field measurements indicated that the maximum recorded headwater level was at Elevation 521.2 m (Fig. 1). The contraction joints between the arch blocks have been opening gradually. In order to study the effect of the headwater on the arch structure, the finite element model was modified and analyzed six times. The modifications were based on varying the length of the opening of the contraction joints from zero meters (joints closed) to 10.7 m (Elevation 512 m). The following cases were considered.

i) Contraction joints closed
ii) Contraction joint opening length 3.06 m (El. 522.7 - 519.64 m)
iii) Contraction joint opening length 6.11 m (El. 522.7 - 516.59 m)
iv) Contraction joint opening length 7.64 m (El. 522.7 - 515.06 m)
v) Contraction joint opening length 9.17 m (El. 522.7 - 513.53 m)
vi) Contraction joint opening length 10.7 m (El. 522.7 - 512 m)

In the analysis, special consideration was given to the smeared crack introduced in the finite element model at the base of the downstream face of the arch. The smeared crack was considered active when the base of the downstream face of the arch was in tension in the cantilever direction and was inactive when it was in compression.

In addition to the hydrostatic load, the dead load due to the self-weight of the concrete was considered for the analysis of the spillway.

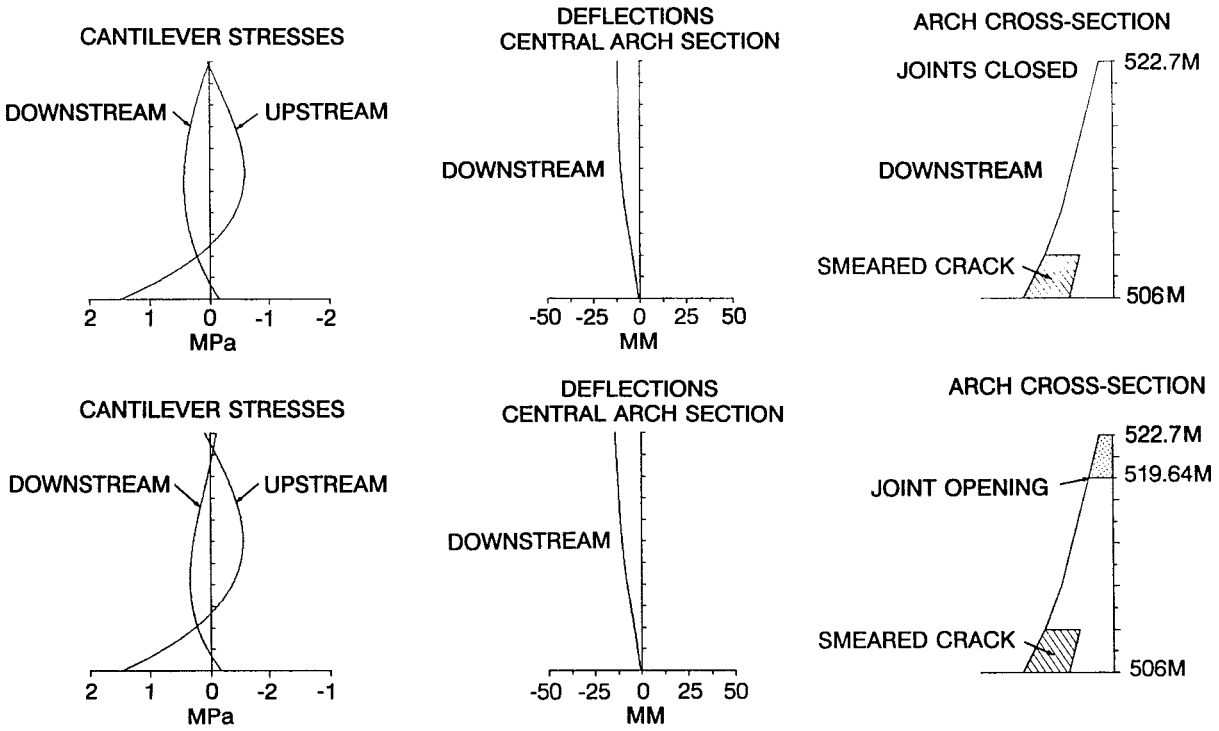

Figure 3. Cantilever Stresses and Deflections Due to Gravity and Hydrostatic Loads. Case (i) and (ii)

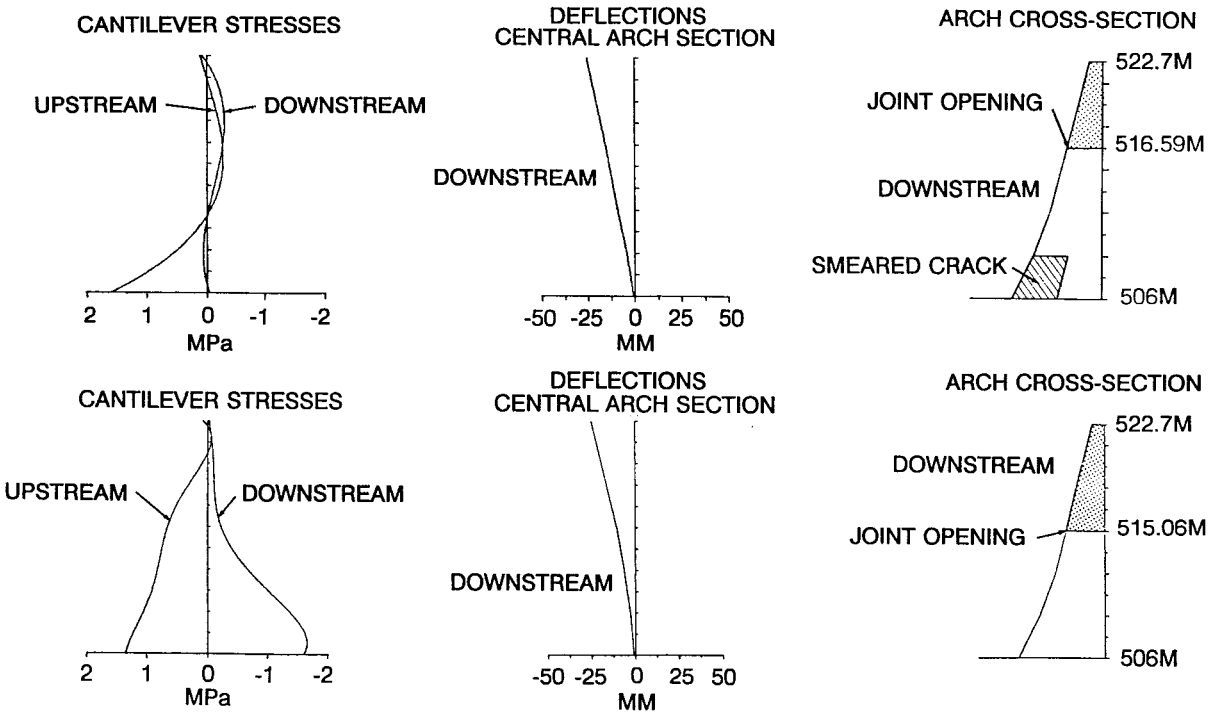

Figure 4. Cantilever Stresses and Deflections Due to Gravity and Hydrostatic Loads. Case (iii) and (iv)

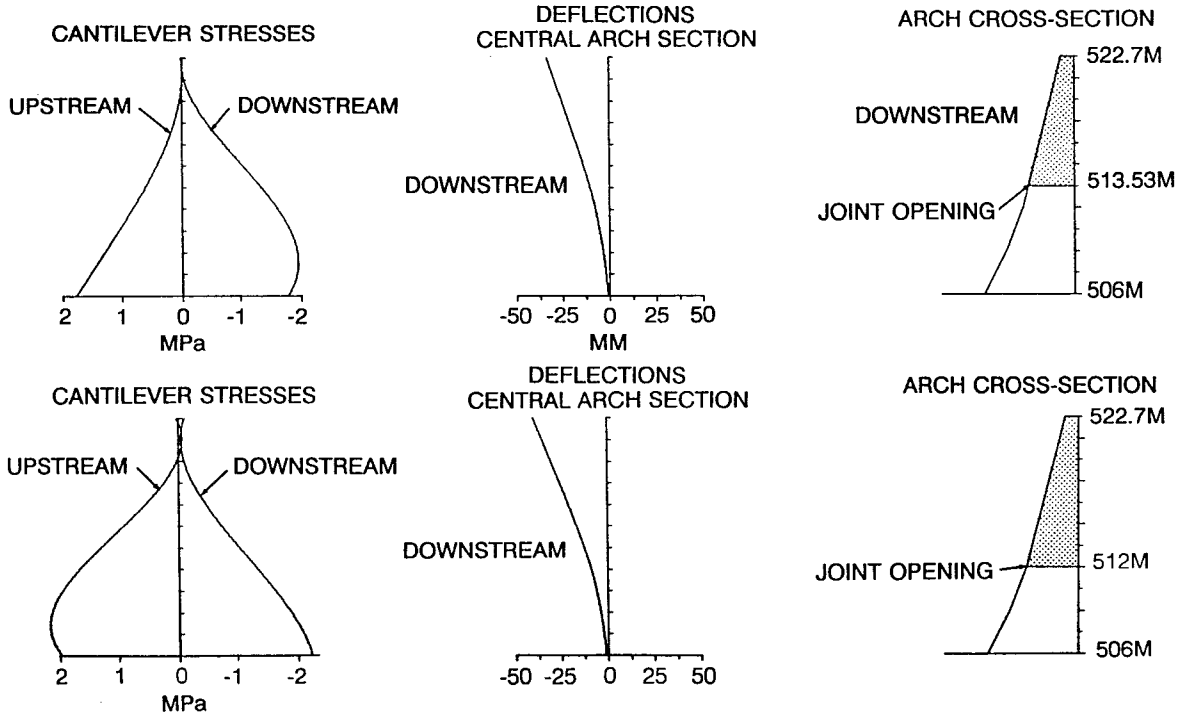

Figure 5. Cantilever Stresses and Deflections Due to Gravity and Hydrostatic Loads. Case (v) and (vi)

Discussion of Results

The maximum stresses and deflections for the above analysis cases are shown in Figures 3 thru 5. These are stresses in the cantilever direction at the center of Block 2 (Fig. 1) and deflections of the center section of the arch.

The load on an arch dam is being resisted by both the arch action and the cantilever action. Figure 3 (joints closed) shows cantilever stress distribution of a typical monolithic arch dam. As the length of the joint opening increases, cantilever action becomes more prominent. When the joint opening length reaches 7.64 m (Case IV) cantilever compression is developed on the downstream side of the dam and the smeared crack is closed. At the same time, tension appears in the upstream side. As the opening length continues to increase large tensile stress is developed over a substantial area on the upstream side. These stresses could induce horizontal cracking at the upstream face of the structure.

Two-Dimensional Stability Analysis

A conventional two-dimensional stability analysis of the spillway was performed under the effect of the gravity and water loads. This two-dimensional model simulates the arch blocks when the contraction joints are open and the shear keys are disengaged. The purpose of the analysis was to determine the critical cantilever height for which a free-standing closure block becomes unstable. The headwater elevation was assumed to be at 521.2 m. The cross-section of the arch was considered to be under the effect of the gravity load, the water load, and the uplift pressure. The analysis indicated that for a cantilever height of 4.59 m or less, the closure blocks are stable. When the cantilever height is greater than 4.59 m, the blocks become unstable.

It should be noted that the two-dimensional stability analysis is a very conservative analysis for this type of structure.

Conclusion

A study was performed to determine the effect of the hydrostatic load on the Fontana Emergency Spillway taking into account the length of the contraction joint opening. The headwater level was assumed to be at Elevation 521.2 m. A three-dimensional finite element analysis indicated that, when the contraction joints were opened below the Elevation 516.59 m, substantial tensile stresses were developed in the cantilever direction of the arch at the base of the upstream face. A conventional two-dimensional stability

analysis indicated that when the contraction joints opened below Elevation 518.11 m, the closure blocks could become unstable.

Based on this study, it is recommended that the length of the contraction joint opening be monitored on a regular basis. The joints shall be grouted to restore the arch action when the opening length exceeds 4 m.

References

1. "Fontana Project - Emergency Spillway Evaluation" by J. L. Golden, Tennessee Valley Authority (TVA) Internal Memo, September 29, 1989.

2. "Petrographic Examination of Drilled Cores Taken from the Fontana Emergency Spillway", R. C. Mielenz, December 1990.

3. "Finite Element Analysis of Reinforced Concrete - Arthur H. Nilson et al. (eds.), ASCE Task Committee Report, New York, 1982.

4. "Fontana Project - Emergency Spillway Arch Structure" by C. D. Ragsdale, TVA Internal Memo, January 26, 1984.

5. "Fontana Emergency Spillway, Case Study", C. H. Yeh, C. Wagner, J. Niznik, V. J. Zipparro, M. Kaltsouni, International Workshop on Dam Safety Evaluation, Grindelwald, Switzerland, April 26-28, 1993.

MODIFICATION AT HIWASSEE DAM DUE TO CONCRETE GROWTH PROBLEMS

by
Vann A. Newell[1], David T. Tanner[2], Charles D. Wagner[3]

INTRODUCTION

Hiwassee Dam is experiencing concrete growth caused by an alkali-aggregate reaction (AAR). The AAR in this case is the alkali-silica type associated with excessive alkali in the cement and a micaceous quartzite (siliceous) aggregate used in the concrete. This concrete growth has resulted in high stresses and deflections within the dam. These stresses and deflections have caused major problems.

The most noticeable problems are:

1. The nonoverflow blocks have deflected into the spillway openings causing the spillway gates to bind. This will continue to be an annual problem if the deflections of the nonoverflow sections are allowed to continue or unless the spillway gates are redesigned to allow for additional deflection.

2. Closed contraction joints in the spillway bridge putting the bridge under a stress condition that it is not designed for. The bridge deck at this time is in a state of longitudinal stress.

3. Structural cracking of the upper portion of the dam, particularly at the abutments. Additionally, the stresses at the abutments are approaching unacceptable limits.

PROJECT DESCRIPTION

Hiwassee Dam is located on the Hiwassee River at river mile 75.8 in Cherokee County, North Carolina. It

---

1 Civil Engineer, BSCE, MSCE, Member ASCE
2 Civil Engineer, BSCE, MSCE
3 Manager of Civil Engineering, BSCE, PE, Member ASCE
Tennessee Valley Authority, 3S Signal Place
1101 Market Street, Chattanooga, TN. 37402

is approximately 20 miles downstream from Murphy, North Carolina and 105.3 miles upstream of Chickamauga Dam.

Construction of Hiwassee Dam started on July 15, 1936 and dam closure was made December 31, 1940. Hiwassee Dam is a 307 foot high and 1,287 foot long concrete gravity structure. It consists of a main spillway with seven radial gated bays, nonoverflow sections at the abutments, four sluices and a power intake section with a 2-unit hydroelectric plant. The dam impounds a reservoir volume of 434,000 acre-feet at elevation 1526.5 (top of radial gates) and provides 365,000 acre-feet of flood control storage capacity when headwater is at minimum pool elevation 1415.

FINITE ELEMENT MODEL

A three-dimensional linear-elastic model of the dam and foundation was developed using ANSYS. Gravitational, thermal, reservoir and AAR loads were applied to the model. Loading induced by the AAR was applied as an additional thermal load.

The Finite Element Model (FEM) was constructed using the ANSYS preprocessor PREP7. A simple solid (geometric) model was constructed initially. Meshing of the solid model was accomplished by using primarily 8-node isoparametric bricks (ANSYS STIF45 elements). In order to establish the degree of mesh refinement, a convergence study was done on the original model starting with an 8 elements per volume mesh. Gravity, reservoir and thermal loads were applied and the model analyzed. Stresses and deflections were plotted at various locations. This process was repeated using progressively finer meshes until the stresses and deflections converged to constant value. A mesh of 27 elements per volume was deemed to be sufficiently refined.

The AAR loading was incorporated into the model by adding a second thermal load to the entire volume of the dam. The AAR load applied was proportional to the average annual concrete temperature at each location. This assumption was used because laboratory data has shown clearly that AAR is accelerated by higher temperatures. In laboratory tests, the rate of growth noticeably increases at temperatures above 70 degrees. It was therefore assumed that if the average temperature was less than 65 degrees, the AAR growth would be minimal. Temperature data from TVA report (1950) was used to calculate a weighting factor for AAR loading throughout the model. The weighting factor was based on the monthly temperatures. Petrographic analyses of cores from the no growth and high growth regions have confirmed the validity of the assumptions. Growth extensometers were also installed to verify the assumptions and provide long-term growth monitoring.

The maximum growth appears at the downstream face where the concrete temperature is consistently high. The AAR was modeled as thermal strain. The model was calibrated by adjusting the value of the artificial temperature until the calculated plumbline deflections approximated the deflections measured in 1987 and the calculated transverse and vertical stresses approximated the measured stresses. The coefficient of thermal expansion was adjusted in the longitudinal direction until the calculated longitudinal stresses approximated the measured stresses. The longitudinal expansion coefficient was reduced since the high longitudinal stresses restricted AAR growth in the longitudinal direction. Confinement factors were also included in calculation of the growth rate in blocks 8 and 16 with less confinement applied at the free spillway face of each block.

ALTERNATIVES (Figure 1)

Using the information gained from the FEM and other options to solve the problems of concrete growth (See Page 1), three primary alternatives were developed.

Alternative A: Posttensioning of the dam, cutting of four slots and reestablishing the spillway gate's operational capability. End slots would be cut to just above the foundation while center slots would be cut to approximately 40 feet below the spillway crest.

Alternative B: Posttensioning of the dam, cutting of slots at each abutment, reestablishing the spillway bridge expansion joints and modifying the end spillway gates to allow for 25 years of additional deflection.

Alternative C: Same as Alternative "A" except that the central slots would be cut just below the level of the spillway crest.

Alternative B was selected as the best remedial measure to combat the concrete growth problem at Hiwassee. This alternative was changed after overcoring stress test in Block 16 showed high longitudinal stresses in the vicinity of the spillway bridge deck's structural girders. Due to these high stresses, the decision was made to cut the center slots at Blocks 7/8 and 16/17 to relieve stresses in the spillway bridge deck.

The new alternative was to posttension the dam in the fall of '92, cut the center slots at Blocks 7/8 and 16/17 (slots 3 and 4 respectfully) in the winter of '92. Monitor the movements at slots 3 and 4 for the next year and recut the slots, if needed, and cut abutment slots at Blocks 2/3 and 24/25 (slots 1 and 2 respectfully) in the winter of '93 - '94.

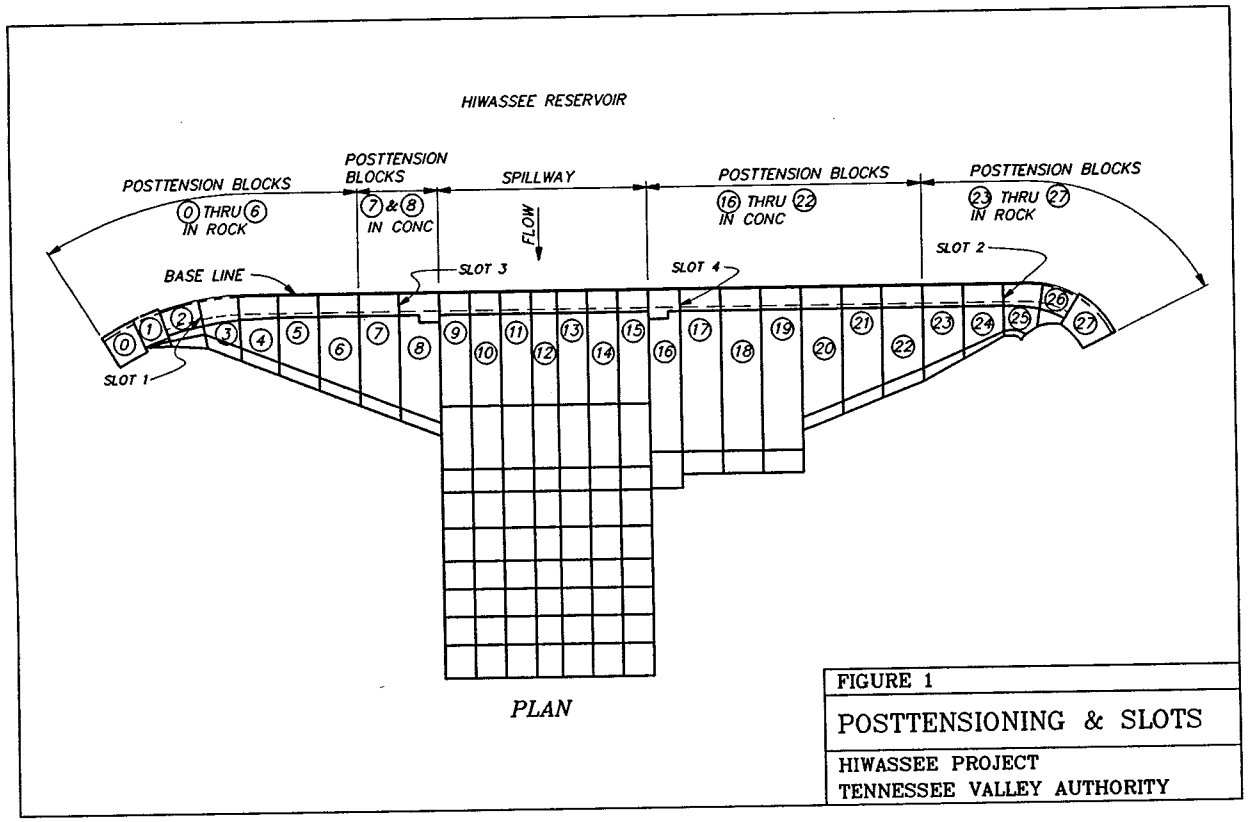

FIGURE 1

POSTTENSIONING & SLOTS

HIWASSEE PROJECT
TENNESSEE VALLEY AUTHORITY

POSTTENSIONING (Figure 2)

Posttensioning of Hiwassee Dam will serve three purposes. The first is to stabilize the upper portion of the dam during a seismic event. The dam was analyzed for the MCE assuming a fully cracked section at the base of the stem at elevation 1519.23. This analysis showed that the upper portion of the dam during this seismic event would be unstable. The second is to prevent shearing of the concrete block lift sections into the slots as stress is being relieved by the wire saw cutting operation. The third is to add compressive forces into the dam in an attempt to restrict concrete growth. Posttensioning of the dam started August 28, 1992 and was completed on December 23, 1992. The posttensioning consists of 140 tendons with thirty, 7-wire strands each with alternating anchor depths of 40 to 50 feet. The tendon anchors were set and grouted and then tensioned to the desired loading. The tendons were loaded between 25 to 35 percent of ultimate strength to allow for future stress from concrete growth. Seven days later, a lift-off test was performed to check the loading. After the testing, the tendon tails were cut off and second stage grout was placed to the top of the hole, then the anchor head recesses were filled with concrete. These tendons are located in two rows parallel to the axis of the dam.

INSTRUMENTATION AND MEASUREMENTS

The original instrumentation that was installed during construction of Hiwassee Dam and still functioning today includes gallery drainage weirs, plumblines and uplift cells.

An extensive instrumentation program has been initiated for the purpose of monitoring deflections, stresses and closure rate during the cutting of slots 3 and 4 (center slots) to verify the FEM analysis and assumptions for the model and gain valuable information that can be used in the cutting of slots 1 and 2 at the abutments in the winter of '94. This instrumentation consists of critical and non-critical instruments. The critical instrumentations will be read a minimum of every 6 hours during the first cut at slots 3 and 4. The critical instrumentation includes convergence meters, crackmeters, jointmeters, strain gages and stressmeters. The non-critical instrumentation will be read before and after each pass of the wire saw. The non-critical instrumentation includes growth extensometers, tape extensometer points on the roadway deck, inclinometers, closure points on the upstream and downstream faces of the dam and plumblines. A spillway pier survey will be made before and after the cutting of slots 3 and 4.

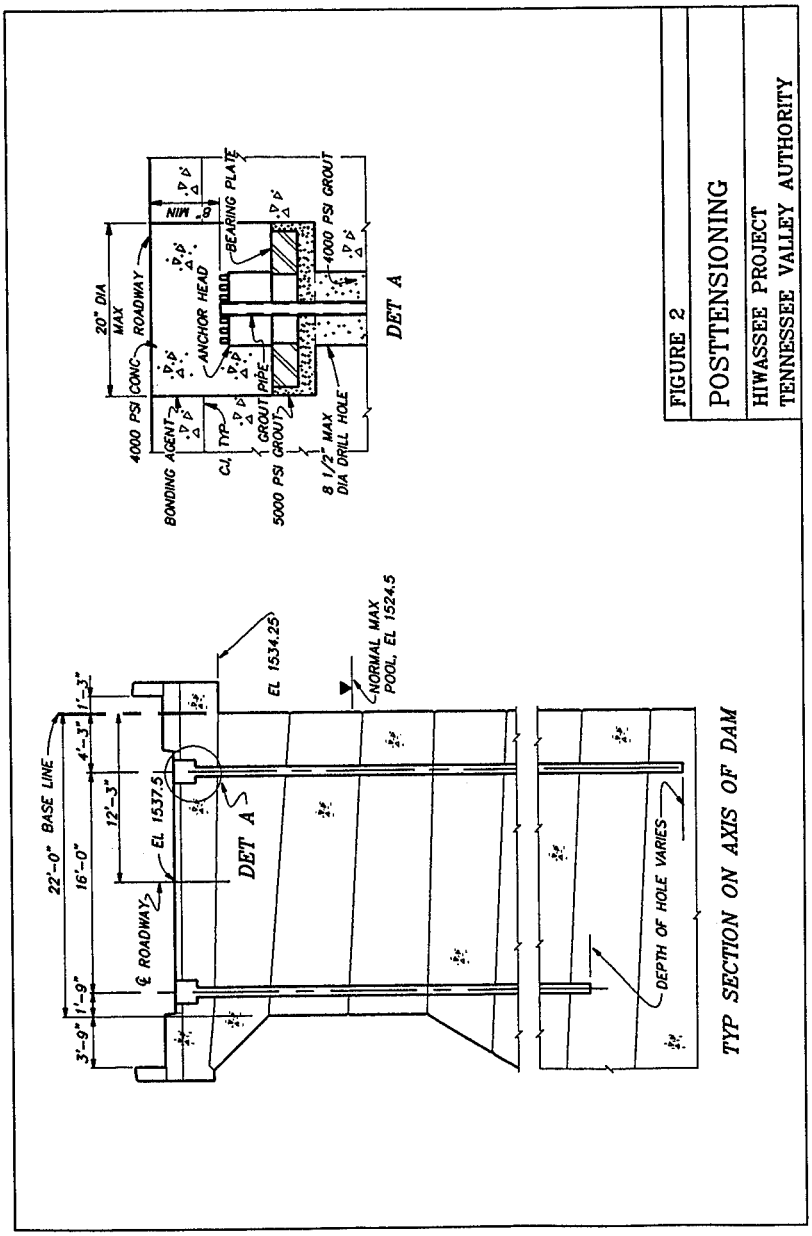

FIGURE 2

POSTTENSIONING

HIWASSEE PROJECT
TENNESSEE VALLEY AUTHORITY

SLOTS 3 AND 4 (Figure 3)

The finite element model was analyzed for the center slots at varying depths from 35 to 75 feet. It was decided to cut one-half inch slots 50 feet deep at blocks 7/8 (slot 3) and 16/17 (slot 4). Based on the finite element analysis, the calculations indicate that approximately 0.73 inch of elastic rebound at the top of the spillway edge elevation 1537.5 will be provided when the slot is cut to full depth. The slot cuts will be made in blocks 8 and 16 because the joint in these blocks should be relatively free of form steel. The cutting of the slots shall be accomplished by a series of passes. The initial two passes shall be 50 feet in depth with two subsequent passes 20 feet in depth. Additional cutting may be required to achieve the desired opening. To minimize undesirable stress concentrations and binding of the wire saw, the cutting operation at blocks 7/8 and 16/17 will run simultaneously and must stay within 2.5 feet of each other during cutting.

The wire saw cutting operation will stay above the operating level of the reservoir to minimize the risk of contaminants dropping into the reservoir. Containment of the slurry will be provided by a recirculation system on the upstream and downstream faces of the dam. This system collects the concrete slurry and pumps it to holding tanks on top of the dam. These holding tanks have baffles in them to help settle out the concrete materials from the water. The water then drops into a clean water tank ready to be used again.

When the slots are cut, the water seals of the dam will also be cut. To reseal the dam, a rubber sleeve seal will be utilized. This rubber sleeve seal will be placed 5 feet below the wire saw cut in the existing 6-inch diameter formed well and filled with water to seal the slot opening. Before the seal is placed, a mechanical packer will be put into the 6-inch diameter formed seal well 15 feet below the bottom of the wire saw cut, then grout will be placed 10 feet above the mechanical packer for the seal to rest on.

SLOTS 1 AND 2 (Figure 4)

Cutting of two abutment slots will relieve stresses in the dam caused by AAR and the geometry of the curved abutment sections. These slots will be located at Blocks 2/3 and 24/25 with cut depths of approximately 45 feet and 60 feet respectfully.

The wire saw cutting operations will make two passes in each block. The first pass will follow the block joint down to the desired depth with the second pass starting 8 inches over from the joint at the top (EL 1537.5) and taper down to 3 inches at the bottom. The

FIGURE 3

SLOT 3 AND 4

HIWASSEE PROJECT
TENNESSEE VALLEY AUTHORITY

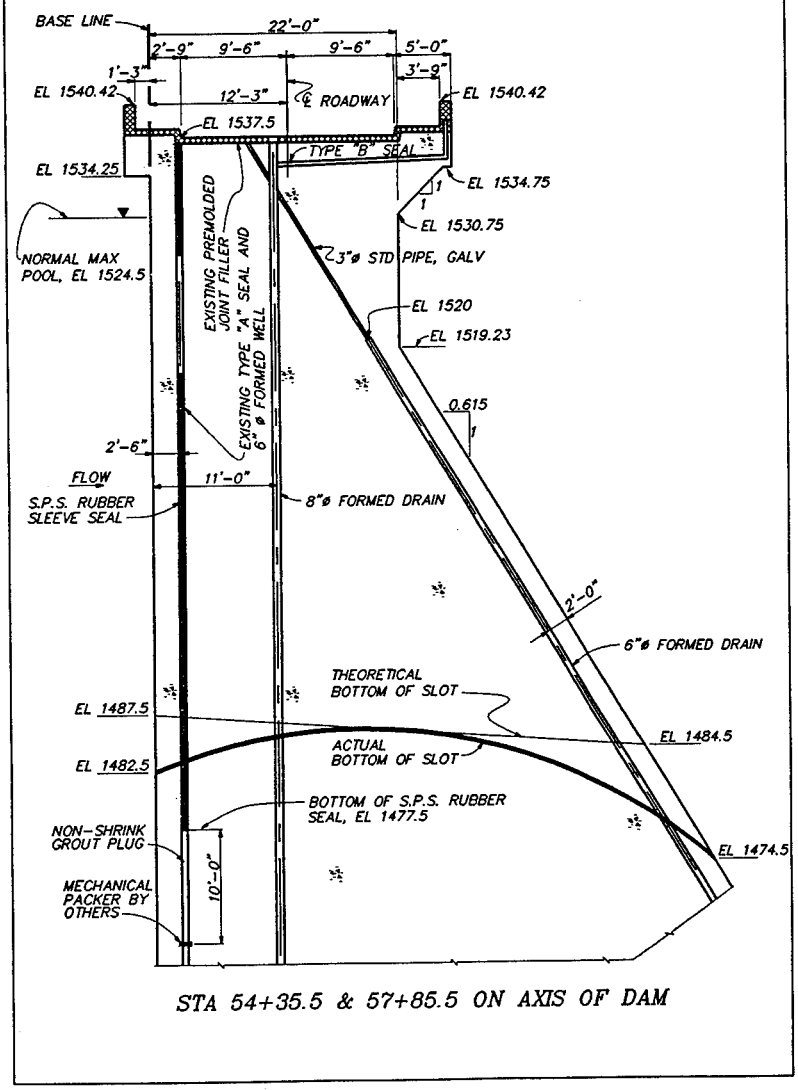

FIGURE 4

SLOT 1 AND 2

HIWASSEE PROJECT
TENNESSEE VALLEY AUTHORITY

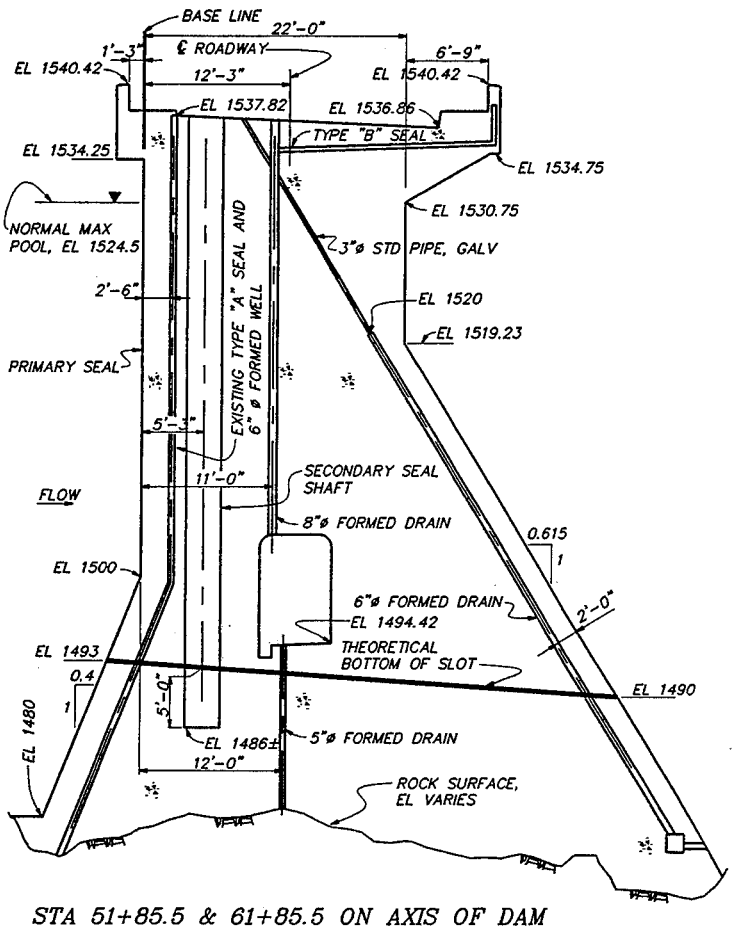

cuts will be made in Blocks 3 and 24 because less miscellaneous steel will be encountered in these blocks. The stem section of concrete will be removed by breaking sections out at the lift joints and lifting them out of the slots using a crane. Below the stem in the mass of the dam, the concrete will be broken up with drill hammers and water jetted out to the downstream face of the dam for collection and proper disposal.

Before the slots can be cut, a blister cofferdam will be installed on the upstream face of the dam. This cofferdam will have a interior radius of 4 feet, will tie into the foundation rock and have a top elevation of 1525 feet. This cofferdam will allow for normal reservoir operations during the slot cutting and also provides additional protection for the upstream seals.

Sealing of the dam after the slots have been cut will be provided by a primary seal on the upstream face of the dam. A secondary seal will be provided in a 3 feet by 3 feet shaft located 5 feet and 3 inches into the dam from the upstream face.

SPILLWAY GATES

The gates will have temporary adjustments made to them after the cutting of slots 3 and 4 to ensure adequate seal closure and operation of the seven spillway gates. During an interim period between the cutting of slots 3 and 4 and the Fall of '93 an engineering study shall be carried out to develop a long-term solution for the gates. The modification assessment of the spillway gates will include skinplate edges, rubber seals, guide rollers and embedded gate guide/seal plate channels.

FUTURE REMEDIAL MEASUREMENTS

Future modifications that will be required to correct the AAR growth problems over the next 25 years will include: Closure at slots 3 and 4 will be monitored for the next year. If closure is in the order of or approximately 1/4 inch by June '93, the 1/2 inch slots will be recut in winter of '93/'94 and the larger 8-inch slots will be cut in the winter of '94/'95. Instrumentation will be installed in the summer of '93 to monitor the cutting of the 8-inch slots at blocks 2/3 and 24/25 in the winter of '94. Modification of the spillway gate seals, piers and bridge bearing anchor bolts will be performed during low pool in '94. Monitoring of all instrumentation will be maintained year around. This schedule takes advantage of the best time of the year for each activity. It also spreads the financial burden over three fiscal years.

GUIDELINES FOR EVALUATING AGING PENSTOCKS

Charles S. Ahlgren [1] M. ASCE

Abstract

A Task Committee consisting of members of the Hydropower Committee of ASCE's Energy Division is currently producing a document for publication entitled, "Guidelines for Evaluating Aging Penstocks". This paper will summarize the contents of this document scheduled to be complete and ready for publication in January 1994.

Introduction

Penstock safety is an increasing concern among the owners of hydroelectric projects and regulatory agencies. Because many fabrication techniques and construction methods have been employed in constructing penstocks and the fact that documentation on these is rather scarce, the ASCE Energy Divsion, Hydropower Committee has commissioned a task committee with the charge of producing a publication to guide engineers in evaluating penstocks of older construction. The final draft of the document is almost complete. Entitled, "Guidelines for Evaluating Aging Penstocks," it is scheduled to be published by ASCE sometime in 1994.

Many hydroelectric facilities in the United States are over 40 years old and in need of repair and rehabilitation to bring them up to present day standards for safety and efficiency. These needs are often driven by economic or regulatory issues. During the project relicensing process, for example, the owner must demonstrate that the plant will be operated safely and efficiently throughout the next licensing period. The project engineering and economic studies that provide the backup information

[1] Civil Engineer, Pacific Gas and Electric Co., One California Street, Room 1730D, San Francisco, CA 94106.

for these determinations often include recommendations for plant improvements and modifications to improve efficiency and reliability of the facility. A costly penstock replacement could have a significant impact on the project economics and the project life itself. The engineer should therefore apply the combination of yesterday's knowledge and standard practices together with today's sophisticated analyses techniques and codes before making recommendations which have such far-reaching impacts.

Evaluation of older hydroelectric facilities is often hindered by the lack of documentation on the facility available for the engineer to review. Compounding this problem is a similar lack of available data on industry standards of the day. These two key components must then be carefully reconstructed and with the application of today's state-of-the-art technology, before the adequacy of the existing penstock can be determined with accuracy. It is the intent of this document to provide the bridge between the older technology used to originally design these aging penstocks and the new technology that is in use today and provide guidelines for making determinations of acceptability.

Also, the fabrication and construction of penstocks has progressed through a tremendous technology advancement during the twentieth century. During this time many materials and fabrication processes have been used; some successfully and some not so successfully. The guide will cover three basic types of penstock: *steel, concrete, and wood stave.* Penstocks of more modern construction such as fiberglass have not been included. Past design codes, criteria , and construction practices are discussed. Present day inspection techniques, design and analyses methods, and their acceptability based on both past and present day codes and standards is discussed.

In view of the fact that most civil rehabilitation of hydroelectric facilities is driven by age, the Committee has determined that this guide should be focused on penstock fabrication and construction before 1950. Therefore, for the purposes of this document, the Committee, has defined the term *"Aging Penstocks"* denote penstocks constructed prior to 1950. However, the techniques and practices discussed here are applicable all types of penstocks of newer and older construction.

General Guidelines

The publication discusses general guidelines that will help the engineer in gathering background data, preparing for a site visit or inspection, and evaluating conditions. This background data check will give the engineer the necessary information to evaluate the past performance based on the its operation history. It can also give the engineer a knowledge of the intent of the original designers. This type of information is particularly helpful in evaluating projects for expansion, upgrade, or life extension. In knowing the limits imposed on the original system, the engineer

may form a good basis with which to build on if he expects to recommend modifications or replacements to upgrade or extend the life of an aged facility.

Engineering documentation typically found in the owners records is discussed. This typically would include design criteria, engineering drawings, specifications and supplier documentation. The types of operations documentation that may be available to the engineer are also described. These include leakage and settlement data, slope stability instrumentation data, equipment changes, documentation of past failures and their causes, and penstock hydraulic pressure transients.

Personal safety issues typically encountered during an inspection of this type are briefly discussed to give the reader a feel for what may be involved depending upon the level of detail required for the inspection. This issue is very important, but can also lead into an expensive endeavor. Therefore, the cost of inspections that require significant safety measures must be weighed against their benefits; but at no time shall it be acceptable to forgo any safety requirements for an inspection.

Although the final evaluation of any condition is left to the judgment of the individual engineers performing the inspection, the document discusses the typical features that should be inspected and gives some incite into their important aspects.

Steel Penstocks

Most aging penstocks are steel. However, several different types of steel penstocks exist as a variety of fabrication methods have been used in the construction. The most common methods are riveted, forge-welded, arc welded, and combinations of these. Steel pipe was typically formed in 20-foot to 40-foot sections. Because dependable portable arc welding technology was not readily available until the 1960's, the individual cans were typically interconnected in the field by a riveted circumferential joint; either a butt strap type or bell and spigot type.

Although some have been found to be supported on cast steel rollers, most above ground penstocks are supported on reinforced concrete saddles spanning 120 degrees of the shell's circumference. Each saddle was typically free to allow sliding of the pipe along the saddle top. An expansion joint was installed between each anchor block to allow for thermal expansion and contraction of the steel shell. More modern constructions may employ the use of steel ring girders welded to cans that are interconnected by sleeve type mechanical couplings.

Partial or fully buried was also a common steel penstock configuration. A fully buried installation did not usually include any type of saddle and did not typically include expansion joints between the anchor blocks as thermally induced loads were not of concern due to the insulating effects of the ground. However, this type of penstock is particularly susceptible to corrosion as both sides of the shell are exposed to corrosive environments.

The inspection of riveted steel penstocks should focus on wall thinning. The existing condition of the riveted joints in the penstock may be approximated by visually inspecting the area for rust and or excessive leakage. There is no reliable method of performing non-destructive examinations (NDE) on a riveted joint to the extent of determining its strength. If severe joint degradation is suspected, sections of pipe must be removed and tested to determine joint efficiency; otherwise published or calculated values of joint efficiency may be used; however, this does not account for any degredation due to aging effects such as corrosion.

In addition to wall thinning, a welded penstock must also be inspected for flaws in the parent and weld metals. Steels manufactured prior to World War II are particularly brittle at colder temperatures (less than 40 F). This often leads to sudden ruptures initiated at locations of weld flaws or cracks during or after transient events such as load rejections.

Special areas of concern in the analysis of an exposed steel penstock include supports or saddles, anchor blocks, expansion joints, bolted type sleeve connections, stiffener rings, and bifurcations. The evaluator must take into account the effect of these specials upon the system. This sometimes involves complex calculations to estimate the state of stress at or near some of these specials.

Buried steel penstock evaluations must consider, in addition to the above, the added effects of thrust rings and seepage rings.

The physical assessment, or field inspection, of a steel penstock includes a visual inspection, some non-destructive examination (NDE), and collection of material samples for testing. The visual assessment of steel penstocks involve mainly a corrosion assessment; focusing on an assessment of pitting and corrosion by-product, but should also include a complete walk down of the penstock alignment and careful inspection of all appurtenances such as saddles, manholes, expansion joints, and anchor blocks taking care to notice leakage, signs of movement or distress such as cracking of concrete, slumping of the ground, or dimpling of the penstock shell. The NDE examination involves ultrasonic measurements of wall thickness and flaws in the parent and weld metals. Collection of coupons may be required to assess the materials for yield and ultimate tensile strengths, joint efficiencies, chemical composition, and fracture toughness or ductility.

Using data obtained from field investigations, the engineer should proceed with a stress analysis and fracture mechanics analysis, if the penstock is of welded construction. The interpretation of all the historical, operational, field investigation, and engineering analysis data should be assembled into a final report with recommendations based on the existing physical condition of the pipe as it relates to the existing and postulated future loading conditions the penstock is likely to be subjected to in the future.

Concrete Penstocks

Concrete penstocks are not as common as steel. Generally low head applications are found. Only reinforced concrete pipe is covered as pre-stressed concrete pipe is of a more modern vintage.

The basic types of reinforced concrete pipe construction can be classified as exposed, cut and cover or buried, and tunnel liners. The exposed pipes are either pre-cast or cast in place sections supported on cradles or bedded on prepared earth or sand and gravel up to the spring line. Cut and cover pipes are those which are buried in a trench on a prepared bed or foundation usually of sand. Tunnel liners can be considered a special case of buried, cast in place concrete pipes.

Over the years, reinforced concrete pipe has been designed using a number of codes, standards, design guides, and many articles, theories, and design methods. Most of the methods used, focus on calculating the load induced on the pipe by the surrounding soil or rock and any surcharge loading, such as motor vehicle traffic. The effects of this external loading upon the pipe shell often requires a complex engineering analysis. The structural design of the wall and its reinforcement are generally based on the working stress design method (WSD); with the allowable concrete compressive stress at 45% of ultimate and the allowable steel stress at 50% of yield.

The field inspections associated with concrete pipes and tunnel liners focus on visual assessments of the geometry, alignment, concrete and reinforcement, joints and appurtenances. Particular attention is paid to cracked or misaligned joints, cracking in the wall of the pipe, and any leakage that may be found.

The condition of the concrete is of prime importance. Colder climates often take their toll on these structures subjecting them to freeze-thaw deterioration. Chemical reactions to sulfates or alkali aggregate reactions are common as the technology to avoid them may not have been available at the time of construction. Coring of the concrete for compressive strength testing and petrographic analysis may be necessary for documentation of the structural analysis. A sample of the concrete reinforcing steel may also have to be removed for strength testing.

As with other types of penstocks, the data from the field inspections and the historical data, are assessed, combined and applied to the structural analysis. Recommendations are then formulated based on the results of engineering analysis and judgment as to the past performance of the structure and the postulated future performance with expected loading scenarios.

Wood Stave Penstocks

Perhaps the least understood of all penstocks is the wood stave. It may be considered a specialized technology and for that reason, the engineer would do well to retain a qualified consultant to inspect and assess the penstock.

Wood stave pipe is fabricated from a number of longitudinal wood staves that are assembled side by side and wrapped with steel bands, similar to a wooden barrel, to form a circular cross section or pipe. These pipes are of low head and found generally where the site access for construction is particularly difficult; such as environmentally sensitive areas or along the top of a ridge surrounded on two sides by steep slopes. The savings in extensive mitigation or labor costs related to site access improvement for construction purposes is the main advantage of wood stave pipe. Materials can be brought to the site in a piece by piece fashion and assembled largely by hand; virtually eliminating the need for cranes or other heavy rigging.

Wood stave pipe is supported on saddles or cradles of reinforced concrete or wood. Leakage is common as the bands tend to loosen somewhat over the years. The pipes are generally designed to flow with low pressure heads. The strength coming from the threaded steel rods or bands which hold together the staves.

The main cause of degradation of wood stave is rot usually; caused by alternating wetting and drying of the material. Because wood is prone to rotting problems, buried sections of wood stave penstock are not common. As the pipe is typically exposed in remoted locations, falling rocks or trees are a common source of damage because the the wood staves are not strong enough to resist impacts.

Inspections of wood stave pipes or penstocks focus on the visual aspects of the wood staves and their end joints. The wood often degrades in and around the areas where the ends of the staves are spliced by butt joints with metal connectors. A collection of small samples of wood are taken to check the condition of the material throughout the cross section of the stave. Special attention should be given to the condition of the supports and the wood staves immediately adjacent to them to detect any structural distress caused by discontinuities. And all damage to the pipe, past and present, caused by foreign objects should be noted and assessed.

Following the inspection and laboratory testing of samples, an assessment is formed as to the structural integrity of the pipe. This is primarily based on the condition of the wood staves and steel bands. If limited repairs cannot bring the pipe into line with industry accepted standards, then replacement may have to be evaluated. However, a replacement evaluation must take into account the use of other materials such as steel in the replacement scenario. Modern construction techniques may negate the necessity of wood as a material in favor of a scheme incorporating a more durable and less maintenance intensive material which would exhibit a longer life span.

The Art of Assessment

The engineering assessment of an aging penstock is a multi-disciplinary effort involving the fields of structural engineering, corrosion, metallurgy, materials technology, and geotechnical engineering. All these different disciplines must be combined in order to make a complete assessment of any penstock system. Perhaps the most important aspect, however, of the whole study is the field investigation. Data obtained from site inspections is applied to the analysis and assessment of structural adequacy for any penstock.

Actual measured dimensions for diameter and wall thickness should be used where ever possible. Existing wall thickness should be measured at enough locations along the penstock so that a statistical distribution may be developed so that a general wall thinning value based usually on a percentage of nominal wall thickness can be applied throughout the length of the penstock. A high level of confidence should be applied to this function; perhaps 97.5% or 2 standard deviations from the mean.

A similar approach can be used when developing the strengths of materials used in fabricating steel and concrete penstocks. Samples of material can be obtained and tested. Most codes and standards give allowable stresses based on material strengths as specified in standards such as those developed by ASTM. These standards dictate certain minimum material strengths be assured by the manufacturer. This assurance is based on a percentage of tested samples being at or greater than the minimum acceptable strength for the material. Similar to the approach used by manufacturers, a statistical analysis of testing results from samples of the penstock material may be used to determine minimum ultimate tensile and yield strengths for use in analysis. This unique approach actually resurrects a material specification from an actual sample of the material and ensures that the basis of the codes and standards, the nature of the material, is kept intact for the future engineering analyses and assessments. It may also be extended to determining joint efficiencies.

The final assessment of safety or structural adequacy for the penstock is usually based on a comparison of a calculated factor of safety (FS) to an acceptable FS for various loading conditions. The FS against failure is typically developed for stress, brittle fracture, and stability of anchor blocks in the normal, emergency, and extreme loading conditions. The loads for the normal condition should be developed from actual historical data, if available, on penstock pressures rises during load rejections. This historical data is usually available for one or two locations along the penstock alignment. However, using this limited data to calibrate an hydraulic transient computer model will yield reliable maximum pressures at other locations along the penstock. This model can also be used to simulate other loading conditions that may occur due to malfunction or failure of the powerhouse equipment. Current industry accepted design guidelines for penstocks call for increased allowable stresses and reduced FS for these more unlikely loading events.

Conclusion

In conclusion, the assessment of aging penstocks should be the product of a thorough historical search to determine the operating history of the plant, a site or plant inspection of the interior and exterior of the penstock to the detail deemed necessary by the project engineer, and an engineering analyses to combine the two. The assessment should utilize all available information on the existing structure. Factors of safety should be developed utilizing these methods. Recommendations should be developed based on current industry accepted codes and standards with the knowledge of what would constitute an acceptable risk for safety and reliability. The intent of these codes and standards would be preserved if the inspection data were extrapolated in keeping with modern day manufacturing processes. The engineer should always be aware of the basis upon which the codes and standards used in the assessment were developed. In doing do he can assure that his assessment is realistic and has not been slanted in such a way as to be either too liberal or too conservative.

HYDRO PUBLIC SAFETY AWARENESS: ONE UTILITY'S APPROACH

Lisa Hildebrand [1]

Abstract

Washington Water Power (WWP), an electric and natural gas utility with nine hydroelectric facilities in eastern Washington, northern Idaho, and western Montana, recognizes its social responsibility to educate the public regarding potential hazards on and around its sites. In addition to its upstream & downstream warning systems, including boater safety devices, warning signs, and fences, WWP is in the midst of a continuing effort to increase hydro public safety awareness.

Introduction

WWP's goal is to ensure public safety through its long-term commitment to a program of safety information, education, and training. By involving and educating the public, the company strives to meet or exceed all regulatory safety requirements, and to reduce accidents with a cost-effective public safety program. In an era in which million-dollar lawsuits are commonplace, we believe that money invested in a properly designed public safety effort is well spent.

EAP's and CABEX "90"

Part of this effort includes the interaction, involvement, and cooperation of local agencies and residents in the improvement and execution of the utility's EAP's (Emergency Action Plans) for each of its hydroelectric facilities. An excellent example of this involvement was CABEX "90," a September 1990 tabletop and functional exercise testing the EAP for WWP's Cabinet Gorge Dam (Figure 1) in northern Idaho.

---

1 Emergency Action Plan (EAP) and Public Safety Coordinator, The Washington Water Power Company, E. 1411 Mission, Spokane, WA 99207.

All hydroelectric Emergency Action Plans are tested at least once each year in an annual drill, which consists of notification phone calls to agency planholders, describing a simulated dam failure emergency. However, Washington Water Power was one of the first utilities selected by FERC to implement a tabletop and actual functional EAP exercise. (A functional exercise is the highest level test that does not require the total activation of licensee and cooperating agency emergency management field personnel and facilities.) This situation required WWP to actually create and develop its own exercise format for its Cabinet Gorge Dam, which later served as a model for other companies' EAP exercises. (Licensees must now hold a minimum of at least one functional test on one of their projects every five years.)

A hydro safety team was organized, holding orientation meetings with both company personnel and local agencies (e.g., police, fire, disaster & emergency services). The team familiarized these people with WWP's dam safety program, the purpose and content of the EAP and CABEX exercises, participants' respective roles during the exercises, and the establishment of notification priorities.

Figure 1 - Cabinet Gorge Dam

The tabletop and functional exercises were held on the same day. Their purpose was to assure the proper execution of the EAP during a dam failure, and ensure the safety and welfare of persons and property downstream through agency cooperation.

During the tabletop exercise, the sixty participants clarified their notification responsibilities, identified priorities for evacuation, and inventoried their existing resources.

The functional exercise divided the participants into the following groups at five different tables: state and federal agencies, local residents and resort owners, local emergency services, WWP interoffice personnel, and WWP plant operators. Temporary wall partitions were erected to isolate each group; telephones and radios provided communication between tables. The exercise achieved a high level of realism by timing the responses of the various groups to simulated stress-imposed events during a two-hour disaster scenario.

Participants were given an opportunity to critique the exercise using both oral and written feedback. Through involvement in the exercise, the agencies learned to recognize the benefits of communication and cooperation with each other, and to identify areas of improvement in both WWP's Cabinet Gorge EAP as well as in their own internal emergency plans.

Television and Radio Commercials

To further increase hydro public safety awareness, three different hydro safety commercials were developed during 1992 for radio and television presentation. The 30-second commercials, Fishing Above a Dam, Fishing Below a Dam, and Playing Below a Dam, feature many of WWP's new hydro warning signs (more than 250 new signs have been installed since June 1992), which now include safety pictographs. Designed primarily for children and non-English speaking recreators, the pictographs portray boaters, swimmers, hikers, and / or fishermen in the center of "slashed circle" / international "do not" symbols (Figure 2).

The commercials urge the public to obey the warning signs ("Stay Out • Stay Alive") and heed boater safety barriers and other restraining devices. They especially emphasize the dangers of swift currents around dams, and the sometimes sudden discharges of water from spillgates during normal operations.

Figure 2 - Hydro Safety Sign near Upper Falls HED

Hydro Safety Brochure, Print Ads, and Other Publications

An illustrated, six panel Hydro Safety Brochure, detailing potential hazards above and below hydroelectric dams, was mailed to more than 250,000 customers with their July 1992 bills. This free brochure has also been placed in numerous fish and game supply outlets, for distribution to other recreators. In addition to reminding the public to heed warning signs, restraining cables, and bouy lines, the brochure offers general water safety tips, such as always wearing an approved Personal Floatation Device, and avoiding alcohol consumption when boating or swimming.

WWP print ads concerning hydro safety have also been featured in various newspapers throughout the company's service territory, and in the 1992-93 Washington Department of Wildlife Game Fish Regulations pamphlet.

Washington Water Power is always willing to provide free safety articles for organizational newsletters and other publications. One example, appearing in a recent issue of Waterfront Review (a recreational newsletter published by a local realtor), is an article titled "Rollin' Down the River (Safely)." The article, dealing with boating, swimming, and fishing safety near hydroelectric facilities, reached approximately 10,000 Pacific Northwest lake and riverfront property owners.

School Program

Initiated during the autumn of 1992 was The WWP Energy Show , an interactive program for upper elementary students. Using employee volunteers, the one hour program ties into the school science curriculum, and contains eight energy and safety modules, including "Playing Above and Below a Hydro Dam." It features team activity boards and a large "hands on" power model.

For each module, a two-minute video is shown. Divided into teams of four or five individuals, the students work together to answer moderator questions pertaining to the video. For example, during the hydro segment, the children are asked to circle warning signs on their 34" x 17" team activity pads. They also identify a boater restraint, draw the two places near a dam where the current is most dangerous, and indicate which of several fishermen are in a safe place.

Using a spinner, one group of students is then chosen to present their answers to the rest of the class. Afterwards, that same group receives recognition by adding pieces to the highly colorful "Energy Model." To highlight the hydro module, the students add three miniature hydro warning signs and a boater restraining device.

At the conclusion of the presentation, the class is given take-home family activity books, rulers, and "Partners in Safety" buttons. By the end of the 1992-93 school year, The WWP Energy Show will have been featured in over 250 different area schools to approximately 6,500 students.

Partners in Safety

Washington Water Power's efforts in the hydro public safety area are only one part of its overall Partners in Safety program. The Partners in Safety program also deals with electric and natural gas safety, and uses a combination logo (Figure 3) featuring a lightning bolt (general electricity), waves (hydropower), and a natural gas flame. Communicating the idea that public safety is everyone's responsibility, the logo proclaims, "WWP and You -- Partners in Safety."

Is the Program Successful?

No safety program will completely eliminate accidents. Although Washington Water Power has consistently displayed a superior hydro safety record, an unfortunate incident occurred in late July 1992.

A teenager ignored large red-lettered pictographs and warning signs prominently displaying "KEEP OUT" and "DANGER," and jumped a fence at WWP's Post Falls Dam. He subsequently fell off a cliff along the river, and was seriously injured. (He did eventually recover.)

The following week, a local television station ran a special news segment discussing the accident. However, instead of reacting negatively, the station depicted WWP's past and continuing hydro safety efforts, including mention of the company's school safety program, and footage of warning signs, fences, and hydro safety brochures. A clip from one of the recent WWP hydro safety commercials (Playing Below a Dam) was also shown.

The segment concluded with shots of a "STAY OUT • STAY ALIVE" sign and the following newscast commentary: "The signs warn of the risks of jumping over the fence and onto the rocks. It's a message that, for some reason, is still sometimes ignored. It's a message that you can't miss -- unless you try."

Conclusion

Washington Water Power feels that its hydro safety program is an important part of its overall "hydro mission." The company believes that the program will continue to prove its worth by further reducing accidents through heightened public awareness and by generating positive public response toward WWP safety efforts, as illustrated by the Post Falls incident.

Figure 3 - "Partners in Safety" Logo

DAM SAFETY INSPECTION OF SPILLWAY AND SLUICE GATE OPERATING MACHINERY AT TVA DAMS

By Tommy McEntyre[1], Darle Parker [2], and David Hegseth[3]

Abstract

The vast majority of TVA's 53 dams have spillway gates and/or sluice gates. These gates have various types of hoisting and/or operating machinery. Reliable operation of this machinery is vital to flood control operations. For this reason, inspection of the machinery is an important part of the dam safety inspection program at TVA.

Introduction

As owner of 53 dams, TVA has a formal dam safety inspection program. Recognizing the importance of having reliable flood control equipment, inspection of the spillway and sluice gate operating machinery is a vital part of this program.

Formal inspections by mechanical and electrical engineers are conducted at 2 1/2 year intervals and monthly inspections are made by plant personnel.

Plant personnel use a site specific inspection checklist prepared by the engineering department. While most of the items on the checklist are inspected monthly, some items are designated for less frequent inspection (quarterly or semiannually). The visual inspections look for obvious damage and oil or water leaks. The completed checklists are sent for review to the Hydro Engineering office which is responsible for dam safety.

During the 2 1/2 year formal inspections, the mechanical and electrical features are inspected simultaneously. Site specific checklists are also used for these inspections

[1] Electrical Engineer, Hydro Engineering Services, TVA
[2] Mechanical Engineer, Hydro Engineering Services, TVA
[3] Civil Engineer, Hydro Engineering Services, TVA

and are useful tools for documenting the results of the inspections. The field inspections are preceded by a review of monthly inspection checklists, previous inspection reports, and historical data.

ELECTRICAL INSPECTION

Periodic testing of the electrical features varies as a function of plant equipment. This electrical equipment consists of:

a. Fixed in place hoisting equipment.
b. Traveling gantry crane/traveling car equipment.
c. Hydraulic pump systems.

Various electrical test instruments are necessary to conduct the electrical inspection. The test equipment used consists of:

a. Insulation Resistance Meter
   A battery powered, digital display, 500vDC insulation meter is used to measure insulation resistance of motors and cables.
b. Digital Volt/Ohmmeter with Temperature Probe
   This test instrument is used to take point voltage measurements and temperature measurements. The temperature measurements are used for insulation resistance temperature correction purposes.
c. Clamp-on Ammeter
   A battery powered, digital display clamp-on ammeter is used to take single point current measurements.
d. Portable Data Acquisition System
   The data acquisition system is used to record phase currents and phase to phase voltage for the hoist equipment under test. This data is stored in non-volatile memory to be downloaded by computer.

The plant inspection consists of visual inspection of motors and controllers before operation. Visual inspection consists of assessment of control enclosures, conductor raceway system, motor housing, control switches, limit switches, and pressure switches associated with the equipment under test. Deterioration is noted on inspection checklists. The visual inspection also notes the operation of enclosure and motor winding heaters. Conditions are noted which may result in maintenance recommendations regarding required maintenance, personnel safety, or possible equipment replacement.

Prior to operational testing of the equipment, the insulation resistance of the power feeder cables and hoist motors is measured. The power feeder cables tested are, for the most part, 480 vAC circuits and the following criteria is used to evaluate the condition of the cables:

a. Cable measurements are corrected to 15.6 degrees.
b. Motor measurements are corrected to 40 degrees Celsius.
The data is corrected in accordance with IPCEA and IEEE criteria.

The data collected is analyzed for abnormally low readings and is also compared to prior inspections to determine if downward trending is occurring. Use of the trending data has proven valuable because persistent downward trends in insulation resistance normally provides warning of impending trouble. Abnormally low readings or large changes in readings from a previous inspection may command immediate attention requiring cable replacement or motor refurbishment.

The most common failure mode observed is related to water or oil contamination of insulation. Pin holes or cracks that develop as insulation ages can provide a low resistance path for leakage currents. Collection and analysis of trend data for insulation resistance from inspection of cables and motors have proven valuable in detection and prevention of potential failures.

After completion of the visual inspection and electrical cable/motor insulation testing, operational testing is performed on the gate machinery. This testing is conducted concurrently with the mechanical testing. Electrical test data collected consists of phase current and phase-to-phase voltage measurements. The data is collected with a Rustrak Ranger II[1] data logger.

Depending upon the size of the electrical load to be measured, various sets of current transformers are used to measure phase currents. Use of different ranges of current transformers allows accurate scaling of the collected data while providing sufficient range to capture motor inrush currents. The data logger is configured to record data at a fast scan rate to enable capture of motor inrush currents. A single phase-to-phase voltage measurement is logged to reflect the effect of motor operation upon the power feeder.

Duration of the data collection varies according to the specific test performed. The data logger is configured with sufficient memory to allow capture of most gate

[1] Rustrak Instruments, East Greenwich, Rhode Island

open/close cycles conducted during an inspection. Collection of entire gate cycles can allow signature curves to be developed for comparisons to all subsequent inspections.

Provided in figure 1 is data collected at Chickamauga Dam during an inspection. The machinery consists of a gantry crane with a lifting beam used to raise a wheel gate. Power is supplied to the gantry crane via a collector rail arrangement. During a gantry travel operation it was discovered that areas existed in the collector rail where the collector shoes were not transferring power to the crane. A single phasing condition was occurring where two phase conductors were drawing excessively high currents and the phase-to-phase voltage sagged. Maintenance was performed on the collector rail and collector shoes to resolve this problem.

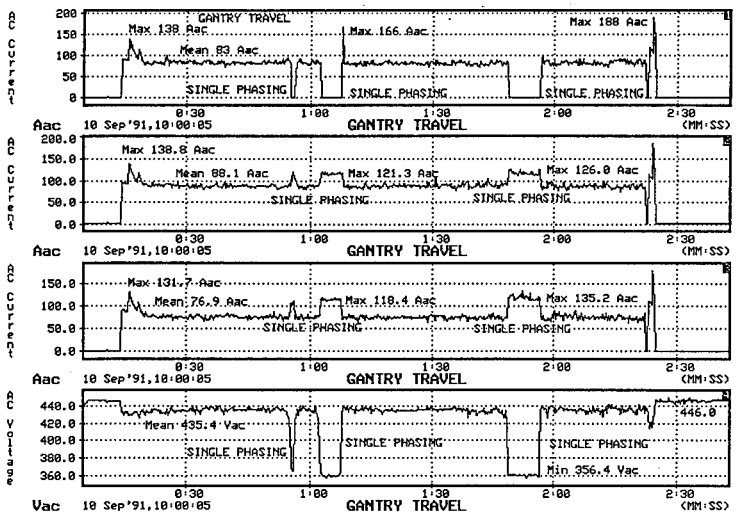

Figure 1 : Chickamauga Gantry Crane Travel

Figure 2 indicates a complete gate open cycle for Gates 1 and 2 at Fontana Dam. The machinery consists of a fixed hoist arrangement with a radial spillway gate. This graph indicates the signature motor inrush current and decay. It also shows a decrease in motor current as the gate approaches the fully opened position.

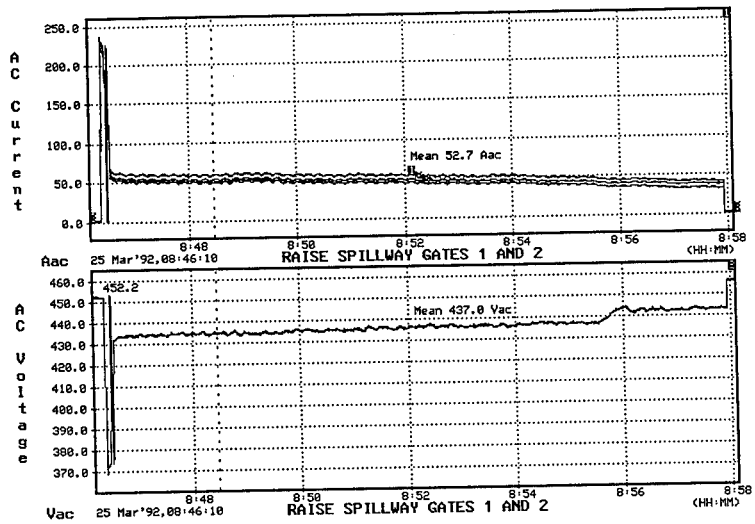

Figure 2 : Fontana Spillway Gates 1 and 2 - Raise Operation

MECHANICAL INSPECTION

A typical mechanical inspection includes an initial visual examination and a lubrication check of all the respective gate operating machinery components. The visual check is done to identify any obvious or apparent damages; to check for seal leaks; to note exterior paint conditions; and to ensure all components, machinery guards and bases are secure. A detail lubrication inspection is then done to verify proper gear box oil levels and adequate greasing of machinery couplings, bearings, and journals.

Fixed Gate Hoist

One type of gate operating machinery is the fixed hoist. The fixed hoist, characteristic of a radial spillway gate, is comprised of a central drive unit connected by floating shafts and flexible couplings to two hoisting arrangements. The drive unit consist of an electric motor, motor brake, and worm gear reducer mounted on an embedded frame[1]. The hoist arrangement consist of large parallel shaft reducers connected on the output side through large flexible couplings to integral

sprocket/drum-shafts that are supported by pillow block bearings[1]. A wire rope, anchor or roller type chain is used to lift a respective gate.

After the visual inspection has been completed, the drive and hoist gear reducers are checked for and drained of condensate and their oil levels verified. The inspection plates on these units are removed and the internal gearing examined for alignment, wear or damage. All shaft and motor couplings and bearings are checked for adequate lubrication. Covers are removed from the sprockets and the sprockets and chain examined. The motor brake covers are removed and the brakes checked for correct adjustment, alignment and wear of pads and wheels.

After the lubrication checks have been completed the equipment is test operated. Depending on whether a gate is under head or dewatered, the gate is raised to a partial or full open position and then closed. During operation, all rotating components are checked for excessive run-out, reducers and bearings are checked for unusual noises, and the motor brakes checked to confirm disengagement when energized.

Traveling Hoists

A second type of gate operating machinery is the traveling hoist. The traveling hoist is characteristic of a radial or vertical lift spillway gate. Two electrically driven hoist cars are provided to ensure having one in operating condition at all times[2]. Each traveling hoist consists of a structural steel frame deck and machinery that is mounted on four double flanged wheels[2]. The gate hoisting equipment has two drums, one mounted at each end of the structural frame deck[2]. Anchor type chains connect the gate to the hoist drums during a gate operation. The driving equipment for moving the car along two crane rails is mounted near one end of the structural frame and below the frame deck surface.

After the visual checks are completed, the hoist and travel drive worm reducers are checked for and drained of condensate and their oil levels verified. The travel drive train and wheels are checked for alignment and wear. Inspection plates are pulled on the hoist pinion and gear cases to check condition of and verify the gears are adequately lubricated. All hoist journals, motor bearings and couplings are checked for adequate lubrication. The hoist drive and travel drive motor brakes are checked for adjustment and condition of the shoes and wheels.

After all mechanical checks have been completed the traveling hoists cars are test operated. During the operation, the travel drive unit and wheels are observed for proper operation, and all rotating components for excessive run-out. The reducers; pinion and gear drives, motors and bearings are checked for unusual noises. The hoist and travel motor brakes are observed to verify proper disengagements when energized.

Gantry Crane

Another type of gate operating machinery is the gantry crane and lifting beam. The gantry crane, characteristic of vertical lift spillway gates, consist of a structural steel frame with four 2-wheel trucks and driving machinery[5]. The crane travels on crane rails on the intake and spillway deck. Two cranes are provided, one for use on the intake and one for use on the spillway[5]. The cranes may be transferred from one use to the other by swapping the lifting beams[5]. The cranes have trolleys with hoists, wheel trucks, and driving machinery which travel in an upstream and downstream direction on rails mounted on the gantry frame[5].

The connection between the gantry crane hoist and the spillway gate is the lifting beam. The lifting beam is connected to and operated through the main hoist drums by wire rope. The lifting beam is equipped with pairs of lifting links attached at each end of the beam for engaging the lifting hooks on the gate. Torque motors mounted on the crane trolley, operate these links through cables, gears, and shaft mechanisms.

After the visual checks have been completed, all of the gantry, hoist, and trolley worm and pinion gear reducers are checked for and drained of condensate, and their oil levels verified. All the brake shoes and wheels are checked for adjustment, wear and damage. All the inspection plates on the gantry wheel trucks, the hoist, and the trolley drive worm gear reducers and pinion gear cases are removed. The internal gearing is checked for alignment, tooth wear, corrosion and damage. The hoist drums, sheave blocks, and wire ropes are checked for condition and wear.

After the mechanical checks have been completed the gantry crane and lifting beam are test operated. Prior to lifting any gates, the crane trolley and gantry are traveled in both directions to check operation of the controls, and for unusual noises in the hoist and drive units. All the trolley, the hoist, and gantry drive brakes are observed for proper operation. The lifting beam is raised and lowered to check hoist controls and actuation of lifting links. During the gate handling, the crane hoist functions and hoist controls are monitored for improper operation.

Differential Control Valve

A final type of spillway gate operating machinery is the differential control valve. The differential control valve is used in combination with a motor operator for the operation of a drum type gate. The motor operator regulates the intake of water through a gate valve and into the drum gate chamber[6]. The control valve regulates the discharge from the chamber[6]. The buoyancy of the drum gate causes it to rise or lower in accordance with the water level inside the chamber. The mechanism consists of the differential control valve, a cable connecting a pilot valve integral to the control valve with a weighted anchorage that rests upon an adjustable support table; a counterweight; and two sheaves over which the cable passes between the

valve and anchorage[6]. One sheave is free to turn and is mounted on the gate end hinge pin[6]. The other sheave is mounted at the end of an operating arm that is rigidly connected to the gate hinge pin that moves with the gate[6].

The visual examination and lubrication check includes the gear operator and stem, cable, cable sheaves, operating arm, shaft assembly, shaft bearings and keys, gate position and limit indicator control, the pilot valve and the differential valve body.

After the mechanical checks have been completed the motor operator and the differential valve are test operated. During operation the intake gate (normally open) is cycled closed and back open to check for unusual noises or improper operation of the gear operator. The differential valve is checked by presetting the gate limit control and then verify that the control mechanism will maintain the spillway gate at the predetermined discharge elevation.

Motor Operator

One type of sluice gate operating machinery is the motor operator. The motor operator, characteristic of a slide type gate, consists of an electric motor, actuator (gear-train) unit, limit switches and/or torque switches, stem, stem nut, declutching lever, manual hand wheel and a operator floor stand. The operating stem supported by wall brackets and guide bearings, provides the connection between the gate and the motor operator.

After the mechanical checks have been completed the motor operators are test operated. Depending on whether the gate is under head or dewatered, the gate is raised to a partial open or full open position and then closed. During operation, the gear motor operator functions and operator stem movements are observed for any improper operation and unusual noises.

Hydraulic Operator

A second type of sluice gate operating machinery is the hydraulic operator. The hydraulic operator is characteristic of a slide type gate. The operating system consists of two hydraulic pumps with pump motors (one is back-up), a hydraulic storage tank, various piping and valves, and push button controls for raising and lowering of a gate[4]. The hoist is mounted directly above the gate on the bonnet of the gate frame[3]. The hydraulic piston shaft is connected to the gate by a steel operating stem[3]. A stem extension with a cone shape head is fitted to the upper end of the stem[3]. The extension projects through the top head of the hydraulic cylinder and engages a gate hanger when the gate is in full up position[3]. The gate hanger prevents the gate from drifting down to a closed position should there be any leakage around the piston seal rings[3]. The hanger is released by manually exerting a downward pull on a spring and chain attached to the hanger counterweight[3].

After the visual and lubrication checks have been completed the hydraulic system operator is tested. Several slide gates are raised and lowered, either under balanced or unbalanced head conditions. During a gate operation, the system pressures and relief valve settings are checked to assure proper operation at designated pressures. The pumps are checked for unusual noises or seal leaks. The hydraulic cylinders are checked for oil or water leaks from around the cylinder rod packing.

After completion of the inspection, formal reports are written. If repair or maintenance work is recommended, it is recorded on a "Maintenance/Repair Form" with recommended completion date and accompanies the report to the responsible individual. All recommended maintenance and repairs are kept in a database. After repairs are complete, the completion date is noted on the "Maintenance/Repair Form" by the responsible individual and returned to the engineering office for updating in the database.

REFERENCES:

[1] Tennessee Valley Authority, The Nickajack Project, Technical Report No. 16, U. S. Govt. Print. Office, Washington: 1972, p. 55.

[2] Tennessee Valley Authority, The Cherokee Project, Technical Report No. 7, U. S. Govt. Print. Office, Washington: 1946, p. 57.

[3] Ibid., p. 58.

[4] Ibid., p. 59.

[5] Tennessee Valley Authority, The Guntersville Project, Technical Report No. 4, U. S. Govt. Print. Office, Washington: 1941, p. 81.

[6] Tennessee Valley Authority, The Norris Project, Technical Report No. 1, U. S. Govt. Print. Office, Washington: 1940, p. 90.

Dam Safety of Hydroelectric Projects in Thailand

Yin Au-Yeung, F. ASCE[1]
and
Taweesak Mahasandana[2]

Abstract

The current safety inspection and evaluation of existing hydropower project dams in Thailand is presented in this paper. Remedial measures and rehabilitation works performed for a high hazard dam after the dam was identified as having serious safety deficiencies also discussed.

Introduction

There are thirteen large scale hydroelectric projects in Thailand. These projects are owned, operated and maintained by the Electricity Generating Authority of Thailand (EGAT), a semigovernment organization responsible for large electricity generating facilities. A summary of these projects is given in Table 1. Smaller or provincial level power generation facilities are handled by the Department of Energy Development and Promotion (DEDP). The dam heights of EGAT hydroelectric projects range from 32 meters to 154 meters. The highest and oldest is the Bhumibol Dam, a concrete arch gravity structure with a power plant installed capacity of 535 MW. The Bhumibol Dam was completed in 1964. The general consultant for this project was Sverdrup & Parcel International Inc., of St.Louis, Missouri and Engineering Consultants Inc..(ECI) of Denver, Colorado.

For design and construction of new hydropower projects involving large dams, EGAT follows the normal international practice to engage an international board of consultants (IBC) to oversee the safety and behavior of the dam and reservoir during design and construction of the project until after the first filling of the

[1]Vice President, Engineering Consultants, Inc. (**ECI**), 5660 Greenwood Plaza Blvd., Suite 500, Englewood, Colorado 80111

[2]Director, Hydropower Engineering Department, Electricity Generating Authority of Thailand (EGAT), Bangkok, Thailand

reservoir. However, there was no formal dam safety inspection and evaluation performed by EGAT on any of their dams until 1978, when overtopping of the center core occurred at the Ubol Ratana dam in Khon Khaen province due to an extraordinarily large flood flow entering the reservoir. EGAT assembled and dispatched an emergency inspection team to the site and conducted emergency repairs on the dam.

Since the incident at Ubol Ratana, EGAT has established a comprehensive dam safety regulation and program for safety inspection and evaluation of their dams. The current EGAT dam safety program is structured similar to the SEED program presently enforced by the U.S. Bureau of Reclamation.

This paper discusses the details of the development of the EGAT's dam safety inspection and evaluation program, the dam safety regulation,the institution and organization arrangement and the implementation of the dam safety evaluation for hydropower projects which now serve as models for other large dam owners in Thailand. Highlights on the rehabilitation of the Ubol Ratana dam are also presented.

Table 1 Summary Data of EGAT's Large Dams

Name of Dam	Dam Type	Dam Height (Meters)	Crest Length (Meters)	Power-plant Installed Capacity (MW)	Age (years)
* Srinagarind	RF/impervious core	140.0	610	540	12
* Bhumibol	Concrete arch gravity	154.0	486	535	29
* Sirikit	Earth Fill	113.6	800	375	18
Khao Laem	RF/concrete face	90.0	910	300	8
Rajjaprabha	RF/impervious core	95.0	730	240	6
* Ubol Ratana	RF/impervious core	32.0	800	25	28
* Sirindhorn	RF/impervious core	42.0	940	36	22
* Bang Lang	RF/impervious core	85.0	422	72	12
* Chulabhorn	RF/impervious core	70.0	700	40	21
* Nam Pung	RF/impervious core	40.0	1,720	6	28
Mae Chang	RF/impervious core	40.0	760	N/A	11
Tha Thung Na	RF/impervious core	30.0	840	38	11
Huai Kum	RF/impervious core	35.5	282	1.06	13

Remarks: Age as of 1993
RF = Rockfill
* = Dam inspected under the 1980 inspection program

Extreme Flood of 1978

Several large flood events have occurred in northeast Thailand. The most devastating one occurred in October,1978 when Typhoon Kit struck the Nam Pong

Basin and produced heavy rain fall over the watershed upstream of the Ubol Ratana dam resulting extreme floods in the Ubol Ratana reservoir.

This flood produced an inflow flood peak of 8,633 m^3/s in the reservoir and a routed outflow through the spillway of 3,800 m^3/s which was 40% above the design capacity. During the flood event, the reservoir had risen to El. 183.74 m (MSL), which was 0.24 m above the top of the clay core, causing significant flow through the filter. Overtopping of the clay core lasted for over 13 hours. Leakages were observed on the downstream face of the dam at elevations 181.5 and 173.0 and also in the powerhouse walls. Although the dam remained intact after the flood, the flood event caused substantial damage to the dam and properties in the Nam Pong River basin. Another large flood also occurred in the Nam Pong Basin in September of 1980. However this flood was far less severe than the 1978 flood.

Initial Dam Safety Inspection and Evaluation Program

Even though EGAT had carried out intensive inspections for the Ubol Ratana dam after the incident at Ubol Ratana in 1978 EGAT and conducted informal inspection for other dams, there were no official regulations,procedures and organization structure for safety inspection and evaluation of dams owned by EGAT.

EGAT understood the urgent need for formalizing and institutionalizing a safety inspection and evaluation program of their dams. In September,1980 Engineering Consultants Inc.,(ECI) of Denver, Colorado was contracted by EGAT to organize and perform a dam safety inspection and evaluation of eight large and older dams owned by EGAT. These dams are listed in Table 1. Review and evaluation of EGAT's dam safety practice and field inspection and evaluation of the eight large dams were carried out by ECI during two months from September 10 through November 10,1980. In December 1980, the consultant submitted recommendations on EGAT's dam safety practice and improvements needed with regard to organization and management,operation policy and technical aspects. Assessments on the general condition of the eight dams inspected also were presented. Safety deficiencies of each dam were identified along with remedial actions required to overcome these deficiencies.

Dam Safety Regulations

In 1982, EGAT organized the Civil Maintenance Department to take responsibilities for all EGAT dams and enacted the Dam Safety Regulation.on and safety evaluation of their dams. The regulation covers four major aspects of dam safety activities as discuss below:

1. **Data Collection.** The Hydro-power Engineering Department is responsible for the collection of all data and technical reports during the investigation, feasibility study and design period and submittal of this data to the Civil Maintenance Department.

The Hydro-power Construction Department is responsible for the collection of all data and technical reports occurring during the construction period and submittal of this data to the Civil Maintenance Department.

Data and technical reports for period after the completion of the project are the responsibility of the Dam Superintendent and he will submit all this data to the Civil Maintenance Department. The task of data analysis and evaluation lies with the Civil Maintenance Department.

2. **Field inspection and safety evaluation of existing dams.** Visual and safety evaluation of existing dams will be carried out by a Dam Inspection and Safety Evaluation Committee. The Committee consists of the following members:

- Chairman (the Director of Civil Maintenance Department)
- Superintendent of the Dam
- One representative from each of the Hydropower Construction, Hydropower Engineering, Mechanical Maintenance, Electrical Maintenance and Efficiency Control departments
- Chief of Power House and Transmission System Civil Maintenance Engineering Division
- Chief of General Civil Maintenance Division
- Chief of Dam Maintenance Engineering Division
- Chief of Civil Maintenance Engineering Division

The Civil Maintenance Department is responsible for collecting the name list of experienced personnel as appointed by the departments involved and submit the names to the General Manager for approval. Frequency of inspections are twice a year for dams less than two years old; once every year for dams between two and five years old; and once every two years for dams older than five years. The Committee is responsible for producing an inspection and evaluation report within 120 days from the date the committee was appointed.

3. **Dam maintenance and emergency measures.** The responsibility for maintenance of a dam rests on the Dam Superintendent or the region responsible for that dam. The regular maintenance activities are detailed in the dam operation and maintenance manuals. In case unusual events occur, such as rapid rise of reservoir water level which may cause severe hazard ,the dam superintendent or his designated representative shall immediately report to the Civil Maintenance Department and the Power System Control Department for necessary action.

Dam Inspection Program

The inspections of dams and their appurtenant structures are performed regularly by the Dam Inspection and Maintenance Division under the Civil Maintenance Department and Dam Inspection and Safety Evaluation Committee.

Although it is not specified in the dam safety regulations, the Dam Inspection and Maintenance Division conducts analysis of dam instrument data and carries out regular field inspection of all dams based on its own schedule. These inspections

are in addition to the formal inspection perform by the Dam Inspection and Safety Evaluation Committee. The Dam Inspection and Maintenance Division also carries out special inspection when the situation warrants.

Major activities organized for the inspection program of the Civil Maintenance Department to carry out regular inspections for existing dams are maintain inventory of data on all dams; perform hazard classification for dams; develop procedures for inspections; perform field inspections of dams; provide technical advice and support on inspection activities; and provide dam safety training.

Three types of dam inspection are implemented under the existing program. They are the informal ,the special and the formal inspections.

The informal inspection is regularly conducted by the Dam Inspection and Maintenance Section for each dam. The inspection involved the reading and taking data of dam instruments and visual observation of the dam. A monthly report is prepared and submitted to the Dam Inspection and Maintenance Division and Civil Maintenance Department for record and follow up actions,if required.

The special inspection is required only under the occurrence of unusual event at or near the dam site such as extreme full reservoir level with continuing heavy rainfall in the watershed or a strong earthquake struck the area.

The formal inspection is performed by the Dam Inspection and Evaluation Committee in accordance with the criteria and schedule set forth in the Dam Safety Inspection regulation.

Emergency Preparedness Plan

A detailed emergency preparedness plan is prepared for each dam under high hazard classification. The plan is closely coordinated and operated in concert with the evacuation plan which is prepared by the National Interior Department.

Rehabilitation and Modification of Ubol Ratana Dam

In February 1982 the Federal Republic of Germany through Kreditanstalt fur Wiederaufbau (kfw) granted one million Deutsche Mark for EGAT to study the flood control and reservoir operation of Ubol Ratana Dam. Subsequently EGAT engaged Salzgitter Consult GmbH,a Germany engineering consulting firm and TEAM Consulting Engineers Co,Ltd,a Thai engineering consulting firm to carry out the Ubol Ratana Dam-Flood Protection Study. A final report of the study was submitted to EGAT in March,1983.

The study concluded that due to the rapid change in land use in the watershed upstream from the dam, the original spillway inflow design flood which was based on 1,000-year frequency flood event is not adequate and the dam and its appurtenant works need to improve and upgrade to accommodate safely the

Probable Maximum Flood (PMF). The study further recommended increasing the dam height by 3.1 m and dam length by 110 m and spillway discharge capacity by 40% from 2,500 m3/s to 3,500 m3/s. No change was suggested for power generating facilities. A comparison of before and after modifications are shown below:

Dam:	Before Modification	After Modification
Type	Rockfill	Same
Reservoir Normal Flood level	El. 182.00	El. 186.60
Crest Level	El. 185.00	El. 188.10
Crest Length (with spillway)	775 m	885 m
Crest Width	6.0 m	Same
Height	32.0 m	35.1 m
Maximum Base Width	120.0 m	Same
Embankment Volume (m^3)	515,000	580,000
Upstream Slope	1:3, 1:1.5	Same
Downstream Slope	1:2	1:1.3, 1:1.5
Spillway		
Type	Radial Gate Open Chute	Radial Gate Orifice
Number of Gates	4	4
Dimension (Width x Height)	19.5 x 6.0	12.0 x 7.8
Design Flood Discharge	2,500 m^3/s	3,500 m^3/s
Sill Level	El. 176.00	El. 171.00

In addition to the above mentioned structural improvements to the dam, the study also recommended to provide two non-structural measures to ensure the safe operation of the spillway and the reservoir. These non-structural measures are: 1) to develop reservoir operation rule curves for normal condition and during floods; and 2) to establish and install a flood forecasting and warning system for the reservoir.

Dam modification

Based on the recommendations of the study,the existing dam crest was raised from El. 185.00 to 188.10 and extended the crest length from 775 m to 885 m with a constant crest width of 6.0 m. Construction of the modified dam was accomplished in 3 stages as shown in Figure 1. The first stage provided rockfill of downstream slope of the dam, the second stage was removal of the exiting dam crest between El. 180.00 to El. 185.00 and the third stage was completion of embankment from El. 180.00 to El. 188.10.

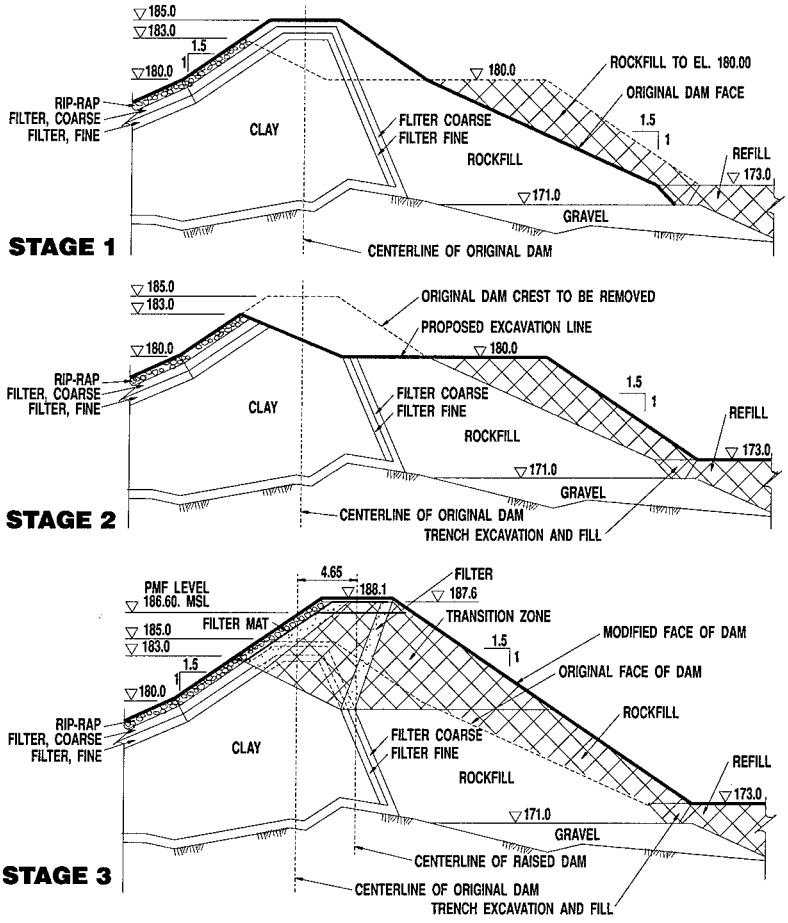

FIGURE 1
METHOD OF DAM MODIFICATION

Modification of spillway structure

The original gated concrete open chute spillway had to be partly removed and rebuilt as a gated orifice spillway with 4 radial gates of 12.0 m x 7.8 m capable of discharging 3,500 m^3/s. The gated orifice spillway equipped with one emergency gate, one gantry crane, and an automatic gate operation system. The cross sections of the original and the modified spillway structure are shown in Figure 2.

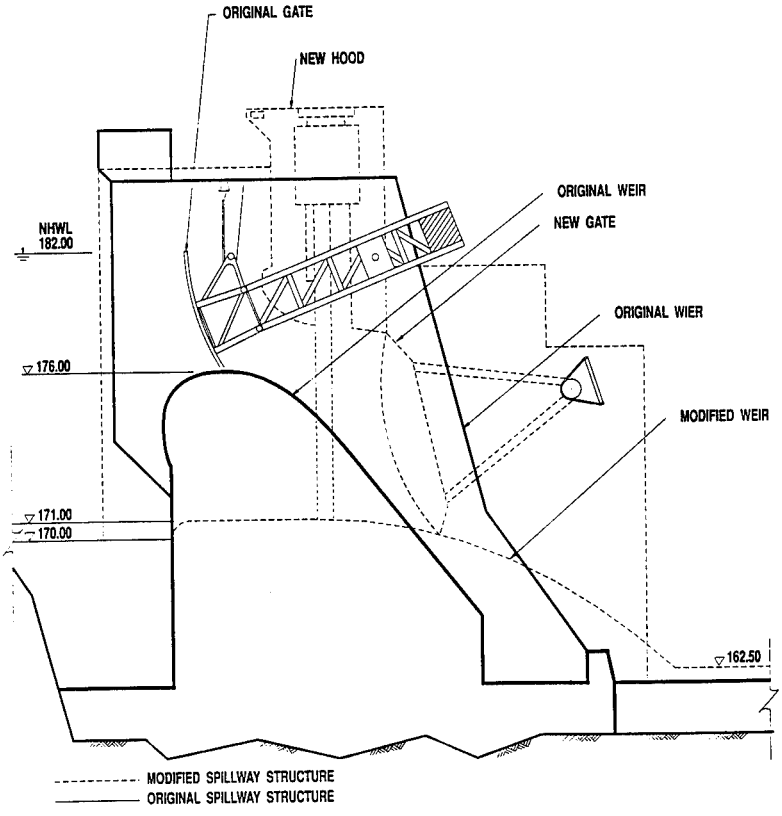

FIGURE 2
CROSS SECTION OF ORIGINAL AND MODIFIED SPILLWAY STRUCTURE

Construction and completion of the modification works

The civil work contract was awarded on November 26,1984 and all civil work were completed and officially accepted by EGAT on June 5,1987. All spillway gate automatic operation systems were installed and tested by March 3,1988.

Benefit from modification

The modifications made to the Ubol Ratana dam provide the dam with adequate safety against major floods including the PMF. The modified dam/spillway system also provide a higher level of flood control for areas downstream of the dam.In addition to drastically increase the physical integrity of the dam and flood control benefits, because the increase in the dam height and the improved reservoir operating policy and procedures, water requirements for double cropping of 40,700 ha of rice in downstream irrigation areas can now be fully met.

Soda Dam: Influence of Reservoir Silt Deposits on the Uplift Load

by Guy S. Lund, M.ASCE[1], Howard Boggs M.ASCE[2] & Dave Daley[3]

Abstract

A study was performed for Soda Dam, a concrete gravity dam with deep reservoir silt deposits, to determine the uplift load on the dam. The study consisted of a) review of the foundation drain pressure data and procedures used to collect this data, b) field investigations, and c) computer analyses to verify the uplift load during normal conditions, the change in uplift during the increased PMF reservoir water elevation, and foundation drain effectiveness. Dam safety criteria normally requires that the uplift pressure head at the upstream heel of the dam be equal to the full reservoir head and any reduction in water pressure due to silt deposits is neglected. Investigations showed, however, that the water pressure at the upstream heel of Soda Dam is less than full reservoir head due to the less permeable silt deposits in the reservoir.

The insitu foundation water pressure data, determined through the field investigations, were used calibrate a finite element seepage analysis through the silt and foundation rock. The model was used to determine the uplift pressure at the heel during the unusual PMF reservoir condition. The insitu foundation data and seepage analysis results were used to evaluate the foundation drain effectiveness at Soda Dam using the computer program **CRFLOOD™**, a numerical model developed for Electric Power Research Institute (EPRI) to estimate the uplift pressure distribution in a crack and the effectiveness of drains intersecting these cracks. The results showed that the drain effectiveness decreased for the PMF reservoir water elevation. The uplift load, however, was less than the allowable uplift load determined in previous structural stability analyses. Thus, because of the silt, the reduced effectiveness of the drains will not effect the stability of the dam during the PMF loading condition and the dam is expected to have adequate safety against sliding for all assumed loading conditions.

Introduction

Soda Dam is located on the Bear River adjacent to U.S. Highway 30 in southern Idaho about 5 miles west of Soda Springs, Idaho. Construction of the concrete gravity dam was

[1] Project Manager, ECI, 5660 Greenwood Plaza Blvd., Suite 500 Englewood, Colorado, 80111 (303) 773-3788

[2] Consulting Engineer,P.O.Box 338, Arvada, Colorado 80001

[3] Project Engineer, PacifiCorp, P.O.Box 26128, Salt Lake City, Utah 84126

completed in 1925. The dam was built in a narrow canyon with a steep left abutment, flat center section and moderately sloped right abutment.

Soda Dam is a concrete gravity structure 433 feet long with a maximum structural height of 103 feet. The concrete dam consists of a 210-foot-long non-overflow gravity section, a 109-foot-long integral powerhouse section, and a 114-foot-long gated overflow spillway section. The typical non-overflow gravity section has a crest thickness of 10 feet, a vertical upstream face, and a downstream face that is vertical extending 10 feet down from the dam crest then slopes at 0.53 horizontal to 1.0 vertical. The uplift pressure is reduced by 3.5 inch diameter drains spaced at 20 foot centers, which extend into the foundation from the north (non-overflow section), central (powerhouse section), and south (spillway overflow section) drainage galleries.

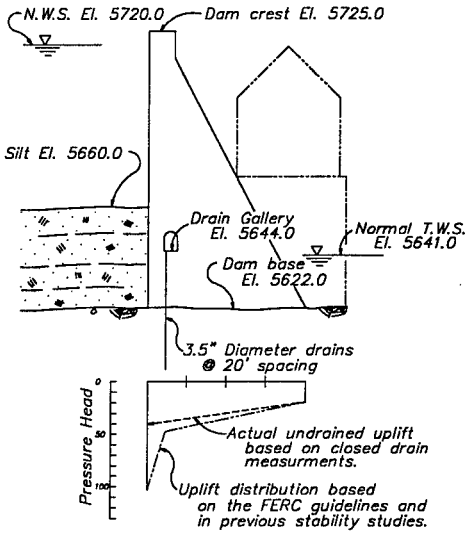

Figure 1 - Revised uplift distribution based on undrained pressure measurements.

A three-dimensional structural stability analysis, presented in the Soda Dam Structural Stability Report *(ECI, April 1992)*, used available data from the drains to compute the uplift load in accordance with the Federal Energy Regulatory Commission (FERC) guidelines *(FERC, 1991)*. The drain effectiveness was determined using the drain pressure readings at the dam during normal operating conditions. During the Probable Maximum Flood (PMF) the drain effectiveness was assumed to be equivalent to the normal load. The analysis indicated that a significant portion of the base may crack during the PMF loading condition and increase the uplift load. Therefore, further study was required to verify the magnitude of the PMF uplift load.

Review of Drain Data

The most recently available drain pressure records were reviewed and are summarized in Table 1. The standard procedure used to record the drain pressure at Soda Dam revealed that the drain pressure measurements were for an undrained uplift condition (drains are inoperable). The standard procedure was to close off the discharge for each drain and measured the pressure after the uplift equalized. The equalizing process may take as long as 15 minutes for some drains, therefore, the dam operators usually closed off the discharge for all of the drains in the gallery before recording any of the pressure readings. Closing off the discharge for all the drains results in an undrained condition in the foundation and a full uplift load acting on the dam. Research has shown that there is no time lag reduction for internal hydrostatic pressure (uplift) in the foundation *(Grenoble, 1991)*.

TABLE 1
Drain Pressure and Discharge Readings

Description	Non-Overflow Section	Powerhouse Section	Overflow Spillway Section
Average measured pressure, at drain gallery	4.5 lb./in^2	4.5 lb./in^2	1.0 lb./in^2
Extrapolated pressure, at dam/foundation interface	8.0 lb./in^2	14.1 lb./in^2	12.3 lb./in^2
Average discharge, per drains	0.07 ft^3/sec	0.124 ft^3/sec	0.03 ft^3/sec

This information can be used to compute an expected uplift pressure distribution along the dam/foundation contact. The expected uplift pressure at the heel is calculated by linearly extrapolating the known pressure at the drains and the downstream toe of the dam. The result is an uplift head of about 40 feet at the upstream heel of the powerhouse section, as shown in Figure 1.

The drained uplift pressure at the drains will be less than the undrained value. The observed discharge from the drains at Soda Dam suggests that the head at the drains is approximately equal to the difference in elevation between the drainage gallery and the interface.

Field Investigations.

A field investigation program was performed under the supervision of PacifiCorp Electric Operation and consisted of recording the silt elevation in the reservoir, installation of piezometers to record uplift pressure at the dam/foundation contact, and installation of piezometers to record drain pressure in the galleries of the dam *(Sergent, 1992)*.

Silt Investigation. The investigation determined that the silt in the reservoir varies from 40 feet in depth at the powerhouse section to 20 feet deep at the non-overflow section of the dam. Samples taken from the base of the silt are high in clay and relatively dry. This suggests that the silt is forming an less permeable boundary. This boundary results in a reduced flow through the silt, and a corresponding reduced uplift pressure at the dam/foundation interface. This agrees with the conclusions reached from review of the undrained pressure readings taken at the gallery drains and discussed in the previously. These studies indicate that the uplift pressure at the heel of the dam would be less than full reservoir head.

Reservoir Piezometers. Two pneumatic piezometers were installed in the silt upstream of the dam in each of two drill holes; drill hole **B-1** located near the center of the powerhouse section, and drill hole **B-2** located near the right portion of the powerhouse section (the maximum section of the dam). One piezometer was installed in the silt layer near the silt/foundation contact, and one was installed in the foundation rock about 1.5 feet away from the upstream heel of the dam.

Measurements showed that the piezometer located near the heel of the dam in drill hole **B-1** had a recorded insitu pressure of 22 lb/in^2. This is equivalent to 51 feet of head and is less than the reservoir head of 90 feet for the piezometer elevation. The piezometer located near

the heel of the dam in drill hole **B-2** had a recorded insitu pressure of 16 lb/in^2. This is equivalent to 37 feet of head and is less than the reservoir head of 94 feet for the piezometer elevation. The insitu water pressure in drill hole **B-2** near the heel is about equal to the calculated water pressure, based on the undrained pressure readings taken from the gallery and discussed previously.

Drain Piezometers. The pressure readings were recorded for closed drains to verify that the pressure measurements from galleries in the dam were for an undrained condition. The results confirmed that these measurements were for undrained conditions, and not the drained condition.

Next the drain pressures were recorded for selected open drains. The average readings for the central gallery (powerhouse section) are 10 lb./in^2, about 23 feet of head, and is approximately equal to the difference in elevation between the central gallery and the dam/foundation contact.

Seepage Analysis

Seepage Analysis. The two-dimensional finite element analysis (FEA) was used to study the water pressure distribution within the foundation rock *(GEO-SLOPE, 1992)*. The purpose of this study was to determine the increase in foundation water pressure at the heel due to the increase in PMF reservoir water surface. The FEA model extended upstream, downstream, and below the dam a distance equivalent to 210 feet, approximately two dam heights. Both the foundation rock and silt were included in the model.

The foundation permeability was determined based on data collected during previous investigations *(Harza, 1990)*. In 1989 a core drilling and testing program was conducted for the concrete and foundation rock. From numerous water tests the average foundation permeability was determined to be approximately 1100 feet/year.

The permeability of the silt in the reservoir was estimated to be 200 feet/year, based on the U.S. Bureau of Reclamation (USBR) values for unconsolidated silty clays with mixtures of sand *(USBR, 1987)*.

Two reservoir loading conditions were studied; the normal water surface elevation and the expected PMF water surface elevation.

Usual Load Condition, **USLC**	Normal reservoir water surface elevation 5720.0
	Normal silt elevation 5660.0
	Normal tailwater surface elevation 5641.0
Unusual Load Condition, **UNLC**	PMF reservoir water surface elevation 5735.0
	Normal silt elevation 5660.0
	PMF tailwater surface elevation 5665.0

The initial analysis, simulating the usual loading condition USLC, was made to calibrate the model. The total pressure head on top of the silt layer upstream of the dam was set to 62 feet, equal to the difference between the normal reservoir water surface elevation 5720 and the top of silt elevation 5660. The total pressure head on the foundation rock downstream of the dam were set to 19 feet, the difference between the normal tailwater surface elevation

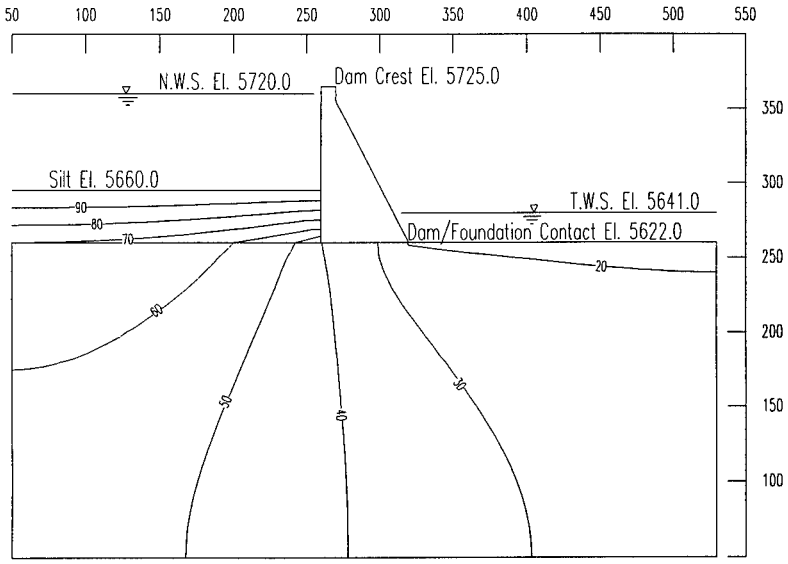

Figure 2 - Usual Load USLC Foundation Water Pressure Contours (feet of head)

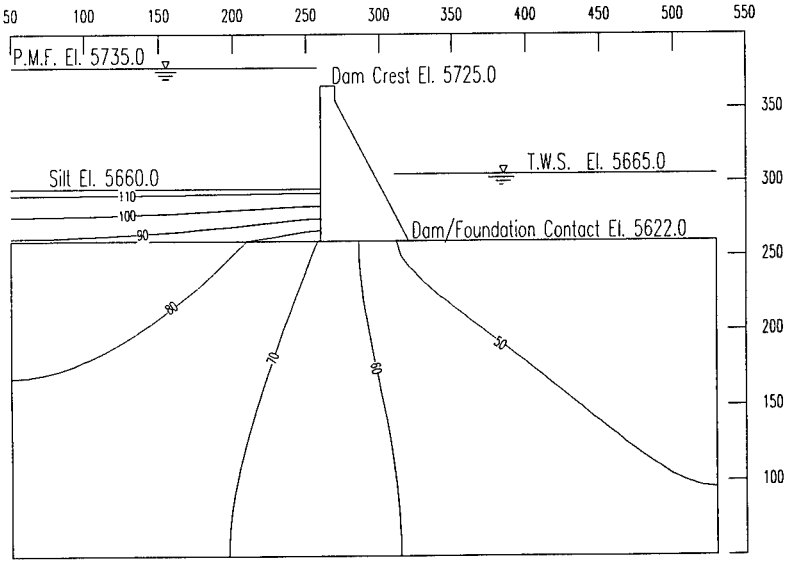

Figure 3 Unusual Load UNLC Foundation Water Pressure Contours (feet of head)

5641 and the foundation elevation 5622. The results from the analysis were compared to the recorded insitu conditions at the dam and verified the accuracy of the FEA model.

The seepage analysis for the unusual loading condition UNLC, increased the total pressure head to simulate the PMF overtopping. The total pressure on the silt layer was increased to 75 feet, equal to the difference between the PMF reservoir water surface elevation 5735 and the top of silt elevation 5660. The total pressure head on the foundation rock downstream of the dam was increased to 43 feet, the difference between the PMF tailwater surface elevation 5665 and the foundation elevation 5622. The model was re-analyzed to determine the change in foundation water pressure at the upstream heel of the dam.

Seepage Analysis Results

The water pressure contours resulting from the seepage analysis are shown in Figure 2 for the usual loading conditions USLC and Figure 3 for the unusual loading conditions UNLC.

The water pressure results from the seepage analysis at the heel of the dam increased from 40 feet during load USLC to 70 feet of head during load UNLC. It should be noted that this 30 foot increase in head is greater than the 15 foot increase in reservoir water surface elevation.

The foundation pore-water pressure head for the usual and unusual loading conditions are summarized in Table 2.

TABLE 2
Seepage Analysis Results

Location	Usual Load Condition USLC	Unusual Load Condition UNLC
	(feet)	(feet)
Upstream Heel	40	70
Drain	23	43
Downstream Toe	19	43

Uplift Analysis

The computer program **CRFLOOD™** *(EPRI, AP-101596, Beta Test)* was used to determine the effectiveness of the foundation drains. The crack model measured 40 feet wide (to include two drains spaced at 20 foot centers) by 60 feet long (distance between the heel and the toe) and included the effect of two 3.5 inch diameter drains.

The loads applied to the uplift model simulated the usual loading condition, USLC. The uplift pressure head at the heel was set equal to 40 feet, simulating the expected head based on the results from the seepage analysis and the measured undrained uplift conditions discussed previously (Figure 1). The pressure head at the toe was set equal to 19 feet. The effective drain diameter was set equal to 3.5 inches and had a pressure head of 23 feet. The effective aperture (crack) width was set equal to a constant 0.032 inches and the roughness was assumed to be 0.0. The results were verified with the known insitu conditions.

The next step in the uplift analysis was to increase the loads to simulate the unusual loading condition, UNLC. The uplift pressure head at the heel was increased to 70 feet based on the results of the seepage analysis. The uplift pressure head at the toe was increased to 43

feet, equal to the difference between the PMF tailwater and the foundation surface. The pressure head at the drain was also increased to 43 feet. The effective aperture width and effective drain diameter remained the same as in the previous analysis. The model was re-analyzed to determine the increase in the uplift load.

The final step on the uplift analysis was to study the effects of different effective crack widths and drain spacing for the usual loading condition, USLC.

Uplift Analysis Results

The uplift load and drain discharge for the usual and unusual loading conditions USLC and UNLC are summarized in Table 3. The uplift load is the product of the water pressure in the crack and the 40 foot by 60 foot cracked area. The uplift includes the influence of the cone-of-depression.

TABLE 3
Uplift Load and Drain Discharge

Load	Drain Spacing (feet)	Effective Aperture Width (inches)	Uplift Load (kips)	Drain Discharge (ft^3/sec)
USLC	20	0.032	4012	0.132
UNLC	20	0.032	7644	0.200

The results from the **CRFLOOD™** uplift analysis show that the uplift load during the usual load USLC and the unusual load UNLC will be less than the uplift load used in previous studies which was based on the FERC guidelines. Figure 4 compares the computed uplift load to the assumed uplift load.

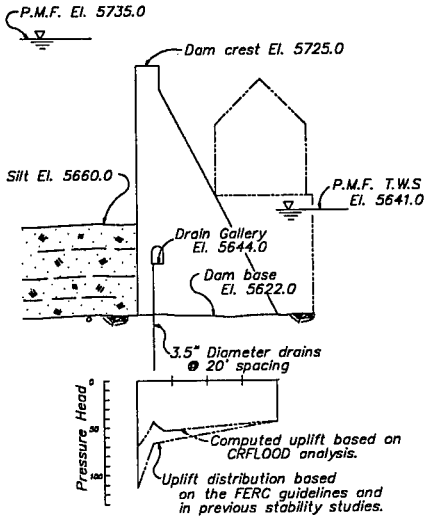

Figure 4 - Computed uplift distribution for Unusual Load UNLC.

The uplift load and drain discharge versus effective aperture width and drain spacing is summarized in Table 4.

TABLE 4
Effects of Aperture Width and Drain Spacing

Drain Spacing (feet)	Effective Aperture Width (inches)	Uplift Load (kips)	Drain Discharge (ft^3/sec)
20	0.05	4019	0.350
20	0.02	4078	0.030
20	0.005	4081	0.0005
No Drains	0.038	4425	0.0
20	0.038	4012	0.132
5	0.038	3392	0.062

The results of the sensitivity analysis indicate that the effective crack width does not significantly effect the uplift load for an effective drain diameter of 3.5 inches. However, the increase in crack width does increase the discharge per drain. The narrower aperture increases the friction loss in the crack, which results in a reduction in the cracks flow velocity. The wider crack allows as much flow as the drain can handle resulting in an increased discharge.

The results of the analysis show that the uplift load remains relatively constant for the change in effective aperture width. Research has shown that the uplift remains the same over the crack plane for different aperture widths if flow in the cracked are is laminar *(Illangasekare, Tissa H., Uplift Reduction using Drains, WaterPower '91)*. The results show that the flow around the drain is laminar for an effective aperture width of 0.005 inches and is turbulent upstream of the drains for an effective aperture width of 0.05 inches. Turbulence can reduce drain effectiveness and increase the uplift load. The results of the analysis indicate that the 3.5 inch diameter drain is large enough to prevent an increase in the uplift load.

The results of the analysis also show that by increasing the number of drains would decrease the uplift load acting on the dam. The uplift analysis indicates that the present drainage system is 9 percent effective (9 percent less uplift load than an undrained condition). This could be increase to 23 percent effective if additional drains were installed at 5 foot intervals. The uplift analysis indicates that the uplift loads acting on the dam are much less than the assumed uplift loads used in previous studies and based on the FERC guidelines. The previous studies showed that the dam was stable for larger uplift loads. Therefore, additional drains are not required to improve stability.

Conclusions

Three separate studies including a) review of foundation drain pressure data and procedures used to collect the data, b) field investigations, and c) computer analyses were performed to determine the uplift load during the usual and unusual loading conditions. Each study indicates that the uplift loads used in previous structural stability analyses for the usual and unusual loading conditions were conservative. The major conclusions are summarized below:

1. Further review of drain data and the procedures used to collect the drain pressure data indicates that the drain pressure measurements are for an undrained uplift condition. The pressure head at the heel of the dam can be computed using linear extrapolation of the known pressure at the toe and drain locations. The computed water pressure at the heel is less than the corresponding reservoir pressure at that elevation due to the less permeable silt deposits in the reservoir. These results also indicate that the actual uplift load will be less than the uplift load used in previous structural stability analyses which were based on the FERC guidelines.

2. Field investigations showed that the silt level in the reservoir is above the foundation rock.

3. Pressure measurements taken from piezometers located at the heel of the dam show that the water pressure at the heel is less than the reservoir water pressure for that elevation. This indicates that the silt layer in the reservoir is less permeable than the foundation rock and reduces the pressure at the heel of the dam.

4. Pressure measurements taken from piezometers located in open and closed drains verified that the drain measurements were for undrained uplift conditions.

5. The results from the two-dimensional finite element seepage analysis of the silt and foundation rock showed that the uplift head at the heel increases from 40 feet for the usual loading condition to 70 feet during the unusual PMF loading condition. This is less than the PMF reservoir head of 113 feet. The 30 foot increase in head at the heel, however, is greater than the 15 foot increase in the reservoir water surface elevation.

6. The results from the **CRFLOOD™** uplift analysis indicate that the uplift during the unusual load UNLC will be less than the uplift load used in previous studies and based on the FERC guidelines. The previous studies showed the dam to be stable for larger uplift loads. Therefore, the dam should be stable under the actual uplift conditions and no further measures are required to stabilize the dam with respect to uplift.

7. The results from the **CRFLOOD™** uplift analysis indicate that the drain spacing of 20 foot centers is 91 percent effective (reduces the undrained uplift load by 9 percent). Results indicate that the drain effectiveness could be increased to 23 percent by drilling additional drains at 5 foot centers. However, based on the results of this and previous stability studies this remedial measure is not necessary.

List of References

ATC Engineering Consultants, Inc., "Report on Soda Dam Structural Stability Analysis", Denver, October 1992.

FERC Guidelines. Federal Energy Regulatory Commission, Office of Hydropower Licensing, "Engineering Guidelines for the Evaluation of Hydropower Projects", Washington, D.C., April 1991

Electric Power Research Institute (EPRI), **CRFLOOD™** , AP-101596, Beta Test, 1992.

GEO-SLOPE International Ltd., SEEP/W User's Guide, Calgary, Canada, 1992.

Grenoble, B. Alex, Craig W. Harris, and Douglas I. Morris, Measurements of Time Lag in Concrete Gravity Dam Foundations, WaterPower 91.

Harza Engineering Company, "Supporting Design Report - Stability Improvement Project for Oneida, Dam", Chicago, April 1990.

Sergent, Hauskins & Beckwith, Report for: Piezometer Installation Project, Soda Point Dam and Oneida Dam Located on the Bear River in Southeast Idaho, Salt Lake City, 1992.

Underweight, Lad B., and Norman A. Dixom, "Dams on Rock Foundation", in Rock Engineering for Foundation and Slopes, American Society of Civil Engineers (ASCE), New York, 1977, pp125-146.

U.S. Department of the Interior, Bureau of Reclamation, Design Standard No. 13, Chapter 8, 1987.

The Automated Instrumentation Monitoring System At The Bad Creek Pumped Storage Project

Edwin C. Luttrell, P.E. [1]

Abstract

The hydroelectric industries continuing focus on safety directs increasing emphasis on the need for reliable and responsive instrumentation monitoring systems. Such a program must deal with large numbers and diverse types of instruments, manage large quantities of data, and yield readily interpretable results. Availability of new computerized automated monitoring equipment has made these goals achievable. The Bad Creek Pumped Storage Project employs an automated data acquisition system (ADAS) integrated with manual systems to monitor the performance and assure the safe reliable operation of three large embankment dams, an underground powerhouse, and tunnel network.

The central element of the Bad Creek instrumentation program is the PC controlled ADAS which monitors instruments and stores the resulting data. Distinct features of the system include its interface and data exchange with the plant control system allowing direct plant operator involvement and its communication link to the engineering support staff located 290 kilometers from the station. In this way, critical parameters are continuously monitored by station personnel while more routine functions such as database management and report production can be conducted at the central engineering offices.

In excess of 150 instruments are linked to ADAS covering a physical area exceeding 2000 acres. The ADAS architecture consist of the central network PC with thirteen remote measurement and control units. These remote units have local intelligence which allows them to function independent of the network computer. Telemetry for communication within the network is accomplished by a combination of

[1]Senior Engineer, Duke Power Company, 500 South Church Street, Charlotte, NC 28201-1006.

function independent of the network computer. Telemetry for communication within the network is accomplished by a combination of radio, hardwire, and fiber optic links. Instruments which are polled manually form the additional component of the overall program. Automated parameters associated with the dams include piezometric levels, seepage flow quantities, stress measurements, and rainfall. Penstock pressure (internal and external) is monitored. Numerous other parameters such as deformation of the embankments are integrated with the ADAS data to form the total instrumentation system database. The post processing of this data forms an essential component of the overall system. The ADAS computer maintains preset alarm levels for selected instruments and trigger of these alarms precipitates operator action through the link to the overall plant control system. The bulk of the data is processed at the central engineering office utilizing PC based programs to generate clear graphic based reports.

This paper describes the evolution of the Bad Creek instrumentation monitoring program and its vital role in the safe operation of the station. Performance during initial filling and early plant operation are discussed and specific examples are used to illustrate the systems functional capabilities. Methods and software tools employed to manage the large quantity of data collected by the monitoring program are described. Lessons learned during the system development, procurement, installation, and operation are presented.

Introduction

The Bad Creek Project is a 1068 MW pumped storage hydroelectric facility located in Oconee County, northwestern South Carolina. The upper reservoir is created by two large dams and a saddle dike, and has a surface area of 1.5 km^2 when at full pond, elevation 704 m. The upper reservoir has a usable storage volume of 37,726,000 m^3 within the 48.8 m draw down zone. Lake Jocassee, a 29.9 km^2 reservoir empounded in 1974, serves as the lower reservoir. The plants four reversible pump-turbines are located in a underground powerhouse.

The three embankments which form the upper reservoir have a typical cross-section consisting of an impervious central soil core supported by a rockfill shell. An internal filter system collects and controls seepage and provides a transition between zones of diversely graded material. The principle performance concern associated with the embankments is stable operation during the rapid pool draw down that is a normal loading condition. Numerous geotechnical instruments are located within the dams to monitor their performance. Physical dimensions of the dams are given in Table 1.

Water from the upper reservoir reaches the underground powerhouse via a vertical shaft and power tunnel with an overall length of 1390 m and diameter of 9 m. The power tunnel transitions into four penstock segments leading to the units located in the powerhouse chamber. The powerhouse cavern is located 168 m below ground and is 22.5 m wide, 50 m high, and 132 m long. Drains are drilled into the rock mass and specific geologic features in the penstock area to relieve any build-up of pressure at the powerhouse wall. The four units draft tubes reduce into two tailrace tunnels which run approximately 335 m to the lower reservoir and a submerged discharge structure.

It was recognized that detailed monitoring of the civil features of the project would be required to assure safe plant operation. To this end, an extensive geotechnical instrumentation package was incorporated into the design of the project.

Table 1

Structure	Length (m)	Height (m)*	Volume (m^3)
Main Dam	786.6	109.7	9,670,497
West Dam	276.8	51.8	764,654
East Dike	292.6	27.5	339,922

* At Centerline

Instrumentation Program

The Bad Creek geotechnical instrumentation program is used to monitor the operational performance of the embankment dams, natural rims, power tunnel system, powerhouse cavern, and related areas and parameters. The program evolved throughout the design and construction phases to address generic performance parameters and to target specific physical features and parameters which were identified during the construction phase of the project. Table 2 provides a delineation of the types and numbers of instruments along with the principle features they monitor.

Table 2

Instrument Type	Number	Project Feature
Vibrating Wire Piezometer	136	Dams, Tunnels
Twin Tube Hydraulic Piezometer	14	Dams

Pneumatic Piezometer	16	Dams, Tunnels
Open Standpipe Piezometer	45	Dams, Reservoir Rim
Earth Pressure Cells	5	Main Dam
Weirs	14	Dams, Reservoir Rim
Parshall Flume	3	Dams
Displacement Monuments	72	Dams
Cross-Arm Settlement	5	Main Dam
Sondex (Settlement)	14	Dams
Inclinometers	29	Dams, Project Wide
Single-Position Borehole Extensometer	32	Powerhouse Cavern
Strong Motion Accelerograph	2	Main Dam

Early in the development of the instrumentation package, the concept of automating the polling of selected instruments was adopted. This influenced decisions such as the selection of piezometer type, where it was felt that vibrating wire instruments could be most easily automated. It was also recognized that the tremendous anticipated volume of collected data, either automated or manual, would have to be linked to an overall data management and evaluation process if it was to truly be a functional tool in the monitoring and evaluation of the safe performance of the project features.

ADAS Overview

To assist in the tasks of monitoring and data management associated with the instrumentation program, an automated data acquisitions system (ADAS) is utilized at the Bad Creek project. The system consists of remotely intelligent Measurement and Control Units (MCU's) networked into a central microcomputer (PC) containing the system software. Individual instruments interface with the system at the MCU. Communications between nodes (MCU's) on the network is either by radio, hardwire, or fiber optic data link. Figure 1 provides a simplified overview of the system architecture. The design of the ADAS incorporates the following features and capabilities.

- Remote reading of sensors (instruments) at predetermined time intervals or real time, forced polling by user.

- Processes and converts data to engineering units, computes mean values, or maximum-minimum during a defined time window.

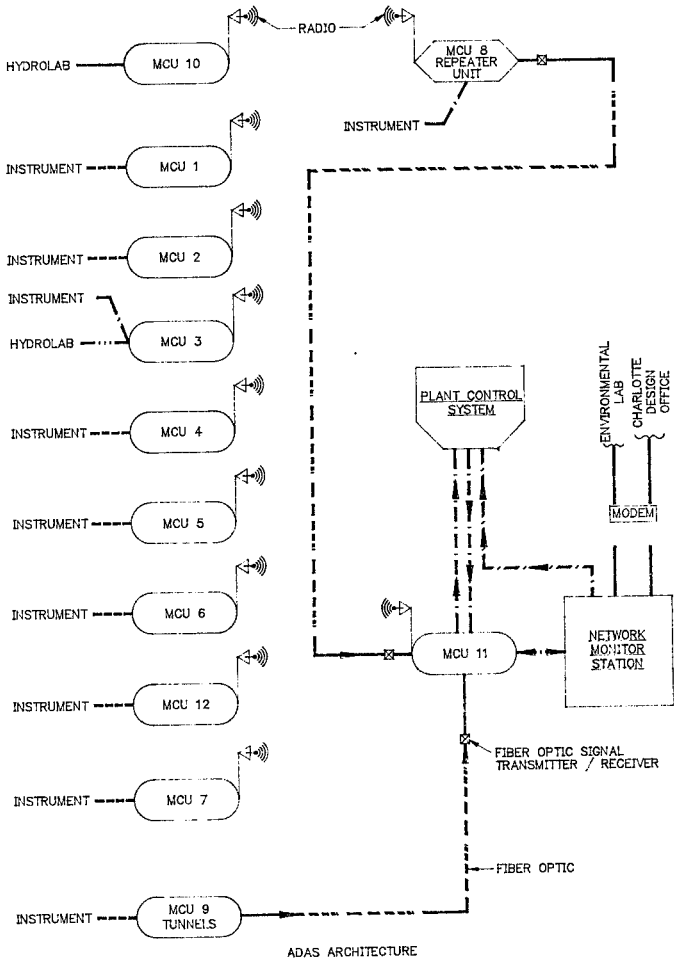
RADIO
HYDROLAB
MCU 10
MCU 8
REPEATER
UNIT
INSTRUMENT
INSTRUMENT
MCU 1
INSTRUMENT
MCU 2
INSTRUMENT
HYDROLAB
MCU 3
INSTRUMENT
MCU 4
INSTRUMENT
MCU 5
INSTRUMENT
MCU 6
INSTRUMENT
MCU 12
INSTRUMENT
MCU 7
INSTRUMENT
MCU 9
TUNNELS
PLANT CONTROL
SYSTEM
ENVIRONMENTAL
LAB
CHARLOTTE
DESIGN
OFFICE
MODEM
MCU 11
NETWORK
MONITOR
STATION
FIBER OPTIC SIGNAL
TRANSMITTER / RECEIVER
FIBER OPTIC
ADAS ARCHITECTURE

FIGURE 1

- Measurement and control units are remotely intelligent and can read and store data even if there is a communications link failure. Remote units are battery powered with solar recharge. Electronics minimize power consumption. Individual MCU's may be accessed by portable computer to download data or upload software modifications.

- Stores historical data on the microcomputer storage media (hard drive). File structure allows easy subsequent processing to aid in data interpretation.

- System can be configured for threshold and rate of change alarms for any parameter which is being monitored.

- The ADAS is linked to the Bad Creek plant control system allowing the exchange of data collected by the two systems. For example, penstock piezometric levels and rainfall are ported to the plant control system from ADAS while reservoir level and penstock pressures are passed to ADAS from the plant control system. The ADAS alarms may be passed to the plant operators console, globally or for individual parameters. This interface allows the operator to utilize ADAS selectively without the need to monitor the complete system continuously.

- The system may be controlled and programmed remotely. Data is transferred by this link to the plant engineering support staff located in Charlotte, N.C., 290 kilometers from the station. The remote communications capability can also be utilized by the equipment supplier to assist with software upgrades and trouble shooting of system problems.

- In the event of problems, all instruments are installed in a manner which allows for manual data collection.

- The system has considerable inherent flexibility. Each MCU is modular, with the ability to be configured to read most instrument signals including vibrating wire, 4-20 mA, and voltage outputs. Future expansion is easily accommodated.

The equipment used at Bad Creek is the Geomation System 2300 manufactured by Geomation, Inc., in Golden, CO. There are twelve Measurement and Control Units (MCU's), ten at the dams, one underground and one at the controlling PC, the Network Monitoring Station (NMS). In excess of 150 instruments are connected to the ADAS, principally vibrating wire piezometers, but including weir and flume level sensors, water quality modules, water temperature sensors, and a rain gauge. Polling times for the various instruments varies and may be easily

Data Management/Post Processing

In order for the information from a geotechnical instrumentation program to serve its role in the assurance of safe performance of project components, a well organized, responsive data management program must be in place. At Bad Creek, the data management program has evolved through the construction, start-up, and early operation phases of the project. A flow chart showing the data processing paths is shown below.

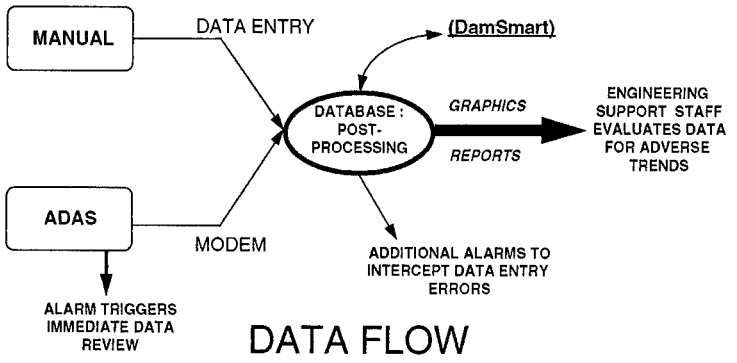

FIGURE 2

As can be seen, the ADAS data and that which is collected manually is moved into a database within the DamSmart computer program developed by Woodward-Clyde, Inc., Processing options within DamSmart include alarm/threshold levels, tabular reporting, time-history, x-y, and contouring graphics. More complex presentation graphics options are possible using custom developed AutoCad templates.

The data management program utilized for the Bad Creek project provides for timely reporting, plotting and interpretation of collected data. This allows the engineering support staff to review and interpret results, looking for significant performance trends. This would include changes over time which would not immediately trigger a threshold alarm set at some point in the system. This human link remains the most vital component of any instrumentation program, even an automated one.

Operational Performance

The operational performance of the ADAS and the overall geotechnical instrumentation program during construction, plant start-up, and initial operation has been good. The program has evolved as the need for improvements was recognized. A brief listing of "lessons learned" in the process are delineated below.

- A complex instrumentation program, including the ADAS portion requires maintenance and oversight by qualified personnel. Procurement of an ADAS system should include on-site vendor training in system maintenance and operation.

- The data management program should be designed and necessary software and hardware procured up front to allow personnel to grow into the overall instrumentation program as it is installed and operated. Careful planing is required to determine the needed personnel resources.

- Attention to detail during the installation of individual instruments is vital. The cost of an instrument is insignificant compared to installation or replacement cost. Use the most robust, highest quality components. A particular lesson at Bad Creek was the need for armored cable for vibrating wire piezometer leads to withstand construction and in-place stresses in a high embankment.

- The group responsible for reviewing and evaluating data must allocate sufficient resources to review the instrumentation data in a timely manner.

The geotechnical instrumentation program at Bad Creek was installed incrementally as construction progressed. During this phase the embankment dams were the primary area of focus. Parameters measured included embankment pore pressures used to assure safe fill placement rates. Other data was collected by ADAS and manual means to establish "baseline" characteristics for various parameters.

The first real "test", and perhaps the most important function of the ADAS and instrumentation program, was the monitoring during the initial filling of the tunnels and upper reservoir. Careful preparation and planning for this phase of the project was essential to its successful completion. This preparation included the creation of a controlled filling plan and the development of performance envelopes for each of the instruments. These envelopes of "allowable" values were established by analytical means such as FEM analysis of the embankments and by review of the filling performance of similar projects and structures. With the assistance of the ADAS, daily reports were readily available to the filling team. Considerable additional manpower would have been required if the ADAS capabilities had not been available. Initial reservoir filling was completed without significant difficulties.

An example of the value and versatility of the ADAS can be found in the early operational monitoring of the piezometers located along the steel lined penstock section just upstream of the powerhouse. These instruments help evaluate the effectiveness of cut-off measures in place to help prevent the build-up of hydrostatic pressure at the upstream wall of the powerhouse. Early on during plant operation, these pressures began to rise significantly. By looking at additional parameters tracked by ADAS, temperature and pool level, superimposed with pressure, it could be seen that the pressure rise was related to thermal changes. Figure 3 shows this seasonal trend. The flexibility in looking at multiple data parameters greatly simplified the evaluation of the situation.

Conclusion

Rapidly evolving advances in geotechnical instrument technology have made Automated Data Acquisition a practical alternative to manual collection of data. Such a system can be made an integral part of a hydroelectric facility geotechnical performance monitoring/safety program. A well designed system will be flexible and expandable as well as streamline data management. Evaluation to determine the feasibility of such a system must include the cost to train personnel to install, operate and maintain these complex systems. A commitment consistent with that given to any other essential plant component is required to insure success.

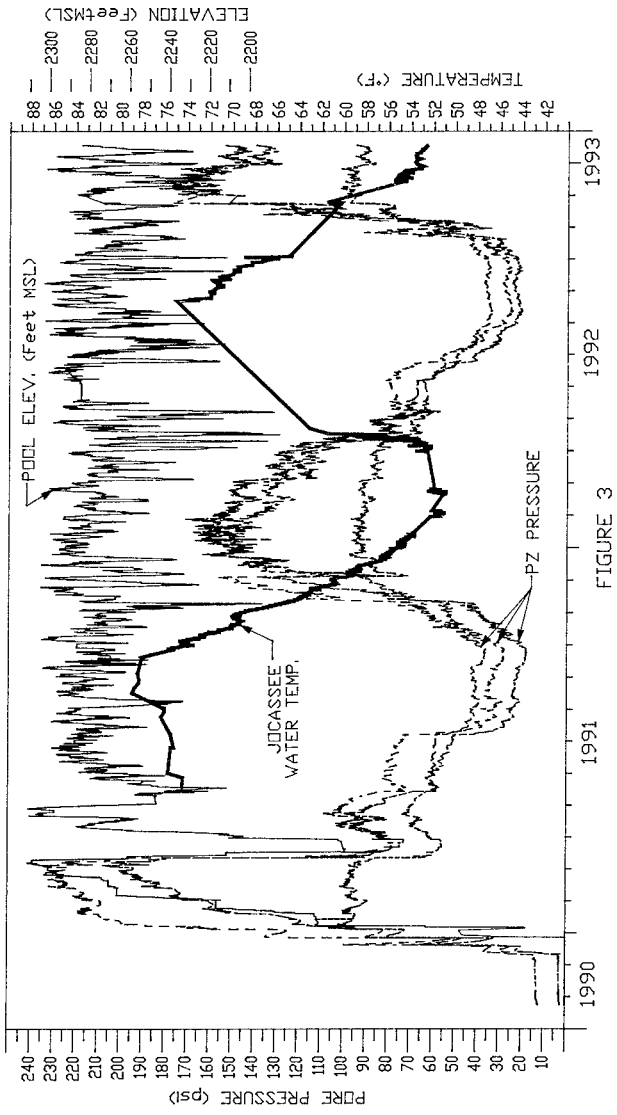
ELEVATION (FeetMSL)
2300
2280
2260
2240
2220
2200
TEMPERATURE (°F)
88 86 84 82 80 78 76 74 72 70 68 66 64 62 60 58 56 54 52 50 48 46 44 42
POOL ELEV. (Feet MSL)
JOCASSEE WATER TEMP.
PZ PRESSURE
PORE PRESSURE (psi)
240 230 220 210 200 190 180 170 160 150 140 130 120 110 100 90 80 70 60 50 40 30 20 10
1990
1991
1992
1993

FIGURE 3

Automating Instrumentation at Navajo Dam

Stan B. Mattingly, P.E. 1)

Introduction

With over 300 instruments and structural behavior monitoring points, Navajo Dam, located in northwestern New Mexico, is one of the Bureau of Reclamation's most instrumented dams. This fact underlies the desire of Reclamation personnel to automate the process of data gathering, reporting and evaluation.

Construction of Navajo Dam and Reservoir was completed in 1963. The dam is a zoned earthfill embankment with a structural height of 402 feet and a crest length of 3,648 feet. As a part of Reclamation's Colorado River Storage Project (CRSP), the reservoir is operated for delivery of water for irrigation on the Navajo Indian Irrigation Project, minor irrigation water needs downstream, municipal and industrial water contracts, and flood control on the San Juan River.

In 1984, Reclamation's safety evaluation of Navajo Dam concluded that modifications to the dam should be considered. Seepage occurring through the abutments of the dam posed a safety risk to the structural integrity of the dam. A corrective action study was prepared in 1985 recommending actions to control the seepage. A drainage tunnel in the right abutment and a diaphragm wall keyed into the left abutment were recommended. The tunnel and the diaphragm wall were constructed in 1987 thus completing the safety rehabilitation. A powerplant to be operated by the City of Farmington, New Mexico under FERC license was also constructed in 1987.

Instrumenting and Monitoring the Dam

A large array of instruments and monitoring devices were installed at Navajo Dam as a part of its

1) Civil Engineer, Water Operations Branch, Durango Projects Office, Bureau of Reclamation, P.O. Box 640, Durango, Colorado 81302

construction and during the dam rehabilitation. The system included 3 drain monitoring meters, 79 embankment and structural measurement points, 40 hydraulic piezometers, 81 internal vertical movement instruments, 9 observation wells, 20 porous-tube piezometers, 10 seepage measurement weirs and gages, 26 slotted-pipe piezometers, 258 water quality measurement points and 10 wells where 15 vibrating wire instruments were installed.

The drainage tunnel has 7 pressure and 32 flow meters on the drill hole drains and a total-tunnel-flow rectangular weir. The diaphragm wall was instrumented with 19 wells containing 30 vibrating wire piezometers and 4 inclinometers.

In 1988, the Bureau's Denver Office, Co. Structural Behavior and Instrumentation Branch staff began a program of automating the collection of data from surface seepage flow weirs, selected porous-tube piezometers, nearly all slotted-pipe piezometers and all vibrating wire piezometers. The automation equipment included 6 master control units (MCU) on the dam top, a network monitoring station (NMS), a phone link from the Denver Office to the NMS, and PERK software on an HP-45 which loads and saves data. At the same time, a modem for data transmission to the Durango Projects Office, Co. was installed. All other instrument and monitoring points not involved in the automation program are read manually.

Dam Instrumentation Data Processing Scheme

Personnel and equipment are involved at three key locations: the Denver Office, the Durango Projects Office, and at Navajo Dam, N.M.

The data processing scheme is as follows: the instrumentation and monitoring data are gathered at the dam, recorded to the databases at the Durango Projects Office and the Denver Office, graphed and charted with instrument plots and the latest reading and any alarms are reported.

The database for the automated instruments in the Denver Office is stored on the Bureau's CYBER computer. A phone link from the Denver Office to the NMS at the dam tells the NMS to upload the data through satellite transmission by blocks to the HP-45. The HP-45 saves the data for later uploading to the CYBER. Plots can then be created from this database for engineers at the

Structural Behavior and Instrumentation Branch in the Denver Office.

A VAX computer at the Durango Projects Office stores the data from the automated instruments after it accesses the NMS at the dam via a modem. The manually read instrument data is pulled into the same VAX database by importing the data from pre-created spreadsheets which are filled out by the recording technicians at the dam. These spreadsheets are also electronically transmitted to the Denver Office via VAX MAIL for use by monitoring engineers in the Denver Office.

Involvement by the Durango Projects Office for Monitoring Instrumentation at Dam

The Durango Projects Office engineers became increasingly involved in the monitoring program of Navajo Dam when it became apparent that with the amount of instrumentation and monitoring equipment at both Navajo Dam and at all Reclamation facilities, Durango Projects Office staff wished to assist the Denver Office staff in dealing with the data review. The Denver Office Structural Behavior and Instrumentation Branch staff are ultimately responsible for monitoring and reporting problems for Reclamation facilities throughout the western United States. Continuing discussions between the Denver Office staff and Durango Projects Office personnel resulted in the evolution of the present system.

Another reason the Durango Projects Office maintains involvement in the dam monitoring program is because of the political need to keep public agencies responsible for administration of downstream areas along the San Juan River up to date on events at the dam.
24 hour monitoring is a part of the Bureau's efforts to communicate with local governments.

Durango Projects Office Problem Monitoring System

This system involves the scheme as discussed above but with Durango Projects Office engineers becoming more involved in the line of reporting. All data is reviewed and graph plotted by a technician in the Durango Projects Office Water Operations Branch. The technician then rechecks any anomalous readings with the instrument reading technician at the dam. If the data is found to be accurate, the Durango Projects Office technician then

reviews the reports and plots with the supervisor of the Water Operations Branch. A decision is made on whether or not to contact Denver Office engineers based on the findings and interpretation of reports, charts and graphs. In this way, the amount of effort that Denver Office personnel have to attribute to Navajo Dam monitoring can be reduced and yet there is sufficient review by qualified personnel of the dam monitoring data.

Automation of Data and Instrument Alarm Reporting and Graphical Analysis at the Durango Projects Office

Several methods of data review are available at the Durango Projects Office. Alarm reports are generated weekly giving current status of individual instruments compared to a pre-set alarm threshold. The latest 5 readings are also reported by running a procedure to extract this information from the database. There are two ways of plotting the data. One involves the transmitting of the manually read instrument data to the Denver Office CYBER computer, running a program to create plot output files, multiple instrument plotting these time-series graph files on a TECTRONIX computer terminal and screen dumping these plots to a thermal-process paper plotter for a paper copy.

This plot method has a weakness in that some of the data would not be transmitted either on its way to or from the CYBER computer in the Denver Office. Hence, erroneous plots would result. This led to frustration by Durango Projects Office reviewers and the creation of an alternative way of plotting. This involved creation of a CALMA CADD program to plot the data in conjunction with development of a database routine that creates the files in the format that the CADD program can plot. These time-series graph plot files are created directly from the VAX database at the Durango Projects Office and thus eliminating the link to the Denver Office. Multiple instrument plots are created within CADD on a VAXStation 3100 and postscripted to a laser printer at the office to obtain a paper copy.

Development and Use of CALMA CADD Data Plotting Program

As explained earlier, there were problems with a plotting routine involving the Bureau's CYBER computer, the phone transmission of the plot files and inadequate hardware and plotting equipment in the form of the TECTRONIX. This led to a proposal of a plotting program

which engineers at the Durango Projects Office could have local control over and embrace state-of-the-art technology. The proposed system would also have to be simple enough to be used by personnel with little computer experience or training.

The first and second problems were overcome by accessing the data on the local Durango Projects Office database. The data stored on the local VAX computer is accessed and arranged into files with the necessary pre-defined format by DATATRIEVE. DATATRIEVE is a relational database management (rdbm) software package.

Menu-driven programs to operate the DATATRIEVE and the CADD programs were required to solve the last problem. Engineers and programmers worked to create a menu-driven VAX command screen which upon entry of the appropriate choice (a single keystroke and a "return" keystroke) at the computer terminal would operate the database program, perform the required data sort and create files in the pre-defined format. This command screen gives a user the ability to select: (1) output of alarm reports, (2) 5 latest readings reports or (3) creation of multiple instrument time-series graph plot files.

To obtain the time-series graph plots involves the use of CALMA CADD. CALMA CADD is a CAD system for which custom programs can be written. Once the graph plot files have been generated, a user can then initiate a CAD session on the VAXStation 3100. The user types in the program name at the CAD prompt and the program begins. Choices of families of instruments and whether multiple or single instruments will be plotted can then be selected by the user. The program will then plot the time-series graph on the screen and give the user the option of either outputting the results shown on the screen to a laser printer or creating a drawing and plotting this on a drum pen plotter at a selected scale. This gives the user the capability of obtaining 8-1/2" x 11" size laser prints or any size drawing plots complete with standard Bureau drawing border and titleblock for formal presentation.

Future Improvements in Automated Reporting and Plotting Using State-of-the-Art Technology

The system in use in the Durango Projects Office could be improved further by use of a WINDOWS based graphics data analysis package interfaced with the database. This type of system would offer improvements in the reporting and time-series plotting of the data. Durango Projects

Office personnel will obtain X-window terminals in early 1993.

Engineers in the Durango Projects Office are continuing discussions with the Denver Office staff in an effort to be able to access the Denver Office database and thereby eliminating the need for duplicate databases. The proposed process would be for Durango Projects Office personnel to obtain a copy of the Denver Office database management software (TECHBASE). This would allow the engineers in the Durango Projects Office to access the Denver Office database directly and with the assistance of the X-Window terminal plot data reports and graphs directly to the terminal in Durango.

CALMA CADD is a very powerful tool for viewing three-dimensional objects with its multiple window view screen layouts. This is an advantage which CALMA CADD has over other currently available CAD software packages. CALMA CADD has been proposed for use to produce three-dimensional plotting of subterranean dam water level isopach plottings. This would involve creating a terrain model by the CADD program which describes the surface of the subterranean water level on any given date. This terrain model would in turn be contoured through use of the Civil/Site software available as a part of CALMA CADD. With the program routine at a user's disposal, this type of analysis can become automated.

Instrumentation data for other projects would be put into a database specifically set up for that project. This data will be accessed through the data report output and graph plot programs and reviewed much as the program for Navajo Dam.

Use of Geographic Information Systems (GIS) shows great promise for automating the reporting and evaluation processes. GIS offers 3-dimensional analysis and graphical presentation in many of the same ways that CADD would be able to. GIS has advantages over CADD programs in that specialized CADD programs to graph and plot the results do not need to be developed and maintained. GIS ties directly into both a database where reports can be generated and a graphical mapping interface where evaluation results can be displayed.

Conclusion

Automation of the instrumentation and monitor reporting has been shifted from a central management function to a local management priority. This shift has

and will assist in reducing the time required for developing reports and getting dam information to decision makers. This in turn will reduce safety risks to the public by allowing more time to take action if necessary.

The Design and Installation of Dam Failure Monitoring Equipment for the Southern California Edison Company System of Dams

C. Michael Knarr, Member[1]
Thomas J. Barker[1]
Stephen F. McKenery[2]

Introduction

In accordance with a FERC (Federal Energy Regulatory Commission) mandate, the So. Calif. Edison Co. ("SCE") has recently installed an extensive monitoring system for detection of a dam failure in each of its dam systems. The company has two separate systems of dams. One of the systems is on the west side of the Sierra Nevada Mountain Range, just east of Fresno, California. The other is on the east side of the Sierras near the cities of Bishop and Lee Vining, California. There are 10 dams on the west side and 11 dams on the east side which required monitoring for dam failure. The total volume of water stored on the west side is 566,000 acre-feet, which provides for 1,000 megawatts of hydro generation. The system is considerably smaller on the east side of the Sierra Nevada's, where a total capacity of 61,000 acre-feet is available with a generation capacity of 52 megawatts.

Each of these dam systems, the east and the west, has its own dam failure monitoring system, and each acts independently from the other. This paper briefly describes how SCE implemented the FERC guidelines for installation of a dam failure monitoring system, including the method for detecting an imminent or actual failure of a dam. It also discusses the design and installation of the systems and equipment and

[1]Sr. Engineer, Southern California Edison Co., Rosemead, California
[2]Project Manager, Southern California Edison Co., Rosemead, California

describes how set points indicating failure of a dam were established. A description of the computer logic used to provide equipment failure warnings and alarms, and how these are handled by personnel when they occur, is presented. The paper discusses how the sites within each system were integrated into a central processing unit.

The paper also describes the differences between the west side and the east side systems and, in particular, the larger power requirements of the west side system. These systems were installed in very remote, high altitude, rugged terrain offering many challenges. Problems which came up during the design and construction phases of the projects are discussed. Lastly, the additional capabilities of the equipment for future applications are presented.

Implementation of FERC Guidelines

The FERC guidelines require that a surveillance system be installed that includes instrumentation and telemetering facilities to provide a continuous reading of headwater and tailwater levels at an operations control center that is manned 24 hours a day, every day throughout the year. SCE's compliance with these guidelines was to install systems which would reliably detect a potential or imminent failure so that downstream inhabitants could be evacuated. In order to do this, instruments have been placed at each dam to detect unusual changes in water level in the reservoirs (headwater) and at appropriate downstream (tailwater) locations. Signals from these devices are then telemetered to the main operations center for alarm dispatch to the appropriate public officials for early warning and possible evacuation of inhabitants. In addition, at remote campgrounds and other inhabited areas, pole-mounted sirens were installed to provide early warning for occupants.

Three methods are used for detection of a dam failure and are applied according to site specific characteristics:

1. An indication of extremely low reservoir level,
2. An indication of extremely high tailwater level, or
3. A rapid rate of change in reservoir level.

The first method is used to monitor very small forebay type dams where normal operation requires that the level be maintained within a strictly controlled band. These dams are also used as tailwater monitors for upstream dams, in which case Method 2 is utilized. Any substantial excursion outside of the normal operating band is a basis for operator alarming.

The second method is used for dam tailwater sites where the normal operation of the upstream dam maintains the gaging station level within a strictly controlled band. Any substantial increase above this normal operating band used in conjunction with headwater monitoring is a basis for operator alarming.

The third method is used for all other reservoirs where, during normal operations, the reservoir levels may vary substantially, but at controlled (and, typically very slow) rates.

The detection is done with level sensing pressure transducers and remote terminal units (RTU's) located at each reservoir. These RTU's are tied into a central processor at the dam system's main operations center. Some of the RTU's are tied in through local controller's (LC's) located at key installations. SCE's operations centers are manned 24 hours a day, so complying with that part of the FERC guidelines was already in-place.

With the exception of the small forebay dams, all dams have two set points determined by rate of change of reservoir water level. The initial alarm set point (minor alarm) alerts the operator that there is an immediate need to make close observation of the dam site. The major alarm set points, which vary for each dam, require the Company's main operations center to promptly alert public safety officials of the emergency conditions in accordance with the company's previously established Emergency Action Plan. All alarm set points for reservoirs are for measuring a downward rate of change in water level. An alarm occurs if the reservoir water level drops by the number of feet within or less than the time period specified.

The small forebay dams have major alarm set points at reservoir minimum elevation levels. When the water level drops to this elevation or below, an audible and visual alarm will require the operator to notify EAP agencies of a dam failure. When the reservoir is being drawn down to this level for maintenance/operational reasons, the alarm is disabled until refilling begins to prevent false alarming.

A few of the reservoirs also have minor alarm set points at their maximum water elevations. These will be acting as tailwater monitors for upstream dams. When the water level rises to this elevation or above, a warning alarm requires the operator to immediately check the headwater monitor of the dam for which the tailwater alarm sounded.

The tailwater gaging stations have alarm set points at elevations

such that when the water level rises to this elevation, a warning alarm requires the operator to check the dam's headwater monitoring system to determine if there is an indication of a dam failure.

System Design

The systems on each side of the mountain range are conceptually the same. Pressure transducers are used to sense reservoir level and are placed at the lowest level of the dam. An analog pressure (level) signal is received by the RTU, which then digitizes and converts the data to engineering units for processing. The transducers are connected to the RTU via special sealed and vented cabling, which runs from its location at the bottom of the reservoir up to the RTU cabinet near the dam. The cabling is buried below the ground surface above the water line, and anchored with steel or concrete devices on the bottom of the reservoir below the water line. The scheme for a typical installation is shown in Figure 1.

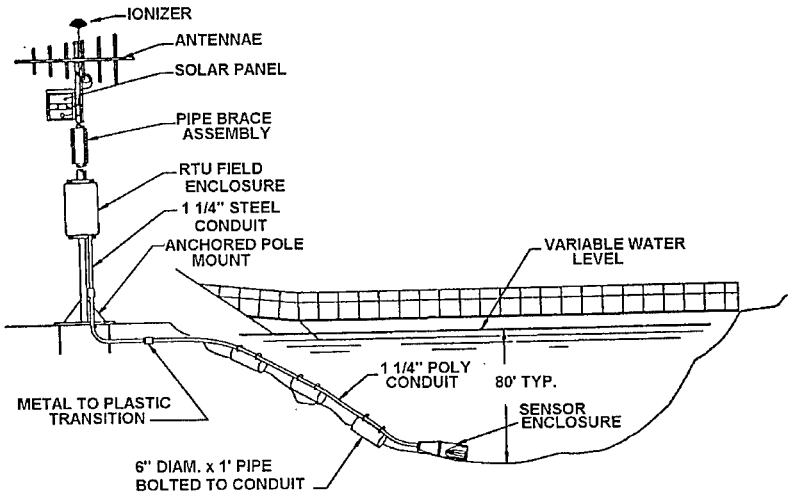

Figure 1. Typical Installation

The dam sites on both sides of the Sierra range have RTU's which continuously monitor reservoir level via two pressure transducers (one for redundancy) and have communication systems which transmit the collected data to a central processing computer at the main operations center for the system. On the eastern system of dams, the

RTU's not only collect the raw data from the transducers, but also process the data and determine an alarm condition before transmitting to the host computer at the main operations center. The RTU compares the rate of change of the level values to a predetermined algorithm. If the level rate of change exceeds a predetermined rate, an alarm condition message is transmitted to the central computer at the main control station indicating the trouble. In addition, each RTU transmits site data to the central computer once every 15 minutes for archival purposes and to confirm that the RTU and communication link are operating properly. The central computer receives all communications from the RTU's either directly or through repeater stations. On receipt of alarms from the RTU, the alarm condition is displayed on the system monitor and annunciated to the operator via the main annunciator panel.

On the west side system, compatibility with existing plant control equipment was maintained by using or expanding existing hardware. The existing system uses OPTO 22 I/O equipment to collect the data. As this I/O equipment does not have the capability to analyze the data, every four seconds the raw data is transmitted to local controllers (LC's) which collect data from several RTU's. These LC's are HP1000 microcomputers located at various hydro plants in the system. These computers format the data for transmission to the system operations center processor. At the operations center, the data from the LC's is received every 15 seconds by another HP1000 microcomputer. This microcomputer is used to interface with the main computer (CDC mini-computer) at the operations center. The main computer then runs the alarm checking algorithm and processes the data in a similar manner as the host computer for the eastern dam system.

One of the other major differences between the two systems is in the telecommunication systems. Because of the very rugged terrain of the east side dam system, a satellite system was originally selected for communications. However, during the installation phase of the project, the company that was to provide the satellite service experienced financial problems and was forced to go out-of-business, and the project had to fall back to a radio system for its communication link. VHF radio transceivers operating in the 153 Mh range with four radio repeater sites were used to link all eleven dams with the central operations center. These radios are powered by small 1.5 amp solar panels with a 45 amp hour gel cell battery back-up. The power requirement at these sites is primarily determined by the frequency (15 minutes) of the communication interval (except in an alarm condition) and duration (approximately 1 second) of routine communication between each RTU and the host processor. These are relatively small requirements

compared to the west side dams.

On the western side of the Sierras, there is an existing automation system for remote operation of the hydropower generating stations. This system utilizes conventional telephone circuits (wire or microwave) for inter-processor communication. The new dam monitoring system is integrated into this communication network. However, because of the high frequency operation (in the 950 Mh range), the remote sites, which do not have wire or microwave circuits, use the Motorola DARCOM radio system. This system is on-line continuously at about 20 to 30 watts power consumption and is transmitting site data every 4 seconds for processing at the main operations center. This high power consumption, in addition to the need for uninterrupted, continuous operation for 15 days, necessitated the use of large solar panels (6-3 amp panels) and a whole cadre of batteries (8-88 amp hour gel cells).

One of the other differences in the systems is the type of main controller used at each of the central operations centers. On the east side of the Sierras, all processing and alarming is done with an IBM industrial PC utilizing the QNX real time operating system. On the west side, the main controller, as previously noted, is a CDC mini-computer. The west side could have used an industrial PC as well. However, during design, operators complained that they already had enough to watch on the main boards and would prefer to have monitoring and alarming from the existing system and boards.

The algorithm that was used for advisory and alarming functions to the local operator is shown below. This algorithm executes in the master controller at the main operations center on the west side dams and in the local site RTU'S on the east side dams.

1. Raw data is collected from the primary and secondary level sensors once every 15 seconds. If the data is not available due to a communication link failure, the current data is set equal to the last available good data and the operator is advised of the communication failure.
2. The data is then converted to engineering units.
3. The data is then checked to determine if it is out of range. If it is out of range, the current data is set equal to the last available good data and the operator is advised.
4. For those sites with primary and secondary level indications, the data is checked for signal agreement. If the data differs by more than 2%, the operator is advised.
5. If the reservoir level is being checked and has

exceeded the extreme low level setpoint, an alarm is activated in the operations center.

6. In locations where level rate of change is being monitored, the data from the primary and secondary levels is shifted into moving window buffers of eight values ranging from the current value to the eighth oldest value.

7. The average of the 4 oldest values in the buffer is calculated and the same for the 4 newest values in the buffer.

8. The absolute value of the difference in the oldest and newest running average is calculated.

9. The difference in the averages is then compared with the associated dam alarm limit. If it exceeds the limit, an operator alarm is activated, and in some remote locations sirens are activated.

10. The difference is compared with the associated dam advisory limit. If it exceeds the limit, the operator is advised.

11. The cycle is then repeated .

Installation

Installing systems on both sides of the Sierra range at the same time was not an easily managed job, especially with both systems being different. Different contractors were hired for the work on each side of the mountain range and were hired to furnish both equipment and installation. As usual, each contractor had his own way of conducting business. It is our opinion that the contractors knew their equipment for the most part, but were not well versed in how to install the equipment. The rugged, mountainous and remote conditions were difficult to work in, and the contractors most likely did not understand the logistical problems associated with this.

Aside from the managerial and logistical problems, the physical installation was fairly simple and straight forward, except for the installation of the cabling in the bottom of the reservoirs. Boats were used to move the conduit out onto the lake in the proper location and then the conduit was lowered into place with steel pipe and/or concrete anchor blocks using divers. The conduit on-shore was buried for protection from traffic and vandalism.

Problems Encountered During Design and Installation

The remote and rugged mountainous conditions posed significant

design and installation challenges. Perhaps the most significant of these was the establishment of communication links between the various monitoring sites and the main operations centers. At the beginning of project design for the east side dams, establishing satellite communication links required a preliminary topographic map study, and then field tests to determine if reliable satellite communication paths could be established from the dam sites, which for the most part, were in deep canyons surrounded by high mountains. Through individual site assessments, locations for the satellite transceivers were found. In locating these sites, consideration was given to protection from rock and snow slides, vandalism, solar reception, maintenance access and foundation conditions. Consideration was also given to the length of the cable run from the site RTU to the location where the level transducers had to be placed, which, in most cases, was near the dam outlet structure (usually the greatest depth of water at the dam). When the satellite system was abandoned (for reasons noted previously), the surveys had to be conducted again to establish VHF radio paths. In this case, not only did the dam sites have to be tested, but repeater sites had to be established as well in order to get the signals out of the mountains and down to the operations center. The radio paths for the west side dams were established in a similar manner.

Another significant challenge was the design and installation of the pressure level transducers and cabling. The cabling needed to be continuous for moisture protection since it is vented cable. It also needed to be secured in place, capable of resisting ice drag during lake thawing and light enough to be installed in remote locations. The transducers were housed in a pipe section at the end of the cable conduit. This scheme is shown in Figure 2. The cables were housed in polyethylene pipe which was anchored with steel pipe or concrete block weights. The polyethylene pipe is very tough and is cable of extreme distortion, which may occur during ice break-up. It is also lightweight, so that transporting and installing it in remote sites was significantly easier. One feature to note about this installation is that, if a transducer fails, it will be left in-place, and a new cable in its own conduit will be installed. There is no easy way to pull new cable through the existing conduit without the use of divers.

Two of the dam sites are located in U.S. Forest "wilderness areas." Access to one of the sites required a 4-mile hike up an unmarked trail to the 11,000 foot elevation. The trail starts at the end of a 45 minute, 4--wheel drive. The other site involved a 15 minute ride up a cable tram, a ten minute ride across a lake, a ten minute ride up a second tram, a 20 minute ride across a second lake, and finally a one

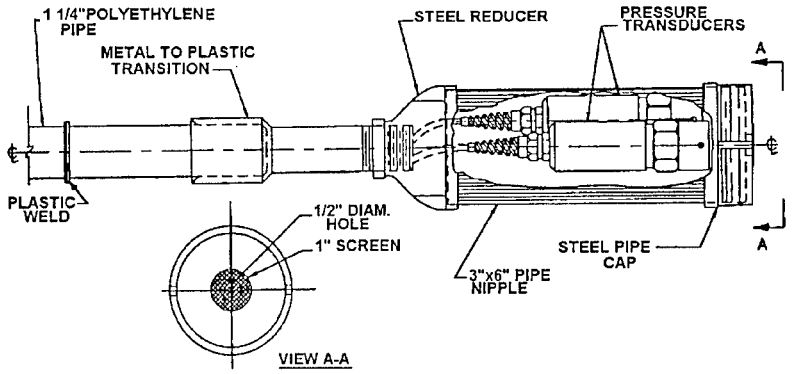

Figure 2. Transducer Casing

hour hike. Approval was finally given during the implementation phase of the project by the U.S. Forest Service to allow construction at these dams. The Forest Service was reluctant to have anything built in the wilderness areas. Normally, the U.S. Forest Service does not allow any type of power equipment into wilderness areas as well. However, in this instance, they did authorize the use of a portable generator for drilling anchorage holes in the rock. Pack animals were used to carry the equipment and materials up to the site, and some trail improvement had to be done in order to do this.

Another important design aspect of the projects was in selection of the appropriate power requirements for the different field conditions. 110 VAC power was used when available. However, for the remote sites, selection and sizing of photovoltaics and batteries were a challenge. The first part of this process was in estimating how long a specific site might be without sunlight, and then making it long enough to provide some conservatism in the battery storage capacity. This was addressed by estimating the maximum time for sunlight blockout, and then adding to it an allowance for accessing the site during storm conditions. Fifteen days of reserve battery storage was considered sufficient to cover these conditions. The second part of the process was sizing the solar panels and batteries for solar blockout and power drain for the 15 day period. This was a mathematical problem and relatively straight forward to solve.

Future Applications

The computers and RTU's that were installed have additional capacity for other monitoring and controlling functions that may be desired in the future. This additional capacity is available in the existing equipment as the new systems did not utilize all of the capacity of the standard electronics that were installed. The communication circuits are capable of handling these future applications as well. Some of the possible applications include meteorological data collection, instream flow monitoring and control, and dam gate control. These applications can be added to the existing equipment without interfering in the function of the existing dam monitoring systems.

Use of Advanced Technologies in Michigamme River Basin PMF Analyses

Mark S. Woodbury[1], A.M., ASCE, Douglas T. Eberlein[2], and Nicholas Pansic[3], M., ASCE

Abstract

Probable maximum flood analyses were recently updated for two of Wisconsin Electric's hydroelectric developments on the Michigamme River in Michigan's Upper Peninsula. The study incorporated comprehensive data collection and analysis including updated soil surveys, aerial reconnaissance, satellite image analysis, and digital map data. Unit hydrographs were developed using Clark's Method. Results of an updated PMP study for the region were incorporated into the Corps of Engineers HEC-1 flood hydrograph package to develop sub-basin hydrographs, which were routed using the NWS DAMBRK dynamic routing program to develop the PMF hydrographs for the two dams. CAD and GIS systems were used extensively in analysis of basin parameters and generation of modeling inputs. Results show a significant reduction in the PMF peak and volume at both projects.

Introduction

Wisconsin Electric Power Company (WE) owns and operates a system of 13 hydroelectric plants on the Menominee River and its tributaries in northeast Wisconsin and Michigan's Upper Peninsula, including the Way and Michigamme Falls projects on the Michigamme River. Previous probable maximum flood (PMF) studies based on the generalized probable maximum

[1]Hydrologist, Harza Engineering Company, 233 South Wacker Drive, Chicago, IL 60606

[2]Project Engineer, Wisconsin Electric Power Company, 333 W. Everett St., Milwaukee, WI 53201

[3]Associate and Head, Special Projects, Harza Engineering Company, 233 South Wacker Drive, Chicago, IL 60606

precipitation (PMP) given in the U.S. National Weather Service Hydrometeorological Reports (HMRs) numbers 51 and 52 concluded that the appropriate inflow design flood (IDF) for both developments is the PMF. Because the previous PMF was developed primarily for use in determining the appropriate IDF, WE sought to refine the PMF estimates to determine the most economical means to comply with Federal Energy Regulatory Commission requirements to accommodate the flood.

WE contracted with Harza Engineering Company to re-estimate the PMFs using state-of-the-art technology and the results of a recent Probable Maximum Precipitation Study for Wisconsin and Michigan conducted by North American Weather Consultants for the Electric Power Research Institute and the Hydro Users Group of Michigan and Wisconsin (EPRI/HUG). Anticipated changes in the FERC PMF guidelines were also considered in selecting methods for the study.

Refinements over previous studies were achieved by gathering additional data, increasing the number of sub-basins in the model, improving the unit hydrographs, using the updated PMP study, and expanding the use of dynamic flood routing techniques. Implementation of the new methods was successful in reducing the peak flood flows by about 40%. Significant changes in the new PMP estimation procedures account for more than one-half of this reduction. Compliance costs for modifications to accommodate the reduced PMFs at these sites will be considerably reduced due to this study.

Data Collection

Development of the PMF model required data collection to assist in defining sub-basins, estimating retention loss parameters, determining sub-basin runoff characteristics, and estimating parameters for channel and reservoir routing. This included acquiring recent soil survey data, USGS topographic maps covering the basin, and corresponding digital quad maps. Satellite imagery covering the basin was obtained for three separate dates to aid in determining land cover and other basin characteristics.

Two site visits were made, one at the outset of the study, and another after initial basin characterization was complete. Both visits included an aerial reconnaissance to aid in selection of sub-basins and verification of land cover estimates made from the satellite imagery. These visits corresponded roughly with the dates of the satellite imagery, which aided in comparison of the results. Cross-section surveys were also made at various locations along the Michigamme River for use in dynamic flood routing. Historical records and project data were obtained from WE, in addition to digital USGS gaging data from Harza's hydrologic database.

Basin Characterization

The review of USGS topographic maps and the information gained during the aerial reconnaissance were the most important components in defining and selecting the number of sub-basins for the model. Eight sub-basins, each with unique features, were ultimately selected to characterize the 720 square mile basin. Analysis of the satellite imagery confirmed that further subdivision of the basins would not improve the definition of the model. The sub-basin boundaries were delineated on the topographic maps and digitized for analyses using a geographic information system (GIS).

Retention Loss Estimation

Basic infiltration characteristics of the soils were identified from the soil surveys and incorporated into the GIS. Analysis of the satellite imagery was performed to estimate the land cover characteristics within each sub-basin. A procedure was developed to assign infiltration rates to each unique combination of land cover and soil type. A GIS overlay of the soil and land cover information was used to perform the analysis. The average infiltration rate was then computed for each sub-basin. Infiltration during the PMP was computed in the HEC-1 model using the uniform loss rate method.

Unit Hydrographs

Clark's method of unit hydrograph development was used to characterize runoff from each sub-basin. Because adequate rain gages and unregulated stream gaging stations were not available in the basin, time of concentration (T_c) and storage constant (R) parameters were estimated by correlating watershed parameters from similar basins in the region. Isochrones (lines of equal travel time to the outlet of each sub-basin) were drawn on the topographic maps, taking into account the presence of wetlands and minor drainage systems within each sub-basin. These were then digitized in the GIS, from which time-area histograms were prepared for each sub-basin, indicating the relative rate at which sub-basin area begins to contribute to direct runoff. The values of T_c and R, along with the time-area histograms and sub-basin areas, provided the necessary inputs for unit hydrograph computation in the HEC-1 model.

Basin PMP Estimation

Results of the EPRI/HUG regional PMP study were used to develop a 72-hour PMP storm for the basin. The method of storm development is similar to the procedure outlined in HMR 52. An important difference, however, is in the orientation of the storm. The HMR 52 procedure allows the storm to be oriented for maximum precipitation over the basin. If this orientation deviates

more than 40 degrees from the preferred orientation for the region, a reduction factor is taken on the PMP depths for the storm. The EPRI/HUG procedure allows the storm to be oriented a maximum of 50 degrees from the preferred orientation. This prevents the use of a storm alignment that is not representative for PMP type storms. The axis of the Michigamme River basin is oriented approximately 10 degrees to the east from north, while the preferred storm orientation for the basin is 280 degrees. The placement of the elliptical storm pattern is shown in Figure 1. As shown, the storm does not align closely with the basin when rotated within the specified limits. This resulted in an additional reduction in basin PMP beyond the lower PMP values found in the EPRI/HUG study.

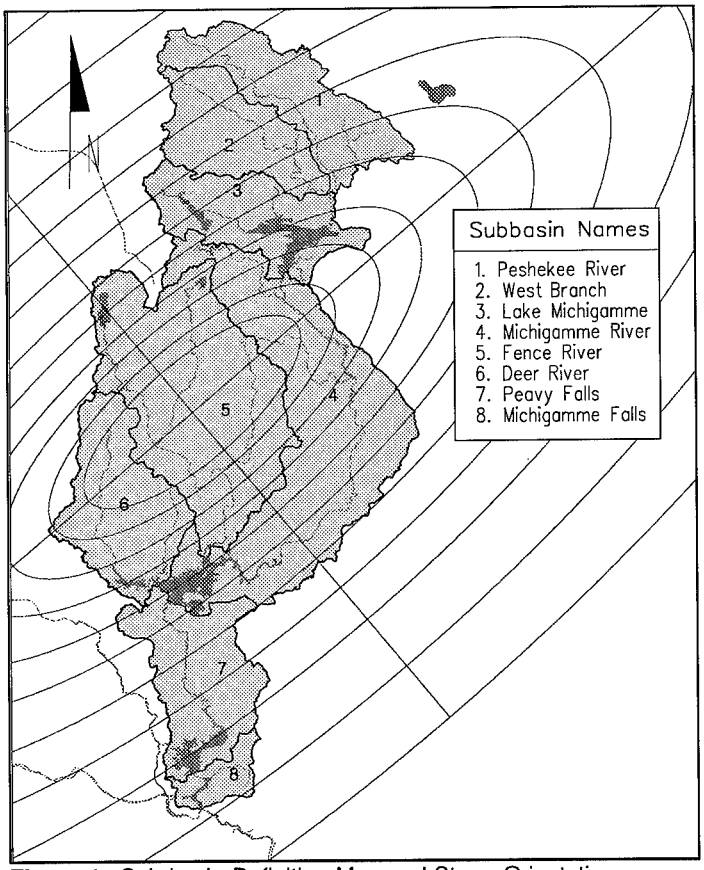

Figure 1 Sub-basin Definition Map and Storm Orientation

After determining the location and orientation of the storm, the GIS system was used to determine the contributing area from each isohyet for the individual sub-basins. The 72-hour precipitation and temporal distribution of precipitation increments were computed for each sub-basin and included in the HEC-1 model.

PMF Model Description

The structure of the PMF model was dictated by the number and location of sub-basins. A schematic diagram of the PMF model is shown in Figure 2. Oval shapes and solid lines represent computation and combination of sub-basin hydrographs in the HEC-1 model. Dashed lines and triangles represent dynamic channel and reservoir routing using the NWS DAMBRK model.

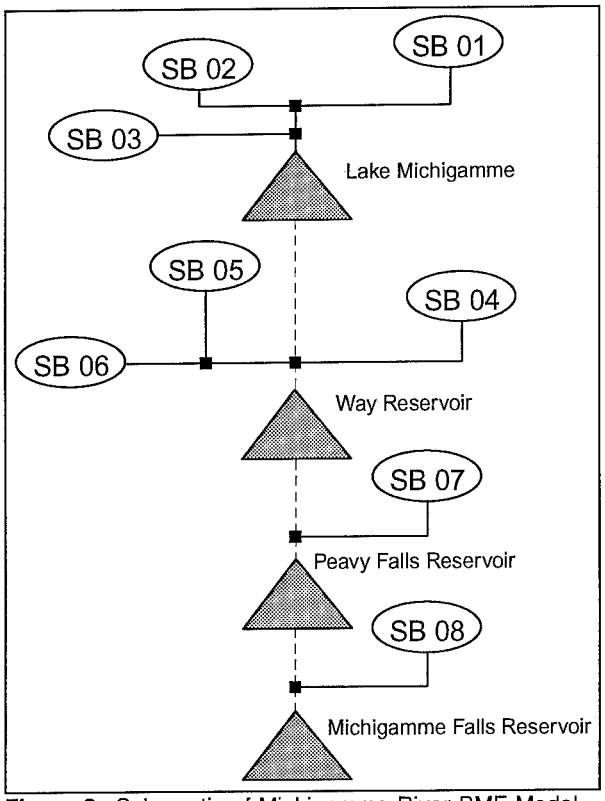

Figure 2 Schematic of Michigamme River PMF Model

The channel from Lake Michigamme to Way Reservoir was previously modeled using Muskingum routing in the HEC-1 model. Modeling this reach with the DAMBRK model resulted in increased storage and attenuation in Lake Michigamme, increased travel times through the channel, and additional channel storage and attenuation due to the presence of marshlands adjacent to the channel. This delayed the arrival at Way Reservoir of peak flow from the first three sub-basins, flattening the hydrograph and reducing the peak inflow. Figure 3 shows the hydrograph at Way Dam, together with the previous PMF hydrograph. The relative shapes of the hydrographs show that the reduction in PMF peak discharge is greater than the reduction in PMF volume.

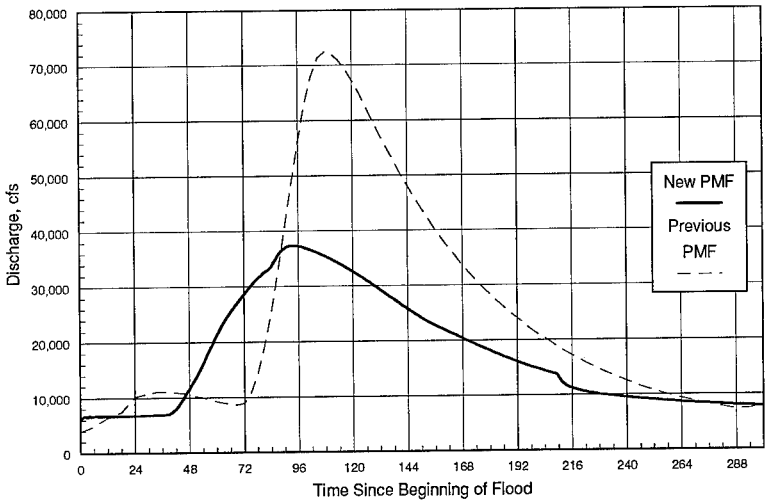

Figure 3 PMF Inflow Hydrographs to Way Dam

Conclusions

Because this study was performed as part of an overall plan for compliance with FERC requirements for spillway capacity at Way and Michigamme Falls Dams, a basic methodology was chosen that would be acceptable to FERC. To maintain the adequacy of spillway expansion designs while controlling the costs of modifications, an expanded level of detail and advanced technologies were employed in the PMF analyses. While the updated PMP study was perhaps the most important factor in reducing the peak discharge, the revised unit hydrographs, infiltration parameters, and routing model significantly impacted the shape and volume of the new PMF hydrograph. These factors will have a significant impact on the nature and cost of spillway upgrades at Way and Michigamme Falls Dams.

A Guideline for the Determination of Probable Maximum Flood for Civil Works

John J. Cassidy[1], Samuel L. Hui[2], Jerrold W. Gotzmer[3] and Douglas I. Morris[4]

Abstract

Guidelines are presented for the development of probable maximum flood (PMF) hydrographs for civil works. The development of these Guidelines was sponsored by the Electric Power Research Institute and cofunded by the Federal Energy Regulatory Commission. The Guidelines provide detailed procedures and considerations for the development of inflow PMF hydrographs primarily intended for use in the assessment of dam safety. It is assumed that full information on the site-specific probable maximum precipitation is available for the PMF calculation. The intent of the Guidelines is to provide for uniform procedures for PMF hydrograph development which will hopefully result in an increased degree of consistency in the work of hydrologic engineers. Although they were written by the Bechtel Corporation, the Guidelines were reviewed in detail by a peer committee appointed by EPRI. After review by consultants and representatives of the industry, FERC intends to make the Guidelines a part of their Engineering Guidelines for the Evaluation of Dam Safety.

Introduction

In the assessment of dam safety it is generally necessary to develop an inflow probable maximum flood (PMF) hydrograph for the assessment of safety of dams whose failure would result in a hazard to life and/or great economic loss [FERC 1987]. The inflow PMF hydrograph must then

[1] and [2] Manager and Chief Hydrologic Engineer, respectively, Hydraulics/Hydrology Group, Bechtel Corporation, San Francisco, California 94105.
[3] Senior Hydrologic Engineer, Federal Energy Regulatory Commission, Washington, DC.
[4] Project Manager, Electric Power Research Institute, Palo Alto, California, 94303.

be routed through the reservoir to determine the maximum resulting reservoir elevation and the maximum flow past the dam. Thus, the development of the inflow PMF hydrograph has an important effect on the assessment of the safety inherent in the operation of the dam. Although many PMF inflow hydrographs have been developed for dams throughout the United States, the procedures used in the hydrologic development and the results, in terms of peak flow rate and timing, have been variable. Part of this variability is due to the fact that hydrology, at its current state of art, is far from an exact science because of the large number of variables that affect surface runoff.

A workshop on probable maximum precipitation (PMP) and PMF, sponsored by the Federal Emergency Management Agency (FEMA) and held at Berkeley Springs, West Virginia in April, 1989, defined a number of research topics that could improve hydrometeorological estimates of PMP, particularly for some regions of the U.S. In addition it recommended that a standard be developed for the computation of PMF hydrographs [FEMA 1991]. As a result of the recommendations of that workshop, the Electric Power Research Institute (EPRI) sponsored the development of a set of guidelines for the development of PMF hydrographs for civil works; the project was cofunded by the Federal Energy Regulatory Commission (FERC). The intent of EPRI was that experienced and competent hydrologists, by following the Guidelines, would be able to produce PMF hydrographs with a maximum of consistency.

Although this paper is of necessity too short to completely describe all of the procedures which are recommended in the Guidelines, it does summarize the specific considerations which were covered.

General Overview of The Guidelines

While recognizing that a number of methods can be used for the development of an inflow PMF hydrograph, the Guidelines recommend that unit-hydrograph theory be used and, in particular, that the U.S. Army Corps of Engineers program HEC-1, Flood Hydrograph Package [HEC-1], be used in the application since that program has been widely used for such developments and the experience so achieved is valuable.

The Guideline was prepared specifically for drainage basins up to 10,000 square miles in area although the size of the drainage area is not necessarily a limiting factor. It provides recommendations for review of the project and the pertinent drainage area, the hydrologic and project-specific data to be obtained, the analysis and use of that data in the development of the required unit hydrographs, and the development of the inflow PMF hydrograph using the unit hydrographs, and the routing of the inflow PMF to

obtain the maximum resulting reservoir level and the maximum flow rate passing the dam. Guidelines are provided for the subdivision of drainage basins when desirable and for the development of unit hydrographs for basins where the available hydrologic data is totally adequate to provide confidence in computation of the PMF hydrograph. In addition, guidelines are provided for the development of unit hydrographs when less-than-adequate hydrologic data is available from gages within the basin.

Snowmelt contributions are considered in both the analysis of historic flood data and in the development of the PMF hydrograph using developed unit hydrographs.

Specific procedures and methods are recommended throughout the Guidelines and are summarized in a procedural flow chart. Potential problems and specific considerations that should made are enumerated in the form of *Caution* statements through-out the text. Although the Guidelines are specific and recommend specific methods, they do not need to be rigidly applied. The Guidelines recognize that there are other entirely valid methods in existence which may be readily available and may be entirely satisfactory for application to the project. For such cases the Guidelines state that such methods may be used but must be documented and their applicability verified.

Acquisition and Review of Field Data

The most vital of all of portions of the development of the inflow PMF hydrograph is the acquisition and review of the available project and hydrologic data, since the data obtained will affect not only the procedures to be followed in developing the PMF hydrograph, but the final results as well. A field visit to the project and to the drainage area is vital and should be used to obtain information on the project and drainage basin as follows:

- Type, capacity, condition, and operating history of the spillway, its gates, and the outlet works.
- Hydrologic conditions in the drainage basin including soil types, type and extent of cover, and general hydrologic use.
- Existence of upstream dams, their type, spillway and outlet-works capacity, and operating policy during passage of extreme floods.
- Geologic and/or soil features of the drainage basin that may have an important effect on runoff characteristics such as areas having unusually large infiltration rates (large impermeable areas such as rock outcrops) or areas having smaller than average infiltration rates such as marshes, lakes, areas covered with deep sand or fractured basalt, or areas which are closed and do not contribute to runoff.

During field reconnaissance, for an existing project, operating personnel should be interviewed to obtain first-hand history of operations during passage of extreme floods as well as eye-witness accounts of flood levels and records of operations and/or flood flows. It is particularly important to obtain information about operations during passage of the historic floods identified in the search for hydrologic data.

Soil characteristics for the basin are an important requirement. The Guidelines that the soils in the basin be classified in terms of the U.S. Soil Conservation Service (SCS) hydrologic types A, B, C, and D where A soils are highly porous with large minimum rates of infiltration and D soils are tight with correspondingly low minimum infiltration rates. The characterization of the soils can be done from soil maps sometimes available from state offices of the SCS or from the digital State Soil Geographic Data Base available from the SCS National Cartographic and GIS Center in Fort Worth, Texas.

Acquisition and Review of Hydrologic Data

All historic floods which have been recorded within and near the basin should be identified in order to identify the rainfall and streamflow data which must be obtained. All raingages which exist or have existed within and near the basin should be located and rainfall data for the storms which produced the historic floods should be obtained. Stream-flow records for the historic floods should also be obtained for all stream-gages located within and below the drainage basin.

If some of the historic floods were influenced by snowmelt, or if the critical PMP is apt to fall in the season when a snowpack can be expected in the basin, it will also be necessary to obtain snowmelt records for snow courses within and near the basin.

All data must be carefully reviewed for quality as well as its adequacy for the purpose of determining the required unit hydrographs or the inflow PMF hydrograph.

Development of the Unit Hydrographs

It is desirable to have concurrent rainfall and streamflow records for at least four or five historical floods which have occurred on the basin. The floods selected for analysis should always be the largest and most severe of the historic floods for which records are available.

It will be necessary to make a judgement as to whether or not the available data is sufficient to allow confidence in the computation of unit

hydrographs and the inflow PMF. Special treatment is required for basins for which data is inadequate, which may include basins for which both raingages and streamgages are located in the basin, but the historical data is sparse.

The Guidelines recommend that Clark's unit hydrograph be used for all unit-hydrograph computations because it is included in the HEC-1 package and a good deal of experience is available for its use

(Basins With Adequate Data)

Basins with adequate data will have concurrent rainfall and streamflow records for a least four large historic floods within the basin. For these cases unit hydrographs can be readily developed using the existing data and no special treatment will be required.

(Basins with Inadequate Data)

The Guidelines make three recommendations for basins for which available hydrologic is inadequate to provide confidence in the computation of unit hydrographs and the inflow PMF hydrograph.

1. A regional approach is recommended in the Guidelines. Since regional studies can be time consuming and expensive an initial attempt should be made to locate previously developed unit hydro-graphs or unit-hydrograph parameters which are applicable for the basin and can be used with confidence. Regional water-resource agencies should be contacted to determine if the results of regional studies may be available. If the results of such studies are available, a unit hydrograph should be developed and tested by using it to reconstitute a historic flood.

2. If a suitable synthetic unit hydrograph or applicable unit-hydrograph prove not to be available, hydrologic data and basin characteristics must be obtained for gaged basins in the region of interest. Clark unit hydro-graphs must be developed for those basins; a relationship between the Clark unit-hydrograph parameters R and T_c and physical basin characteristics, such as area, slope, and stream length, should be investigated using statistical regression analysis (R is the Clark unit-hydrograph reflecting storage in the basin and T_c is the basin's time of concentration). Once a satisfactory relationship has been developed, a unit hydrograph for the basin of interest can be formulated. The Clark unit hydrograph is recommended for this analysis, because it has been used frequently in regional analyses in the United States and the parameter $R/(T_c + R)$ has been found to often be a constant for a region.

3. For drainage areas smaller than 100 square miles, the Guideline recommend that the U.S. Soil Conservation Service synthetic unit

hydrograph be used to develop the inflow PMF hydrograph.

(Subdivision of the Basin)

In many cases, for gaged or ungaged basins, it will be necessary to subdivide the drainage basin in order to develop a satisfactory inflow PMF hydrograph. Subdivision will be required when:

- Rainfall on portions of the basin deviates strongly from the average due to orographic effects.
- Portions of the basin have significantly different infiltration characteristics than the average.
- Upstream reservoirs exist whose storage will significantly effect the PMF hydrograph's characteristics.
- Physical characteristics of the basin, such as slope or cover, differ strongly from the average.
- Streamgage data exists for more than one gage within the basin.
- Snow covers only a portion of the basin.

When the basin is subdivided, streamgage records will generally not be available for each subarea. For such subareas a synthetic unit hydrograph may be used. Routing of streamflow between subareas will be required; either the Muskingum or the Muskingum-Cunge method may be used. The combination of unit hydrographs for the subareas and the routing process provide a "runoff model" which is used to develop the inflow PMF hydrograph.

Representative Unit Hydrographs

The historical floods identified should be divided into those used for calibration and those used for verification of unit hydrographs. In general the largest of the floods should be included in those used for calibration while the second largest should be included in those used for verification. Unit hydrographs should be developed for each calibration flood and verified for each verification flood. A representative unit hydrograph must be chosen that provides the best possibility of accurately computing an inflow PMF hydrograph. Generally this will be the one which best duplicates the peak flow of the largest historic flood. For subdivided basins, it will be the "runoff model" which must be calibrated and verified.

Non-linear Effects

The unit-hydrograph theory assumes that peak flow rate of runoff is linearly proportional to excess rainfall. However, the runoff process is known to be non linear and considerations should be given to the need for adjustment of the unit hydrographs used for these non-linear effects. If only

channel routing effects are considered, the lag time associated with larger floods will be shorter than small floods because the flood-wave velocity increases as depth in the channel increases. Increases in channel depth also produce a compensating effect if the channel rises out of its banks and significant out-of-bank storage is created; storage reduces the peak rate of flow by delaying the downstream progress of the flood wave. The Guidelines consider non-linear corrections in the following way on the basis of documented research [Pilgrim 1988]:

- When the historic floods, used in the unit-hydrograph analysis, were clearly out of bank and significant over-bank storage existed, no increase in the unit-hydrograph is required.

- When the historic floods, used in the unit-hydrograph analyses, were not clearly out of bank, but significant overbank storage would result during the PMF, an increase in the unit-hydrograph peak of up to 15% should b considered.

- If the cross sections of the stream channels in the drainage basin are V-shaped the unit-hydrograph increases in the unit-hydrograph peak of up to 20% should be considered.

Development of Hydrologic Criteria for the PMF

When using the calibrated and verified unit hydrograph or "runoff model" to compute the PMF inflow hydrograph, it will be necessary to consider potential operation of the project as well as possible antecedent and coincident floods. Antecedent floods affect basin infiltration rates, initial abstractions of rainfall, and the starting elevation of the reservoir when the PMF enters. The Guidelines make recommendations for such events.

(Infiltration)

Applicable minimum infiltration rates should be assumed to occur during the PMP. A minimum infiltration rate for each subarea analyzed should be established using the applicable minimum rate for the SCS hydrologic soil type established for the subarea. Infiltration rates determined during the unit-hydrograph analyses can be a guide in selecting the applicable minimum infiltration rate, but can be much greater if the basin was dry before the historic storm occurred.

(Operation of the Project)

It will be necessary to carefully evaluate the operating history of spillway gates and outlet works of the project to establish the policy to be followed during passage of the inflow PMF. If flashboards or stop logs are normally used on the spillway during operation it will be necessary to know

the dates when they are in place and when they are removed. If they are normally in place during the season when the PMP would occur, the spillway and/or outlet works capacity must be set accordingly. Considerations must also be given to the possibility that gates may be inoperable during the PMF or that operators may not be able to reach the gates during a severe storm in order to carry out emergency operations.

(Snowmelt)

If the critical PMP can be expected to occur during a season when snowpack can be expected on at least a portion of the basin, a 100-year snowpack should be assumed to occur. Temperatures at the snowline and a lapse rate should be assumed in accordance with historical values which have occurred during major snowmelt-influenced floods of the past.

(Initial Reservoir Elevation)

In some areas of the U.S. lesser storms often precede major storms by one to three days. Such storms will often saturate the basin, causing infiltration to occur at minimum rates, and raise the reservoir surface to a higher-than-average elevation. The Guidelines make four alternative recommendations to allow for adequate conservatism in routing the inflow PMF through the reservoir:

1. The reservoir may be assumed to be at its annual maximum normal operating level when the inflow PMF begins;

2. Or, assume that the inflow PMF is preceded by a flood due to a 100-year rainfall on the basin. At the beginning of this antecedent flood, the reservoir level is assumed to be at the normal operating level for the season as given by the reservoir operating rule curve.

3. Or, the reservoir may be assumed to be at the maximum operating level for the season as given by a "wet-year" operating rule curve at the time the inflow PMF begins.

4. Or, a detailed study of antecedent floods may be made in order to arrive at the magnitude and lead time applicable for a reasonable flood which may occur prior to the beginning of the inflow PMF.

FERC will consider the dam to be safe from a hydrologic standpoint if the inflow PMF can be passed without endangering the dam or its appurtenances during at least one of these scenarios.

(Routing of the PMF)

The inflow PMF should be routed through the reservoir initially assuming that the pool is level. However, considerations should be given to

the use of fully dynamic routing if the reservoir is long and narrow. Level-pool routing assumes that the flood wave traverses the reservoir instantaneously, which is generally not the case.

Conclusions

These Guidelines have been developed in an attempt to increase consistency and repeatability in the development of PMF hydrographs for civil works. The methodology recommended is neither new nor unique but have been proven, generally accepted, and documented by the profession. Although the initial draft of the Guidelines has been completed, they are expected to be a living document subject to change as experience in their use accumulates and newer, better hydrologic procedures are developed through research and practice.

References

Federal Energy Regulatory Commission (1987), Engineering Guidelines for the Evaluation of Hydropower Projects, 0119-2, Washington, D.C.

Federal Emergency Management Agency (1991), Probable Maximum Precipitation and Probable Maximum Flood Workshop, Proceedings of the Workshop, May 1- 4, Washington, D.C.

Pilgrim, D.H., I.A. Rowbottom, and G.L. Wright (1988), "Estimation of Spillway Design Floods for Australian Dams," Transactions, 16th Congress of the International Commission on Large Dams, San Francisco, California.

EXTREME RAINFALL PROBABILITIES

George A. Harper[1], Member, A.S.C.E.,
Thomas F. O'Hara[1], and
Douglas I. Morris[2]

Abstract

A method to estimate probabilities of extreme rainfalls for a specific duration and areal coverage was developed. The method uses a rainfall data base which includes all hourly and daily rainfall data collected by the NCDC. Rainfall contour maps at selected low probability levels and rainfall frequency relationships were developed for the study area. Results indicate that the method can be used along with other techniques in the determination of Probable Maximum Precipitation (PMP) values for specific basins or regions.

Although the study was performed for 24-hour duration, 2,590 km^2 (1,000 mi^2) areal rainfalls, the method can be applied to other durations and areas. However, there is a lower limit on area size which is dependent on rainfall station density.

Introduction

A methodology was developed to investigate the viability of estimating probabilities of extreme rainfalls using daily and hourly rainfall data that could be used, along with other techniques, in site-specific PMP evaluations. A recent site-specific PMP estimate (Board of Consultants, 1987) included consideration of the 10^{-6} annual probability rainfalls along with storm transposition results in setting a site-specific PMP value for a Probable Maximum Flood (PMF) study of a dam.

---

[1]Principal Engineer, Yankee Atomic Electric Company
580 Main Street, Bolton, MA 01740-1398

[2]Project Manager, Electric Power Research Institute,
3412 Hillview Avenue, Palo Alto, CA 94303

The method presented here uses all available hourly and daily rainfall data in the study area to produce more reliable probability estimates for extreme rainfall events at a particular location. This type of analysis applies the concept of trading space, i.e., the many sites, for time to effectively increase the length of record at any individual site.

At present, high hazard dams and other critical facilities such as nuclear power plants, are evaluated to a flood resulting from the PMP. This flood is commonly referred to as the PMF. Various National Weather Service (NWS) reports present generalized PMP values for different durations and areal coverage. These NWS estimates are typically in the format shown in Figure 1. The figure shows the 24-hour, 2,590 km^2 (1,000 mi^2), all season PMP estimates east of the 105th meridian.

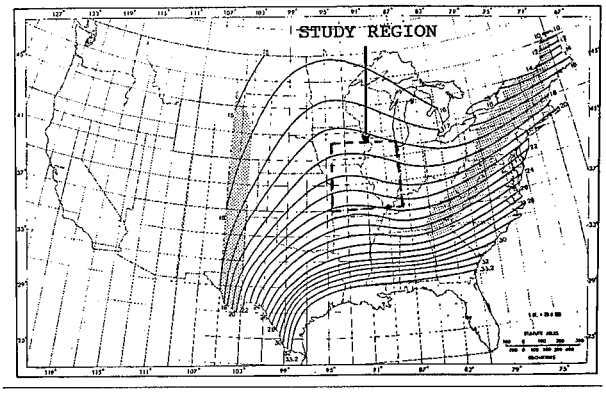

FIG. 1. All Season PMP (in.) for 24 Hours, 2,590 km^2 (1,000 mi^2) From Schreiner and Riedel (1978)

Today many facility owners are opting to have a site-specific PMP estimate developed for their project area. The attractive feature of a site-specific study is that a more detailed evaluation of possible PMP producing mechanisms and, therefore, a more definitive PMP estimate can be made versus simply relying on generalized estimates.

This study investigated a new methodology for use in site-specific PMP evaluations. A test study region, not subject to orographic effects, of 258,974 km^2 (100,000 mi^2) in the central United States was chosen for methodology development. This area is shown on Figure 1. For this demonstration study the 24-hour duration, 2,590 km^2 (1,000 mi^2) areal rainfalls were chosen for evaluation.

Rainfall Data Base

The rainfall data base included all hourly and daily rainfall data collected by the National Climatic Data Center between 1949 and 1988, giving a total period of record of 40 years. The rainfall data base was obtained on CD-ROM (Compact Digital Read Only Memory) format from a private vendor. Previous to 1949 the data base is not completely digitized and, therefore, is not available on the CD-ROM format.

All rainfall recording stations within an area of about 323,718 km^2 (125,000 mi^2) were used. This data region was selected larger than the study area to minimize edge effects.

The daily rainfall values were converted to hourly values using an inverse distance weighting algorithm. The two closest hourly stations in each of the four quadrants surrounding the daily station location, as shown in Figure 2, were used to estimate the hourly rainfalls at the daily station location. The estimates were adjusted so that the sum of the hourly estimates matched the actual observed 24-hour value. To avoid processing data that could not possibly impact low probability rainfall estimates a lower bound cutoff value of 5 mm (0.2 inches) was specified and no daily rainfalls below this cutoff were processed. A computer program, CNVRTDH, was written to perform the daily to hourly rainfall conversion.

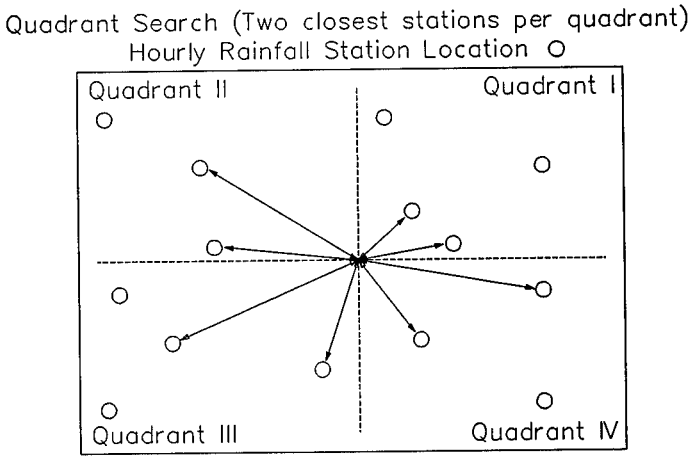

FIG. 2. Quadrant Search Used in Program CNVRTDH

Data from 417 daily recording stations were converted to synthetic hourly records using CNVRTDH. In addition, a total of 302 actual hourly recording stations were available in the study region for a total of 719 data sets.

At any given time during the study period, active rainfall station density in the study region averaged about one station per 622 km^2 (240 mi^2).

The raw data base includes two data flags which were considered throughout all data processing. A flag for missing data indicated that between two specified time periods the station was temporarily out of service. A flagged station was not used in any calculations during the out of service period and was replaced by the next closest station. The other flag of interest was for accumulating data. During this specified time period only the total rainfall was recorded and hourly or daily information was not available. Again when this occurred another closest station with valid data was used in its place.

Basin Annual Maximum Series

The study area was subdivided into 100 approximately square basins, in a 10x10 array, each with an area of 2,590 km^2 (1,000 mi^2). A computer program, BASRAIN, was written to generate the annual maximum series for each of the 100 individual basins for the 40-year study period. The computer code could readily be modified to handle other more complicated geometric basin shapes.

The program first subdivides each basin into 100 subbasins. The closest rainfall recording station to each of the 100 subbasin centroids is then determined. If any of the stations are found to have missing or accumulating flags, the next closest station is reassigned to the subbasin.

For each hour during the study period the basin rainfall is estimated using a modified Thiessen polygon method. The Thiessen polygon method is based on perpendicular bisectors of the lines connecting nearby stations to form a polygon around each station. The area of the basin within a polygon is assigned rainfall equal to that polygon's station. In this study, the polygons were approximated by assigning each of the 100 subbasins the rainfall from the nearest station. The procedure is shown in Figure 3. Results using the polygon approximations were nearly identical to the traditional polygon approach.

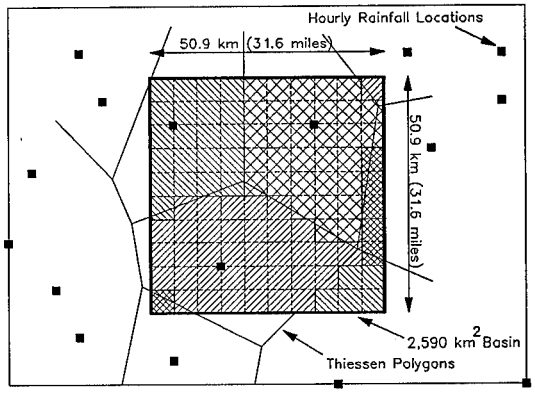

FIG. 3. Hourly Rainfall Estimation for Basins Used in Program BASRAIN

The highest 24-hour consecutive rainfall total during the year is the annual maximum value for the year. The entire set of 40 values over the period of record make up that basin's annual maximum series.

The 10x10 basin array which formed the study area could be placed down with some leeway onto the slightly larger data region. It was acknowledged early on in the study that basin placement may require careful consideration. The concern was that actual 24-hour, 2,590 km^2 (1,000 mi^2) extreme rainfalls could be missed if an historical maximum 2,590 km^2 (1,000 mi^2) rainfall was split into two or more basins. To address this issue a literature search was performed to identify major 24-hour, 2,590 km^2 (1,000 mi^2) rainfall values from published depth-area-duration (D-A-D) charts.

For several major events, the program BASRAIN was used to search out these events. Table 1 presents several events and the published D-A-D as well as BASRAIN calculated rainfalls. As seen the program was able to find the correct date of occurrence and most of the rainfall, varying between about 70 to 95 percent of the published D-A-D value. The lower rainfalls found are due to the fact that the program was using square shaped basins versus the actual storm shape of the D-A-D and the published latitude-longitude storm centers may not be optimally positioned. From this analysis the 100 basin array was located on the study area so as to reproduce the highest rainfall. This was referred to as DROP 1. Subsequently BASRAIN was rerun twice for other array centerings to determine the sensitivity of the results to basin array location.

TABLE 1

Major Historical 24-Hour, 2,590 km^2 Rainfalls
in Study Area Between 1949 and 1988

End Date	24-Hours, 2,590 km^2 Rainfall	
	Published D-A-D	BASRAIN
10/10/54	9.5	6.7
6/15/57	11.0	8.7
6/28/57	9.4	8.7
7/13/57	8.7	8.3
9/13/61	7.1	5.2

Individual Basin Frequency Analysis

A frequency analysis was performed for each of the individual basin annual maximum series. Annual probability of occurrence levels of interest were chosen as 10^{-1}, 10^{-2}, 10^{-3}, 10^{-4}, 10^{-5}, 10^{-6} which correspond to return periods of 10^1, 10^2, 10^3, 10^4, 10^5, and 10^6 years, respectively.

For this project, it was decided to use the L-moment methodology as described in Hosking (1990). The L-moment method provides an objective approach to select the appropriate statistical distribution.

Recent applications of L-moments are described in Adamowski et al. (1990) and Schaefer (1990). FORTRAN routines which greatly facilitated the use of the method of L-moments were provided in Hosking (1991a). Various IBM FORTRAN routines were incorporated into the computer programs written for the frequency analyses. To evaluate which statistical distribution would be used in the frequency analyses a theoretical L-moment ratio diagram was prepared after Hosking (1991b). The L-moment ratio diagram is a graph of L-Skewness versus L-Kurtosis. The L-moments for each of the 100 individual basins were computed. The basin L-moments were plotted on the L-moment ratio diagram as shown in Figure 4. It was determined using several statistical tests that basin L-moment data pairs most closely plot around the generalized extreme value (GEV) relationship. Therefore, the GEV distribution was chosen for the frequency analyses.

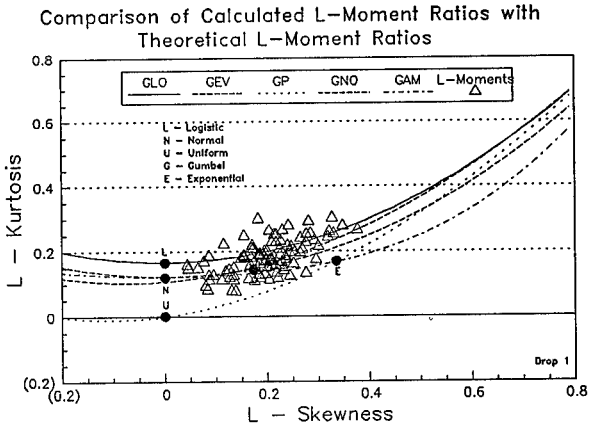

FIG. 4. L-Moment Ratio Diagram and Individual Basin L-Moments

A computer program, GEVFIT, was developed and a rainfall frequency relationship was developed for each basin. Rainfall depth contour plots across the study area similar to those described below for the regional analysis were prepared.

At low probability levels the variability in the rainfall estimates precluded producing meaningful contour plots.

Regional Frequency Analysis

A regional frequency analysis uses data from many sites to produce more reliable quantile estimates for extreme events at a particular site. This type of analysis uses the concept of trading space, i.e., the many sites, for time to effectively increase the length of record at any individual site.

Regional frequency analyses using L-moments are described in Wallis (1989), Hosking and Wallis (1990), Adamowski et al (1990) and Schaefer (1990). FORTRAN routines to perform these analyses using L-moments are described in Hosking (1991a).

For the regional study, the individual basin L-moments were combined to produce one set of regional L-moments. The regional GEV parameters and the quantiles were then estimated from the regional L-moments. Individual site quantile estimates are the product of the site mean of the annual maximums and the regional quantile estimates. Contour plots of rainfalls at annual probability levels of 10^{-3} and 10^{-6} are shown in Figures 5 and 6.

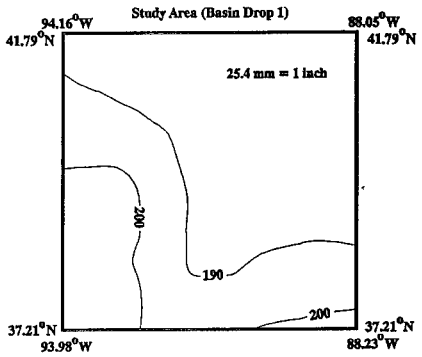

FIG. 5. 10^{-3} Annual Probability Rainfall Contours (mm)

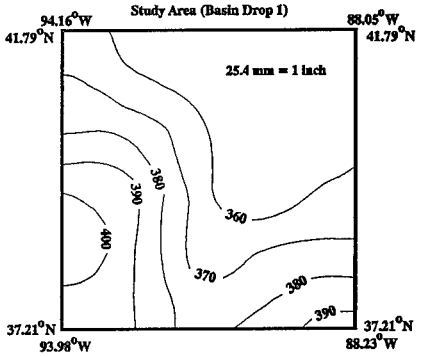

FIG. 6. 10^{-6} Annual Probability Rainfall Contours (mm)

All 100 basin rainfall probability relationships are plotted on Figure 7 along with the mean for the entire study area.

Results from the other two basin array centerings show that the regional frequency results are not very sensitive to placement of the basin array.

Results

Results of the study are shown on Figures 5 through 7. These figures show the 24-hour, 2,590 km^2 rainfall estimates associated with various probability levels. At a given probability level, the rainfall estimates increase to the south. The increase from the northern to the southern limits of the study area is about 10 percent. This increase is slightly less than the increase indicated in Figure 1.

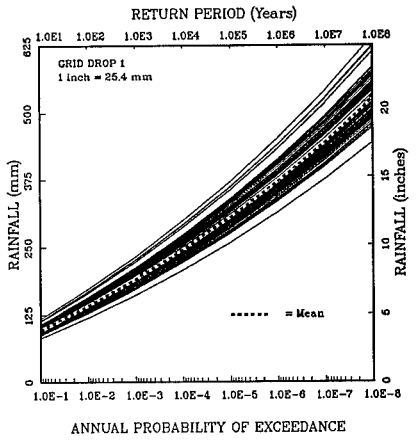

FIG. 7. Basin and Study Region Mean 24 Hour 2,590 km^2 Rainfall Frequency Relationships

Comparing the NWS estimates for the 24-hour 2,590 km^2 PMP in Figure 1, which range from 18 inches (457 mm) to 22 inches (559 mm), to the mean probability relationship shown in Figure 7 implies that the annual probability of the NWS PMP estimates in the study area are on the order of 10^{-8}.

Summary & Conclusions

A method to estimate the probabilities of extreme rainfalls for a specific duration and areal coverage was investigated. The method uses a rainfall database which includes all hourly and daily rainfall data collected by the NCDC. Contour plots and frequency relationships were developed as shown in Figures 5 through 7. Comparison with NWS PMP generalized estimates for the same duration and area implies the annual probabilities of the NWS PMP to be on the order of 10^{-8}. This methodology should be useful in the determination of site-specific PMP estimates. Contour plots similar to those shown in Figures 5 and 6 at various probability levels would be a valuable supplementary guide to estimating PMP magnitude and variation from one region to another. A recent site-specific PMP estimate (Board of Consultants, 1987) included consideration of the 10^{-6} annual probability rainfalls along with storm transposition results in setting a site-specific PMP value for a PMF study of a dam.

Acknowledgments

This study was performed under contract to the Electric Power Research Institute (EPRI). The EPRI contract project manager is Mr. Douglas I. Morris. The L-moment FORTRAN routines used in the frequency analyses were made available by Mr. J.R. M. Hosking of the IBM Research Division. The research project was originally conceived by the late Dr. Vance A. Myers who also served as project consultant during the early phases of the project.

APPENDIX REFERENCES

Adamowski, K., and Pilon, P.J., and Alila, Y. (1990). "Regional Analysis of Annual Maxima Precipitation." International Workshop on Urban Rainfall and Meteorology, St. Moritz, Switzerland, 2-4 December 1990.

Board of Consultants (1987). "Calculation of the 24-Hour PMP for the Upper Deerfield Drainage Above Harriman Dam." New England Power Company, Westborough, MA, 243 pp.

Hosking, J.R.M. and Wallis, J.R. (1990). "Regional Flood Frequency Analysis using L-Moments." Research Report RC-15658, IBM Research Division, Yorktown Heights, NY, 12 pp.

Hosking, J.R.M. (1990). "L-Moments: Analysis and Estimation of Distributions using Linear Combinations of Order Statistics." J. R. Statist. Soc. B, 52, No. 1, pp. 105-124.

Hosking, J.R.M. (1991a). "Fortran Routines for Use with the Method of L-Moments, Version 2." Research Report RC 17097, IBM Research Division, Yorktown Heights, NY, 117 pp.

Hosking, J.R.M. (1991b). "Approximations for Use in Constructing L-Moment Ratio Diagrams." Research Report RC 16635, IBM Research Division, Yorktown Heights, NY, 3 pp.

Schaefer, M.G. (1990). "Regional Analyses of Precipitation Annual Maxima in Washington State." Water Resources Research, Vol. 26, No. 1, pp. 119-131.

Schreiner, L. C. and Riedel, J. T. (1978). "Probable Maximum Precipitation Estimates, United States East of the 105th Meridian." Hydrometeorological Report, No. 51. National Weather Service, National Oceanic and Atmospheric Administration, U.S. Department of Commerce, Washington, DC, 87 pp.

Wallis, J.R. (1989). "Regional Frequency Studies using L-Moments." Research Report RC 14597, IBM Research Division, Yorktown Heights, NY, 16 pp.

PROBABLE MAXIMUM PRECIPITATION STUDY FOR MICHIGAN AND WISCONSIN: PROCEDURES AND RESULTS

Edward M. Tomlinson[1] and Doug Morris[2]

INTRODUCTION

Probable Maximum Precipitation (PMP) is defined by the AMS Glossary as:

> "The theoretically greatest depth of precipitation, for a given duration, that is physically possible over a particular drainage area at a certain time of year."

Since the mid-1940's, several government agencies have developed methods to calculate PMP estimates for various sections of the United States. These agencies include the National Weather Service, Army Corp of Engineers and the Bureau of Reclamation. The PMP estimates derived are used to calculate the Probable Maximum Flood (PMF) which, in turn, is used for hydraulic design purposes.

Hydrometeorological Report #51 (HMR 51) provides generalized PMP values for various area sizes and durations for US locations east of the Rocky Mountains.

The Hydroelectric Users Group of Wisconsin-Michigan and the Electric Power Research Institute sponsored a regional study to determine PMP values for Wisconsin and Michigan. This study incorporates regional considerations for the Great Lakes area and addresses PMP estimates for all-season and for the cool season storms.

[1]Chief Scientist, North American Weather Consultants, Subsidiary of TRC Environmental Corp. 1293 West 2200 South, Salt Lake City, Utah 84119

[2]Project Manager, Hydroelectric Generation and Renewable Fuels EPRI, 3412 Hillview Ave., Palo Alto, California 94303

The study continued the basic approach used in prior studies to estimate PMP. This methodology includes the following:

- Identifying major flood producing storms which have occurred over and adjacent to the study region
- Maximizing each storm's precipitation
- Moving the storm's precipitation pattern over the study region, adjusting for geographic and meteorological variations (This procedure is called transpositioning)
- Analyzing the largest precipitation amounts by enveloping the rainfall amounts

This methodology was updated with computer applications and refinements to the moisture parameterization. The goal was to maintain as much continuity as possible with previous studies while providing more reliable PMP estimates for the study region.

REGIONAL TOPOGRAPHY

The study domain lies within the Great Lakes region of the United States mid-west (approximately 82°-93°W, 41.5°-47°N). The topography is characterized by low, rolling hills covered by forest or farmland. The topography is not significant enough in elevation to affect precipitation patterns and large scale weather phenomena. The proximity to the large inland lakes, do exert some control on local climate, weather patterns, and precipitation amounts.

The largest storms that have occurred within the study domain and immediate surrounding area form the data base necessary to develop PMP estimates. Storms from surrounding areas with similar meteorological controls may be transposed into the study domain when it can be established that these storms, with appropriate adjustments considering topography and available precipitable water, could have occurred over the study domain. The boundaries of the storm search area are the transposition limits defined by significant topography or changes in meteorological controls such as available atmospheric moisture.

The major data set utilized to determine the largest rain events of record were the precipitation observations archived by the National Climate Data Center (NCDC), in Asheville, North Carolina. Other sources included the

storm list from HMR51 and various documents from state climatologist offices.

Analyses of these data identified the largest storms which have occurred within the storm search area. Seventeen of the 25 storms identified had previously been listed in HMR 51. Additionally eight cool season storms were identified, i.e., storms which could have occurred during the times of year with snow covered or frozen ground conditions. Figure 1 shows the storm locations.

STORM DEPTH-AREA-DURATION ANALYSIS

The purpose of a depth-area-duration (D-A-D) analysis is to determine the depth and areal extent of precipitation over various temporal intervals for a particular storm event. That analysis provides the hydrologist and/or engineer with storm precipitation data which can be uniformly compared to similar events and may be used for various hydrologic scenarios. In this study, the methods used in past D-A-D analyses are kept fundamentally intact, but the procedures used to derive the final product have been refined. The new procedures are enhancements which take advantage of computer-based technology, and advanced statistical techniques, increasing the objectivity and efficiency of the D-A-D analyses.

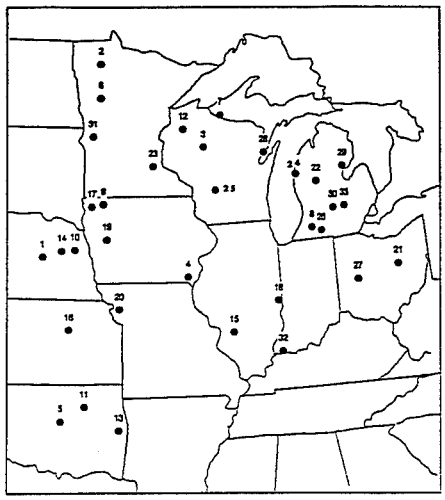

Figure 1. Storm Locations

PRECIPITATION DATA PROCESSING

The data are compiled for all existing stations within the storm area. Both hourly and daily data are acquired to provide the maximum density of stations. Data sources are not constrained to official records but all precipitation totals are considered from any source if they are reliable and consistent.

In order to create a more dense grid of hourly values for the storm region, weather data from daily or cooperative stations (those stations which report a single precipitation total each day) were processed to provide hourly precipitation values.

The approach taken in this study was to develop an objective technique which identifies the best correlated hourly stations to be used in producing consistent, reliable and reproducible hourly distributions. The statistical procedure evaluates the relationship between the daily totals reported by the various hourly stations and the single daily station. The correlation is based upon which hourly stations over the period of record best correlate with the precipitation observed at the daily station. After the relationships are developed, the storm data are entered and a distribution of hourly values at each daily station is established for each day of the storm.

GRIDDING AND CONTOURING TECHNIQUE FOR RAINFALL ANALYSIS

Distributing the rainfall over the domain of interest has historically been performed using the Theissen polygon method. Although this method could be used in a computer application, increased spatial resolution and application of non-linear interpolation techniques are possible using a gridded approach. The capability of readily available computer resources for storing and manipulating these large amounts of data and the availability of objective contouring software led to the development of a gridded technique for spatially distributing the rainfall data. This approach provides a consistent grid for all storms and provides for non-linear interpolation.

A relatively fine grid with uniform spacing is defined over the storm domain. The hourly data are interpolated to the grid points using kriging interpolation. Kriging provides a more consistent distribution than linear or inverse square techniques. The commercially available software package Surfer was used for determining the hourly rainfall values at each grid point. A grid analysis was completed for each hour of the storm. This

procedure provided a set of hourly data sets with the same grid point locations.

For each grid point identified in a file, hourly values are compiled creating a time series of hourly values for each grid point. Using these hourly series, the largest contiguous 6, 12, 24, 48 and 72 hour periods are identified.

This procedure yields an area for each precipitation depth increment and the largest contiguous values for the various time increments. These data are then plotted on semi-log paper to produce D-A-D curves.

STORM MAXIMIZATION

The HMR 51 procedures for storm maximization uses a representative storm dewpoint as the parameter to represent available moisture for a storm. The storm precipitation amounts are maximized using the ratio of precipitable water based on the storm representative dewpoint to precipitable water based on a maximum dewpoint climatology. The HMR 51 procedure was followed in this study with several refinements in determining dewpoint values. Average dewpoint values were used instead of persisting and various temporal periods (i.e., 6, 12 and 24 hour) based on precipitation durations were used.

There were several factors which were of concern in using the existing 12 hour persisting maximum dewpoint climatology to maximize the storms identified in the storm search. The published climatology is a combination of several analyses, previously performed at different times and by different organizations. Since complete documentation was not available for these separate studies, issues such as consistent periods of record, quality control, meteorological analyses of representativeness for storm development and analysis procedures were not known.

The use of observed maximum dewpoints for finite periods of record instead of return period values has disadvantages. The observed maximum dewpoints fluctuate depending on the particular period of record used and on the length of the period of record. Generally return period values are more stable and reliable, provided that an adequate period of record is available.

A third concern was the use of 12 hour values. Many storms identified in the storm search had precipitation periods much shorter (4-6 hours) or much longer (24-72

hours) than 12 hours. Analyses of the inflow moisture on a time scale consistent with the precipitation duration provides a more realistic estimate of available storm moisture. For the shorter storms, the 12 hour value includes data for air masses not involved in the precipitation event. For longer storms, dewpoint values based on periods longer than 12 hours should better represent the continuous moisture being supplied to the storm.

The procedure for developing the new maximum dewpoint climatology involved the authors working directly with the NWS Hydrometeorology Branch. The study team acquired and performed quality control on the hourly station data acquired from the National Climate Data Center (NCDC) and extracted the highest two dewpoint values for each station for the months of March through October for each year in the period of record. These were then statistically processed to provide return values for the maximum dewpoints by month. The new climatology includes values consistent with the various temporal periods used in the PMP study, i.e. 6, 12 and 24 hours. Additionally, both average and persisting maximum dewpoint values were derived. New climatologies were computed for the months of March through October for use in maximizing the warm season storms.

Storm Dewpoint Procedure

In order to characterize a storm, its moisture inflow must be quantified. This involves determining the amount of moisture in the air inflow feeding the storm, the direction and velocity of the air inflow moisture, and the length of time that a particular moisture air mass is available to the storm. Historically, the inflow moisture has been characterized by its surface dewpoint temperatures. An analysis of soundings taken during storm periods showed that the adiabatic assumption for computing precipitable water approximates the actual precipitable water computed from the soundings. Therefore, this study continued to use surface dewpoint temperatures as an indication of the moisture content of the inflow air mass.

To identify the inflow moisture for each storm, surface and upper air analyses, and precipitable water charts were examined. Hourly dewpoint temperatures for the inflow area upwind from the storm center out to several hundred miles were also obtained. From that information, the dewpoint temperatures associated with the inflow air mass were determined.

Once the moisture advection vector was established, stations with hourly dewpoint observations along the vector were used to determine the storm dewpoint. Dewpoint values for stations along the vector where rain was occurring were not used. For the stations and periods selected, a representative storm dewpoint was determined. That could have been an average of several stations, or a single station along or in the general area of the vector (WMO, 1986).

Adjustments to Older Storms

When using average dewpoints to describe the storm inflow moisture, an inconsistency existed between the older storms on the storm list (Numbers 1-17) and the modern storms (Numbers 18-25). The earlier storms used 12 hour persisting dewpoints to characterize moisture inflow. As previously discussed, the approach used in this study was to derive storm inflow moisture based on average, rather than persisting dewpoints. Furthermore various temporal periods were used, i.e., 6, 12 and 24 hours. The older storms, which used 12 hour persisting dewpoints, are inconsistent with the use of the average maximum dewpoint climatology. Since our storm list is much smaller than desired, eliminating the older storms was not considered to be feasible. Instead a procedure to provide average dewpoint values for the older storms was developed.

To quantify the storm dewpoint differences, each modern storm was analyzed in a manner consistent with the procedure used with the older storms to determine 12 hour persisting dewpoints. This analysis has provided correlations between 12 hour persisting storm dewpoints and average storm dewpoints for both Mesoscale Convective Systems (MCS) and synoptic storms. To be conservative, the adjustments are decreased from the analyses results. The eight degree difference indicated for MCS type storms has been decreased to five degrees. A similar consideration is made for the synoptic type storms. The three degree difference is decreased to two degrees. The adjusted representative storm dewpoints are used with the new maximum average dewpoint climatology to maximize the storms.

ENVELOPMENT

Maximization and transposing provides an indication of the maximum total amount of precipitation that a particular storm could have produced over the region of interest. These values alone do not provide assurances that PMP values are provided for the particular basin sizes and durations since some of the maximized values

could be less than PMP. By enveloping the values resulting from the maximization and transposing of the maximum totals from all the major storms, values indicative of the PMP magnitude will result (WMO, 1986).

Enveloping is the process of selecting the largest value from a set of data. This technique provides continuous smooth curves based on the largest precipitation values from the set of maximized and transposed storm rainfall data values. The largest precipitation amounts provide guidance for drawing the curves.

This enveloping procedure addresses the possibility that for certain sizes and durations, no significantly large storms have been observed which provide large enough values after being maximized and transposed. The result of this procedure is a set of smooth curves which maintain continuity among temporal periods and areal sizes.

The envelopment process was used twice in PMP determinations for this study. The first application was in determining the D-A-D curves. A curve was drawn for each time period. Envelopment was used in constructing those curves such that low values at particular area sizes were increased to provide a smooth transition from one area size to another. The curves were constructed such that there were no values for any area size which exceeded the value for a smaller area for the same duration.

The second application of enveloping was during the construction of the final PMP maps. This process provided spatial continuity over the grid. In general, little adjustment was required but slight envelopment provided a smooth analysis for most cases.

GREAT LAKES EFFECTS ON PRECIPITATION

The most significant effect of the Great Lakes on PMP storms is on-shore convergence, which can contribute significantly to localized precipitation. Several small scale storms along the shorelines of the Great Lakes demonstrate this effect. Although none of these events are the major storms that determine the PMP values for this study, they represent significant amounts of rainfall over short periods and small areas.

These small scale storms occurring along the shoreline should not be transposed to other locations since the storm dynamics would not include the on-shore convergence contributions. Storms which have occurred elsewhere and

are transposed to the affected shorelines areas need to be adjusted to account for the increased storm dynamics. The following adjustment are recommended for the region within 30 miles of the affected shorelines:

6 & 12 hr, 100 square mile PMP values.....add 10%
6 & 12 hr, 200 square mile PMP values.....add 5%

RESULTS

PMP maps were produced for the Michigan and Wisconsin region for area sizes ranging from 100 to 10,000 square miles and for time periods of 6, 12, 24, 48 and 72 hours. A separate set of PMP maps were produced for cool season storms. Figure 2 shows the warm season PMP map for the 1,000 square mile area for 48 hours. Figure 3 shows the cool season PMP map for the same area and duration.

The regional PMP values resulting from this study vary from those obtained from HMR 51. The differences vary from approximately 20% smaller values for small areas and short durations to approximately 2% increase for large areas and long durations. These differences are primarily due to the more detailed treatment of the moisture maximization and the new dewpoint climatology.

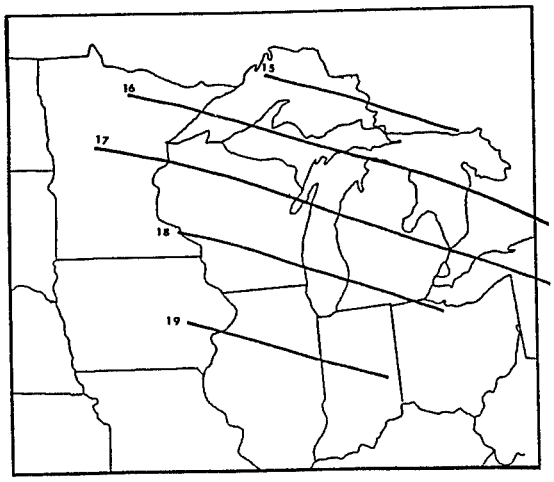

Figure 2. Warm season PMP (in.) for 48 hr 1,000 mi^2

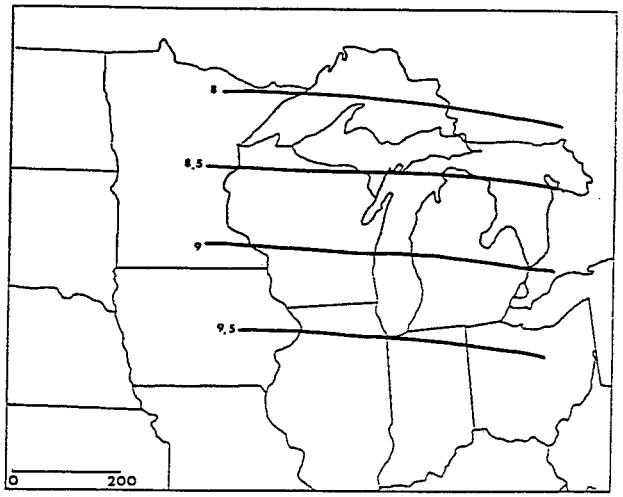

Figure 3. Cool season PMP (in.) for 48 hr 1,000 mi^2

REFERENCES

World Meteorological Organization, 1986: Manual for Estimation of Probable Maximum Precipitation (2nd Ed.), WMO - No. 332, Geneva, Switzerland, 250 pp.

CG-DAMS SOFTWARE: DAM STABILITY CASE STUDIES

Peter R. Barrett(1), H. Foadian(2), L. Zhang(3),
Y. R. Rashid(4), D.I. Morris(5)

Abstract

This paper illustrates applications of the CG-DAMS program written specifically for stability safety evaluations of concrete gravity dams. The code automates the prediction and evaluation of the dam's strength and stability under extreme flood and earthquake loading. The program has the general capability of predicting potential cracks anywhere in the dam and foundation structure; however, its primary application is in the analysis of crack propagation along the dam-foundation interface. CG-DAMS' automated procedure for gravity dam stability analyses provides a fast, easy to use, and more accurate representation of the true dam behavior over the traditional trail-and-error cracked base analysis method. The code uses an automated finite element approach taking into account the material and geometric properties of the specific dam analyzed.

CG-DAMS analytically computes any initiation, propagation, and arrest of cracks. The code uses an enhnaced version of the smeared crack material model derived orginally by (Rashid 1968) which determines if cracking will take place in accordance with a strain based cracking criterion. If cracking occurs, the normal stresses across the open cracks are reduced to zero and the forces (and thus stresses) around the cracks are redistributed. Loading is incrementally applied to allow for this redistribution of forces. The material model of the dam-rock interface using the same capabilities along with accounting for the cohesion and coefficient of internal friction in evaluating the stability of the dam. Reservoir and tailwater loads

---

(1)ASCE Member, Senior Engineer, Anatech Research Corp. 5435 Oberlin Drive, San Diego, CA 92121
(2)ASCE Member, Project Engineer, ANATECH Research Corp.
(3)Research Engineer, ANATECH Research Corp
(4)President, ANATECH Research Corp
(5)Project Manager, Hydroelectric Generation, EPRI, P.O. Box 10412, Palo Alto, CA 94303.

are incremented based on the upstream and downstream water depths such that a single analysis predicts the dam behavior under normal, 1/2 PMF (Probable Maximum Flood) and full PMF load.

Applications of the method for gravity dams include hydrostatic and seismic loading conditions based on FERC's guidelines. The code runs on 386/486 PC's under the DOS operating system with a minimum of 4 Megabytes of RAM. Graphical input and output are accessed through pull-down input menus where the analysis type, geometry, loading (including reservoir, tailwater, uplift, pseudo-dynamic, crest and bucket forces), and material properties are defined. Site-specific data for the reservoir, dam and foundation materials, and structural dimensions, input by the user, can be viewed graphically immediately after input.

Introduction

One of the major tasks in licensing and relicensing concrete gravity dams is evaluating the dam's structural integrity. In almost all cases, the governing criterion that must be met is sliding stability. When performing stability evaluations, the most important parameter to calculate is the extent of cracking along the interface between the dam and its foundation. Current practice varies from hand calculations using the "gravity method" to finite element calculations using general purpose software. The gravity method assumes the dam deforms like a rigid beam which can introduce significant error for many dam cross-sections. The application of general purpose finite element software accurately models the relative stiffness of the dam and foundation, but usually requires considerable training, extensive manpower efforts and generally a trial and error process of predicting the dam-rock interface crack length. Both methods require substantial engineering efforts in defining and developing the model and loading conditions and evaluating the analysis results. CG-DAMS (Barrett, 1992) was developed to both automate the stability analysis process so that stability evaluations will not always require a finite element specialist and to provide a more accurate analysis tool which incorporates recent research activities. The software was developed by ANATECH Research Corp. through funding from the Electric Power Research Institute's Hydroelectric Generation Program. CG-DAMS is a two-dimensional finite element based code developed specifically for analyzing the stability of concrete gravity dams. The menu driven software prompts the user for input of the dam's geometry, loading (using input commands such as reservoir and tailwater elevations), and site-specific material properties of the dam and foundation. The analysis results are illustrated graphically, with a separate table summarizing the results and providing the sliding stability factor of safety.

Example analyses presented in this paper are used to demonstrate CG-DAMS' unique capabilities. Spillway and nonoverflow cross-sections are analyzed for PMF hydrostatic loading, including the effects of silt loads, crest pressures, bucket forces, tailwater loading, and drain effectiveness. Input and output processing routines simplify the definition of loading by using dam engineering terminology. Specific cracking of the dam-rock interface reflects the interface tensile strength input by the user (generally zero for licensing calculations). General cracking in the dam and foundation is also computed. The analyses are illustrated through cracking orientation plots, stress contours, and deflected shape plots. The analysis summary table includes the computation of the sliding stability factor of safety.

Example Analyses

The engineer choosing to evaluate a dam's structural safety using CG-DAMS initially needs only obtain drawings with dimensions of the dam's geometry. Next, one or more cross-sections are selected for analysis. The engineer is now ready to follow a seven stage procedure to evaluate the dam's strength and stability.

1) Choose Analysis Type
2) Choose Library Model
3) Input Geometric Data
4) Input Material Properties
5) Input Loading Conditions
6) Execute the Analysis
7) Evaluate the Analysis Results

1) The second item in the main menu for CG-DAMS is used to choose the analysis to be performed. Choices for analysis include elastic or cracking for either static or pseudo-dynamic loads. The user must also choose whether to include the effects of crack roughness and whether thermal stresses will be included (Details on the codes capabilities can be obtained from the CG-DAMS User's manual). For this example, a static cracking analysis will be performed without the effects of the rough crack or thermal loads.

2) The appropriate library model is selected that meets the geometric constraints of the cross-section to be analyzed. Generally all standard nonoverflow and spillway cross-sections can be adapted to one of the library models. It is important to emphasize the strength of having these library models, since when applying the finite element method, constructing a finite element mesh is generally the most tedious task. CG-DAMS automates this process through the use of library models. The library models can be stretched or contracted to model almost any dam cross-section. Figure 1 illustrates the library model used to define a typical example nonoverflow dam cross-section.

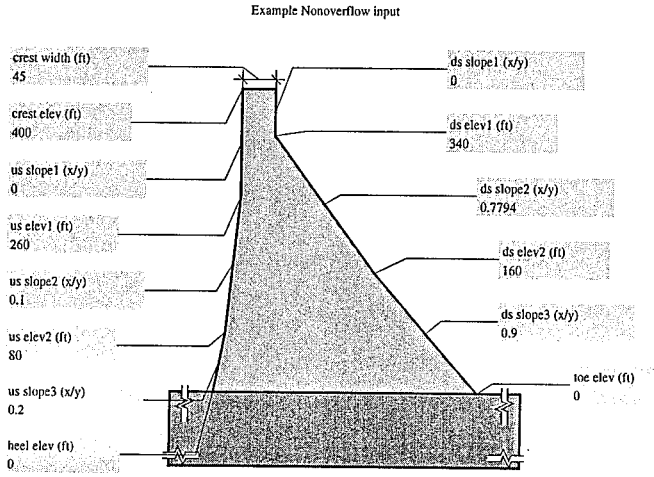

Figure 1. Example Nonoverflow Library Model Input Screen. Generic Data can be Modified to Fit Most Standard Cross-Sections.

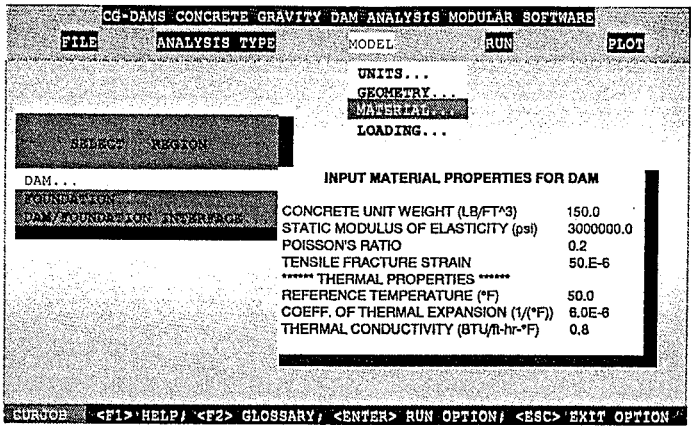

Figure 2. Example Input Screen for Material Property Data Entry

3) Once the library model has been selected, the user simply enters elevations and slopes into the appropriate boxes on the screen to define the unique geometry of the dam to be analyzed. After entering the data, the program immediately redraws the dam cross-section to provide a visual check of the user's input. This is a very powerful feature, since most engineers spend many hours trying to find typographical errors created during mesh generation procedures. CG-DAMS features seven different library model cross-sections which can be used to model almost all standard nonoverflow and spillway dam cross-sections. The code also offers mesh generation capabilities so that users can generate their own finite element models which can also be easily adapted to analyze similar dam cross-sections.

4) Once the geometry of the dam has been prescribed, the next item to define from the model menu is the material properties of the dam, foundation, and interface. Figure 2 illustrates one of the input windows provided to enter this data. The user steps from line to line after each data entry. Default values are provided as examples. If data such as the Modulus of Elasticity of the foundation material is unknown, the user can easily run several analyses varying this parameter to evaluate its sensitivity on the sliding stability of the dam. This point is significant, since the faster one can generate analysis results, the more time that can be spent on engineering. If the dam analyzed does not meet the required factor of safety, analyses can easily be performed to determine the most influential parameters causing the overstress.

5) Defining loads on the dam is the next step in the analysis process. Visual verification of the entered reservoir and tailwater loads is performed with graphic checks similar to defining the dam geometry. Figure 3 illustrates the reservoir, silt and tailwater loads for an example nonoverflow cross-section. Since, the solution technique used by CG-DAMS increments the reservoir loads as a function of water depth, the user can obtain results for Normal, PMF (Probable Maximum Flood) and any other water elevation in between with a single analysis. Water pressure under the dam (uplift load) is also illustrated on this input screen along with the location and efficiency of internal drains. The profile of the uplift pressure is based on either the Federal Energy Regulatory Commission's guidelines (FERC 1991), the user's piezometer data, or CRFLOOD (Chinnaswamy 1992). CRFLOOD is an EPRI sponsored, experimentally verified, numerical tool used to predict flow and uplift pressure distribution in gravity dams. CG-DAMS also provides earthquake analysis capabilities through its Pseudo Dynamic loading option. Hydrodynamic loads are computed using Chopra's simplified method (Fenves 1986). Data entry for seismic loading has been greatly simplified, requiring only the magnitudes of design ground acceleration, since all other input

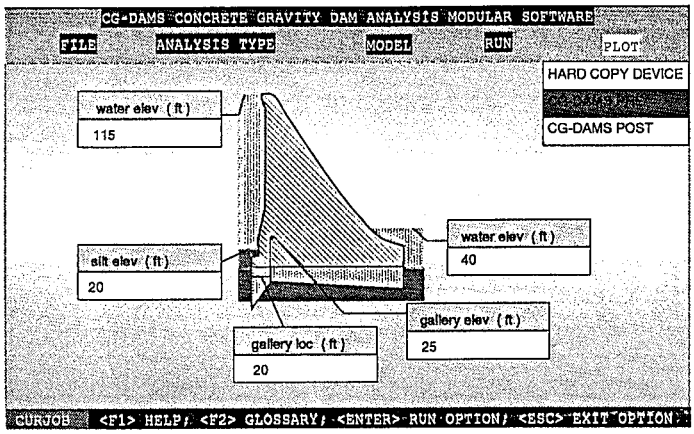

Figure 3. Example Loading Input Data Illustrated on the Modeled Dam Cross-section

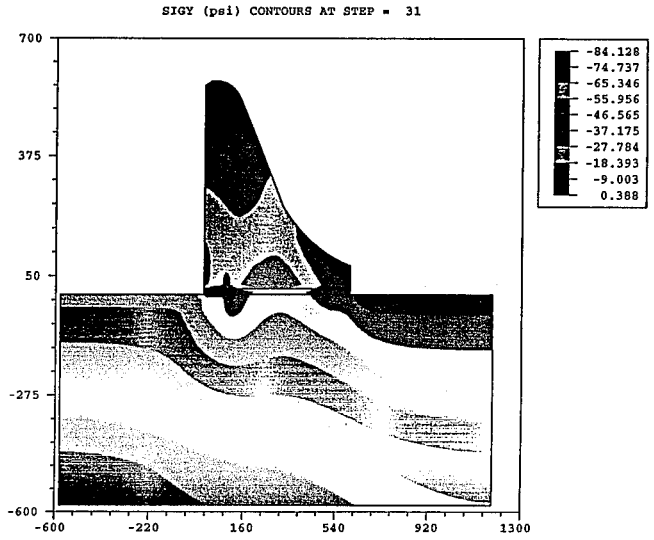

Figure 4. Vertical Stress Contour Plot From PMF Reservoir Loading Cracking Analysis.

parameters are calculated by CG-DAMS internally. In addition to reservoir loads, CG-DAMS also allows for the application of concentrated forces, such as ice, post-tensioning tendon loads, and crest and bucket forces. Steady state thermal loads can be included in the analysis using graphical input screens for surface temperatures, conductivities, and coefficients of thermal expansion. The code provides a loading summary for each analysis so the user can quickly verify the data input through the menus. The entire package of graphical input screens allow the user the ability to generate a complex computational model complete with material properties and boundary conditions in a matter of minutes.

6) The incremental analysis techniques used by CG-DAMS do not require any interaction by the user. Reservoir, tailwater, uplift, etc. are changed automatically to reflect increases in reservoir depth and/or dam-rock interface crack. The user simply defines the load steps where detailed results are required. However, if the user wants to monitor how the tailwater and headwater are increased relative to each other one can easily change the loading sequence such that each of the different loadings are increased at different rates.

7) The CG-DAMS post-processor was developed for the specific analysis of concrete gravity dams. Crack pattern plots, stress contours, and deflected shape plots are created to aid in interpreting the analysis results. Figure 4 illustrates the vertical stress distribution for the example dam and foundation subjected to PMF loading. The tensile stress zone at the heel of the dam indicates the presence of a dam-rock interface crack. The computed dam-rock interface crack length and corresponding sliding stability factor of safety is summarized at pre-defined steps prescribed by the user. Figure 5 illustrates a summary table that supplies a quick reference of the critical input data and analysis results. The input data consists of nominal dam dimensions and elevations of the reservoir and tailwater. The results consis of the length of dam-rock crack (if any) and the net componet forces on the dam along with the sliding stability factor of safety. In addition to providing an executive summary of individual analyses, these tables can be extremely useful in comparing and documenting parametric evaluations.

Computer Hardware Requirements

CG-DAMS-PC is a menu driven program that runs on 386/486 PC's under the DOS operating system. The program requires a computer with a minimum of 4 Megabytes of RAM and at least 25 Megabytes of hard disk space to load the software and perform licensing stability analyses of library models and/or similar cross-sections. A VGA or super-VGA monitor is required

example summary table

01/15/93
09:49:00.10

Dam Geometry	Results	Units
Crest elevation	400.00	ft
Base elevation at heel	0.00	ft
Base length	317.00	ft
Water Elevations		
Reservoir surface elevation	400.00	ft
Silt elevation	200.00	ft
Tailwater surface elevation	100.00	ft
Backfill elevation	0.00	ft
Uplift Data And Drain Location		
Upstream uplift pressure	173.33	psi
Downstream uplift pressure	43.33	psi
Drain elevation	60.00	ft
Drain location	30.00	ft
Drain efficiency	0.85	
Interface Properties		
Unit cohesion = c	100.00	psi
Internal friction angle = phi	45.00	deg
Crack Length		
Cracked length = t	43.60	ft
Uncracked length = l	273.40	ft
% of base cracked	13.75	
Uplift Force		
Initial uplift at start of analysis	-2661.83	kip/ft
Final uplift at end of analysis = U	**-2874.45**	**kip/ft**

Foundation Normal Forces	Results	Units
Reservoir vertical load on foundation	14592.01	kip/ft
Tailwater vertical load on foundation	2496.00	kip/ft
Other vertical forces on foundation	0.00	kip/ft
Dam Normal Forces		
Dam dead load	9635.33	kip/ft
Reservoir normal load (inc. silt)	0.00	kip/ft
Tailwater normal load (inc. bkfl)	250.25	kip/ft
Other normal forces	0.00	kip/ft
Total normal forces = n	**9885.58**	**kip/ft**
Dam Lateral Forces		
Reservoir lateral load (inc.silt)	5443.81	kip/ft
Tailwater lateral load (inc.bkfl)	-312.46	kip/ft
Other lateral forces	0.00	kip/ft
Total lateral forces = v	**5131.35**	**kip/ft**
Shear Friction Factor of Safety		
Q=(cl + (n+U)tan(phi))/v	2.13	

Figure 5. Example Summary Table of a Full Reservoir Analysis of the Nonoverflow Model Illustrated in Figure 1.

to display on-screen graphics. Hard copies are generated for either postscript or HPGL compatible printers.

Acknowledgments

CG-DAMS was developed by ANATECH Research Corp., San Diego, California. Many individuals contributed to the code development, and their efforts are greatly appreciated. Primary contributors are Peter R. Barrett, Hoss Foadian, Randy J. James, Y. R. Rashid, Frank Wong, and Liping Zhang. We greatly appreciate the support and cooperation of the people and organizations who through their use and review have made this software possible.

Peter Barrett has recently left ANATECH and joined Computer Aided Engineering Associates, Inc., 398 Old Sherman Hill Rd., Woodbury, CT. 06798, (203) 263-4606

References:

Barrett, P.R. et. al., "CG-DAMS Concrete Gravity Dam Analysis Modular Software, User's Manual," Electric Power Research Institute, RP2917-12, December 1992.

Chinnaswamy, C., Illangasekare, T., Amadei, B., "CRFLOOD: A Numerical Model to Estimate Uplift Pressure Distribution in Cracks in Gravity Dams," University of Colorado, Dept. of Civil Engineering, Electric Power Research Institute, EPRI No. TR-101671, 1992.

"Engineering Guidelines for the Evaluation of Hydropower Projects, Department of Energy, Federal Energy Regulatory Commission," FERC 0119-2, Office of Hydropower Licensing, April 1991.

Fenves, G., Chopra, A.K., "Simplified Analysis for Earthquake Resistant Design of Concrete Gravity Dams," Report no. UCB/EERC-85/10, Earthquake Engineering Research center, University of California, Berkeley, Calif., 1986.

Rashid,Y.R., "Ultimate Strength Analysis of Prestressed Concrete Pressure Vessels", Nuclear Engineering and Design, Volume 7, pages 334-344, 1968.

Hydro-electric Machine Condition Monitoring
A Technical Proposal and Business Argument

D.E. Franklin[1]
B.C. Pollock[1]
J. Laakso[2]

Abstract

Since early in 1990, both Powertech and the B.C. Hydro Apparatus Department have been involved in a strategic effort to "conceive an overall plan for hydro plant machine condition monitoring and to determine areas where R&D investment in technology can cost-effectively accelerate the implementation of condition driven maintenance". Results of this effort has produced several documents and a comprehensive proposal on the subject. The work has clearly identified that there is a great opportunity to reduce costly outages, improve predictive maintenance capabilities, and get more value out of hydro generating equipment through the intelligent application of new sensing and monitoring technologies. After establishing the justification for potential savings in the area of MCM, Powertech and B.C. Hydro examined the state-of-the-art of this technology. The available systems and technology did not meet the requirements of hydro monitoring, primarily due to the low speed of the units (i.e. usually less than 300 rpm), lack of appropriate facilities for implementing diagnostics, and a general lack of an Open Systems Architecture for both software and hardware. Consequently, a plan was devised to permit a consortium of utilities, R&D affiliate organizations, and technology companies to participate in a program to develop and implement the required technology for this program.

Introduction

This paper provides a technical overview of a proposed Machine Condition Monitoring (MCM) System for Hydro. Key issues are explored to provide support for the financial justification and the technical merits of the

[1]Powertech Labs Inc., 12388 88th Avenue, Surrey, B.C., Canada, V3W 7R7
[2]B.C. Hydro, E07, 6911 Southpoint Drive, Burnaby, B.C., Canada, V3N 4X8

program. A modular approach is presented which permits development flexibility, and an opportunity for manufacturers to develop technology components using their own financial investment.

Improved performance in areas of reliability, efficiency and availability can only be achieved through a better understanding of the internal fault mechanisms which develop in equipment. In many instances technology is available to measure/monitor these mechanisms on-line and detect changes in machine performance. Changes from normal acceptable baselines can form the essential information necessary to detect and diagnose progressing fault conditions. If used effectively, this new knowledge can permit timely money saving decisions to be made to predict time-lines to failure, implement effective maintenance strategies, and reduce the risk of costly immediate and secondary damage which would result if problems progress undetected. Technical experts within B.C. Hydro, Powertech, and other utilities have identified the frequency and severity of failures in a wide range of hydro-electric subsystems. These were ranked in terms of overall impact based upon reported hours of forced outages and on judgment by operating staff. This historical data has provided a solid direction for prioritizing the importance of monitoring particular equipment subsystems.

Future monitoring systems designed using the latest technology must aspire to a new level of performance and flexibility, beyond that of current systems. A plan of approach has been defined to utilize the latest technological developments and implement a comprehensive monitoring system for the hydro generation area. The proposed system is modular, providing flexibility, expandability, and the diagnostic capability necessary to achieve an effective MCM system.

General Description of Proposed MCM System

A careful examination of both perceived and documented equipment problems was conducted with the goal of designing a cost-effective monitoring system tailored to the unique requirements of hydro-electric generating equipment. When trying to "sell" a new idea it is important to address the realities, and, the perceptions of the end-user. A modular plan was devised which would allow the flexibility, expandability and distributed processing capability necessary to achieve a cost-effective MCM system, in an efficient project format. Such a system design would also permit development and funding leverage flexibility, and utilize all available utility expertise. Leading manufacturers of MCM technology could also invest their own development dollars to manufacture the required monitoring modules in compliance with the overall MCM platform standards.

The following Monitoring Modules were identified to cover the full monitoring requirements of a hydro-electric generating unit:

1. Bearing Module
2. Brushgear Module
3. Generator Windings Module
4. Turbine Module
5. Governor Module
6. Excitation System Module
7. Environment Module
8. Master Information and Diagnostic System (System Data Manager and Display)

A system layout diagram for these modules is included in Figure 1.

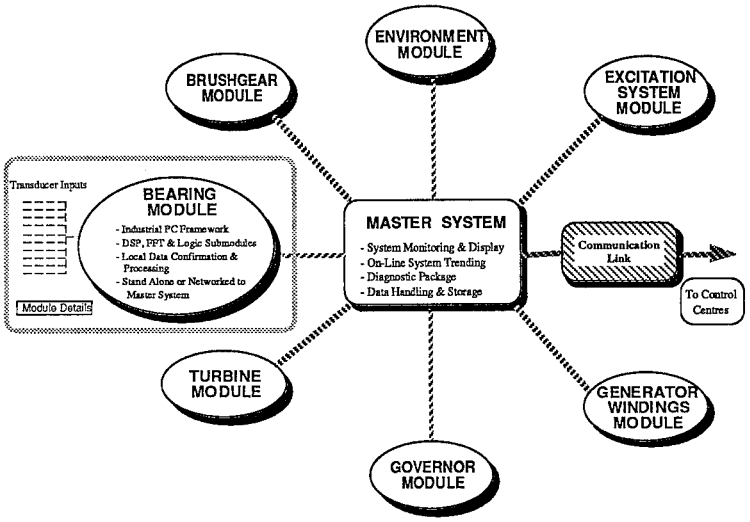

Figure 1: Modular Layout of Proposed Hydro MCM System

This system modularity will allow monitoring strategies to be developed for individual plants based on their own cost/benefit analysis, while maintaining utility and industry wide standards for implementing monitoring technology.

Proposed Approach

A building block approach is desirable to enable development flexibility for tackling a large project, both from a technical and funding leverage point-of-view. Standardization of communication protocol, networking, multi-tasking, and graphical operator interfaces are all

essential elements of the proposed Machine Condition Monitoring System. Consideration has been given to allow flexibility of configuration for both small and large plant monitoring requirements. Expanding monitored parameters and/or machines should not unduly effect the response time of the host system. The system architecture will enable ease of expansion and permit flexibility for the full utilization of new technological advancements.

Proposed system features include:

1. Modular subsystem monitors
2. Advanced diagnostics
3. Multi-tasking
4. Networking
5. Graphical User Interfaces (GUIs)
6. High confidence data for operational decisions
7. Development flexibility
8. Ease of system expansion
9. Clear upgrade path based on industry accepted Open System standards

System End Users

The end users of the MCM system can be grouped into three categories:

1. Operators and maintenance personnel not trained in machinery diagnostic analysis techniques. This group will be primarily concerned with overall levels, lists of conditions that have exceeded pre-set alarm levels, and trends of overall data levels.

2. Plant or maintenance engineers who have some basic training in machinery diagnostic analysis techniques. These individuals will require access to dynamic data such as orbits, vibration spectra, and waterfall plots (i.e. for vibration analysis). Their primary interest will be in planning maintenance activities and correcting operational problems.

3. Corporate rotating machinery specialists who review design-related machinery problems and establish corporate monitoring criteria. These individuals will require all the information available and the ability to perform complex calculations and correlations necessary to produce specific recommendations.

Each of the MCM system user groups must be involved in the defining of specifications for their specific function. B.C. Hydro has initiated a program to examine these issues as part of their contribution to the Master System pre-Consortium work.

Goals and Objectives

New monitoring systems developed using the latest state-of-the-art technology must aspire to a new level of performance and flexibility, beyond that of current systems. Goals and objectives of the preferred approach are outlined below with reflections on the short-coming of earlier systems in these areas.

Goal 1: Optimized Cost/Benefit Approach toward Machine Monitoring

Historical Difficulty

Documented causes of untimely costly outages are often not carefully examined to identify and prioritize the costs and benefits necessary in selecting what should be monitored.

Proposed Approach

To be useful, MCM systems must be designed from the ground up. Cost/benefit considerations must drive the selection of what is to be monitored and how the data will be utilized for diagnostic purposes. The proposed approach has evolved from a careful consideration of what has traditionally caused the greatest number of lost generating hours firstly on B.C. Hydro equipment, and secondly on other Canadian hydro-electric generating equipment. This approach, coupled with the direct involvement of B.C. Hydro production supervisors, has resulted in the establishment of a firm foundation for maximizing the return-on-investment for implementing new monitoring techniques.

Goal 2: Information Quality Versus Quantity

Historical Difficulty

Too little data has been acquired for diagnostic purposes.

Proposed Approach

Operators desire more effective, less complex systems. The proposed monitoring strategy will utilize both existing technology in new ways, while delivering benefits from new innovative technologies never before utilized for hydro-electric applications. The emphasis of this new approach is to provide accurate quality information rather than an overburden of excessive data. Data integrity requires no false alarms, however, alarms when there should be alarms. Graphical operator interfaces must be intuitive, easy to use, and optimize available information for the user.

Goal 3: Advanced Diagnostics

Historical Difficulty

Traditionally, little or no diagnostics other than alarm thresholds have been implemented to identify potential developing problems. Often valuable troubleshooting expertise has been limited to a few key people,

who are usually senior engineers in high demand. When these key people leave due to retirements or other employment opportunities, a valuable resource is lost to the company.

Proposed Approach

Machine Condition Monitoring in the form of flexible, modular distributed diagnostics can form an important step in keeping this special information where it can be of greatest benefit; with the generation equipment. The proposed system permits valuable troubleshooting expertise to be utilized within advanced diagnostic packages tailored to solve specific hydro-electric machinery problems.

Goal 4: Development Flexibility and System Expandability

Historical Difficulty

Commercial monitoring systems tend to bring too many raw data signals to one location. This results in a processing bottleneck which may slow system response times and limit data manipulation capabilities. These systems tend to be inflexible for expansison and force limitations upon the users.

Proposed Approach

Flexible Open System Architecture design using industry and utility accepted standards is necessary to ensure the long-term maintainability of MCM systems. Modularity of design is also required to allow customized monitoring strategies for different sizes of equipment. These features are fundamental to the proposed Hydro MCM system.

Benefits

General

To obtain financial justification for MCM, B.C. Hydro conducted an evaluation of historical system performance. The study determined that for B.C. Hydro, the five key benefits of applying MCM technology include:

1. Value of Increased Capacity through Overgating
   - In certain situations the nameplate capacity may be exceeded while ensuring minimum impact on equipment life and Maintenance costs. MCM provides the necessary tools to make this a potential sustainable benefit.

2. Energy Value from Utilizing Spill
   - Overloading to use excess water
   - Reducing Water Spill associated with Unit Outages

3. Reduction of Maintenance Costs
   - Reduction of Planned Maintenance Activities
   - Preventing Repair cost from primary and secondary damage

4. Life Extension for Aging Equipment
   - End-of-life prediction to utilize the full service life of components

5. Improved Equipment Efficiency
   - On-line data establishes optimum operating conditions

In addition to these key benefits, many other financially tangible and intangible benefits were identified.

Determining some potential savings possible through the application of MCM technology may be subjective in nature. The savings can only be estimated through a careful examination of the cause of historical failures and an estimate of how preventable future occurrences of these problems might be if appropriate monitoring technology is applied. This assessment must also consider the "bath tub curve" for equipment life which describes how the probability of a forced outage and maintenance costs increase as a particular machine approaches its design life.

Value of Increased Capacity: Overloading

A B.C. Hydro Case Study - Revelstoke Generating Plant

In the fall of 1991, B.C. Hydro was faced with an excess of water at their Revelstoke generating plant on the Columbia River. This plant has 4 generating units, each with a nameplate rating of 465 MW. A decision was made to increase monitoring activities and run the units at an additional gate opening of 6.4% (4.1% overload) above their previous full-gate setting. Three units (G1, G3 and G4) were run for 20 days and produced a combined 58 MW of "extra" generating capability. Over the period this amounted to an additional 17,040 MWh of generation. At an assumed value of energy of $0.031/kWh this would be worth CAN $528,000.

The potential for increasing the installed capacity of plant without building new plant offers a tangible value in terms of deferred building scenarios.

The Revelstoke exercise demonstrated the value possible in safely capitalizing on overload ratings. *Condition Monitoring technologies are necessary to ensure that there is no undue risk to equipment if overloading is to be a sustainable benefit.* In the years to come, utilizing this potential for additional capacity during peak times will become an increasingly attractive. The proposed MCM system is designed to provide the necessary technology to capitalize on both this opportunity, and other opportunities as utilities move toward a predictive/ preventative mode for their maintenance activities.

Water Spill Associated with Unit Outages

The reduction of untimely unit outages is becoming increasingly more important as demand for power grows and installed plants continue to age. Considerable effort has been spent by B.C. Hydro to determine the value of outage prevention. Maintenance outage statistics for all Canadian utilities were examined to assess the primary causes of the outages and determine the value of preventing outages from a power loss perspective. The results of this evaluation for the B.C. Hydro system are described by major subsystem in Figure 2.

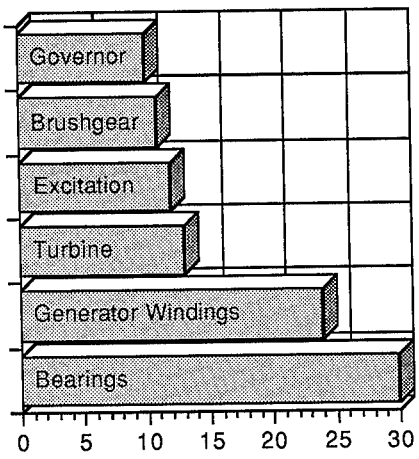

Hydro-electric generating equipment subsystems
Forced and Maintenance Outage Time (%)
for BC Hydro (1985 to 1989)

Figure 2

In assessing the preventability of particular unit outages one must consider:

1. The detectability of problems which lead to equipment outages
2. Lead time before a failure
3. Whether the level of MCM technology on a particular unit is sufficient to detect the problem.

Furthermore, the impact of a forced outage must be assessed in terms of importance of particular plants and units. A classification scheme can be used to identify the importance of particular units from a system perspective.

These classifications could include:

1. Class I (Critical, not-spared): This classification refers to a machine that is not spared and that will result in immediate total or partial loss of generation when the machine is shutdown.
2. Class II (Critical, spared): This classification refers to a machine that is spared, but that will result in a complete or partial, but not immediate, loss of generation when the machine is shutdown.
3. Class III (Non critical): This classification refers to a machine that will not immediately affect generation. Repairs to the machine can be made without the loss of generation.
4. Class IV (Problem Units): This classification refers to a machine that is identified as requiring maintenance or that has a recurring maintenance problem. This is a catchall for machines that should receive special attention for some reason, but that are not necessarily critical to generation.

It should be noted that some site specific restrictions and demand side factors may limit possible savings.

An estimate of value associated with Outage Reduction was obtained for B.C. Hydro through an evaluation of water spilled due to unit outages. This is water which was sent down the spillway that could have gone through a turbine had the unit been available. If the volume of water is converted to MWh based on the ratings of the particular outage units, an estimate of the potential value for reducing Outages may be obtained. Determining the portion of this spill which may be utilized requires a substantial amount of Engineering Judgment based on individual Utility related issues and the classification categories identified above.

Additional Benefits

In addition to the primary benefits identified previously, many other benefits of MCM were identified for B.C. Hydro. A list which is by no means exhaustive, is included below:

1. Improved Risk Management of Critical Run-of-the-river plants
2. Early detection/correction of problems
3. Extending the time between Outages in contrast to calendar based maintenance activities
4. Improved unit availability

5. Establishment of databases on Machine Characteristics, useful for Design Improvements, Product Selection, and Maintenance Information
6. Environmental Monitoring/Protection
7. Improved Safety
8. Enhancement of Operational and Maintenance Skills
9. Reduced need for spare parts
10. Improved Outage planning

Summary

An effective Machine Condition Monitoring system must be specifically tailored to meet the requirements of plant operators and plant maintenance engineers. The system must be developed to provide a key tool to reduce outages, optimize maintenance practices, and build confidence in the condition and safety of generating equipment through data integrity.

Each utility should investigate the business potential of investing in MCM technologies based on the value of increased capacity, increased energy, reduced maintenance, equipment life extension and improved operating efficiency.

A modular system was described which addressed many of the requirements of a future MCM system for the hydro generation area. Features, Objectives and Benefits of such a system were described to provide the justification for investing in the application of MCM technology.

GRINDING MANIPULATOR FOR CAVITATION REPAIR

Randy Wallman[1]
Gary Gusberti[2]

ABSTRACT

This paper is a case history concerning the Research & Development of a manipulator used for grinding during cavitation repair work on propeller turbines and draft tube liners. This research work was carried out between December of 1987 to September 1992.

The primary reasons for developing this manipulator were to reduce operator fatigue, associated back injuries, and to increase productivity. In many cases, cavitation on fixed blade propeller and Kaplan units occurs on the low pressure side of the blades and subsequent repairs require the operators to grind in an overhead position. Research began in late 1987 with a conceptual design study contracted to a private contractor. Randy Wallman acted as the project manager for the private contractor with key personnel from Manitoba Hydro assisting in design and testing. Development work was carried out over 4 models, PROTOTYPE1 through PROTOTYPE4. Testing and evaluation was conducted primarily at the Winnipeg River Stations. PROTOTYPE4 has been successfully tested and has shown grinding times reduced by as much as 50% and has drastically reduced the effort required by the operator. A better surface was also achieved due to the consistent grinding pressure.

[1]Randy Wallman, Consultant, 511-1734 St. Mary's Road, Winnipeg, Manitoba, Canada, R2N 1G8, 204-735-2329

[2]Gary Gusberti, Engineer, Manitoba Hydro, P.O. Box 815, 820 Taylor Ave., Winnipeg, Manitoba, R3C 2P4, 204-474-3194

INTRODUCTION

Initial work began in 1987 in response to a growing problem identified with cavitation grinding. The problem was operator fatigue associated with overhead and vertical grinding on propeller units and the draft tubes during cavitation repair work. A grinder operator must support a 4 to 6 kg. grinding tool in an overhead position when repairing the blades. This requires substantial physical effort and can cause serious back injuries over time. Productivity and safety were also key factors in researching a better method. The research project was limited to grinding only because welding and material removal by air arcing or plasma arc are much less fatiguing and less time consuming.

The private contractor was hired to investigate a robotic solution to this problem. A study was carried out and conclusions drawn showed that some form of self supporting manually assisted device could be built in lieu of a fully automated approach. A conceptual design study was initiated to identify possible design alternatives. Dr. Mark Friedman, the Director of the Robotics Institute at Carnegie Mellon University was hired to assist with conceptual design. Twelve possible designs were submitted and the working group chose one conceptual design as a starting point.

PROTOTYPE1

Manitoba Hydro's Research & Development committee initiated a prototype development contract to build a model suitable for laboratory testing.

The first manipulator consisted of a 915 mm. arm designed to be supported by tack welding a fulcrum to the underside of a turbine blade. Force was applied via a spring load wheel assembly acting against the blade surface. A "Thor" vertical pneumatic grinder was attached to one end of the arm via a floated bearing assembly. The fulcrum was designed to rotate in a 360 degree pattern. A slide mechanism was designed to move the grinder in a linear fashion. 305 mm of linear travel was available by moving the grinder in and out in a manual fashion. Testing was conducted on a mock up turbine blade in the overhead position.

Results showed that the spring load wheel assembly did not provide adequate force control and due to the complex nature of the blade curvature the pressure wheel did not

contact the blade at all times. It was mutually decided that further development was necessary to achieve the desired results.

PROTOTYPE2

Still working under the same contract, the private contractor designed and built the PROTOTYPE2. The primary difference with this model was that a pneumatic cylinder (76mm diameter by 152mm stroke) was employed to apply the grinding pressure in lieu of the pressure wheel assembly. Another pneumatic cylinder (25.4mm diameter by 305mm stroke) was mounted on the linear arm extension to provide 305mm of travel for the grinder. Controls were added to the grinder to allow the operator to move the grinder in the linear mode by pushing a button on either side of the grinder handles. A pressure control system was also adapted to the grinder to regulate the amount of force applied to the grinding surface.

At this point, a key safety feature was introduced. A hole was drilled into the grinder exhaust cavity to supply the air pressure to the 76mm pneumatic cylinder which applied the force. Therefore when the grinder was activated the arm would push against the blade with the grinding stone spinning at the required 6000 rpm. When the grinder handle was released, the exhaust pressure would also be eliminated, and the arm would lower away from the blade surface. The safety aspect of this design is that the grinding stone is always travelling at full rpm before it reaches the blade surface and conversely when the grinder is stopped the arm gently lowers from the blade.

At this point the project showed promise. It demonstrated that a pneumatically powered arm could be safely controlled by an operator in an overhead position.

PROTOTYPE3

The purpose of this phase was to construct a model suitable for field testing and incorporate the ideas generated from the testing and evaluation of the previous prototypes.

PROTOTYPE3 incorporated a 152mm x 102mm aluminum chassis 1168mm in length supported by a 559mm fulcrum. A quick disconnect system was developed to allow easier installation and removal of the system. The linear

travel was increased to 559mm incorporating a 25.4mm diameter rod-less cylinder. (Field testing proved the rod-less cylinder design to be insufficient to support the weight of the grinding tool when used in the vertical position, a lead screw design was substituted and proved effective.) The 76mm diameter by 152mm stroke pneumatic cylinder was also incorporated into this design to provide the grinding force. A regulator was mounted to the grinder to allow the operator to choose the appropriate grinding pressure. Control of the linear travel was accommodated through a "twist grip" arrangement on the grinder handle. The operator simply turned the grip in either direction to move the tool in and out. Rotational travel on the fulcrum was manually operated. A bearing assembly allowed relatively free travel.

A key design improvement was the grinder support arm. In previous prototypes, the arm was attached to the side of the grinder via a floating bearing assembly. This allowed some free travel but when the force was applied, the grinding operator had to correct the stone orientation to allow it to grind in a level position. This was due to the fact that the floating bearing assembly did not apply the force directly down the centre line of the stone.

To solve this problem, Mark Rosheim, a robotic wrist design engineer was hired by the private contractor. A number of concepts were formulated between the parties and a detailed design was completed based on the best solution. The result significantly improved the tool's performance. The grinding shaft was lengthened to accommodate a spherical bearing assembly which attached to a support arm. This allowed the grinder to move in a rotational manner for either overhead or vertical grinding situations.

An Ingersoll-Rand 99V hand held vertical air grinder was used on the PROTOTYPE3. It generates approximately 2.4 KW (3.2 hp.)

Field testing of the PROTOTYPE3 showed grinding times reduced in many cases by over 50% as well as improved surface finish. Testing was primarily conducted on the draft tube liner during a main unit overhaul and runner replacement at Pine Falls Generating Station under the supervision of Mr. Jim McNeill, Mechanical Maintenance Supervisor.

The PROTOTYPE3 was also used at the Selkirk Generating

Station to wire brush a coating on the condensate return tank. The tool was used on the overhead portion of the tank through about 90 degrees of arc, an area in which extreme fatigue and poor productivity were being encountered. Good results were attained with constructive feedback from the site personnel.

PROTOTYPE4

PROTOTYPE4 is the result of the testing of all previous models and incorporates design features to further improve productivity and worker conditions. Primary improvements included the following:

1. The addition of a 6 KW (8 hp) air motor to drive the grinding stone. Tests showed that further horse power could substantially increase productivity.

2. The addition of an Axial Drive Assembly. This allowed the operator to move the grinder in both the linear and rotational modes. A pneumatic brake assembly was incorporated to give the operator a choice of either manual or powered operation.

3. The weight of the PROTOTYPE4 was reduced by 9kgs. to facilitate easier installation. The Axial Drive Assembly was also designed to be installed separately to make it easier. The PROTOTYPE4 was reduced in length by 305mm from the PROTOTYPE3.

4. The linear travel arm was made telescopic to reduce the overall length. Linear travel increased to 610mm.

5. Due to the fact that 2 modes of operation had to be handled by the operator a new air logic system was developed. The twist grip was eliminated an replaced by a lever assembly controlled by the operators thumbs. A toggle switch located on the right handle changes the function of the lever assembly to either linear or axial drive.

6. An improved attachment method was developed in lieu of the PROTOTYPE3 design. Tests on PROTOTYPE3 indicated difficulty in "seating" the attachment spigot due to grinding dust. The improved attachment method employs a "bayonet" system with a locking collar.

TRACKING SYSTEM

A tracking system was developed for the PROTOTYPE4. It is designed for use when performing grinding operations during a unit removal. In the case of rerunnering the units on the Winnipeg River System, a stainless steel overlay is placed around the circumference of the draft tube liner as a preventative measure to reduce future cavitation damage. The TRACKING SYSTEM reduces set up time by increasing the work envelope. The TRACKING SYSTEM has a 914mm. travel and is attached by tack welding 2 spigots to the surface of the liner. This eliminates the need for the attachment rings used on PROTOTYPE4 and saves time during re-positioning. One setup of the TRACKING SYSTEM is equivalent to 3 set ups of the PROTOTYPE4 spigot mount.

TESTING PROTOTYPE4 IN THE FIELD

The PROTOTYPE4 has been in service since the summer of 1991. This model was tested under field conditions at the Pine Falls Generating Station during the Unit #5 overhaul and rerunnering. In this application, it was used to grind a band of stainless steel, welded around the entire circumference of the draft tube liner. The band was 356mm wide by approximately 16000mm long and was required to prevent cavitation damage to the draft tube liner just below the new runner. The band was built up in the normal manner using the mig welding process with 308L stainless steel .035" diameter wire and scarfed with a plasma arc torch. The PROTOTYPE4 was supported vertically using the TRACKING SYSTEM. (See Picture #1) From observations and comments from the site personnel using the tool and the writers, the grinding time was at least 50% faster with this system and considerably less fatiguing. The main objectives of this research project has been met, however some small refinements were required to the tool.

Modifications were made to the PROTOTYPE4 during the winter of 1991 to improve the control system. Manitoba Hydro did not have an opportunity to further test the system at that point in a field condition, however, a comparison test was performed at the Great Falls Generating Station on February 13, 1992 in which the PROTOTYPE4 was compared to a regular grinder in a simulated cavitation repair situation. The test consisted of grinding an area 266mm by 216mm on the underside of a piece of old turbine blade. The test area was built up with stainless steel simulating a cavitation

repair. A hydro worker experienced in cavitation repair work was selected to grind both areas. It should be noted that conditions were arranged to ensure the hand grinder was favoured thereby insuring the results would be conservative. This included using the hand grinder on the slightly smaller and less pronounced test area and using the hand grinder first to avoid any fatigue factor.

The results showed a definite productivity increase of 25% over the conventional hand grinding method. Rest period intervals were reduced by about half when using the PROTOTYPE4 with the operator indicating very little fatigue. Several of the stops were made to check the work and dress the stone. The stone appeared to require fewer touch ups and the finished surface was smoother with the PROTOTYPE4.

The PROTOTYPE4 was also used at Ontario Hydro's Kipling GS in February 1992. (See Picture #2)

SEVEN SISTER FALLS UNIT OVERHAUL

A runner replacement was conducted at Manitoba Hydro's Seven Sister Falls Generating Station in August of 1992. An additional PROTOTYPE4 and TRACKING SYSTEM were constructed for this job. In total, there were 2 PROTOTYPE4's and 2 TRACKING SYSTEMS utilized. The systems were used to grind a band of stainless steel, welded around the entire circumference of the draft tube liner. The band was 254mm wide by approximately 16000mm long and was required to prevent cavitation damage to the draft tube liner just below the new runner. The band was built up in the normal manner using the mig welding process with 308L stainless steel .035" diameter wire.
The band was not scarfed with a plasma arc torch in this application in order to prevent "hard spots" resulting from the heat transfer of the plasma torch. These hard spots were found to require more time to grind. Also to reduce the requirement for a second welding pass to cover areas that had been scarfed beyond specifications.

Manitoba Hydro personnel noted no appreciable difference in the amount of grinding force required to remove an equivalent amount of welded material between the job conducted at Pine Falls where scarfing had taken place and the current job.

Observations made during the Seven Sister rerunnering regarding the performance of the PROTOTYPE4 and TRACKING SYSTEM are as follows:

1. Operators experienced an inconsistent grinding force during the extension and retraction of the linear drive on the PROTOTYPE4. Testing showed that as the linear travel increased, it was difficult to precisely control the grinding force. In an attempt to alleviate this condition, an improved air regulation system was incorporated to the pressure cylinder of the PROTOTYPE4 to provide a more accurate method of controlling the force applied to the grinding stone. It has a faster response to minimize overshoot, a smaller pilot valve motion, and a constant bleed system.

2. Operators confirmed that the overall weight of the both the PROTOTYPE4 and the TRACKING SYSTEM must be reduced to improve set up time. Currently, installation of the TRACKING SYSTEM and PROTOTYPE4 require 3 operators.

3. Improvements are necessary to the "bayonet" connection between the PROTOTYPE4 and the TRACKING SYSTEM. Once coupled, the system is secure, however, during uncoupling a more convenient safety release is required to prevent occasional jamming.

4. A 165mm spring is currently used to hold the grinding motor in an approximate level position with relation to the grinding surface. This spring is connected between the grinding arm and motor assembly. Testing showed that the spring needed to be adjustable in order to compensate for varying positions of the grinding wheel in relation to the surface. An adjustable spring/shock absorber system is being considered.

5. A change was made to the TRACKING SYSTEM for this job. Gimbal mounted attachment plates were added to both ends to allow free 360 degree motion. Therefore only one end had to be removed at a time when repositioning. The other end swung through a 180 degree arc and was re-welded in a level position. Set up time was reduced by approximately 50%.

CONCLUSION

The research and development project to design and fabricate a tool to reduce the fatigue during cavitation grinding has been a success. A human amplifier grinding tool has been developed that not only reduces the fatigue of grinding, but improves productivity, safety, and quality.

ACKNOWLEDGEMENT

We would like to thank all the people who worked on this project to make it a success with special acknowledgement to:

Jim McNeill	Manitoba Hydro, Mechanical Supervisor
Roger Ludwick	Manitoba Hydro - R & D Dept.
Hazel Monkman	Manitoba Hydro - R & D Dept.
Jim Melvin	Manitoba Hydro - Export Services
W.L. Pawlikewich	Manitoba Hydro - Hydro Generation
David Schaldemose	Consultant
Dr. Mark Friedman	Carnegie Mellon University
Mark Rosheim	Ross-Hime Designs

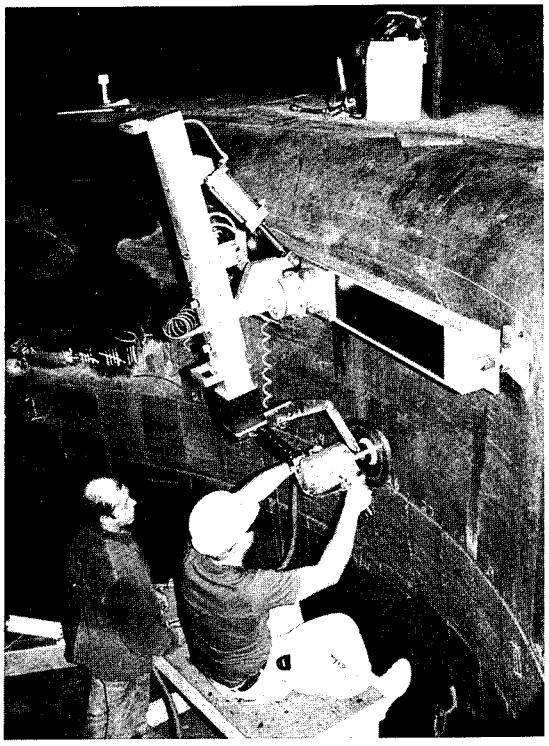

Picture # 1, PROTOTYPE4 and TRACKING SYSTEM in use at Pine Falls GS, July, 1991

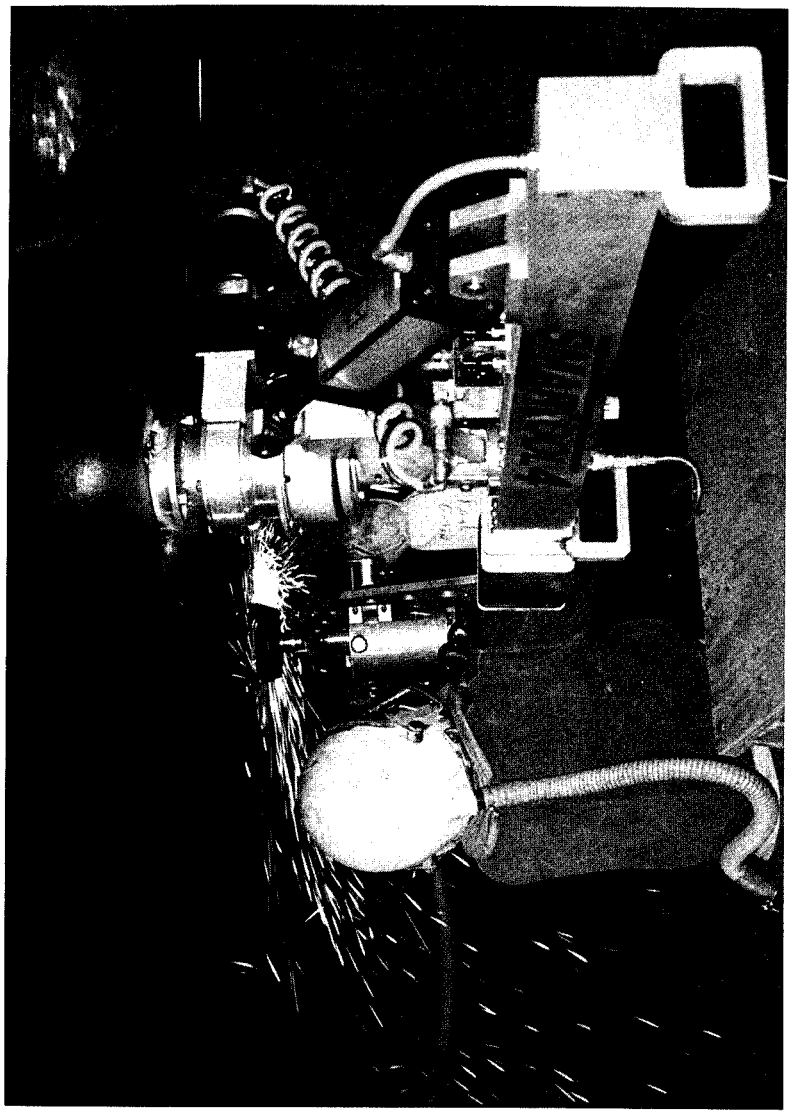

Picture #2, the PROTOTYPE4 in service on underside of Kaplan runner blade, Februray 1992.

Advances in Runner Design for Turbines and Pumpturbines using a Numerical Test Rig

E. Goede [1]
M. Eichenberger [2]
A. Sebestyen [3]

Abstract

The numerical design process used at Sulzer Escher Wyss to optimize turbine runners as well as impellers for pumpturbines is described. Examples are given for different types of machines. The question of accuracy of a numerical design is discussed.

Introduction

Upgrading as well as rehabilitation of existing generating stations is nowadays an increasing business and in many cases a great challenge for the designer. In that field the numerical flow simulation is a key tool to optimize the performance and cavitation behavior of the hydraulic turbomachine. The term *numerical test rig* is here introduced to indicate the way in which the numerical flow simulation is used today. The difference to the classical design process - definition of hydraulic shape, fabrication of model runner, tuning in model test - is only that this work is done today completely on the computer. This does not mean that the physical test facility is now obsolete. For large machines or if a great number of turbines are involved in the upgrading project, it is still needed to perform fine tuning on a physical test rig and to verify the performance.

In order to upgrade an existing turbine or pumpturbine, the main task is the development of a new runner or impeller to replace the old ones, whereas mostly the stationary parts of the hydraulic turbomachine remain unchanged. In such a case a runner design must be taylormade to fit into the machine and to achieve the required hydraulic performance as well. Here the numerical test rig is the fast and flexible method to develop appropriate technical solutions.

1 Head CFD and profile design,
2 design engineer,
3 specialist CFD, all Sulzer Escher Wyss, PO Box, CH-8023 Zurich, Switzerland

Of course, a good design has to take into account the influence of the stationary machineparts that will affect the performance of the runner. In fact, more and more components of the hydraulic turbomachine are now covered by the numerical flow simulation instead of calculating only the flow through the runner. In addition, viscous flow calculation is now applied if necessary. This is important especially for upgrading projects, where sometimes the old machine components are of unusual or poor design compared with the state-of-the-art technology. For example, old drafttubes tend to be unstable under some operating conditions. Here, the design of a new runner can be of some risk, if the influence of the critical components is not known and therefore not taken into account.

In short, one main advantage of the numerical design is to be able to control the pressure distribution on the hydraulic shape of the machine and therefore, to optimize it. This makes clear, why the following applications can be tackled successfully:

1. Operational problems with existing turbines or pumpturbines (i.e. cavitation) can be analysed and often be solved with a new runner design.

2. Potential for upgrading can be determined by performing a numerical flow analysis for an existing machine. If the discharge can be increased, the power output of the turbine can normally be increased in the range of 15 to 20% only by replacing the old runner with a new design, fig. 1.

3. If the operating conditions in a power station have changed over the years (head or tailwater level), with a new runner the hill chart can be shifted to match the new conditions.

4. The hydraulic efficiency can be increased through optimization of pressure distribution and flow field as well.

These tasks are summarized in fig. 2.

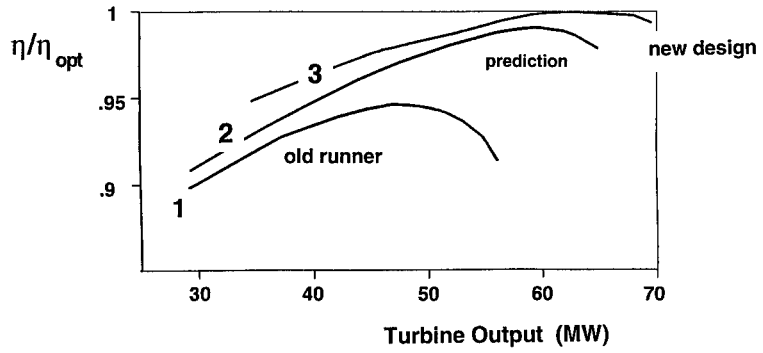

Fig. 1: Upgrading of Francis-turbine Saaheim, Norway, H = 268 m

(1) old runner, field test prior runner replacement
(2) predicted turbine performance with the new runner
(3) turbine performance with new runner, model test stepped up

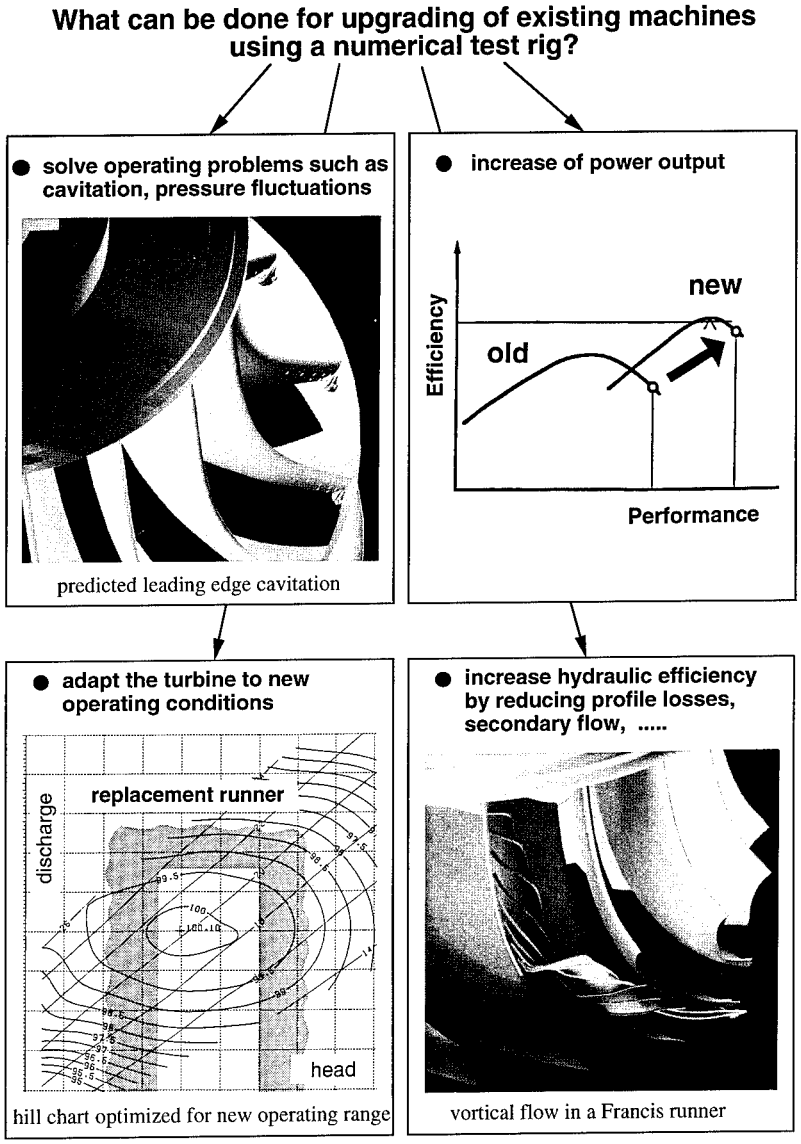

Fig. 2: Field of activities for a runner design based on numerical flow simulation

Numerical runner design process

The numerical design of turbine runners or impellers for pumpturbines at Sulzer Escher Wyss is based on numerical flow simulation using a 3-dimensional Euler method [1,2]. The solution of the Euler equations of motion makes sure the conservation of mass and momentum within the computational domain. If necessary, depending on subject or operating condition, Navier-Stokes flow calculation [3,4] is added to capture turbulence effects within the fluid flow as well as skin friction.

Since one has to deal with field methods, the flow channel must be discretized, here using the finite volume technique. This leads normally to a mesh size in the range from 10.000 cells for an Euler to 60.000 for a Navier Stokes application. Therefore, with CFD (computational fluid dynamics) the data flow is immense, and to find the right information to make sound decisions to improve the design is not an easy task.

However, the flow simulation is not the only part of the design process. The whole design procedure for numerical runner optimization is much more complex and consists at least of the following steps:

1. Define the runner geometry, that is the hydraulic shape, fig. 3,
2. generate a computational mesh for that geometry,
3. define the flow conditions and fluid properties according to operating point,
4. perform the flow simulation,
5. evaluate the numerical solution.

Based on step 5, a new runner shape is defined, and loop 1-5 is repeated until the pressure distribution is perfect and the required performance is obtained. Normally, this process is time consuming, tedious, and it requires a high level of technical expertise after all. But if the right software tools are put together to streamline the described process, the numerical runner design can be efficient and fast enough to motivate the designer to do an excellent job. One of these tools we describe in the next chapter.

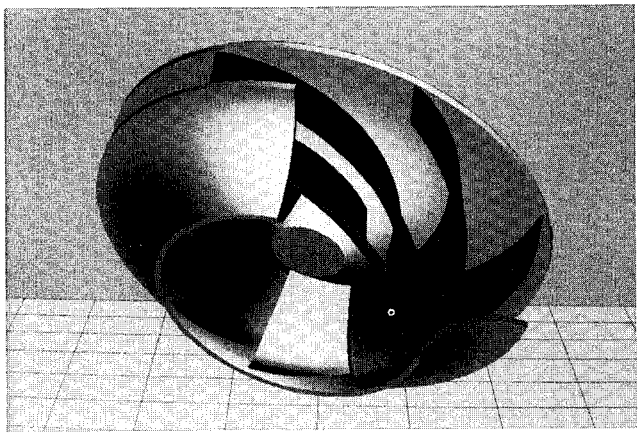

Fig. 3: Numerically optimized impeller for a reversible pumpturbine

Real Time Blade Generator

The advent of new powerful workstations made it possible to develop software suitable to define the runner blade shape in real time. The development of such a tool was initiated at Sulzer Escher Wyss not only to increase productivity of the runner design. More important, experience made before with the conventional method showed some shortcomings: In the past a designer had to work on different tasks at different time. As an example, it was difficult for the designer to forsee how the vent area was influenced if the profile thickness or blade curvature were changed, and so forth. Now, in real time, the designer is much more aware what he is doing when he is reshaping his blade. Here some details about the new method. As usually done [5], the blade shape is defined by specifying

- axisymmetric "streamlines",
- conformal mapping of profile meanlines,
- thickness distribution of blade profiles,
- blade inlet and outlet angles from band to crown, and so on,

now using Bezier polynomials and cubic interpolation as well. The corresponding graphics are provided in different windows on workstation screen, as shown in fig. 4. Each window is coupled with each other. In fact, if a changement is made in one window, all other graphics are immediately recalculated and redrawn. For instance, if the blade inlet angles are changed to improve leading edge cavitation indicated by the flow simulation, the consequences on the conformal mapping can be controlled easily. At the same time, the resulting blade is shown as a solid body in order to get a feeling for the real 3-D blade contour.

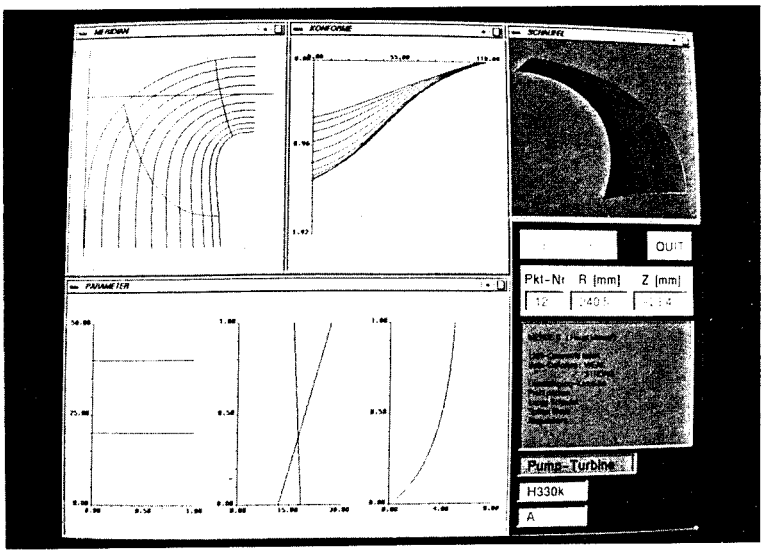

Fig. 4: Real time blade generator for the design of turbine runners and pumpturbine impellers

Hydraulic Design of a Pump-Turbine with Variable Speed

The operation of a pump-turbine at constant rotational speed has some drawbacks for both modes of operation. In pump mode the power input for the pump is roughly fixed for a given head, but sometimes the operator would like to use a different power. In turbine mode the machine cannot be operated at best condition, the turbine operates often at part load with severe losses in hydraulic efficiency. Here the use of variable rotational speed offers considerable technical adventages: For a given head, the pump can be run with variable power consumption, and the turbine can be used with maximum efficiencies according to the hill chart. As shown later, at part load a gain in effeciency of 20 % and more can be realized.

In specific terms, shown in fig.5, a constant speed operation can be represented by ψ=const. characteristics (dotted lines). Variations of power, expressed by the power coefficient $\lambda \approx \varphi.\psi$, are basicly possible at constant speed, achieved by the variation of the flow coefficient φ.

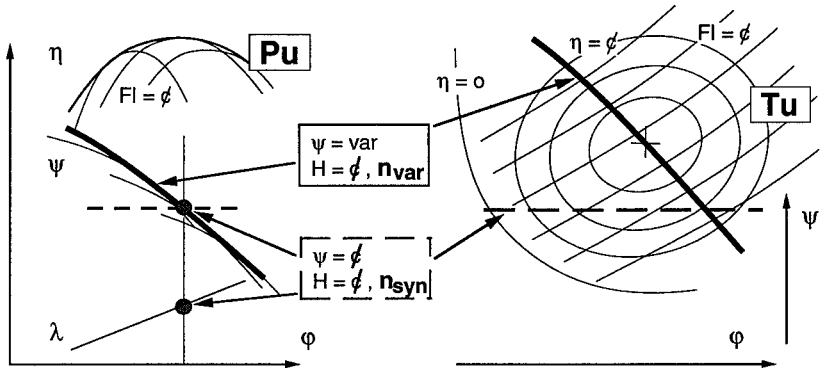

Fig. 5: Characteristics of a pumpturbine in specific terms
pump mode left, turbine mode right

1. Turbine mode

According to fig.5 it is obvious that with a variaton of λ a considerable drop in efficiency results at decreasing flow coefficient. However, turbine operation with variable rotational speed (n_{var}: full line in fig.5) leads to a respectable variation of pressure coefficient and enables to achieve turbine characteristics with much higher efficiencies at part load than with constant speed operation.

2. Pump mode

The variation of power for constant rotational speed is highly restricted. According to fig. 5 there is only a single operating point on the envelope satisfying ψ=const., so that λ=const. results. The guide vane throttling enables only few power-control of the pump, the pump efficiencies descent steeply as a result. In other words, there is no suitable way for a useful variation of the power in pump mode at constant speed. To change the power consumption in pump mode, a variable speed is necessary .

Following the above discussion, a pump-turbine with variable rotational speed was designed with use of numerical flow simulation. Compared with an existing machine the task for the new design was as follows:

- shift the turbine characteristics to 7% more power output,
- pump characteristics (ψ–ϕ) should be unchanged.
- shift the cavitation-characteristics in pump mode to 7% higher power (proportional to discharge),

The task has been accomplished by using purely CFD-tools. For turbine mode flow calculations were carried out with a 3-D Euler-code, pump operation was analysed with a Navier-Stokes code.

In order to verify whether the design goals have been achieved, the following graphics are prepared. First, fig. 6 makes clear that for both the existing and the new impeller the pump characteristic is the same, whereas the turbine characteristic has been shifted to higher discharge as required. In addition, for turbine mode, the difference in guide vane opening is given as a consequence of the different impeller contours.

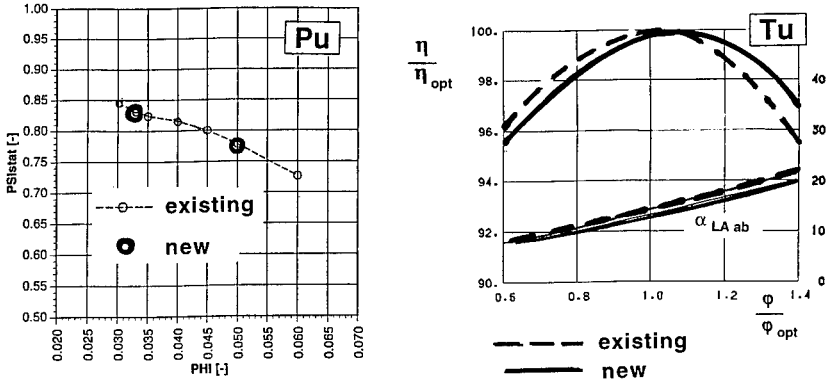

Fig. 6 : Machine characteristics for pump as well as for turbine mode, existing impeller vs. new design
pump mode left, turbine mode right

In pump mode the operating range is limited by leading edge cavitation at impeller inlet, either on blade suction side for low discharge or on blade pressure side for high discharge. To test the cavitation behavior of the new design at full load, the calculated pressure distribution is given in fig. 7 for blade pressure side at impeller inlet. The results are compared with those obtained for the existing machine. It turns out that, at homologous operating conditions, the existing and the new impeller have the same cavitation patterns indicated by low pressure peaks at leading edge below vapor pressure. Therefore, a shift of the new cavitation limit to higher discharge has been achieved as required.

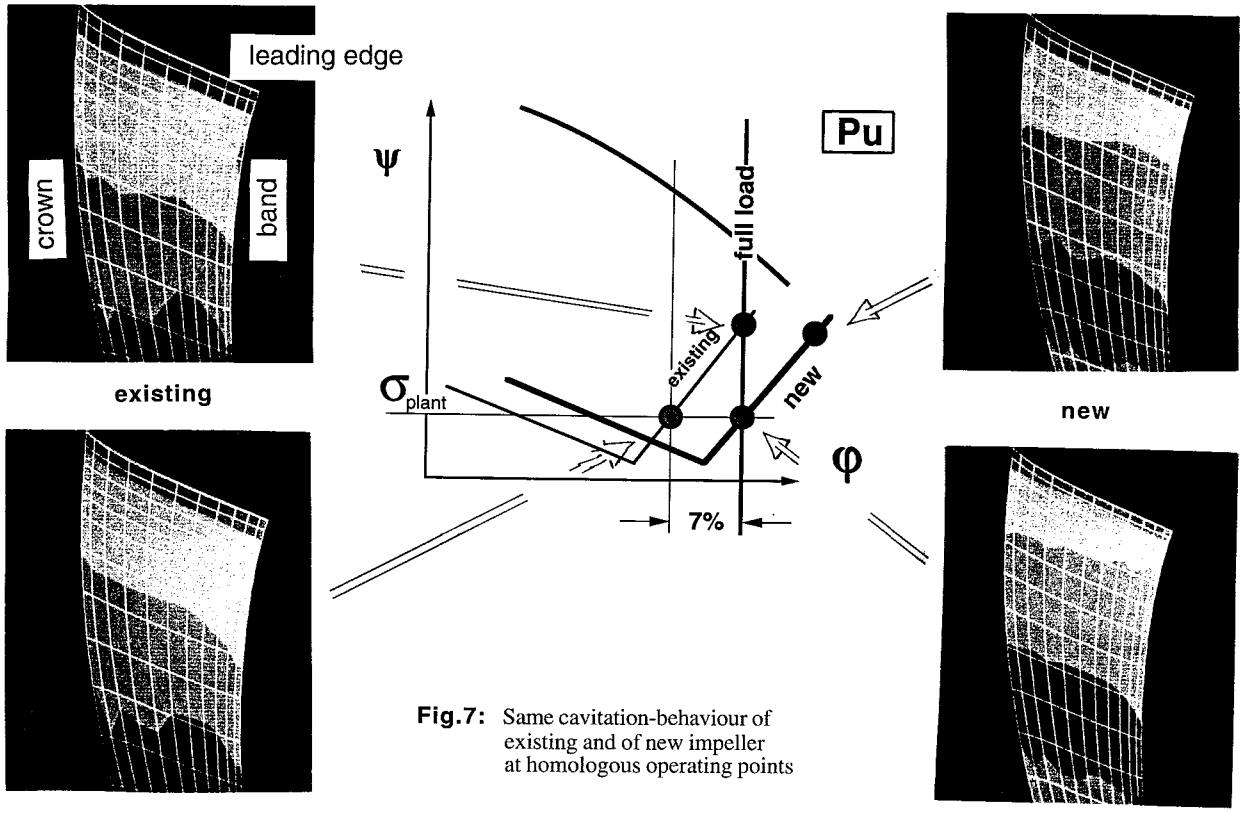

Fig.7: Same cavitation-behaviour of existing and of new impeller at homologous operating points

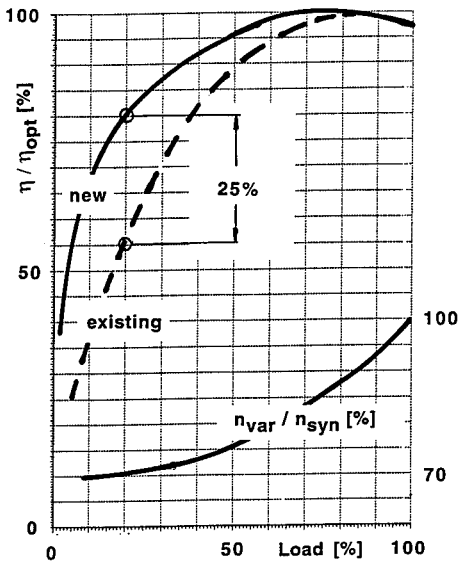

Finally, we present for the new design the predicted hydraulic efficiencies for turbine operation at constant speed compared with that at variable speed. For high turbine loads there is nearly no difference between the two concepts, as shown in fig. 8. However, for turbine operation at part load, especially for very low loads, a big gain in efficiencies can be realized. In fact, up to 25% higher turbine power can be generated with the same amount of water when using variable speed instead of using constant speed. Therefore, for an existing pumped storage plant in which the turbine often runs below 50% load, the concept of variable rotational speed can be a very attractive alternative.

Fig. 8 : Predicted efficiency for turbine mode
existing impeller with constant speed n_{syn}
new impeller with variable speed n_{var}

Conclusion

For upgrading of existing generating stations as well as for hydraulic design of new machines the numerical flow simulation is a key tool to optimize the performance and cavitation behavior of the hydraulic turbomachine. The term *numerical test rig* was introduced to indicate the way in which the numerical flow simulation is used today: Definition of the hydraulic shape, construction of turbine runner or pump-turbine impeller, tuning with flow simulation - is done completely on the computer.

As an example, it has been shown that, to design a pump-turbine impeller, it is possible to shift the cavitation characteristics in pump mode to higher discharge without influencing the ψ–ϕ-characteristics. At the same time the turbine output can be increased. This challenging example shows the flexibility and the potential of the CFD based runner design. However, the numerical runner design is a complex process, and it is not easy to bring it effectively to work. In this context, a new real time blade generator has been described that represents a further step to increase productivity and quality as well.

This does not mean that the physical test facility is now obsolete. For large machines or if a great number of turbines are involved in an upgrading project, it is still needed to perform fine tuning and to verify the predicted performance.

Nomenclature

D_1	[m]	runner diameter
g	[m/s^2]	gravitational acceleration
H	[m]	head
Q	[m^3/s]	discharge
n	[rpm]	rotational speed
η	[%]	hydraulic efficiency
$P = \rho g H Q$	[MW]	performance
c	[m/s]	absolute velocity
w	[m/s]	relative velocity
$Kc = c/(2gH)^{1/2}$	[-]	specific absolute velocity
Kw	[-]	specific relative velocity
Ku	[-]	specifische periferal velocity
Kc_m	[-]	specific meridional velocity
Kc_u	[-]	specific periferal component of absolute velocity
α	[°]	absolute flow angle
β	[°]	relative flow angle
incidence angle	[°]	flow angle relative to the blade at leading edge
deviation angle	[°]	flow angle relative to the blade at trailing edge
σ		cavitation number
$\psi_1 = H / (u_1^2/2g)$	[-]	head coefficient
$\varphi_1 = Q / (u_1 \pi/4 D_1^2)$	[-]	flow coefficient
$\lambda_1 = \psi_1 \varphi_1 \eta$	[-]	specific machine performance in turbine mode
$\lambda_1 = \psi_1 \varphi_1 / \eta$	[-]	specific machine performance in pump mode

References

[1] E. GOEDE, R. CUÉNOD: *Numerical Simulation of Flow in a Hydraulic Turbine.* SULZER Technische Rundschau 4/1989

[2] E. GOEDE, R. CUÉNOD, H. KECK, J. PESTALOZZI: *3-Dimensional Flow Simulation in a Pump-Turbine.* ASME Winter Annual Meeting 1989, San Francisco

[3] E. GOEDE, A. SEBESTYÉN, A. SCHACHENMANN: *Navier-Stokes Flow Analysis for a Pump Impeller.* IAHR Symposium 1992, Sao Paulo

[4] V. DEHENAU, G.D. RAITHBY, B.E. THOMPSON: *Prediction of Flows with Strong Curvature and Pressure Gradient Using the k - e Turbulence Model.* J. Fluids Engineering, Vol. 112, pp. 40-47, 1990

[5] H. KECK, E. GOEDE, J. PESTALOZZI: *Experience with 3-D Euler Flow Analysis as a Practical Design Tool.* IAHR Symposium 1990, Belgrade

DESIGN CRITERIA AND QUALITY REQUIREMENTS FOR LARGE TURBINES

Hermod Brekke

ABSTRACT

The paper gives a brief description of the accept criteria for material defects in large hydraulic turbines. The accept criteria are based on fatigue life time, choice of materials and the design philosophy for the machines.

Also the risk of not fulfilling the important safety requirement of leakage before rupture in pressurised stress carrying parts of large turbines is discussed.

The requirement of tolerances and rigidity to keep small clearances in large high-head machines in order to establish a valid scale effect formula of efficiency will also be discussed.

The last part of the paper includes a brief presentation of a part of the authors work in the scale effect discussion.

INTRODUCTION

Water turbines have been developed in the direction of large units with increased specific speed designed for higher heads. There has also been a demand for a wider range in operation both in head and output.

Because high head hydropower is very suitable for peaking operation, sudden variations in operation and frequent stopping and starting has increased the danger of material fatigue both in rotating parts and stationary pressurised stress carrying parts.
Many old turbines are in operation and care must be taken in refurbishment work and inspection to detect growing material defects due to fatigue.

In the design of new machines the level of working stresses has increased and in machines built after 1960, high strength steel has been used. The rised stress level has increased the risk of not fulfilling the requirement of leakage before rupture in stress carrying pressurised parts in case fatigue propagation has increased the size of hidden smaller material-defects.

Life time - and safety philosophy, choice of materials and production procedures as a basis for the design criteria are discussed in the following chapters.

The problems of deflections in large high head machines has become very important in order to obtain a reliable scale effect formula of efficiency from the model test to the prototype. The author is looking forward to a discussion in this field because some confusing divergences between scaled up model efficiency and the efficiency measurements of the prototype efficiency has been observed. The authors work in previous discussions has been included in the last chapter of the paper.

Professor, Hydraulic Machinery, The Norwegian Institute of Technology

MATERIAL DEVELOPMENT, WORKING STRESSES AND MATERIAL DEFECTS

The pressurised stress carrying parts designed for maximum stress will be the spiral case including the stay ring for Francis turbine and distributor for Pelton turbine. The development of weld able high tensile strength fine grain steel plates have substituted the heavier cast steel design and reduced the number of working hours on turbine production per MW turbine output dramatically. This development can also be illustrated by showing the reduction in weight per MW of the spiral cases of hydraulic homologues high head turbines designed during a period over 20 years. The data is received from the Norwegian turbine manufacturer KVAERNER.

A similar development can be seen in all kinds of turbines, were the stress will be the dimensioning parameter. It should be noted that the strength of the materials has been increased by a factor of 2 from cast steel to fine grain steel.

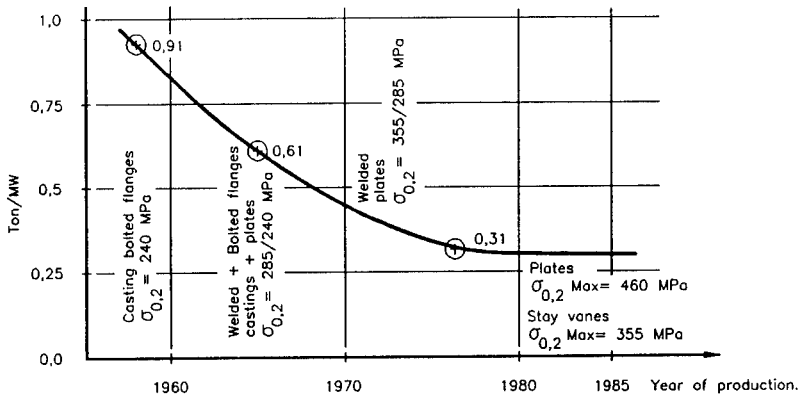

Figure 1 Weight reduction per MW of spiral cases of high head Francis turbines.

However, when increasing the working stresses the danger of fractures from material defects increases. Special attention must be paid to weld defects, in particular cracks which is difficult to detect by X-ray inspection. Fatigue crack growth from sharp corners of defects or cracks which may reach critical crack sizes followed by an unstable fracture, must be avoided by reducing the allowable working stresses.

Safety factors against yelding and/or ultimate stress for the material used are not alone a safe criterion against fracture for high tensile strength steel. Fracture mechanics theory must be taken into consideration and acceptance criteria for defects must be established. It must also be distinguished between acceptable defects in production of a new turbine part and the critical crack size which may be a result of fatigue crack growth starting from undetected defects, during operation.

A crack grown by fatigue must be detected and repaired before the critical size is reached. The inspection of machines in operation is because of this very important.

ACCEPTABLE DEFECTS IN WELDS AND BASE MATERIALS

Basically the stress carrying parts in a Francis turbine are statically loaded. However, if a valve is installed in front of a turbine which is in peaking operation the stress carrying parts on the turbine may be loaded and unloaded 3 times per day which during a life time of 50 years leads to approximately 50 000 cycles totally. In addition minor stress amplitudes caused by pressure oscillations in the penstock from the turbine regulating will be superimposed.

The following criteria then may be established:

1. The statical working stresses must be limited to a value which gives a critical crack size large enough to penetrate the plate. (Leakage before rupture)

2. An acceptable material defect in a new machine shall be so small that it does not grow to a size which leads to unstable fracture (rupture) within 20 000-50 000 loading cycles (i.e.. pressurising and depressurizing)

3. On the other hand a non acceptable defect in a new machine must not be so small that it may be overlooked during inspection by Ultrasonic-, X-ray-, Magnaflux, Penetrate liquid (Dye check) or other methods

4. The stress level including local stress concentration and residual stresses from welding or casting, which has influence on the crack growth, must be limited to a level which makes it possible to fulfil 1, 2 and 3

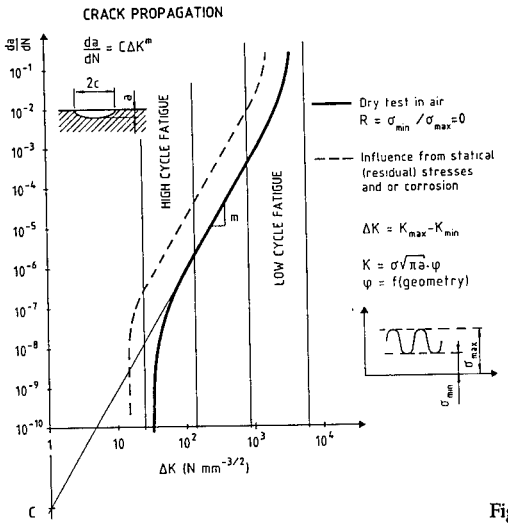

Figure 2 Paris

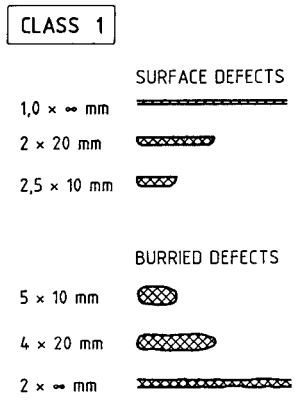

Figure 3 Acceptable cracks for lifetime of 50 000 cycles σ = 180 MPa

Unfortunately the fatigue crack propagation speed on cyclic load in homogeneous material has not decreased even if the toughness and strength have increased. A reliable direct connection between impact tests and crack propagation speed has not been proved so far. However, the ultimate fracture are greatly influenced by the brittleness of the materials.

The fatigue crack propagation is today normally presented in Paris diagrams based upon an increasing number of measurement of crack propagation under cyclical load for different materials and weld deposits. In figure 2 a Paris diagram is shown qualitatively as a function of the values of m and C which are material constants determined from fatigue tests of base materials weld deposit and heat affected zone (HAZ) of different steel qualities. Even if no improvement of fatigue in homogeneous high tensile strength steel has been proven, the quality improvement by less defects has increased the fatigue life time. However, it should be noted that a tough material has a larger resistance against unstable fracture so the critical crack size is larger i.e.. higher crack tip opening displacement (CTOD) as explained later.

The Paris equation yields:

$$da/dN = C\Delta K^m$$

and

$$\Delta K = K_1 - K_2 = (\sigma_{max} - \sigma_{min})\sqrt{a}\,\phi$$

where ϕ is a geometric factor, m and C may be chosen to C = 10^{-11} and m = 3.0 as a conservative mean value according to data for steel of different qualities. In figure 3 calculated acceptable defects in a new turbine for a number of cycles up to 50 000 and stresses up to σ_{max} = 180 MPa are shown where the critical crack size is assumed to have a depth of a_{cr} = 100 - 150 mm for ductile materials with the critical crack tip opening displacement measured to COD = $\delta_{cr} \geq 1.0$ mm.

For high cycle fatigue of runners it seems to be proven that no crack propagation occurs if $\Delta K \leq K_{th}$ (K_{th} = fatigue threshold value). This value will be discussed later in this paper.

THE CRITICAL CRACK SIZE IN PRESSURISED PARTS

The critical crack size which leads to unstable fracture may be determined based upon crack tip opening displacement - (COD) - tests of base materials and welds (Anderson 85). It should be noted that the influence from residual stresses and stress concentration around the area where the crack or defect is located, is of great importance for determination of the critical crack size (Dawes 85).

Normally materials for turbines are of the ductile type including both elastic and plastic deformation of the crack tip before propagation, depending on the strength of the material and the level of the working stress. However, it has been proven from COD - tests that a high tensile strength steel combined with a high working stress level allows for smaller critical crack sizes than a lower tensile strength steel with lower working stress. However, the smaller critical crack depth may partly be compensated by thinner shells which give leakage for smaller crack depths, but large units will get thick plates.

How to calculate the critical crack size is very well described in (Dawes 85). The calculation is based upon several large scale tension tests of different materials where crack tip opening displacement, crack length and the mean stress in the plate have been measured. How to define an unstable or critical crack size by this method is illustrated in figure 4 and may be defined as follows:

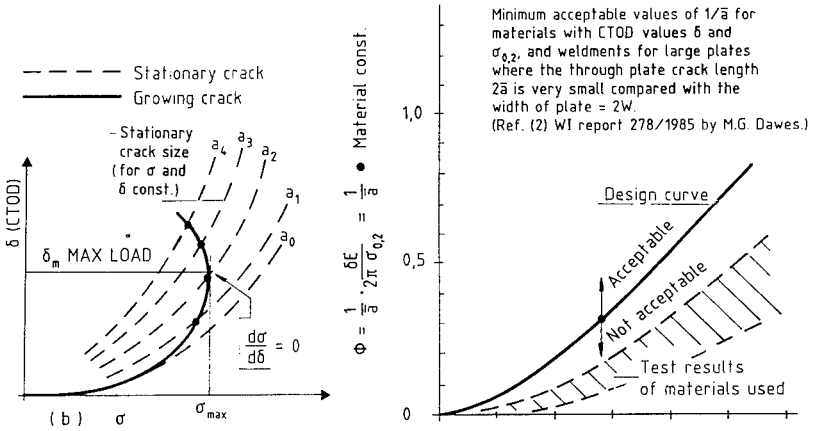

Figure 4 Critical crack size.

Figure 5 Design curve for allowable crack.

A stable crack under static load can only be increased by increasing the working stress in the material where the crack is located.
As the crack grows it will finally reach a size where no increase in the stress is necessary to increase the size of the crack opening i.e.. $d\delta/d\sigma = 0$. This will be the critical crack size or CTODC value and total fracture occurs if the stress is not decreased.

In figure 5 is shown the design curve based upon a dimensionless COD value δ as a function of applied local stress around the crack tip.

The dimensionless value for welded ferritic steel yields:

$$\phi = (1/\bar{a})(\delta E/(2\pi\sigma_{0.2}))(1-2\bar{a}/(2w)) \qquad (1)$$

When substituting for δ by δ_{cr} (= critical CTODC value which is the value where fracture occur). The second term represents a material constant. The last term includes the length $2\bar{a}$ of a through plate crack and the plate width 2w. For a relatively small crack-size/plate-width ratio the last term in eq. (1) may be neglected. The σ_1 value in figure 5 is the working stress including an eventual stress concentration factor K_{sc} and residual stress in the weld. Following equations should be used for post weld heat treated welds with nominal stress = σ.

Weld and heat affected zone:

$$\sigma_1 = \sigma K_{sc} + 0.25\sigma_{0.2} \qquad (2)$$

In a plane plate with ground weld K_{sc} = 1.0. For welds without post weld heat treatment:

$$\sigma_1 = \sigma K_{sc} + \sigma_{0.2} \qquad (3)$$

By means of σ1 and the know values of $\sigma_{0.2}$ (or yield stress), the elasticity modules (Young's modules) E and the critical crack tip opening displacement of the material $\delta = \delta_{cr}$ = DTODC the critical value of a through plate length = $\bar{a}_{max}$ may be found by means of the value of $\phi = f(\sigma_1/\sigma_{0.2})$ taken from figure 5.

Then one gets:

$$\bar{a}_{max} = (1/\phi)\delta_{cr}E/(2\pi\sigma_{0.2}) \qquad (4)$$

Because a short through plate crack = $\bar{a}$ is not a normal shape of a defect, corresponding values of surface cracks and a buried crack must be found. Corresponding values of crack depths for different crack depth/length ratios for surface crack and for buried cracks have been found by fracture mechanical theory and experiments as presented in (Dawes 85).

By means of the shown procedure one can now determine the statical working stress which allows for a crack through plate thickness for given values of the critical CTODC in the plate and welds used. As stated earlier in this paper the following statement should be made For safety reasons the critical crack should penetrate the plate before rupture i.e.. $a_{max} \geq s$.

It should also be noted that some not published reports show very low values of COD in a narrow heat affected zone (HAZ) even after heat treatment of the weld for high tensile strength steels with $\sigma_{0.2}$ > 355 mPa. For example CTODC values down to δ_{cr} = 0.02 have been measure in the HAZ in K welds in small test samples for plate qualities with $\sigma_{0.2}$ = 460 mPa after post weld heat treatment. However, COD test of wide plate specimens have indicated that the tougher material adjacent to the heat affected zone normally stops the crack also for the K type notch because the narrow HAZ is never straight enough to lead the crack in the brittle material in a normal weld. Thus the δ_{cr} values increase. Further experiments in the future may hopefully prove this indication.

From this chapter following conclusion may be drawn:

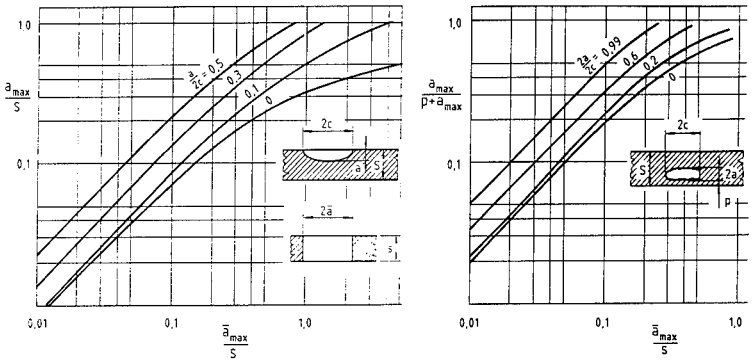

Figure 6 Elliptic cracks compared with through cracks.

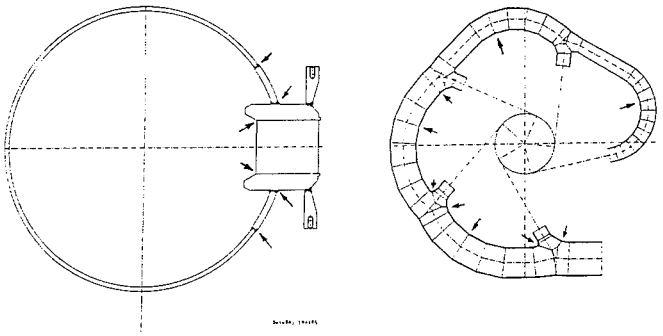

Figure 7 Critical points in spiral case and distributor

It will be very difficult to increase the maximum working stresses above 200 MPa for large turbines parts exposed to loading cycles above 20 000 in lifetime if leakage before rupture shall be fulfilled.

Due to the residual stresses and the hardening effect of high tensile strength steels, welds should be post - weld heat treated if the machine will be in peaking operation.
For Pelton turbine distributors the bend joints on the inside will be the critical point, and for Francis turbine spiral cases the critical points will be the joint between the plates and the stay ring as well as the welds joining the stay vanes and the stay ring where care should be taken because no leakage will indicate cracks in this place. (see figure 6 and figure 7).

PARTS EXPOSED TO HIGH CYCLE FATIGUE

Pelton runners:

Both runners and also guide vanes specially in reversible pump turbines, will be exposed to high cycle fatigue passing 10^{10}-10^{11} cycles with relatively low stress amplitudes. Casted Pelton runner in 13 % Cr 4 % Ni alloy steel have been thoroughly discussed in (Brekke 84) and this paper will give a brief discussion of the 16 % Cr 5 % Ni quality which has been used for fabricated Francis runners because no preheating is needed and the cavitation resistance is excellent (Brekke 86).

As explained earlier in this paper the threshold value in the Paris diagram has been defined for an infinite number of cycles to be $\Delta K_{th} = 50$ Nmm $^{-3/2}$ for R = 0.3 (Brekke 84) and in the literature (Grein 86) a higher value $\Delta K_{th} = 72$ Nmm$^{-3/2}$ for R = 0.5 has been found for 13 % Cr 4 % Ni alloy steel.

Fabricated Francis runners:

For large turbines also the high head runners may be fabricated. For low head runners electroslag welding has been adopted because of capacity limitation of the foundries. Now and then blade cracking in Francis runners and reversible pump turbine runners has been reported. The reason for fatigue cracks will always be found in a material defect often combined with residual stresses from welding and high cycle stress amplitudes created by the wakes behind the guide vanes or Von Karmas vortexes.
For low head runners mechanical resonances in the runner itself may also lead to fatigue cracking. For rigid high head runners possible resonances may occur from chock wave resonances in the hydraulic system while mechanical resonances normally will not be the reason except in special cases.
Based upon various strain gauge measurements on the runner blades of Francis turbines following conclusion may be drawn:

1) The main frequency of the stress amplitudes in the runner which always will be found in the blades of a Francis runner will be $f = Z \cdot n / 60$ Hz where Z = the number of guide vanes. (A multiple of guide vanes number and the runner blade number may also give a stress peaks for higher frequencies (see fig. 6 where higher frequencies are superimposed 24 guide vanes and 30 blades, 6 x f can be found).
2) The Stress amplitudes are normally moderate and maximum peak to peak values have been measured to about $\Delta\sigma = 40$ mPa on the blade a outlet adjacent to the shroud.
3) If blade cracking occurs, the reason may be high residual stresses in the runner and/or blade resonances to either the main frequency $(f = z\,n / 60)$, a multiple of the main frequency or Strouhals number of the blade outlet flow.

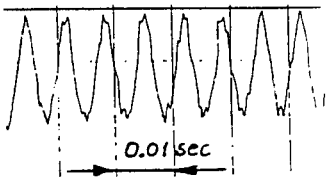

Figure 8 Recorded stress amplitudes on outlet of a runner blade in a 180 MW, 420 m, 375 RPM Francis turbine.

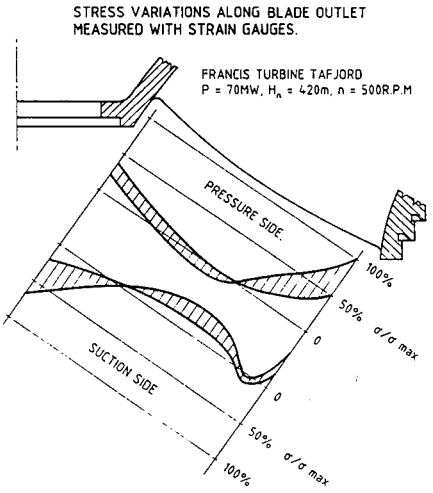

Figure 9 Stress variation measured on a Francis turbine.

In figure 8 typical recorded stress amplitudes with a frequency 150 Hz are shown for a 375 RPM high head Francis turbine with 24 guide vanes and 30 runner blades included splitter blades. In figure 9 is shown the variation of statical stresses superimposed with amplitudes on the outlet edge of a runner blade on another smaller low specific speed Francis turbine. The maximum stress amplitudes normally occur at the blade outlet close to the band on the runners for these Francis turbines. For a reversible pump turbine with a low number of longer blades the critical zone normally will be at the high pressure side i.e.. the turbine inlet side. Acceptable criteria for linear surface defects could be a maximum length 1.5 mm and a depth 0.5 mm.

The quality requirement to fulfil this requirement will be possible with careful welding practice. In the middle of the through thickness of the blade welds the stress amplitudes are normally strongly reduced because of the dominating bending stress amplitudes in the blades and buried cracks with sizes up to 2.5 x 2.5 mm or 10. x 1.5 may be accepted in the middle of the thickness with the same safety as a 1.5 x 0.5 mm surface crack.

THE DEFORMATION AND FLEXIBILITY OF LARGE MACHINES

The deformations in large turbines will always cause problems due to leakage flow. Large tip clearance of Kaplan runners and axial clearance between head covers and the guide vane end faces will always cause losses in efficiency.

Special attention should be paid to the leakage caused by the guide vane clearance in low specific speed Francis turbines. It should also be noted that an increased efficiency may be obtained in a model by a careful production without waviness and sealed clearance between guide vanes and the facing plates of the covers. It should be noted that even 0.1 mm clearance decreases the efficiency in the model so care is often taken by reducing the clearance to zero in the model.

In the prototype, however, the deformation of the head cover and bottom cover may be relatively large in an order of 1.0-1.5 mm in a pressurised turbine. Rigidity of the covers cost money and the price must be kept low due to competition. The clearance of non-pressurised covers is normally made within given tolerances in the order of 0.05-0.25 mm for a high head turbine. However, variations within normal tolerance may lead to variation in efficiency of homologous turbines. This phenomena has been studied by increasing the clearance gap step wise on prototypes followed by efficiency tests as shown by (Brekke 88). In figure 10 is shown the loss in efficiency caused by too loosely prestressed bolt in the bottom cover of a high head Francis turbine where the prestressing of the bolts reduced the clearance by 0.35 mm.

The efficiency scale effect code does not include any rules about the described clearance gaps. In the struggle of increasing the model efficiency small clearances or seals have been used between the guide vanes and the covers on the model turbines. In figure 11 the best efficiency of three model turbines and several prototypes of different sizes, but with the same specific speed are shown.

The best model efficiency presented in fig. 11 is obtained with sealed guide vane clearance. A 0.6 % increasing in efficiency is obtained compared with the model tested with normal clearance. The poorest efficiency has been obtained by a model made with surface finish, waviness and clearances homologous to the maximum tolerance of small prototypes. If the best efficiency of a model with rough surfaces and large guide vane clearances homologous to small prototypes is compared with the best efficiency of the prototypes, following scale effect formula seems to be valid:

$$\Delta\eta = \left(1-\eta_{t_1}\right)\left(1.064-0.54\cdot{}^{*}\Omega\right)\left[1-\left(Re_{t_1}/Re_{t_2}\right)^{0.2}\right] \qquad (5)$$

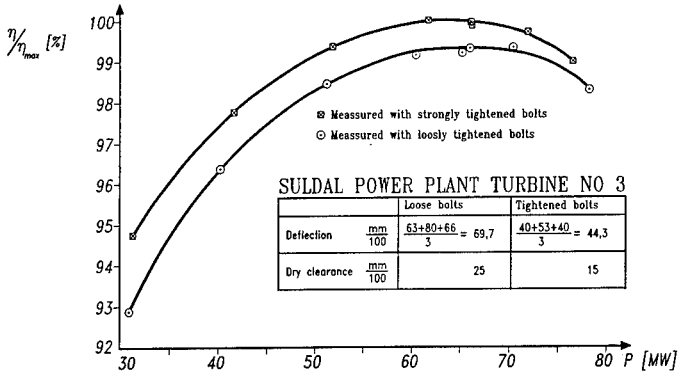

Figure 10 Difference in efficiency caused by to loose prestressing of bolts in bottom cover of a high head Francis turbine.

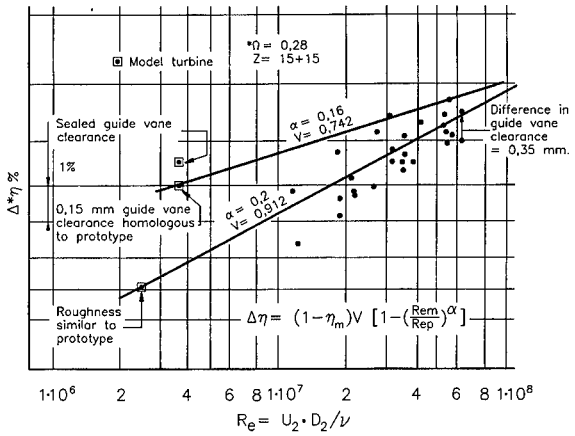

Figure 11 Results of thermodynamic efficiency on prototypes and model efficiency.

The formula in eq. (5) will also be valid for the scale effect between small and large prototypes. However, by comparing modern model turbines with prototypes with Re = $5 \cdot 10^7$ one finds a different scale effect, but for a small prototype no scale up effect of efficiency can be found (see fig. 11).

CONCLUSION

The reliability and availability of Francis and Pelton turbines depend on the quality and weld ability of the materials and the general design. It is important to improve the development of materials for plates with large thickness for welding without heat treatment and still obtain acceptable fracture mechanical results. Runners should be made with defects small enough to guarantee a life time of 10^{11} cycles. It is most important to

make the models with clearance gaps and surface smoothness homologous to the values of the pressurised prototypes. A most important detail concerning the efficiency is the guide vane clearance gaps in high head Francis turbines. This gap should be measured on pressurised prototype at site and on the end clearance model. Standard codes for tolerances should be developed.

ACKNOWLEDGEMENT

The author thanks Kværner Energy A/S for admission to material published in this paper.

REFERENCES

(Anderson 85) T. L. Anderson. Elastic - Plastic Fracture Assessments based on COD. WI report 276/1985.

(Dawes 85) M. G. Dawes. The COD Design Curve Approach: Limitations, Finite size and Application. WI report 278 1985.

(Brekke 84) H. Brekke. "A General Study on the Design of Vertical Pelton Turbines" Proceedings Thirty-five years of Turbo institute. Ljubliana 1984.

(Grein 86) H. Grein. Inspection Periods of Pelton Runners. Proceedings, IAHR, Stirling 1986.

(Brekke 86) H. Brekke. "Design and Material Quality for High Head Turbines" Proceedings IAHR, Montreal, 1986.

(Brekke 88) H. Brekke. "The Influence from guide vane clearance gap on efficiency and scale effect for Francis turbines" Proceedings IAHR, Trondheim Norway 1988.

SYMBOLS

a	=	crack dept (mm)	P	=	power MW
C	=	constant in Paris equation	H_n	=	net head
m	=	exponent in Paris equation	n	=	speed RPM
N	=	number of cycles			
K	=	stress intensity factor $Nmm^{-3/2}$			
ΔK	=	stress intensity factor amplitude			
σ	=	stress (MPa) (N/mm^2)			
ϕ	=	geometry factor and design constant			
δ_{cr}	=	critical crack tip opening displacement (mm)			
COD	=	crack tip opening displacement (mm)			
E	=	young modules, elasticity modules ($2.07 \cdot 10^5$ N/mm^2)			
D	=	pipe diameter (mm)			
S	=	plate thickness (mm)			
Z	=	number of guide vanes			
R	=	$(\sigma_{min}/\sigma_{max})$			

C, Cr Ni, N, V, Nb, S = chemical symbols in composition

A REVISIT TO DATA PROBLEMS AND DATABASES*

Shou-shan Fan, Ph.D.**

(* The discussions in this paper represent the views of the author and may or may not be the views or positions of the Federal Energy Regulatory Commission or its staff.)

I. INTRODUCTION

Data has become an essential part of our life. Hydrologic data are the basic information we need to successfully plan, design, and operate any water resources development.

In modeling, adequate data also are critically important for modelers and users. To the modelers, data are critical in developing models; to the users, adequate data are absolutely necessary for calibrating, verifying, and running the models.

A nine-agency Sedimentation Work Group, chaired by the author, has proved these points in a joint evaluation of computer sedimentation models, developed in the United States (Fan, 1988).

In general, data adequacy problems are of three major types--quantity, quality, or both. Data quantity and data quality problems are closely related and are usually treated together.

In my experience, the major cases involving data problems are: (1) monitoring; (2) sampling; (3) uncertainty and errors; (4) database management; (5) treatment, analysis, and interpretation; (6) processing and transmission; and (7) presentation.

Because of page limits and the complexity of the problems, I am limiting this paper to the first four problems. For each of the four problems, the discussion will be very brief, and serving only as a road map to the problems. In depth details of these four problems and a discussion of the remaining three problems will be covered in future publications.

** Special Assistant, Office of Hydropower Licensing, Federal Energy Regulatory Commission

II. DATA MONITORING

The data we need are often nonexistent or not readily available. We usually have to collect a great deal of field data ourselves. But data collection can be complex, expensive, and time consuming. Therefore, in resolving data problems, we need to determine the worth of data by balancing the need, accuracy, and cost-benefit ratio of the plan.

In designing a data monitoring program, we must at least answer these questions:

1. What parameters must be monitored?
2. What gages or instruments should be used?
3. Where should the gaging station be located and how many gages do we need at each station?
4. How many stations are needed, how should they be distributed, and how should they be operated?

These questions are essentially network problems. The answers to these questions are not easy. They are not general, vary from problem to problem, and are site-specific.

The answers depend primarily on how well we understand the characteristics of the problems we study. Other critical factors are local environment, economics, and budgets.

Often we do not know exactly how to select the parameters that describe the phenomena or how to accurately measure the parameters once we select them. For example, channel roughness is one of the most important parameters in stream flow and sedimentation studies, but there is no accurate way to account for its true value.

At present, the best we can do is to approximate a time and a spatial, invariable average through indirect ways, using known values of channel geometry and flow characteristics.

For flows in a fixed-bed channel, channel geometry is a random variable in a spatial domain, independent of the flows. In an alluvial channel, however, the problems become much more complicated: channel geometry is random in both the spatial and the time domains and interacts continuously with random flows.

III. OPTIMAL DATA SAMPLING

Sampling and monitoring are closely related and are often used interchangeably. When a data collection plan is made, these two problems must be solved together.

Some scientists therefore consider the two as one problem; strictly speaking, however, sampling and monitoring problems are distinct.

In this paper, monitoring problems usually deal with instrumentation and networking (data collected by more than two gages or at two or more stations). Sampling problems, on the other hand, deal with accuracy and the length of records obtained at a single gaging station.

As we know, many natural phenomena are recorded in continuous analog form. To analyze these voluminous data, we usually rely on digital computers. To do that, we must first map a sampling plan and then digitize the analog data at a predetermined sampling intervals.

In a sampling plan designed to analyze ocean waves propagating in a harbor, the author demonstrated that sampling interval, record length, and the error associated with the analysis are closely interrelated (Fan, 1968). As shown by the analyses, the narrower the time interval, the higher is the resolution and the shorter is the data length required.

Adopting a narrow time interval or a high frequency may cost greater effort and may create aliasing (folding frequency) problems that worsen the data's quality. Therefore, to balance these complicated interrelationships, we need to find an optimal sampling interval and a corresponding optimal record length.

IV. DATA STORAGE, RETRIEVAL AND DATABASE

After engineers collect voluminous data, data management-storing and retrieving data cost effectively-immediately becomes a critical issue. Database application is a modern technique that can help minimize, and perhaps solve, expensive data management problems.

In this paper, a database is defined as an orderly collection of all information, stored in a single, integrated system. In a speech to scientists in Taiwan, the author stressed that a good database must be user friendly, expandable, dynamic, and adaptable to any major foreseeable changes (Fan, 1976).

Generally, establishing a database has several major advantages: the information in the database (1) can be retrieved rapidly, accurately, and often cost effectively; (2) can show the need of correcting inaccurate, inconsistent, and redundant historical data; and (3) can be accessed simultaneously by multiple users.

To design a database, we should do the following:

1. Identify data elements and set up a data dictionary and a data directory
2. Define file requirements and develop master and subordinate files with known file characteristics and given data elements
3. Select objectives and plan future changes
4. Evaluate the need for a current system and for future expansion
5. Map a plan and schedule for developing the database
6. Develop programs controling input and output to measure the database's performance in retrieval efficiency and storage utilization
7. Develop test programs with complete documentation
8. Plan a security system, using backfiles and data recovery techniques, to protect data, equipment, programs, and documentation
9. Plan database modifications and cleanup strategy
10. Plan system audits and evaluate results

V. DATA ERRORS AND PROPAGATION

Most errors are primarily of two kinds--accidental and systematic. These two errors are quite distinct in nature.

Accidental errors are random in occurrence and magnitude. These errors may take either a positive or a negative sign. In fact, the probability of having a positive sign equals the probability of having a negative sign. These errors can often be eliminated by averaging repeated measurements under the same conditions.

Systematic errors are invariable and have the same magnitude under any condition. They are often caused by natural, instrumental, and personal factors.

Systematic errors are often cumulative. By comparing these errors with independent results, we can easily remove them once they are detected.

Furthermore, when a value is computed and indirectly derived from several parameters that are erroneously measured, the value's errors are compounded. The extent of these compounded errors can usually be determined through using calculus, if the relationship between the computed value and its component parameters can be represented by an equation that is differentiable.

VI. UNCERTAINTY, RELIABILITY, AND RISK

When we collect and use data, there is always a degree of uncertainty. Uncertainty and reliability are complementary: when uncertainty is zero, the data are reliable; when nothing about the data is certain, the data are totally unreliable.

Although uncertainty and risk are often used interchangeably, they are different. Risk is predictable; uncertainty is not.

Uncertainty is the event for which risk cannot be predicted. Risk is the probability of an undesirable event. Thus, when risk is zero, the event is certain; when risk is infinity, the event becomes totally uncertain.

Despite the great achievements in scientific research, we still do not thoroughly understand many natural phenomena. Uncertainty exists in almost every hydrologic investigation and every data monitoring program (Fan, 1984). Under these circumstances, the best we can expect in data collection and monitoring is an approximate value.

VII. CONCLUSIONS

1. Data is an essential part of our life.

   To engineers, adequate hydrologic data are important for successfully planning, designing, and operating any water resources development. To the modelers, data are critical in developing models. To the model users, data are absolutely necessary for calibrating, verifying, and running the models.

2. The data we need are often nonexistent or not readily available. We usually have to collect a great deal of field data ourselves. But data collection can be complex, expensive, and time consuming; sometimes, for a small project, may not be economically justified.

3. Despite enormous accomplishments by many scientists, we still do not thoroughly understand the physics underlying many real phenomena. In data collection and modeling, uncertainties are everywhere, we may never know the true value we are seeking. Under these circumstances, the best we can expect to get is only an approximate value.

4. We believe we can statistically determine optimal sampling intervals and corresponding optimal record lengths.

5. Most data errors are of two kinds--accidental and systematic. Accidental errors are random and can be eliminated through repeated samplings. Systematic errors are invariable and cumulative; they can easily be removed, once they are detected, by comparing them with independent results.

6. Database is a modern technique that can help minimize, and perhaps totally solve, the expensive data management problems.

VIII. REFERENCES

1. Fan, Shou-shan, (1968), Diffraction of Wind Waves (A Directional Spectrum Approach), Report HL-1-10, Hydraulic Engineering Laboratory, University of California, Berkeley, CA.

2. Fan, Shou-shan, (1976), Streamflow Computerization and Databases, Invited Speech, Sino-American Joint Commission on Rural Reconstruction, Taipei, Taiwan.

3. Fan, Shou-shan, (1984), Scientific Evaluation of Probable Maximum Flood Related Studies of Upper Deerfield River, Massachusetts and Vermont, Draft Staff Report, Federal Energy Regulatory Commission, Washington, D.C.

4. Fan, Shou-shan (Editor), (1988), Twelve Selected Computer Stream Sedimentation Models Developed in the United States, Interagency Sedimentation Work Group, published by Federal Energy Regulatory Commission, Washington, D.C.

RESEARCH AND DEVELOPMENT PROJECTS TO EVALUATE NON-CHEMICAL METHODS FOR CONTROL OF THE ZEBRA MUSSEL (DREISSENA POLYMORPHA)

By A. Garry Smythe[1] and Cameron L. Lange[2]

ABSTRACT

The zebra mussel (Dreissena polymorpha) is a macrofouling organism that has recently been introduced into North America. Since its introduction into Lake St. Clair in 1986, it has spread throughout the Great Lakes and has entered major river systems including the Mississippi, Susquehanna and Hudson River drainages. Once introduced into a new waterbody, the mussel's numbers can drastically increase and quickly cause significant biofouling. Every facility that uses infested raw water is at risk. At present, chemical control has been the most widely used approach, however, inherent environmental effects and difficulties in the environmental permitting of chemical agents have imposed limitations to their practical use to control mussels in hydropower facilities. Non-chemical options for the control of zebra mussels in hydropower and other facilities need to be developed. Acres has been involved in several research and development projects to study non-chemical technologies to control the zebra mussel. Four non-chemical technologies were studied in flow-through test stand systems constructed within utility facilities on Lake Ontario. Three of the four technologies tested used equipment that was purchased or leased from various manufacturers and were "off the shelf" items. The non-chemical technologies that were evaluated were centrifugal separators, automatic backwash filters, in-line high speed mixers, and low voltage electric fields. The first three approaches could be used to protect service water lines while the latter would have applicability for protection of trashracks. Each of these technologies could be utilized at hydropower facilities.

The projects to study centrifugal separators, in-line high speed mixers, and automatic backwash filters were funded by New York State Electric and Gas Corporation and the Empire State Electric Energy Research Corporation (ESEERCO) and its member utilities. The low voltage electric field study was supported by Rochester Gas & Electric Corporation and ESEERCO.

[1]A. Garry Smythe, Environmental Technical Director, and
[2]Cameron L. Lange, Senior Environmental Scientist, Acres International Corporation, 140 John James Audubon Parkway, Amherst, NY 14228-1180

INTRODUCTION

The zebra mussel (Dreissena polymorpha) is a freshwater macrofouling species that has recently been introduced into North America. This mussel has the potential to biofoul raw water intake systems, limit recreational use opportunities and alter the aquatic environment. The zebra mussel is a small bivalve mollusk that utilizes a byssal apparatus to strongly affix itself to virtually any hard, non-toxic surface. Due to the mussel's early life history and an affinity to moving water, raw water systems in hydropower facilities are especially vulnerable. Attached mussels can foul trashracks and reduce conduit diameter which increases head loss and reduces flow. In extreme cases, complete blockage can occur. Mussels can foul metering equipment including pressure and level monitors. Clumps of mussels (druses) that release from trashracks or inner walls of pipes can penetrate further into a raw water system where they may become lodged and block smaller diameter pipes. Service water and fire protection systems are especially vulnerable.

The zebra mussel was first documented in the Laurentian Great Lakes of North America in 1988 (Herbert et al. 1989). Based on the size and other characteristics of the mussels collected, they were probably introduced sometime in 1985 or 1986. The mussels rapidly increased their range and by 1990 were present in all of the Great Lakes. From 1990 to present, the zebra mussel extended its range outside the Great Lakes drainage system through canal interconnections and by human-mediated overland dispersal mechanisms. Through 1992, zebra mussels have been found in the Hudson, Susquehanna, Ohio, Tennessee, Mississippi, Cumberland and Arkansas River systems.

Zebra mussels cannot be kept out of raw water systems at hydroelectric facilities by conventional means such as trashracks or conventional strainers. Although these may remove zebra mussel adults and druses, early life history stages will readily pass through these barriers. The zebra mussel belongs to the only genera of freshwater mussels that has a free-living larval stage that is capable of suspending itself in the water column for a significant period. North American studies have determined that the fecundity of some larger females may exceed 1,000,000 eggs (Nichols and Kollar, 1991). The onset of spawning may occur when water temperatures reach about 7°C (Moore, 1991) although European literature suggests that the minimum spawning temperature is 12°C (Sprung, 1989). Fertilized eggs become free-living larvae (veligers) within a few days. Veligers then remain in the water column for at least one to three weeks (Lewandowski, 1982a and 1982b; Sprung, 1989). At hatching, zebra mussel veligers are about 60 microns long. When the veliger is about 180 to 200 microns, it reaches a stage that is capable of settling (Sprung, 1989). Once settled, if conditions are suitable, the veliger produces byssal threads and transforms into the characteristic adult form. Densities of about 125,000 zebra mussels per square meter have been observed on substrates in a hydroelectric facility on the Mohawk River in upstate New York.

At present, the physical removal of adults, along with chemical and thermal methods, has been the primary means of controlling zebra mussels in a power generating facility's raw water system. Each of the presently available technologies has drawbacks to its practical use. Physical removal methods such as scraping,

pigging, or hydrolazing are time consuming and may require outages or some loss of generation. Chemical and thermal methods, although they can be biologically effective, may result in environmental impact. Regulatory requirements often limit the biological effectiveness of these methods as well as increase the cost of successfully controlling zebra mussels by these means. In fact, the use of any chemical control agent is not allowed at many small low head hydropower facilities since a National Pollutant Discharge Elimination System (NPDES) permit is required. Non-chemical options for control of zebra mussels in hydropower and other water use facilities need to be developed.

In 1991 and 1992, four potential means of non-chemical control were evaluated by the authors. These were (1) high speed, in-line mixing devices, (2) low voltage electric fields, (3) centrifugal separators, and (4) automatic backwash, in-line filters. This paper provides background on each of these technologies as it pertains to zebra mussel control, presents the procedures utilized to evaluate each technology, and summarizes the results of the evaluation of each technology.

IN-LINE HIGH SPEED MIXERS

Background on High Speed Mixers

High speed mixers, such as Waring Blenders, are widely used in microbiological applications to disrupt or break cells. Cell disruption can be caused by direct contact with the blender blades (i.e. mechanical damage) or by the tearing action created by the high shear stress which results from high velocity mixing (i.e. hydraulic damage). It was hypothesized that commercial, large scale, high velocity/high shear agitators used in-line could similarly damage zebra mussel veligers. In 1992, a study was conducted to test this hypothesis. The potential application for this equipment would be for protection of fire service and high/low service water pipelines from zebra mussel macrofouling.

The primary objective of the study was to determine whether in-line high-speed mixers would kill a significant percentage of settleable size zebra mussel veligers (i.e. 180 microns or larger) as they passed through the unit. An assessment of the mortality of smaller, younger veligers was a secondary objective.

Three different types of equipment were tested to evaluate their relative effect on veliger mortality. The high-speed mixers selected for this study were: the Lightnin' Line Blender, the Ross Emulsifier, and the Chemineer Agitator. The Lightnin' Line Blender unit that was evaluated was a three-inch, 30 gallons per minute, 0.5 horsepower, 1,725 rpm model. The Chemineer Agitator unit that was tested was suitable for mounting on a six-inch flange and included a four-inch radial impeller, 0.75 horsepower and 1,745 rpm. The unit was provided with a special maximum shear radial flow impeller. The Ross Emulsifier unit that was tested was a horizontal, 1.5 inch inlet, one-inch outlet, 66 gpm, 1.5 horsepower, 3,450 rpm model.

In-Line High Speed Mixer Tests

The evaluation of the three in-line mixers was conducted at the New York State Electric and Gas Corporation's Kintigh Station. The facility is located near Lake Ontario in Somerset, New York. The test apparatus was designed and constructed to simulate in-line operation of the test equipment but allowed for significant control over test flows and pressures. Water for this system was drawn from a tap off of the facility's existing fire protection system. Water for the fire protection system was drawn from Lake Ontario and prefiltered through 1 mm mesh travelling screens. The tap was capable of providing up to 1,140 liters per minute (300 gpm). For the mixer study, the tap supplied approximately 115 to 415 liters per minute (30 to 110 gpm) through each of the two legs of the test apparatus. The piping and equipment layout of the apparatus was designed so water flow was homogeneously distributed between the test leg that contained the mixers and the control leg.

For biological testing, treated (i.e. passed through the mixing equipment) and control samples were simultaneously collected in separate 0.5 m, 63-micron mesh plankton nets. Typically, samples were collected over 10 to 15 minutes and volumes collected ranged from 945 to 4,685 liters. The samples were analyzed using dissecting microscopes. Estimates of the total number of live and dead veligers in a sample were calculated. The density of veligers in each sample was also determined. A total of 26 valid paired (treated and control) samples were collected and analyzed.

Results of In-Line High Speed Mixer Tests

A total of six tests were used to evaluate the effect of the Lightnin' Line Blender on zebra mussel veligers. There were no significant differences in the density (paired t-test, $p<0.05$) or percent mortality (Wilcoxon signed ranks test, $p<0.05$) of either settleable or non-settleable zebra mussel veligers between treated and control samples.

Similar results were obtained in the analysis of the data collected during the eight tests run on the Chemineer Agitator.

A total of 12 tests were used to evaluate the effect of the Ross Emulsifier on zebra mussel veligers. The Ross had a significant effect ($z = -2.824$, $p = 0.0047$) on veliger mortality, but had no effect on overall density. Overall, there was a 13 percent reduction in the number of living non-settleable form veligers in the treated samples over the control, however, 45 percent of the veligers were still alive when the treated samples were analyzed. A 14 percent reduction in the number of living settleable sized veligers in the treated samples was also observed, but 42 percent of the settleable sized veligers were still living when the treated samples were analyzed.

These results indicated that none of the mixers tested have any applicability to zebra mussel control. Eventhough there was significant observable mortality in the tests conducted on the Ross unit, this unit obviously could not be used alone to control zebra mussels. If used in conjunction with chemical treatments, a 14

percent reduction in viable settleable veligers would not appreciably impact either the frequency or the amount of chemical required to control the settled mussels.

LOW VOLTAGE ELECTRIC FIELDS

Background on Electric Fields

Soviet, Canadian and U.S. investigations have demonstrated that high voltage electric fields can kill zebra mussels, but power costs are prohibitive (Mackie, et.al. 1989). Other investigations have also shown that low voltage fields, when applied for long durations, are effective on veligers (Claudi and Wianko, 1991; Michaud, 1991). The effects of economically feasible voltages on zebra mussel attachment, when applied for short durations, has not been previously documented. It was assumed that if an electric field was of sufficient intensity, the settling stage veligers would not attach while under the influence of, and for a short time after, exposure to the field. Water flow would carry the veligers away from the protected structure. In 1991, the authors performed a preliminary study to determine whether low voltages, when applied to a structure, would prevent settlement of zebra mussels. In 1992, the authors continued the study using somewhat higher but still economically reasonable voltages.

Electric Field Tests

The evaluation was conducted at RG&E's Russell Station in Rochester, New York. The test apparatus consisted of a head tank designed to evenly distribute water flow and veligers through four test flumes. A flow-through system that used Lake Ontario water, which was known to contain veligers, was employed.

Test arrays that simulated trashracks were used. In 1991, two types of electrode array configurations were employed. Type 1 utilized the entire array as one electrode. Type 2 was configured so alternating plates in the array were opposite electrodes. In 1992, only the Type 1 configuration was used. The flow in the test flumes was held constant at about 0.5 fps. With this flow and the configuration of electrodes, the veligers remained under the influence of the electric field for about 0.3 to 0.8 seconds.

In 1991, four concurrent low intensity electric field tests were conducted using various amplitudes of DC, pulsed DC and AC voltages. In 1992, only AC voltage was applied and only two tests were run. The maximum voltage tested was 250 VAC. Periodic microscopic examination of the test racks for zebra mussel attachment was conducted.

Results of Electric Field Tests

There was no detectable effect of the low voltage electric field applied during the 1991 tests. In 1991, uncontrollable veliger density variations in the test troughs, and low overall settled veliger densities may have obscured any electric field effects. The DC voltage appeared to attract mussels, and if real, this phenomenon may have practical application in disposable surface protection techniques.

Results of the 1992 studies were inconclusive due to the extremely low densities of settled mussels observed on the test and control racks. Insufficient data were obtained to determine whether the higher applied voltage had any effect on veliger settlement. Low rates of veliger settlement were observed throughout Lake Ontario in 1992.

CENTRIFUGAL SEPARATORS

Background on Centrifugal Separators

Centrifugal separators are used at many raw water facilities to remove solids from source water. Separation of solids from liquids occurs in these units due to forced sedimentation which occurs as a result of the high centrifugal force created within the unit. The larger and heavier solids are thrown against the inner side wall and are propelled to the underflow where they are discharged along with a relatively small volume of water. The major volume of the incoming liquid passes through the overflow and continues through the system. In 1991, a study was conducted to determine if centrifugal separators could remove settleable sized zebra mussel veligers from a raw water system.

Centrifugal Separator Tests

Two models of centrifugal separators were tested in-line at NYSEG's Kintigh Station. The models tested were the Lakos Super Separator and the Krebs Desander. The test apparatus, with minor modifications, was as described for the high speed mixer evaluations. Biological samples were concurrently collected from the underflow and overflow of the separator units in separate 0.5 m, 63 micron mesh plankton nets. Zebra mussel veliger densities were determined by morphological stage (i.e. settleable or non-settleable) by use of a dissecting microscope.

Results of Centrifugal Separator Tests

Results of the centrifugal separator study indicated that the Lakos Separator design provided relatively low separation values (approximately 20 percent) whereas the Krebs Desander provided a mean separation efficiency of approximately 50 percent for the settleable umbonal form veligers. Separation of non-settleable (D-form) veligers was very poor for both the Lakos and Krebs units. Overall, the results indicated that the average separation efficiencies for settleable sized zebra mussels by the single Krebs unit are less than 100 percent. However, separation efficiency could be boosted by placing units in tandem. A supplemental control method such as an automatic backwash filter (or chemical treatment) could be used to complement the separator. It is possible that prefiltering with a centrifugal separator may minimize the potential for clogging associated with fine mesh filter media. A potential engineering drawback to the use of centrifugal separators (in retrofit situations) is that their operation results in an appreciable pressure drop across the unit. Some installations may require the addition of a small, in-line booster pump to offset this pressure drop.

AUTOMATIC BACKWASH FILTERS

Background on Automatic Backwash Filters

Automatic backwash filters are widely used to remove particles from flowing water. To effectively exclude zebra mussel veligers, very fine mesh filter media is necessary which could result in unmanageable clogging effects. Since 1991, Ontario Hydro and the New York Power Authority have been testing various filters to exclude zebra mussel veligers from their hydroelectric facilities. Their goal is to exclude all zebra mussel veligers, regardless of size, from the water. In 1992, the authors evaluated two previously untested self-cleaning filter designs that appeared to have the greatest potential for zebra mussel control. The main goal of the work performed was to test the filters with the largest mesh possible that would exclude all settleable size mussels while allowing smaller organisms and debris to pass through the system. This would minimize clogging of the filter units.

Automatic Backwash Filter Tests

Two models of automatic backwash filters were selected for testing. One model was the Kinney motorized self-cleaning strainer that has a cylindrical strainer body which consists of a rotating drum that contains numerous strainer elements. The other model tested was the Bromm backwash filter assembly which consists of an outer sleeve of filter media fitted over a cylindrical core frame. Testing was conducted at NYSEG's Kintigh Station and utilized the same apparatus used to evaluate the in-line high speed mixers.

To test the Kinney strainer, raw water which contained zebra mussel veligers was passed through the strainer that had either a nominal 40, 95, or 115 micron media installed. Both nominal 60 and 100 micron filter material was evaluated for the Bromm filter. Standard 0.3 m, 63 micron mesh plankton nets were used to concurrently collect samples upstream and downstream of the filter unit. Samples were biologically analyzed to determine the density of veligers by morphological form (i.e. settleable or non-settleable forms). During high debris loading periods, an analysis of clogging rates was conducted by determining the time that it took for the pressure across the unit to become large enough to trigger an automatic backwash cycle.

Results of Automatic Backwash Filter Tests

The densities of settleable and non-settleable size veligers in paired treated and control samples were used to evaluate the effect that a particular filter and mesh had on reducing the number of zebra mussel veligers in the raw water flow.

A large and significant difference (paired t-test, $p<0.05$) was found in the density of settleable size veligers in treated and control samples collected from the Kinney strainer fitted with 40 micron mesh. This filter removed 99 percent of the veligers. The Kinney strainer,when fitted with 95 micron or 110 micron mesh, did not significantly reduce the number of veligers in the raw water flow, however.

The Bromm filter fitted with a 60 micron mesh sleeve significantly reduced both settleable and non-settleable size zebra mussel veligers from the raw water flow. Ninety-six percent of the settleable size veligers and 74 percent of the non-settleable size veligers were removed by the filter. The Bromm filter fitted with 100 micron mesh did not remove a significant percentage of veligers from the flow.

Preliminary tests on filter media clogging were conducted during high debris load periods. Results indicated that clogging would be manageable for all filter media tested, however, the potential for clogging should be determined on a site-specific basis.

CONCLUSIONS

The need for protection of facilities from the macrofouling zebra mussel through use of non-chemical technologies is evident since current and future environmental regulations restrict the applicability of chemical controls, especially at hydroelectric facilities. The rapid range expansion of the zebra mussel and its life history characteristics place the vast majority of U.S. hydroelectric facilities at risk.

Of the technologies evaluated by the authors, the automatic backwash filters and centrifugal separators show the most promise. The in-line high speed mixers did not display a level of effectiveness that would warrant future testing. The results of the low voltage electric fields were inconclusive so future testing may be warranted.

The evaluations of the four physical control technologies described in this paper were preliminary in scope and did not assess the full range of operating parameters that may be encountered in actual replications. Although the test conditions attempted to evaluate each technology based on the optimization of readily controllable test parameters, the effect of all potential conditions was not made. Prior to the widespread application of any of the technologies, more testing should be carried out both in controlled test environments and in pilot project installations.

ACKNOWLEDGEMENTS

The projects to study centrifugal separators, in-line high speed mixers, and automatic backwash filters were funded by New York State Electric and Gas Corporation (NYSEG) and the Empire State Electric Energy Research Corporation (ESEERCO) and its member utilities; Central Hudson Gas & Electric Corporation, Consolidated Edison Company of New York, Inc., Long Island Lighting Company, New York Power Authority, Niagara Mohawk Power Corporation, Orange and Rockland Utilities, Inc., and Rochester Gas & Electric Corporation. The low voltage electric field study was supported by Rochester Gas & Electric Corporation and ESEERCO.

REFERENCES

Claudi, R. and P. M. Wianko. 1991. Summary of Ontario Hydro's 1990-1991 zebra mussel research program. Presented at the Electric Utility Zebra Mussel Control Technology Conference, Itasca (Chicago), Illinois, October 22-23.

Herbert, P.D., B. W. Muncaster, and G. L. Mackie. 1989. Ecological and genetic studies on Dreissena polymorpha (Pallas): A new mollusc in the Great Lakes. Can. J. Fish. Aquat. Sci. 46:1587-1591.

Lewandowski, K. 1982a. The role of early developmental stages in the dynamics of Dreissena polymorpha (Pall.) (Bivalvia) in lakes. I. Occurrence of larvae in the plankton. Ekol. Pol. 30:81-110.

Lewandowski, K. 1982b. "The role of early developmental stages in the dynamics of Dreissena polymorpha (Pall.) (Bivalvia) populations in lakes. II. Settling of larvae and the dynamics of numbers of settled individuals. Ekol. Pol. 30:223-286.

Mackie, G. L., W. N. Gibbons, B. W. Muncaster, and I. M. Gray. 1989. The zebra mussel, Dreissena polymorpha: A synthesis of European experiences and a preview for North America. Ontario Ministry of Natural Resources, Water Resources Branch, Great Lakes Section. Queen's Printer, Toronto, Ontario.

Michaud, D. 1991. Personal communication. WI Electric Power Co., Milwaukee, WI.

Moore, S.G. NY Zebra Mussel Clearinghouse. 1991. 1991 veliger sitings. IN: Dreissena polymorpha Information Review. New York Zebra Mussel Information Clearinghouse, New York Sea Grant Extension. Volume 2, Number 3, May/June.

Nichols, S.J. and B. Kollar. 1991. Reproductive cycle of zebra mussels (Dreissena polymorpha) in western Lake Erie at Monroe, Michigan. Presented at 34th Conference on Great Lakes Research, International Association of Great Lakes Research, Buffalo, New York, June 1991.

Sprung, M. 1989. Field and laboratory observations of Dreissena polymorpha larvae: Abundance, growth, mortality and food demands. Arch. Hydrobiol. 115:537-561.

Prioritizing PG&E's Environmental Research for Hydropower

Steven F. Railsback[1], M. ASCE, Ellen H. Yeoman[2], and Thomas R. Lambert[3]

Abstract

A prioritization process was developed to identify the environmental issues that most affect relicensing costs, regulatory concerns, and aquatic and wetland ecosystems of Pacific Gas and Electric Company's hydroelectric generating system. The prioritization method used numerical criteria that are designed to use data and semi-quantitative information on hydro projects and their environment to rate the importance of each issue. The process identified instream flows and stream temperature as the highest priority issues, for which additional planning will identify specific study topics of greatest benefit. Some issues of national and regional importance were determined to have low research priority. During the planning process, trends in how hydro is regulated in California were identified.

Introduction

Purpose. This paper presents methods used to prioritize aquatic and wetland environmental issues affecting Pacific Gas and Electric Company's (PG&E's) hydroelectric generating system. The prioritization is the first step in development of a strategic plan for PG&E's environmental

[1]Consultant, P. O. Box 8248, Stanford, CA, 94309.

[2]Environmental Program Manager, Research and Development Department, Pacific Gas and Electric Company, 3400 Crow Canyon Road, San Ramon, CA, 94583.

[3]Senior Consulting Biologist, Technical and Ecological Services, Pacific Gas and Electric Company, 3400 Crow Canyon Road, San Ramon, CA, 94583.

research and development (R&D), which is one component of an overall R&D program for hydropower. A secondary purpose of this paper is to present trends in how hydropower is regulated; these trends were identified in a regulatory analysis used in the prioritization process.

PG&E's hydroelectric system. PG&E provides electric service to most of northern California, delivering approximately 100,000 gigawatt-hours (GWh) per year (Fig. 1). PG&E generates approximately 55,000 GWh per year; approximately 25% of this generation is hydroelectric. PG&E operates 71 powerhouses and holds 29 Federal Energy Regulatory Commission (FERC) licenses. The system includes approximately 170 individual dams or diversions, mainly on streams draining the western slope of the Sierra Nevada. Much of PG&E's hydro R&D is focussed on the 12 projects that are scheduled for relicensing between 1995 and 2010; these 12 projects produce 45% of the company's hydroelectric power.

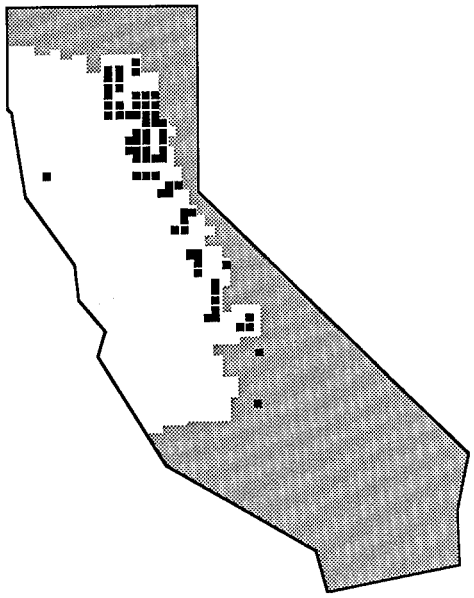

Figure 1. PG&E's service area (in white) and hydroelectric powerhouses.

PG&E's research program. PG&E spends approximately $50 million (or 0.5% of revenues) annually for R&D in support of the company's electrical and natural gas operations. In recent years, about $5 million annually has been spent on environment, health, and safety programs, many of which support hydropower. Examples of PG&E environmental studies include a long-term evaluation of how changes in stream flow affect trout populations; participation in the Electric Power Research Institute's COMPMECH program, which is developing innovative trout models at a PG&E site; studies of how fish use

thermal refuges in mountain rivers; and testing of sediment flushing flow evaluation methods.

In 1991 PG&E's R&D Department completed a strategy for PG&E research, the *Hydro Strategic Technology Plan* (HYSTEP, Tello et al. 1991), to address the company's long-term hydro generation goals and business objectives. HYSTEP defines the mission for future hydro R&D and analyzes key issues facing PG&E and the hydro industry. HYSTEP identifies enhancement of natural resources and the environment as one of five major R&D issues.

Research planning for aquatic and wetland issues discussed in this paper is part of the environmental portion of the HYSTEP program. The environmental research plan will identify specific R&D studies to be conducted as funding becomes available. This purpose is being met by (1) prioritizing aquatic and wetland issues to identify the ones that most affect the hydro generation system (the focus of this paper), (2) identifying weaknesses (e.g., uncertainties and high costs) in the mitigation currently used for the highest priority issues, and (3) identifying R&D studies that would improve mitigation methods by reducing their cost, improving their ability to protect the environment, or reducing potential regulatory concern. The plan is designed to maximize the benefits of R&D spending by funding projects with the highest potential benefits to PG&E and the environment, especially during the upcoming relicensing efforts. Two important secondary purposes of the strategic plan are to (1) justify the hydro R&D budget by showing the potential benefits of research and by showing that funding will be spent efficiently, and (2) integrate R&D with PG&E's hydro operating and licensing efforts to ensure that R&D efforts meet the company's needs.

Methods

The process for prioritizing environmental issues described in this paper (and summarized in Fig. 2) followed these steps:

(1) Identify issues that are candidate subjects for R&D studies,
(2) Design numerical criteria for prioritizing issues,
(3) Acquire information on environmental characteristics of hydro projects for use in assigning values to the criteria,
(4) Develop semi-quantitative cost and environmental impact scores for use in assigning values to the criteria,
(5) Develop regulatory concern scores for use in assigning values to the criteria,
(6) Review methods and data by a steering committee, and
(7) Determine numerical priority values for each issue.

The issues with the highest priority values are identified as most important to the PG&E hydro system and, therefore, the most important potential R&D topics.

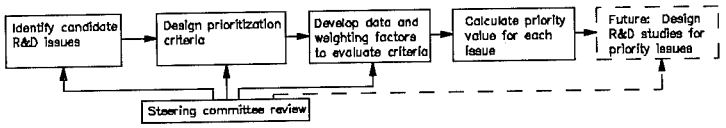

Figure 2. R&D issue prioritization process.

Identification of candidate R&D issues. The first step in the prioritization process was to list environmental issues that occur at PG&E projects; these issues are candidate subjects of R&D studies. The comprehensive list included (1) issues that commonly arise during licensing of hydro projects (e.g., instream flows, water quality, lake levels, fish passage), (2) basic processes that control stream and reservoir ecosystems (e.g., primary and secondary biological production in streams and reservoirs), (3) hydro effects on riparian zones and wetlands created by reservoirs and conveyances, and (4) unique issues that have occurred at PG&E sites (e.g., control of undesirable fish species, conflicts over which species to manage for, sedimentation problems). This list included 46 aquatic and wetland issues that were defined and prioritized.

Design of prioritization criteria. The prioritization criteria, or the basis for ranking environmental issues by how important they are to PG&E's hydro system, were designed to reflect regulatory and company objectives. Designing criteria was the most important part of the prioritization process because it established the basis for identifying the most important issues for R&D, and because it incorporates the company's business objectives in the process.

The California Public Utility Code allows utilities to charge ratepayers for research when the objectives are to reduce generating costs or reduce environmental impacts. PG&E's hydro operating objectives, as stated in internal plans, include cost-effective power generation, full compliance with regulatory requirements and building trust with regulatory agencies, and conduct of business in an environmentally sensitive manner. In accordance with these regulatory and company objectives, three criteria for prioritizing research issues were designed to reflect how much each issue affects (1) costs for environmental studies and mitigation (including lost generation), (2) regulatory concerns and compliance, and (3) aquatic and wetland environments.

The three criteria were designed so that each can be given a numerical value for each environmental issue, and the issues with the highest criteria values have the highest priority for R&D planning. Criteria were based on (1) the number of projects where the environmental issue does, or could, occur; and (2) the relative importance of the issue, compared to the other environmental issues. This general design was varied for each of the three criteria according to the kinds of projects where the criterion is relevant and the kind of information available on the importance of issues. Weighting factors were used to reflect how important each of the three criteria are to PG&E.

The cost criterion indicated, for each issue, the study and mitigation costs to PG&E resulting from relicensing the 12 projects whose licenses will expire before 2010. (The criterion was based on relicensing because most study and mitigation requirements are determined during relicensing.) Values for the cost criterion were assigned, for each environmental issue, by multiplying (1) the percent of the 12 projects to be relicensed where the issue occurs or is expected to occur, by (2) a cost score that represents the relative cost of mitigating the issue when it occurs. The cost scores had values between zero and one, and their values are discussed below.

The regulatory concern criterion indicated the likelihood of each issue being the focus of regulatory actions (e.g., have studies, negotiation, or mitigation required) during relicensing. The criterion was therefore based on the percent of projects to be relicensed where each issue could occur (i.e., the environmental resources or conditions that could lead to regulatory concern are present), and the current and future regulatory importance of the issue. The current regulatory importance was based on how much authority resource agencies have to regulate an issue and how much emphasis agencies have given to the issue. Future changes in regulatory importance were based on trends in environmental management practices and expected changes in laws. The regulatory concern criterion was assigned a value, for each issue, by multiplying (1) the percent of the 12 projects to be relicensed where the environmental resources associated with the issue occur, by (2) the combined current and future regulatory importance scores for the issue. The combined regulatory importance scores had values between zero and one, as discussed below.

The environmental impact criterion indicated the effect of each issue on the natural environment. Because this criterion reflected concern about the environment and not cost or regulatory concerns, it was based on the effects of the issue at all PG&E projects, not just those being relicensed. The environmental impact criterion was evaluated for each issue by multiplying (1) the percent of all PG&E projects where the issue occurs by (2) an environmental impact score that represents the environmental

importance of the issue where it occurs. The environmental scores are discussed below.

Acquisition of information on environmental characteristics of hydro projects. Assigning values to the prioritization criteria required information on the environmental issues and resources at PG&E hydro projects. Three kinds of data were assembled for each of the 27 hydro projects included in the prioritization study: (1) physical characteristics (e.g., the number of dams and diversions, operating modes, size of facilities), (2) environmental resources present (e.g., fish communities, wetlands, recreational resources, endangered species), and (3) environmental issues that have arisen, or are expected to arise. An issue was defined to occur at a project if (1) the issue is the subject of licensing or regulatory concern or controversy; (2) studies on the issue have been requested or conducted by FERC or resource agencies; (3) mitigative measures are, or are expected to be, provided for the issue; (4) the issue is the subject of a specific FERC license article; or (5) the project is believed to cause impacts related to the issue that may deserve study or mitigation. The environmental data were obtained primarily from PG&E biologists who are familiar with each project, and from company reports and documents.

Development of cost and environmental impact scores. The scores used to represent the relative mitigation cost and environmental impact of each issue were semi-quantitative values based on the judgement of PG&E staff. The scores were not based on cost or environmental data because (1) mitigation costs and environmental impacts are difficult to quantify for many issues, (2) there is high variability in the mitigation cost and environmental impact of an issue among projects of different size and design, and (3) there were too few actual data to evaluate the scores for many issues. Given the inability to base these scores on measured values, a specific basis for estimating scores was developed. For example, cost scores were developed by identifying the most expensive issues to mitigate and estimating the relative cost of mitigating other issues. The environmental impact score for an issue was based on the assumption that minimal mitigation exists, and reflected impacts on native ecosystems at a watershed scale. After the basis for scores were agreed to, members of a steering committee (discussed below) used their experience and judgement to rate the relative mitigation cost and environmental impact of each issue. The values obtained from the steering committee were reviewed in a meeting; committee members then rated each issue again and the revised ratings were averaged to obtain the values used in the prioritization ranking.

Development of regulatory concern scores. Semi-quantitative scores reflecting the regulatory importance of each issue were based on an analysis of current and future hydropower regulation. A current regulatory importance score was based on the authority for agencies to regulate each issue provided by existing laws and current practices of regulatory and resource agencies. The authority for agencies or FERC to regulate specific issues was evaluated by reviewing existing laws and policies related to hydropower. The current regulatory practices and priorities of agencies were estimated from data collected by the Electric Power Research Institute and the Department of Energy (e.g., Hunt Assoc. 1991; USDOE 1991) and from experience with the licensing process. A regulatory trend score was based on potential changes in the laws regulating hydropower, and observed trends in environmental management and regulatory concerns and policies. Information on potential changes in laws was obtained from hydro industry literature, PG&E staff that track regulatory activity, and the Edison Electric Institute. Trends in regulatory practices were observed from recent policy initiatives, management actions, and research programs at the state and federal level.

The current regulatory importance score and the regulatory trend score for each issue, which were determined from the regulatory review, each had values between zero and ten. The two scores for each issue were then added (and normalized by dividing by the maximum score among all issues) to obtain an overall regulatory importance score that gives equal weight to the current importance and the expected trend.

Steering committee review. A steering committee was formed to guide the prioritization process. The committee included staff from the PG&E departments that operate hydro projects, manage FERC licensing and regulatory compliance, and conduct environmental studies. This committee served three main purposes: (1) to provide a company-wide consensus that the methods were appropriate, (2) to establish (through weighting factors, discussed below) the relative importance to PG&E of the three prioritization criteria, and (3) to evaluate the relative cost and environmental impact of each issue (through cost and environmental impact scores, discussed above). The steering committee has been essential to successful R&D planning.

Determining numerical priority values for issues. The numerical priority values of environmental issues were used to identify the most important issues for future R&D. The prioritization values are the sum of the values for each of the three criteria, weighted by factors that reflect the importance of each criterion to PG&E.

Weighting factors were used to reflect the strategic importance of the three criteria to PG&E's hydro operations. The weighting factor for each criterion had a value between zero and one (and the sum of the three weighting factors equals one); the higher the weighting factor for a criterion, the more important it was in PG&E's decision-making process. Selection of weighting factors was based on company values and so was conducted by the consensus of the steering committee.

The numerical priority value for each issue was calculated by multiplying the numerical value of each criterion by its weighting factor, and summing the three weighted criteria values. The final priority value for an issue is summarized by the equation:

$$PV = W_C[P_{ri} \times S_C] + W_R[P_{rr} \times (S_R + S_{RT})] + W_E[P_i \times S_E]$$

where PV is the weighted priority value for an issue; W_C, W_R, W_E, are the weighting factors for relicensing cost, regulatory concern, and environmental impact; P_{ri} is the percent of projects to be relicensed between 1995 and 2010 where the issue occurs, P_{rr} is the percent of projects to be relicensed where environmental resources associated with the issue occur, and P_i is the percent of all PG&E projects where the issue occurs; S_C is the cost score (divided by the highest value of S_C among all issues), $S_R + S_{RT}$ is the sum of the current regulatory importance score and the regulatory trend score (divided by the highest value of this sum among all issues), and S_E is the environmental impact score (divided by the highest such score among all issues). The priority value PV has a value between zero and one for each issue, with higher values meaning higher strategic importance of the issue.

Results

General results of the prioritization process and the regulatory analysis are presented here. The complete prioritization of environmental issues was specific to the PG&E system and is not necessarily applicable elsewhere.

Prioritization results. The numerical prioritization process described in this paper identified two issues as clearly having highest priority for R&D planning: instream flow for fish habitat and stream temperature. Instream flow and water temperature issues occur at almost all PG&E hydro projects, are among the most expensive issues to mitigate (because of the power generation losses resulting from flow releases), are of high concern to regulatory agencies, and are considered very important to the environment.

A number of other issues received priority values that were relatively high, although significantly less than the values for instream flow and water temperature. These issues ranked highly usually because they have relatively high mitigation costs, are considered environmentally important, and because they occur at roughly half of PG&E's hydro projects.

An important result of the prioritization process is the identification of issues that have little effect on the hydro system. Several issues that are considered highly important nationally or within California were identified as having low priority for PG&E. Issues associated with anadromous fisheries received low priority values, even though PG&E is currently building an expensive anadromous fish passage facility on the Eel River. The priority values for anadromous fish issues are low because they occur at a small fraction of PG&E's projects; it appears appropriate to continue addressing these issues on a site-specific basis instead of through the R&D program. Dissolved oxygen is a common mitigation issue nationally (USDOE 1991), but occurs at few PG&E projects and is therefore a low R&D priority.

Regulatory analysis observations. The analysis of regulatory practices conducted for this study observed the following general trends in how hydropower is regulated.

(1) The fish and recreation issues currently of highest regulatory importance (e.g., instream flow, passage, water temperature, lake levels) will continue to be the primary concerns of regulatory agencies in hydro licensing.

(2) Assessment and mitigation of cumulative and large-scale impacts will continue to increase in regulatory importance. Assessments will more commonly address impacts at the watershed level instead of just looking at local effects of hydro on streams; this change is driven by changes toward broader ecological thinking and by the development of technology for studying large-scale impacts. This trend is not necessarily bad for hydropower, as it may result in more equitable and more efficient mitigation of some impacts.

(3) Water quality regulation will become more comprehensive, with increased use of biological water quality indicators, more emphasis on nonpoint-source pollution, and less reliance on conventional water quality criteria that are easier to demonstrate compliance with.

(4) Biodiversity will increase in importance as a regulatory and environmental management objective; as a result there may be less emphasis on sport fisheries and more emphasis on preservation of habitat for native and nongame fish, and preservation of nonfish species.

(5) Regulation of wetlands is likely to change, but it is not yet clear what the change will be. New legislation may clarify the authority to regulate wetlands; however, new legislation may allow classification of wetlands by their ecological importance, which could result in less regulation of wetlands created by hydro projects.

(6) Post-licensing changes in mitigation requirements are increasingly common. Monitoring requirements, post-licensing studies, re-opening of licenses, and other changes are making environmental management of hydro projects more of a continual process than a periodic event that occurs during licensing.

Conclusions

The prioritization process described here enables PG&E to focus its R&D efforts on the issues that have the greatest effect on its hydro generating system. The highest priority issues will be examined in detail to determine the greatest weaknesses in the mitigation methods currently in use. Opportunities for research at PG&E sites, or for cooperative research at other sites, will be evaluated, and a list of high priority studies will be developed. Well-designed studies that strengthen the mitigation methods for high priority issues will provide the greatest payoff for investment in R&D, which is important both for meeting corporate management objectives and for justifying R&D budgets.

The strategic planning process has also fostered communication among the PG&E departments involved in hydro operations, licensing, and R&D, helping assure that future R&D is relevant and cost-effective.

Appendix--References

Hunt Assoc. 1991. Lessons learned in hydro relicensing (1984-1989). EPRI report GS-7324, prepared by Richard Hunt Associates for the Electric Power Research Institute, Palo Alto, California.

Tello, J. C., E. H. Yeoman, and ?????. Hydro Strategic Technology Plan, HYSTEP - Vision 2000: Power in Partnership with Nature. PG&E Department of Research and Development, San Ramon, California.

U. S. Department of Energy (USDOE). 1991. Environmental mitigation at hydroelectric projects, Volume I. Current practices for instream flow needs, dissolved oxygen, and fish passage. DOE/ID-10360, USDOE Idaho Field Office, Idaho Falls, Idaho.

Oxygen Transfer Similitude for the Auto-Venting Turbine

by Eric J. Thompson[1] and John S. Gulliver[2], Members ASCE

Abstract

A similitude relationship for gas transfer in an auto-venting turbine with specific reference to scaling between a homologous turbine model and a full size installation has been developed from oxygen transfer data from a turbine model and physically realistic theories. An empirical fitting process based upon discrepancies in predicted behavior caused by bubble coalescence and air core formation was performed to increase scaling accuracy. The final result is a similitude equation which satisfactorily predicts gas transfer efficiency in a full scale prototype from known model behavior.

Introduction

Because hydroelectric installations frequently release water from the lower depths of reservoirs where dissolved oxygen (DO) concentrations are often quite low, it is not uncommon to find tailwater discharges with minimal dissolved oxygen concentrations. The concerns for low DO associated with hydroelectric installations primarily include preservation of aquatic habitat. Under anoxic conditions, several problems may develop which endanger the lives of fish and other aquatic lifeforms; trace metals and nutrients may be released from sediments, high concentrations of hydrogen sulfide may result from anaerobic biodegradation, and the pH of the water body may

[1] Research Assistant, St Anthony Falls Hydraulics Laboratory, University of Minnesota, Mississippi River at Third Ave. S.E., Minneapolis, MN 55414. (612) 627-4588.

[2]Associate Professor University of Minnesota, Dept. of Civil and Mineral Engineering and St. Anthony Falls Hydraulics Laboratory, (612) 627-4600

drop (Wilhelms et. al., 1987). Dissolved oxygen concentrations approaching zero will create extensive mortality of fish and other components of the aquatic biota.

To reduce or eliminate the impacts of low DO the U.S. Army Corps of Engineers, The Tennessee Valley Authority, The Southwestern Power Administration, The U.S. Bureau of Reclamation, and others (March et al, 1992) have been researching various means of increasing DO concentration in hydroelectric tailwaters. One of the most attractive techniques investigated was the auto-venting turbine (AVT).

The AVT operates by aspirating air through openings inside the turbine where pressure is subatmospheric (March and Waldrop, 1991), thus eliminating the requirement for equipment to inject the air. To improve air flow, research has been performed on hub baffles which may be installed immediately upstream of the injection ports to further reduce pressure at the port outlet, and increase the air flow of each port.

For maximum oxygen transfer efficiency, the injection ports are placed at locations of high turbulence. To establish a point where maximum turbulence occurs, air injections have been made at various locations including the turbine runner edge, the draft tube cone, the discharge ring, and many others (March et. al., 1992).

One component of the research comprising the AVT project has been the development of scaling criteria for the auto venting turbine under these various configurations. It is the purpose of this paper to develop a similitude relationship for the gas transfer that occurs in an auto-venting turbine with specific reference to scaling between a homologous turbine model and a full size installation, regardless of the turbine operating conditions. The relation is developed with oxygen transfer data from a turbine model and physically realistic theories. The relation is confirmed with data from the full scale installation.

The similitude relationship could be improved with further data and some well planned experiments. Therefore, this report represents an initial investigation of model/full-scale similitude for oxygen transfer in the auto-venting turbine.

Theory

Mass Conservation

The basis for the auto-venting turbine scaling relation is mass conservation. The mass conservation equation applied to bubbles in a liquid takes the following form

$$\frac{dC}{dt}=K_L'\frac{A'}{V}(C_s-C) \qquad (1)$$

where C = the mean concentration of dissolved oxygen in the water, measured in the control volume, t = time, K_L' = the liquid film coefficient for bubble-water oxygen transfer, which is a function of time, A' = the surface area of bubbles, also a function of time, V = control volume corresponding to A and C measurements, and C_s = the saturation concentration at equilibrium between the bubble and water.

Assuming that C_s remains constant, equation 1 can be integrated to give

$$-\ln\left[\frac{C_s-C_U}{C_s-C_d}\right]=\int_{t_d}^{t_u}K_L'\frac{A'}{V}dt=K_L\frac{A}{V}t \qquad (2)$$

where C_U and C_d are concentrations measured upstream of the point of ventilation, and downstream of the location where the bubbles leave the flow (tailwater) respectively, and t is the residence time of the bubbles in the flow, or the time of contact. K_L and A are mean values of K_L' and A', weighted by their impact on bubble-water oxygen transfer.

If we define transfer efficiency as

$$E=\frac{C_d-C_U}{C_s-C_U} \qquad (3)$$

and we define a specific surface area as

$$a=\frac{A}{V} \qquad (4)$$

then equation 2 can be rewritten in the following form:

$$\ln(1-E)=-K_L a t \qquad (5)$$

For similarity between a turbine model (1) and the full-scale turbine (2) the following must be true:

$$\frac{\ln(1-E_1)}{\ln(1-E_2)}=\frac{(K_La t)_1}{(K_La t)_2} \tag{6}$$

To develop equation 6 into a more useful form, the liquid film coefficient, the specific surface area, and the time of contact will be investigated in detail in the following sections.

Determination of a K_L Scaling Relationship

In 1981, Azbel developed an analytical expression for the liquid film coefficient that applies to bubbles in a bubble swarm. He began with Levich's theoretical expression for the air-water mass flux from a spherical bubble

$$V\frac{dC}{dt}=2\left[\frac{\pi D v_r}{d_b}\right]^{1/2} d_b^2 (C_a-CH) \tag{7}$$

where D = diffusivity of the compound (oxygen) in water, v_r = velocity of the bubble relative to the liquid phase, d_b = bubble diameter, C_a = concentration of gas in the bubble, and H = Henry's Law constant.

Azbel then developed an expression for v_r in a turbulent flow field by assuming that the flow is composed of equal sized bubbles that are uniformly spaced. The relationship has a characteristic velocity and characteristic length that are properties of the turbulent flow field (Azbel, 1981)

$$v_r=\frac{U^{3/2} d_b}{2(\nu L)^{1/2}}\frac{1-\phi}{(1-\phi^{5/3})^{1/2}} \tag{8}$$

where U = a characteristic velocity of the large eddies, ν = the kinematic viscosity of the liquid, L = a characteristic length of the large eddies, and ϕ = the gas void fraction.

Substituting equations 7 and 8 into equation 1 for a single bubble results in the following expression for K_L.

$$K_L=\frac{(1-\phi)^{1/2}}{(1-\phi^{5/3})^{1/4}}\frac{D^{1/2}U^{3/4}}{(L\nu)^{1/4}} \tag{9}$$

For the auto-venting turbine, $U \propto Q/d_t^2$ and $L \propto d_t$, where d_t = the diameter of the turbine runner. Therefore, the scaling relationship between two homologous turbines for liquid film coefficients would be

$$\frac{K_{L1}}{K_{L2}}=\left[\frac{1-\phi_1}{1-\phi_2}\right]^{1/2}\left[\frac{1-\phi_2^{5/3}}{1-\phi_1^{5/3}}\right]^{1/4}\left[\frac{D_1}{D_2}\right]^{1/2}\left[\frac{Q_1 d_{t2}^2}{Q_2 d_{t1}^2}\right]^{3/4}\left[\frac{\nu_2 d_{t2}}{\nu_1 d_{t1}}\right]^{1/4} \quad (10)$$

Development of a scaling criterion for specific surface area

As stated earlier, the specific surface area, a, is dependent upon the diameter of bubbles in the control volume. The mean bubble diameter, d_b, for a shear flow in an auto venting turbine draft tube is a function of the maximum bubble size the shear forces will allow. Large bubbles when introduced into the draft tube are rapidly broken down by the shear forces in the flow, until the bubble size is sufficiently small that the surface tension forces are significant enough to restrict any further breakdown in bubble size.

Hinze (1955) experimentally studied the larger bubble sizes in rotating concentric cylinders and proposed that this bubble size is

$$d_b=k\left[\frac{\sigma}{\rho}\right]^{3/5}\epsilon^{-2/5} \quad (11)$$

where d_b = the volumetric mean bubble diameter, k = a constant of proportionality, σ = surface tension, ρ = density of water, and ϵ = rate of turbulent kinetic energy dissipation per unit mass.

Assuming that turbulent velocities scale with the mean axial velocity, the dissipation of turbulent kinetic energy is approximated by

$$\epsilon \propto \frac{U^3}{d_t} \propto \frac{Q^3/d_t^6}{d_t}=\frac{Q^3}{d_t^7} \quad (12)$$

Therefore, equation 11 may be written as

$$d_b \propto \left[\frac{\sigma}{\rho}\right]^{3/5}\frac{d_t^{14/5}}{Q^{6/5}} \quad (13)$$

If one notes that the specific surface area is related to the gas void ratio and bubble diameter through

the relation for surface area and volume of a sphere, the following proportionality arises

$$a \propto \frac{\phi}{d_b} \tag{14}$$

Therefore a scaling relation in the form of equation 10 can be developed from the insertion of equation 13 into equation 14.

$$\frac{a_1}{a_2} = \left[\frac{\phi_1}{\phi_2}\right]\left[\frac{\rho_1}{\rho_2}\right]^{3/5}\left[\frac{\sigma_2}{\sigma_1}\right]^{3/5}\left[\frac{Q_1}{Q_2}\right]^{6/5}\left[\frac{d_{t2}}{d_{t1}}\right]^{14/5} \tag{15}$$

Contact Time

The contact time of the bubbles in the flow, t, is proportional to the length traveled between upstream and downstream measuring points divided by velocity. The length traveled should scale with runner diameter in homologous turbines. As mentioned previously, velocity scales as discharge divided by runner diameter squared.

$$t \propto \frac{d_t}{Q/d_t^2} = \frac{d_t^3}{Q} \tag{16}$$

Or in similitude form,

$$\frac{t_1}{t_2} = \left[\frac{d_{t1}}{d_{t2}}\right]^3\left[\frac{Q_2}{Q_1}\right] \tag{17}$$

Similitude Relation

If one notes that for homologous turbines the flow rate, Q scales as

$$\frac{Q_1}{Q_2} = \frac{n_1 d_{t1}^3}{n_2 d_{t2}^3} \tag{18}$$

where n = turbine rotational speed, then equations 6, 10, 15, and 17 can be combined and simplified into the following relation for gas transfer in homologous auto-venting turbines.

Deficiencies in the Similitude Relationship

The Tennessee Valley Authority working with Voith Hydro have constructed a working 1/11.7 scale model of an existing auto-venting turbine. The purpose was to develop and verify scaling relationships before a new AVT model runner was built and scaled to a full size auto-venting

$$\frac{\ln(1-E_1)}{\ln(1-E_2)}=\left[\frac{1-\phi_1}{1-\phi_2}\right]^{1/2}\left[\frac{1-\phi_2^{5/3}}{1-\phi_1^{5/3}}\right]^{1/4}\left[\frac{\phi_1}{\phi_2}\right]$$
$$\left[\frac{D_1}{D_2}\right]^{1/2}\left[\frac{\nu_2}{\nu_1}\right]^{1/4}\left[\frac{\sigma_2}{\sigma_1}\right]^{3/5}\left[\frac{\rho_1}{\rho_2}\right]^{3/5}\left[\frac{n_1}{n_2}\right]^{19/20}\left[\frac{d_{t1}}{d_{t2}}\right]^{13/10} \quad (19)$$

turbine runner at Norris Dam. The raw data resulting from tests run by TVA are expressed in figures 1 - 4, and are used to illustrate the complexity of modelling oxygen transfer similitude in an AVT.

Bubble Coalescence

Equation 19 describes a linear relation between ln(1-E) and a, as long as ϕ is small. For the AVT, ϕ is usually less than 0.05, therefore the relationship between (1-E) and ϕ can be expressed as

$$\ln(1-E) \propto \phi \quad (20)$$

Examination of operational data for both the auto-venting turbine prototype and model, however, has shown that the relationship between ln(1-E) and ϕ is not linear as would be expected from the preceding relations. Figure 1 shows measurements taken from an auto-venting turbine model operating at different speeds while figure 2 represents curves fit through the data to better emphasize the nonlinear nature of the relation by elimination of scatter.

The decreasing change in efficiency (nonlinear behavior of Fig. 2) with increasing gas void ratio is believed to be caused by bubble coalescence. Normally, bubble coalescence is incorporated by fitting the ln(1-E) term to ϕ^{η} where η is normally between 0.6 and 0.8 (Azbel 1981).

Air Core Formation

Individual bubble coalescence could not describe the reduction in DO transfer efficiency with increasing rotational speeds. A reasonable hypothesis describing this behavior is that at high rotational speeds, strong radial pressure gradients caused by swirl drive bubbles to the center of the draft tube where they coalesce into an air core comprising the majority of the air volume. The resulting reduction in surface area serves to limit the transfer of oxygen to the water in the draft tube and causes the low efficiencies evident in figure 4.

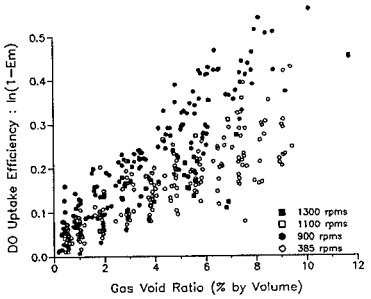

Figure 1: Measured DO Uptake for Turbine Model

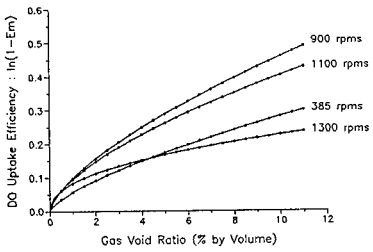

Figure 2: Curves fit to DO Uptake for Turbine model, taken from figure 1

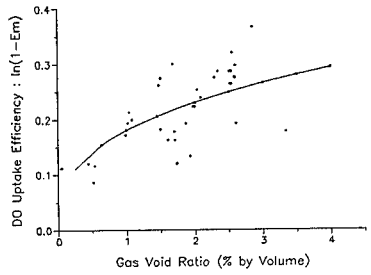

Figure 3: Measured DO Uptake for Turbine Prototype

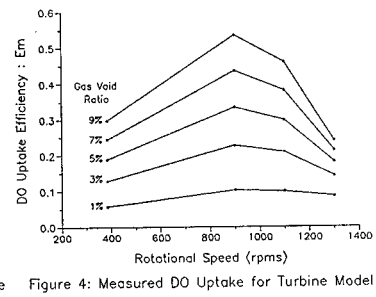

Figure 4: Measured DO Uptake for Turbine Model at Selected Gas Void Ratios, taken from fig. 2

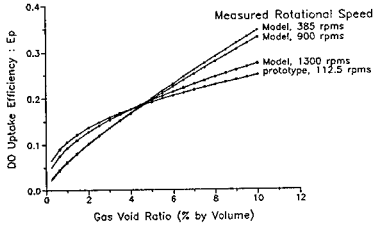

Figure 5: Predicted DO Uptake Scaled to the Model Runner Diameter and to 385 rpms

The maximum transfer efficiency occurs at approximately 900 rpms in the model. It can be surmised that the location at which an air core forms is highly dependent upon rotational speed at higher rpms. The greater the speed, the greater the pressure gradient, and the greater the force which seeks to drive the bubbles to the draft tube center. The less time the air exists as a bubble swarm, the less oxygen transfer will occur.

Verification of Similitude Relation

To account for the deficiencies in the similitude model equation 26 has been fitted to the data with additional empirical terms accounting for air core formation and coalescence.

$$\frac{\ln(1-E_1)}{\ln(1-E_2)} = \left[\frac{1-\phi_1}{1-\phi_2}\right]^{1/2}\left[\frac{1-\phi_2^{5/3}}{1-\phi_1^{5/3}}\right]^{1/4}\left[\frac{\phi_1}{\phi_2}\right]^{\eta}\left[\frac{D_1}{D_2}\right]^{1/2}\left[\frac{\nu_2}{\nu_1}\right]^{1/4}$$

$$\left[\frac{\sigma_2}{\sigma_1}\right]^{3/5}\left[\frac{\rho_1}{\rho_2}\right]^{3/5}\left[\frac{n_1}{n_2}\right]^{19/20}\left[\frac{d_{t1}}{d_{t2}}\right]^{13/10}\left(\left[\frac{1-\tanh(\alpha n_1-\beta)}{1-\tanh(\alpha n_2-\beta)}\right]\left[\frac{d_{t2}}{d_{t1}}\right]^{1/2}\right) \quad (21)$$

For the Norris model and prototype turbine, α = 1/385 rpms, β = 1100/385, and η = 0.72.

Figure 5 shows predicted DO uptake efficiencies for the data represented in figures 1, 2, and 3 scaled by equation 21 to the conditions of a turbine model operating at 385 rpms. As can be seen, equation 21 provides a reasonable degree of overlap between curves and therefore allows for relatively accurate prediction of DO transfer efficiency between this turbine model and the prototype. Because of the empirically fitted coefficients, however, there is currently no guarantee that the similitude relationship will be valid for a different turbine. Research is continuing in this area.

Acknowledgements

We would like to thank Paul Hopping, Mark Mobley, and Tom Brice of the Tennessee Valley Authority for sharing their AVT data with us. We would also like to thank Steven Wilhelms for his continuing encouragement and support. This paper is based upon research supported by the Reservoir Water Quality Branch of the US Army Engineer Waterways Experiment Station and by the Minnesota State Legislature ML. 89, Chapt. 335, Art. 2, Sec. 1, Subd. 6 as recommended by the Legislative Commission on Minnesota Resources.

References

Azbel, D. (1981), Two Phase Flows in Chemical Engineering, Cambridge University Press, Chapts. 3 and 7.

Hinze, J. O. (1955), "Fundamentals of the Hydrodynamic Mechanism of Splitting in Dispersion Processes," American Institute of Chemical Engineering Journal 1(3) pp. 289-295.

March, P. A. and W. A. Waldrop (1990), "Technology Development for Auto-Venting Turbines," Air-Water Mass Transfer, S. C. Wilhelms and J. S. Gulliver, Eds., ASCE, pp 506-511 New York, NY.

March, P. A., T. A. Brice, M. H. Mobley, and J. L. Cybularz, Jr. (1992) "Turbines for solving the D.O. Dilemma," Hydro Review, 11(1) pp. 30-36.

Wilhelms, Steven C., M. L. Schneider, and Stacy E. Howington (1987) Improvement of Hydropower Release Dissolved Oxygen with Turbine Venting, U.S. Army Engineer Waterways Experiment Station, Vicksburg, MISS.

NIAGARA RIVER FLOW FORECASTING SYSTEM

Ken Lacivita[1] Ion Corbu[2] Francis Kwan[1] Randy D. Crissman[3] , M. ASCE

Abstract

The flow of the Niagara River depends mainly upon Lake Erie water levels. While these water levels are generally stable when averaged over a weekly or monthly period, sudden changes in wind speed, wind direction and barometric pressure can cause dramatic variations in hourly lake levels and thus in Niagara River water flows. The prediction of these changes in flow is important to the real-time operation of the hydraulic generating facilities located along the river.

A Niagara River Flow Forecasting System has been developed based on a hydrodynamic storm surge model for Lake Erie. The system uses real-time and forecasted weather data from eight weather stations located around the lake, as well as real-time lake level readings.

Introduction

The hydroelectric generating facilities located along the Niagara River are very significant resources for both Ontario Hydro and the New York Power Authority. The combined systems have a total installed capacity of approximately 4,700 MW. Because of their importance, a series of models are used to optimally dispatch and

[1]Engineer-Operations, Ontario Hydro, Power System Operations Division, 5775 Yonge Street, North York, Ontario M2M 4J7.

[2]Section Head, Ontario Hydro, Power System Operations Division, 5775 Yonge Street, North York, Ontario M2M 4J7

[3]Senior Hydraulic Engineer, New York Power Authority, Niagara Power Project, P.O. Box 277, Niagara Falls, New York 14302.

maximize the value of energy of the system over a daily time period (North, Lacivita and Corbu, 1988 and 1990). The effectiveness of these models relies upon a continuously updated near-term forecast of Niagara River flows.

The Niagara River flow is stable relative to many other rivers since flow variation is mainly dependent upon Lake Erie level changes rather than upon seasonal climatic conditions. However, wind and barometric pressure differences over Lake Erie can cause substantial short-term level changes (Bedford and Dingman 1982, Hamblin 1979, and Platzman 1963) resulting in significant variations in Niagara River flows. In general, a 0.3 m (1 ft) change in Lake Erie elevation at the mouth of the Niagara River results in a corresponding change in river flow of approximately 566 cms (20,000 cfs). An example of an extreme event was on December 2, 1985 when the elevation at this location rose by 2.19 m (7.2 ft) over an eleven hour period, resulting in an increase in Niagara River flow of 5,100 cms (180,000 cfs). Certain meteorological conditions can also cause the elevation of the lake to decline, resulting in a reduction in river flow. These variations can have considerable effects on the operation of the hydroelectric generating facilities located along the river.

An accurate near-term river flow forecast would permit the existing models to issue optimal reservoir dispatch plans, resulting in an increased value of energy. To improve the near-term inflow forecast of the river, a Lake Erie hydrodynamical model was adopted for use during real-time operation. This paper describes the implementation of the Niagara River Forecasting System. Major sections of the paper include a description of the hydrodynamic model, a statistical analysis of surges, details of the meteorological data link, a description of the on-line programs required for real-time operation and of the operational process.

Description of the Niagara Generating System

The system is comprised of the Niagara River, a control structure, the Grass Island Pool (GIP) Reservoir, and hydroelectric generating facilities (Figure 1).

The Niagara River is a 58 km (36 mile) international waterway connecting Lake Erie to Lake Ontario. The difference in elevation between these two lakes averages 99 m (326 ft). The flow entering the Niagara River is not controlled and is dependent on the elevation of Lake Erie at the mouth of the river. While the mean monthly flows are well regulated by the upper Great Lakes, with the long-term flow averaging 6,000 cms-hrs (212,000 cfs-hrs), daily and hourly flows can vary significantly. This is explained by the effects of extreme winds and barometric pressure differences over Lake Erie which can cause substantial short-term level changes at Fort Erie.

The river drops dramatically over the Niagara Escarpment forming the Horseshoe

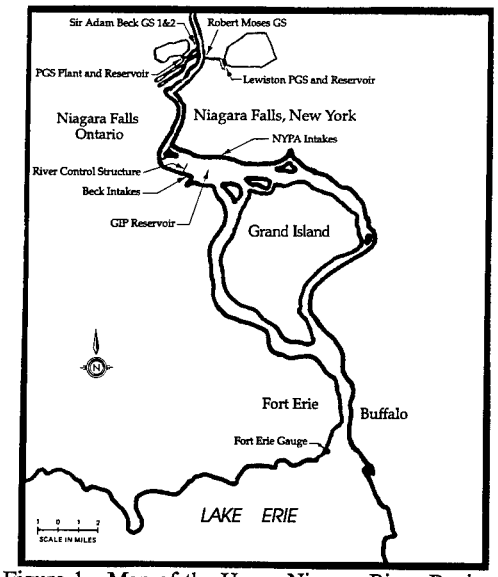

Figure 1. Map of the Upper Niagara River Region

and American Falls. Since these represent major tourist attractions, their flows are strictly regulated by the provisions outlined in the 1950 Treaty between Canada and the USA. The flow of water over the Falls is controlled by a structure consisting of 18 gates which extends approximately half way into the river. This structure has resulted in the formation of the partially controlled GIP Reservoir, having a storage capacity of 9,900 cms (350,000 cfs). This reservoir enables water, in excess of Treaty requirements, to be stored within specified constraints. River flow in excess of Treaty requirements can be used for power production purposes.

The hydro generating facilities located along the Niagara River consists of seven generating stations having a total installed capacity of approximately 4,700 MW, two man-made reservoirs and the GIP Reservoir.

Statistical Analysis of Surges

A statistical analysis of large surges at Fort Erie was performed (Camacho, 1989) for the 22 year period between 1966 and 1987, in which historical data was readily available. For the purpose of this analysis, a surge was defined to have occurred whenever the change in Fort Erie elevation, during a day, exceeded 0.3 m (1.0 ft) or whenever the change in elevation from one hour to the next exceeded 0.06 m (0.2 ft). The analysis was used to identify time periods in which to calibrate, test and validate the model. It was also used to get a better understanding of surges by

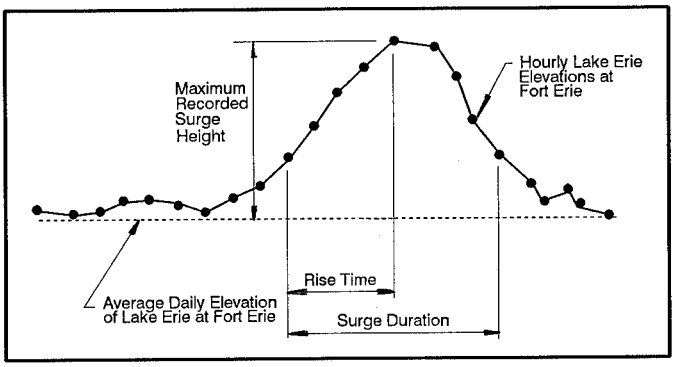

Figure 2. Definition of Surge Characteristics

identifying the time and frequency of occurrence, surge height, surge duration, and surge rise time. The definitions of these characteristics are illustrated in Figure 2.

Surges have been classified into two types. Type I surges are positive surges which cause the elevation of Lake Erie at Fort Erie to rise. These surges are caused predominately by south-westerly winds. Tables 1 and 2 show the results of the Type I surge analysis. Approximately two thirds of the total positive surges during this period, occurred between October and January.

Table 1 - Positive Surges at Fort Erie (1966 to 1987)

Month	Number of Surges	Mean Duration (hrs)	Mean Rise Time (hrs)	Mean Max. Surge (ft)	Mean Max. Surge (m)
January	53	7.6	4.1	2.75	0.84
February	16	4.0	2.4	2.29	0.70
March	28	4.4	2.6	2.46	0.75
April	25	6.3	3.0	2.74	0.84
May	8	3.1	1.9	2.08	0.63
June	14	2.8	1.9	1.94	0.59
July	4	4.0	3.0	1.90	0.58
August	7	3.0	2.1	2.10	0.64
September	12	3.7	1.8	2.17	0.66
October	28	5.5	2.7	2.43	0.74
November	47	5.8	3.2	2.84	0.87
December	72	6.6	3.2	2.68	0.82
	314	5.7	3.0	2.57	0.78

Table 2 - Exceedence Probabilities For Positive Surges

Exceedence Probabilty (%)	Surge Height (m)	Surge Height (ft)
1	1.847	6.06
5	1.400	4.59
10	1.177	3.86
90	0.482	1.58
95	0.451	1.48
99	0.393	1.29

Type II surges are negative surges which cause the elevation of Lake Erie at Fort Erie to decline. These types of surges are caused predominately by north-easterly winds. The distribution pattern of Type II surges is consistent with that of Type I (ie., approximately two thirds occurred in late fall and early winter). However, the frequency and maximum magnitude of Type II surges were much lower than the Type I surges (ie., 54% and 40% respectively).

Hydrodynamic Model

The Niagara River Flow Forecasting System employs a free-surface, one-layer, two-dimensional finite difference model for Lake Erie. The model was developed in Canada by the National Water Research Institute (Simons and Lam, 1982). A single Richardson lattice is used for its computational grid with the depth of water below mean lake level (H) and the free-surface elevation above mean lake level (Z) defined at the centre of each grid square. The currents (U,V) are represented by vertically-integrated water transports per unit width. X-components (U) are defined at the centre of the left and right sides of the grid square, while Y-components (V), are defined at the lower and upper sides of the grid square. Bathymetry of the lake is determined by the depth array (H), with the depths being zero at the shoreline.

The model computes the free-surface elevation above mean lake level (Z) for given wind stresses. In the following equations used by the model, nonlinear accelerations are neglected:

$$\frac{\partial U}{\partial t} = fV - gH\frac{\partial Z}{\partial x} - BU + \tau_{sx} \qquad (1)$$

$$\frac{\partial V}{\partial t} = -fU - gH\frac{\partial Z}{\partial y} - BV + \tau_{sy} \qquad (2)$$

$$\frac{\partial Z}{\partial t} = - \frac{\partial U}{\partial x} - \frac{\partial V}{\partial y} \qquad (3)$$

where: t = time; x,y are the horizontal coordinates; Z = the upward displacement of free-surface of grid from mean level; U,V are the components of vertically integrated current; H = the depth of grid from mean lake level; B = the bottom stress coefficient; f = the Coriolis parameter; g = the gravitational acceleration; and τ_s = the wind stress.

The wind stress at the surface (τ_s) is given by the following equation:

$$\tau_s = C_d \frac{\rho_a}{\rho_w} W^2 \qquad (4)$$

where: C_d = the drag coefficient; ρ_a = air density; ρ_w = water density; and W = wind vector.

A linear relationship is used for bottom stress (B).

$$B = a/H \qquad (5)$$

where: a = 0.01 to 0.05 (cm/sec).

The model has a time step of 240 seconds and a grid size of 10,000 meters (32,800 ft). The number of grid squares total 40 in the x-direction and 18 in the y-direction. Under normal conditions, a drag coefficient of 0.0025 is used for Lake Erie. This value is modified in real-time, during the winter, to take into account the effects of reduced drag caused by ice coverage of the lake.

Meteorological Data Link

A link between Ontario Hydro's Meteorological (MET) computer, located in Toronto, and the Niagara River Control Centre (NRCC) computer, located in Niagara Falls, was established to allow for the exchange of data required to run the model. Every hour, the MET computer is scheduled to dial into the NRCC computer and download a file consisting of on-the-hour instantaneous values of wind speed, wind direction, air temperature and atmospheric pressure for eight weather stations located around Lake Erie (Figure 3). These weather stations include six inland stations (Buffalo, Erie, Cleveland, Toledo Rondeau and Simcoe), and two automated stations (Longpoint and Southeast Shoal).

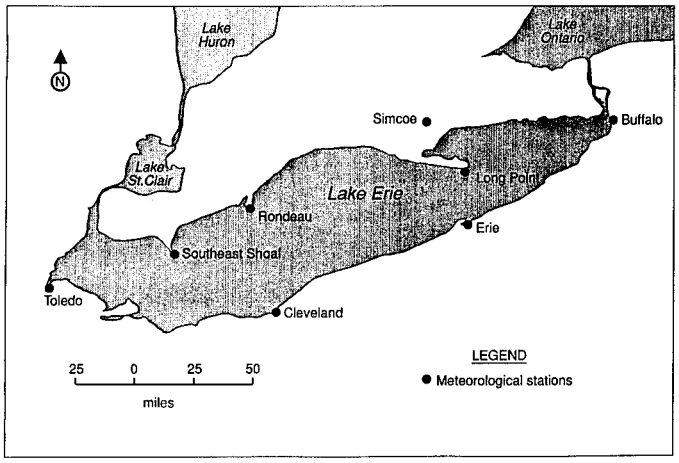

Figure 3. Location of Meteorological Stations

In addition to the above real-time data, a 48 hour forecast of Niagara River flows, generated by the MET Office Planning Model, is also transmitted through the link. The forecast is generated by a one-dimensional finite difference model (Gillies and Punhani, 1976) and its output is given in the form of 8-hour average flows. A heuristic approach is used to combine this information with the 6-hour operational forecast, to produce a 24 hour flow forecast used for daily planning purposes.

Data received from the MET Office is stored in the NRCC data base, where it is retrieved by the on-line programs for use by the Flow Forecasting System.

On-Line Programs

A number of on-line programs have been developed to automate the real-time operational process. The major programs include the Meteorological Monitoring, Meteorological Input, and the Lake Level Input Programs (Figure 4).

The Meteorological Monitoring Program reads the most current meteorological data from the NRCC data base and displays it on screen. This data consists of wind speed and direction, air temperature, and atmospheric pressure recorded at the eight weather stations. The program automatically updates the screen whenever new data is transmitted to the data base. The program is primarily used by NRCC staff as an early warning indicator for high winds. Changes in wind speed and wind direction throughout Lake Erie are continually being monitored to give advance notice of potential storm surge conditions.

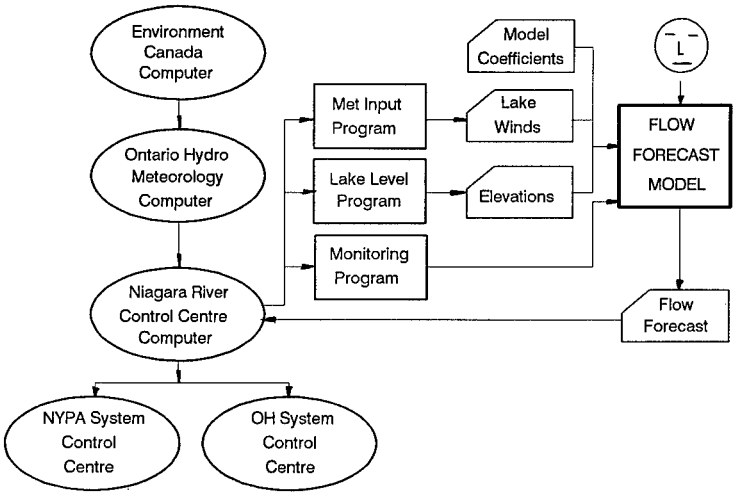

Figure 4. Flow Chart for the Niagara Flow Forecasting System

The Meteorological Input Program generates an input file required by the Flow Forecasting System. The program reads the latest 72 hours of meteorological data from the NRCC data base and uses an averaging algorithm to calculate

representative values of wind speed and direction, for Lake Erie, for each of the 72 input hours. Provisions have been made in the program to handle missing and/or erroneous data as well as for the unavailability of weather stations. This program is also run automatically, every hour, as new meteorological data is transmitted into the data base.

The Lake Level Input Program reads the real-time, minute-to-minute Lake Erie elevation file from the NRCC data base and calculates hourly values of representative lake levels. These values are essential inputs into the Flow Forecasting System as they ensure proper calibration.

Flow Forecasting Process

The Niagara River Flow Forecasting System is an hourly process which begins with the downloading of real-time and forecasted meteorological data from the MET Office. Once this data has been transmitted, the model automatically spawns a series of subprocesses which calculate the Flow Forecast Model's input (ie., 72 hours of representative winds and representative Lake Erie elevation to initialize

the model). In addition, an automatic run of the Flow Forecasting System is also initiated using the previous hour's default settings and a 6-hour forecast of winds based on persistence of the current hour's wind speed and direction. This automatic run is triggered both on the hour and whenever updated meteorological data is received from the MET Office.

The performance of the Forecasting System in real-time operation is dependent upon the ability of NRCC staff to make reasonable forecasts of wind speed and wind direction for the six hour forecast period. To assist them in making this forecast they are provided with access to hourly real-time meteorological data from the various Lake Erie weather stations, and twice a day updates of forecasted wind data provided by the MET Office. This information, along with continually updated marine weather forecasts for Lake Erie issued by the Coast Guard, allow the NRCC Operators to make reasonable wind forecasts.

The model also allows the drag coefficient to be modified on-line, in order to account for the effects of reduced drag caused by ice coverage of Lake Erie. During the winter, frequently updated Lake Erie ice surveys are available to NRCC staff. By inputting the percentage of ice coverage for the lake, the model will automatically adjust the drag coefficient.

Other features of the model include provisions for up to three simulation runs. Various wind scenarios can be input and compared to determine their effect on the elevation of the lake at Fort Erie and the corresponding Niagara River flows.

An example of model performance is shown in Figure 5. This validation test of the model compares the Lake Erie elevation forecast at Fort Erie, during the December 2, 1985 storm, with actual lake level readings.

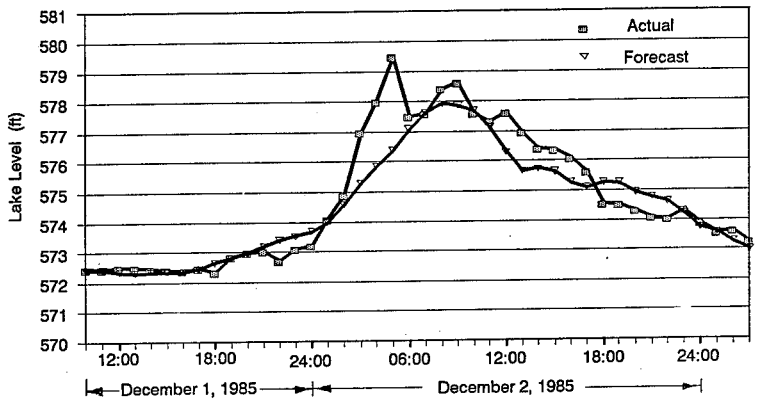

Figure 5. Example of Model Performance

Conclusions

The Niagara River Flow Forecasting System has been developed for real-time operation based on a hydrodynamic storm surge model for Lake Erie. The system, which is currently in production at the Niagara River Control Centre, forms part of a series of models which aid in the dispatching of water to maximize the value of energy over a daily time period.

Acknowledgements

The authors would like to acknowledge the National Water Research Institute and the Canadian Climate Centre of Environment Canada for use of the hydrodynamic model.

References

Bedford, K.W., and Dingman, J.S., "Model Intercomparison of Lake Erie Storm Surge Resonance Predictions," Proceedings of the ASCE Conference on Applying Research to Hydraulic Practice, Jackson, Mississippi, August 17-20, 1982.

Camacho, F., "Hourly Forecast Models for the Lake Erie Elevations," Ontario Hydro Research Report, November 1989.

Corbu, I., North, H., and Lacivita, K., "Development Work for the Niagara Generating System," Proceedings of the International Symposium on Water Resources Systems Application, Winnipeg, Manitoba, June 12-15, 1990.

Gillies, D.K.A., and Punhani, A.L., "Dynamic Forecasting of Lake Erie Water Levels," Ontario Hydro Research Report, 1971.

Hamblin, P.F., "Great Lakes Storm Surge of April 6, 1979," International Association Great Lakes Research, 1979.

North, H.A., Lacivita, K., and Corbu, I., "Application of DDDP to Determine the Optimal Daily Operation of the Niagara Generating System," Proceedings of the 3rd Water Resources Oper. Man. Workshop, Fort Collins, Col., June 27-30 1988.

Platzman, G.W., "The Dynamic Prediction of Wind Tides on Lake Erie," Meteorological Monographs, September 1963.

Simons, T.J., and Lam, D.C.L., "A Two-Dimensional X-Y Model Package for Computing Lake Circulations and Pollutant Transports," National Water Research Institute, Canada Centre for Inland Waters, Burlington, Ontario, Canada, 1982.

SENSITIVITY ANALYSIS OF DESIGN AND OPERATIONAL CHARACTERISTICS OF RESERVOIRS

M.A. Mimikou[1], P.S. Hadjissavva[2], Y.S. Kouvopoulos[2], and H. Afrateos[3]

Abstract

Regional effects of greenhouse warming on water resources and water management systems are assessed for a mountainous region of central Greece, by using plausible hypothetical scenarios of temperature and precipitation change. The operation of a hydropower generation scheme in the area is simulated under the assumed climate change scenarios and new risk levels are estimated with respect to firm water and energy supply. Increase of reservoir storage volume is examined as a means to maintain guaranteed supply levels.

Introduction

Growing atmospheric concentrations of carbon dioxide and of other trace gases are expected to alter the heat balance of the Earth and cause global climatic changes by increasing earth temperature. This effect, known as the greenhouse effect, as well as its impacts on the

[1]Associate Professor, [2]Research Associates, [3]Research Assistant
Division of Water Resources, Hydraulic and Maritime Engineering
Civil Engineering Department
National Technical University of Athens
5, Iroon Polytechniou 15773-Athens, Greece

regional hydrological cycle and the subsequent effects on the quantity and quality of water resources, have gained widespread interest. Recent research strongly suggests that significant temporal and spatial alterations will be caused in the various forms of water resources and associated water management works. This fact raises the possibility of dramatic environmental and socio-economic dislocations. In this paper an attempt is made to evaluate the regional climate change impacts on some critical water management issues, such as reservoir storage and hydroelectric production by analysing their sensitivity to plausible climatic change scenarios.

Data used

The study area lies in the central mountainous region of Greece, about 39° 30' N. It comprises four drainage basins, the Mesohora basin, the Sykia basin, the Pyli basin and the Mouzaki basin, listed in order of decreasing elevation. As can be seen on the map of the area in Fig. 1, the first two basins are associated with the upper Acheloos River, whereas the other two are associated with the Portaikos and Pliouris Rivers respectively. Also, the first two are purely mountainous, while the other two lie on the east slopes of the mountain range towards the Thessalia Plain and are more humid. Four multi-purpose reservoirs each one at the outlet of each basin will be constructed in the area and will operate as a system. The ultimate goal is to transfer water from the upper Acheloos River to the Thessalia Plain for irrigation purposes and hydroeloctric production. The dam-sites are shown in Fig. 1.

A network of hydrometeorological stations is satisfactorily operating in the region and has provided the necessary information in terms of monthly flows, precipitation, temperature, relative humitity, sunshine duration and wind speed, for the operation of the watershed simulation conceptual model (Mimikou et al., 1991_b). The locations of the observation stations are indicated in Fig. 1.

Regional Hydrological Effects

Climatic change

The effects of climate change on surface runoff were estimated by a monthly water-balance model. The underlying idea was that variations of the key climatic parameters precipitation P and temperature T, produce significant changes on the hydrological cycle of a basin, that can be

reproduced by watershed simulations. Scenarios of climatically changed P and T can either be deduced from running general circulation models (GCM) or from reasonable hypotheses. In our case, relying on GCM outputs was considered improper mainly because of the very coarse resolution of the grid they operate on. Secondly, different GCM estimates of precipitation change over the greater region are often inconsistent regarding both magnitude and direction of change.

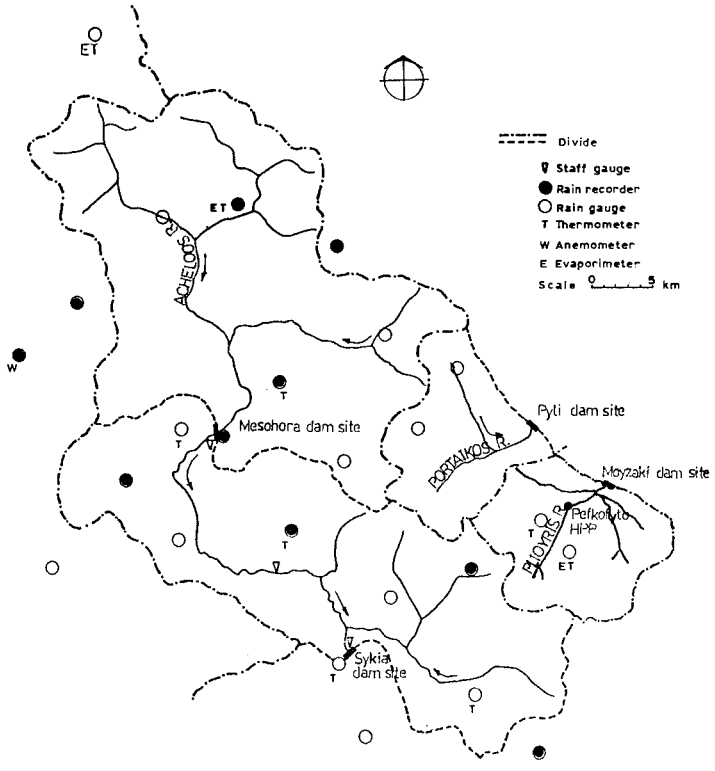

Figure 1. General plan of the study area.

Therefore, working with a number of hypothetical scenarios of climate change was preferred as more suitable for the purpose of sensitivity

analysis of runoff which was pursued rather than a prediction in itself (Gleick, 1986; Dooge, 1989; Mimikou et al., 1991_b).
Scenarios of climate change were produced by combining climatically affected time series of precipitation and temperature. These were obtained from reasonable hypotheses, well within the scope of current state climatological predictions regarding equivalent CO_2 doubling; uniform increases of 1, 2 and 4 C^o over the historical temperature time series were assumed to obtain three temperature scenarios, whereas for precipitation, five scenarios were constructed by assuming uniform percent change of the historical time series by +20%, +10%, 0, -10% and -20%. The temperature and precipitation scenarios thus derived combine into 15 climatic scenarios.

Watershed simulation

The model employed for watershed simulations was specially developed to make the most of the available field data (Mimikou et al., 1991_b). It operates on a monthly basis and it includes routines simulating the basic components of the hydrologic cycle at the catchment scale. The model produces estimates of monthly surface runoff, soil moisture content and of groundwater storage.

The model was calibrated and satisfactorily tested for its spatial and temporal robustness on three basins of the study area in the 16 year period of available hydrometeorological records. The Mouzaki basin was excluded from calibration due to lack of sufficient runoff data. Therefore, the study of watershed response to climate change was restricted to the other three basins. However, since the Mouzaki reservoir plays an important role in the water management project, estimates of climatically affected runoff were also made for this catchment on the basis of a profound similarity between the Mouzaki basin and the satisfactorily gauged Pyli basin (PPC, 1986).

Regarding its performance, the model was shown to accurately reproduce the annual flows and adequately so the monthly flows. Snow accumulation and snow melt runoff were also satisfactorily predicted both in
timing and in magnitude. Finally, parameter values obtained through the calibration procedure were explained and qualitatively justified by the specific morphological characteristics of each basin.

To obtain climatically affected time series of runoff I_t, the climatic scenarios previously described were fed into the model. Base run results, i.e. for no change of precipitation or temperature served as a basis of comparison, instead of the historic time series of runoff, for uniformity reasons. These runoff series I_t constituted the reservoir inflows scenarios corresponding to the fifteen hypothetical climatic change scenarios and were further used in the reservoir simulation

models. Details concerning the hydrological effects of climate change on runoff and soil moisture can be found in previous publications (Mimikou, M. and Kouvopoulos, Y. 1991; Mimikou et al., 1991_b). Some results indicating the extreme sensitivity of the mean winter and summer runoff for the Mesohora, Sykia, and Pyli basins are shown in Table 1, as percent deviations of the above runoff quantities from normal (i.e. base) run.

TABLE 1. Percent changes of seasonal surface runoff

Drainage basin:	**Mesohora**		**Sykia**		**Pyli**	
Runoff quantity:	**mean summer**	**mean winter**	**mean summer**	**mean winter**	**mean summer**	**mean winter**
Base run value (mm):	88	447	101	508	84	621
$\Delta T=1^oC$						
$\Delta P=$ -20%	-49	-24	-44	-22	-22	-25
-10%	-38	- 6	-33	- 6	-11	-12
0%	-27	-11	-21	10	- 1	2
10%	-14	28	- 9	26	11	13
20%	- 1	44	4	41	21	30
$\Delta T=2^oC$						
$\Delta P=$ -20%	-57	-17	-52	-18	-23	-15
-10%	-48	2	-42	0	-12	-12
0%	-39	20	-32	17	- 2	2
10%	-30	38	-22	33	9	16
20%	-20	55	-11	49	20	30
$\Delta T=4^oC$						
$\Delta P=$ -20%	-63	-16	-58	-19	-24	-27
-10%	-55	3	-49	0	-13	-14
0%	-48	23	-40	17	- 3	- 1
10%	-39	41	-30	34	8	13
20%	-30	59	-20	51	18	27

Change Impacts on Design and Operational Characteristics of Rererevoirs

Water management scheme

The reservoirs to be constructed in the study area are indicated in Fig. 1. Starting from upstream, the Mesohora reservoir is designed to guaranteed power production only. The Mesohora power plant will be located at the tail of the downstream Sykia reservoir. A minor fraction of the water collected there will be released through a power plant at the toe of the Sykia dam as firm water supply into the downstream portion of the Acheloos River basin. Most of the water volume collected in the Sykia reservoir will be transferred at a guaranteed annual rate to the Mouzaki basin.

At the downstream end of the diversion tunnel, the flow will be passing through the Pefkofyto power plant. The Mouzaki reservoir is designed to guarantee both energy production and firm water supply to the downstream Thessalia Plain for irrigation purposes.

The operation of this system of reservoirs is simulated by a monthly water balance equation under various constraints concerning storage volume, outflow from the reservoir and energy production. A detailed description of the reservoir simulation models, and approach used, can be found elsewhere (Mimikou et al., 1991_a).

Impacts on firm water and energy supply levels

The impacts on firm water and energy supply levels were estimated by a probabilistic assessment of the risk involved under the various climatic scenarios (Mimikou et al., 1991_a). The monthly flows I_t, either historic or climatically affected, were used as inputs to a stochastic model of the AR(2) type to generate synthetic series of inflow spanning 50 years, equal to the duration of the project economical life. The calibration of the AR(2) model was done by using the standard Box and Jenkins procedure (Box & Jenkins, 1970). For each climatic scenario, the historic record included, a multitude of synthetic inflow series were thus fed into the system operation simulating model, and the relative frequencies of monthly failures, or risk values, were estimated for various combinations of primary energy E and firm water supply W. A failure was considered to occur when either of the produced quantities failed to meet the preselected demand. As this kind of analysis implied a convolution between two and three (W, E) sets for the Sykia and Mouzaki reservoir respectively, to limit computer time the simplifying assumption was made that when operation of a certain reservoir was

simulated for a set of (W, E) pairs, all upstream reservoirs in the system would then operate at their design values for W and E.

The risk analysis conducted under current climatic conditions revealed that the probability of an operation failure at the examined reservoirs, associated with the design values for W and E, was well below 1% for all of them. However, the risk level as a function of (W, E) appeared much more sensitive in the case of the Mouzaki reservoir, with a tendency to grow rapidly as E increased.

The results of the sensitivity analysis on the probability of failure associated with the design values of E for the Mesohora (as only power generation is guaranteed there), and W and E for the Sykia (power plant at Pefkofyto), and Mouzaki reservoirs under the 15 hypothetical climate change scenarios are listed in Table 2.

TABLE 2. Sensitivity analysis of risk (%) for the design values of energy and water yield under climate change.

Climatic scenarios	Mesohora HPP	Pefkofyto HPP	Mouzaki HPP
Current climatic conditions	0.35	0.04	0.33
$\Delta T=$ 1 ^{o}C			
$\Delta P=$ -20%	21.43	26.99	51.40
-10%	7.02	5.92	13.77
0%	1.50	0.88	1.35
10%	0.56	0.03	0.16
20%	0.33	0.03	0.04
$\Delta T=$ 2 ^{o}C			
$\Delta P=$ -20%	21.92	27.28	49.37
-10%	9.01	6.95	15.12
0%	3.77	1.05	1.56
10%	1.74	0.31	0.38
20%	0.61	0.07	0.03
$\Delta T=$ 4 ^{o}C			
$\Delta P=$ -20%	25.29	32.99	53.65
-10%	11.15	9.90	20.54
0%	4.43	1.38	2.47
10%	2.10	0.30	0.28
20%	1.07	0.02	0.04

By examining these calculated risk values it is generally observed that reservoir operation failure is affected rather by precipitation reduction than by temperature increases. Under the same precipitation reduction, downstream reservoirs exhibit larger risk levels than upstream ones, owing to an increasing sensitivity of risk from the Mesohora to the Mouzaki reservoir. This is explained by the cumulative effect of upstream failures transferred downstream, in combination with the pronounced sensitivity of the Mouzaki reservoir discussed previously. Regardless of the temperature increase, precipitation increases do not significantly improve risk levels, while precipitation reductions significantly and disproportionately raise the risk levels. Regarding temperature increases alone, the Mesohora reservoir appears to be relatively more sensitive than the other two, owing to the previously mentioned intensification of the already high seasonality of runoff in conjunction with its comparatively smaller storage capacity. When temperature increases combine with precipitation reductions then they become in effect marginal, mostly so in the case of the Sykia and Mouzaki reservoirs.

The risk levels for water and energy supply were shown to be unacceptably high under conditions of reduced precipitation, even by 10%. However, increasing net storage volume of the reservoirs compensates for this effect of precipitation reduction. To obtain an idea of how much should the net storage volume be increased in order the design firm water and energy yield be maintained at tolerable risk levels, the upstream Mesohora reservoir was examined under precipitation reduction scenarios. Results indicated that radical increases of net storage volume, sometimes greater than 100% are required for the design energy production to be met with tolerable risk levels. Precipitation reductions were found to play the important role, whereas the effect of warming appeared to be marginal as compared to that of precipitation decreases.

Conclusions

Climate change effects on various forms of water resources, such as surface runoff and soil moisture, in mountainous catchments of central Greece are shown to be very important.

The climatically affected runoff causes dramatic increases of the risks associated with the annual firm water and energy supply levels from the system of reservoirs in the study area, particularly when precipitation decreases are involved. The effect of temperature rise on risk levels appears to be marginal. Downstream reservoirs appear to be more sensitive than upstream ones. Radical increases of reservoir

storage volume are required to maintain guaranteed water and energy supply levels from reservoirs.

Acknowledgements

The work presented here is part of a major research project jointly funded by the General Secretariate for Research and Technology, and the Greek Ministry of the Environment, Physical Planning and Public Works.

References

Box, G. & Jenkins, G. (1970). *Time Series Analysis-Forecasting and Control.* Holden Day Series, San Francisco.

Dooge, J.C.I. (1989). Effect of CO_2 increases on hydrology and water resources. In: *Carbon Dioxide and other Greenhouse Gases: Climatic and Associated Impacts.* (R. Fantechi & A. Ghazi, Eds.), Kluwer Academic Publishers, London.

Gleick, P.H. (1986). *Regional Water Availability and Global Climatic Change: The Hydrologic Consequences of Increases in Atmospheric CO_2 and other Trace Gases.* Ph. D. Dissertation, University of California, Berkeley.

Mimikou, M.A., and Kouvopoulos, Y.S. (1991). Regional Climate Change Impacts. In: I Impacts on water resources. *Hydrol. Sc. J.,* **36, 3, 6:** 247 - 258.

Mimikou, M.A., Hadjissavva, P.S., Kouvopoulos, Y.S. & Afrateos, H. (1991_a). Regional climate change impacts - II. Impacts on water management works. *Hydrol. Sci. J.* **36, 3, 6:** 259 - 270.

Mimikou, M., Kouvopoulos, Y., Cavadias, G. & Vayiannos, N. (1991_b). Regional hydrological effects of climate change. J. *Hydrol.,* **123:** 119 - 146.

Public Power Corporation of Greece (PPC), (1986). *Hydrologic Design on Portaikos and Pliouris Rivers in the Thessaly Plain.* PPC Report. Athens (in greek).

REAL-TIME FLOW FORECASTING ON THE SALUDA RIVER WATERSHED

George Kanakis, Jr.[1], A. M .ASCE, and Robert A. Laura[2], M. ASCE

The Saluda Watershed, located in the northwest portion of South Carolina, covers approximately 2,200 square miles and contains the Saluda Dam, which creates a reservoir known as Lake Murray. This reservoir has a normal pool elevation of approximately 360 feet above mean sea level (MSL) and has a surface area of 48,000 acres. This paper summarizes the development of a flow-forecasting model to monitor the response of the lake level to antecedent weather conditions in order to predict inflows and control reservoir elevations in real-time.

The flow forecasting system has three main components. The first component is an automated real-time database to collect and maintain hydrologic data via modem from a network of telemetered gages in the watershed. The second component is a dynamic, linked, hydrologic and hydraulic model for creating rainfall and runoff hydrographs and for carrying out dynamic hydraulic calculations. The third component is a system manager, which controls computer operations, synthesizes the data, directs the flow of calculations, and generates reports.

An automated real-time database was developed based upon a network of ten streamflow gages, eleven rainfall gages and one elevation gage in the watershed. The United States Geological Survey (USGS) maintains these gages as part of their geostationary operational environmental satellite (GOES) network. These gages record data at one hour intervals and transmit the data to the central USGS computer in Columbia, South Carolina at four-hour intervals.

[1]Project Engineer, Law Environmental, Inc., 7375 Boston Blvd., Suite 200, Springfield, VA 22153.
[2]Senior Civil Engineer, South Florida Water Management District, West Palm Beach, FL 33416.

The gage locations provide broad coverage across the watershed. One water-elevation gage is located in Lake Murray near the Saluda Dam. Ten streamflow gages, located in major tributaries, provide base flows for the hydrologic model and boundary conditions for the hydraulic model. Eleven rainfall gages provide loadings for the hydrologic model.

The system manager uses the BLAST communication protocols to link with the USGS central computer system six times per day. The timing of the computer link coincides with the regular transmission from the gages.

Custom script programs were developed within the BLAST software to establish a link between our computer and the USGS computer and to download data in automatic operation. We maintain the data base in a file conforming to the American Standard Code for Information Interchange (ASCII) format. We also developed custom software to check the data for errors before loading the database. Since the primary purpose is flow forecasting, the system manager only keeps data for a one month period. After one month, the data is deleted and replaced with the current day data.

The database also contains forecasted information on rainfall and operations of the dam. The system manager establishes a communication link with the National Weather Service (NWS) computer facility in Atlanta, Georgia to download precipitation forecasts automatically. The precipitation forecasts augments the gage data in the basin network and provide estimates for predicting runoff in the watershed. Precipitation forecasts consists of daily predictions for two 24-hour periods covering the current day and the following day. The system manager displays the rainfall forecast in a graphical format on the computer screen. The forecast from NWS may be used in the database or the user may enter other values.

Dam operations include spillway opening schedules, and turbine flow schedules. The hydraulic model uses the dam operation schedule for boundary conditions. The use can optimize the dam schedule by simulating different alternatives and choosing the most effective combination of gate opening schedule and turbine flows in order to meet the operating requirements of the dam.

The system manager uses the Basin Runoff and Streamflow Simulation (BRASS) model to conduct hydraulic calculations and flow forecasting. The Savannah District of the Corps of Engineers originally developed the BRASS model, which was revised and enhanced for this study in order to provide the following capabilities; continuous simulation of infiltration potential, generation of runoff hydrographs, storage reservoir routing, dynamic streamflow routing, and dam failure simulations. BRASS is a package of program modules to simulate the hydrologic and hydraulic response of watershed and river systems. BRASS has a hydrologic model

to distribute rainfall, determine the Soil Conservation Service (SCS) curve number, base flows, and runoff using the SCS curve number equations for rainfall using the infiltration capacity of a basin. This hydrologic model is linked with the NWS dynamic wave operational model (DWOPER), which is a flow routing model solving the one-dimensional St. Venant equations of unsteady flow.

The BRASS model, developed in this study, has two segments: an upper segment upstream of Saluda Dam and a lower segment downstream of the dam. The upper segment consists of seven sub-basins for hydrograph generation and storage routing, and approximately 50 miles of dynamic streamflow routing reaches. The lower segment consists of approximately 57 miles of dynamic streamflow routing reaches. The study area includes the Saluda River, Broad River, and Congaree River as well as the watershed areas that contribute runoff to these rivers.

The upper segment determines the lake response for forecasted dam operations and rainfall events. The lower segment determines downstream effects, flows and flow elevations, resulting from upstream conditions.

Most of the gages in the database are in the upper segment of the BRASS model, in order to provide data for the runoff calculations. Streamflow gages in the lower segment provide boundary conditions for DWOPER. Seven sub-basins in the upper segment collect rainfall data from the gage network to be used for calculating runoff. The computed runoff hydrographs provide boundary conditions for the dynamic routing. The dynamic routing is split into two segments to take advantage of the special downstream boundary condition routines for simulating dam operations and failure. BRASS saves the computed downstream hydrograph of the upper segment for use as the upstream boundary condition of the lower segment.

The system manager has six primary functions to integrate model operations. The first function creates and maintains a database of historical gage data. The second function creates and maintains a database of forecasted precipitation and dam operating schedules. The third function performs flow forecast simulations. The fourth function provides a mechanism for reporting and displaying the information in the database and the results of the flow forecast simulations. The fifth function provides disk and file maintenance with a regular backup procedure. The sixth function is a system status display.

The system manager integrates the functions described previously into a "user friendly" system of menus. The system manager combines a package of custom programs written in FORTRAN, BASIC, and DOS.

This model runs on a desktop computer that is compatible with an International Business Machine (IBM) personal computer (PC), using State-of-the-Art hardware and software. This model can easily be adapted to other river systems, and is a powerful tool for monitoring hydrologic and hydraulic conditions in the Saluda Watershed in real-time.

Monte Carlo Simulation Techniques for Predicting HydroPower Performance

Mr. John P. Cross[1]
Member, A.S.C.E.

Introduction

Traditional methods of predicting anticipated production of hydroelectric facilities have focussed on the evaluation of historic streamflows within the context of plant design and efficiency. This approach results in the projection of an average annual production which is then factored into various financial projections for the facility. At times the question is raised as to a "best" case and a "worst" case scenario for a facility. Normally, the flow records are scanned and the low flow and optimum flow year are selected. The flows from these two years are then modeled with respect to the facility design and the resultant production is considered as the "best" and "worst" case scenarios.

The question that inevitably faces the individual reviewing these results and evaluating the financial viability of such a site for construction, acquisition or other capital expenditures is how often these events occur. What level of confidence is associated with this average flow? How often should a low flow year be anticipated? How often should a year be anticipated that will significantly exceed average flow predictions? Traditionally, the best response has been simply one of a "feel" for the site. A review of the flow histories may provide the trained observer with a sense that the flows at the site are generally consistent or they may indicate a flashy situation with significant variations from year to year. Often in an investment analysis this intuitive feel has been translated into the required rate-of-return for the site. The more stable the flow is at a site, the lower the

---

[1] Regional Civil Engineering Manager, Beling Consultants, Joliet, Illinois

acceptable rate-of-return became as the flow risk was deemed to be less significant. Conversely, on sites with great annual flow variations, higher rates-of-return were required to account for the increased level of risk. While such an approach does satisfy the need for a sense of the financial performance of a site, it does not address the problem in an analytical manner and provide any type of measurable projection of anticipated performance.

Statistical Analysis of Performance

One solution to this problem would be to create a performance model for each year of flow history. This set of production results could then be analyzed statistically to determine a mean, median and a standard deviation. The standard deviation indicating a range on either side of the mean defining a 68% confidence interval for the annual production. By taking the required production to meet the financial requirements of the project against the distribution curve it would be a simple matter to evaluate the percentage of years when it would be anticipated that the cash flow from the project would not meet the cash requirements.

The solution noted in the preceding paragraph would seem to resolve the problem being faced in that it provides a statistically determinate model against which financial decisions can be made. However, the question that must be asked is whether twenty to fifty data points create an adequate sample set from which reasonable conclusions can be drawn. In general, a sample size should be larger than the selected set by a factor of twenty to fifty. If a financing period of twenty years is selected, an appropriate sample set should be in the range of four hundred to one thousand data points or years in this analysis. Obviously, no site exists where four hundred to one thousand years of flow data has been recorded.

Monte Carlo Method Applicability

This does not mean that no statistical method can be of assistance in the modeling of performance. Rather, the attention of the analysis must be moved from a limited (twenty to forty) number of data points or years to a larger data set. That larger data set would be composed of the daily flows experienced at the site. In that case, forty years of flow would create a sample set with nearly fifteen thousand data points. Yet, it would be inappropriate to simply determine the mean daily flow and construct a confidence interval around that flow and evaluate the financial performance of the site based on a daily production multiplied by 365

days. Such an analysis would ignore the reduced performance of the turbine and generator during low flow periods or the high flow limitations of the design.

The goal then is to utilize the daily flows to increase the size of the sample set, yet still evaluate the performance of the site based on daily production across an entire year. It is possible to do this if the daily flows are used to create a stochastic model of the streamflow. A stochastic model is a model that takes into account both the random and time dependent nature of any event, in this case streamflow. The model predicts the event at any given point in time by analyzing the prior event and the statistical "history" of similar events. Each generated model is triggered by a random variable to start the sequence. The result is that a synthetic or predicted streamflow can be generated from a statistical analysis of existing streamflow information. By seeding this prediction with numerous random variables, multiple streamflow scenarios can be created. These created streamflows are the product of a data set with an adequate number of data points to predict streamflow within acceptable confidence levels.

The bottom line is that instead of modeling the twenty year performance of a hydroelectric site against forty years of data, a synthetic data set of over one thousand years of data can be created against which the modeling can take place. Such an approach is common in statistical modeling and is known as the Monte Carlo Method.

Introduction to the Monte Carlo Method

The Monte Carlo method allows for the creation of an approximate numerical answer to a specific, concrete problem. The essence of the method is that an analog of the relevant situation is created and the process is simulated to generate a body of data from which the desired information can be extracted.

As an illustration of how the Monte Carlo method works, suppose that a manufacturer annually purchases a lot of fifty components from an outside vendor. These components require a greater tolerance than typically specified by the manufacturer. Upon inspection it is found that ten of the components are outside the range of tolerances required for the component. The manufacturer agrees and states that it is true that based on their production methods one-sixth of the components purchased will be outside the required tolerances.

The critical question is how likely is it that more than ten of the components will be out of tolerance in any given lot. One way to solve this problem would be to take fifty dice and throw them simultaneously one thousand times. On each throw the number of dice showing a one is counted and then the number of throws where the "one count" exceeds ten is tallied. This tally is then divided by 1000 to indicate the probability that more than 10 components will be outside tolerance.

The implementation of the "model" testing does not have to be performed by repetitive rolling of dice. Rather, any series of analogous events can be repeated and the results studied as long as the events are truly analogous to the actual situation being studied. The Monte Carlo method is not the definition of the mathematical model of the physical event, but rather the technique of using the model repetitively to generate a larger sample that can be analyzed through the use of standard statistical tools.

The Application of Monte Carlo Techniques to Streamflow Modeling and Hydroelectric Power Production

The value in utilizing a Monte Carlo simulation to model streamflow is that a large number of scenarios can be examined to determine the probability of an actual streamflow condition occurring. The technique has been used to model groundwater conditions and reservoir capacity factors, but limited work has been done in applying this approach to hydroelectric development. Hydroelectric development is perhaps an even more natural arena for this activity than other areas of hydrology. Granted that in a reservoir filling scenario care must be taken to assess the probability of a scenario of events occurring that would cause overfilling and a potential failure condition, but safety factors can be included in the design to cover these possibilities. But with respect to hydroelectric power development a financial factor also presents itself. It is not just that accurate projections of flows are required to size the plant, but that the constructed site must also be able to supply adequate cash flow to satisfy debt service during the early years of operation. By accurately modelling the site and predicting performance it is no longer necessary to say "the average flow at the site should have no problem in supporting the debt", but rather be able to say, "there is only a six percent probability that the site will not support its debt service in the first ten years of operation."

Stochastic Modeling of Streamflow Data

In order to create a series of streamflow models from which power production can be derived, it is necessary to model the mathematical relationship used to generate the streamflow data. It is assumed that the starting point for such an analysis is the existence of at least twenty years of daily flow data for the site under study. This data may be directly available from a nearby stream gauge, the combination of data from several stream gauges or generated from nearby gauges and then proportionalized against the relative drainage areas.

This flow data is the basis of a stochastic model of the streamflow at the site. As stated earlier, a stochastic model is a model that takes into account both the random and time dependent nature of an event. Unlike simply rolling dice where each event is an isolated act, the flows at a point on a stream are related statistically to the flow occurring a day earlier and the time of year that the flow occurs.

The actual mathematical model that expresses this univariate condition is:

$$Y = \bar{y} + [R(x,y)\,(X - \bar{x})\,\sigma(y) / \sigma(x)] + t\,\sigma(y)\,(1 - R(x,y)^2)^{.5}$$

where:

Y	=	present daily flow
X	=	previous daily flow
$\bar{y}$	=	mean present daily flow
$\bar{x}$	=	mean previous daily flow
$\sigma(y)$	=	standard deviation of the present daily flow
$\sigma(x)$	=	standard deviation of the previous daily flow
R(x,y)	=	serial correlation coefficient of the two successive daily flows
t	=	a random number between -1 and 1

From this model a series of annual flows can be constructed to create the synthetic set of flows used in the Monte Carlo model. In general the use of modern computing resources allows a minimum of a thousand years of synthetic streamflows to be easily generated for use in the analysis.

Relating Streamflow Predictions to Power Production Estimates

Each of the one thousand annual streamflow data sets can be evaluated for power production potential by simply running the flow through a simple algorithm. This power production algorithm should relate power production to turbine efficiency over a range of flows, take into account any minimum release criteria at the site, reduce production if an increase in tailwater elevation occurs during peak flows and adjust for periods of non-production during high flow periods due to equipment inundation.

The result of the analysis will then be power production in kilowatt-hours for each of one thousand years. These production quantities form a distribution that can be defined in terms of mean, median, standard deviation and variance. It then becomes possible to speak of the site having the probability of some percentage of being able to meet its debt service and cash flow requirements. From the design standpoint, the sizing of the generating equipment may be modified to better "catch" the variability of the flow at the site and increase potential production or narrow the equipment operating ranges to increase efficiency.

Integrated Financial Modeling

After constructing the model of the streamflow it is possible in the computer model to directly integrate the financial aspects of a site's performance so that the results of the analysis are not produced in kilowatt-hours, but in dollars generated. The advantage of such an integration is two fold. First, payment variations based on season or splits between energy and capacity components can be model directly rather than averaged over the year. Secondly, a probabilistic assumption can be added to the rate of escalation of any variable pricing mechanism. In effect, if it is felt that over the life of a contract the average increase in the energy component may be four percent with a variation of three percent, this can be modelled in the analysis. After the streamflow is constructed, a similar calculation can be performed with a random number seed to project an annual variation is purchase price.

The major difference in the financial portion of the projection is that it is not based on any historic trends, but rather on a random selection from an arbitrarily determined prediction of future power rates. This may seem little different than the normal assumption of an escalation factor in a financial analysis,

however in this case the resultant cash flows are a function not only of an average escalation rate, but also the anticipated annual level of variation from that average rate.

Multiple Site Scenarios

The applicability of the Monte Carlo method is not limited to viewing one hydroelectric site at a time. Much to the contrary, the technique can be easily utilized to examine multiple sites simultaneously. Such multiple site viewing is of great advantage in two situations. First, if several plants are located in the same drainage or watershed the same flow generation when properly scaled for each site can generate the production model using same year data for the entire thousand year time span. Obviously such a modeling must take into account additional flow sources or drainage area, but the same stochastic model can be maintained across all sites to provide the required consistency of data for the statistical evaluation.

Secondly, an entire portfolio of sites for a developer or organizational entity can be modeled to predict whether the composite effect of all sites is to provide adequate cash flow to meet the requirements of the total debt service. Such an analysis should have the effect of providing an increased level of assurance to lending institutions or investors resulting in a reduced coverage ratio on the extended funds. In this analysis, separate flow models are constructed for each site predicting the flow independently in each production model. However, one of the major challenges in this type of analysis is to adequately take into account the effect of regional or national weather patterns. This investigation is ongoing but it is tentatively felt that the historic flow data from each site must be aligned to the same year so that the serial correlation coefficient is consistent between sites. In addition, the random number seed used to generate the flow histories in each model should be the same to give the impact of the similar timing. This is an area requiring further research and investigation.

Overview of the Computer Model

The computer model currently exists in several versions written in either BASIC, FORTRAN or C for an MS-DOS based computer. The BASIC version is used for experimentation related to quick code changes and the impact model variations. The C and FORTRAN versions are more difficult to modify for varying site conditions but provide more efficient processing and a reduction in the required computer time. No attempt has been made to create a user-friendly

version of the program that simply accepts user commands to determine the analysis parameters. Rather, because of the complexities between the operating parameters of various sites and the formats of available flow information, each site has been developed as a "rewritten" program.

Executions time on a 25 megahertz machine with a math coprocessor have been in the range of ten to twenty minutes for a model generating 1000 years of data from twenty years of flow records for a single site.

Single Site Case Study

To illustrate the use of the model, a site was analyzed for which twenty years of flow data was available. The site, located in the western United States, had a median flow determined to be 1500 cubic feet per second utilizing a typical flow duration curve methodology. When the turbine selection criteria was applied to this typical flow an annual generation of 12.64 gigawatt-hours was anticipated. This analysis indicated that cash generated by the project would not satisfy the debt obligations of the project.

When daily flows were used to create the statistical parameters to predict one thousand annual flows, the results were significantly different. A mean annual power generation of 14.32 gigawatt-hours was predicted with a standard deviation of 2.83 gigawatt-hours. When factored into a financial performance model it was seen that there existed a probability of 11% that the project would not be able to meet its cash flow and debt service obligations in any given year, but that over the twenty year life of the project financing there existed only a 4% probability that the project would be in a cumulative cash deficit position.

Conclusion

The Monte Carlo method of analyzing a series of streamflows produced through stochastic modeling is a valuable tool for evaluation of the anticipated production of hydroelectric power facilities. Its use provides a greater definition of the level of confidence that is reflected in viewing an annual power generation value. As such it should be used for the evaluation of potential capital investments and site value assessments along with the more traditional approaches to predicting power production and financial value.

Applications and Limitations of the USBR "Method of Successive Subtraction of Subbasin PMP Volumes" for Critical Storm Development for Dam Safety Hydrologic Assessments

Ed A. Toms[1]

ABSTRACT: This paper discusses the application of the USBR "Method of Successive Subtraction of Subbasin PMP Volumes" to compute the critical storm for regions that are classified orographic within the Rocky Mountain region. It is critical to evaluate the spatial and temporal distribution of the Probable Maximum Precipitation (PMP) when evaluating the hydrologic safety of an existing dam. Inappropriate procedures used to develop the critical storm pattern can result in large rehabilitation costs not required if the storm characteristics were studied in more detail. A sensitivity analysis was performed to estimate what effect basin area and shape has on the selection of the critical PMP storm using the USBR method. The PMP is estimated using the HMR 55A and the resulting Probable Maximum Flood (PMF) is computed by the rainfall-runoff simulation model HEC-1. Based on the sensitivity analysis, conclusions are developed for the use of the method within the Rocky Mountain region.

Two case studies are presented illustrating the USBR method. The application of the USBR method to the case studies differs with respect to the watershed characteristics and areal and temporal distribution of the PMP storm. The first case study involves a 15 square mile urbanized

[1]Hydrologic/Hydraulic Engineer; Engineering Consultants (ECI) 5660 Greenwood Plaza Blvd., Suite 500; Englewood, Colorado 80111 Telephone (303)773-3788.

watershed located in New Mexico. The second case study involves a 1000 square mile Northern Colorado mountainous watershed.

INTRODUCTION

In the Rocky Mountain Region (between the Continental Divide and the 103rd meridian) PMP storms are influenced by mountain orographic effects due to the upslope weather conditions as illustrated in Figure 1. The areal distribution of the design storm should be estimated based on subbasins or design points rather than a generalized watershed method.

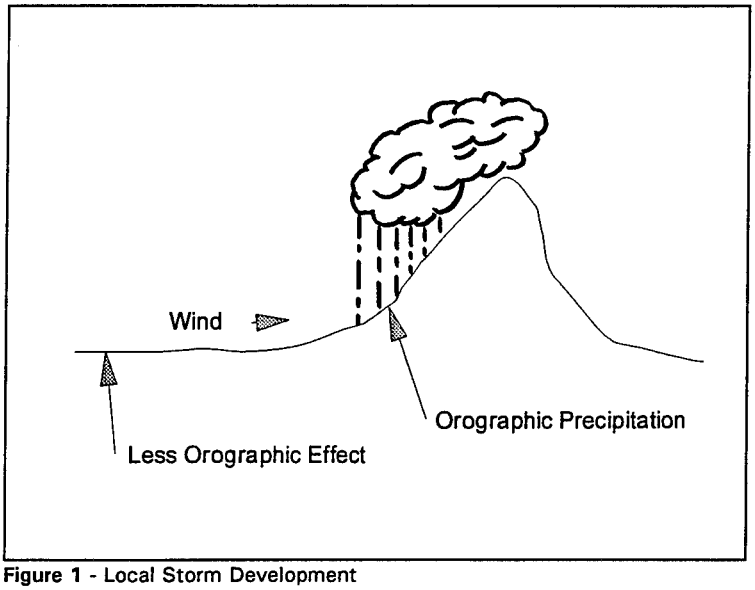

Figure 1 - Local Storm Development

Using a generalized storm pattern over a watershed is an overly conservative approach to compute the hydrologic response of the watershed. The generalized storm pattern will tend to over estimate the hydrologic response for large watersheds. The smaller the watershed, the lesser this holds true because of the storm characteristics within the geographical area of study. The over estimation of the hydrologic response could possibly led to unnecessary dam improvements to meet state dam safety standards.

STORM CHARACTERISTICS

Within the Rocky Mountain Region, investigations have shown that the PMP for small areas and short durations are not likely to occur in a general storm [HMR 55A (1988)]. The local or convection storm concept is used in western PMP studies to describe an intense, short duration storm occurring in isolated areas. East of the 105th meridian, previous studies [HMR 52 (1982)] have concluded that the general storm controls PMP for all durations.

A local storm can be comprised of one (simple) or multiple (complex) storm cells. Simple local storms usually affect smaller areas, have a higher intensity, and produce greater amounts of precipitation over smaller areas than a larger general or cyclonic storm. The areal extend of a simple local storm is characterized by a 6 hour duration and the total storm area is generally less than 500 square miles [HMR 55A (1988)]. Complex local storms generally have a duration longer than 6 hours and a total storm area will be greater than 500 square miles [HMR 55A (1988)]. A complex local storm also will have a duration less than 24 hours and the total storm area will be less than a few thousand square miles.

A general storm event is primarily caused by the large scale vertical motion associated with weather fronts caused by pressure systems. The areal extent of the storm is typically larger than 10,000 square miles. The total duration of the storm is one or more days. The precipitation is steady rather than high intensity bursts.

DESIGN STORM

The design storm is the estimate of the rainfall amount spatially and temporally distributed over a particular drainage basin that is used in the development of a PMF. The PMP is used to develop the PMF. The PMP is the theoretical greatest depth of precipitation for a given duration that is physically possible over a given size storm area at a particular geographical location at a certain time of the year.

DAM SAFETY HYDROLOGIC ASSESSMENT

The hydrologic assessment of a dam structure is a study addressing the probable performance of the project during future extreme flood conditions. Because the actual timing and magnitude of future flood events are indeterminate, such assessments cannot be based on rigorous analyses but must be made by analyzing the probable function of the project during hypothetical design floods [Safety of Existing Dams (1983)]. Several storm characteristics affect the outcome of the hydrologic assessment: Storm Placement; Subbasin Distribution; and Temporal Distribution.

Several storm placements should be considered in order to determine the critical storm location. Generally, placing the storm center near the downstream end of the drainage area will produce the most critical condition for peak inflow but not for maximum volume. This is caused by the lack of basin storage which includes channel and floodplain storages. The maximum storm volume will be generated when the storm is located in the upper portion of the drainage area.

Watersheds are usually divided into smaller subbasins because of flow patterns, hydrologic conditions, and subbasin property characteristics. Several methods can be used to develop the areal rainfall distribution over the subbasins. One method is to transpose the PMP isohyetal pattern to the drainage area and determine the depth-duration curves for each area. Another procedure is to position the critical storm location by hydrologic methods and derive depth-duration curves for successively large areas. This is the bases of the USBR method and is described in the next section.

Temporal distributions are presented in several publications [Safety of Existing Dams (1983)][USBR (1989)] which can be used effectively for this geographical region. An indepth analysis can be performed using historical rainfall distributions and sensitivity analyses on the different storm patterns.

SPATIAL DISTRIBUTION USING THE USBR METHOD

For areas that are not effected by topography or nonorographic regions of the geographical area, the spatial distribution criteria described in HMR 52 can be used [HMR 52 (1982)]. For orographic areas a procedure called "successive substraction of subbasin PMP volumes" can be used to distribute the storm over the watershed [USBR (1989)].

The procedure is based on the averages of the storm precipitation calculated for the watershed and those required for subbasins and combined subbasins. The basic equation for the procedure is as follows:

$$P_T A_T = P_1 A_1 + P_2 A_2 + \ldots + P_n A_n$$

Where:
P = Average Precipitation
A = Subbasin Area

The above equation equates the storm volume $P_T A_T$ over an area A_T to the summation of the storm volumes over the subbasins A_1 through A_n. The critical hydrologic response for the watershed is computed for various subbasin centers of the storm.

If the storm is assumed to be centered over subbasin 1, the areal distributed precipitation would be computed for subbasins 2 and 3 by the following equations:

$$P_2 = \frac{P_{1,2}\,A_{1,2} - P_1\,A_1}{A_2}$$

Where :
$P_{1,2}$ = *The average precipitation for the combined area of subbasins* 1 *and* 2.
$A_{1,2}$ = *The combined area of subbasins* 1 *and* 2.

$$P_3 = \frac{P_{1,2,3}\,A_{1,2,3} - P_{1,2}\,A_{1,2}}{A_3}$$

Where :
$P_{1,2,3}$ = *The average precipitation for the combined area of subbasins* 1, 2 , *and* 3.
$A_{1,2,3}$ = *The combined area of subbasins* 1, 2, *and* 3.

The storm is then assumed to be centered over subbasin 2 and then subbasin 3. The hydrologic responses of the watershed for the different spatial distributions are then tested by hydrologic simulations, and the distribution generating the largest peak discharge is considered the critical storm distribution.

CASE STUDIES

Two case studies are presented to illustrate the USBR method. The first case study is a 15 square mile watershed located in Albuquerque, New Mexico. The second case study is a 1,000 square mile watershed located in northern Colorado.

Case Study One: The 6-hour local PMP storm was developed for the 15 square mile urbanized Bear Canyon watershed. The study area is affected by an upstream watershed of approximately 10.5 square miles that extends east from Tramway Boulevard to the crest of the Sandia Mountains at an elevation of 10,680 feet. The area from the base of the Sandia Mountains

to the peak consists of extremely steep slopes. The area from Tramway Boulevard east to the base of the Sandia Mountains has slopes increasing to ten percent. This area is primarily undeveloped, except for a low-density residential development. The area downstream to the North Diversion Channel consists of mild to medium slopes ranging from 1 to 5 percent.

There are two flood detention facilities on the arroyo: John Robert Dam and Arroyo del Oso Dam. The watershed was divided into two basins defined by the dams. The contributing watershed area into John Robert Reservoir is 10.5 square miles and the contributing watershed area into Arroyo del Oso is 13.7 square miles including the area above John Robert Reservoir.

Three cases were analyzed for the local PMP storm: the storm centered over John Robert watershed, the storm centered over Arroyo del Oso watershed , and the storm centered over the combined watershed (one watershed method). The adjusted 6-hour local PMP values for the different scenarios are presented in Table 1.

Table 1 - Adjusted 6-Hour Local PMP Values

Case	John Robert Watershed (in)	Arroyo del Oso Watershed (in)	Comment
1	15.75	12.21	John Robert Watershed
2	14.72	15.36	Arroyo del Oso Watershed
3	14.88	14.88	One Watershed Method

The hydrologic response of the watersheds were computed using HEC-1. The peak discharges into the reservoirs are presented in Table 2. The values are very close to each other. This is caused by the wide spreading of the isohyetal lines given in the HMR 55A. The watershed is located on the outer edges of the orographic area which is also reflected in the wide

spreading of the isohyetal lines. The areas are too small relative to the isohyetal pattern to effectively use the USBR method.

Table 2 - Reservoir Peak Inflow for the Local Storm PMF Analysis

Case	Peak Discharge John Robert Reservoir (cfs)	Peak Discharge Arroyo del Oso Reservoir (cfs)	Comment
1	47,078	50,291	John Robert Watershed
2	42,904	46,910	Arroyo del Oso Watershed
3	47,440	49,506	One Watershed Method

Case Study Two: The second case study is for the 1,000 square mile Cache la Poudre mountainous watershed west of Fort Collins, Colorado. The watershed is divided into three main basins: Upper North Fork, Lower North Fork, and Cache la Poudre. The analysis was performed for the 72-hour general PMP storm. There are two large reservoirs located within the watershed which divide it into the three main basins.

Halligan Reservoir is located on the Upper North Fork of the Cache la Poudre River. Seaman Reservoir is located 12 miles downstream of Halligan Reservoir on the North Fork of the Cache la Poudre. The drainage area at Seaman Dam is approximately 555 square miles including approximately 349 square miles lying above Halligan Dam. The remaining 445 square miles makeup the main stem of the Cache la Poudre. The North Fork of the Cache la Poudre flows into the main stem approximately 2 miles downstream of Seaman Dam.

Three critical storm locations were analyzed to compute the maximum peak discharge into Seaman Reservoir. The critical storm locations included a storm centered over Halligan Watershed, Seaman Watershed, and the two combined watershed. Table 3 lists the adjusted PMP values for the 72-hour general storm.

Table 3 - Adjusted 72-Hour General PMP Storm Values

Case	Halligan Watershed (in)	Seaman Watershed (in)	Comment
1	25.5	19.8	Halligan Basin
2	19.9	29.4	Seaman Basin
3	23.4	23.4	One Basin

The hydrologic response for the watersheds was computed using the SCS curve number method. The storm centered over the Halligan Basin produced the critical peak inflow into Seaman Reservoir. Table 4 lists the results of the hydrologic simulations.

Table 4 - Peak Discharges

Case	Halligan Reservoir	Seaman Reservoir	Comments
1	283,515	377,842	Halligan Basin
2	211,918	375,202	Seaman Basin
3	246,027	376,824	One Basin

There was a large difference between the inflows into Halligan Reservoir compared with the inflow into Seaman Reservoir. Halligan Watershed has the larger area between the two which contributed more flow to the system.

CONCLUSIONS

The USBR method to distribute a PMP storm event is an effective and simple procedure. Four major factors influence the use of the method which include basin area, isohytal pattern, the watersheds orientation to

the isohytals, and the relative location of the watershed within the orographic region.

REFERENCES

Hydrometeorological Report No. 52 (1982). National Weather Servive, Silver Spring, Md.

Hydrometeorological Report No. 55A (1988). National Weather Service, Silver Spring, Md.

Safety of Existing Dams - Evaluation and Improvements (1983). Committee on the Safety of Existing Dams, Washington, DC.

U.S. Bureau of Reclamation (USBR 1989). *Flood Hydrology Manual*,United States Printing Office, Denver, Colorado.

Flood Frequency Analysis with FOS Distributions

S. Rocky Durrans, AM ASCE[1]

Abstract

Distributions of fractional order statistics (FOS distributions), which may be viewed as pre-asymptotic extreme value distributions, have been recently suggested (Durrans, 1992) as plausible models for frequency analyses of hydrologic data. In this paper, we examine these distributions more closely and consider several reasons why they should be of interest to hydrologists.

Introduction

Analyses of the magnitudes and corresponding frequencies of floods provide basic information for design and evaluation of most types of hydraulic structures. Methods for performance of these analyses have been the subject of a considerable amount of research but, in spite of the existence of some institutionalized approaches such as those recommended by the U.S. Water Resources Council (WRC, 1981) and the U.K. Natural Environment Research Council (NERC, 1975), there has yet to be a consensus reached with respect to an appropriate technique.

Recently, a committee under the Water Science and Technology Board of the National Research Council was established to study the problem of extreme flood estimation and to make recommendations related to needed research. As noted in the report of that committee (NRC, 1988), there exist three generally recognized approaches to

[1]Assistant Professor of Civil Engineering, The University of Alabama, Tuscaloosa, Alabama 35487-0205.

estimation of extreme flood magnitudes. The first of these consists of estimation of a "probable maximum flood" and is a methodology that has been applied worldwide. Despite its name, however, it does not provide estimates of the probabilities that are needed in risk assessment studies. The second approach to flood estimation is to perform statistical analyses of observed streamflow records. This is the classical approach and dates to the early 20th century. The third approach consists of statistical analysis of meteorological data with employment of some type of model to make the physical transformation to runoff. There is a fairly recent belief that the greatest potential of this latter technique has to do with regionalization, the thought being that differences in flood frequency distributions from one site to another are due primarily to physical differences in the catchments rather than in the meteorology. The NRC committee did not identify a single preferred algorithm for computing the probabilities of floods of interest. Instead, it recommended that estimates be made using both flood-based statistical techniques and runoff modeling methods, the rationale being that increased insight relevant to decision making will be gained from both types of information.

In this paper is considered the problem of flood estimation using the first of the two methods endorsed by the NRC, namely that of statistical frequency analysis. Within this category of methods, one may differentiate between parametric and nonparametric techniques, and within each of those subcategories, one may also identify any number of specific algorithms and/or schools of thought. For example, in the category of parametric techniques for statistical analysis of floods, one may identify two schools of thought. The first, as reflected in the WRC (1981) recommendations, advocates use of a distribution within the exponential class (the log Pearson type 3). The second school, which is exemplified by the recommendations of the NERC (1975), prefers use of distributions lying within the extremal class. Both classes of distributions have been found to be suitable in certain cases, but not in all. That is, there is no single method that can be universally applied.

In some cases, theoretical support exists for selection a particular distributional form. The central limit theorem for instance, depending on how it is interpreted, suggests that either the normal or lognormal is an appropriate choice (Chow, 1954). Similarly, since interest is often focused on extremes, the (asymptotic) results of extreme value theory point to and support utilization of extreme value distributions. The theoretical underpinnings provided by the central limit theorem and extreme value

theory are, at least superficially, convincing arguments for support of a particular type of distribution, especially if that distribution is also known to be robust. When these arguments are scrutinized more closely, however, certain shortcomings come to light. The central limit theorem implies that the distribution will be Gaussian or lognormal when the number of contributing effects is large. Extreme value distributions, in a similar manner, are based on asymptotics. It is often the case, however, that convergence to asymptotic forms may be quite slow. Fisher and Tippett (1928) stressed the extremely slow convergence to the EV-1 of the distribution of the extreme order statistic in samples drawn from Gaussian populations, and J.R. Stedinger (personal communication, 1992) has found that convergence is even slower when the population is lognormal (and hence more flood-like than the Gaussian distribution). In cases where convergence is slow, the adequacy of asymptotic approximations is open to question (NRC, 1988).

Even in situations where asymptotics may be invoked, the question of whether to employ extreme value theory or the implications of the central limit theorem still arises. Adoption of either theory effectively forsakes the other. This is true because the central limit theorem points to distributions in the exponential class whereas extreme value theory indexes members of the extremal class. This schism is presently irreconcilable because the two classes are mutually exclusive of one another. That is, member distributions of one class are not embedded as special cases of members of the other class.

In light of these observations, the writer has initiated a research effort to study the efficacies of distributions of fractional order statistics (FOS), which may be interpreted as pre-asymptotic extreme value distributions, for flood frequency analysis. These distributions not only retain (and actually improve on) the theoretical basis that makes extreme value theory so attractive, they also embed as special cases members of the exponential class of distributions. In effect, FOS distributions are capable of bridging the gap between the exponential and extremal schools of thought; it is quite conceivable that they may in fact obviate the need to make a choice between those schools.

It should be remarked that the generality of FOS distributions referred to in the previous paragraph is really of only secondary importance, and should serve only to amplify one's interest in them. Of primary importance is the fact that they have the same theoretical basis as does extreme value theory, and that they are capable of

modeling that portion of the skewness-kurtosis space in which flood populations are thought to reside. They also, unlike alternative models, contain a parameter that can be interpreted in terms of an observable physical phenomenon. Because of this, they occupy a unique niche among competing alternatives.

Distributions of Fractional Order Statistics

The theory of order statistics provides for evaluation of the exact distribution function of the k-th smallest element, i.e., the k-th order statistic, in a random sample of size n drawn from a known initial distribution (David, 1981). In particular, the distribution function $G(x)$ of the n-th, or largest, order statistic is

$$G(x) = F^n(x) \tag{1}$$

The term $F(x)$ in this expression denotes the initial distribution function and n is the sample size. $G(x)$, for finite n, is a pre-asymptotic extreme value distribution.

For the forms of the initial distribution that are of the greatest practical interest to hydrologists (but not for all forms), the asymptotic extreme value distributions arise as the sample size n in (1) grows without bound. The particular form of the asymptotic distribution that arises, be it EV-1, EV-2, or EV-3, depends on the behavior of the tail of the initial distribution. If the tail is of an exponential type then an EV-1 arises, if it is of a Cauchy type then one obtains the EV-2, and if is is bounded then an EV-3 is yielded.

As described by Durrans (1992), the development of the class of FOS distributions is based on the same fundamental idea that underlies extreme value theory. The primary difference is that the exponent n in (1) is interpreted not as an integer-valued sample size, but rather as a real-valued parameter that must be estimated from an observed data sequence (this is the reason for the name "fractional order statistics"). Letting γ ($\gamma > 0$) represent the real-valued and unknown counterpart of n, individual members in the class of FOS distributions may be defined as

$$\Lambda(x) = F^{\gamma}(x) \tag{2}$$

The notation $\Lambda(x)$ has been introduced here to avoid confusion with $G(x)$. The density function corresponding to (2)

is found by differentiation and is

$$\lambda(x) = \frac{d\Lambda(x)}{dx} = \gamma F^{\gamma-1}(x) f(x) \qquad (3)$$

where $f(x) = dF(x)/dx$ is the density function of the initial distribution. Different members of the class of FOS distributions are obtained by making different selections of the initial distribution F. For example, one might take F as the normal distribution, as the lognormal, or as the gamma or any other distribution.

It may be recognized that the definitions of FOS distributions as given by (2) and (3) are rather general and are valid as long as the initial distribution is a valid probability distribution. The initial distribution may be discrete, continuous, or otherwise. Another point that may be noted is that the development of (2) and (3) began with the distribution of the largest order statistic. Alternative definitions of FOS distributions could be based on the smallest order statistic, or on any other order statistic. FOS distributions based on the smallest order statistic, for example, would be of interest for low-flow studies.

FOS Distributions in Hydrology

There are several reasons why FOS distributions should be of interest to hydrologists. These have already been alluded to in the introduction, and are discussed in more detail in the following paragraphs.

The first, but probably not the most important, reason for interest in FOS distributions is their generality. As noted earlier, this reason is really of only of secondary importance, but is worthy of mention. Similar reasoning has been cited often in order to justify use of the GEV distribution (Jenkinson, 1955). Singh (1988) has noted that Klemes (1972), in contrasting the physical and systems approaches to the study of hydrology, has made the remark that the two schools of thought often seem to be like hostile camps. A similar analogy may be made in the context of flood frequency analysis between those who hold to the class of exponential distributions and to those who espouse the extremal class. If a distribution, or class of distributions, could be found that would unify these schools by embedding as special cases members of their respective classes, it could be applied with the confidence that it would "default" to the appropriate class depending on the statistical properties of a modeled data sequence. In effect, and much like the Wakeby, the distribution could

be viewed as a "grand-parent" (Houghton, 1978).

It may be contended that the class of FOS distributions may be viewed as representing such a class of grand-parents. By starting with a known initial distribution $F(x)$, and by letting the parameter γ in (2) take on finite and positive but increasingly large values, one obtains a complete family of distributions extending from the initial distribution to the attracting asymptotic extreme value distribution (assuming that it exists). Consider, for example, the Pearson type 3 as a choice for $F(x)$. This distribution embeds as special cases (and hence so does $\Lambda(x)$) the complete gamma family, including the exponential distribution, as well as the normal distribution (as a limiting case). Since the Pearson type 3 falls within the domain of attraction of the EV-1, the FOS distribution would also include not only that limiting distribution, but also the entire spectrum of pre-asymptotic distributions leading up to it. In effect, a simple generalization of the Pearson type 3 permits it to represent many of the distributions that have been commonly applied in hydrology.

A second, and much more important, reason why FOS distributions should be of interest is that they are capable of modeling that portion of the skewness-kurtosis space in which flood (and rainfall) populations are thought to reside. This in turn implies that they may be capable of explaining the separation phenomenon (Matalas et al., 1975; Houghton, 1978; Beran et al., 1986). In the case of precipitation data, Wallis (1982) and Schaefer (1990) have found that skewness-kurtosis plots developed from observed data lie close to the EV-2 limb of the theoretical curve for the GEV distribution. There appears to be a belief that flood populations lie in this region as well. Related to this, Lettenmaier et al. (1987) provide a degree of incentive for use of pre-asymptotic distributions with their statement that

> Distributions with heavier tails than the GEV family will all lie above the GEV [skewness-kurtosis] curve, as will the pre-asymptotic distribution of the largest from a finite number of random variates, each drawn from a heavy-tailed or mixed distribution. The pre-asymptotic distribution of the largest of a finite number of random variates drawn from light-tailed distributions, on the other hand, lie below the GEV curve.

It is evident therefore that FOS distributions (which are pre-asymptotic extreme value distributions) are capable of modeling that portion of the skewness-kurtosis space that is of interest.

A third reason why FOS distributions should be of interest to hydrologists may be outlined as follows. It is generally accepted that flood events arise in response to differing causative effects. To acknowledge and account for this, flood frequency analysts have typically resorted to use of mixture distributions. In fact, this is a fundamental basis for the introduction of the two-component extreme value (TCEV) distribution (Rossi et al., 1984; Beran et al., 1986). While FOS distributions are not themselves mixture distributions, it is believed that they do have some relevance in this context. By definition, flood frequency analysis concerns itself with extreme events, usually the single largest flood magnitude within each calendar or water year. It is easy to argue that the distribution of these large runoff rates is probably very much different than that of the more common events that occur during the course of the year.

In the context of flood frequency analysis in general, and extreme value theory in particular, this observation that large runoff events are distributed differently than are more common events, along with the realization that there are typically only a few severe storms per year which would give rise to realizations from the large flood event distribution, may be employed to subject the use of asymptotic extreme value distributions to some well-founded criticism. Indeed, whatever physical basis may be possessed by extreme value distributions is arguably forsaken if one chooses to employ the asymptotic form for flood analysis (there simply are not enough events per year for the asymptotic form to take hold). Only when the pre-asymptotic form is employed should an extreme value distribution used for flood analysis be considered to have any physical meaning. This very point, while not stated explicitly, is alluded to by Wallis and Wood (1985) and by Lettenmaier et al. (1987).

This discussion implies that the parameter n in (1), or the parameter γ in (2) and (3), can be interpreted as the number of "large" storm events per year. This quantity, while governed to a somewhat by the infiltration characteristics of the soils in a catchment, is largely governed by meteorological factors. Also, since this number of large storms will vary from year to year (it is a random variable), it would seem reasonable to employ its expected value. Since this quantity in turn is real, as opposed to integer-valued, this provides a rationale for use of a real-valued parameter γ rather than the integer-valued parameter n. In summary, the fractional order parameter γ can be interpreted in a physical sense as the average number of "large" storms per year. Since this quantity is probably relatively stable over at least a

limited geographical region, it would appear as though an opportunity exists to try to regionalize on this parameter.

Conclusion

There has for many years been a desire on the part of hydrologists to reconcile the differences between deterministic and probabilistic, or stochastic, modeling efforts (see, e.g., Salas et al. (1980) and Binley et al. (1991)). This desire is also reflected in the recent NRC (1988) study dealing with estimation of flood probabilities. It is arguable that FOS distributions, because of the physical interpretability of one of their parameters, represent a positive step in the direction of this goal. What is needed at this point is to make an assessment of their performance measures relative to what can now be obtained by use of other contemporary methods. In summary, it is believed that the most significant contribution of this work will lie in the effort to provide some physical basis for flood frequency analysis without resorting to derived distributions procedures of the types discussed by Eagleson (1972) and Moughamian et al. (1987).

Cited References

Beran, M., J.R.M. Hosking, and N. Arnell. (1986) Comment on Two-Component Extreme Value Distribution for Flood Frequency Analysis by F. Rossi, M. Fiorentino, and P. Versace." Water Resources Research, 22(2), 263-266.

Binley, A.M., K.J. Beven, A. Calver, and L.G. Watts. (1991) Changing Responses in Hydrology: Assessing the Uncertainty in Physically Based Model Predictions. Water Resources Research, 27(6), 1253-1261.

Chow, V.T. (1954) The Log Probability Law and Its Engineering Applications. Proceedings, American Society of Civil Engineers, 80, 536-1 to 536-25.

Durrans, S.R. (1992) Distributions of Fractional Order Statistics in Hydrology. Water Resources Research, 28(6), 1649-1655.

Eagleson, P.S. (1972) Dynamics of Flood Frequency. Water Resources Research, 8(4), 878-898.

Fisher, R.A., and L.H.C. Tippett. (1928) Limiting Forms of the Frequency Distribution of the Largest or Smallest Member of a Sample. Proceedings, Cambridge Philosophical Society, 24(2), 180-190.

Houghton, J.C. (1978) Birth of a Parent: The Wakeby Distribution for Modeling Flood Flows. Water Resources Research, 14(6), 1105-1110.

Jenkinson, A.F. (1955) The Frequency Distribution of the Annual Maximum (or Minimum) Values of Meteorological Elements. Quarterly Journal of the Royal Meteorological Society, 81, 158-171.

Klemes, V. (1972) Comment on "Mathematical Models of Hydrologic Systems by J.C.I. Dooge." Proceedings of the International Symposium on Modeling Techniques in Water Resources Systems, May 9-12, Ottawa, Canada, Vol. 3, 701-705.

Lettenmaier, D.P., J.R. Wallis, and E.F. Wood. (1987) Effect of Regional Heterogeneity on Flood Frequency Estimation. Water Resources Research, 23(2), 313-323.

Matalas, N.C., J.R. Slack, and J.R. Wallis. (1975) Regional Skew in Search of a Parent. Water Resources Research, 11(6), 815-826.

Moughamian, M.S., D.B. McLaughlin, and R.L. Bras. (1987) Estimation of Flood Frequency: An Evaluation of Two Derived Distribution Procedures. Water Resources Research, 23(7), 1309-1319.

NERC. (1975) Flood Studies Report. Natural Environment Research Council, London.

NRC. (1988) Estimating Probabilities of Extreme Floods: Methods and Recommended Research. National Research Council. National Academy Press, Washington, D.C.

Rossi, F., M. Fiorentino, and P. Versace. (1984) Two-Component Extreme Value Distribution for Flood Frequency Analysis. Water Resources Research, 20(7), 847-856.

Salas, J.D., J.W. Delleur, V. Yevjevich, and W.L. Lane. (1980) Applied Modeling of Hydrologic Time Series. Water Resources Publications, Littleton, Colorado.

Schaefer, M.G. (1990) Regional Analyses of Precipitation Annual Maxima in Washington State. Water Resources Research, 26(1), 119-131.

Singh, V.P. (1988) Hydrologic Systems: Rainfall-Runoff Modeling, Vol. 1. Prentice Hall, Englewood Cliffs, NJ.

Wallis, J.R. (1982) Probable and Improbable Rainfall in California. IBM Research Report RC 9350, Yorktown Heights, New York.

Wallis, J.R., and E.F. Wood. (1985) Relative Accuracy of Log Pearson III Procedures. ASCE Journal of Hydraulic Engineering, 111(7), 1043-1056.

WRC. (1981) Guidelines for Determining Flood Flow Frequency. Bulletin 17B, U.S. Water Resources Council, Washington, D.C.

RUNOFF MODELING ON A BASEFLOW-DOMINATED WATERSHED

Ellen B. Faulkner[1], Gary M. Schimek[2] and David S. McGraw[3]

Abstract

Numerous hydrologic studies have been conducted to estimate the Probable Maximum Flood (PMF) at five hydroelectric projects on the Au Sable River in northern Michigan. Although it has been gaged for over 40 years, this 4,216-km^2 (1,628-mi^2) basin has never experienced a flood greater than approximately 140 m^3/s (5,000 ft^3/s). Factors apparently contributing to the lack of historic flooding are the almost complete forest cover, the deep sandy glacial soils, and the poorly developed drainage network. In this study, a small gaged subbasin of the Au Sable River was selected for an intensive modeling effort using the Agricultural Research Service's KINEMAT watershed model. The KINEMAT model was selected for its spatially distributed structure, which retains areal diversity in soil types and other hydrologic features. The model was calibrated and used to predict the subbasin PMF. These results, in turn, were used to infer an equivalent spatially averaged infiltration loss rate for the Probable Maximum Storm and then to estimate the PMF at the five project sites.

Introduction

Six Consumers Power Company hydroelectric projects are located on the main stem of the Au Sable River in northern Michigan. Each project, under Federal Energy Regulatory Commission (FERC) regulations, requires adequate spillway

[1]Project Engineer, Water Resources Department, Mead & Hunt, Inc., 6501 Watts Road, Madison, Wisconsin 53719-1361

[2]Hydrologist, Northwest Hydraulic Consultants, 22017 70th Avenue South, Kent, Washington 98032

[3]Engineer, Water Resources Department, Mead & Hunt, Inc., 6501 Watts Road, Madison, Wisconsin 53719-1361

capacity to safely pass the Probable Maximum Flood (PMF) at the project site. As of early 1989, five of the six projects were considered to have inadequate spillway capacity by this criterion. The spillway capacities at the five projects range from approximately three to ten times the flood of record. Since 1989, several hydrologic analyses have been performed to improve the estimate of the PMF, which appeared questionably high in light of the flooding history of the river. The study described here was undertaken to determine a PMF consistent with the known hydrologic characteristics and history of the Au Sable River.

The Au Sable River Watershed

The Au Sable River drains a 4,216-km^2 (1,628-mi^2) watershed in the northwest of Michigan's Lower Peninsula. The river flows from west to east, discharging to Lake Huron at the city of Oscoda. The drainage area is sparsely populated and almost entirely forested, with moderate relief and poorly developed drainage patterns. The predominant soils are sands as much as several hundred feet deep.

The river is gaged at Mio, Michigan, at a drainage area of 3,300 km^2 (1,273 mi^2). At this gaging station, the maximum flow for the 41-year period of record is 124 m^3/s (4,380 ft^3/s). A 50-year gage record also exists for the Au Sable River at Grayling, at a drainage area of 285 km^2 (110 mi^2); the flood of record at this station is 8 m^3/s (274 ft^3/s). Shorter gage records for other tributaries to the Au Sable are characterized by a similar absence of significant flood events.

Previous Runoff Modeling Approaches

Since 1983, several modeling studies have been conducted to evaluate the PMF at the Au Sable River hydroelectric projects. All used the HEC-1 watershed model (U.S. Army Corps of Engineers, 1987). The model was developed for the Five Channels project, third downstream of the five projects, with the understanding that due to the small storage and negligible intervening drainage area, the PMF estimate at Five Channels would be applicable to the other projects as well. In the initial study, unit hydrographs were calibrated at the Mio gage and transferred to the intervening basin area. The lack of historic floods in the gage record hindered unit hydrograph calibration and precluded any realistic verification or calibration of loss rates. Later studies retained the initial study's unit hydrograph structure but took a variety of approaches to estimating runoff losses. These approaches fall into two general categories: those using the Soil Conservation Service (SCS) Runoff Curve Number and those using known infiltration rates of the watershed soil groups.

The 1983 model study predicted a PMF of approximately 1,530 m^3/s (54,000 ft^3/s) at Five Channels Dam. This version of the model used an SCS Runoff Curve Number estimated manually from generalized state soil and land use maps. Subsequent studies included varying the assumed antecedent moisture condition as provided in SCS literature and obtaining a precise estimate of the Curve Number through satellite image processing (Mettel, 1991). These efforts produced PMF estimates ranging from 547 m^3/s (19,000 ft^3/s) to the original estimate of 1,530 m^3/s (54,000 ft^3/s) and emphasized the extreme sensitivity of the model to reasonable variations in runoff parameters.

Because of this sensitivity in the SCS methods, much of which was due to the distinction between three possible antecedent moisture classes, another analysis was performed using documented saturated infiltration rates of the basin soils. This analysis, like the others, was conducted with the existing HEC-1 basin model but substituted the Green-Ampt moisture accounting procedure for the SCS methods used previously. The Green-Ampt loss rate calculation reduces to a constant loss rate when the soil is saturated and infiltrates water at a steady rate (U.S. Army Corps of Engineers, 1987). Saturated infiltration rates of the basin soils and the percent of the basin covered by each soil were determined from the database developed in the satellite image soil study. Area-weighted basin average Green-Ampt parameters were then calculated. When the Probable Maximum Precipitation (PMP) was applied to the new watershed model, the resulting PMF estimate was only 170 m^3/s (6,000 ft^3/s), hardly larger than the flood of record. Closer inspection of the model calculations revealed that the entire runoff hydrograph was caused by precipitation falling on lakes, roads, and other impervious surfaces.

A review of the model input data further clarified the source of these unsatisfactory results. While approximately ten percent of the basin soils had infiltration rates low enough to generate runoff from the PMP, the remaining 90 percent were capable of infiltrating water at rates far greater than the PMP intensity. The process of averaging the rates over all the basin soils produced an average rate that, while lower than the highest infiltration rates represented in the basin, was still high enough to allow all of the PMP to infiltrate. The soils that would be expected to generate some runoff during intense storms were obliterated, in the model, by the averaging procedure.

Defining the Problem

Although the Green-Ampt modeling effort produced obviously flawed results, these results shed a great deal of light on future modeling needs. The failure of the Green-Ampt modeling approach was not in the infiltration theory, but in the use of spatially *averaged* parameters to describe a spatially *distributed*

process. While not unique to the Au Sable River basin, this problem was especially pronounced because of the extreme contrast between the runoff-producing soils—apparently few in number but hydrologically critical—and the more common, highly permeable upland soils.

In order to represent the runoff processes in the Au Sable River basin with any realism, a model would need to accomplish several goals. First, it must preserve the spatial diversity of the watershed soils, permitting hydrologically sensitive areas to generate runoff while allowing the great majority of the basin soils to infiltrate rainfall at characteristically high rates. Second, while thus reflecting local detail, it must be useful for predicting the design flood at a large river basin scale. Finally, especially since it would be a significant departure from previous methods, it should be verifiable against historic hydrologic records.

Meeting the first goal required selecting a model that would permit spatial detail within the constraints of actual data availability. The second and third goals were met by selecting a small representative sub-watershed and developing a calibrated detailed model for it, and extending the calibration results to the entire Au Sable basin within the HEC-1 model structure.

KINEMAT Model

The Agricultural Research Service's KINEMAT watershed model was selected for its "partially distributed" model structure, which enables the user to describe a watershed as a group of linked planes and channels (U.S. Department of Agriculture, 1990). Each plane is defined on the basis of land cover, soils, and slope and by its position in the flow network. A plane receives overland flow from one or more upslope planes and discharges to a downslope plane or a channel. For a plane to contribute water to the basin outflow hydrograph, it must have runoff-producing soils and be hydraulically connected to the channel, without intervening high-permeability areas. Overland and channel flows are then routed by the kinematic wave method to the basin outlet. This structure is not as rigidly data-intensive as a "fully distributed" (i.e., grid cell) model, allowing the hydrologist to define the level of spatial detail appropriate to the available data and study needs.

KINEMAT Model Calibration and Equivalent Averaged Loss Rate

The East Branch of the Au Sable River, gaged at a drainage area of 189 km^2 (73 mi^2), was chosen as a representative subbasin for KINEMAT modeling (Figure 1). The distribution of soil types and land cover for the East Branch subbasin was found to be similar to the distribution for the Au Sable River basin as a whole. It was also found to be the best available subbasin for detailed

Au Sable River Basin Showing Location of East Branch Subbasin

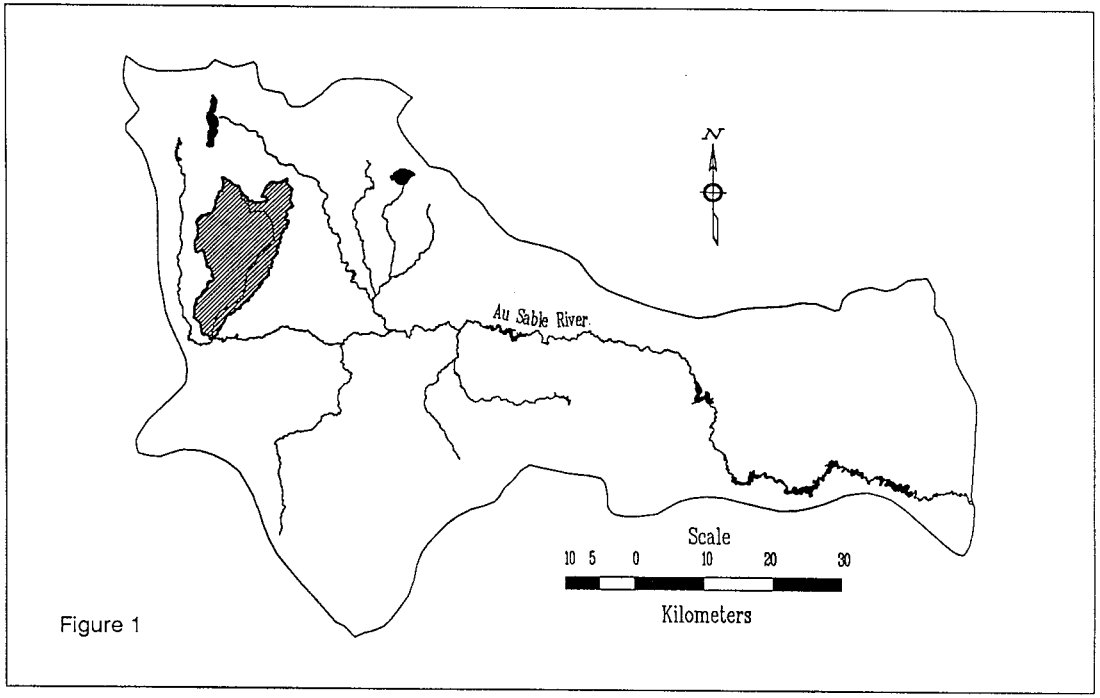

Figure 1

study because of the proximity of rain gages and the availability of hourly flow data. The East Branch basin (unlike some other candidates) was further distinguished by having at least one recorded flood hydrograph that could be confidently attributed to direct runoff from a severe rainstorm. Finally, the relatively small size of the East Branch subbasin made it the best gaged candidate for the KINEMAT model, which is designed for small rural drainages.

The model structure was developed based on soil, land cover, and topographic maps. Subdivision based on these characteristics resulted in a 89-element representation of the watershed (Figure 2). As a starting point, each plane element was assigned soil infiltration parameters as suggested by the Michigan state soil database and the Agricultural Research Service (U.S. Department of Agriculture, 1990).

The flood of record for the East Branch watershed is 6 m^3/s (207 ft^3/s), but due to an extremely high baseflow component, this event did not lend itself to runoff model calibration. The best available flood event for calibration occurred in July 1984 and peaked at 4.5 m^3/s (158 ft^3/s). The flood peak resulted from an 11-hour, 8-cm (3-inch) rainfall.

Calibration was achieved by testing systematic variations in the infiltration parameters of soil types. The calibration proved to be insensitive to the assumed parameters in the sandy upland soils, as they produced little or no runoff throughout the reasonable parameter range. However, some soil groups found in the uplands were also represented in valley bottoms adjacent to streams, in areas designated as wetlands on topographic maps. By virtue of their topographic position (and possibly local impermeable layers) these areas can be assumed to have much lower infiltration potential than the upland soils. The runoff hydrograph calibration—in terms of both timing and volume of runoff—responded well to changes in the infiltration parameters for these soils. This adjustment is consistent with current theories of runoff generation, which maintain that the runoff-contributing area of a basin is generally far less than the entire area and occurs where the land surface approaches the seasonal or short-term saturated zone (Beven, 1991). The calibration hydrographs (with baseflow removed) are shown in Figure 3.

The calibrated KINEMAT model was then used to predict the East Branch runoff hydrograph resulting from the PMP. This hydrograph peaked at 24 m^3/s (860 ft^3/s), excluding baseflow contributions. This was the first step in determining an equivalent basin-averaged loss rate that could be transferred to the whole-basin HEC-1 model.

The averaged PMP loss rate could not be inferred directly from the 1984 flood, because the true area-averaged loss rate is a function of the storm's intensity. Suppose, for example, that the great majority of basin soils have infiltration capacities of 12 cm/hr and a few have zero infiltration rates. Then a 1-cm/hr

East Branch Au Sable River
KINEMAT Model Elements

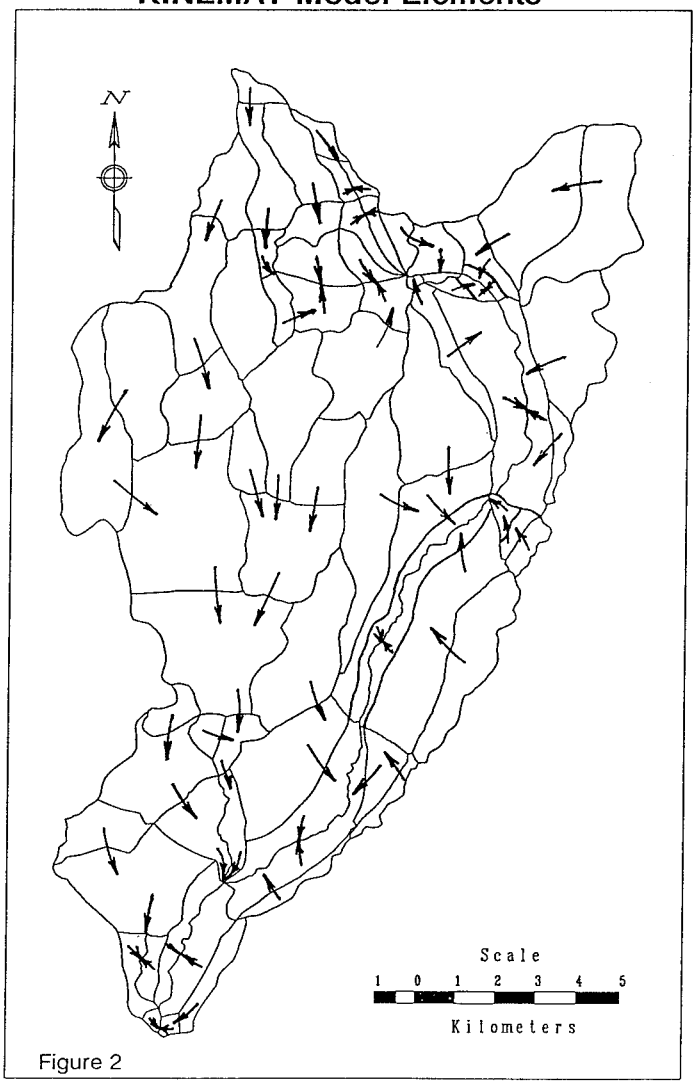

Figure 2

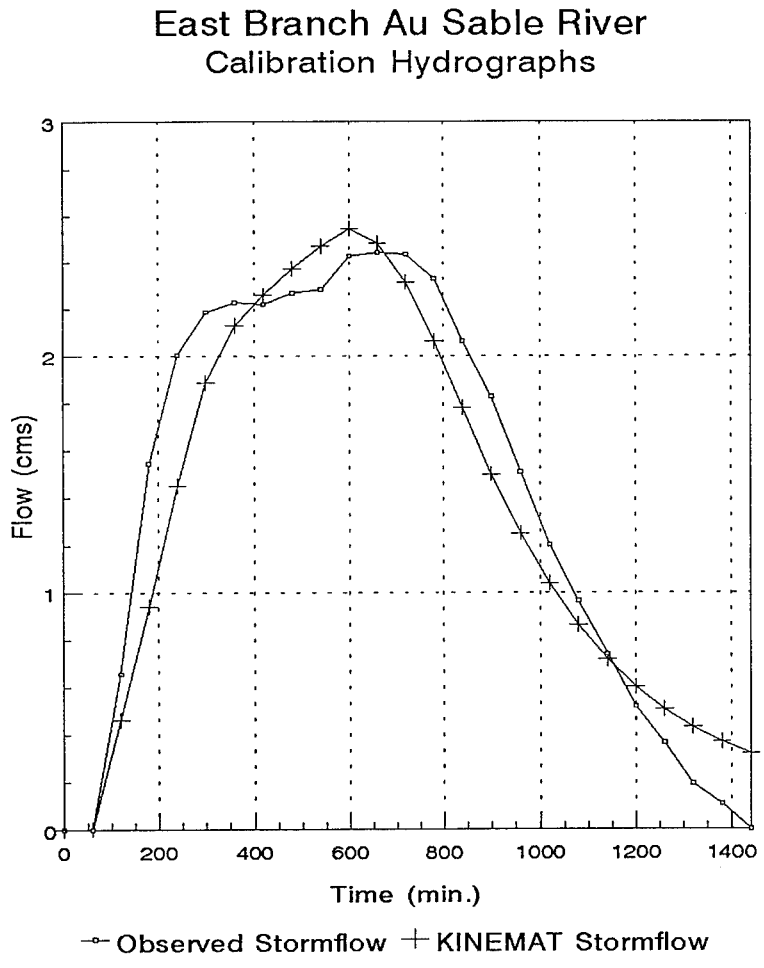
East Branch Au Sable River
Calibration Hydrographs
Flow (cms)
0
1
2
3
0
200
400
600
800
1000
1200
1400
Time (min.)
Observed Stormflow
KINEMAT Stormflow

Figure 3

storm, a 2-cm/hr storm, and a 10-cm/hr storm will all produce some runoff from the impermeable soils. However, back-calculation of the area-averaged loss rate will yield a loss rate of less than 1 cm/hr for the smallest storm, almost 2 cm/hr for the 2-cm/hr storm, and almost 10 cm/hr for the largest storm. Similarly, the equivalent area-averaged loss rate for the 1984 flood on the East Branch subbasin is not the same as the area-averaged loss rate for the PMP.

The KINEMAT PMF hydrograph was then entered into a HEC-1 model of the East Branch subbasin to calibrate an equivalent area-average constant loss rate. The equivalent PMP loss rate was found to be 5.6 cm/hr (2.2 in/hr), which is considerably less than the area-averaged rate of approximately 13 cm/hr (5 in/hr) determined for the Green-Ampt modeling study.

Probable Maximum Flood Determination at Five Channels Dam

The calibrated constant loss rate of 5.6 cm/hr was transferred to the whole-basin HEC-1 model with the PMP as rainfall input. The resulting runoff hydrograph was then superimposed on an assumed baseflow flood (with "baseflow" used loosely to describe all flow except direct overland runoff, including quick-return shallow subsurface flows). As modeling shallow and deep subsurface flows was not practicable for this study, the baseflow flood was taken from an outer envelope of historical baseflow-dominated floods.

In addition to using modified loss parameters derived from the KINEMAT modeling study, this analysis departed from earlier studies in using new PMP values. The depth-area-duration relationship for the PMP in Michigan and Wisconsin was modified in a 1992 study supported by the FERC and the Electric Power Research Institute (North American Weather Consultants, 1992). The new study presented an Au Sable River PMP depth approximately 15 percent less than that used in previous studies.

The resulting estimate of the PMF at the Five Channels project was approximately 283 m^3/s (10,000 ft^3/s). It should be noted that this estimate applies to warm-season conditions, the possibility of frozen soils being considered in a separate analysis. A flood of 283 m^3/s is more than twice the flood of record. The statistical estimate of the 100-year flood at the Five Channels project is approximately 133 m^3/s. Of all previous studies, the closest reasonable estimate was provided by the SCS curve number method using the satellite soil study and a low antecedent moisture condition (Mettel, 1991). That study's estimate of 547 m^3/s (19,000 ft^3/s) is comparable to the present study results, considering that the 1992 reduced PMP values were not then available.

Conclusions

The KINEMAT/HEC-1 model study included the most detailed effort to date to model hydrologic processes on the Au Sable River. Previous studies had demonstrated the necessity of investigating these processes at a detailed, spatially distributed level; but the size of the Au Sable River basin precluded complete detailed analyses of the entire area. By using the East Branch subbasin to represent the runoff processes of the entire basin, the detailed modeling component of the study was kept to a manageable level. Modeling results throughout the study, including the model calibration and the PMF determination, were consistent with the basin's hydrologic history and lessons learned from previous studies.

References

Beven, Keith, 1991. "Spatially Distributed Modeling: Conceptual Approach to Runoff Prediction." In *Recent Advances in the Modeling of Hydrologic Systems,* David S. Bowles and P. Enda O'Connell, Eds. Kluwer Academic Publishers, Dordrecht, Netherlands.

Mettel, M. Carson, 1991. "Satellite Imagery Refines PMF Determination." In *Waterpower '91: Proceedings of the International Conference on Hydropower,* David D. Darling, Ed. ASCE.

North American Weather Consultants, 1992. *Probable Maximum Precipitation Study for Michigan and Wisconsin.* Electric Power Research Institute Research Project No. 2917-29.

U. S. Army Corps of Engineers Hydrologic Engineering Center, 1987. *HEC-1, Flood Hydrograph Package, Users Manual.*

U. S. Department of Agriculture, Agricultural Research Service, 1990. *KINEROS, a Kinematic Runoff and Erosion Model, Documentation and User Manual.* ARS-77.

Use of NETWORK Flood Routing Model To Reduce PMF's at LCRA Dams

by John Lee Rutledge, P.E.[1]
Richard K. Frithiof, P.E.[2]
Kathryn M.Ozment, P.E.[3]

Abstract

A standard procedure for developing Probable Maximum Flood (PMF) hydrographs, using the Corps of Engineers' HEC-1 Flood Routing Model, consists of the calibration of empirical routing methods using historical flood data. These routing parameters are then assumed to be constant over all levels of flow up to and including the PMF. In the majority of cases this involves a significant extrapolation of calibrated parameters. The present results of research indicate that extrapolating empirical stream flow routing parameters from historical level floods up to PMF levels may be overly conservative. In a descriptive sense, this is due to the assumption that floodwave routing parameters which are calibrated from flows that consist of 70 to 90 percent in bank flow, also apply to flows that are 70 to 90 percent out of bank flow. The propagation of such floodwaves are different and the extrapolation of empirical routing parameters does not take these differences into account.

Dynamic wave flood routing models, such as NETWORK, developed by the National Weather Service, can more accurately estimate the impacts

[1]Associate, Freese and Nichols, Inc. 4055 International Plaza, Suite 200, Fort Worth, Texas 76109-4895
[2]Senior Engineer, Lower Colorado River Authority, P.O. Box 220, Austin, Texas 78767; (512) 473-4057.
[3]Engineer III, Lower Colorado River Authority, P.O. Box 220, Austin, Texas 78767; (512) 469-6861.

of the different flow engines. This will tend to give a more dependable estimate of design level storms and has also shown tendency to reduce the magnitude of the results. Both models have been used in the calibration and development of the PMF for a proposed reservoir, and for the update of PMF for eight existing reservoirs. Both models were calibrated from historical storms and the information used to develop the PMF hydrograph. Use of the dynamic wave model tends to reduce the peak flows from the HEC-1 results and therefore could provide a reduction in the estimated cost of the construction or rehabilitation project being considered.

The paper presents an overview of the two flood routing techniques as well as the results of the case studies involved. Comparison of the results of flood determination on six dams operated by the Lower Colorado River Authority will be presented in greater detail because of the extensive calibration and comparison of the floods at these dams. Preliminary estimates of total savings in the projects, as a result of using NETWORK, are about $30 million.

Introduction

The Lower Colorado River Authority (LCRA), based in Austin, Texas, operates a system of six dams and reservoirs in series on the Colorado River in central Texas for the uses of hydropower, water supply, and flood control. These dams are from upstream to downstream, Buchanan Dam, Inks Dam, Wirtz Dam, Starcke Dam, Mansfield Dam, and Tom Miller Dam. The existing dams were built between 1938 and 1951. Tom Miller Dam is actually a reconstruction of the older Austin Dam. Austin Dam was originally built in 1893 by the City of Austin. The dam had experienced two failures before the LCRA took responsibility, by agreement with the City of Austin, for reconstruction and operation of the dam in 1939. All six dams are considered high hazard dams by the Texas Water Commission, the state dam safety regulating agency. By current TWC regulations the dams need to pass 100% of the Probable Maximum Flood (PMF) without overtopping.

In 1991, the LCRA completed a comprehensive hydrologic and a preliminary structural review of their dams to determine their status of compliance with TWC regulations. Utilizing computer models HMR52[1] for the rainfall distribution and HEC-1[2] for the flood routing, estimates of the PMF for each dam were developed. Based on these results, a preliminary structural evaluation of the dams was performed. All of the dams, with the exception of Mansfield which is the only flood control dam in the series, were found to

be hydraulically inadequate. The structural review indicated that four of the dams were structurally inadequate in that they could not pass the PMF without structural instability. Of these however, Starcke Dam was found to be structurally adequate as it was still stable even with significant overtopping.

Initial Findings

The most upstream of the six structures is Buchanan Dam, which forms Lake Buchanan. The combination multiple arch and gravity dam has a maximum height of 145 feet and is used for hydropower and water supply, but does not have significant flood control storage. The dam has a total drainage area of 19,350 square miles, 12,647 square miles of which are controlled by the S.W. Freese Dam. The San Saba River, with a drainage of 3,046 square miles is the primary contributor during the PMF as the critical storm location was primarily centered over this tributary drainage area. The initial PMF determined that the dam had a peak discharge of 1,099,400 cfs with 4.85 feet of overtopping. Only about 60% of the total discharge could be passed through the dam's four spillways, while the rest was passed over the top of the dam.

The next dam in line, the Roy Inks Dam, a 96-foot high gravity dam that provides hydropower and water supply. It is located only four miles downstream of Buchanan Dam. It has only an additional 40 square miles of incremental drainage area, and therefore its PMF is completely controlled by the discharge of Buchanan. It was initially found to have a peak discharge of 1,096,700 cfs with 10.40 feet of overtopping.

The next dam in series is the Alvin Wirtz Dam, which forms Lake Lyndon B. Johnson, with a total contributing drainage area of 24,390 square miles. The dam is an 118-foot high earth fill embankment with a concrete core wall. It has ten radial gates that form the service spillway. Similar to Buchanan, the critical storm location for Wirtz Dam is on a primary tributary, the Llano River which contributes 4,443 square miles to the drainage area of Wirtz dam. The initial PMF had a peak discharge of 1,419,500 cfs with 11.55 feet of overtopping.

The Max Starcke Dam which forms Lake Marble Falls, is located a short distance downstream from Wirtz Dam. It is a concrete gravity dam 99 feet high, and similar to Inks, it forms a smaller hydropower and water supply reservoir that has only 35 square miles of incremental drainage area. Its PMF is completely controlled by the discharge from Wirtz Dam, and was initially found to have a peak discharge of 1,414,400 cfs with 34.7 feet of

over-topping. This dam was found to be structurally stable even with the extreme overtopping.

The next dam in series is Mansfield Dam which was built by both the Bureau of Reclamation and LCRA. This is the only flood control reservoir in the series. It is also used for hydropower and water supply. The dam, which is a concrete gravity dam and earthen embankment, has a maximum height of 266 feet and 2,050,000 acre feet of flood control storage. It has a total drainage area of 26,230 square miles with the Pedernales River providing the primary incremental drainage area. Because the dam is designed for flood control, the PMF is primarily storage controlled, and the critical storm location is centered over the majority of the drainage area downstream of the Freese Dam. The initial PMF had a peak discharge of 806,000 cfs with 0.70 feet of free board. This was the only dam that was found to be hydraulically adequate.

The last dam in the series is Tom Miller Dam, located 20 river miles downstream from Mansfield. Similar to Starcke and Inks Dam, it has a small incremental drainage area of 110 square miles, and its PMF is completely controlled by the discharge of Mansfield. The initial PMF estimate included a peak discharge of 804,800 cfs with 4.2 feet of overtopping. The 85-foot high dam is a combination of masonry concrete and earthen sections with 9 radial gates and an uncontrolled ogee spillway.

PMF Update

In 1990, the LCRA retained Freese and Nichols to complete the review of the dam structures and to review potential alternatives for modifications to meet state regulations. As part of the proposal, Freese and Nichols recommended that the LCRA review the possibility of updating their PMF analysis to include the use of the model NETWORK[3]. This model was developed by the National Weather Service and is ideal for routing flood discharges through most naturally occurring channels.

The recommendation was adopted based on LCRA's review of the basin. As noted earlier, Lake Buchanan has only minimal flood storage capacity. The initial PMF analysis reflected that the dam would be overtopped by five feet. These results indicated that the level of flooding is directly related to the peak inflow. As a result, any reduction in the flood peak would reduce costs associated with design and construction of required rehabilitation measures. It was apparent that the river channel upstream of Lake Buchanan contained characteristics which were conducive

to the benefits which could be gained through the use of the NETWORK model. They include reaches where minimal channel slope and significant overbank storage could easily attenuate a flood peak. In addition, the area upstream of the confluence of the Colorado and San Saba Rivers would experience much higher flood levels from backwater effects than could be simulated by any of the other methods. These higher levels translate into more peak attenuation due to more water going into temporary storage.

NETWORK Comparison

NETWORK is an update of the original DWOPER[4] model and is very similar to the more commonly used DAMBRK[5] model. These models perform routing simulations utilizing dynamic wave methodology. The models utilize the full St. Venant equations in establishing river conditions at each computation point within a model run. The implicit computational solution technique is employed within the models.

It is possible, through use of dynamic wave models, to better simulate flood discharges. These models are able to more accurately reflect floodwave propagation than some of the other, more simplistic, routing techniques. The more simplistic models do tend to produce more conservative results. However, the amount of conservatism is very much related to the system being analyzed. A review of flood records of the river being studied can give an insight on which model needs to be employed.

Typically, a dynamic wave model requires a considerably greater amount of input and calibration data to attain the increased accuracy. It also involves a greater amount of time to produce the calibrated running model. Even after it has been setup, additional modifications are typically required for model stability as the flood routings are executed. The benefits to be potentially gained are especially evident where construction may be required. The effort put into utilizing a dynamic wave model can more than pay for itself by reducing the cost of rehabilitating a structure.

The typical steps taken in the development of a design storm include the use of a few major floods of record for the calibration of the routing parameters. These flows are typically at a level which would consist of primarily channel flow with a significant amount of overbank flow. Once routing parameters have been calibrated for the historical storm, these parameters are then assumed to apply to the design flood level. However, if the design storm is the PMF, its floodwave characteristics will likely be predominantly those of overbank flow. On a major river, with a large

drainage area, the design flood can be expected to have a significantly higher flow than the maximum flood of record. In this situation, a dynamic wave routing model, such as NETWORK, will likely provide a more accurate estimate of the magnitude of the design storm. Where the actual floodwave is more influenced by overbank rather than channel flow, empirical models, such as are found in HEC-1, when calibrated for a floodwave with mostly channel flow characteristics, will tend to overestimate the peak flow of the design storm. Use of the dynamic wave flood routing model will tend to reduce this conservatism by more accurately estimating the design storm flood level.

Previous Experience

Prior to the LCRA project, Freese and Nichols had updated the PMF for one proposed reservoir and two existing dams. All had shown significant reduction in the PMF level and, thereby, in the cost of construction or rehabilitation of the dams involved. The first study was of the proposed Belzora Landing Dam located on the Sabine River near Hawkins, Texas. This study was done as part of a feasibility study for the Sabine River Authority of Texas in 1988[6]. The calibrated parameters for HEC-1 resulted in a peak PMF at the dam site of 384,000 cfs. The DWOPER model calculated an estimated 332,000 cfs peak PMF flow at the dam site, a reduction of about 13 percent. It was estimated that if the HEC-1 PMF had been used in the study, it would have added approximately $1.5 million to the cost of the dam and spillway.

The second project involved Eagle Mountain Dam northwest of Fort Worth, owned by Tarrant County Water Control and Improvement District Number One. It had been found by the Texas Water Commission to have a peak PMF discharge of 271,000 cfs with a 2.1 feet of overtopping of the embankment. An update of the PMF using the DWOPER model resulted in a peak discharge of 229,200 cfs without overtopping. The use of the dynamic wave model verified that the dam meets state criteria and saved approximately $500,000 of modification costs that would have been needed.

The third project was for the Lake Arlington Dam in Arlington, Texas. The previous study had estimated that the dam could pass only 52 percent of the PMF. The peak inflow calculated by the dynamic wave model for the PMF was 311,400 cfs, which is 11 percent less than the peak of 346,000 cfs calculated in the previous report. Utilizing the dynamic wave procedures for channel routing reduced the PMF level by over two feet, and reduced the cost of modifications by about $500,000.

Lower Colorado River Authority Dams

The drainage areas for the six LCRA dams were divided into 41 subbasins. Eleven subbasins were used for the Colorado River, while 3, 11, 11, and 5 subbasins were used for the four major tributaries, Pecan Bayou, the San Saba River, the Llano River, and the Pedernales River, respectively. Other than a constant initial flow in the NETWORK model of 5,000 cfs, no contribution from the drainage area upstream from the S.W. Freese Dam was considered. This was verified during the analysis to determine critical storm locations for the updated model.

For the Colorado River, 250 cross sections were used in the NETWORK model to describe 289 miles of the river channel from the U.S.G.S. gauge near Winchell at the U.S. Highway 377 bridge to the Tom Miller Dam. In addition, 17 cross sections were used to describe the 13.6 miles of Pecan Bayou from the U.S.G.S. gauge at Mullin to its junction with the Colorado River. The 116 miles of the San Saba River from the U.S.G.S. Menard gauge to its mouth were described using 69 cross sections. The Llano River downstream from the U.S.G.S. Junction gauge is 110.2 miles to its mouth on the Colorado and was described using 82 cross sections. 87.7 miles of the Pedernales River, from the U.S.G.S. gauge near Fredericksburg to the Colorado River, was described using 80 cross sections.

The LCRA, in their previous work, had found that three different Probable Maximum Flood events would have to be modeled to determine PMF levels for the six reservoirs. It was found that the PMF for Buchanan Dam would also apply to Inks Dam. Likewise, the PMF for Wirtz Dam would apply to Starcke Dam and the PMF for Mansfield Dam would apply to Tom Miller Dam. As noted earlier, the incremental drainage areas for Inks, Starcke, and Tom Miller Dams are minor.

For the Highland Lakes chain, Lake Buchanan and Inks Lake showed dramatic reductions in PMF levels. The original PMF estimate for Buchanan was elevation 1030.20, which is 4.85 feet over the crest of the dam. The updated model using the NETWORK channel routing lowered this PMF level to 1024.9, 0.5 foot below the top of the dam. Inks Dam also showed a significant reduction in the PMF level with a new PMF estimate of 919.2, which is 3.0 feet below the top of the dam. The previous estimate was elevation 932.60, which overtopped the dam by 10.40 feet. About 4.0 feet of the 5.3-foot reduction at Buchanan and 10.8 feet of the 13.4-foot drop at Inks were a direct result of the NETWORK model application. The remainder of the difference was due to adjustments in the uniform loss rate derived in the

updated calibration. The dramatic difference due to the NETWORK model can be traced to the modeling of the discharges at the confluence of the Colorado and San Saba Rivers. The critical storm was centered over the San Saba River. Though this left significant precipitation over the Colorado River, the majority of the flows were from the tributary. As a result, the peak flow from the San Saba was significantly reduced because of backwater as the large area on the Colorado River became temporary storage. This is a good example of how a dynamic wave model can better simulate the actual movement of water.

The Wirtz Dam showed no change in the PMF level of 849.4, which overtops the dam by 11.55 feet. The revised PMF for Starcke was virtually unchanged as the PMF level dropped from 793.2 to 793.1. However, the revised level has 34.6 feet of overtopping. Similar to Buchanan, Wirtz had the primary contribution of flow from a tributary, the Llano River. The Llano River itself does not exhibit characteristics which would benefit from a dynamic wave simulation. In addition, because of its confluence with the Colorado River taking place within the confines of Lake LBJ and because the ability of the flow to spread upstream was limited by Inks Dam, gains similar to those for Buchanan Dam were not realized.

The PMF routing at Mansfield Dam is storage controlled because of its large flood storage volume. The estimated PMF level for Mansfield was lowered from elevation 752.70 to 752.0 which is 1.4 foot below the top of the concrete gravity section. The revised PMF for Mansfield Dam resulted in a larger runoff volume due to the use of smaller subbasins in the fringe areas of the drainage area. By itself, this would have raised the peak level by 0.7 feet. However, the final peak level was actually reduced by 0.7 feet, due to adjustments in the Mansfield Dam spillway discharge rating curves. The adjustments were based on actual measurements during the flood of record which occurred during the study and also from adjustments in the operating schedule of the spillway due to the flatter hydrograph calculated by NETWORK. Even though the peak level was lower, the peak discharge was increased as a result of the changes. In this instance, because the peak elevations were dictated by storm volume more than peak inflow, the increased accuracy in routing the hydrographs using a dynamic wave simulation did not have a major impact on the PMF levels. The revised PMF level at Tom Miller Dam is elevation 522.2, an increase of one foot from the previous estimate. This revised level is 5.2 feet over the top of the earth embankment portion of the dam. The increase in the level at Tom Miller Dam is primarily due to the adjustments in the planned operating scheme and adjustments in the rating curve at Mansfield.

The results of the analyses on the LCRA dams was dramatic for two of the six structures. The affects of the update of the river routing to the NETWORK model on the remaining four were minimal. The study of rehabilitation alternatives for the structures is continuing. From preliminary estimates, it appears that the cost reduction for stabilizing Buchanan and Inks Dams for the lower design elevations is approximately $30 million.

III. CONCLUSION

The channel routing methods currently used in HEC-1 are accepted standards of river routing procedures. Many situations exist where these methods are suitable and provide sufficiently accurate results. However, there are a variety of cases where these methods, when calibrated from historical events, may give inaccurate estimates of design level floods. These would include any situation where a design level flood will experience significantly different floodwave characteristics than the historical flood, such as,

a. Significantly different roughness coefficients between the channel and overbank,

b. Considerable storage in the overbank area from adjacent draws, creeks, and tributaries,

c. Significant impact from highway or railroad embankments,

d. Floodplain areas that are wide and flat, relative to the channel, or

e. Significant backwater effects associated with tributaries that contribute a significant portion of the flows.

Given these conditions, the empirical methods have a tendency to underestimate both the amount of attenuation and the travel times, resulting in a potentially over-conservative design storm estimate. The routing techniques used in the available dynamic wave models can reduce this conservatism by more accurately describing the design flood characteristics. This can potentially result in considerable cost savings in the design or rehabilitation of dams and their spillways.

Prior to the LCRA projects, dynamic wave models had been used by Freese and Nichols to update the PMF for one proposed reservoir and two existing dams. In all three cases, the use of the dynamic wave models resulted in a reduction of the PMF and a corresponding reduction in the cost

of construction or rehabilitation. These estimated savings ranged from $500,000 to $1.5 million.

The use of the NETWORK model for an update of the PMF on the Lower Colorado River Authority's six dams dramatically reduced the PMF levels on two of the dams, and had little impact on the other four. Preliminary estimates indicate that the effort initiated to update the PMF hydrographs will result in a reduction in rehabilitation costs for Buchanan and Inks Dams of about $30 million.

LIST OF REFERENCES

1. U.S. Army Corps of Engineers, Hydrologic Engineering Center, HMR52, Probable Maximum Storm (Eastern United States) User's Manual, March 1984.

2. U.S. Army Corps of Engineers, Hydrologic Engineering Center, HEC-1 Flood Hydrograph Package, January 1985.

3. Fread, Danny L., DWOPER/NETWORK, National Weather Service Operational Dynamic Wave Model, Users Guide, National Weather Service, National Oceanic and Atmospheric Administration, U.S. Department of Commerce, Silver Spring, MD, June 1982.

4. Fread, Danny L., National Weather Service Operational Dynamic Wave Model, User's Guide, National Weather Service, National Oceanic and Atmospheric Administration, U.S. Department of Commerce, Silver Spring, MD, June 1982.

5. Fread, Danny L., Office of Hydrology, National Weather Service: DAMBRK The NWS Dam-Break Flood Forecasting Model, Silver Spring, Maryland, 1984.

6. Freese and Nichols, Inc., "Feasibility Report on the Belzora Landing Dam and Reservoir," prepared for the Sabine River Authority of Texas, 1988.

7. Lower Colorado River Authority and RAC Engineers and Economists, Reevaluation of Probable Maximum Floods for LCRA's Highland Lakes Projects, February 1991.

Use of Mainstream Computing Platforms for Power Plant Control

Robert J. Hughes[1]

Abstract

Software based control systems for powerplants are moving away from proprietary systems to solutions based on commonly available, mainstream computer hardware and software components. The feasibility of this progression to "open-systems" has been enabled by the emergence of widely used standards in the general computing industry.

Use of Mainstream Computing Platforms for Hydro Control

Control systems for powerplant applications have gradually evolved from solely providing hardware to include increasing amounts of software. For new projects, software is likely to be present in some degree. In fact, many new plants employ software extensively in the control scheme.

Within the realm of software based systems, a progression is being made from embedded software, running on proprietary, specialized hardware, to "off-the-shelf" software running on commonly available computing platforms. This progression has significantly changed the way many owners and vendors are approaching the design and implementation of hydroelectric controls.

The most recent trend has been away from proprietary hardware, which is used only for a particular vendor's control system. Instead, many vendors and customers are favoring the use of commonly available hardware. These new developments are much more aligned with the general computing industry to utilize computing platforms that are widely available and used for many applications. This trend is occurring because of the competitive economics and additional features that are provided by this type of system.

[1] Project Lead Software Engineer, ABB Phoenix Controls, 22310 20th Ave. S.E., Bothell, WA 98021, (206) 483-4288

The most progressive systems run on widely used computer hardware and software platforms such as the Microsoft MS-DOS compatible computers, or the UNIX operating system running on commonly available workstation computers. The important distinction of these systems is that they make significant use of de facto standards. In this context, a de facto standard is a type of hardware or software that is so widely used that other vendors' hardware and software products are compatible with it, either inherently or by design. An example of this type of system can be found in the reference (Bogert and Hughes 1992).

Besides running on widely available or de facto standard computers, it is important for a control system to support a wide variety of controllers and I/O devices. This is significant because many types of controllers and I/O devices are available and are already installed in plants where control system upgrades are planned.

The effect of these trends is that many new control systems are a mixture of personal computers, control system software, I/O devices or controllers, network products, and mainstream applications. The design and implementation of finished control systems becomes a system integration task. The feasibility of mixing these components is greatly enhanced by "open-systems."

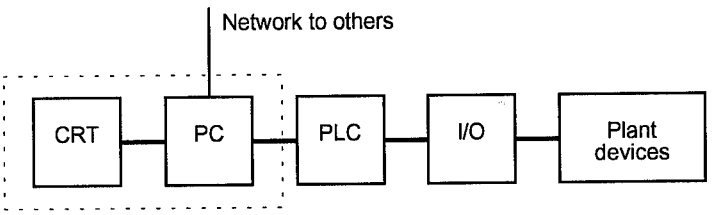

Figure 1. Typical control system block diagram. This paper focuses on the part of the control system in the dotted box.

Definition of an Open-System

An open-system is typically described as having standardized interfaces allowing components from different vendors to work together. A more practical definition for the power plant owner, however, is that it allows off-the-shelf hardware and software from unrelated vendors to be easily integrated to form a system.

There is much debate over what genuinely qualifies as an open-system. It is important that the powerplant owner has a clear definition of an open-system because today, "open" is as much overly used to describe systems as "user friendly" was to describe products a few years ago. The key to actually

benefiting from an open-system is to focus on the aspects of openness that are relevant to the control systems user.

The technical definition of an open-system, as defined by IEEE, is "a system that implements sufficient open specifications for interfaces, services, and supporting formats to enable properly engineered applications." Many of the technical discussions surrounding open-systems focus on adherence to sanctioned standards by ANSI, OSI, IEEE and others. The most ambitious open-systems standard is POSIX which stands for "portable operating system interface for computer environments." POSIX attempts to define a standard interface between the computer software application and the computer operating system and hardware. The idea is that if a software application complies with the POSIX standard, then, with little effort, it can be made to operate on any computer platform that supports POSIX.

Because POSIX is such an ambitious specification, its development is a substantial undertaking and is not completed. The fundamental problem is that the de facto standards are changing rapidly, as is the case with almost anything relating to computing technology. Thus, the POSIX specification cannot keep up with advancing technology.

In addition, the most active growth segment for powerplant controls involves the use of micro-computers (hereafter referred to as the personal computer or PC). POSIX, on the other hand, is most relevant to workstations and minicomputers. The de facto standard operating systems for PCs are not now POSIX compliant nor is it likely that they will be in the future. (Typical business users do not care if their office PCs comply with POSIX, but they do have to be DOS, Windows, and OS/2 compatible.) Consequently, the de facto operating system standards overshadow the sanctioned standards in defining an open-system for control system applications. The control system user needs to identify the de facto standards to maximize the potential of the open-system.

Currently, the de facto operating system standards for the PC are Microsoft MS-DOS, MS-Windows, and OS/2. For networking hardware, Ethernet and Token Ring are standard, with Ethernet dominating the market. For PC network software, NET BIOS is widely used. TCP/IP is extensively used on networks connecting computers other than PCs .

For mini-computers and workstations, UNIX is the de facto standard operating system. UNIX is also available for the PC compatibles but commands a very small share in that market. The POSIX standard is modeled after UNIX. This makes UNIX the easiest path to POSIX compliance.

Some of the leading control system vendors have chosen to vigorously follow the PC de facto standards. These systems use commonly available personal computers for the hardware platform. The software uses DOS, Windows, OS/2, and UNIX. Some systems even support a mixture of these within a single control system. The use of de facto standards makes it possible to use hardware and software from different vendors to implement control solutions and allows the user to receive the benefits of an open-system.

Advantages of Open-Systems

Some functional areas are basic to the control system and must be an integral part of the control system software. Other areas involve support functions, data input/output, reporting and analysis, data archival, and networking system software. These latter functional areas are well suited to open-system solutions.

The open-system allows the best and most appropriate hardware and software components to be integrated to form the control system. This reduces the dependence on any single vendor. Additionally, the individual components can be upgraded over time without requiring the replacement or upgrade of the entire system.

No single component vendor can solve all of the problems of the control system user. Due to differences in features and the various requirements of the system, a vendor who tries to solve all of the problems will likely solve none of them very well. This is true first, because the needs are too diverse to be supported by one system, and second, because the size of the control system market is too small to support "from the ground up" development.

One of the limitations to single vendor solutions, stated above, is the market size. Mainstream applications, such as spreadsheets and database managers, do not have this limitation since they are supported by such a large market. Spreadsheet programs, for example, are of very high quality, loaded with features, and inexpensive relative to their capabilities. A control system vendor could only hope to implement a small portion of the features found in these mainstream applications into their products. Because of their relatively small market, the cost of doing so would be prohibitive in light of the benefits.

The solution to this problem is for the control system vendor to allow these mainstream applications to be used with their product. One way of doing this is for the control system vendor to develop a special interface to a given product. The problem with this method is that only the one product, and typically only a specific version, is supported. A better way is to develop an interface that supports multiple products, even ones that may not exist at the time the control system software is developed. In addition to allowing mainstream applications to be used, this approach allows the use of niche market products, and even those which have been custom developed. Using de facto standards enables this solution.

In some cases, the mainstream applications add to the functionality of the system as implemented by the control system vendor. In others, the control system vendor has chosen to drop their own development of a function in favor of the third party product. The best example is the use of a commercially available spreadsheet for report generation. The formatting flexibility and graphical presentation capabilities of the modern spreadsheet surpass anything that could realistically be developed by the control system vendor. Thus, some system vendors have discontinued development of their own report generator and now identify a particular spreadsheet as the system's report generator. It is an increasing trend by control system vendors to use third party products in place of internally developed ones.

Figure 2 shows an example of a control system being implemented as a multi-vendor solution. In this example, the computers are from company A, control system software from company B, PLCs from C and D, operating system from E, network from F, the spreadsheet program from G, and on-line help system from H.

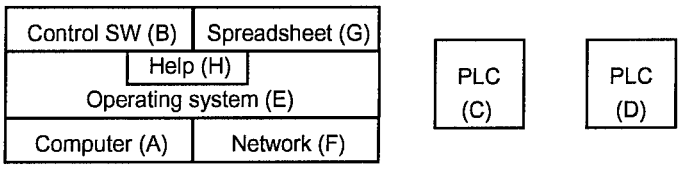

Figure 2. Multi-vendor solution

Perhaps the most significant benefit of open-systems is the ability to add functions to meet new requirements **after** the system is installed. This ability is a key benefit and test of an open-system. Examples of unanticipated new requirements include adding new types of controllers or I/O devices, mapping displays, windowing support, network file server, extended networks, tieing to another control system, or using a new type of computer hardware. The key to practical open-systems is the ability to add new, unanticipated features.

Enabling Technologies for Open-systems

A key to making open-systems work is allowing different applications or discrete functions to work together, as with a control system using a spreadsheet. To make the generalized interaction of all applications possible it is necessary that there be a widely used de facto standard for this interaction. Two technologies that have emerged in this role are the Graphical User Interface and computer networking. Both make open-systems a practical reality. The GUI has done this by allowing applications on the same computer to interact. Networks have allowed applications running on different computers to interact to form a much more capable system. Together these complimentary technologies allow complex control systems to be built using off-the-shelf components.

Previously, the de facto standards provided by standardized hardware platforms and operating systems have allowed for the creation of a wide variety of applications. For example, there are literally thousands of applications available for PCs using the MS-DOS operating system. Similarly, there are a large number of applications for UNIX and even Digital Equipment's VMS operating system. These operating systems have a large enough installed base to attract significant development effort. One thing that almost all of these applications have in common is that they are self-contained, providing all their own functionality, except that furnished by the

operating system. Only with the advent of GUI and network technology have applications begun to interact with each other.

The Graphical User Interface (GUI), as typified by MS-Windows, is generally recognized as providing improved graphics, easy to use user interface, and the ability to run multiple windows simultaneously on a single monitor (CRT). The benefit to open-systems is that GUIs define a way for different applications running on the same computer to interact with each other. In the MS-Windows environment this is known as Dynamic Data Exchange (DDE). DDE allows applications to exchange data while both are running. Users of Windows business applications are familiar with DDE in that it allows data, like the result of a spreadsheet calculation, to be dynamically updated in a word processing application. This same method can be used to link data between any two applications that have been written to support DDE. The applications involved do not need to have been developed with any prior design knowledge of the other. Thus, GUIs provide de facto standards for allowing different applications running on the same computer to interact.

Computer networks allow applications on different computers to communicate at relatively high speeds, and over almost unlimited configurations. The high speeds permit well-designed software to utilize the network without undue delays. The data routing ability of the network allows the data to get from computer A to B without the need to write the application for a specific network configuration.

Users of office applications are most familiar with electronic mail as a network application. In this case, a single application runs on many different computers and allows each computer running the application to communicate with every other. This is similar to the method used by many control products in which the application can be run on several computers, and each computer can exchange control data over the network.

It is also possible for different applications to communicate with each other over a network. For example, electronic mail software from different manufacturers can exchange mail messages if both are written to support the same message handling standard. At this time, there are few applications that can communicate over a network with applications other than those provided by the given vendor. However, this is an area that will see expanded development in the future.

The combination of GUI and networking technologies potentially allows almost any application anywhere to communicate with any other. MS-Windows provides for this with NetDDE which allows data exchange between applications running on different computers to interact the same way as they would using DDE on a single computer. X-Windows has always been a network based GUI system. Thus, it also allows similar interaction.

GUI Systems as State of the Art

The GUI has introduced many advantages to control systems that utilize it effectively. The most significant is the ability for unaffiliated applications to work together. Other significant benefits include better presentation to the

user, standardized interface, and the ability to present new types of information.

A GUI is not a requirement of an open-system. However, the GUI is significantly increasing the viability of open-systems by expanding their technical capabilities and by providing a mass market de facto standard. The most interesting technical aspect of GUIs for open-systems is the ability of applications to communicate using a standard method: DDE for MS-Windows, and "links" for X-Windows.

DDE or "links" are the methods typically used by control software to allow a spreadsheet to serve as the report generator. Since DDE allows the two-way exchange of data between applications, essentially any application that supports DDE can exchange information with the control system. The application used with a control system does not have to be developed specifically for use with that control system. (The capabilities described for DDE generally apply to X-Window's links. DDE is mentioned primarily due to its larger installed base.)

Another significant benefit of GUIs is the standardization of software interfaces such as printer drivers, video display systems, and graphical input devices. This standardization allows the freedom to use the almost any device, from the most basic dot matrix printer, to a high resolution, full color printer. Likewise, video display systems of varying resolutions can be used. Graphical input devices such as image scanners allow graphical images to be incorporated into control system displays, such as maps, equipment diagrams, and non-Roman characters.

Combining software interface and windowing technologies together allows some new types of information to be displayed on the control system. For example, position the cursor over a power plant's step-up transformer, click the mouse button, and a smaller window appears over part of the current window. This window contains a diagram of the transformer, scanned in using an inexpensive hand held scanner. Along side this diagram could be all of the telemetered values for the transformer phase voltages, currents, temperatures, etc. This is just one example of what GUI technology brings to the open-system.

Networking as a Key Technology

Besides allowing applications on different computers to interact, modern networking technologies increase the flexibility of a control system by allowing any one system to be configured in innumerable ways, e.g., from a small single unit plant to a unified multi-plant system. In order to realize these benefits, the control systems must be able to utilize industry standard networking hardware and software.

Networks are an area in which the sanctioned standards, IEEE 802.3 and 802.5, and the de facto standards are one and the same. The IEEE standards for Ethernet and Token Ring networks are used to define the hardware. For networking software, NET BIOS is the de facto standard most relevant to control systems using PCs.

Many control systems use proprietary networks. These networks are usually limited to the features that can be developed by the control system vendor. Use of the IEEE standard networks, however, provides all the benefits of using mainstream networking products. When the IEEE standard networks and the de facto standard network software are used, the control system can be configured in almost endless ways. All of these benefits can be obtained transparently by the control system.

Local Area Network (LAN) technology can be used for the plant and any structures in the immediate vicinity (within 10000 meters). This allows the hardware for data acquisition and control, operator interface, data archival, etc., to be placed wherever appropriate and convenient. Bridges, repeaters, routers, remote access products, and Wide Area Network (WAN) products allow multiple plants to be networked together. At a minimum, this allows data sharing between sites. A greater benefit is the ability to control and monitor multiple plants from a single control room. Control system maintenance functions can be performed from a central site as well.

Effective use of networks favors a distributed configuration. This is one in which several smaller computers are used to implement a control system instead of one bigger one. A distributed control system using standardized networks can be scaled from a small, single unit plant, to a large multi unit, multi plant system.

Networking also makes it possible to use completely different types of computers in the same system. This is called a heterogeneous system. Besides providing flexibility of the original control system implementation, heterogeneous systems allow the use of contemporary computers to enhance an existing system, instead of having to use the same type of computers as originally installed.

One area that still remains to be solved is getting control systems from different vendors to work together in a system. Currently, the vendor's systems do not readily communicate with each other over the network, although they can coexist on the same network. Hopefully, this situation will change as the market matures.

Integration of Mainstream Applications

The integration into the control system of mainstream applications such as the spreadsheet, word processor, database manager, artificial intelligence, file server, etc., allows the capabilities of the control system to be extended to well beyond what is provided by the control system software. Some of the most imaginative and useful innovations will take place in this area by allowing the control system to include the characteristics of these applications.

The GUI makes it feasible to integrate the control system with off-the-shelf, mainstream applications. This is done using DDE, shared disk files, and application-to-application communication over the network. With a GUI, the ability to display the control system in one window and a different application in another window allows both applications to be used at the same time. In a

well-implemented system, the user is not necessarily aware that different applications are being used. The applications' windows have the appearance of being part of the same system.

The spreadsheet has already been mentioned as being a report generator. Another spreadsheet use is for engineering studies. Real time data from the control system can be automatically placed in the spreadsheet cells. The graphic display capabilities of the spreadsheet can be used to display information in ways not possible with the control system alone. In addition, with two-way data exchange, algorithms, such as generation optimization, can be calculated using a spreadsheet and the results sent to the control system as set points.

The context sensitive help tools of the GUI can be used to describe operational criteria for a selected device. For example, click on a help button, and a window is displayed showing the device's operating criteria. Alternatively, use a word processor, which in turn may be linked to a control system.

A file server can be transparently integrated into a system to allow centralized management of displays, database, help system, spreadsheets, etc. A database manager can be used to archive data in a format that is usable to other systems such as maintenance record tracking. Run time information for the plant could be piped into the database of the maintenance system.

This are just a few examples of how applications can be integrated into the control system. With an open-system and continued technological development, even more possibilities for integration of mainstream applications will be possible.

Conclusion

The use of computer based monitoring and control for powerplants is an increasing trend. Accompanying this trend is a move away from proprietary systems to those built using de facto standard software and hardware. This progression to open-systems allows the best and most appropriate hardware and software components from unrelated vendors to be easily integrated to form the control system. However, in order to realize the advantages of an open-system, the components of the control system must adhere to de facto standards for software and hardware and be able to work with other vendor's equipment.

The open-system can be tailored to meet the current needs of the powerplant with minimal custom development. After installation, the owner will benefit because the system will allow changes that are not anticipated when the system is implemented.

Appendix I. References

Bogert, John M., and Hughes, Robert J. (1992) "Hydro Plant Control Systems: The State of the Art." Hydro Review, XI(6), October 1992, HCI Publications, Kansas City, MO, 16-24

THREE–DIMENSIONAL NUMERICAL ANALYSIS OF HEAD LOSS IN A BIFURCATION PIPE FLOW

Charles C. S. Song[1], Jianming He[2] and Xiang Ying Chen[3]

ABSTRACT

Flow in the intake bifurcation pipe system of a pump–storage hydraulic power plant has been studied numerically by solving three–dimensional compressible hydrodynamic equations, together with Smagorinsky's subgrid scale turbulence model. The detailed flow characteristics in the bifurcation pipe system under both generating and pumping operation conditions will be described in this paper.

The bifurcation pipe system consists of two bifurcators. The computed cases include the physical model condition with relatively low Reynolds number of $Re=2.5x10^5$ and the corresponding prototype with a high Reynolds number up to $4.2x10^7$. The effect of the sickle plates installed at each bifurcator is also assessed. Detailed three–dimensional flow pattern is simulated successfully. The computed head loss is in good agreement with the experimental data.

1. INTRODUCTION

Bifurcation pipe is widely used in daily life and industrial applications as a basic component of fluid conveyance net works. A typical example is the bifurcating penstock of a multi–unit hydroelectric power plant. Energy loss due to flow separation and vortex shedding in the bifurcation pipe system plays an important role in determining the energy efficiency of the power plant. The vortex loss, commonly called minor loss, is strongly associated with the geometry of the junction. Presently, the bifurcation pipe design is mostly based on some empirical formula and physical modeling. But it is very difficult to obtain detailed flow information using current experimental techniques. It is also difficult to extrapolate the model testing results to the corresponding prototype condition due to the scale effect.

[1]Professor, [2]Research Associate, [3]Research Assistant, *St. Anthony Falls Hydraulic Laboratory, Dept. of Civil and Mineral Engineering, University of Minnesota, Minneapolis, Minnesota* 55414, *U.S.A.*

In recent years, Computational Fluid Dynamics (CFD) method is increasingly applied to many fluids engineering practices. It is believed to be an effective and less costly tool for engineering design of complex flow configurations. However, the CFD method has never been directly employed to bifurcator design due to its complex geometry.

The large eddy simulation approach based on the compressible hydrodynamic Navier–Stokes equations has been developed and successfully applied to various flow problems (Song and Yuan, 1989; He and Song, 1991; He and Song, 1992). This paper describes the application of this method to the flow through a bifurcation pipe of a pumped storage hydroelectric plant. Both the generating and pumping modes are analyzed. By changing the Reynolds number, both small–scale model case and the corresponding prototype condition are computed. In addition, the effect of the sickle plate installed at the junction is also assessed. The section–averaged head loss in all computed cases is discussed in detail.

2. GOVERNING EQUATIONS

In water resource engineering, most flows can be considered to be at low Mach number state, for which the time evolution can be adequately described by a compressible hydrodynamic (previously called weakly compressible) flow model (Song and Yuan, 1988):

$$\frac{\partial p}{\partial t} + K \frac{\partial u_j}{\partial x_j} = 0 \tag{1}$$

$$\frac{\partial u_i}{\partial t} + \frac{\partial}{\partial x_j}(u_j u_i) + \frac{1}{\rho}\frac{\partial p}{\partial x_i} = \nu \frac{\partial^2 u_i}{\partial x_j \partial x_j} \tag{2}$$

where $K=\rho a_0^2$ is the bulk modulus of fluid elasticity, and a_o is the sound speed.

The pressure time–derivative term in the continuity equation, which is zero in incompressible flow model, is retained to represent the effect of compressibility and the fast acoustic transport mechanism.

For turbulent flow, the large eddy simulation approach is adopted. By means of the box filter operation over a small control volume in space (Deardorff, 1970), the momentum equation can be written as:

$$\frac{\partial \bar{u}_i}{\partial t} + \frac{\partial}{\partial x_j}(\bar{u}_j \bar{u}_i) + \frac{1}{\rho_o}\frac{\partial P}{\partial x_i} = \nu \frac{\partial^2 \bar{u}_i}{\partial x_j \partial x_j} - \frac{\partial \tau_{ij}}{\partial x_j} \tag{3}$$

where $P = p + \frac{1}{3}\overline{u_k' u_k'}$ is a modified pressure, and $\tau_{ij} = \overline{u_i' u_j'} - \frac{1}{3}\delta_{ij}\overline{u_i' u_j'}$ is the subgrid scale turbulence shear stress.

The simplest and most widely used subgrid model of the small–scale turbulence is due to Smagorinsky (1963).

$$\tau_{ij} = -\nu_t \left(\frac{\partial \bar{u}_i}{\partial x_j} + \frac{\partial \bar{u}_j}{\partial x_i}\right) \tag{4}$$

and

$$\nu_t = (C_s\Delta)^2 \, (\bar{S}_{ij}\bar{S}_{ij})^{1/2} \qquad (5)$$

where C_s is a model coefficient, $\bar{S}_{ij} = \frac{\partial \bar{u}_i}{\partial x_j} + \frac{\partial \bar{u}_j}{\partial x_i}$, and Δ is a length associated with the filter. For brevity, the bar will be dropped out in the following expressions.

The governing equations are solved numerically using the well–known explicit finite volume method based on MacCormack's predictor–corrector scheme (MacCormack, 1969).

3. PROBLEM DEFINITION AND BOUNDARY CONDITIONS

3.1 Problem Definition

A typical bifurcation pipe is the penstock bifurcator system of a hydropower plant, shown as Fig. 1, where the bifurcation pipe has two bifurcators, forming three branches indicated as P1, P2, and P3, respectively. P0 to P3 also represent the stations where section–averaged pressure and velocity were measured in a small–scale model experiment. There are two sickle plates which are installed between the main pipe and branch 3, and between branch 1 and branch 2, respectively. The sickle plates are designed for guiding the flow so that flow rate could be distributed equally to the three branches without using a valve control at generating mode, and stabilize the flow from each branch at pumping mode. Hence their design is very important for the function of the bifurcation pipe system.

The computation domain is bounded by the measured sections, as indicated in Fig. 1. The used total number of grids is 22x24x247=130,416.

Combined the operation conditions with and without the sickle plates for the small–scale model and the prototype conditions, there are six cases which are computed in this study:

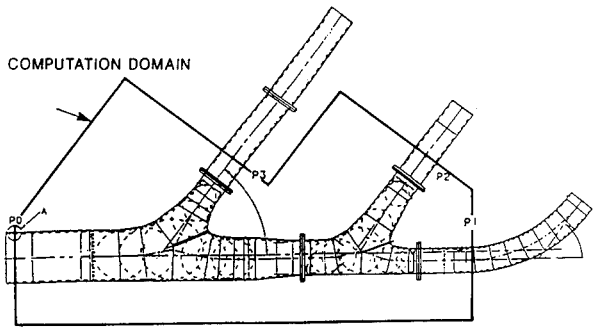

Fig. 1 Schematic of a penstock bifurcation pipe system in the intake section of a pump–storage hydropower plant.

(1) model case at generating mode with sickle plates, Re=2.5x10^5;
(2) model case at generating mode without sickle plates, Re=2.5x10^5;
(3) model case at pumping mode with sickle plates, Re=2.5x10^5;
(4) model case at pumping mode without sickle plates, Re=2.5x10^5;
(5) prototype condition at generating mode with sickle plates, Re=4.24x10^7;
(6) prototype condition at pumping mode with sickle plates, Re=3.23x10^7.

3.2 Boundary Conditions

To avoid the necessity of using extremely small grids near solid wall, a wall function, or a partial slip condition, is applied (Yuan et al., 1991). The log law is assumed to hold near the wall for the time averaged velocity:

$$\overline{u} = 2.5\ \overline{u}^*\ \ln\ |\ 9.0\ \overline{u}^*\ y/\nu\ | \tag{6}$$

where $\overline{u}^* = \text{sign}(\overline{\tau}_w)(|\overline{\tau}_w|/\rho)^{1/2}$ is the time averaged wall shear velocity, $\overline{\tau}_w$ is the wall shear stress, and the bar here represents a time–averaged value. Considering the effect of wall curvature, the boundary condition for pressure is

$$\frac{\partial P}{\partial n} = \rho(V_b^T)^2/R \tag{7}$$

where n is the unit outwards norm, R is the radius of curvature of the wall, and V_b^T is the tangential velocity on the wall.

At upstream, the velocity profile can be given using desired condition. In the present case, a power law $u/u_o=[(D-2r)/D]^{1/7}$ is assumed for considering the fact that the inflow is already fully turbulent in each case. In addition, the following conditions are also specified at the upstream end,

$$v = w = 0,\ \frac{\partial P}{\partial x} = 0 \tag{8}$$

At far downstream, it is assumed that

$$\frac{\partial u}{\partial x} = \frac{\partial v}{\partial x} = \frac{\partial w}{\partial x} = 0 \tag{9}$$

The pressure at downstream may be given a constant.

4. COMPUTED RESULTS AND DISCUSSION

(1) Model case at generating mode with sickle plates, Re=2.5x10^5;

Figs. 2(a) and (b) show the flow field on the symmetrical plane around the two bifurcators. They are computed in one full domain, but plotted separately. It is known from Fig 2(a) that the flow around the first bifurcator is quite smooth, and the sickle plate appears to play a role of pushing a little more fluid into the branch since small separation zone is

noticed behind the plate in the main pipe. In Fig. 2(b), however, a large stall eddy occurs at the inlet of branch 2, which results in a large fluid blockage and energy loss in the branch. Similar to that in a diffuser flow (He and Song, 1991), the flow separation is caused by the sharp diffusion of the boundary from the main pipe to P2. Contrary to the effect of the sickle plate at the first bifurcator, the sickle plate in the second bifurcator appears to block fluid to branch 2. Fig. 3 shows the energy balance (including friction loss and minor loss), based on section–averaged value, where the main pipe means from station 0 to station 1; side pipe 1 is branch 3; and side pipe 2 is branch 2. Apparently, the linear drop part of the total energy distribution is mainly due to the friction head loss, while the sudden drops at each bifurcator represent the minor head loss. As may be expected, this figure shows that main minor energy loss occurs at the second bifurcator.

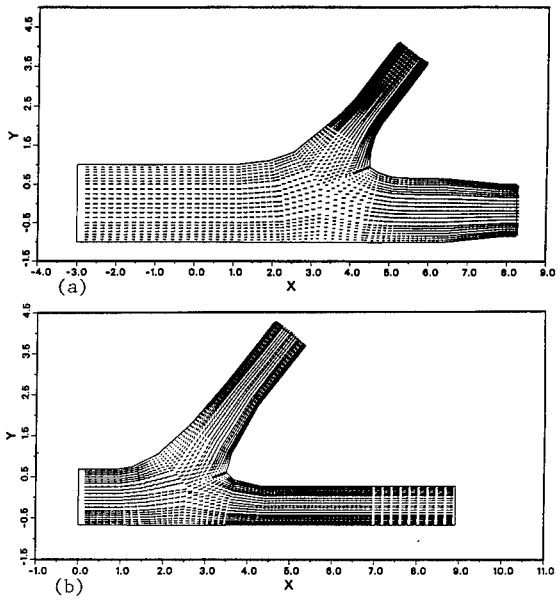

Fig. 2 Velocity field on the horizontal symmetrical plane at generating mode with sickle plates, (a) the first bifurcator; (b) the second bifurcator, Re=2.5x10^5.

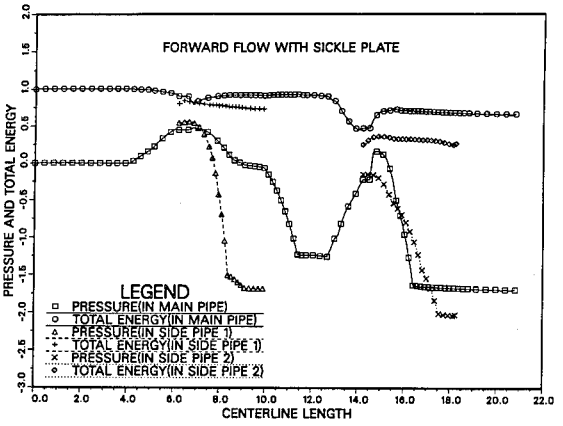

Fig. 3 Section–averaged energy balance along the pipe centerline at generating mode with sickle plates, Re=2.5x10^5.

(2) Model case at generating mode without sickle plates, Re=2.5x10^5;

The computed result shows that the stall eddy at the second bifurcator becomes a little smaller than that in the case with the sickle plate. Apparently, the existence of the plate makes the inlet to branch 2 smaller. Therefore, the sickle plate at the second bifurcator strengthens the fluid blockage at branch 2, and thus leads to more energy loss.

Table 1 Flow Quantities in the Model Cases at Generating Mode

With sickle plates (design case), Re=2.5x10^5				
	Station0	Station1	Station2	Station3
Velocity	1.003	1.503	1.503	1.503
Pressure Coef.	0.000	–1.698	–2.058	–1.683
Loss Coef.(Cal.)	0.000	0.440	0.772	0.424
Loss Coef.(Exp.)	0.000	0.310	0.674	0.453
Without sickle plates, Re=2.5x10^5				
	Station0	Station1	Station2	Station3
Velocity	1.002	1.503	1.503	1.503
Pressure Coef.	0.000	–1.721	–2.033	–1.698
Loss Coef.(Cal.)	0.000	0.483	0.764	0.429
Loss Coef.(Exp.)	(Not available)			

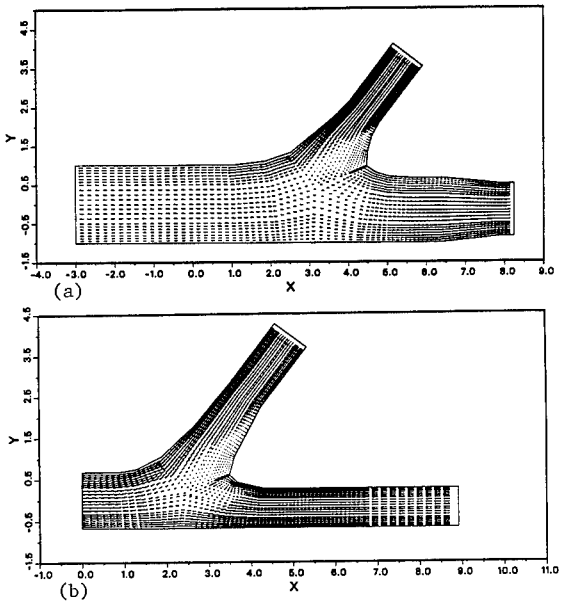

Fig. 4 Velocity field on the horizontal symmetrical plane at pumping mode with sickle plates, (a) the first bifurcator; (b) the second bifurcator, Re=2.5x10^5.

A summary of some computed flow quantities in above two cases and comparison with the model experimental data (WRPC,1991) are listed in Table 1. The experiment was conducted in laboratory with the sickle plates. The energy loss is referred to station 0. Generally, it appears that a fair agreement between the computation and experiment is achieved. As one may expect, the energy loss at the first bifurcator is almost the same in the two cases, but more head loss in branch 1 and less loss in branch 2 are noticed. The results

also show that the head loss difference in each branch due to the sickle plates is mainly caused by the pressure difference. Generally speaking, the effect of the sickle plates at generating mode on the flow field and head loss is not very significant.

(3). Model case at pumping mode with sickle plates, Re=2.5x10^5;

Fig. 4 shows the time–averaged flow field on the symmetrical plane in this case. At the pumping mode, the contraction section at the generating mode becomes diffusion section. Similar to the transitory stall flow in a diffuser, the largely–diffused boundaries result in large flow separation in all branches, and strongly unsteady vortex–shedding and stall–washout can be found in the stall regions. These worse flow behaviors also lead to big energy loss in the flow system, especially in branches 2 and 3, as shown in Fig. 5.

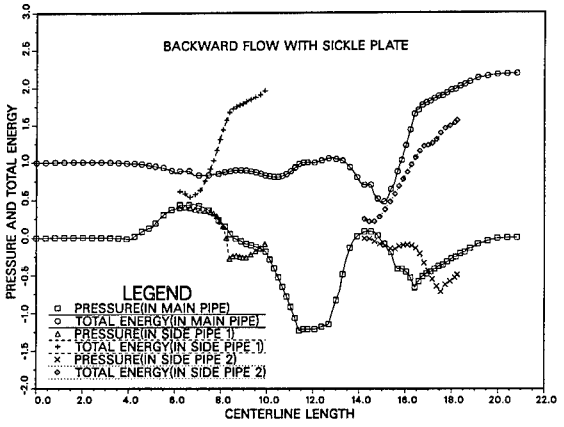

Fig. 5 Section–averaged energy balance along the pipe centerline at pumping mode with sickle plates, Re=2.5x10^5.

(4). Model case at pumping mode without sickle plates, Re=2.5x10^5;

The computed result shows that the sickle plates do not make the time–averaged flow separation and stall region significantly different. But the sickle plate at the second bifurcator dose make the unsteady flow more stable. Therefore, more energy loss occurs at the second branch, compared with the case with the sickle plate.

A summary of some computed flow quantities in the model cases at pumping condition and the model experimental data (WRPC, 1991) are listed in Table 2, where minus represents the flow in reverse direction. It seems that the head loss at each branch is a little over–predicted. It is probably caused by the strong unsteady vortex shedding, which is very difficult to predict accurately.

Table 2 Flow Quantities in the Model Cases at Pumping Mode

With sickle plates (design case), Re=2.5x10^5				
	Station0	Station1	Station2	Station3
Velocity	−0.996	−1.477	−1.423	−1.427
Pressure Coef.	0.000	−0.098	−0.395	−0.318
Loss Coef.(Cal.)	0.000	−1.084	−0.591	−0.718
Loss Coef.(Exp.)	0.000	−0.983	−0.464	−0.630
Without sickle plates, Re=2.5x10^5				
	Station0	Station1	Station2	Station3
Velocity	−0.973	−1.472	−1.423	−1.421
Pressure Coef.	0.000	0.340	−0.722	0.187
Loss Coef.(Cal.)	0.000	−1.508	−0.263	−1.206
Loss Coef.(Exp.)	(Not available)			

(5) Prototype condition at generating mode with sickle plates, Re=4.24x10^7;

As mentioned before, one of the advantages of numerical method over the experiment is that numerical method can directly simulate prototype condition just by changing the Reynolds number. At normal case, it is impossible to conduct an experiment at the same Reynolds number as that in the prototype. The large change in Reynolds number do affect flow quantities, especially on head loss, even in the high Reynolds number range as considered herein. Therefore, it is very difficult to convert an experimental result at low Reynolds number into the prototype condition at high Reynolds number.

Fig. 6 shows the computed energy balance along the pipe centerline in the prototype case at generating mode with sickle plates. The Reynolds number of 4.24x10^7 is based on a normal operation condition of the

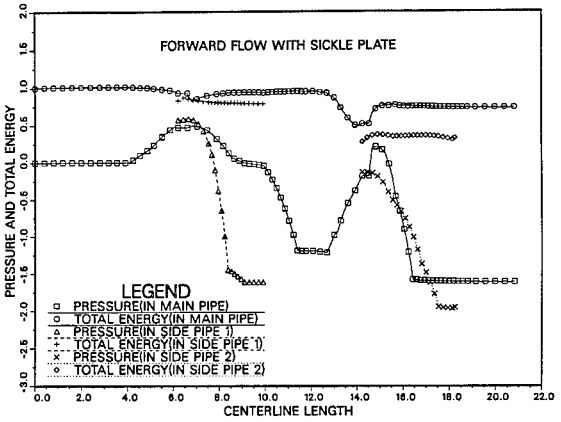

Fig. 6 Section–averaged energy balance in the prototype along the pipe centerline at generating mode with sickle plates, Re=4.24x10^7.

pump–storage power plant. Compared with the similar case at model condition in Fig. 3, it is hard to find a significant difference between the two cases except the friction loss. It is shown that the energy slope is a little smaller in Fig. 6 due to the increase of Reynolds number. Therefore, the increase of Reynolds number dose reduce the head loss although it changes the flow pattern very little. The summery of the flow quantities in this case is listed in Table 3.

(6) Prototype condition at pumping mode with sickle plates, $Re=3.23x10^7$;

Similar to the generating mode, the prototype condition at pumping mode has less head loss than the corresponding model case, as shown in Fig. 7. The computed flow quantities in this case are summarized in Table 3.

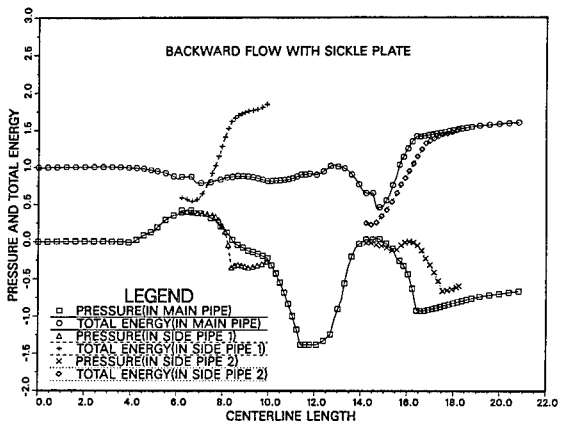

Fig. 7 Section–averaged energy balance in the prototype along the pipe centerline at pumping mode with sickle plates, $Re=3.23x10^7$.

Table 3 Flow Quantities at the Prototype Condition with Sickle Plates

Generating mode, $Re=4.24x10^7$:				
	Station0	Station1	Station2	Station3
Velocity	1.003	1.503	1.503	1.503
Pressure Coef.	0.000	–1.610	–1.984	–1.608
Loss Coef.(Cal.)	0.000	0.351	0.693	0.349
Pumping mode, $Re=3.23x10^7$				
	Station0	Station1	Station2	Station3
Velocity	–0.978	–1.477	–1.423	–1.427
Pressure Coef.	0.000	–0.272	–0.540	–0.430
Loss Coef.(Cal.)	0.000	–1.911	–0.471	–0.605

CONCLUSIONS

The fact that there is large head loss in branch 2 at generating mode and in branch 1 at pumping mode is apparently due to the appreciable flow separation that occurs at the second bifurcator.

Based on the computed results, the sickle plate at the first bifurcator does not make a significant difference in energy performance at generating mode , but it reduces the energy loss in branch 3 at pumping mode by stabilizing the unsteady separated flow. The sickle plate at the second bifurcator plays a favorable role in reducing head loss at both modes.

Prototype condition has about 15% less overall head loss than the model case due to the increase of Reynolds number.

By comparing with available experimental results, the computed results show that the numerical method is capable of predicting the energy performance of a general bifurcation pipe.

ACKNOWLEDGEMENTS

This research was sponsored by Sinotech Foundation for Research & Development of Engineering Sciences & Technologies, Taipei, Taiwan. The computer time was granted by the Minnesota Supercomputer Institute of the University of Minnesota. The authors are grateful for their support. The second author would also like to recognize the support of the 1992–1993 Minnesota Supercomputer Institute research scholarship for preparing this paper.

REFERENCES

Deardorff, J. W., 1970, "A numerical study of three–dimensional channel flow of large Reynolds numbers," *J. Fluid Mechanics*, Vol. 41, Part 2, pp. 453–480.

He, J., and Song, C. C. S., 1992, "Computation of turbulent shear flow over a surface–mounted obstacle with large eddy simulation," *Journal of Engineering Mechanics, ASCE*, Vol. 118, No. 11, pp. 2282–2297.

He, J., and Song, C. C. S., 1991, "Numerical simulation and visualization of two–dimensional diffuser flow," *Experimental and Numerical Flow Visualization*, FED–Vol. 128, ASME, pp. 355–362.

MacCormack, R. W., 1969, "The effect of viscosity in hypervelocity impact cratering," *AIAA Paper* No. 69–354.

Smagorinsky, J., 1963, "General circulation experiments with primitive equations," *Month Weather Review*, Vol. 91, No. 3, pp. 99–164.

Song, C. C. S., and Yuan, M., 1990, "Simulation of vortex–shedding flow about a circular cylinder at high Reynolds numbers," *Journal of Fluids Engineering*, Vol. 112, pp. 155–161

Song, C. C. S., and Yuan, M., 1988," A weakly compressible flow model and rapid convergence methods," *Journal of Fluids Engineering*, Vol. 110, pp. 441–445.

Water Resources Planning Commision (WRPC), Ministry of Economic, Taiwan, ROC, 1991, "Report on hydraulic model tests of penstock bifurcators of Mingtan pumped storage project," 42–T–08.

Yuan, M., Song, C. C. S, and He, J., 1991, "Numerical analysis of turbulent flow in a two–dimensional nonsymmetric plane–wall diffuser," *Journal of Fluids Engineering*, Vol. 113, pp. 210–215.

Development of an Integrated Hydraulic-Electrical Model for Hydropower Plant

Angus Simpson[1] , Michael Gibbard[2] and John McPheat[3]

Abstract

An integrated model for describing the dynamic response of the hydraulics, governor and electrical systems associated with hydropower plant is described. An accurate representation of the elements in the hydraulics system including reservoirs, tunnels, penstocks, bifurcations, open or closed surge tanks, valves, multiple turbines, and pumps has been incorporated in the model. Various governor types can be modeled. In addition, elements in the electrical system that can be modeled include generators, their controllers, transmission lines, transformers and loads. The integrated model may be used to determine the behavior of the system following a large magnitude disturbance, for example, load rejection or load acceptance at the hydropower plant. The model should provide a useful tool to planning engineers in deciding the range of possible sizes for penstocks and layout options that may be considered.

Introduction

Traditionally Civil Engineers plan the layout, penstocks, power tunnels, surge tanks and other water-hammer control devices for hydropower plants. One important factor in determining the diameter of the penstock for supplying water from the reservoir or diversion to the hydropower plant is the systems' dynamic response to small magnitude disturbances. In addition the performance of the entire system following a large magnitude disturbance must be considered. Adequate numerical models exist (usually developed by Civil or Mechanical Engineers) for

[1] Senior Lecturer, Dept. of Civil & Environmental Engineering, GPO Box 498, University of Adelaide, South Australia 5001

[2] Assoc. Prof., Dept. of Electrical & Electronic Engineering, GPO Box 498, University of Adelaide, South Australia 5001

[3] Research Officer, Dept. of Civil & Environmental Engineering, GPO Box 498, University of Adelaide, South Australia 5001

modeling the water-hammer events in the conduit system and water-hammer control devices associated with a hydropower plant. Often these models also incorporate the detailed description of the governing system. Usually the electrical system is modeled in a simplistic way to simulate load rejection or load acceptance at the plant. Conversely, detailed electrical system models for dynamic events are available (usually developed by Electrical Engineers). Often these models have simplified models for representation of the hydraulic system. As a result it has never been possible to investigate fully and in detail the behavior of the hydraulics systems, and the interaction between the hydraulics, the governors and the electrical power system. Often, specific questions based on cost, operational or environmental considerations require answers which are dependent on details of model results. This paper presents details of a comprehensive integrated numerical model in which the hydraulics system dynamics and electrical system dynamics (including the governor) and their interactions are modeled in detail. An integrated modeling approach should enable a planning or design engineer to investigate such things as:

(i) detailed assessment of whether a surge tank is necessary
(ii) whether a smaller diameter penstock can be selected
(iii) the analysis of stability and operational problems and their remedies
(iv) co-ordination of the governor parameters with those of the hydraulic and electrical systems

Software for simulating the dynamic behavior and interaction between the hydraulic and the electric power system when a hydropower plant is subject to a large magnitude disturbance has been available for some years (e.g. PSS/E Power System Simulator - Power Technologies 1989). However, as acknowledged by the software providers, the computer models do not attempt to provide a high degree of exactness for any given plant, but rather they represent the principal effects inherent in hydropower plants of conventional configuration. Furthermore, such models are not intended to be used in studies of the detailed behavior of individual plants.

Modeling of the Hydraulic Systems' Dynamics

Stability problems in regulating water turbines are caused mainly by disturbances in the hydraulics system. Dynamic effects in the hydraulics system can be modeled using either rigid water column theory or elastic water column theory. Rigid water-column theory has been used in a number of models for the integrated hydraulic-electrical behavior of hydropower plant (Hovey 1960; Hirano and Kuwabara 1979; Chaudhry 1970). A rigid column model is an approximation of the dynamic behavior in the hydraulics system and is often inadequate especially in systems involving long penstocks. Taking into account the water and penstock elasticity provides a more accurate representation of the hydraulic dynamics during water-hammer events (Brekke 1974; Chaudhry 1980).

In the developments described in this paper, a flexible water-hammer model (or model of the dynamic behavior of the hydraulics system) has been incorporated within an integrated model including the governing and electrical systems. Any piping configuration can be modeled including reservoirs, power tunnels, penstocks, branches (e.g. bifurcations, trifurcations etc.), open and closed surge tanks, valves, pumps, and multiple turbine units (McPheat et al. 1992). In addition looped configurations involving draft tubes from different machines leading to a common downstream surge tank can be modeled. Currently both Pelton wheel and Francis turbines can be modeled. Up to 10 turbines in parallel can be accommodated. Steady-state flows are solved for in the hydraulics system and turbines by solving the resulting set of non-linear equations by an iterative Newton-Raphson technique. The dynamic behavior in the hydraulic system is governed by a set of hyperbolic partial differential equations. A common solution method is the method of characteristics. The governing set of equations for a boundary condition (e.g. a Francis turbine) during the transient event usually leads to a set of non-linear equations which are also solved using an iterative Newton-Raphson solver.

The flexible structure of the integrated model allows for detailed studies of the dynamic behavior of both the hydraulic and electrical systems and the interaction between them and between generating units. Each turbine unit and its associated hydraulics is modeled individually. For example, the following details may be considered by using the integrated model:

(i) the effect of variations in tunnel and penstock diameters and inside surface roughness
(ii) the effect of an open surge tank or a closed surge chamber
(iii) bifurcations, trifurcations etc.
(iv) individual machines
(v) tail race open surge tanks or closed surge chambers
(vi) manufacturer supplied characteristics for turbines or valves
(vii) various governor models (e.g.PID control, water compensation -Hitachi)
(vi) water column separation

The software is user-friendly allowing various configurations of the hydraulic system, associated parameters and characteristic curves to be entered through simple menus.

Modeling of the Electrical Power System

The model of the electrical power system includes generators, their controllers, transmission lines, transformers and loads (Arrillaga and Arnold 1983; Stagg and WI-Abiad 1968). Included in this model are fossil-fuel

prime-movers and their governors. The controllers for a generator comprise the automatic voltage regulator, the excitation system and, in some cases, a power system stabiliser. There may be significant variations in frequency and voltage during the transient. As a result, the active and reactive power demand of the loads may be selected to be frequency and/or voltage dependent (CIGRE 1990). Transients in the hydraulic system may last many tens of seconds and thus it will be necessary, as a future development, to include boiler dynamics in a long-term model of the system.

A range of disturbances is accommodated by the electrical system software. These include the various types of major faults (e.g. three-phase), line switching and loss of generation or loads.

Integration of the Models of the Hydraulic and Electrical Systems

In the step-by-step solution of the integrated system, three groups of differential equations, together with the solution for the variables in the hydraulic system, are solved simultaneously at each time-step. The first group of differential equations is that describing the motion of the turbine/generator shafts of each machine:

$$\frac{2H}{\omega_o}(\omega_o+\omega')\frac{d\omega'}{dt} = P_{turb} - P_{elec} - P_{loss} \qquad (1)$$

in which H = inertia constant of the unit (MWs/MVA), ω_o = synchronous speed (elec rad/s), ω' = deviation from synchronous speed of ω_o (elec rad/s), P_{turb} = mechanical power supplied by turbine, P_{elec} = electrical power provided by generator, P_{loss} = power losses in the generator (the powers are in per unit on generator base MVA).

The second group of differential equations describes the behavior of generator internal voltages, the automatic voltage regulators, the turbines and governors of fossil-fuel units and any load dynamics. The third group of differential equations represents the dynamics of the wicket-gate servo motor, servo amplifiers and the governor, including, for example, a PID control algorithm. The inputs for this set of equations are the turbine speeds and the speed or load set-points.

The three groups of differential equations are combined to give a set of first order differential equations of the form

$$\frac{dx_i}{dt} = f(x_1, x_2, x_3, \ldots, x_n, u_{ref}) \qquad (2)$$

in which $x_1,\ldots,x_n$ are the unknowns states and u_{ref} are controller setpoints.

This set of of first order differential equations (Eq. 2) is solved using a predictor/corrector method. The procedure for solving the differential equations and the algebraic equations for both the electrical network and the turbine is as follows.

From the load flow of the electrical power system, the steady-state electrical power outputs of the generators are supplied to the program. To these values are added the generator losses to obtain the turbine torques at synchronous speed. Given fixed reservoir levels, the following are calculated including the steady-state heads, flows and gate openings in the hydraulic systems. The step-by-step integration of the non-linear differential equations of the governors and electrical system then proceeds. At each time-step the following steps are implemented.

1. Using the generator voltages and rotor angles calculated at the previous time-step, the electrical system software calculates the complex bus voltages at the current time-step.

2. Knowing the voltages and network admittance matrix, the electrical power output from each generator, P_{elec}, is calculated.

3. Given the values of ω' (speed deviation) and y (wicket-gate position) from the previous time-step, the hydraulic system software calls a Newton-Raphson solver routine to calculate six unknowns for each turbine. These variables are v (dimensionless flow), H_{pu} (head upstream of the turbine), H_{pd}, (head downstream of the turbine), WHH (normalised head drop across the turbine), WBB (normalised mechanical torque produced by the turbine) and x (dimensionless abscissa position on the turbine characteristic curves).

4. The torque developed by each turbine, P_{turb}, is calculated from the variables determined in step 3. The P_{turb} value is used in the torque differential equation (Eq. 1).

5. The program moves to the next time step, beginning again at step 1. This procedure is followed for the duration of the simulation study.

Case Studies

In order to demonstrate the capabilities program, the results of two simulation examples using the integrated computer model (HAMMER) are presented below. The first network simulated appears in Fig. 1. This network is based on a network modeled by Wylie and Streeter (1983).

The network modeled by Wylie and Streeter featured an upstream reservoir, tunnel and turbine discharging to an open tailrace downstream of the draft tube. The network in Fig. 1 behaves in the the same way, but also

features a downstream pipe and reservoir. The downstream pipe has a large diameter to simulate the effects of the open tailrace at the end of the draft tube. Data describing the network appears in Tables 1, 2 and 3. Units for this first case study example are U.S. Customary as used by Wylie and Streeter. HAMMER is able to use either U.S. customary or metric units.

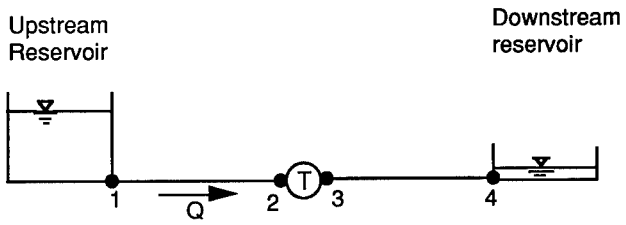

Figure 1: Hydraulic Network Modeled for Case Study (Example 1)

Table 1: Network Data (Example 1)

Upstream node	Downstream node	Length (ft)	Diameter (ft)	Friction factor	Wave speed (ft/s)
1	2	410	18	.013	4100
3	4	410	1000	.013	4100

Table 2: Reservoir Data (Example 1)

Reservoir	Head (ft)
1	258.3
2	0

Table 3: Turbine Data (Example 1)

Rated Flow:	4025 cfs
Rated Head:	269 ft
Rated Torque:	3.03×10^6 lb-ft
Rated Speed:	200 rpm
WR^2:	3.55×10^6 lb-ft^2

The transient is caused by a change in the electrical power output from the turbine. A step change occurs, changing the output power from the steady state value of 61.7 MW to 44.8 MW. Figure 2 shows the HGL upstream of the the turbine during the first 20 seconds after the power change. The figure compares the Wylie and Streeter (1983) results and the HAMMER results.

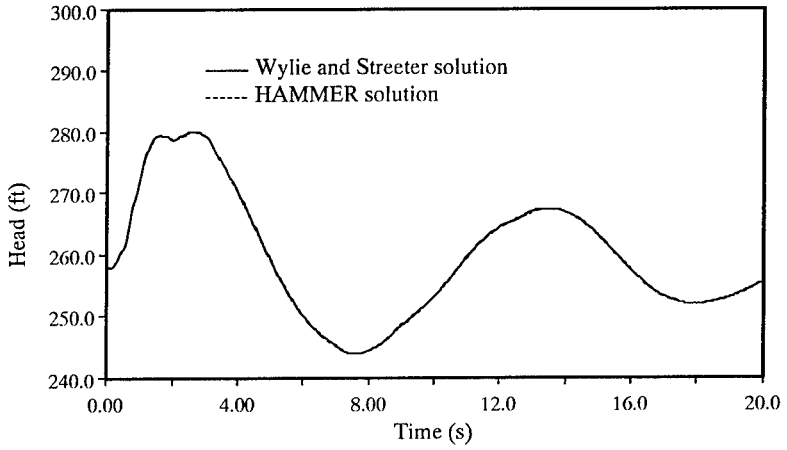

Figure 2. HGL Upstream of the Turbine (Example 1)

A second example network has been modeled in order to show that HAMMER can handle multiple turbine problems. This network, shown in Fig. 3, is very similar to the first network modeled. In fact, it is two of these turbines in parallel, together with a pipe leading to the upstream reservoir.

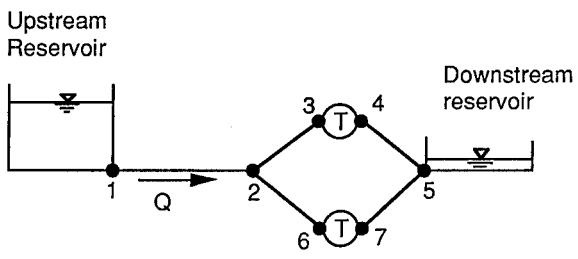

Figure 3. Layout of the 2 Turbine System

Tables 4, 5 and 6 give the data for the 2 turbine system.

Table 4: Network Data (Example 2)

Upstream node	Downstream node	Length (ft)	Diameter (ft)	Friction Factor	Wave speed (ft/s)
1	2	8200.	1000.	.013	4100.
2	3	410.	18.0	.013	4100.
2	6	410.	18.0	.013	4100.
4	5	410.	1000.	.013	4100.
7	5	410.	1000.	.013	4100.

Table 5: Reservoir Data (Example 2)

Reservoir	Head (ft)
1	257.7
2	0

Table 6: Turbine Data (Example 2)

Rated Flow:	4025 cfs
Rated Head:	269 ft
Rated Torque:	3.03×10^6 lb-ft
Rated Speed:	200 rpm
WR^2:	3.55×10^6 lb-ft^2

The transient for example 2 is caused by the same step change as before (61.7 MW to 44.8 MW) on turbine 1. Turbine 2 remains at a constant power output of 61.7 MW. The resulting HGL upstream of each of the two turbines are shown in Fig. 4.

Conclusions

An outline of an integrated model for the detailed simulation of the hydraulic, electrical and governor systems for hydropower plants has been presented. The model is very flexible and allows any configuration of penstocks, tunnels, reservoirs, multiple-turbines, and surge tanks to be investigated. In addition the electrical system can be modeled in detail. This type of model should provide the capability to investigate the behavior of the entire system when subjected to large magnitude disturbances. The interaction between the individual sub-systems and the systems' response when a surge tank is incorporated or a different type of governor is used may also be investigated. A predictor/corrector scheme has been used to solve the governing set of non-linear first order differential equations which describe the turbine behavior during the transient event. The computer

model should provide a useful tool to hydropower planning and design engineers.

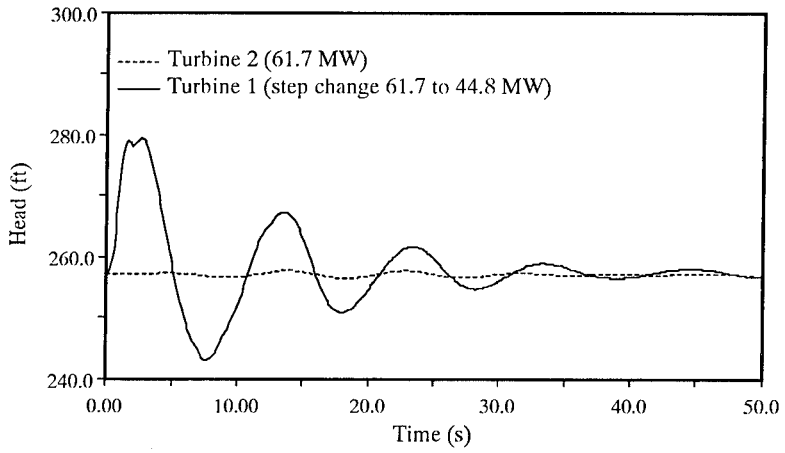

Figure 4. HGL at Upstream of Each of the Turbines

Acknowledgements

The funding support of the Australian Electricity Supply Industry Research Board (AESIRB) is gratefully acknowledged. The AESIRB has funded this research over the period 1991 to 1993. The provision of the electrical system dynamics software and advice by Dr. A.M. Parker of the University of Adelaide is also gratefully acknowledged.

References

Arrillaga, J. and Arnold, C.P. (1983). "Computer modeling of electrical power systems. " John Wiley and Sons.

Brekke, H. (1974). "Stability studies for a governed turbine operating under isolated load conditions." Water Power, Sep., 333-341.

Chaudhry, M. H. (1970). "Governor stability of a hydroelectric power plant." Water Power, April, 131-136.

Chaudhry, M. H. (1980). "A nonlinear mathematical model for analysis of transients caused by a governed Francis turbine." 3rd International Conference on Pressure Surges, Canterbury, England, March, 301-314.

CIGRE Study Committee 38. (1990). "Load modeling and dynamics." Electra, No. 130, pp 123-141, May.

Hirano, K., Kuwabara, T. (1979). "Recent control systems for hydropower plants." Hitachi Review, Vol. 28, No. 4, 193-198.

Hovey, L. M. (1960). "Optimum adjustment of governors in hydro generating stations." The Engineering Journal, Nov., 64-71.

McPheat, J., Simpson, A. R., Gibbard, M. (1992). "Integrated dynamic modelling of hydro-electric power plants-progress on development of a water-hammer computer model." Research Report No. R91, Department of Civil Engineering, University of Adelaide, South Australia, 36 pp.

Stagg, A.W. and Wl-Abiad, A.H. (1968). Computer methods in power system analysis. McGraw Hill International Editions.

Wylie, E.B. and Streeter, V.L. (1983). "Fluid transients." FEB Press, Ann Arbor, Michigan.

Upgraded Control System for Vianden Hydro Plant

Authors: Ralf Brosowski, Karl-Ludwig Holder and Mathias Krecké,
Sales and Project Manager*, Chief Engineer of Control System** and Manager of Electrical Department***
Co-Author & Presenter: Wolfgang Butz, Sales and Project Manager+

Abstract

The conventional control system at the Vianden power station in Luxembourg, one of the largest and most important pumped-storage plants in Europe, is replaced by a computerized control system. This presentation describes the concept and technical features of the new system, and the resulting improvements for station operation and management.

Introduction:

The 1.000 MW Vianden pumped-storage station, built to produce peak power, is connected to the German RWE-Energie AG grid and represents an important link in the Western European interconnected network.

RWE-Energie AG, the largest power supply company of Germany, provides the Vianden station with the required pumping energy and receives, during peak load periods, the power generated by Vianden. In practice, the operation of the power station is exclusively determined by a central dispatching center in Germany, depending on the momentary load demand.

* Marketing and Sales Service, Dept. KW/H1, ABB Kraftwerke AG, Hydro-Power Division, Kallstadter Strasse 1, D-6800 Mannheim 1, Germany
** Engineering Department, Dept. KW/H4, ABB Kraftwerke AG, Hydro Power Division, Kallstadter Strasse 1, D-6800 Mannheim 1, Germany
*** Société Electrique de l`Our S.A. BP 37, L-2010 Luxembourg
+ Marketing and Sales Service, Dept. KW/H2, ABB Kraftwerke AG, Hydro-Power Division, Kallstadter Str. 1, D-6800 Mannheim 1, Germany

Vianden is operated by the Société Electrique de l`Our (SEO) and has been in operation since 1964, with a conventional control system; this included automatic sequence control by relays which have been used to operate the powerplant in a safe and reliable manner. At the time of its installation, this relay technology was the most advanced and reliable solution for a hydro plant control system.
Automatic control of the sequences, and a number of diagnostic and optimizing functions, have become standard for modern control systems. Therefore, SEO decided on a step-by-step modernization programme for the Vianden control system, taking into account the periodic overhaul and maintenance works for the units. A contract to renew the complete control system was awarded to the Hydro-Power Division of ABB Kraftwerke AG, Germany in 1989.

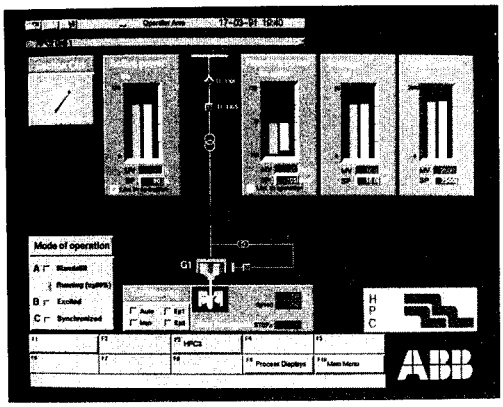

Pict. 1.
Process display:
Unit Control

HPC concept

Based on recent hardware and software technologies ABB has developed the powerful HPC (Hydro Power Control) concept. The HPC concept is suitable both for new installations and for the refurbishment and renewal of existing control systems, such as at Vianden. The principal design of the HPC concept for Vianden is a hierachical structure, complying with the control task pyramid shown in Fig. 1.
At the bottom of the control pyramid, the group (unit) control level has been defined to cover all the functions for control, supervision and protection of the various sections of the plant.
These independent control units represent the generating sets, power lines, switchyards, auxiliary systems and so on.
This distribution of functions to independent control units means that a single fault will have a minimal influence on the total control system,and therefore increases the availability of the control system and the whole plant.The station control level covers the overall control and self-diagnostic functions of the different computers and the more common plant control functions, such as:

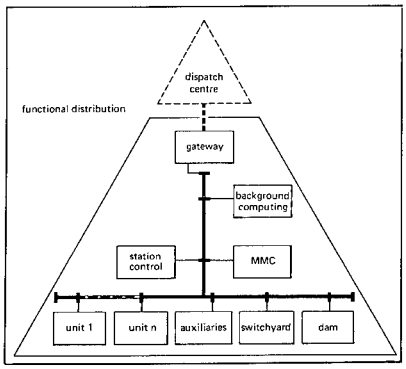

Fig. 1.
HPC control task pyramid bottom-up design.

* joint control of the units;
* water level control;
* control of the spillway gates;
* overall energy and water calculations;
* acquisition of water data and building data and
* trend analysis of water and energy values.

In addition to the station control level, advanced color graphic workstations provide all the information from the unit and station control levels. These MMC stations (man-machine communication) are connected to the same high speed communications network, with a capacity of 10 Mbit/sec, to which the unit and station control level microcomputers are also connected.
The MMC systems (local and/or central) incorporate the following functions:

* presentation of process displays;
* dialogues for controlling the power station;
* event and alarm handling;
* trend data and trend displays;
* report functions;
* display print-out;
* system supervision of all computers and input/output boards and
* display design and integration.

For energy management, statistical analysis, reports, power production planning and long term archiving of plant data, a background computer (station management computer) can also be connected to the control network.
Software modifications required at any control level can be carried out at any time (on-line) by one central programming system connected to the communication network.

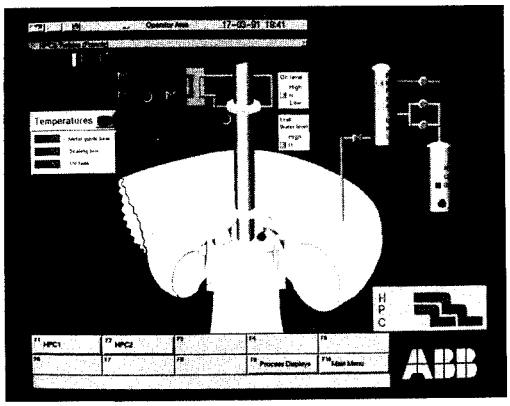

Pict. 2.
Process display:
Turbine control

The approach at Vianden

The replacement of a conventional control system by a decentralized computerized system in a plant which is in operation not only involves technical challenges, but requires careful logistical scheduling; it also involves re-education of staff and integration of the new control philosophy.

The main improvements achieved with the new control system, compared with the old system, will be a better diagnostic capability for the control system itself, for the automatic start/stop and transfer sequences, and for the units. Furthermore, the education of the plant operation staff in using the computer technology will not only influence plant operation, but also reduce administration and statistical paperwork which will become more and more computerized.

Functional requirements

A particularly important requirement for pumped-storage plant control systems is the need for fast control actions to enable quick and safe startup and transfer sequences.
Because of the large number of starts and transient conditions of a pump-turbine unit, all the mechanical components, such as the bearings, runner blocks, generator rotor, pressure valves and so on, are heavily loaded; therefore, supervision of all these systems is an essential function of an intelligent control system to prevent failure. The typical measurement elements for preventive supervision are vibration sensors, temperature detectors and noise analysers; measurement of execution times for a complete sequence and the steps of a sequence are also made. Statistical data and related curves help to identify disturbances and modifications in the behaviour of the

unit and its hydraulic/mechanical systems. Discovering these disturbances at an early stage avoids expensive repair work and costly down-time of the unit.
The general requirements for a peak load plant such as Vianden demand a very high availability of the plant, which implies a reliable control system with redundant control circuits where appropriate diagnostic routines for the control functions, including admissible operator actions in each situation, improve the overall control and availability of each generating set.
With the new system at Vianden, for example, up to ten units can be started at the same time in different modes, several times each day. Each start of a unit in a new operating mode generates approximately 200 events and numerous commands.
All events are registered on the local and central MMC systems for operator information and for trouble shooting analyses. A major requirement to help the plant operator make correct decisions rapidly in critical situations, such as process faults, is the concentration of the events and alarms. This system reduces the information and communication on that fault section to important messages only, so that the operator can easily manage the situation.

Control system structure

The Vianden complex consists of three main plant components: the underground plant with nine 100 MW units; a separate tunnel plant with the 200 MW pump-turbine and the small powerplant at the dam of the lower reservoir, with two 3 MW units. The new control system connects these plants with fibre-optic links to a local area network (LAN).
The LAN system is the backbone of the new control system. Principally, it is a LAN bus system, but physically it is a star configuration of independent fibre-optic cables.
According to the HPC concept, process stations for local control functions, MMC stations for supervision and plant operation, and one background computer system for long term data archiving and plant management functions, are connected to the LAN. All the systems are based on powerful 32-bit microprocessors with multitasking operating systems of high efficiency, with short response times.
Two process stations for the units and for the essential functions of the station auxiliaries are installed, to improve availability (one system is for emergency back-up functions).
The MMC stations in the central control room are also duplicated, not only for redundancy, but also because of the manifold tasks of the operators. One additional mobile station has been supplied, which can be connected locally to each process station. With that system, the same plant information and operation functions as in the central control room can be made available all around the plant.

Unit control

All the related surroundings for the units have been completely renewed. The old local unit control board for the units has been replaced by the new one consisting of 10 cubicles. All the sensors and actuators have also been replaced by new systems.

The control principles for each unit have not been changed. Two control levels have been defined:

* local unit control (machine-hall) and
* central unit control (central control room).

From these two levels, a unit can be started up for the various modes of operation. There are four stable modes of operation for each unit:

* turbine mode (TU);
* pump mode (PU) and
* phase shifting mode (PS);
* standstill (ST).

For the Vianden horizontal shaft units, 13 transfer sequences in addition to the four stable operation modes have been provided, to enable a quick and safe change of operation modes instantly.
Detailed sequence-step elements supervise all transfer actions and in case of failure, a diagnostic system is available to the operator immediately.
Automatic control on the local and central control level for complete sequences or step by step mode is possible. For each unit, one local MMC-system has been connected, showing in detail all the control sequences, including the criteria for the past, present and next control steps.

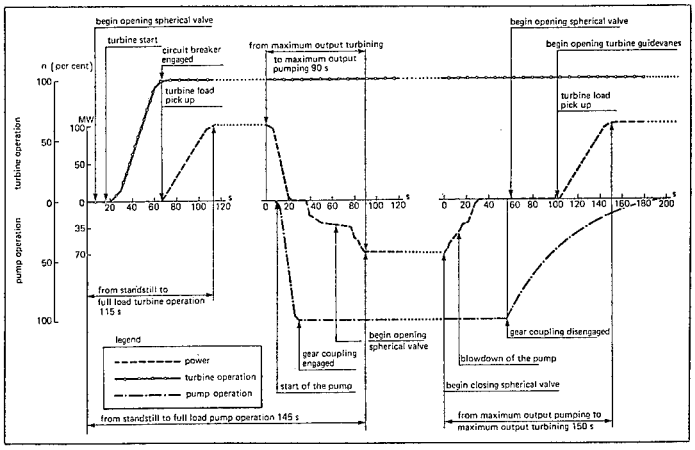

Fig. 2. Mode changing diagram for machines 1 to 9.

Fig. 2. shows the typical transfer curves for one complete transfer procedure from standstill (ST) to turbine mode (TU) and to pump mode (PU), including the stop sequence, with parameters such as speed and opening. It should be noted that these transfer times have been kept very short with the new computerized control system.
In addition, functions have been included which cannot be achieved with conventional relay control (for example, repeating the coupling procedure for coupling the pump to the shaft).
There are three stop sequences, to be selected according to the status of the unit or the kind of failure that has happened:

* quick shut-down (mechanical faults);
* emergency shut-down (electrical faults) and
* normal shut-down.

The local and central control levels for unit control provide for safe operation of each unit. In the local control mode, there is, in addition, a possibility for manual control, using push buttons and instruments on the manual control cubicles, with safety interlockings to avoid dangerous commands to the actuators.
The structure of the automatic control program is arranged so that in each sequence step, the operator can change from automatic to manual control and vice versa. This means that, in the event of any failure in the automatic sequence, the local operator can change to manual control and make the next step manually. After this step, the operator can change back to automatic control and the sequence will continue.

From the central control room, the automatic start/stop programs for changing the operation modes of each unit can be started and stopped by using the station MMC systems or conventional push buttons. In this central control mode, the unit is also completely supervised.
A start/stop command from the German load dispatch center is given to the operator, giving information on how many units have to bestarted and in which operating mode. When the units are connected to the grid, the loading of the units is done directly from the remote dispatch center by sending a load participation factor directly to the turbine governor.
Special functions have been included as diagnostic systems for the supervision of the units, for the start/stop sequences and for the control system itself. All the sequences, for example, have associated indications of preconditions before starting any transfer program, with a possibility of overriding if there are missing conditions.
In the case of sequence failure, all the missing criteria of the next step are displayed. Here also, there is an overriding option for the operator and the possibility of step repeating.
In addition, special history registers (post mortem reviews) are implemented to memorize the situation in the case of a unit failure or a failure of one sequence. With these data memorized in the history register, a high time resolution can be achieved for each

measured value before and after the failure, within a predefined overall supervision time.

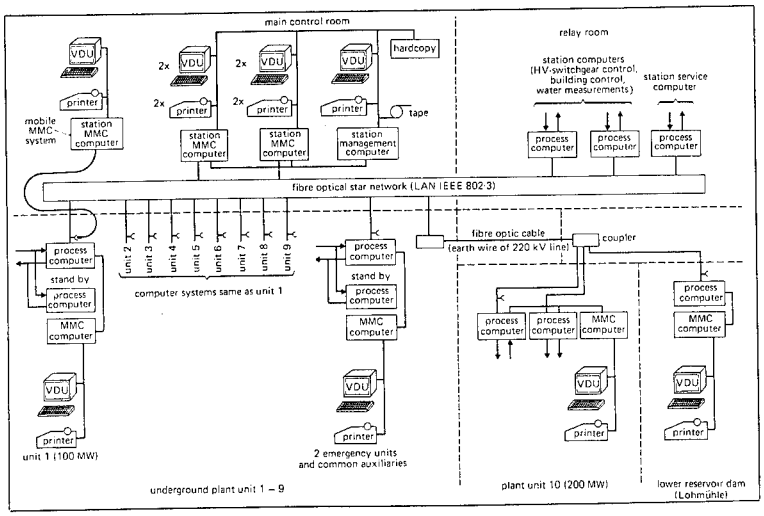

Fig. 3. Principal diagram of computerized control systems.

Only some of the main control and supervisory functions have been highlighted here. The unit process computer is, of course, not only be used for logical control of sequences; the more common control functions such as set point control, selection of temperatures for the conventional recording system and the counter function, have also been provided as standard.

HV switchgear control

The HV switchgear is conventional 220 kV equipment with four busbar segments (Fig. 4). Each segment has one outgoing line to a 220 kV substation near Vianden. The segments can be connected to a common busbar with disconnectors. Operation of the line disconnectors, the busbar disconnectors and the grounding switches is controlled by using the central MMC-systems. All interlocking conditions for operating a disconnector are verified by the computer, and in the event of missing conditions, the operator is provided with details of the situation. Because of the local switchgear configuration and the rather large distances to the remote circuit breakers in the Vianden substation there is a complex interlocking trip system for the unit circuit breakers. This system is supervised and the measurements indicated.

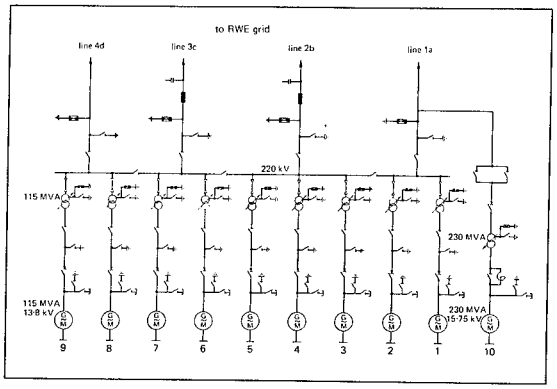

Fig. 4
Single line diagram.

Station service control

The station service of Vianden is a complex system with various power sources. Normally the power is supplied by the 220 kV grid or through a 20 kV incoming line. Two emergency turbine sets also exist and, in addition, the two units of the power plant at the dam of the lower reservoir may be used for auxiliary power supply. Therefore, a lot of control and interlocking functions are necessary for station service.
For the complete station service, two computer systems are used. One system controls the two emergency turbine sets and the drainage system in the machine hall (with a back-up computer for safety reasons), and the second is installed in the main switchgear room.
The communication channels between these two computers is the LAN bus.
A large pumped-storage plant such as Vianden has a lot of station auxiliaries such as an air ventilation system, fire detection and fire fighting systems, a smoke exhaust system, and so on. The new computerized control system improves also the supervision and control of these systems.

Water level measurements and analysis functions

Water level measurements and analysis functions are very important for the pumped-storage plant. The existing systems for measuring water levels in the upper reservoir, the lower reservoir and of the river Our, which flows through the lower reservoir, are used to calculate the actual reservoir volumes and the overflow set point for the lower reservoir dam. These calculated values are also used for electrical energy storage calculation.

Because of the importance of these functions and the complexity of adapting the existing water measurement and indication system, a computer is used for these functions. As well as the calculation and MMC functions, the computer supervises all water measuring systems as far as admissible limits and gradients of the signals are concerned.

Information management functions

A powerful multitasking computer, with large mass memories, is used as background computer for processing the huge volume of input data. The main functions of the background computer are:

* the logging of events, analog signals and computer values for historical logs;
* preparing reports for the power plant management, based on the historical logs (energy and water reports);
* notebook functions for operator logs (shift reports, and so on);
* long-term analysis of process data (long-term supervision of the units and the plant, based on characteristic process data) and
* comprehensive monitoring functions (graphical diagrams and trend curves) depicted by different data.

The background computer, with its comprehensive analysis and diagnostics, plays an important role in the long-term improvement of plant reliability and availability. The open software system architecture will make it easy for the utility to extend the background computer functions. Typical fields could be the implementation of knowledge-based systems for plant optimization and maintenance scheduling. Administrative functions can be added, too.

Conclusion

For many existing plants, modernization is a good investment. A computerized control system offers both increased income by enhancing the efficiency or capacity of the plant and minimized interruption times because of better diagnostics and safer operation.

In summary, the power plant control concept at Vianden meets the old and new hydro power control demands, but also provides possibilities for extensions to meet future requirements of the owner. The HPC concept has been implemented not only in large hydro power plants but also at schemes of smaller size in other parts of the world.

Improving Performance with a Hydro Control System

James Cook[1], James Walsh[2], Jamie Veitch[3]

Abstract

Through the proper use of modern instrumentation, optimal operation of hydroelectric plants under increasing environmental constraints is possible. The Hydro Control System (HCS) discussed here measures on-line turbine-generator performance and provides optimized plant operation by properly allocating required generation among units. The feasibility of one key element of this system has been demonstrated at the School Street hydroelectric plant in Cohoes, New York. Initial tests indicate that performance improvements of at least three to four percent are possible with this element. The HCS system is summarized and a detailed description of the feasibility demonstration and the resulting benefit assessment is provided.

Introduction

IIT Research Institute, Accusonic O.R.E., Inc., and Niagara Mohawk Power Corporation have collaborated to develop a Hydro Control System for optimizing power plant performance. (Hosmer, 1992) An Initial Operating Capability (IOC) version of the system is being implemented at the School

[1]Senior Science Advisor, IIT Research Institute, 4600 Forbes Blvd., Lanham, MD 20706-4324

[2]Senior Project Engineer, Accusonic O.R.E., Inc., Falmouth Heights Road, Falmouth, Massachusetts 02541.

[3]Superintendent, Power Delivery, Niagara Mohawk Power Corporation, School Street Hydro, Cohoes, N.Y., 12047.

Street Plant in Cohoes, New York. This paper addresses a test of one key element of the system, the Tactical Planner, which was recently implemented as a prototype at School Street.

The HCS IOC Functionality

The primary focus of the HCS IOC functionality is optimum allocation of discharge between the penstocks for a hydro project operating in a run-of-the-river mode. Future implementations of the HCS will also include discharge and power following modes. The control process providing these capabilities is referred to as the tactical planner in the full HCS system.

The operation of the IOC system is illustrated in Figure 1. Sensors measuring flows, levels, and powers are acquired by an Accusonic 7432 instrumentation logging system. This data is available on the digital display of the 7432 computer. It is also passed on to a second computer running the HCS IOC software. Here trending analyses are performed and the results are displayed in a graphical format as illustrated in Figure 2.

In addition to displaying the monitored data, the HCS IOC also recommends the necessary plant discharge to bring the pond to a desired level at some specific time. This recommendation is provided as target flows

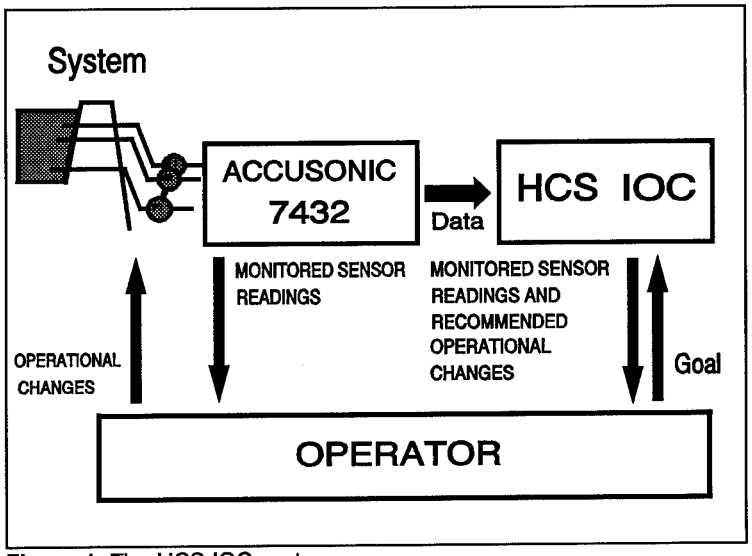

Figure 1. The HCS IOC system.

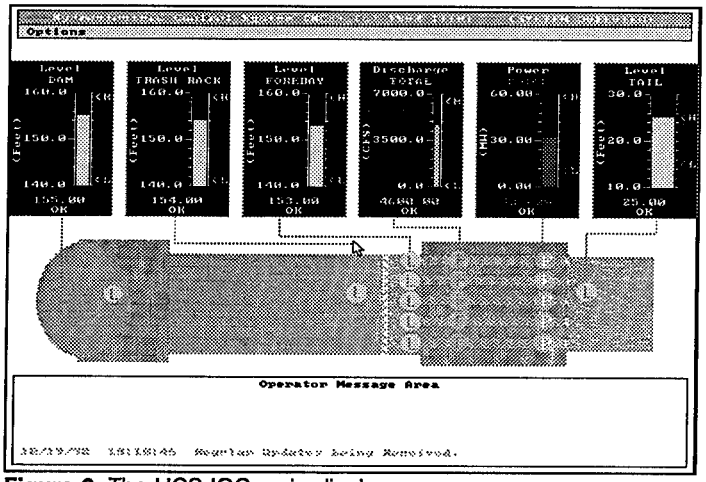

Figure 2. The HCS IOC main display screen.

for specified units so that the level is attained while maintaining optimum overall plant efficiency. The system is only advisory. The operator has to take independent action to invoke the system's recommendations.

Figures 3 illustrates the major system components. The Monitor performs the trending analyses and creates the graphical displays. It also accepts a goal statement from the user which specifies the pond level to be attained by a given time. The total plant flow necessary to meet the goal is continuously compared with the current plant flow.

When the operator feels this comparison indicates the need for a gate change, he can ask the planner to develop a new allocation. The planner provides the operator several options. He can ask it to consider all units or some subset of units, specifying his own loading for those not to be considered or indicating that they are not to be used.

The planner utilizes a database of pregenerated "optimum" solutions to obtain the recommended unit flows. This solutions database is obtained in a two step off-line process as illustrated in Figure 4. First operational data from the plant is used to provide analytical models of the power and efficiency, as functions of gross head and discharge, for each penstock-turbine-generator system. Then these models are used to fill out the solutions database.

Creating the solutions database is the most involved part of the entire process. If all possible combinations of unit flows and gross heads were

represented in the database its size would be impossibly large. To limit its size and keep the time to generate the database within reason several heuristics

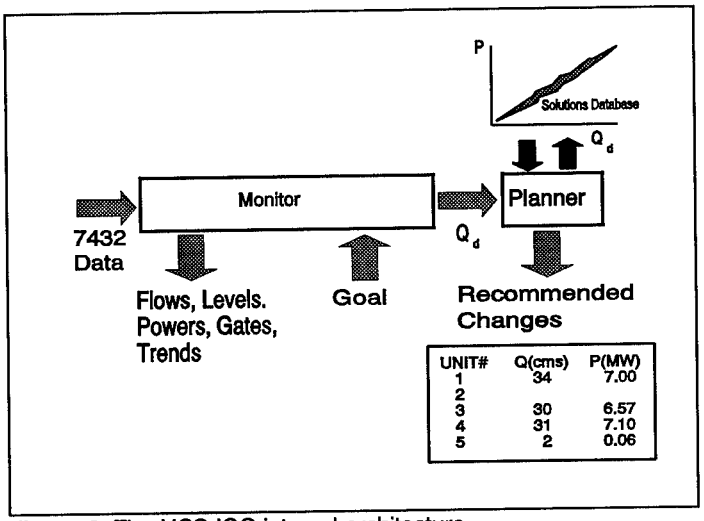

Figure 3. The HCS IOC internal architecture.

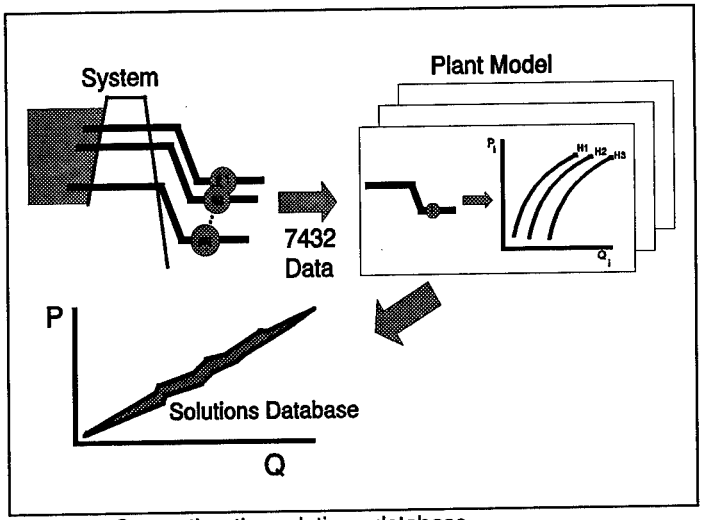

Figure 4. Generating the solutions database.

are used to include only optimum or at least very good solutions. Since the unit characteristics may vary considerably over the range of gross heads, solutions must be obtained at several heads. At School Street the gross head varies from 28.0 m to 29.3 m (92' to 96') and models were developed at three gross heads.

The School Street Hydro Plant

The School Street Hydro facility was constructed in 1913, during the period when many sites were converted from direct mechanical drive to hydroelectric facilities. The existing power canal dating to the mid 1800's was expanded and diverted directly back to the Mohawk River through the hydroelectric plant at the base of Cohoes Falls. Cohoes is located at the confluence of the Mohawk and Hudson Rivers, approximately 12 Km (7 mi.) north of Albany, New York.

The development utilizes the 26 m (85') drop at Cohoes Falls by way of a low, masonry diversion dam and a 1340 m (4400') long canal parallel with the river around the falls. The flow is then passed through a rack house into five penstocks, running almost vertical to the powerhouse. This arrangement results in a gross head of approximately 28.7 m (94').

The powerhouse consists of five vertical Francis turbines with direct connected synchronous generators. Originally designed to develop a total of 34 MW (Units 1-4 @ 6 MW and Unit 5 @ 10 MW), the plant is in the midst of upgrading and generates at slightly over 38 MW during optimum conditions. Three of the four smaller units have had modern design runner replacements in the last four years and the fourth will have a new runner and generator rewind during the summer of 1993. Unit 5 is scheduled to have a runner replacement and rewind in 1994. All auxiliary systems and controls are also being updated.

This powerhouse was originally manned 24 hours a day to maximize the generation potential of the Mohawk River. As is with many developments, the river has become more regulated and present economics dictate a remote operation. Ongoing operation and maintenance is carried out on a scheduled basis, and the plant is manned only 25% of the time. Although there is daily dialogue between the on site traveling operator and the remote operator, the remote operator is attempting to maintain a level pond, canal, and power output while also being responsible for the operation of several other hydro facilities and the electric system in the area. Thus the resulting operation of this hydro plant may not be the optimum for the given flow conditions. The conditions of most concern are those between the lowest flow of operation and the maximum hydraulic capacity of the plant where there are many possible choices for allocating the flows.

This large range of possibilities makes it difficult to make even a reasonably good choice for allocating the flows between units in the most efficient manner. Without the knowledge gained by experienced operators located at the site continuously, it is clear that the selection of the flow distribution is typically only very good as opposed to optimum. This combined with the ever changing physical plant characteristics and abrupt changes such as a new turbine or generator rewind makes the process even more of a best guess method, until much experience is gained.

The School Street Testing

The objective of the test was to determine if the tactical planner would provide improved operational efficiency. The test concept was to compare plant operation using the tactical planner to that obtained with standard operating procedures. The tactical planner provided for the test consisted of a level following mode since the strategic operation of School Street is typically "run of the river," which requires keeping the pond level constant.

A model 7432 collects power, efficiency, head, wicket gate opening, and flowrate for each unit at School Street and periodically logs this data to disk. During the spring and early summer of 1992 data was downloaded and reduced to form the plant model used for the test.

Nine separate tests were performed over a three day period (August 25 - 27, 1992) at different inflows. This was coordinated with other utilities both upstream and downstream. Each test consisted of the following steps:

a) A 1/2 hour period consisting of an inflow change and a load change by Niagara Mohawk operators.
b) An hour of data collection to establish a baseline efficiency.
c) A load change according to the HCS recommendations followed by a 1/2 hour period to allow conditions to stabilize.
d) An hour of data collection to establish the efficiency under the HCS recommended settings.

Unit #2 was not in service since it was being overhauled and the availability of Units#4 and #5 was impacted during the first two days of testing by other maintenance which couldn't be rescheduled. The tests used units 1, 3, and 4 on 8/25; 1, 3, and 5 on 8/26; and 1, 3, 4, and 5 on 8/27.

The allowable range of discharges involving some or all of these four units is from about 17 cms to 156 cms (600 cfs to 5500 cfs). At the very low and high ends of this range the choice of potential operating points is trivial, and the Tactical Planner isn't expected to be able to improve typical operations for

discharges in these regions. In the middle of the range the number of choices is very large. In this region it is often not at all obvious how to set the plant for optimum operation since there are so many possible ways to get a given flow from the combination of units. Thus, in this range the expectation for improved operation is greatest.

Test Results

The results from Test #7 (100 cms - units 1,3,4,5) are probably the most interesting of the nine tests. Figure 5 provides a graphical illustration of the operator and HCS set points chosen for that test. The operator chose a solution which loaded the three best of the four available units, obtaining a good efficiency of 81.3%. HCS chose distinctly different set points, and used all units to improve plant efficiency by 2.2%. This probably was obtained by a combination of avoiding the motoring loss for unit #1 and taking better advantage of the high efficiency of unit #4.

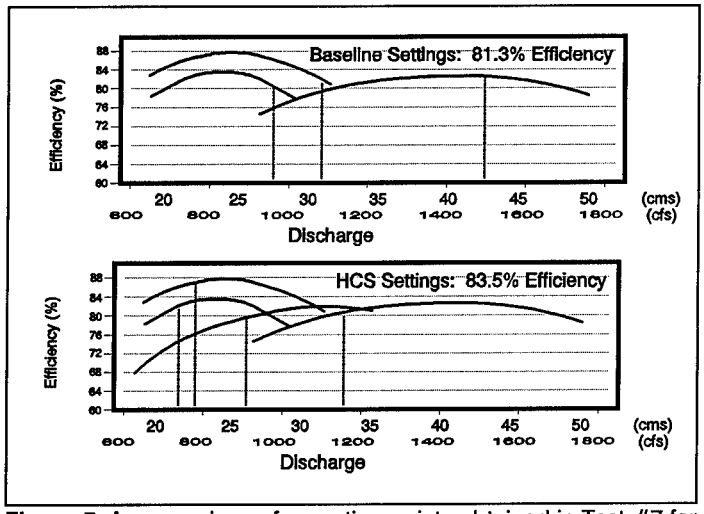

Figure 5. A comparison of operating points obtained in Test #7 for a discharge of 100 cms.

Table 1 contains a summary of the different discharge combinations for each test and the efficiencies obtained. The discharge combinations are given as a percentage of the maximum flow at 28.7 m (94') gross head. The efficiencies are calculated by dividing energy delivered by the maximum energy available. The efficiency improvement averaged 3.3%.

		---- % of Max Flow ------					
Test	Mode	#1	#3	#4	#5	Eff.%	Change
1	Baseline	85	59	100		81.0	
	HCS	100	71	100		78.8	-2.2%
2	Baseline	100	0	85		78.4	
	HCS	90	0	81		80.9	+2.5%
3	Baseline	86	0	0		61.3	
	HCS	0	0	82		72.5	+11.2%
4	Baseline	77	63		97	81.6	
	HCS	95	59		90	83.5	+1.9%
5	Baseline	0	63		91	80.8	
	HCS	79	51		73	82.8	+2.0%
6	Baseline	62	50		0	74.4	
	HCS	0	0		89	76.5	+2.1%
7	Baseline	0	64	98	88	81.3	
	HCS	74	49	70	68	83.5	+2.2%
8	Baseline	75	0	0	68	72.2	
	HCS	0	0	73	74	81.0	+8.8%
9	Baseline	0	0	95	0	68.3	
	HCS	0	0	88	0	69.5	+1.2%

Table 1. A comparison of Baseline and HCS allocation settings.

Benefit Analysis

In any hydroproject there are always many more potential areas for investment than available resources. Thus, a decision to implement a system such as HCS must be made based upon a thorough evaluation of the benefit to be derived. The test results reported have been used to help develop such an evaluation, which is summarized here.

For this case the inflow ranges over which the tactical planner is expected to be able to provide useful improvements are between 35 cms and 135 cms (1200 and 4800 cfs). Using the non-sequential power data derived from the annual flow duration curve for School Street, the increase in MWH available from the tactical planning may be easily calculated. The following Table summarizes the calculation:

Annual (cms)	Flow (cfs)	Prob. of Flow (%)	Baseline MWH	HCS MWH	MWH Gained
135	4800	5	12588	13138	550
120	4200	5	11014	11496	482
110	3800	5	9965	10401	436
90	3200	5	8392	8759	367
85	3000	5	7867	8211	344
75	2700	5	7081	7390	310
70	2400	5	6294	6569	275
55	2000	5	5245	5474	229
50	1800	5	4720	4927	206
45	1600	5	4196	4379	183
35	1200	5	3147	3284	138
Totals			80,509	84,028	3,520

Table 2. The benefit calculations.

Here the first three columns are derived from the flow duration curve. The Baseline MWH is obtained by multiplying the flow by its probability, the average head (assumed to be 28.7 m (94') for School Street), the weight of water, and the average baseline efficiency (75.5% for School Street), and a conversion factor to obtain MWH. The HCS MWH are derived from the Baseline MWH by multiplying by the new efficiency (75.5% + 3.3%) and dividing by the Baseline efficiency (75.5%). The MWH gained is the difference between the HCS and Baseline MWH.

The 3,520 MWH gained represents 4.4% of the total baseline MWH. This represents the expected gain from tactical planning for those times the operation is in the mid range for a multiple unit plant. The annual value of this gain depends upon the value of avoided generation and the size of the plant. For example, assuming an avoided cost of $50/MWH, annual benefits of $175K would be realized.

It is felt that 4.4% is a conservative estimate of the potential improvement. The operators at School Street who provided the baseline settings were

experienced and had been working with the 7432 data for over a year. Their mind set in choosing unit settings was already focused on improved efficiency where possible, and they had the benefit of current models of the individual unit performance. Thus their choices used for the baseline data were often fairly good to start with.

Conclusion

The tests have shown a significant improvement in a 32 MW "Run of the River" plant and have economically justified the IOC implementation. It is important to point out that the benefit discussed here is a product of only one part of the full HCS system. In addition to the tactical planning there are several different areas in which the full HCS system can provide measurable benefits. These include strategic planning to coordinate the operation of several plants, on-line diagnostics to limit unanticipated system degradation, and continuous performance monitoring coupled with a learning component to keep the plant model current.

Thus even greater opportunities for increasing energy production exist. For instance in a storage release facility the strategic capability of the full HCS could be used for retiming the generation to concentrate on peak demand periods and maximizing production during outage times of other plants in the same or neighboring utilities. The performance monitoring alone is likely to continue to become more important in the future with the increasingly stringent environmental constraints being placed on hydro projects.

Many medium sized hydro projects have neither current plant models nor the instrumentation in place to utilize such data efficiently. The unit settings made under such circumstances are often based on a combination of local rules of thumb, loosely based on the original index test data from the specific units involved or from similar units. There are even cases in which such approaches have been automated. Based upon the results reported here, it is felt that such projects could gain an additional five or six percent of the available generation by implementing a system such as HCS.

Reference

C.D. Hosmer, J.T.Walsh, J.M.Audunson, "A New Kind of Advisor for Hydro Plant Operators," Hydro Review, Vol. XI, No.3, June 1992.

RECENT DEVELOPMENTS OF TURBINE GOVERNORS AND CONTROLS

J. Perry Bevivino *

Abstract

Turbine controls advanced dramatically in the 1980's, progressing from relay logic control systems and separate analog or mechanical governors to integrated digital control and governor systems based on a Programmable Logic Controller (PLC).

Innovation in the area of controls was driven in part by developers in the small hydro market, who wanted inexpensive equipment to provide reliable and completely unattended automatic operation. The "big hydro" school of system design which included relay logic controls, mechanical governor systems, and resulted in high costs, came under scrutiny.

PLC systems were found to be an effective plant automation tool. With their flexible programming structure, routines for sequencing auxiliaries, monitoring of permissives and control of start/stop and alarm sequences, the PLC provided reliable equipment at low cost. The demonstrated effectiveness of the PLC for plant automation led to the virtual elimination of relay logic.

The digital based governor, introduced in the mid-1980's, utilizes the advantages of the PLC to provide complete governor capability. Advances in the PLC technology and widespread acceptance of PLC controls made possible the integration of the governor and control system. Lower costs, reduced interconnecting wiring, and interface requirements, as well as smaller space requirements, and the ability to use the remote control systems available for the PLC are some of the benefits of the integrated system.

* Application Engineer/Project Manager, Voith Hydro, Inc., P.O. Box 712, York, Pennsylvania, 17405, Telephone: (717) 792-7000

Specification writers of the 1990's can now choose integrated governor and control systems in the same way that relay logic and analog governors were specified in the 1980's. Whether applied to new turbine projects or the rehabilitation of existing sites, the integrated controller provides a greater level of turbine control than ever before, while reducing costs and maintaining a high level of reliable operation.

I. INTRODUCTION

The hydro industry was overtaken in the 1980's by a wave of new developments in the governor and control fields. Slowly following the lead of other industries, the hydro industry finally shed its reluctance to let electronics and automatic control supplant manual operation.

II. BACKGROUND - THE EARLY YEARS

Anyone who has ever visited a plant built early in this century should appreciate the simplicity of the governor and control systems used at that time. Speed control was provided on almost every unit, through a mechanical governor. The mechanical governor had direct mechanical connections for speed and gate feedback, and developed its output mechanically. Usually, these governors operated at a low oil pressure, and were completely manual in operation. The control systems on these units consisted primarily of an operator who inspected sight gauges and ran the unit. The blade/gate relationship was implemented through a mechanical follower, riding on a metal cam. For many years, the control and governing of a hydro turbine remained simple, hardwired relays for the semi-automatic operation of the turbine auxiliaries, and a mechanical governor for speed control. This type of manual operation was considered quite acceptable, and continued for many years.

Obviously, this arrangement has several drawbacks. First, complete manual operation requires large operating and maintenance staffs, resulting in high labor costs. Second, the mechanical nature of the system does not lend itself to modification or tuning. Something as important as the cam determining the gate blade relationship was fixed and could not easily be changed.

III. ADVANCES IN TECHNOLOGY

Governor Advances:

Over the last few decades, advances in governor technology

followed advances in the electronics industry. Complete mechanical governors with flyballs evolved into mechanical hydraulic governors, which used an electrical signal from a Permanent Magnet Generator or Potential Transformers as a speed input. The electric-hydraulic governor was introduced in the 1960's. This governor used a modular design with custom-designed printed circuit cards that performed the governor calculations and generated the governor output. These governors marked a shift in the reliance on mechanical equipment toward electronics. While this governor was quite successful, it was predicated on the use of proprietary equipment, which made it expensive and difficult to repair. Several types of digital governors were introduced in the 1980's. The early digital governor was designed specifically for governor applications, and included programmable operating parameters, control routines, and a digital gate/blade relationship. The digital governor was made possible by the availability of low cost microprocessors, which were incorporated into a proprietary system.

Control System Advances:

Advances in governor technology were outpaced by control improvements. Hardwired relay logic was used extensively to provide automatic sequencing of auxiliary systems. With the use of timing relays and discrete components, basic automatic control was available to the hydro owner. With older units, the instrumentation was quite simple and the relay logic could be kept simple. However, as time progressed, turbines and their instrumentation began to advance. Thermocouples, vibration probes, and flow switches became more common. This required additional manpower to insure safe operation. Eventually, the control system evolved to include smart annunciators used to indicate alarm and shutdown functions, including sequence of events, and temperature monitors, used to read temperature devices. This type of system proved to be highly reliable, but had several negatives; changes required rewiring, and the number of components made construction expensive.

The emergence of the PLC as a factory automation tool proved to be pivotal in the advancement of hydro controls. The automotive industry pioneered the use of the PLC as a replacement for hardwired logic. Since it was designed as a relay replacement, the PLC performed the same functions of the hardwired relays, while allowing much more flexibility. Ladder logic, which was familiar to most control engineers was used to program the PLC's, allowing many users to quickly learn the programming techniques required.

Unfortunately, this simplicity also proved to be a limiting factor. Most early PLC's had only basic mathematical capabilities. Without higher level math, programming a routine like flow control was extremely complex. The terminals used in the programming of the PLC's were not user friendly, some lacked regular typewriter keypads, and, as anyone who had to use one knows, were very heavy. Advances in microprocessor design allowed newer PLC's to include functions like PID loops, real math, and other functions, while programming software progressed to allow the use of a PC. The use of the PLC provided the ability to perform complex control routines, readily incorporate changes, and interconnect with a wide range of devices.

IV. HYDRO DEVELOPERS AND AUTOMATION

In the 1980's, the hydro industry saw a wave of projects by developers acting as independent power producers. These developers were concerned with maximizing the return on their investment, so maximum generation at the lowest cost was the primary concern. Maximizing income required minimal operating staffs, continuous operation and that the initial investment be kept as low as possible. The strict attention to cost conflicted with the "big hydro" school of hydro design, that required the same system on a 1 MW unit that would be used for a 100 MW unit. Many in the "big" hydro industry had become caught up in the "if it ain't broke don't fix it" school of design, and with their conservative approach, became unwilling to consider new alternatives to the existing systems. No developer could afford to conduct business as usual and still expect to make money on his project. Instead, these entrepreneurs looked for systems to meet the minimum requirements without overspecifying unnecessary equipment.

V. WHAT HAPPENED IN THE 1980'S

The combination of developers searching for low cost automation and the successful introduction of the PLC to the hydro industry around 1980 resulted in the widespread use of PLC based automatic control systems in the hydro industry. The PLC was used to completely automate operation of the hydro turbine, while a separate governor was used to control speed. Automatic routines for starting and stopping the auxiliaries were incorporated into the PLC system. Run-of-the-river plants were operated with water level control, maintaining a preset water level, and allowing plants to operate without full time operators. Providing a separate governor and control system, while technically acceptable, requires substantial

interface during the design, construction and installation of the components.

VI. THE NEXT STEP - THE INTEGRATED SYSTEM

As the 1980's progressed, the electronics industry saw the explosion of the personal computer, and with it, an acceptance of the use of similar tools in automation. This set the stage for the next step of hydro governor and control evolution, which was the incorporation of all controls, including the governor functions into the PLC. The integrated system can include speed control and automatic start/stop sequencing, gate control and operation of pumps and auxiliary systems and checking of permissives. Temperature monitoring, using RTD's or thermocouples, can also be included along with alarm and shutdown sequencing and much more. This approach met with skepticism in the hydro industry, however, as time progresses, the advantages is listed below.

The Advantages of Integrated Systems

- Reduced wiring and interconnection. The combination of the governor and control system reduces the number of components that must be installed and the wiring of those components. It also results in smaller floor space requirements. The complete system can be tested in the factory reducing the amount of problems that can arise when in the field.

- Coordination of design. Since the system is designed as one system no coordination between vendors is required. While this may seem simple, it is much easier to accommodate design changes or other unforeseen developments without many problems.

- Simpler operation and maintenance. Systems with multiple components and locations are usually more difficult to operate and maintain. The integrated system cuts down on the number of components, simplifying operation. Maintenance is simplified by making it easier to master one system and maintain fewer spare parts.

- Adaptability to future control changes. A digital system can be designed to allow the addition of new inputs and control routines. Developments such as adaptive governing or advanced cavitation control or optimization routines, can be incorporated later. This

allows the user to adapt the system hardware and software as needs develop.

- Lower Cost. The advantages in design coordination, hardware requirements, installation, commissioning, future maintenance, and adaptability all lead to reduced costs for the owner.

VII. CURRENT CAPABILITIES

The integrated systems in today's hydro plants, shown schematically in Figure 1, include a wide range of governor and control functions.

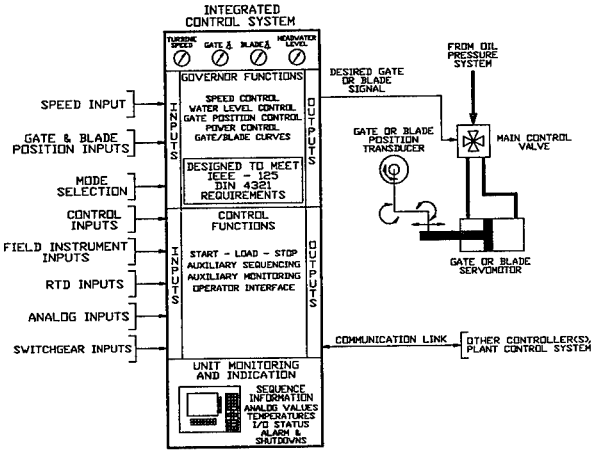

Figure 1
Integrated Control System Functional Schematic

With the flexibility of the integrated approach, the digital system can be designed to include any "governor" or "control" routine necessary for the operation of the hydro plant. Some of the functions commonly included may be:

Operating Modes - Typically associated with governors

Speed Governing - Speed governing or speed droop operation, is used to maintain synchronous speed and to aid system stability.

Speed Regulation - Similar to speed droop operation, except that power feedback is substituted for gate feedback, speed regulation is used to keep power constant.

Power Control - Power Control is used to maintain a desired power output based on an adjustable setpoint, regardless of speed.

Gate Control - Gate position control is used to maintain a gate position based on an adjustable setpoint.

Water Level Control - A preset water level can be maintained based on a setpoint. Turbine flow can similarly be controlled based on a setpoint.

Gate/Blade Relationship - The gate/blade relationship, or cam curve, which selects blade position based on gate and net head, can be implemented.

Gate and Power Limits - The gate limit can be used to prevent operation above or below preset openings. Power limits can be used to protect the generator against overload.

Operating Sequences - Typically associated with control systems

Automatic Start - In an automatic start, prestart conditions are verified, auxiliary systems are started, and poststart conditions are checked. When all conditions are met, the shutdown solenoids are energized, enabling the gates to move. At this point, the wicket gates are opened, settling at speed-no-load. When the circuit breakercloses, an automatic operating mode is engaged until intervention by an operator.

Manual Start - The manual start sequence is similar to the automatic except that the gates are operated manually.

Normal Shutdown - A normal shutdown simply stops the turbine and auxiliary systems in a controlled manner. In this sequence, the system begins to ramp the wicket gates closed at the normal operating rate to the speed-no-load position. The circuit breaker is opened when speed-no-load is achieved. The shutdown solenoids are then de-energized to fully close the gates, and the auxiliary systems are turned off when the unit is at rest. The stop sequence can also include creep detection and brake control.

Fault Shutdowns - Fault shutdowns are variations of the normal stop sequence. In emergencies, the generator breaker and lockout relays trip and the shutdown solenoids are immediately de-energized closing the wicket gates at their fastest rate. A restart is allowed when the fault is cleared and the lockout relay reset. Similar sequences exist where restarting is allowed if the fault clears. For non-emergency faults, from non-critical field devices, a normal shutdown will be initiated and on the breaker trip a lockout relay trip is initiated. A restart is allowed when the fault is cleared and the lockout relay reset.

Partial Shutdown - Partial shutdown is provided when the generator breaker opens without a fault or shutdown input, and will control the turbine gates to maintain rated speed and operate in the isolated mode until a restart is initiated.

Other control sequences including synchronous condenser modes, VAR control, spillway gate interface, time-of-day release, ponding, and creep routines can easily be included in the digital system.

Alarm and Shutdown Annunciation:

Alarm and shutdown annunciation can also be included into the governor and control system. All field devices can be wired directly to the system and identified as status, alarm, and shutdown inputs. For local indication, several options exist, from simple one line data displays to a Man Machine Interface (MMI). In the most advanced version, the display screen can not only replace the traditional lightbox annunciator, but it can also display operating modes and sequence information, all operator setpoints and current analog values, and allow operator input and control. This provides valuable operating and troubleshooting information. The control system should be designed so that loss or failure of the display screen does not affect the operation of the unit.

An advanced display can be designed with an almost unlimited number of screens, which can be customized to meet specific needs. A typical list of screens may include control screens for indication, sequence screens for use while starting or stopping and alarm screens for system annunciation. A time-stamped listing of all current alarms and shutdowns can be provided along with a historical list of all alarm and shutdown information including the time of the occurrence. Even troubleshooting screens, which provide

information on how to correct a fault after it occurs, can be included on a display screen.

Capability for Remote Operation:

One feature of a modern system is the capability to interface with remote monitoring and control systems. Also known as Supervisory Control and Data Acquisition (SCADA), remote systems are particularly useful where the plant is unattended and monitored remotely or in plants with multiple units. Since the integrated digital governor and control system already monitors all field I/O, it is ideal for connection to a remote control system. A typical remote control system can provide remote monitoring of all data input to the control system along with basic control functions like start and stop, data logging, historical trending, alarm indication and automatic reporting.

In the most typical application, a PC is connected via a serial communication link to the control system. In a multiple unit plant, the control systems of several units can be connected via a local area network providing centralized monitoring and joint control capability. The PC software, which can be a commercially available package, is configured as required for each application to provide the control features required. There is a large installed base of PC-based control software that has been developed for applications far more critical than hydro, and these programs can be used successfully on hydro applications without the complicated custom programming or configuration often associated with proprietary software.

IX. CONCLUSION

Specification writers of the 1990's can now choose integrated governor and control systems in the same way that discrete relay logic systems and analog governors were specified in the 1980's. Whether applied to new turbine projects or the rehabilitation of existing sites, the integrated control system provides a greater level of turbine control than ever before while reducing costs and maintaining a high level of reliable operation. Only a separation from traditional thinking is necessary to take advantage of these advances.

On-line Optimal Unit Load Allocation at NEDRE VINSTRA

R. Nylund[1]
O. Wangensten[2]
M. Browne[3]

Abstract

This paper presents a simple solution for automatic settings of optimum load distribution between the five units at Nedre Vinstra. The experience gained, and the benefits of doing so are discussed.

1 Introduction

In Norway practically all electricity production comes from hydropower (99.5%). The production system consists of approximately 500 power stations connected to a national grid.

A major part of energy production comes from plants with big reservoirs and complicated hydraulic systems. The total storage capacity is 2/3 of annual production. Many plants have more than two units, and the units are quite often of varying size and design. Finding the optimum load allocation between the units in such a system for any given condition, is practically impossible without a computer program. This is why we have developed RUNAID® . When a production plan is determined, RUNAID®

1 R. Nylund, Vinstra Kraftselskap, 2640 Vinstra, Norway

2 O.Wangensten, ABB Energi AS, P.O. Box 214 Økern, N-0510, Norway

3 M.Browne, Hydropower Technologies Inc., 1482 Erie Boulevard, Schenechtady, NY

can take over and automatically give optimum setpoints.

2 The owner: Vinstra Kraftselskap

Vinstra Kraftselskap operates Nedre Vinstra powerplant on behalf of its owners; Oslo Energy, Hamar-region Kommunale Energiverk and Stange Kommunale Elektrisitetsverk.

Energy is produced according to orders from the owners. Amounts are agreed on a daily basis, with production specified by the hour. Long time planning (year cycle) is done in a body where owners of all powerplants that are hydraulically interconnected attend. Such meetings take place 2-3 times each year.

The basic task for Vinstra Kraftselskap is to produce a desired amount of energy, at a given time, with a minimum consumption of water.

3 Plant description of: NEDRE VINSTRA

Nedre Vinstra lies approximately 300 km north of Oslo. In 1990 the power station was upgraded. A fifth unit was installed and a new parallel headrace tunnel was provided. Figure 1 shows the waterways schematically.

Turbine 4 and 3 were set in operation 1952/53 and unit 2 and 1 in 1955 and -58 respectively. They are basically of the same design. There are two transformers, one for each pair of generators. Turbine 5 was set in operation in November 1989.

With this installation it is a complicated task to find the optimal load distribution. As can be seen of figure 2, all the assumingly equal turbines (unit 1 through 4) have individual turbine efficiency curves. In finding the best load distribution one must also remember the influence on the neighbouring unit because of a common transformer (units: 1+2 and 3+4) and a partly common, partly individual hydraulic system.

3.1 Control equipment: ABB Master®

Another important change in 1990 was that the existing control equipment was replaced by a new system from Asea Brown Bovery (ABB Master®), ensuring:

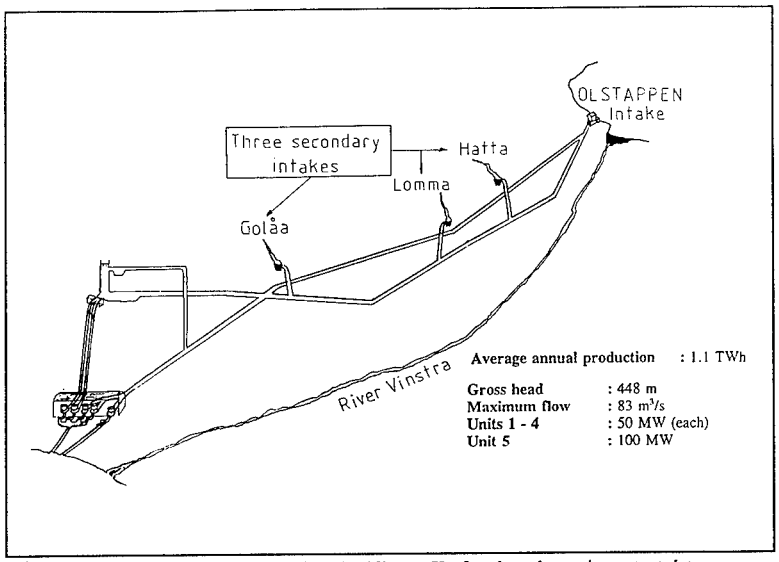

Figure 1: Schematical view of Nedre Vinstra Kraftverk and som important data

1) A higher degree of reliability
2) Added functionality in control-functions
3) Integrated optimization (RUNAID®)

ABB Master® offers functions from both the field of logic and the field of measurement and control. There are also functions for supervision, process optimization and calculation.

Nedre Vinstra has a solution where advanced colour graphic operator stations provide all man machine communication (MMC). The operator performs all tasks using the same MMC. This makes his task easier. Whether he is controlling internal PLC functions or he is running third party software, such as RUNAID® , is transparent to him.

The solution chosen implementing RUNAID® in ABB Master® was to let the control system communicate with an IBM® PC through files. A request for a calculation of optimum load distribution is received through the MMC and written on a file in the PC. In turn this file is read and results return in the same manner.

Optimization is performed either for either:
a) The current situation (single value, flow or output)

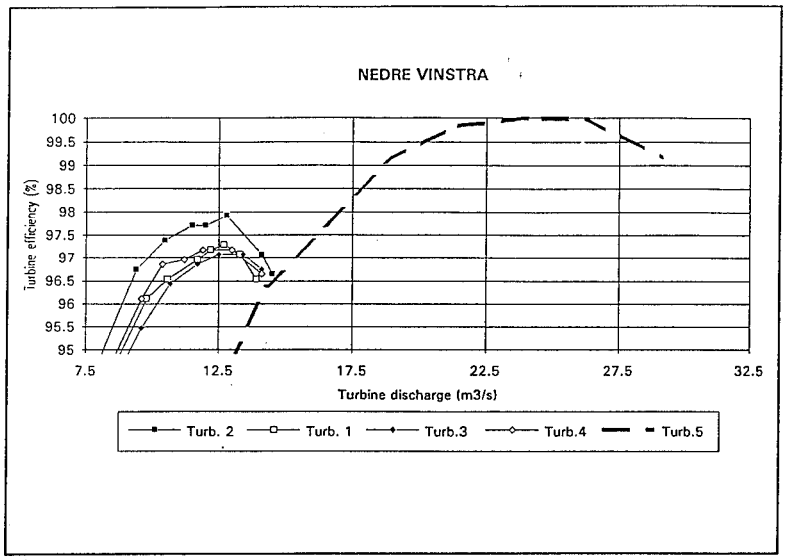

Figure 2: Relative turbine efficiency curves at Nedre Vinstra

b) A one to four day schedule

If the scheduling option is used, the plant can stay unmanned for four days. ABB Master® and RUNAID® will operate the units with optimal load distribution adjusting load on individual units and taking units in and out.

3.2 Software optimizing load distribution: RUNAID®

Hydropower Technologies' software; RUNAID® , is written for the IBM® PC. RUNAID® is a commercially available software package. It can be used as a stand-alone package or integrated with ABB-Master® . It has three functional modules;

1) A numerical model of the powerplant
2) Optimization module A: finding the best load distribution between several units in a powerstation under optional restrictions such as:
   a) Fixed load on any unit (including idle running or standstill)
   b) Maximum load on any unit (fully opened)
   c) Given order of start (and stop)
   d) Forcing operation on any unit

3) Optimization module B: as Optimization module A, but including the time aspect where start and stop costs are included

The numerical model can be used for simulating historical data or planning new powerplants. The optimizations performed give the best load distribution between several units (under stationary conditions) including any of the mentioned restrictions.

The numerical model for NEDRE VINSTRA includes:

a) A complete model of the hydraulic system (any detail can be included)
b) Individual turbine characteristics; efficiency as a function of discharge (influence of head and limitations from maximum opening can be included)
c) Electrical losses such as generators and transformers (any generator and transformer configuration is possible, losses are given as a function of active and reactive load, maximum MVA values can be specified)

In figure 3 the plant efficiency is calculated for a range of discharges with all units in operation and no special restrictions. The result is shown as a function of discharge. At 60 m^3/s we have shown the optimum load distribution. We have also calculated the plant efficiency for an alternative load distribution, giving approximately 1% reduced plant efficiency. The example may seem exaggerated, but we know from other cases that much greater errors can be made due to ignorance or slack routines.

More details about optimization in hydropower production can be found in the paper by Vinnogg/Holt 1989.

4 Experience gained at NEDRE VINSTRA

At Nedre Vinstra the new unit was set in operation 1 november 1989 and the rest of the system autumn 1991. Unfortunately there was a rockfall in the tunnel just after. This postponed normal operation for some time. The period for gaining experience with RUNAID® is therefor only the last year.

Training the staff in the use of RUNAID® took 1 day. Since the staff already had been through an extensive training program to learn the ABB-Master®, they already knew the basics of the MMC. Additional and necessary information covered on this day was; basic knowledge describing the problem in finding optimum load distribution (for motivating staff) and handling RUNAID® (which is very simple).

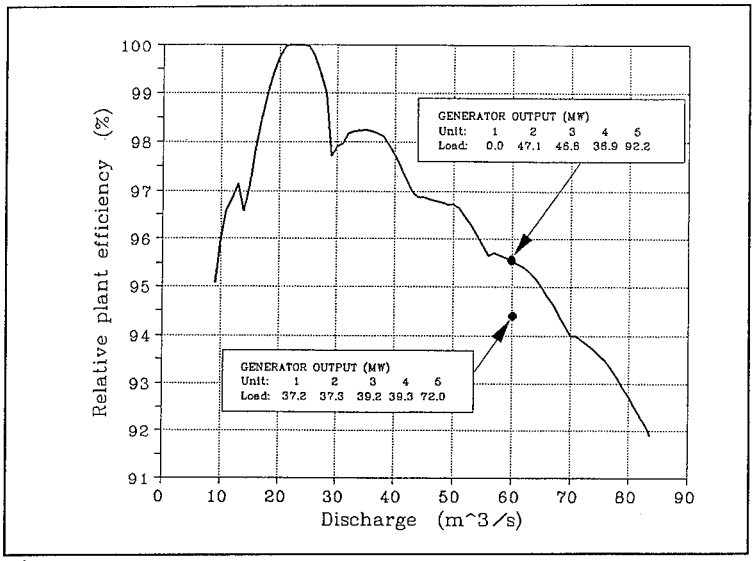

Figure 3: Example of total plant efficiency as a function of flow for Nedre Vinstra

During the first period of operation the staff noticed discrepancies between RUNAID® recommendations and actual values. This will normally be the case. The numerical model will normally have to be adjusted to represents reality. They had been warned about this, and the adjustments were done by the staff themselves. (Important data such as turbine efficiencies and hydraulic headlosses had been measured[4] as a basis for the model)

In the implementation of RUNAID® a pragmatic approach has been followed. During the first period, the staff were present at every change of load or shutdown/startup. Having confirmed that things were functioning as specified, the staff were only present at incidents of shutdown/startup. The next step will be to only attend alerts.

RUNAID® has performed as specified. There have however been two areas which have needed improvement. The algorithm that handles optimization regarding start and stop costs was based on a type of "fuzzy logic". Such an approach will only improve operation in general, but can not guarantee that there can not be better solutions (global optimum). This was

[4] Thermodynamically with an accuracy of typically ± 0.7%

unsatisfactory and this module has been replaced by optimization based on dynamic programming using an algorithm by Bellman 1957.»

There were also some disappointment regarding execution time. There are mainly three contributors to the execution time; software optimization algorithm, hardware processing capacity, communication between ABB-Master® and the PC. The optimization algorithm has been improved and initial computation time was reduced by typically 30%. The PC hardware (an IBM® XT) was equipped with a numerical processor giving a reduction of additional 75%. The communication between hardware and the PC was using a baud rate of 1200 baud, this will be increased to 19200, which presumably will reduce communication time proportionally.

Installing RUNAID® has focused the issue of load distribution. The staff have fully become aware of its importance and it is satisfying for them to have the tools to get the maximum of the available hydraulic resources. They now have the feeling that this part of their job is giving better results.

The computer model in RUNAID® can also be used for educational purposes and "what if" experiments.

Before the new equipment was installed the powerplant was manned 24 hours a day. With the new ABB-Master® and RUNAID® this was reduced to only the eight normal working hours. Staff appreciates not being on duty at night, and the power company save the extra cost of working night-shifts.

5 Cost/Benefit

Some work has been done to determine the value of optimum load distribution. Nilsen 1983 states that for the power plant Nedre Røssåga, with an annual production of approximately 1.8 TWh, the difference between the best and worst starting order of the machines (6 units) is 15,6 GWh annually. This figure was arrived at by simulating 10 years production.

Another approach was used by Hulaas 1989. He has simulated production at Alta Powerplant (two units, annual production 450 GWh) in 1988. His conclusion is that the difference between actual and optimal load distribution was 0.93 GWh annually. It should be mentioned that 1/3 of the year Alta is operating at full capacity so a major part of production can not be improved.

If one assumes that the mentioned examples are typical, then optimal load settings can improve production somewhere in the region of 0.5%. For

Nedre Vinstra this means an annual increase in production of 5.5 GWh which, with todays energy prices, is equivalent to 160.000 USD/year. This in turn means that without including the savings of man hours, the additional investment in automatic setpoints is easily repayed the first year. We consider this to be a careful estimate in the case of Nedre Vinstra because it has a rather complicated hydraulic system and electrical configuration.

A report has been made (Browne 1993) where historical data from Nedre Vinstra have been studied. Every hour the production at each unit is printed. Recordings are from 1990, before RUNAID® was installed. Actual production during 11 weeks were compared to the same production at the same time but using optimum load distribution calculated by RUNAID®. The difference varied from 0 to 1.5% (comparing one week at a time) with an average of approximately 0.5%. This does not prove the savings willbe 0.5%, but is a very clear indication.

6 Conclusion

The prototype for automizing optimum setpoints at Nedre Vinstra is a technically simple solution. The additional cost for such a solution willmost likely repay within the first year by increased production. There are also significant savings in not having the powerplant manned 24 hours a day.

Appendix 1 (reference)

Bellman, R. 1957
Dynamic Programming, Princeton University Press

Browne, M. 1993
Nilsen, E. Nedre Vinstra Kraftverk, Estimates of benefits from Optimum load allocation. HTI-Report no.: 863301, 1993

Hulaas, H. 1989
Nytteverdi av Optimal Drift,Rapport fra en studie av Alta Kraftverk, VR Teknisk Medlemsmøte Kirkenes

Nilsen, T. 1983
Noreng, K. Nedre Røssåga Kraftverk, Tilstandsregistrering og totalvurdering, SINTEF-NHL Rapport nr.: 2 83103, 1983-10-31

Vinnogg, L. 1989
Holt, B.G. Optimization of Power Production based on efficiency Data
Waterpower 1989, Niagara Falls, NY, Aug. 23-25 1989
American Society of Civil Engineers

OPTIMAL UNIT DISPATCH FOR HYDRO POWERPLANTS

Mark A. Severin, A.M.ASCE[1] and Lee L. Wang[2]

Abstract

To aid in modernization studies of hydro powerplants, it is necessary to establish the performance of the powerplant under the present conditions and with modernization of the existing generating units. These performance data will be used to estimate the increases in generating capacity and energy production, and determine the economic attractiveness of each individual modernization concept.

A computer model has been developed and used to derive the overall performance curve for hydro powerplants with multiple units based on the performance data of individual units. To derive the curve, unit dispatch is optimized using a dynamic programming technique for maximum efficiency. Adjustments to the original manufacturer's unit performance curves can be made to represent present-day or upgraded conditions. These adjustments allow for changes in both efficiency and generating capacity.

The model can be used for real-time unit dispatch to maximize power output for a required discharge release, or minimize turbine discharge for a required power output under a known headwater condition.

Introduction

Many existing hydro powerplants have been modernized and upgraded to extend generating equipment useful life and increase equipment capacity

[1]Hydraulic Engineer, Simons & Associates, Inc., 2821 Remington Street, Fort Collins, Colorado 80525.

[2]Associate and Head of Planning Section, Harza Engineering Company, 233 South Wacker Drive, Chicago, IL 60606.

and efficiency. Modernization and upgrade of the existing hydro powerplants will maximize the utilization of renewable resources, and provide low-cost peaking capacity and energy for meeting regional power system demand.

Harza Engineering Company has recently completed two hydro modernization studies including 22 hydro powerplants for the Tennessee Valley Authority (TVA), and 6 hydro powerplants for the Lower Colorado River Authority (LCRA) in Texas. One of the TVA powerplants contains 21 generating units. For these modernization studies, present-day equipment conditions and limitations were established to formulate alternative modernization concepts. Construction and equipment costs for each concept were estimated. Increases in generating capacity, energy production, and associated benefits due to modernization were computed. Economic comparisons of the alternative concepts were made based on the estimated benefits and costs.

A Harza computer model, Unit Dispatch Optimization, was used in the TVA and LCRA studies. This paper briefly describes the model including optimization approach, input requirements, output, and applications.

Model Development

The Unit Dispatch Optimization model was developed to optimize unit dispatch for hydro powerplants with multiple units. The model uses a dynamic programming algorithm to select the optimum combination of units by either of the following two criteria:

- Maximize power output for a given discharge and head
- Minimize discharge for a given power output and head

To optimize the unit dispatch at a powerplant, a family of performance curves is required for each individual unit. Each curve represents the power output vs. unit discharge relationship for a given head. These curves are normally furnished by the equipment manufacturer.

The model allows for adjustment to the original performance curves to account for changes in efficiency and generating capacity. This is useful when conducting hydro modernization studies to develop one family of curves representing downgraded conditions from the original performance and another family of curves representing the proposed upgrade conditions.

Dynamic Programming

Dynamic programming is a multistage optimization problem solving technique. Computational savings result by eliminating non-optimal paths as the solution focuses in on the optimal path. The problem is set up as a series

of known stages for which the state of each stage is an unknown variable. A return function defines the relative worth of each decision (state) at a stage. The overall optimal solution is the combination of decisions which maximizes (or minimizes) the sum of the return functions for all stages.

Dynamic programming is applied to the unit dispatch by assigning a stage to each powerplant unit. For the case where power output is to be maximized for a given discharge, the state variable is the discharge for each unit and the return function is the powerplant output. The optimal solution for a given head and total discharge is the combination of units which provides the desired total discharge while maximizing the powerplant output. For the case where discharge is to be minimized for a given power output, the state variable is unit power output and the discharge return function is minimized. Refinement of the solution is achieved by developing a corridor along the optimal path and repeating the solution at a finer incremental discharge for each unit.

Head Loss and Net Head

Head loss computed by the model is defined by the following:

$$H_l = C\,Q^2$$

where H_l is the head loss in meters, C is the friction loss coefficient, and Q is the discharge in m^3/s. Friction loss coefficients can be defined for each unit as well as for a penstock which is common to all units. For each unit, net head is computed from the following:

$$H = HWEL - TWEL - C_u\,Q_u^2 - C_p\,Q_p^2$$

where H is the net head in meters, *HWEL* is the headwater elevation, *TWEL* is the tailwater elevation, C_u is the unit friction loss coefficient, Q_u is the unit discharge in m^3/s, C_p is the common penstock friction loss coefficient, and Q_p is the common penstock discharge in m^3/s.

If unit dispatch is based on a known discharge, head losses can be directly computed, and tailwater elevation can be computed from a tailwater rating curve. If unit dispatch is based on a known power output, an iterative process is required to determine the head losses and tailwater elevation which result from the optimal discharge.

Data Input Requirements

The input data requirements for the model can be separated into two categories; powerplant data and unit data. Powerplant data consists of the following:

- Number of units
- Friction loss coefficient for a penstock common to all units
- Tailwater rating curve
- Headwater elevation

Data for each unit consists of the following:

- Friction loss coefficient for unit
- Minimum and maximum operating net heads
- Maximum discharge or maximum power output
- Unit performance curves for the range of net heads

Unit performance curves can be input as discharge vs. power output, efficiency vs. power output, or efficiency vs. discharge. Power output can be specified as output from either the turbine or the generator. Efficiency can be specified for either the turbine only or for the turbine and generator combined.

The minimum and maximum operating net heads provide a means of restricting operation of a unit to a range within the limitations of manufacturer's performance curves for the minimum and maximum net heads. This can also allow extrapolation of performance at net heads slightly beyond the limits of curves provided by the manufacturer.

Development of Overall Performance Curves

An example is presented to demonstrate the ability of the model to develop overall performance curves and to optimally dispatch units for a three-unit powerplant. The unit performance curves for Unit #1 and Unit #3 are identical and presented in Figure 1. These units can operate at a range of net heads from 36.6 to 67.1 meters (120 to 220 feet). Unit #2 has a narrower operating range from 42.7 to 61.0 meters (140 to 200 feet) and is presented in Figure 2.

Unit #1 and Unit #3 have recently been upgraded and are more efficient than Unit #2 at net heads greater than 48.8 meters (160 feet) but cannot operate at discharges or power outputs as low as Unit #2.

The overall performance curves are presented in Figure 3. The curves consists of points representing the maximum power output which can be generated for a given discharge at a given net head. Note that the curves at net heads of 36.6 meters (120 feet) and 67.1 meters (220 feet) are restricted to the combined capacity of Unit #1 and Unit #3 because Unit #2 is inoperable under these net heads.

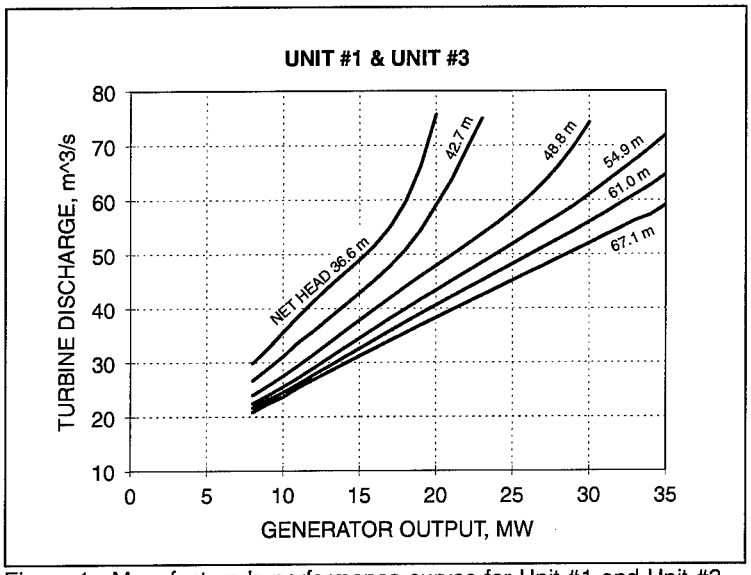

Figure 1. Manufacturer's performance curves for Unit #1 and Unit #3.

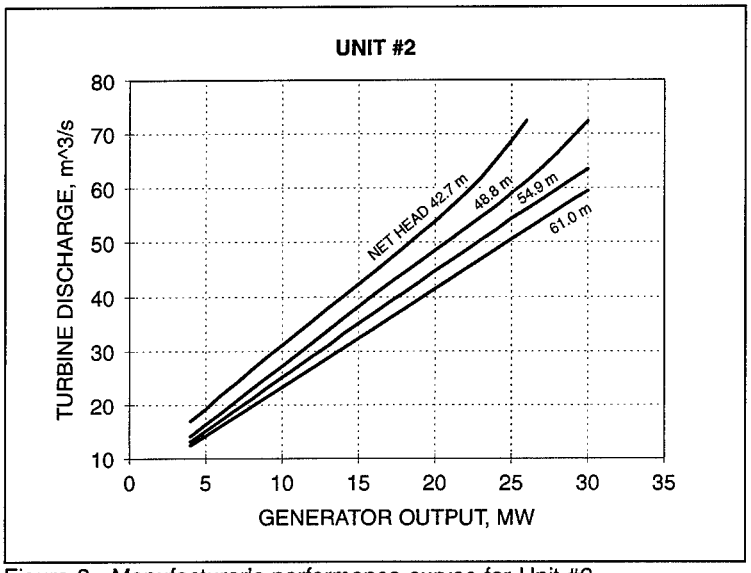

Figure 2. Manufacturer's performance curves for Unit #2.

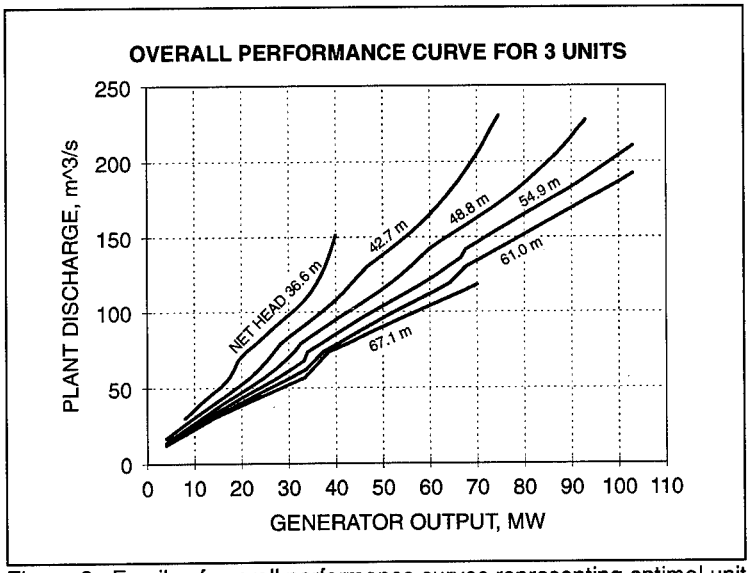

Figure 3. Family of overall performance curves representing optimal unit dispatch for the three-unit powerplant.

This family of curves was developed using original unit performance curves as supplied by the manufacturer. Unit #2 has not been upgraded and its actual performance may not be as efficient as that represented by the manufacturer's curve. It is appropriate to modify the Unit #2 curve using the efficiency adjustment parameters in the model. Unit #1 and Unit #3 do not require adjustment due to their recent upgrade. A new family of overall curves can be developed to represent present-day conditions.

Upgraded Overall Performance Curves

An upgraded unit performance curve for Unit #2 is presented in Figure 4. This figure demonstrates how the model interpolates a performance curve at 45.7 meters (150 feet) net head based on the original manufacturer's curves at 42.7 meters (140 feet) and 48.8 meters (160 feet). An upgraded curve representing an efficiency increase of 3% and a capacity increase of 10% is then developed.

To evaluate the benefit of upgrading Unit #2, average annual generating capacity and energy production of the powerplant under present-day conditions will be estimated. This can be done using a daily simulation model for the powerplant operation.

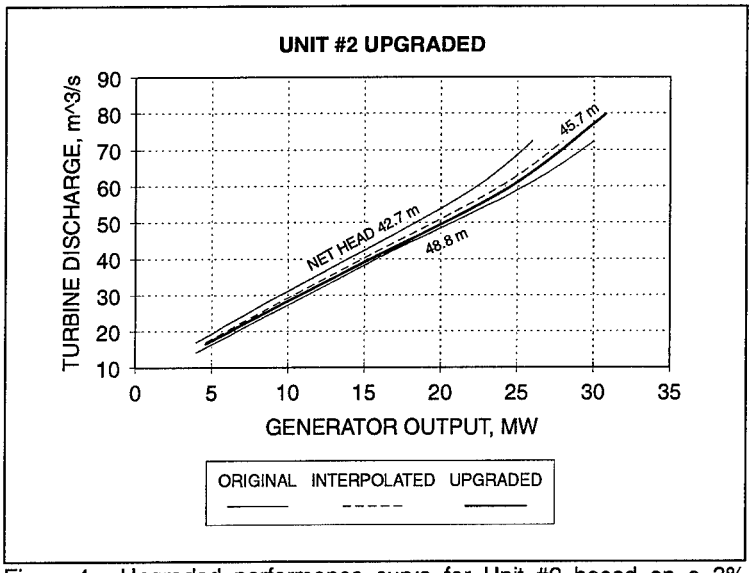

Figure 4. Upgraded performance curve for Unit #2 based on a 3% efficiency increase and a 10% capacity increase.

The expected increase in efficiency and maximum capacity resulting from the upgrading of Unit #2 will be estimated. A new family of overall performance curves will be developed for the upgraded Unit #2 with the performances of Unit #1 and Unit #3 as above. The new family of curves will be used to compute the average annual capacity and energy production for the modernized plant. A benefit-cost analysis will be the final step in evaluating the economic justification of the upgrade.

Real-Time Unit Dispatch

For the real-time conditions, the following parameters must be specified for performing the optimal unit dispatch:

- Required discharge or power output
- Headwater elevation

In addition, the following optional parameters may be specified for each unit:

- Unit availability
- Efficiency adjustment parameter
- Capacity adjustment parameter

The unit availability parameter allows for one or more units to be unavailable due to scheduled maintenance. The model will determine the optimal combination of units using only those which are operable. Several examples of real-time dispatch are presented in Tables 1, 2, and 3.

In Table 1, the optimal unit dispatch was determined for a required power output of 60,200 kW at three different headwater elevations using the original manufacturer's curves. At a low headwater elevation of 195.7 meters (net head of approximately 44.8 meters), all three units were dispatched. At a headwater elevation of 203.3 meters (net head of approximately 52.1 meters), only Unit #1 and Unit #3 were dispatched. At a high headwater elevation of 216.4 meters (net head of approximately 65.5 meters), Unit #2 is inoperable due to a net head limitation of 61.0 meters.

Unit #1 and Unit #3 were dispatched at different settings for the high head case. If the two units had been dispatched equally and each generated 30,100 kW, the overall efficiency would have been slightly lower, and require an additional 0.14 m^3/s (5 cfs) to be released. When Unit #1 and Unit #3 were dispatched equally, their performance differed due to slightly different friction loss coefficients. It should be noted that for all cases, the unit power output is an increment of 100 kW. This accuracy of dispatch is specified by the user.

In Table 2, the optimal unit dispatch was determined at a headwater elevation of 203.3 meters (net head of approximately 52.1 meters) for three different discharge release requirements using the original manufacturer's curves. To satisfy a low discharge of 28.3 m^3/s (1,000 cfs), only Unit #3 was dispatched. For a discharge of 130.4 m^3/s (4,600 cfs), Unit #1 and Unit #3 were equally dispatched. For a high discharge of 178.5 m^3/s (6,300 cfs), the variation in performance among the three units is evident with all three units releasing 59.5 m^3/s (2,100 cfs).

Table 3 summarizes the effect that the upgraded Unit #2 would have on the real-time dispatch. The first case represents the optimal dispatch assuming that the performance of Unit #2 is as originally installed. For the second case, Unit #2 was downgraded to the present-day performance by using an efficiency adjustment to account for a 2% decrease in efficiency. The power generated by Unit #1 and Unit #3 are increased to compensate for the downgraded performance of Unit #2. The proposed upgrade for Unit #2 would result in a 3% increase in efficiency over the original performance and a 10% increase in maximum generating capacity. The optimal real-time dispatch after the upgrade is presented in the third case and requires a release of 2.0 m^3/s (68 cfs) less than the present-day condition for the power requirement of 65,000 kW.

Table 1
Real-Time Unit Dispatch to Satisfy a Power Output Requirement

Input		Output			
HWEL meters	Required Power kW	Unit #	Power kW	Discharge m^3/s	Efficiency
195.7	60,200	1	18,500	49.3	0.856
		2	23,200	59.7	0.889
		3	18,500	49.2	0.857
		Plant	60,200	158.2	
203.3	60,200	1	30,100	65.3	0.900
		2			
		3	30,100	65.2	0.900
		Plant	60,200	130.5	
216.4	60,200	1	33,100	57.2	0.900
		2			
		3	27,100	48.8	0.862
		Plant	60,200	106.0	

Table 2
Real-Time Unit Dispatch to Satisfy a Discharge Requirement

Input		Output			
HWEL meters	Required Discharge m^3/s(cfs)	Unit #	Power kW	Discharge m^3/s	Efficiency
203.3	28.3 (1,000)	1			
		2			
		3	11,281	28.3	0.764
		Plant	11,281	28.3	
203.3	130.4 (4,600)	1	30,028	65.2	0.900
		2			
		3	30,054	65.2	0.900
		Plant	60,082	130.4	
203.3	178.5 (6,300)	1	27,538	59.5	0.907
		2	26,632	59.5	0.877
		3	27,556	59.5	0.907
		Plant	81,725	178.5	

Table 3
Real-Time Unit Dispatch with Unit #2 Upgraded

Input		Output			
HWEL meters	Required Power kW	Unit #	Power kW	Discharge m^3/s	Efficiency
203.3	65,000	1	27,200	58.5	0.907
Original performance when installed		2	10,500	26.9	0.756
		3	27,300	58.7	0.907
		Plant	65,000	144.1	
203.3	65,000	1	27,400	59.0	0.907
Downgraded to present-day performance		2	10,200	27.4	0.721
		3	27,400	58.9	0.907
		Plant	65,000	145.3	
203.3	65,000	1	26,400	56.9	0.904
Modernized to exceed original performance		2	12,100	29.3	0.800
		3	26,500	57.1	0.904
		Plant	65,000	143.3	

Conclusions

Modernization and upgrade of existing hydro powerplants will extend their useful life, and provide additional relatively low-cost peaking capacity and energy production to the power system they serve. Overall powerplant performance curves for present-day and upgraded conditions are needed to estimate the benefits from increased generating capacity and energy production due to modernization. These benefits along with the estimated construction costs of the modernization will be used to rank alternative modernization concepts and select the optimum concept.

The Unit Dispatch Optimization model develops the overall powerplant performance curves by maximizing the power output for a given discharge and range of generating head. The model can also be used by powerplant dispatchers and operators for real-time optimal dispatch to determine which units should be operated and how much power each operating unit should generate to satisfy a given discharge or power requirement at the present reservoir headwater level.

CANADIAN INFLATABLE DAM - A UNIQUE APPLICATION

Richard Slopek, Lloyd Courage[1] and Brian Pelz[2]

Abstract

The Brazeau Development, which is owned and operated by TransAlta Utilities Limited, is located on the Brazeau River approximately 200 km southeast of Edmonton, Alberta, Canada. The main reservoir is impounded by five earthfill dams ranging in size from the 65 m high Main Dam to a 5 m high side dam, a concrete chute spillway and Outlet Works, which controls flows into the 16 km long power canal.

As part of dam safety evaluations carried out by Monenco AGRA, the development was classified in the large dam, high hazard category. In accordance with provincial guidelines this required the development to be able to safely handle the Probable Maximum Flood (PMF). Modifications to the development were required in order to increase spill discharge capacity by approximately 100 %. This paper briefly discusses some of the options evaluated and describe the unique solution that was adopted to allow the development to safely handle the PMF.

Introduction

The Brazeau Development is one of thirteen hydroelectric owned and operated by TransAlta Utilities. The development was commissioned in 1962 and consists of the following structures shown on Figure 1.

The Main Dam, which was constructed with two 4.6 m wide by 6.4 m high oval shaped conduits running through the foundation, is a 65 m high zoned earthfill dam. The conduits were used to divert flows during construction and were intended to be retained as an emergency spillway. However, operation of the conduit regulating gates was found to be

---

[1]Monenco AGRA Inc., Design and Consulting Engineers, 400 Monenco Place, 801 6th Ave. S.W., Calgary, Alberta, Canada, T2P-3W3, (403) 298-4615.
[2]TransAlta Utilities Corp. Limited, 110 12th Ave. S.W., Calgary, Alberta, Canada, T2P-2M1.

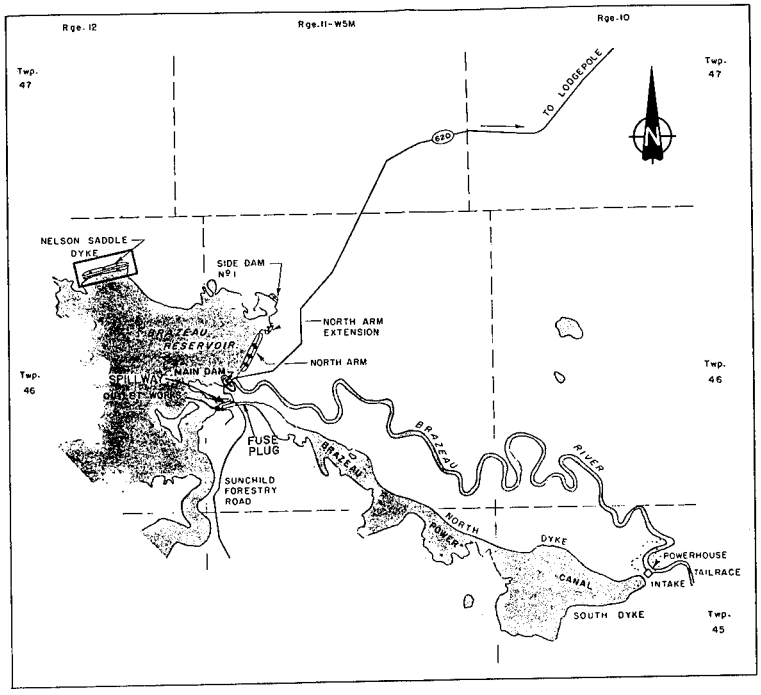

FIGURE 1
BRAZEAU DEVELOPMENT

unsatisfactory. Therefore, in 1969 the conduits were sealed with concrete plugs and a gated chute spillway was constructed.

The North Arm, North Arm Extension, Nelson Saddle Dam and Side Dam No.1 are all homogeneous earthfill structures which impound the main reservoir.

The Outlet Works is equipped with two pump-turbines and two venturi sluices, which are used to convey flows from the main reservoir into the power canal. At low reservoir levels the pumps are used to maintain constant water levels in the canal. When the reservoir approaches its full supply level the pumps are switched to the generation mode to produce power.

The power canal is 16 km long and is contained by the North and South Earthfill Dykes. The intake at the far end of the canal feeds two steel penstocks that convey flows to the powerhouse. The 120 m of head at this

point is used to generate up to 350 MW.

The power canal was also equipped with a fuse plug washout section which in the event of an emergency will breach and ensure that the dykes are not overtopped. The lateral progression of the breach is restricted by steel sheet pile cells located at the abutments of the fuse plug and driven to rock.

Dam Safety Evaluations

In 1985, the initial dam safety evaluations were carried out for the development. At that time, in accordance with the Government of Alberta Dam Safety guidelines, the development, based on hazard and size classification was required to be capable of handling the 3/4 PMF. Subsequent to the initial evaluation, additional studies, including hydraulic model testing of the spillway, dam break and inundation mapping studies, were carried out. Based on the findings of these studies the hazard potential of the development was increased from significant to high due to the effects of downstream flooding. This change in classification required the development to be able to handle the PMF.

The results of the hydrology study for this development established the mid-August flood to be the most critical. The peak mid-August inflow into the reservoir was estimated to be 4280 m^3/s. The inflow hydrograph is shown in Figure 2. The spillway capacity at the time of the study was 1840 m^3/s.

There was insufficient storage capacity to attenuate the flood to the extent that the spillway could handle the
inflows, therefore a study was undertaken to evaluate various alternatives to add emergency spill capacity in order to safely pass the PMF.

Alternatives

The following is a list of the main alternatives, which were examined and a brief description of their more significant aspects and reasons why they were not selected:

Alternative 1 - Changes to the operating rule curves.

The development is basically a pumped storage scheme. Therefore, the reservoir goes through an annual cycle, which requires that the reservoir be drawn down prior to the spring runoff and peak reservoir elevations in the fall. Since the critical time for the PMF is in August changing the operating rule curve for this period would also

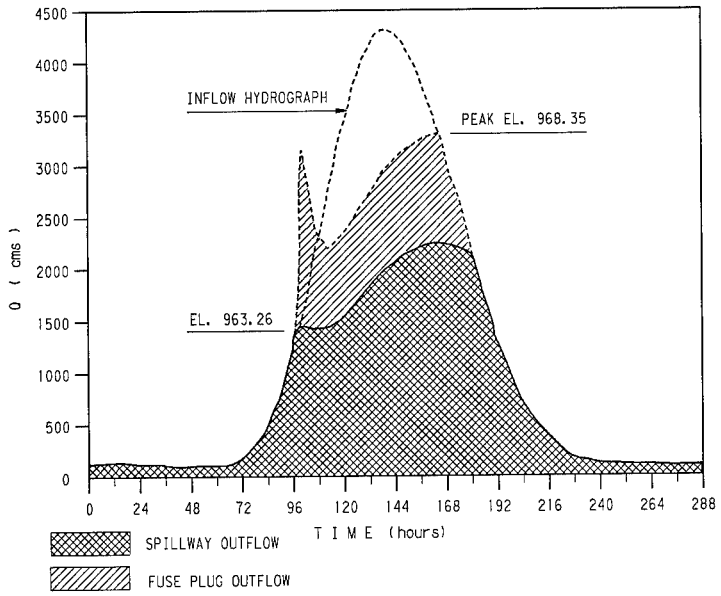

FIGURE 2
INFLOW / OUTFLOW HYDROGRAPHS

affect the levels that the reservoir could be operated at earlier in the year. The changes required to the operating levels in order to gain enough storage to attenuate the PMF resulted in a significant loss to operational flexibility that was not considered to be acceptable.

Alternative 2 - Spillway modifications.

The spillway consists of a control structure with two 15.25 m high and 9.15 m wide vertical lift gates and a concrete chute with a flip bucket. Although the control section could handle twenty-five percent more flow, the chute could not. Even if it could, it was determined that there still would not be sufficient capacity to handle the PMF. Therefore, options such as adding additional bays and lowering sill elevations were studied. The costs associated with this option ranked it low as a possible option.

Alternative 3 - Reactivation of the diversion conduits.

The diversion conduits under the Main Dam were considered as another potential source of emergency spill capacity providing that the problems with the gate operation could be resolved. In addition, the reservoir cannot be drawn down low enough to expose the intake structure.

Therefore, removal of the concrete plug and reactivation of the intake would have to be carried out underwater. Although not impossible this would increased the difficulty and cost of this option making it unattractive.

Alternative 4 - Raising the reservoir retaining structure.

The original design for the development was for a two phase construction approach that would allow the structures to be raised an additional 7 m at some time in the future. The second phase was never executed. Raising of the structures would provide increased spillway capacity and would also provide additional attenuation in the reservoir. Costs associated with this alternative also ranked it low as a possible option.

Alternative 5 - Construction of a main reservoir fuse plug.

Several low earthfill structures are located around the main reservoir that provided potential locations for a fuse plug washout section. However, the foundations at most of the sites were considered to be highly erodible and could result in significant venting of the reservoir following fuse plug operation. The Nelson Saddle Dam, although it is situated on a poor foundation was sufficiently set back from the main reservoir that continued erosion of the foundation was unlikely. This was determined to be the least cost alternative. Unfortunately, if the fuse plug were activated during a flood, water discharged through the breach would enter the Pembina River, which belongs to a different watershed. This option was rejected because interbasin transfer of flood waters was judged to be politically unacceptable.

Alternative 6 - Construction of an inflatable dam.

This option involved the maximization of flows through the Outlet Works to provide emergency spill capacity from the reservoir. The problem was that there was no means to handle the additional inflows into the power canal. For this reason it was necessary to initiate a breach at the existing power canal fuse plug, which has a crest elevation 0.6 m above the canal full supply level. Therefore, additional water had to be placed into storage in the canal prior to breaching of the fuse plug. Due to the size of the canal this was a substantial volume of water that would later add to the discharge from the fuse plug. Figure 2 shows the resulting outflow hydrograph for this type of operation. It can be seen that additional outflow would occur shortly after the fuse plug was breached. This event also occurs early on in the storm resulting in outflows exceeding inflows. This was not an acceptable condition. Therefore, some modifications to this scheme were required. The solution involved the installation of a 3.35 m diameter 100 m long inflatable dam across the power canal.

The Inflatable Dam Alternative

The inflatable dam would be installed in the power canal and would remain deflated during normal operation. It would then be inflated in the event of a flood in order to isolate the storage available in the 16 km long power canal and minimize the amount of water that would be released. Figure 3 shows the general layout in the vicinity of the inflatable dam and fuse plug. The Outlet Works is located approximately one kilometre to the left of the inflatable dam shown in the figure. The main body of the power canal and powerhouse is located to the right. By retaining the power canal and allowing the fuse plug to breach eliminates the large outflow surge shown on Figure 2. This type of operation is the opposite of normal flood control operations when spillway gates are raised or inflatable dams are lowered.

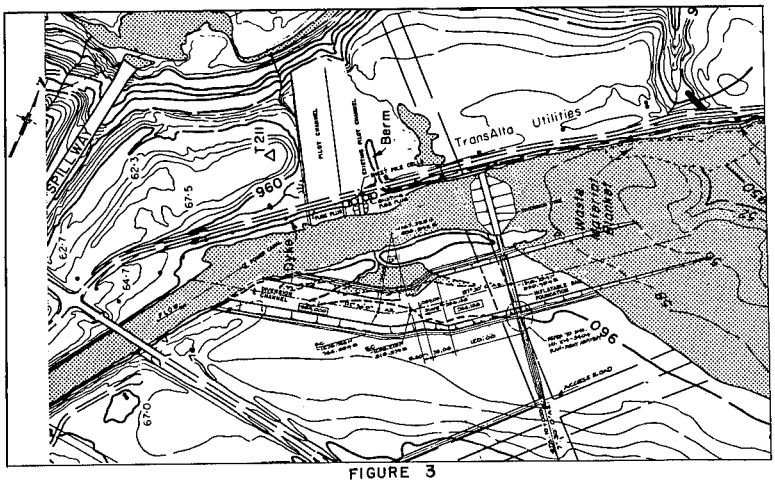

FIGURE 3
GENERAL ARRANGEMENT

Supply of the inflatable dam went out for competitive bids. Bridgestone was the successful bidder. Figures 4 and 5 show the elevation of the inflatable dam looking in the upstream direction back towards the Outlet Works and a cross section through the dam, respectively. On Figure 5, one can see the distinctive fin associated with the Bridgestone design. As not earlier the normal operational direction of flow would from the Outlet Works towards the powerhouse. Note that the fin is pointing in the opposite direction to this normal flow condition.

The reason for this interesting arrangement of the inflatable dam is

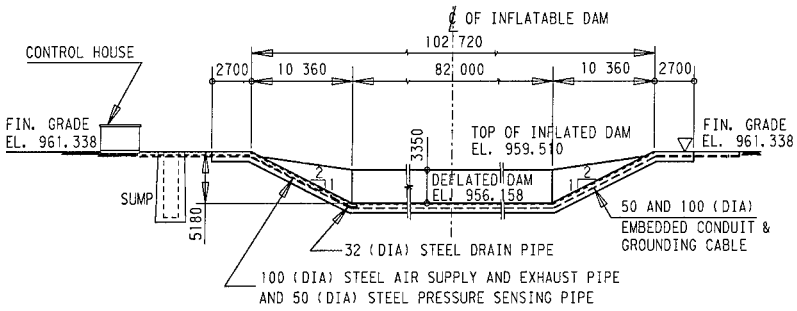

FIGURE 4
INFLATABLE DAM ELEVATION LOOKING UPSTREAM

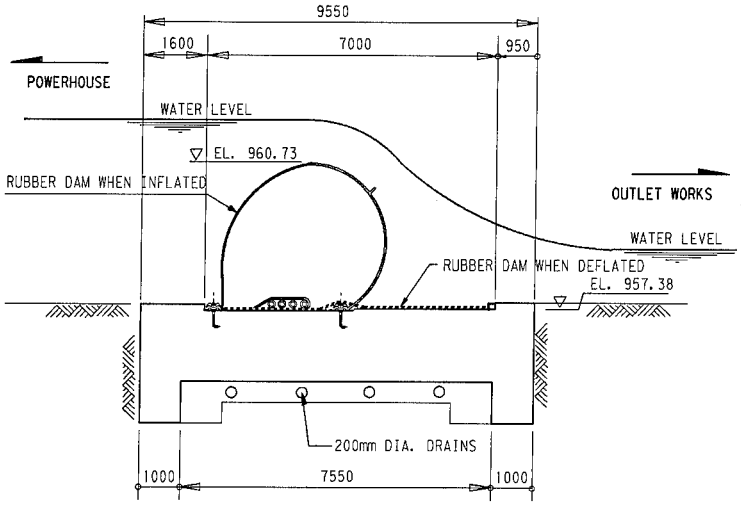

FIGURE 5
INFLATABLE DAM CROSS SECTION

that although the flow for the vast majority of the time would be from the Outlet Works to the powerhouse, during flood conditions if fuse plug operation was required, the flow direction would be reversed.

After the fuse plug has been activated and during post flood conditions, the inflatable dam would be used to regulate flows from the main portion of the power canal out through the fuse plug opening in a controlled manner. The fin arrangement in this case provides better flow characteristics.

This was an important consideration in the design as the outflows shown in Figure 2 would enter the Brazeau River upstream of the powerhouse and the likelihood that powerhouse operation would be lost was high. As the powerhouse is the only means other than the fuse plug for removing water from the power canal this control feature was considered to be essential.

The problems associated with laying the inflatable dam down in the opposite direction to the normal flow was not considered to be a difficult problem to solve and with the double clamping plate system shown on Figure 5, the flow reversal could also be handled. Therefore, this arrangement was adopted.

In order to secure the fin in the check so that flows would not get under the deflated membrane and cause uplift and obstruction to the flow area during normal conditions, a hold down system consisting of eye bolts attached to the fin on the rubber dam and a retractable wire rope was devised to secure the dam.

Final Design and Construction

In order to develop acceptable factors of safety against sliding and overturning measures had to be taken to offset the buoyant effects of the dam when inflated and to reduce uplift beneath the concrete slab. The concrete slab is founded in glacial till and is protected from erosion by gabion mats. During normal operating conditions with the dam deflated there are no loads acting on the structure. When the dam is inflated considerable weight is required to counteract buoyancy and provide adequate stability against sliding. Uplift beneath the slab also contributes significantly to the destabilizing forces. In order to solve this problem and to minimize the amount of concrete required a drainage system to be designed. This consisted of a number of perforated drainage pipes surrounded in a clean processed gravel layer beneath the concrete slab. The drainage pipes were connected to a sump located at the right abutment. In the event that the dam would need to be inflated, the drainage sump would be pumped out and pressures beneath the foundation reduced. In this manner the amount of concrete required in the foundation slab was minimized.

The existing hydroelectric development was maintained in full

operation during the construction period. The general arrangement for the installation of the inflatable dam is shown in Figure 3. The Outlet Works and the main reservoir are located to the left on the figure. Normal flow operation would be from left to right. The existing canal was not closed off by the diversion dyke shown until after the inflatable dam and associated canal work was completed. Excavation of the new canal was carried out behind earth plugs at both ends. After the inflatable dam and canal work was completed in late 1991, the dam was inflated to ensure that the clamping system was secure and no leaks were evident prior to excavating the earth plugs and diverting water through the new canal section. After the new canal section was activated the diversion dyke across the existing canal was constructed.

In addition to the installation of the inflatable dam, other modifications were required to the development to enable it to handle the PMF. This included raising core sections in the main reservoir earthfill retaining structures to ensure their stability when reservoir levels were surcharged above the full supply level. In order to carry this work out it was necessary to expose the top of the core by excavating a trench along the centreline of the structures. An impermeable liner was then installed that tied into the existing impervious core material. As noted earlier in the alternatives section, the concrete chute spillway capacity was limited by the capacity of the chute rather than through the gated control section. A hydraulic model study was undertaken to evaluate the cross waves generated by the centre pier and deflection sills to determine the maximum capacity of the spillway chute. It was determined that the total capacity of the spillway could be increased from 1840 m^3/s to 2265 m^3/s by raising the chute walls.

Commissioning of the Inflatable Dam

The commissioning of the inflatable dam was carried on May 26, 1992. The following is a description of the commissioning procedure that was undertaken. The procedure is also intended to be used for periodic testing to ensure dam operability.

1. The drainage sump pump was activated and the hold down cable was removed.

2. After the sump was dewatered, the dam was inflated with the canal at full supply level (i.e. 3.35 m of head on the dam). Inflation of the dam took less than one hour as required in the design specification.

3. The water level between the inflatable dam and the Outlet Works was lowered. This was done by reversing the flow through the pump turbines in the Outlet Works. Under this differential head and continuous

flow from the main body of the power canal over the inflatable dam and through the Outlet Works, the dam would be deflated back into its normal operating position. The start of the deflation procedure can be seen in Photo 1.

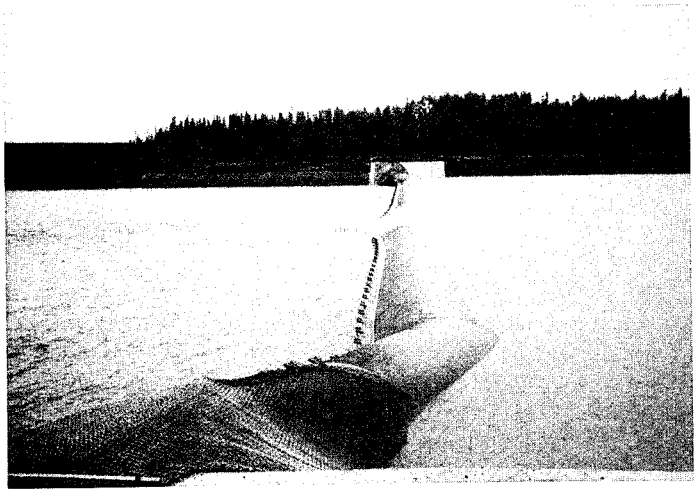

Photo 1
Inflatable dam commissioning test.

Conclusion

The use of inflatable dams is relatively new in North America. The Canadian version provides a unique application of how it can be used for flood control purposes. The combination of modifications, which included the installation of an inflatable dam, raising spillway chute walls and raising impervious cores in earthfill dams, provided the Brazeau Development with the capability of handling the peak PMF inflow of 4280 m^3/s by discharging 2265 m^3/s through the gated spillway and 1360 m^3/s through the Outlet Works/ inflatable dam/ fuse plug arrangement with the remainder of the flows being attenuated in the Brazeau Reservoir.

Acknowledgements

The authors wish to thank TransAlta Utilities Corporation and Monenco AGRA Inc. for their contributions and permission to publish this paper.

CREATIVE CREST CONTROL

Thomas L. Kahl and Stephen T. Ruell[1]

ABSTRACT

Most run-of-the-river hydroelectric stations include overflow spillways to pass river flows that exceed the turbine hydraulic capacity. Frequently these spillways have flashboards that are raised, during periods of normal river flow, to increase the station headpond elevation, and lowered, during high river flows, to increase the spillway hydraulic discharge and mitigate upstream flooding. Traditionally flashboards have been wooden structures that are damaged by high flows, and must be repaired after each flood event. Increasingly automatic flashboard systems comprised of mechanical steel gates or inflatable gates are being used to enhance flashboard performance at both new and existing spillways.

This paper first reviews the experience of Kleinschmidt Associates on three spillways where the operation of wooden flashboards has been improved by installing automatic flashboards or sluice gates. For each of these projects the site conditions and design parameters are discussed, followed by a presentation of the construction and performance to date of the selected system. This paper then summarizes some advantages and strategies useful when evaluating spillway flashboard alternatives.

EXAMPLE 1 - CREST GATES

A 4 MW New England hydroelectric station was constructed in the early 1900s with 2.7m (9 ft) high wooden spillway flashboards. The top 1.5m (5 ft) and the bottom 1.2m (4 ft) of the wooden panels are each separately supported by diagonal downstream struts. During periods of high river flow, if the headpond level increased more than 0.5m (20 in) above the top of the wooden flashboards, the upper section struts would first be pulled to lower the effective spillway crest by 1.5m (5 ft). This was

[1]Engineers at Kleinschmidt Associates, Consulting Engineers, Pittsfield, Maine (207)487-3328

accomplished by using an electrically powered winch to tighten a cable that was looped around the diagonal struts. If the headpond continued to rise, then portions of the lower 1.2m (4 ft) of flashboards would similarly be lowered by a second winch to increase the spillway discharge until the headpond water elevation stabilized. The lower portion of the flashboards would frequently be damaged by the high overtopping flows when the top sections were removed.

Breaching of the bottom portion of the wooden flashboards resulted in a loss of more than 60% of the station's 4.9m (16 ft) of gross head. This level is below acceptable limits for turbine operation and resulted in the station being inoperable for up to several months each year. Although various spillway automation schemes to allow uninterrupted station operation had been investigated since the 1920's, none had proven economically feasible. In 1990, two conditions occurred that finally provided the necessary economic justification for spillway automation.

Design Approach

The first condition was that an approximately 22.9 meters (75 ft) length of the spillway base timber crib construction had deteriorated to the point where major repairs or replacement was necessary. Since, reconstruction was required, this allowed part of the cost of the spillway sill rehabilitation to be considered as a maintenance expense.

The second condition was the determination that hydraulic control of the site discharge during high flows was not at the dam, so automating a portion of the spillway would provide the ability to pass the same river flood flows as the present spillway with all the flashboards dropped. During a review of the site hydraulic conditions by Kleinschmidt Associates, it became evident that under flood river conditions the factor limiting spillway discharge were restrictions downstream of the spillway, rather than the discharge capacity of the spillway crest. This restriction was caused by such items as the piers of a road bridge, backwater from the adjacent powerhouse water discharges, and high bedrock elevations in the riverbed. The calculations showed that approximately 15.2 meters (50 ft) of spillway, with the full flashboard height, would provide enough hydraulic capacity to establish the downstream bridge as the critical hydraulic control. This meant that replacing the 22.9m (75 ft) of deteriorated spillway with gates would provide the same overall discharge capacity, as automating the entire 52.1m (171 ft) long spillway, and at a substantially reduced cost. Final design of the spillway rehabilitation was based on providing 22.9m (75 ft) of gated spillway, with the original wooden flashboards continued along the remaining spillway crest.

Project Construction

Previous studies had revealed that fabricated steel gates offered the lowest total cost for an automated flashboard system. After project funding was confirmed in August 1990, bids were solicited, using a performance specification, for the design and fabrication of automatic steel crest gates. The costs and configurations supplied by various manufacturers were evaluated along with the associated civil costs and operational characteristics. The selected proposal consisted of three separate 7.6m (25 ft) long, by 3m (10 ft) high, bottom hinged steel gates that could be operated in either the full up or full down positions. Each gate is controlled by a top mounted hydraulic cylinder on one end. In September 1990 the gate and general construction contracts were awarded. A cofferdam was installed in October, 1990, and the new concrete spillway and piers replacing the original timber crib portion of the spillway were constructed. The three new steel gates were installed during January, with the entire system fully operational in March, 1991.

Performance

In these first two years of operation the system has not experienced any problems. To date the remaining wooden flashboards have not been breached with river flows up to the 10 year flood. This has allowed uninterrupted station operation and thus has increased power generation and stabilized headpond fluctuations.

EXAMPLE 2 - BOLTON FALLS

The Green Mountain Power Corporation's Bolton Falls hydroelectric station is located on the Winooski River, in northern Vermont. The original timber crib dam, with downstream granite facing, was completed in 1900. In 1986, site revitalization included construction of a new 8 MW powerhouse, a rebuilt intake, and placing a new concrete cap over the granite spillway. As shown in Figure 1, 59.4m (195 ft) of 1.5m (5 ft) high wooden flashboards, with bottom hinged steel framed panels supported by diagonal downstream wooden struts, were installed. The rebuilt crest varied from 4 to 5.4m (13 to 18 ft) in width and was flat except for a 0.2m (8 inch) deep step downstream of the panel hinges.

The performance of the wooden hinged flashboards proved to be problematic. Except for the turbines, the spillway provides the only means of hydraulic discharge at the site. Located immediately downstream of a gorge, the spillway is exposed to concentrated amounts of river borne ice and debris. These rigorous conditions caused the wooden flashboards to drop several times a year and to sustain regular structural damage. The annual spring flows prevented the boards from being raised for several

months each spring. The 1.5m (5 ft) high flashboards, at the full station capacity of 68m^3/sec (2,400 cfs), provides approximately 900 kw of energy production, a significant fraction of the total generation.

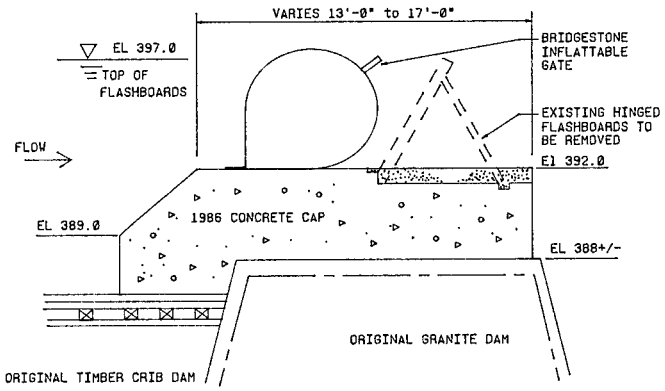

FIGURE 1 - BOLTON FALLS SPILLWAY PROFILE

Design Approach

The exposure of the crest to severe damage from river ice and debris required replacement of the existing wooden flashboards along the entire spillway crest. Feasibility study estimates showed that the flat spillway cross section required only limited field work to adapt to an inflatable gate system.

The fairly new concrete crest was wide and flat, so the lay down space for the deflated bladder was easily provided. The crest would have been difficult to modify for the hinges and hydraulic cylinder mountings of steel gates, as compared to the relatively simple anchorage requirements of the inflatable systems. This resulted in the inflatable gate option providing a 30% savings in direct construction costs compared to mechanical crest gates.

To provide for easier sluicing of debris, a short length of the spillway crest next to the intake, and downstream of the inflated gate support area, was lowered eight inches below the remaining crest. This causes a "notch" in the bladder crest to form at this end of the spillway when deflating the bladder. During trashrack cleaning the operator partially lowers the bladder, creating a flow which pulls much of the intake debris away from the intake and passes it over the spillway.

Construction

Bids for the inflatable bladder systems were solicited in April, 1991, and the Bridgestone Rubber Dam was selected in late May. The abutment modifications, piping, bladder installation and supporting electrical work was bid in August and J. A. McDonald Inc., of Lyndon Center, Vermont, was selected as the general contractor. Construction began in mid-September and the bladder was installed by late October. The electrical and control equipment was installed by mid-November 1991.

Performance

The system has performed well providing significant increases in station electrical production. The elimination of flashboard repair work on the crest has decreased wooden panel maintenance costs and personnel safety risk. The ability to easily sluice intake debris away from the intake has generally reduced the effort required to clean the trashracks from a two person to a one person operation.

The severity of the site conditions at Bolton Falls was illustrated when in March, 1992, 60 year flood and ice jam subjected the inflatable gate to ice blocks in excess of 20,000 kg (45,000 lb). Although the downstream concrete surface of the crest showed areas of impact damage the inflatable gate system showed only a few superficial scrapes.

Two weeks after the flood the bladder received a 1m (3.3 ft) long cut when lying fully deflated to discharge high fiver flows. The cut completely penetrated through the 12cm (1/2 in) thick bladder membrane for the last 50.8cm (2 in). A temporary repair was quickly made by Bridgestone, and they installed a permanent repair later in the summer.

Bridgestone conducted independent testing of the Rubber Dam material in the summer of 1992. The results concluded that the rip could not have been caused by impact from ice and was likely to have been the result of impact from a large sharp rock or metal object passing over the spillway, while the deflated membrane was supported on the horizontal and unyielding surface of the concrete spillway. The sharp object could have obtained sufficient momentum from being embedded in one of the 1m (3.2 ft) thick sheets of river ice that had flowed over the spillway.

A survey of owners of the other Bridgestone Rubber Dam installations in the United States, conducted in September, 1992, confirmed that this was the first occurrence of a cut of this type. It was concluded that two important, site specific, factors contributing to the damage were the broad crested, flat spillway profile that causes a hydraulic drop in the water surface profile over the horizontal crest, and the low 0.5m (1.5 ft.)

headpond elevation to which the water surface was allowed to fall, before the bladder was reinflated. These conditions increased the probability of impact damage to the deflated bladder from floating debris. While inflated, inflatable gates have enough "give" to not be damaged when struck by floating objects.

Presently the bladder control system is being upgraded to allow the bladder to maintain a constant headpond elevation with varying river flows. With this revision the bladder will only be fully deflated when the headpond is at least 2m (6.5 ft) above the concrete crest. This should decrease the probability of future impact damage, since any debris should be carried over the crest well separated from the bladder.

EXAMPLE 3 - ST. REGIS FALLS

The 700 kw St. Regis Falls hydroelectric station, currently under construction, is located on the St. Regis River in northern New York state. This new facility is being built by Azure Mountain Power Company, a private developer, at an existing dam and former mill site. As shown in Figure 2, the new powerhouse and forebay is located adjacent to an existing 32.3m (106 ft) long timber crib dam, equipped with 1.2m (4 ft) high wooden flashboards. These flashboards were previously maintained only for keeping upstream water levels high for recreation.

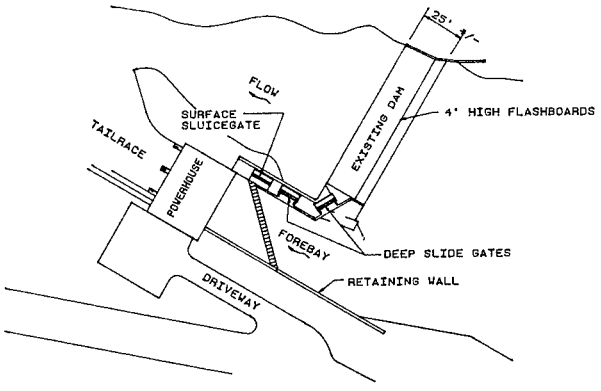

FIGURE 2 - ST. REGIS FALLS SITE PLAN

With redevelopment of the site, the owners are interested in being able to keep the headpond levels high for maximizing power generation, without long periods of time when the boards are out, and with a way to quickly regain control of the river after a flood event where the boards do go out. The site is inside the Adirondack Park and part of the impoundment borders on State Forest Preserve land. Local environmental agencies are interested in more stable pond levels upstream of the site, to preserve wetland areas and wildlife habitat.

The initial hydraulic analysis of the site indicated the existing boards would fail with a river flow of approximately $28m^3$/sec (1,000 cfs), assuming failure begins at two feet of overtopping. This flow is less than the annual flood event, so failure would be expected several times annually. Another concern was in maintaining low headpond levels during flood events, to help with stability of the existing timber crib dam.

Design Approach

To improve the economic feasibility of the proposed station, various methods were investigated to decrease the length of time when the existing flashboards would be breached. Automating the wooden flashboards proved to be undesirable because of the high capital cost and the condition of the timber crib spillway.

During the preliminary stages of the station design, a log Pearson Type III flood flow frequency analysis was performed to determine the probability of various river flows. The 2 year flood event at the site was found to be of $85m^3$/sec (3,000 cfs). Adding two 3m (10 ft) wide by 4m (13 ft) high bottom discharge vertical sluice gates to the new forebay increased the spillway discharge to approximately $96m^3$/sec (3,400 cfs) with two feet of flashboard overtopping. Combining this with the maximum powerhouse hydraulic capacity of $21m^3$/sec (740 cfs) provided a total of $116m^3$/sec (4,100 cfs), which was equal to the 5 year flood recurrence level. This means that in any one year there is a 20% chance that a flood of equal or greater magnitude would occur. While not entirely eliminating breaching of the wooden flashboards this approach provided a significant generation increase and a satisfactory reduction in flashboard maintenance.

In addition, a top discharge slide gate was located adjacent to the trashracks to aid in sluicing debris and ice. Plans for the future include rehabilitation of the dam, which will include installation of hinged wooden boards supported on struts.

Construction

The owner decided to fabricate the gates in his own and local shops. The two vertical steel sluice gates are powered by a hydraulic cylinder, center mounted on the top of each gate. Kleinschmidt Associates provided the detailed design of the gates and hydraulic lifting system, which at the time of this writing (January 1993) are under fabrication. The gates are to be installed in the spring and the station in full operation by August of 1993.

COMPARING ALTERNATIVES

Advantages

When comparing crest control alternatives it is useful to consider the following possible benefits:

1. Increased Energy Production

   A. Maintaining Higher Headpond Elevations

      Automatic systems can maintain the headpond at or above the top of the flashboards and are not like manual flashboards that require the headpond to fall to lower levels before they can be reset. A previous paper by the authors, (Kahl, Ruell 1989), gave an approximate calculation of this potential energy gain. These gains can be easily refined by using a mathematical model incorporating daily average flow values to calculate energy production values for different automation schemes.

   B. Eliminating the Loss of Headpond Storage

      After being breached, manual flashboards generally require the headpond to be lowered to the permanent crest before the flashboards can be reinstalled. After the boards are reinstalled the turbine hydraulic capacity is throttled below the river in-flow until the headpond rises to the top of the flashboards. Automatic flashboards can recover a significant portion of this lost energy since the headpond water level never has to fall below the top of the flashboards.

   C. Flashboard Leakage

      Uncontrolled wooden flashboard leakage can sometimes be economically significant at higher head stations.

D. Intake Blockage

Some stations have significant problems with the intake or forebay becoming blocked by excessive ice and/or debris during certain times of the year. This can be a particular problem for stations on northern rivers that experience significant ice flows during the spring freshet. Automatic flashboards or gates, that can be used to sluice river debris over adjacent spillways and away from the intake, can decrease the length of time that intake blockage curtails turbine operation.

2. Decreased Maintenance Costs

Reducing or eliminating wooden flashboard damage provides a reduction in the labor and materials necessary to repair and periodically replace wooden flashboards. In some cases automatic flashboards also provide the ability to sluice debris over the spillway, thus decreasing trashrack cleaning labor. At some installations, automatic flashboards have converted the intake cleaning operation from a two to a one person operation.

3. Environmental Enhancement

Automatic flashboards or increased gate capacity can reduce or eliminate uncontrolled fluctuations in the headpond water level. This mitigates the spillway's environmental impact by reducing both upstream river bank soil erosion and disturbances to headpond aquatic habitat. Several projects currently under relicensing have proposed automatic flashboards as environmental enhancements in their license applications.

4. Safety

Although it is difficult to evaluate for economics, safety is an important benefit of improving spillway control. Automatic flashboards eliminate the inherently hazardous work of repairing wooden flashboards, thereby decreasing the owners risk exposure to increasing worker's compensation and insurance rates. Most importantly, providing a safer working environment is ethically responsible.

By adding discharge capacity to a site, the flood levels experienced by the structures can be reduced, thus increasing their factors of safety for stability. Conversely, the tendency of maintenance personnel to make wooden boards stronger, so that they do not fail so

often, can reduce the safety factor of a dam due to higher water levels during floods.

Strategies

Although each hydroelectric site is unique, Kleinschmidt Associates has found the following to be useful considerations:

- Understand the Site Hydraulic Conditions

  Example 1 illustrates the importance of confirming what may appear obvious, such as the site's critical hydraulic control cross section.

- Determine the Optimum Length of Spillway Automation

  For longer spillways, automating the entire length of a spillway may not be necessary to obtain most of the benefits.

- Gated Discharge versus Automatic Flashboards

  At sites that are undergoing substantial new civil construction it may be less expensive to provide sufficient hydraulic discharge through smaller gates, deeper in the headpond, than through crest mounted automatic flashboards. Conversely at existing spillways in good condition, installing an automatic flashboard system that has limited cofferdamming and civil construction costs is frequently the least costly way to improve spillway crest control.

- Steel Gates versus Inflatable Gates

  Although it varies between sites, we frequently find that mechanical steel gates present the lowest cost, delivered to the jobsite, uninstalled, compared to inflatable gates. This can result in a lower cost if substantial civil reconstruction is required for other reasons, and the generally more extensive foundation work is already incorporated in the project scope.

  Conversely inflatable rubber bladder systems are usually easier to install and may require less reconstruction cost on an existing spillway crest in good condition.

Reference

1. Kahl, Thomas and Ruell, Stephen (1989) "Flashboard Alternatives Including Rubber Dams", ASCE Waterpower 89 Vol. 1 pp 447-456.

Bottom-Hinged Wood Flashboards

Steven A. Elver[1]

Abstract

This paper will discuss the design, construction and operation of bottom-hinged wood flashboards. These flashboards replace temporary pipe and wood plank flashboards installed on the Schoolfield Dam in Danville, Virginia. This design was chosen over several alternatives, as described within.

Background Information

The low head Schoolfield Dam, located on the Dan River, consists of a 4.5 MW powerhouse, a fish ladder, and a 275 meter long (900 foot) curved ogee spillway. The 7.6 meter (25 foot) high spillway, originally built in 1902, included 0.9 meter (3.0 foot) temporary "pin and plank" flashboards.

The original "pin and plank" flashboards were constructed by stacking (3) - 2x12 planks against vertical 64 mm (2-1/2 inch) steel pipes, 2.4 meters (8 feet) on center, socketed into the concrete spillway crest. The 2x12 planks were 3.6 meters (12 feet) long and lapped 0.6 meters (2 feet) past each pipe. The planks were placed on the upstream face of the pipes and held in place with small straps until water pressure forced them tight against the pipes. The system was designed so the pipe "pins" would fail by bending at the socket support, when floodwater overtopping reached 0.6 m (2 feet). Upon failure, all 2x12 planks were washed downstream.

Based on the Dan River flood frequency, these flashboards failed at a rate of 4 to 6 times annually. Although relatively cost-efficient to reconstruct, a search for an alternative to pin and plank flashboards was undertaken.

Evaluation Criteria

Several alternatives to temporary wood flashboards were investigated. The following criteria were considered for each possible option:

---

[1]Associate, STS Hydropower, Ltd., 111 Pfingsten Road, Northbrook, IL 60062

- **Cost** - Installation, maintenance, and down time costs were analyzed. The alternative chosen had to have a reasonable cost payback compared to operating without any crest control.

- **Reliability** - The new design was required to hold water during normal flow and pass water when flood levels reached 0.5 to 0.75 meters (1.5 to 2.5 feet) above normal, by permit conditions.

- **Adjustability** - With 275 meters (900 feet) of crest control, a staged release would reduce maximum flood levels downstream. For flashboard options, a staged release would also limit flashboard replacement in most flood events.

- **Durability** - Although part of maintenance costs, durability was also evaluated for reconstruction concerns. The Dan River carries numerous trees and other large drift during floods, which could damage crest control structures. Any alternate was to withstand or avoid these forces.

- **Configuration** - Log jam removal after flooding was an important concern. Any structure that caused log buildup would also require log removal mechanisms, with their associated costs.

Alternatives Investigated

Alternatives for raising reservoir elevation range from doing nothing to capital intensive installations such as rubber dams and crestgates.

Raising the reservoir elevation 0.9 meters (3.0 feet) adds approximately 18% to the electrical output of the powerhouse, making some form of structure worth installing.

Taintor gates, permanent flashboards, or drum gates would require numerous abutments along the 275 meter (900 foot) ogee spillway. The associated log cleanups and initial cost concerns eliminated these from consideration.

Rubber dam and hinged hydraulic gate options would reduce log jam concerns. However, concrete rework on the length of the spillway, plus material expenses, made them uneconomical at our 0.9 meter (3.0 foot) height.

Pivoting flashboards are an arrangement where wood flashboards swing on vertical pipes parallel to river flow during floods. This option was eliminated since logs would either jam up on the ends of the parallel panels or they would simply pull the flashboard panel out completely.

A bottom-hinged flashboard section met the criteria for low initial cost, while passing floods without obstruction. The next section discusses how this option fared with the other criteria in our evaluation.

Design of Bottom-Hinged Flashboards

While searching for a solution to our crest control challenge, it became apparent that the chosen option should provide no obstruction to flood flow and should survive any abuse a flood provided. By mounting hinged flashboards on the upstream side of the ogee crest, they would lay submerged as debris scraped on the concrete crest 0.3 meters (1 foot) away.

Another concern of a bottom-hinged flashboard panel was water-tightness of hinge, panels and joints. A 230 mm (9″) wide concrete dumbbell waterstop proved to be an excellent choice for a hinge. Panels were made watertight with inexpensive caulk. Vertical joints were sealed using the same concrete dumbbell waterstop as the hinge.

The most intriguing part of the hinged flashboard option is its structural design. Numerous support concepts were considered before settling on the chain and S-hook option. By adjusting geometries and materials, the Schoolfield Dam design concentrates loading on the steel S-hooks, while the rest of the components stay well below allowable design levels. As flood waters rise, loading on the S-hooks multiplies. This causes failure in a narrow band of flood elevations. The calculations in Attachment A explain the structural design in detail. The graphs in Attachment B explain loading at various reservoir elevations.

The design of bottom-hinged flashboards has two S-hooks per panel. The two hook design provides more stability against racking than a single, stronger hook in the center. Holding the hooks 0.6 meters (2 feet) in from each end better assures that the second hook will fail immediately after the first. Had the hooks been near the ends, a twisting effect could have damaged the panel before it was completely released. Moving the hook connections in from the ends also lowers bending stresses in the wood planks, allowing smaller boards to be used.

For adjustability, different sized S-hooks could be used in different sections of the 275 meter (900 foot) spillway. As a weaker section fails, the reservoir flood elevation recedes accordingly. This extends the amount of time before the next section fails. It often keeps other sections from failing entirely. Flood elevations at failure have been monitored and found to match laboratory results and strength calculations closely.

While the flood recedes, the powerhouse operator opens lower level sluice gates and lowers the reservoir below the concrete dam crest. He has only to swing the flashboard panels into position, adjust the chains, and connect with new S-hooks. This can be accomplished before the flood fully recedes, allowing the reservoir to be filled quickly upon closing of the sluice gates.

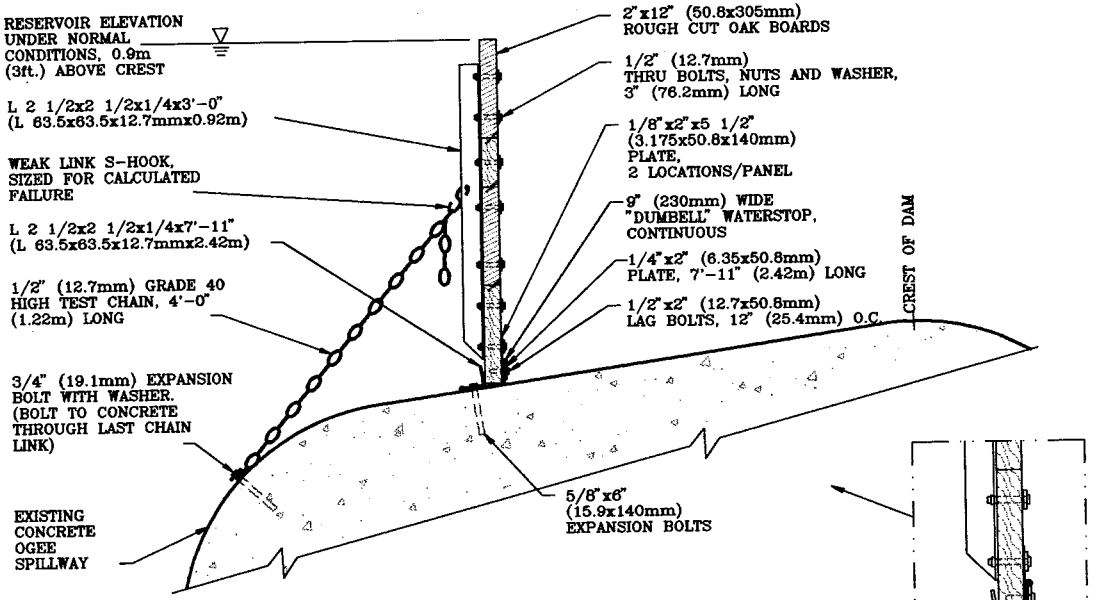

NOTE:
EACH 8' WIDEx3'-6" HIGH (2.44x1.07m) SECTION HAS (2) CHAIN RESTRAINTS, 1 EACH VERTICAL ANGLE.

BOTTOM HINGED WOOD FLASHBOARDS
CROSS SECTION

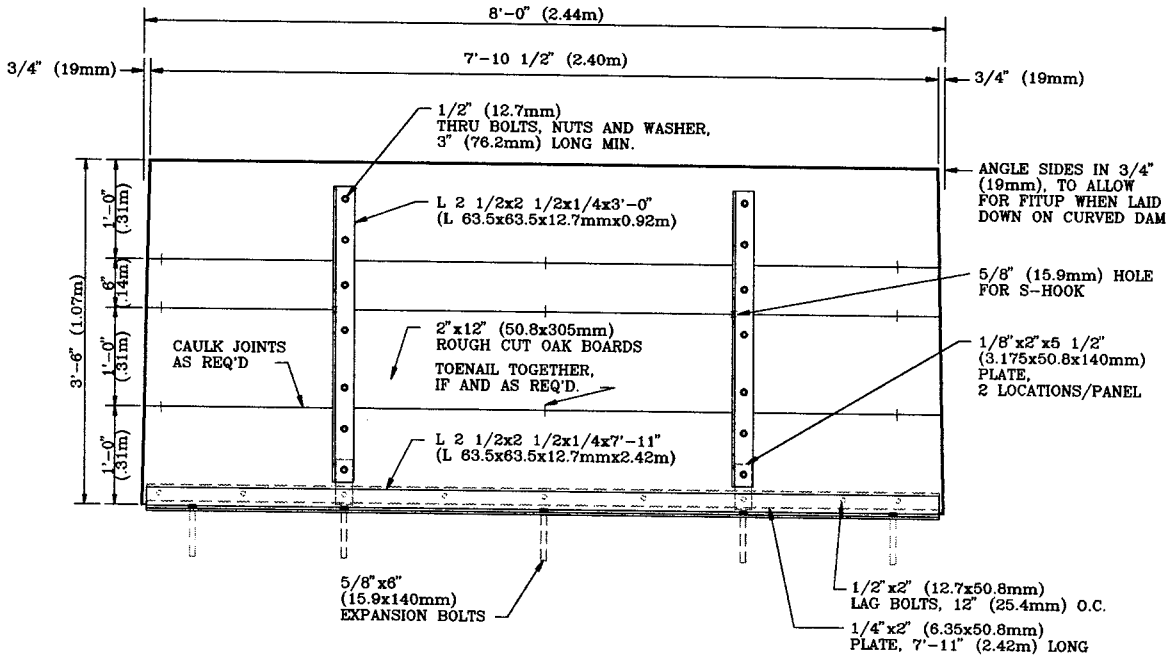

BOTTOM HINGED WOOD FLASHBOARDS
FRONT VIEW, UPSTREAM FACE

S-Hook Laboratory Test Results

S-hook sizing for the flashboard design required test results of actual failure loads. Performed in-house, the following test results were obtained.

	Test Loads at Failure				S-Hook Size
	1	2	3	4	Average
1/4" x 2" STD.	690#	750#	750#	740#	733# (333 kg)
3/8" x 2½" STD.	1330#	1330#	1350#	1330#	1335# (606 kg)
1/2" x 3" STD.	2560#	2580#	2580#	2610#	2583# (1170 kg)
DBL 3/8" X 2½"	2790#	2740#	2770#	2640#	2735# (1240 kg)
1/2" x 5½'Alloy	4190#	-	-	-	4190# (1900 kg)

Since 5/8" standard hooks are not available, it was decided to use both 1/2" x 3" (12.7 x 76.2 mm) and double 3/8" x 2½" (9.5 x 64 mm) S-hooks. Both options fail below the design level of 0.6 m (2 feet) over the flashboards, but are easily available and do not fail too often. (See Attachment B) Alternate suppliers will be contacted, should we desire a stronger S-hook.

Photo #1 - Installation of Bottom Hinged Flashboard Panels

Flashboard Construction

Flashboard panel assembly was accomplished by sending angle and plate shop drawings to a steel fabricator, plus using an on-site construction crew of two. Panels were constructed and stockpiled over a several week period. When the next flood demolished the temporary flashboards, the new hinged panels were ready for installation.

The wall was erected in stages, starting with a 12 meter (40 foot) test section, then progressing about 30 meters (100 feet) after each successive flood. (Installed sections were studied after each flood event to justify the continued installation of the new design).

Actual installation on the ogee spillway required only a concrete drill for fastening the rubber hinge and the steel chains to concrete. Each 2.4 meter (8 foot) section required 7 holes to be drilled, taking about 4 minutes each hole.

The hardest part of the installation was hauling the 160 kilogram (350 pound) panels to their proper location. This was made easier by use of a raft. Each section was slid onto the 1.2x2.4 meter (4x8 foot) raft, pulled in the reservoir along the dam, and dragged off at the proper location.

Flashboard Operation Experience

The flashboards have functioned beautifully for two years. When resetting, the powerhouse operator need only carry a bag of new S-hooks, compared to the previous pipe and plank hauling of temporary flashboard construction.

The panels fail very close to predicted elevations. As shown in Attachment A, the panel geometry concentrates flood forces at the S-hook supports. These S-hooks have proven very consistent in failure load tests, and act accordingly in our installation. This consistency helps control flood levels within permitted limits.

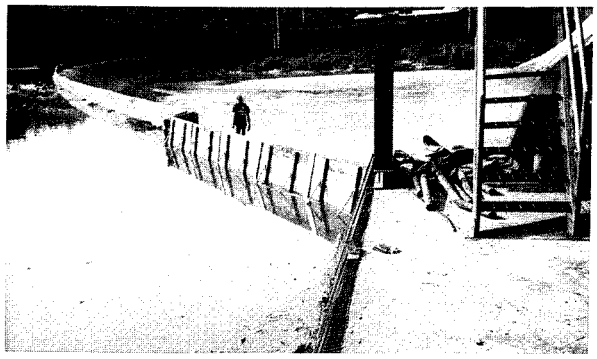

Photo #2 - Raising Water on 12 Meter (40 foot) test section, with temporary flashboards beyond

Bottom-Hinged Flashboard Summary

This alternate to temporary pin and plank flashboards has proven to be a cost-effective choice for the Schoolfield Dam. While other alternatives have merit, the flashboard dimensions of 0.9 by 275 meters (3x900 feet) affect the economies involved.

Bottom-hinged wood flashboards have value in situations where long, low walls are used. They also prevent the buildup of debris on abutments associated with other options. The ease of construction and installation also was appealing.

Regarding durability, all members are designed stronger than the loads applied, with the exception of the weak link S-hooks. Inspection after floods shows all panels to be undamaged, but time will tell how often planks must be replaced due to decay.

This design is being contemplated for other installations, based upon its success at the Schoolfield Dam. Each new spillway will be analyzed for its own characteristics, and the proper alternative chosen accordingly.

ATTACHMENT A

Bottom-Hinged Wood Flashboard Structural Design

This design involves a continuous hinge support at the panel base, and two tension supports per panel. The tension supports are located to carry 90% of the reaction load, concentrating it on a weak link S-hook.

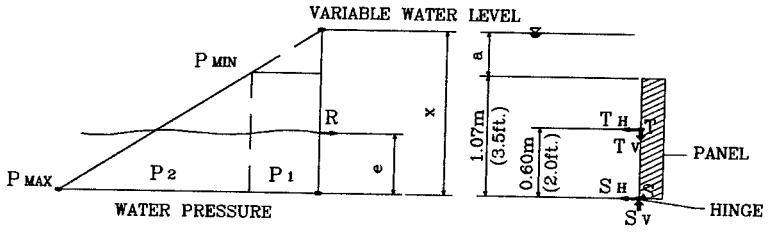

LOADING DIAGRAM

Sample Calculations: For failure when a = 0.60 m (2 ft.)

X = 1.67 m (5.5 ft.)

Pmin = $(9.81kN/m^3)(0.6m)$ = 5.89 KN/m^2 (125 psf)

Pmax = $(9.81kN/m^3)(1.67m)$ = 16.4KN/m^2 (343 psf)

ΔP = 10.5KN/m^2 (218 psf)

R = (5.89)(1.07)+(0.5)(10.5)(1.07) = 11.9KN/m length(819#/ft)

e = [(6.3kN/m x 0.54m) + (5.6KN/m x 0.36m)]/11.9KN/m = 0.45m (1.5 ft.)

ΣM_S=0; T_H = (11.9kN/m)(0.45m)/0.6m = 8.9KN/m length (606#/ft.)

$S_H = R - T_H$ = 3.0kN/m (213 plf)

Calculating chain and S-hook tension, with chain at 45° angle and tributary width = 1.22 m (4.0 ft)...

T = (1.22m) T_H/cos 45° = 15.3kN (3450#)

S-Hook Load = 15.3kN (3450#) @ a=0.60m (2 ft.)

Note that load on S-hook far exceeds hinge load. See Attachment B for design charts.

ATTACHMENT B

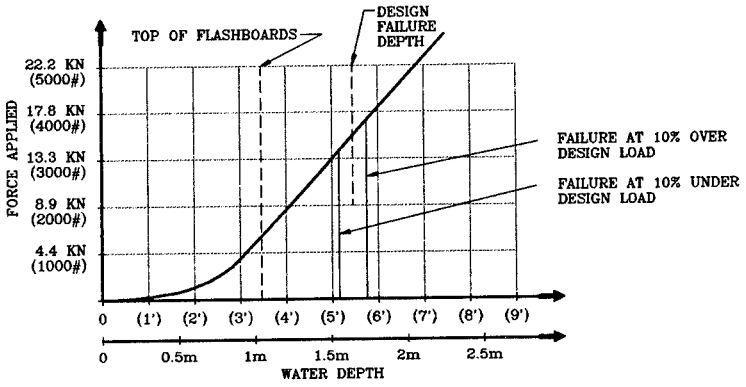

LOAD ON CABLE AND S-HOOK, EA.

STATIC WATER PRESSURE ONLY – NO VACUUM OR IMPACT LOADING

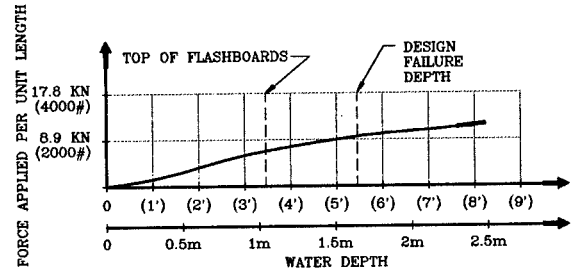

HORIZ. LOAD ON RUBBER HINGE

NOTE SMALL INCREASE IN LOAD WITH INCREASE IN WATER DEPTH

Big Chute Generating Station Redevelopment

I. Lauchlan[1]
W.W. Hall[2]
N.A. Bishop[3]

Abstract

The Big Chute Generating Station is located near Coldwater, Ontario on the Trent-Severn Waterway. This hydroelectric station was originally placed in service in 1909 and has special significance because it was the first owned and operated by Ontario Hydro. The redevelopment includes demolishing the existing four unit 4 MW generating station and replacing it with a new powerhouse and a single 9.9 MW unit. Design work was completed in June 1992. Construction was initiated in 1991 and the station will be in service in November 1993.

This paper describes the special engineering and construction challenges in obtaining environmental approvals and in project development. The Big Chute project is located next to an area of natural and specific interest (ANSI). The area attracts over 100,000 tourists annually, and is adjacent to two marine railways which are a part of the Trent-Severn Waterway. (A marine railway transports boats, barges and ships from a canal at one elevation to a canal at another elevation.) At Big Chute, the old marine railway was constructed by Trent-Severn in 1917 and still operates today. The new marine railway was constructed in 1977 and transports over 10,000 boats each year.

The project was designed to minimize the effect on wildlife, tourism, and

[1] Project Manager, Ontario Hydro, Toronto, Ontario, Canada

[2] Project Engineer, KST Hydroelectric Engineers, Don Mills, Ontario, Canada (A Joint Venture of Klohn-Crippen Consultants Ltd/Stone & Webster Canada Limited/Trow Consulting Engineers Ltd)

[3] Manager of Engineering, KST Hydroelectric Engineers, Don Mills, Ontario

rare plant species in the area. Only winter construction has been planned to eliminate impacts on navigation, requiring careful planning of every detail. A portion of the existing powerhouse will be retained for historic preservation.

Introduction

Feasibility studies for the redevelopment of the Big Chute Generating Station began in the mid-80's. Construction started in October 1991 and the redeveloped project is slated to go in-service in November 1993. The project is located on the Severn River, approximately 140 km north of Metropolitan Toronto.

The project planning and implementation have been largely influenced by the fact that the project area is an environmentally sensitive area and by the large number of tourists who visit the project site. The Big Chute area has been designated as Area of Natural and Scientific Interest (ANSI). The area is known for its outstanding diversity of flora. The ANSI comprises 589 plant species of which 75 are regionally rare, 9 are provincially rare and of these, 5 are nationally rare. The site is located on the Trent-Severn Waterway and is the location of North America's largest marine railway. The marine railway transports boats via a rail car between the tailpool and headpond, a difference in elevation of 17 meters.

Approximately 100,000 tourists visit the site each year, primarily in the summer. Of these, approximately 35,000 are boaters who use the marine railway. Approximately 65,000 land-based tourists visit the site, with most coming to see the marine railways.

The Big Chute Generating Station was the first station owned by Ontario Hydro. The original 3-unit station was built in 1909 by the Simcoe Railway and Power Company. Ontario Hydro purchased the station in 1914 and placed a fourth larger unit in-service in 1919. All of the units were double runner horizontal francis turbines. The powerhouse was constructed of reinforced concrete. Other project elements included a concrete power canal, concrete intake structure and two steel penstocks with a surge tank. The station remained largely unchanged from 1919 to the start of demolition of the station in 1992. The original station utilized a water flow of 37.6 m^3/sec to generate 4.15 MW.

Deterioration of the existing turbine-generator units, as well as the existing structure, necessitated the project redevelopment. Feasibility power studies indicated that the station hydraulic capacity should be increased from the original capacity of 38.7 m^3/sec to 70 m^3/sec for the new station. The increased hydraulic capacity will better match the hydraulic output of the station immediately upstream. The studies indicated that the optimum turbine type is a single unit, full Kaplan, S-Turbine.

Site constraints dictated that the redevelopment project be built within the confines of the existing station. As such, the existing power canal was demolished and a new larger concrete power canal was constructed in its place. An enlarged intake structure replaced the existing intake structure, and a single steel penstock replaced the two original penstocks. The plant layout is shown on Figure 1. The new powerhouse was constructed partially within the limits of the existing powerhouse.

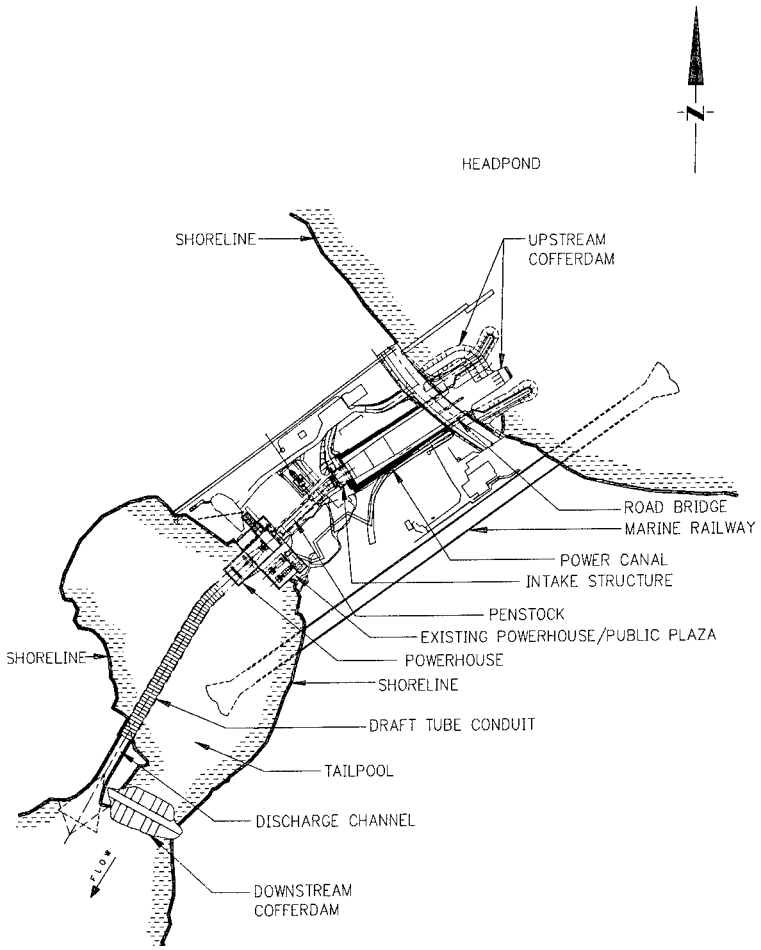

FIGURE 1 : SITE PLAN

In May 1987, Ontario Hydro initiated environmental assessment studies for the redevelopment of the station. In December 1990, Ontario Hydro received the necessary clearances under the Ontario Environmental Assessment Act (EA) and the Federal Environmental Assessment and Review Process.

EA approval included many conditions which were addressed in the design and construction of the station. The conditions included the protection of rare plants, preservation of endangered rattlesnake habitat, and the rescue of fish trapped within cofferdams. The most significant conditions of approval were: 1) requirement for downstream channel improvements, 2) mitigation requirements for impacts to navigation near the marine railway, 3) preservation of the heritage value of the existing station and the natural environment surrounding it, and 4) a requirement that all major construction activities be done in the non-navigation season (mid-October to mid-May). These four conditions had the greatest impact on the project design, cost, and schedule. Each of these issues are discussed individually below.

Downstream Channel Improvements

Increasing the station capacity from 38.7 m^3/sec to 70 m^3/sec will increase currents in the waterway downstream of the station (at the present time, flows in excess of 38.7 m^3/sec are discharged upstream of the station forebay into an adjacent lake which rejoins the Severn River several kilometres downstream of the station). River currents are highest (1.1 m/sec maximum with a flowrate of 38.7 m^3/sec) in a section of the river called Little Chute Channel, which is located 1 kilometre downstream of the station. The conditions of EA approval stipulated that the river currents, after station redevelopment, must be less than the currents which existed prior to redevelopment.

The preferred channel improvement concept called for widening the channel to achieve the required cross section area. However, the conditions of approval stipulated that the visual qualities of Little Chute Channel not be altered. This required that channel improvements be limited to deepening the existing channel. The construction was further complicated by a requirement that all work be done using water based equipment. This requirement was due to the presence of rare plants on the shoreline of Little Chute Channel. Navigation considerations dictated that all work be done in the non-navigation season from mid-October to mid-May.

The Little Chute Channel deepening project included the drilling, blasting and excavation of 12,000 m^3 of Migmatitic Biotite Gneiss bedrock. Blasting was accomplished using holes drilled in a 2 m pattern. A total of 1014 holes were drilled and blasted. Preconstruction water depths ranged from 2 m to 7.5 m. Post construction water depths range from 3.5 m to 7.5 m. The work was completed in the non navigation season utilizing a drill barge containing two drills, a clam

barge, and two rock scows. The maximum velocity in Little Chute Channel after redevelopment will now be 0.7 m/sec.

Navigation Impact

The marine railway loads and unloads boats in the tailpool (See Figure 1). Also, the entire tailpool area is used as a staging area for boats waiting to use the marine railway. To satisfy navigation concerns, it is necessary that the surface currents throughout the entire tailpool area, not be increased as a result of redevelopment. To increase the station discharge by 80% without increasing surface currents, required that a portion of the plant capacity be discharged downstream of the tailpool. To accomplish this, a draft tube conduit was incorporated into the design.

The draft tube conduit will discharge a portion of the turbine flow in the tailpool area by means of openings in the conduit and the remainder will be discharged downstream of the tailpool. Determination of the percentage of the total flow to be discharged into the tailpool must balance the requirements of navigation and water quality requirements. There was a concern that the water quality within the tailpool would be degraded if adequate flushing was not provided.

Determination of what acceptable navigation conditions are and what constitutes acceptable water quality is subjective. For this reason, neither physical or mathematical modelling was considered to be adequately definitive for design. Because of this, a design which allowed for adjustment of the flow within the tailpool was developed. Discharge ports along the draft tube conduit can be opened or closed, by divers, to increase or decrease the percentage of the total flow which is discharged into the tailpool. Once satisfactory hydraulic conditions are achieved during plant commissioning, the discharge ports will remain unchanged in the established configuration.

The original station, which did not include a discharge conduit, discharges station flow at essentially a point source into the tailpool. It is expected that surface currents within the tailpool will be minimized by discharging flow spatially along the draft tube conduit in water depths of approximately 7 m. Therefore, discharge through the conduit of a flowrate equal to the original station flowrate (38.7 m^3/sec) would be expected to improve navigation conditions. However, to be conservative, the initial design is based on discharging 32 m^3/sec into the tailpool and 38 m^3/sec downstream of the tailpool. This represents a 15% reduction in the total flowrate discharged into the tailpool after redevelopment.

Factors influencing the design of the conduit were headloss, construction cost and schedule. The schedule was a significant consideration since the entire civil works of the station must be constructed between mid-October and mid-May.

Early studies suggested the use of three parallel pipelines of 3.66 m. diameter each. This concept was rejected due to concerns that swirl in the turbine discharge would result in uneven flow distribution in the three pipelines. This could result in unstable flow and/or higher than expected headlosses. Because of this, a single conduit design was adopted.

Economic evaluation of the discharge conduit indicated that the headloss should not exceed 400 mm. A single conduit is the most economic solution since a single conduit can meet the required headloss criteria with a smaller flow area than a multiple conduit design. This is because a single conduit has a lower wetted perimeter than a multiple pipeline of equivalent cross sectional area.

The design selected utilized a combination of cast-in-place concrete with precast concrete (Figure 2). The conduit size was established to achieve the required headloss criteria. The selected structural design was based on cost and schedule considerations. The structure is designed for maximum and minimum transient pressures.

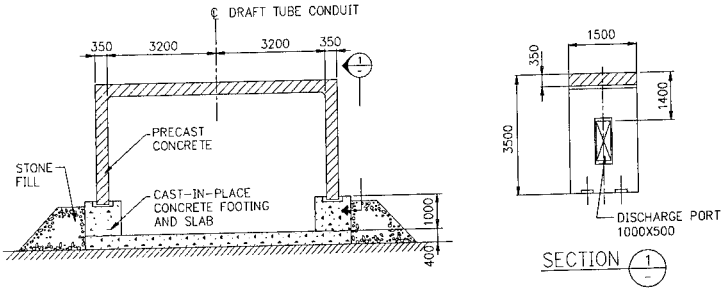

FIGURE 2 : DRAFT TUBE CONDUIT

The design configuration leaves gaps between individual precast concrete units. The gaps were set at approximately 20 mm between units. To supplement leakage through the gaps between precast units, discharge ports are built into the precast panels. Each port is 500 mm by 1000 mm. Flow adjustment is provided by blocking or partially blocking the discharge ports with 500 mm x 250 mm concrete panels. Initially 9 ports will be fully closed and 21 ports will have one-half of the port closed off.

Preservation of Heritage and Natural Environmental Values

Conditions of approval for the project required that the heritage value of the existing station be retained. The existing surge tank tower was identified as a significant feature to be retained. It was decided that, due to the large number

of tourists visiting the area, there was an opportunity to demonstrate how hydroelectric power generation works. A tourist pedestrian observation area or public plaza has been incorporated into the area surrounding the powerhouse. This observation area allows scenic views of the tailrace and operation of the marine railway.

One of the original turbines and two of the existing generators will be retained in place in the original powerhouse. The existing powerhouse roof will be removed and the generator deck level and area surrounding the retained units will become a public plaza. The photograph below shows the extent of the existing powerhouse facilities which will remain as well as the new facilities which are under construction. In addition, turbine runners from the original station will be displayed in the public plaza. Large windows are included in the design of the new hydraulic generating station to provide an opportunity to demonstrate the contrast between the old and new hydroelectric equipment.

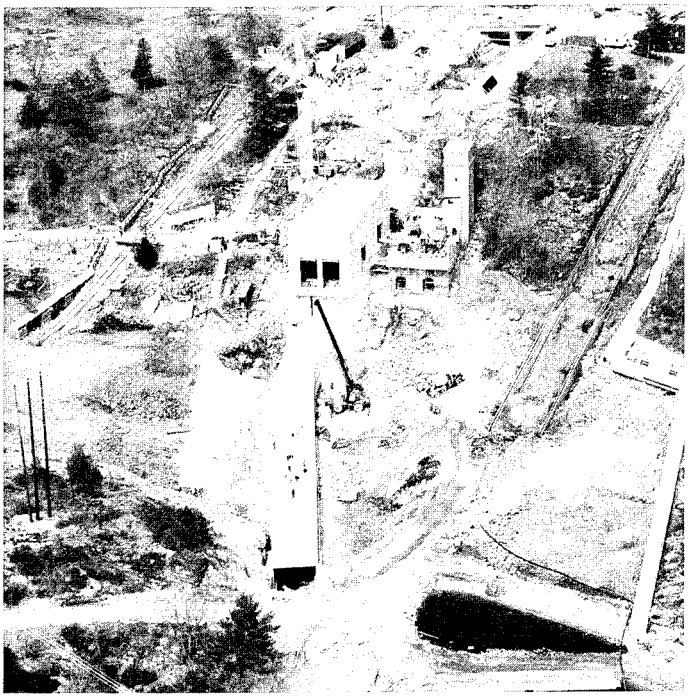

Great care has been taken to ensure preservation of the natural environment. The activities included a video analysis of the Little Chute area using a new technology which would allow before and after construction analysis. This was done so that the "view" would be preserved for those who travelled through this channel by boat. The construction road into the tailpool area was laid out by a botanist rather than an engineer; so that virtually all the rare flora could be preserved. The road allowance was marked by steel stakes to ensure that all travel stayed within the designated approval areas. Extensive silt traps were set up along all travelled areas to prevent construction silt from impinging upon the natural environment. Trees were marked and designated to make sure of their survival. Silt curtains were placed around the cofferdams and silt levels were monitored in the river to ensure that the continued good water quality was available for the fish habitat. Water plants were protected so that they did not become covered with silt.

In areas where construction works had to pass near rare plants, pathways were painted on the snow and access was controlled.

Regular consultations were held with various environment agencies and consultants. As a team, we have been able to preserve the heritage and the environment while providing a new facility for use in the 21st century.

Schedule

The requirement that construction activities be performed between mid-October and mid-May resulted in a very short construction season subjected to harsh winter weather conditions. The work was scheduled in two seasons: the winter of 1991 and winter of 1992.

The first season was used for all construction which did not require shutdown of the existing station. This work included excavation of Little Chute Channel, construction of a new station access road, construction of a new highway bridge accessing the site, and installation of new sluice gates at an adjacent dam.

The second year of construction included essentially all of the stations civil works. The major construction tasks to be completed are:

- Installation of upstream and downstream cofferdams.
- Demolition of existing power generation facilities.
- Drilling, blasting and excavation of 10,000 m^3 of rock.
- Placement of 5,200 m^3 of concrete for the power canal, intake structure, powerhouse, and draft tube conduit.
- Fabrication and installation of a 40 m long, 4.4 m diameter steel penstock.
- Construction of a 4.5 m high x 6.2 m wide by 100 m long draft tube conduit.

- Powerhouse structural steel, precast concrete siding, roofing, powerhouse crane, and turbine embedded parts.
- Construction of a new highway bridge.
- Removal of cofferdams.
- Wet excavation upstream and downstream of the project.

The critical path for the project schedule went through the powerhouse construction. The activities on the critical path included demolition of the existing powerhouse, rock excavation, pouring the concrete substructure, setting the turbine embedded parts and erecting the structural steel/precast concrete siding and steel deck/membrane roof. Completion of the above activities by mid-April was required to allow for cofferdam removal and wet excavation of the tailrace to be completed by mid-May.

To meet the required schedule, the Contractor constructed a 38 m long by 23 m wide enclosure over the entire powerhouse area. The structure included removable roof panels to allow forms, rebar and concrete to be lowered into the powerhouse area. A tower crane with a reach of 50 m provided crane access to the entire powerhouse. The enclosure allowed for work around the clock in the critical powerhouse area. Most of the 3000 m^3 of concrete in the powerhouse was placed in January and February without any lost days due to bad weather conditions. As of the mid-April submittal for this paper, the project is on schedule. All of the civil works are essentially complete and the cofferdams are removed. Final excavation of the intake and tailrace area scheduled for completion by the opening of the waterway on the Victoria Day weekend (May 24).

Conclusion

As with almost all small hydroelectric developments, the Big Chute Generating Station Redevelopment has had a large number of regulatory issues to resolve. In the case of Big Chute, the major issues were navigation and preservation of the original project's heritage values.

Two unique features have been developed to meet the regulatory requirements. The draft tube conduit coupled with downstream channel improvements has resolved the navigation concerns. Retaining a portion of the existing structure and hydroelectric equipment has retained some of the heritage value of the existing structure and also provided an opportunity to demonstrate hydroelectric power to the public.

Development of unique design features coupled with careful scheduling of the project has enabled the project to proceed on schedule and below budget.

DESIGN CRITERIA FOR THE KENTS FALLS PENSTOCK

By Harbinder S. Gill, Chris W. May (Member ASCE)
and Rex C. Powell (Member ASCE)
Acres International Corporation

ABSTRACT

For the design of this welded steel penstock, various combinations of loads were considered to represent the normal load condition, and the construction, intermittent, and emergency conditions. Information from several references was combined to arrive at the allowable stresses in the steel at various locations and under applicable loading conditions. The most conservative approach would be to use the allowable stresses from the requirement of Section VIII, Division 1 of the ASME code for Pressure Vessels. Division 2, which requires a more rigorous analysis, allows higher stress levels but makes no provision for reduced radiographic inspection where high tensile strength is not required. USBR practice is to allow different factors of safety based on whether the loading condition is normal, intermittent, emergency or exceptional. The allowable stresses and inspection requirements were selected by a judicious combination of all these criteria, with due regard to the applicability of each of them, and taking care not to violate the spirit of any. For buckling stability, shear and compression due to bending and axial forces were considered from provisions set forth in the Steel Design Manual published by the United States Steel Corporation. Concepts from this manual, The AISC manual, as well as other sources were combined to develop a method for computing factors of safety against compression buckling. Combined stresses were investigated to ensure that both buckling and shear yield criteria were met.

INTRODUCTION

The Kents Falls hydro project is one of four cascading plants owned and operated by New York State Electric & Gas Corporation, on the Saranac River near Plattsburgh in upstate New York. The 12.4 MW plant has an 820 m long 3.35 m (11 ft) diameter nonembedded penstock. The upper 320 m of the penstock was replaced in 1945. It was determined, in 1991, that the remaining 500 m of the original riveted penstock

Harbinder S. Gill, Project Manager, Chris W. May, Mechanical Engineering Consultant and Rex C. Powell, Supervising Civil Engineer, 140 John James Audubon Parkway, Amherst, NY 14228-1180 (Telephone: 716-689-3737).

required replacement. Several alternatives were considered, including RTR and steel pipes with various methods of support. A preliminary design and cost estimate was used for evaluation of these options.

The selected configuration utilizes continuous a welded steel pipe on ring girder type supports at 19.5 m (64 ft) spacing as opposed to the existing saddle supports spaced every 4.9 m (16 ft). The pipe shell is 9.5 mm (3/8 inch) thick throughout its length, however, as it approaches the powerhouse, the shell is locally thickened to 11.1 mm (7/16 inch) at the ring girders to accommodate higher tensile forces. A corrosion allowance of 1.6 mm (1/16 inch) was applied to the pipe; consequently the design is based on thicknesses of 7.9 mm (5/16 inch) and 9.5 mm (3/8 inch). Static head at the pipe centerline varies from 19.2 m (63 ft) at the upstream end of the new pipe to 46.6 m (153 ft) at the downstream trifurcation. A surge tank is located near the powerhouse to reduce water hammer.

Several guidelines are available for selecting allowable stresses and factors of safety, representing different degrees of conservatism. In order to produce a safe and efficient design, it was necessary to gain an understanding of the background of each source, and select and combine those guidelines considered applicable for the Kents Falls penstock. This paper presents the resulting design criteria that were adopted, along with summarized explanations.

LOADING CONDITIONS

A penstock is subjected to several types of loads over its lifetime. Different combinations of loads were considered in the design process with corresponding safety factors depending on the frequency and likelihood of the load combinations. A discussion of the various design load conditions is as follows:

(a) Normal Loads

- Weight of the steel pipe, weight of water within the pipe, normal operating hydraulic pressures, and other non-transitory external loads such as snow or wind load. Snow and wind loads were based on local building codes and ASCE 7-88. Snow loads effectively increase the weight of the penstock and are not normally considered in conjunction with wind loads.

- Thermal loads due to longitudinal expansion and contraction of the penstock. An expansion joint is normally required between each fixed point on a penstock, such as anchor blocks or fixed pipe supports. The expansion joint must be sized for the maximum anticipated range of thermal movement with the pipe dewatered. For near horizontal gradients the expansion joint is ideally located midway between anchor blocks to minimize thermal loads at anchor blocks, and to minimize movement of the pipe at intermediate supports.

(b) Intermittent Loads

- Under normal operation the circularity of the pipe is maintained by internal water pressure. During the process of filling and draining of the penstock when the pipe is just full or half-full the pipe shell can

undergo flattening and bending, particularly at saddle supports. This was considered as an intermittent load condition.

- Normal operating pressure was added to the surge pressure that results from a total plant load rejection. The surge head is derived from consideration of the pressure wave that is produced when load rejection occurs on all turbines fed by the penstocks (Ref. 1). The wicket gates are assumed to be operating normally at the time. Such an event is historically infrequent at the Kents Falls site and it was considered reasonable to treat it as an intermittent condition.

- Normal operating pressures were added to earthquake loads. Earthquake loads are considered depending upon the location of the project and the corresponding Seismic Risk Zone number (Ref. 2). Vertical and horizontal accelerations are applied as a factor of gravity.

(c) Emergency Loads

- Normal operating loads plus maximum surge resulting from turbine governor malfunction in which the cushioning stroke becomes inoperative and final gate closure occurring at the rate of 2L/a seconds, or less. The parameter, a, is the wave velocity which is dependent on the elastic properties of the penstock as well as constraint from anchor blocks or supports. L is the length of penstock.

(d) Exceptional Loads

- Loads that occur due to malfunctioning control equipment in the most adverse manner. The loads are not used as the basis of design. Precautions must be taken to minimize the probability of occurrence and effects of these loads.

(e) Handling Loads

- Loads that occur during transportation and installation of the penstock should not be overlooked, since they can affect penstock thickness and hence directly impact cost. Parmakian (Ref. 3) derives a simple formula for determining the required minimum penstock thickness based upon the ovalization that occurs when setting an unbraced section of pipe directly on flat ground. For relatively low head projects with large diameter penstocks this formula would be the controlling factor for the penstock thickness. Since handling loads occur only during installation, it is normally more economic to use temporary internal bracing to maintain circularity. This bracing may take the form of either wooden or steel internal spiders located towards each end of the pipe section. This has the added advantage of maintaining circularity during fit up and for welding adjacent sections of pipe. The bracing is not removed until the penstock is fully welded and the installation complete. As a general rule, however, it is not considered prudent to have the penstock thickness less than 9.5 mm (3/8 inch).

ALLOWABLE TENSILE STRESSES

Several guidelines are available for safety factors and allowable stresses, which can be applied to the design of penstocks. Section VIII, Division I of the ASME code for pressure vessels (Ref. 4), generally requires a safety factor of four over ultimate strength, or two over yield strength, whichever is least. Depending on the type of welds and inspection there are further reductions in allowable stresses, based on the joint efficiency. For double welded butt joints, for instance, the recommended joint efficiency is 100 percent if full radiographic inspection is conducted, 85 percent for spot radiography, and 70 percent for visual inspection only. Division 2 (Ref. 5), on the other hand, generally requires a more rigorous analysis and quality control, but allows a safety factor of three. It makes no provision, however, for less than 100 percent radiographic inspection where high strength is not required. USBR (Ref. 6 and 7) practice allows different safety factors for different loading conditions depending on the frequency and likelihood of occurrence of the load combination, as follows:

Normal Condition: The recommended factor of safety (FS) is 3.0 based on the minimum ultimate strength, with the allowable stress not exceeding 2/3 of the minimum yield strength.

Intermittent Condition: Recommended FS is 2.25 over ultimate strength, with the allowable stress no more than 0.8 of the yield strength.

Emergency Condition: Recommended FS is 1.5 over ultimate strength, with the allowable stress not exceeding yield strength.

Exceptional Condition: FS of 1.0 based on the ultimate strength.

No single reference takes into account the loading conditions, degree of inspection and joint efficiency as a whole. The allowable tensions stresses presented in Table 1 give a rational approach to combining these aspects while not violating the intent of each method. For example, if the penstock welds are 100 percent radiographically tested, then ASME Division 2 and USBR agree on the basic factor of safety to be used. Modifications to the safety factor for differing loading conditions, as presented by USBR were considered as a logical extension of the requirements of ASME Division 2. For anything less than 100 percent radiography, ASME Division 1 advocates a greater safety factor with FS equal to 4 instead of 3. As before, the USBR loading conditions were applied but with reduced allowable stresses.

Table 2 shows the actual allowable stresses for ASTM A516 Grade 70 pressure vessel steel selected for the Kents Falls penstock. The steel has an ultimate strength of 483 MPa (70,000 psi) and minimum yield strength of 262 MPa (38,000 psi).

APPLICATION

For relatively high stressed areas of the penstock, it is economic to use 100 percent radiographic inspection to gain the benefit of higher allowable stresses. Low stressed areas of the penstock, such as at quarter-span or near expansion joints, would not require high allowable stresses and may therefore benefit from the reduced cost associated with reduced non-destructive testing.

TABLE 1

ALLOWABLE TENSION STRESSES, F_T

Loading Condition	Description of Non-Destructive Inspection		
	100% Radiographic	Spot Radiographic	Visual Only
Normal	2 F_y /3 but not greater than F_u/3	0.85 F_y/2 but not greater than 0.85 F_u/4	0.70 F_y/2 but not greater than 0.70 F_u/4
Intermittent	0.80 F_y but not greater than F_u/2.25	0.85 (0.80)(3/4) F_y but not greater than 0.85 F_u/3	0.70 (0.80) (3/4) F_y but not greater than 0.70 F_u/3
Emergency	F_y but not greater than 2 F_u/3	0.85 (3/4) F_y but not greater than 0.85 F_u/2	0.70 (3/4) F_y but not greater than 0.70 F_u/2

where: F_y = yield strength of material
F_u = ultimate strength of material

TABLE 2

ALLOWABLE TENSION STRESSES MPa (ksi)
ASTM A516 GRADE 70 STEEL

Loading Condition	Degree of Non-Destructive Inspection		
	100% Radiographic	Spot Radiographic	Visual Only
Normal	161 (23.3)	103 (14.9)	84 (12.2)
Intermittent	210 (30.4)	134 (19.4)	110 (16.0)
Emergency	262 (38.0)	167 (24.2)	138 (20.0)

BUCKLING STABILITY

As part of the overall analysis, and as required by ASME Section VIII, Division 2, (Ref. 5) buckling stability of the shell needed to be investigated. The major stresses for consideration when investigating buckling stability of penstocks are:

- Axial stresses induced by the dead weight of the pipe (for sloped installations only) and thermal expansion;
- Bending stresses induced by the weight of the pipe, water, snow or ice loads, where applicable, and other external loads;
- Shear stresses induced by the same applied loads.

Where the shell tends to bulge around the ring stiffeners due to internal pressure, local bending stresses vary from compression on the outside face to tension on the inside face and are not considered for buckling.

In general, buckling stability of tubes and shells is affected by a number of parameters including:

- Ratio of diameter to shell thickness;
- Ratio of pipe span to radius of gyration;
- Diametral irregularities or imperfections;
- Nature of stresses, such as bending or uniform compression;
- Internal pressure; and
- Boundary conditions.

The mode of compression failure depends principally on the first two parameters and may occur in either the elastic or inelastic range. For long spans, column buckling controls. For intermediate spans, buckling manifests itself in a series of diamond-shaped yield patterns.

It should be noted that several factors have opposing effects on this relationship. Significant out-of-roundness can reduce the critical buckling stress (Ref. 8), while internal pressure tends to stabilize thin shells (Ref. 9). (Paradoxically, internal pressure can contribute to overall column buckling of long tubes (Ref. 10).) However, a number of researchers have shown that critical buckling stress due to bending can be somewhat higher than that for pure axial compression. This is apparently due to the stress gradient within the pipe (Ref. 10). According to Brockenbrough and Johnson (Ref. 8), the increase in buckling strength can be as much as 30 percent.

Buckling stability criteria for tubular and shell structures have been addressed by a number of authors over the years and often correlated with test results. Recommendations presented cover a wide range of complexity and in some cases, limited applicability. It was these authors' intent to select an appropriate set of criteria that is both reasonably conservative and easy to use. The following criteria are based on provisions recommended by Brockenbrough and Johnson (Ref. 8).

Compression

The Kents Falls penstock is an intermediate length tubular structure. In such cases, local elastic buckling of the shell normally controls, and the critical buckling stress is a function of the diameter to shell thickness ratio. The following relationship, established by Plantema in 1946, was used for design:

$$For\ \frac{F_y R}{Et} > 0.20 \qquad f_{crit} = 0.16\left(\frac{Et}{R}\right)$$

where: E = modulus of elasticity (MPa)
R = radius of pipe (m)
t = thickness of pipe shell (m)

This approach compares reasonably well with ASME Section VIII Division 1 (Ref 4) where:

$$f_{crit} = (50\%) \times 0.25\ \frac{Et}{R}$$

for axially loaded cylinders within ASME allowable fabrication tolerances.

Tests by Stephens, et al, 1982 and 1983, confirm Plantema's value for fabricated members in the range D/t = 350 to 450 (Ref. 10). Test specimens had an out-of-roundness limit of one percent, measured by $\frac{D_{max} - D_{min}}{D_{nominal}}$.

At Kents Falls, D/t = 352 and 422 for 9.5 mm (3/8 inch) pipe and 7.9 mm (5/16 inch) pipe, respectively, and the specified out-of-roundness tolerance was 0.5 percent. Consequently, no reduction was taken in Plantema's relationship for potential fabrication irregularities.

According to Marshall (Ref. 10), the factor of safety against compression buckling should be determined in a fashion similar to the approach used in the AISC Manual, Appendix C, where:

$$F_c = \frac{Q_s Q_a \left[1 - \frac{(KL/r)^2}{2(C_c')^2}\right]}{\frac{5}{3} + \frac{3(KL/r)}{8\,C_c'} - \frac{(KL/r)^3}{8(C_c')^3}} \times f_{crit} \qquad C_c' = \left[\frac{2\pi^2 E}{Q_s Q_a f_{crit}}\right]^{1/2}$$

Q_s = Shape Factor = 1
Q_a = Effective Area Factor = 1
K = Effective Length Factor = 1
L = Length of Span (m)
r = Radius of Gyration (m)

For a maximum span of 19.5 m (64 ft) and a pipe thickness of 7.9 mm (5/16 inch):

f_{crit} = 152 MPa (22.0 ksi) $\qquad \frac{KL}{r} = 16.5$

C'_c = 161.4
r = 1.18 m (46.6 in.)

giving $\qquad F_c = \frac{f_{crit}}{1.71}$

A safety factor of 1.71 was therefore applied to f_{crit} in calculating the allowable compressive stress, F_c under normal load. The safety factor is reduced to 1.5 for intermittent load conditions. In no case was F_c allowed to exceed F_T.

Shear

As for compression, shear buckling can also occur in the elastic range (Ref. 8):

$$For\ 10\left(\frac{t}{R}\right)^{1/2} < \frac{L}{R} < 3\left(\frac{R}{t}\right)^{1/2}$$

$$f_{crs} = 0.632E\left(\frac{t}{R}\right)^{5/4}\left(\frac{R}{L}\right)^{1/2}$$

The critical shearing stress, f_{crs}, should be limited to the shear yield strength, $F_y/\sqrt{3}$. For Kents Falls a safety factor of 1.67 was applied to f_{crs} in calculating the allowable shear stress, F_v.

Table 3 summarizes the allowable stresses to be used in design with ASTM A516 Grade 70 steel.

TABLE 3

ALLOWABLE PENSTOCK BUCKLING STRESSES MPa (ksi)
ASTM A516 GRADE 70 STEEL[1]

Loading Condition	Compression (F_c)		Shear (F_v)	
	Thickness mm (in)		Thickness, mm (in)	
	7.9 (5/16)	9.5 (3/8)	7.9 (5/16)	9.5 (3/8)
Normal	88.9 (12.9)	106.1 (15.4)	27.6 (4.00)	34.7 (5.03)
Intermittent	101.4 (14.7)	121.4 (17.6)	30.7 (4.5)	38.6 (5.60)
Emergency	Not critical	Not critical	Not critical	Not critical

[1] 3.35 m (11 ft) diameter x 19.5 m (64 ft) span

COMBINED STRESSES

A continuous pipe supported intermittently will have critical combinations of flexural, shear and local circumferential stresses near the supports. The combined stresses were checked for both yield and overall buckling.

The von Mises-Hencky shear yield criterion was used to check combined biaxial tension and compression with shear at a point of any given penstock or stiffener element:

$$F_T \geq f_e = [f_x^2 + f_y^2 - f_x f_y + 3f_v^2]^{1/2}$$

where: f_e = "equivalent" stress
f_x, f_y = bending or axial stress in the x and y axes, respectively, (tension positive; compression negative).

f_v = shear stress

Buckling stress combinations of the pipe shell were limited at any section of pipe by the following interaction equation:

$$\frac{f_c}{F_c} + \left(\frac{f_v}{F_v}\right)^2 \leq 1$$ where:

f_c = combined and bending stress

The location of critical buckling stress combinations around the penstock circumference varies with the relative magnitudes of axial and shear stresses. As an example, Table 4 shows how the critical buckling stresses interact at a ring stiffener location.

TABLE 4

CRITICAL BUCKLING STRESS INTERACTION
AROUND CIRCUMFERENCE OF
KENTS FALLS PENSTOCK AT RING STIFFENER

α Degrees	Axial Stress f_a MPa (psi)	Bending Stress f_b MPa (psi)	$f_a + f_b$ MPa (psi)	Shear Stress f_v MPa (psi)	$\frac{f_a + f_b}{F_c}$	$\left(\frac{f_v}{F_v}\right)^2$	Combined Interaction
0	5.8 (842)	45.3 (6570)	51.1 (7412)	0	0.56	0	0.56
30	5.8 (842)	39.2 (5690)	45.0 (6532)	11.7 (1695)	0.49	0.18	0.67
60	5.8 (842)	22.7 (3285)	28.5 (4127)	20.2 (2936)	0.31	0.54	0.85
65	5.8 (842)	19.1 (2777)	25.0 (3619)	21.2 (3072)	0.27	0.59	0.86
70	5.8 (842)	15.5 (2247)	21.3 (3089)	22.0 (3186)	0.23	0.63	<u>0.87</u>
75	5.8 (842)	11.7 (1700)	17.5 (2542)	22.6 (3274)	0.19	0.67	0.86
90	5.8 (842)	0	5.8 (842)	23.4 (3390)	0.06	0.72	0.78

where: α = the angle from the vertical pipe centerline to the point of interest
Critical combination underlined

CONCLUSIONS

The resulting analyses produced a cost effective design while meeting the intent of ASME Section VIII and maintaining consistency with the approach taken with allowable tension stresses.

A great number of references are available for selecting buckling criteria for cylindrical shell structures. A reasonably complete list of various proposed equations can be found in Reference 10. The sheer volume of available (and often conflicting) information is, to say the least, cumbersome, and no reference is definitive for structures of this type. These authors have attempted to weed

through the data and present a set of reasonably conservative criteria for the design of intermediate span penstocks.

Thus, in a cost conscious environment, sound engineering judgement, in conjunction with available guidelines and references, and aided by modern computing tools, can today provide designs which are both safe and extremely efficient. A design document that consolidates the design criteria would be a welcome to the industry. ASCE is working towards such a publication.

REFERENCES

(1) Chaudhry, M. Hanif, "Applied Hydraulic Transients," Published by Von Nostrand Reinhold Company, 1979.

(2) Building Seismic Safety Council for the Federal Emergency Management Agency, NEHRP (National Earthquake Hazards Reduction Program) Recommended Provisions for the Development of Seismic Regulations for New Buildings; 1988 edition, Part 1, Provision.

(3) Parmakian, J., "Minimum Thickness for Handling Steel Pipes," Water Power Dam Construction, June 1982.

(4) ASME Boiler and Pressure Vessel Code, Section VIII, Division 1

(5) ASME Boiler and Pressure Vessel Code, Section VIII, Division 2, Alternative Rules

(6) USBR, "Welded Steel Penstocks," Engineering Monograph No. 3.

(7) Arthur, Harold G., and Walker, John J., "New Design Criteria for USBR Penstocks," Journal of the Power Division, Proceedings of the American Society of Civil Engineers, January 1970.

(8) Brockenbrough, R. L., and Johnston, B. G.,"Steel Design Manual," United States Steel Corporation - Steel Design Manual, 1981.

(9) Young, W. C., "Roark's Formulas for Stress and Strain," 6th edition, McGraw Hill, 1989.

(10) Galambos, Theodore V., "Guide to Stability Design Criteria for Metal Structures," 4th edition, Published by John Wiley and Sons, 1988.

TIMBER-CRIB DAM REHABILITATION

by Alan Bondarenko, M. ASCE[1], Paul Martinchich[2], Daniel J. Barton[3], and Paul C. Rizzo, M. ASCE[4]

ABSTRACT

This paper provides the results of engineering investigations and analyses related to the rehabilitation of two rock-filled timber-crib dams. Columbia Dam, located on the Broad River in Columbia, South Carolina has been effectively remediated. Engineering investigations, analyses and the final design, including construction plans and specifications for the rehabilitation of Eastvale Dam, located on the Beaver River near Beaver Falls, Pennsylvania have recently been completed. Construction remediation is scheduled to commence in the spring of 1993. Coincidentally, the original crib structures of both dams were constructed in 1891.

INTRODUCTION

The great popularity for this type of dam during the early era of American history can be attributed to the fact that, with suitable materials, in sufficient supply and being readily available on the local market, timber-crib construction methods provided a quick and economical means for developing communities to satisfy their growing needs for water supply and power. It was known that under conditions of continuous submergence or constant dryness, timber selected from woods having high decay resistant properties yield useful service lives exceeding 50 to 75 years, with minimal maintenance. However, those sections of a dam prone to wet/dry cycles or subjected to damage by floating debris would deteriorate more rapidly necessitating a greater degree of maintenance. One of several types of timber dams, rock-filled timber-crib dams are gravity type structures and are subject to the same analysis against overturning and sliding as other types of gravity dams.

Rock-crib dams were normally constructed of sawed timbers, ten to twelve inches square and laid crosswise to form pens eight to twelve feet apart. These pens were then filled with rock. The timber chosen was usually white oak or yellow pine, both noted for their natural resistance to decay and rot. The cribs were constructed on the bank at a stage where they could be floated in place. Additional timber stringers (those fixed in their direction across the stream) and ties (those with their direction parallel to the flow) were floated to the crib and bolted in place. As the weight of each crib increased with the addition of timber, the cribs

[1] Project Supervisor, Paul C. Rizzo Associates, Monroeville, Pennsylvania 15146.
[2] Engineer, Paul C. Rizzo Associates, Monroeville, Pennsylvania 15146.
[3] Project Manager, Paul C. Rizzo Associates, Monroeville, Pennsylvania 15146.
[4] President, Paul C. Rizzo Associates, Monroeville, Pennsylvania 15146

would sink. Once construction had proceeded to the point where the crib would be resting on the foundation due to its own weight, the cribs would be bolted to foundation rock, and the placement of riprap begun.

The riprap was normally of a size known as "one-or two-man stone." The actual rock size, as the name implies, was limited to what one or two men could carry and place. The placement of rock within the cribs was usually limited to a height of a few feet and maintained below water level simply to enhance stability during construction. The concept was to permit the flow to continue through and over the dam until all cribs were securely anchored in place by bolts and rock. Once this was completed, additional rock was brought in to fill the cribs. The upstream and downstream surfaces of the dam would be faced with timber sheetpiling (one or two rows) to the crest of the dam.

Permanent dams were usually built straight and at right angles to the river. However, other forms such as that used at Columbia and Eastvale Dams were sometimes used. These alternate configurations included a curve of large radius (Eastvale) or straight broken arms as at Columbia inclined to the axis of the river. The intent was to lengthen the crest thereby obtaining a longer spillway. The greater length over which the action of the water was extended minimized the tendency for undermining and facilitated discharging of flood waters.

Rock-crib dams were generally of two types regarding cross section, either stepped or sloped. The bottom width of the dam was sufficient to prevent overturning and its foundation strong enough to resist the associated pressures. The solid rock foundations existing at the dams discussed here minimized concerns with the latter. Rock-crib dams, such as Eastvale, normally had a ratio of bottom width to height in the range of 2.5 to 3.0 to provide for a more gradual drop of the water from pool to pool and to reduce the potential for undermining. However, at Columbia we found that the ratio is just slightly greater than 1.0 in many locations along the dam. This small bottom width to height ratio raises the question of long-term stability; although the 1929 and 1950 concrete remedial work probably enhanced its stability to a certain degree.

COLUMBIA DAM

Project History

The history related to the Columbia Dam is long and complicated. Prior to 1819, commercial navigation along the Broad River, beginning about two miles above Columbia, South Carolina and terminating one mile below, was impossible because of the presence of rapids. A canal - 16 feet wide at the bottom, 28 feet wide at the surface, and 3 feet deep - was completed in 1824 to pass boats around the rapids. A dam was not required for diversion.

With the coming of railroads, the canal was practically abandoned for navigation. Between the years 1840 and 1887, the canal passed through several ownerships and proved profitable to none, each time reverting to the state. Water power from the canal was used for gristmills and sawmills located along the canal and for a small powerhouse that pumped water for the city of Columbia. Major state legislation was passed in 1887 which authorized a substantial increase in the size of the canal and the construction of the dam. In late 1891, the dam and canal improvements were completed. At that time, the canal cross section had been increased to 110 feet wide at the bottom, 150 feet wide at the top, and 10 feet deep.

Columbia Dam, in plan (Figure 1) appearing as three bent segments approximating the letter "L" is slightly longer than 1,000 feet. The original timber-crib section is about 20 feet wide and varies in height from 6 to 19 feet. A powerhouse on the Columbia Canal was completed in 1894. In 1929, a concrete cap and downstream buttresses were added to the dam, and in 1950, concrete aprons were placed between some buttresses (Figure 2). Today, the dam and canal project generates hydroelectric energy and provides municipal water to the city of Columbia. The Columbia Dam, owned by the South Carolina Electric & Gas Company (SCE&G), is licensed by the Federal Energy Regulatory Commission (FERC) as Project No. 1895, and is classified as having a low hazard potential.

In response to a request from FERC, SCE&G retained Paul C. Rizzo Associates to investigate the stability of the dam under static and dynamic conditions. A program for exploratory test pits and geotechnical borings was developed, and laboratory testing on rock and concrete was performed for use in the evaluation of dam stability. Hydrologic and hydraulic analyses included developing a probability of annual occurrence versus flow relationship and a relationship between flow and headwater, and tailwater depths. A computer model for determining stability of gravity dams consistent with FERC guidelines was developed in-house. Conceptual designs for remediation were developed. After review and approval by SCE&G, final plans, specifications, and cost estimates were prepared.

Initial Dam Inspection

An inspection of Columbia Dam was made by Paul C. Rizzo Associates in December 1984, during a period of low river flows. After the dam inspection was conducted, a preliminary stability analysis of the dam was performed. Observations and comments resulting from the inspection and the preliminary stability analysis included:

- The dam did not appear to be in eminent danger of failing at small overtopping depths; however, concern was expressed for safety of the dam when overtopping exceeds ten feet.
- High velocity leakage through the dam, in many cases flowing through pipes, had resulted in minor to major erosion of the dam toe over approximately half of the dam length, reducing overall dam stability.
- A "blowout" of the downstream concrete face was another possible consequence of the excessive leakage coming through the dam.
- Apron concrete, which was placed in the 1950s, was highly deteriorated.
- Decayed timbers were visible along the upstream dam face.

Prior to conducting the dam inspection, it was felt that a major grouting program might be a good first step in upgrading the structure. However, the inspection results suggested that this was not a good idea for a number of reasons. First, the voids in the rock fill appeared to be choked with silt and clay throughout. Secondly, the upstream face was highly pervious

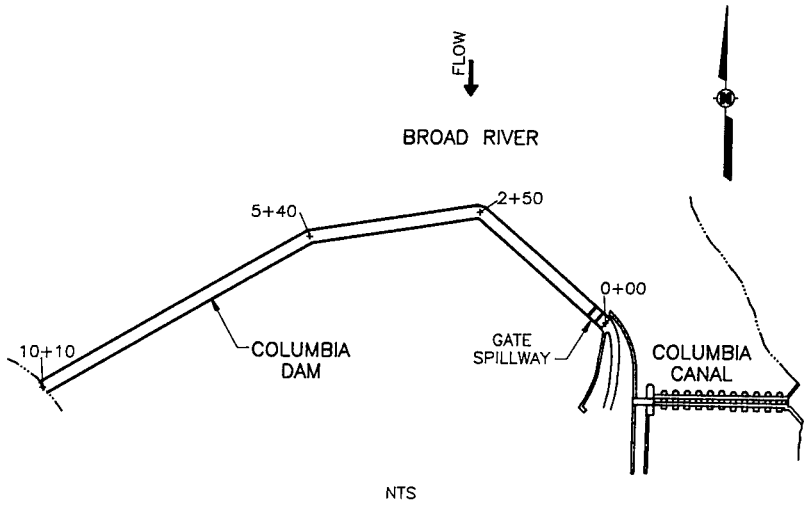

Plan View - Columbia Dam
Figure 1

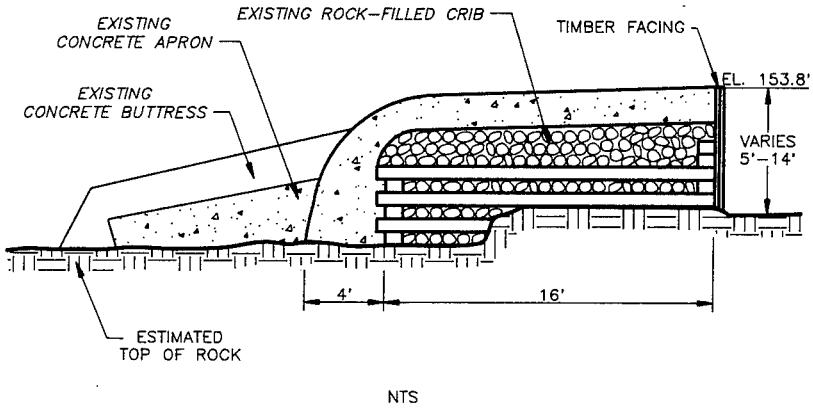

Typical Cross Section - Columbia Dam
Figure 2

Note: Flow is from right to left.

suggesting that any grouting from the crest would eventually find its way, quite rapidly, into the headwater pond. Thirdly, any application of high pressure to displace the grout could cause dangerous pressure increases behind the downstream concrete face.

Hydrologic and Hydraulic Analyses

Fifty-three years of peak stream-flow was available from the USGS gage located upstream of Columbia Dam. Statistical analyses were performed to develop a probability of annual occurrence versus flow relationship at Columbia Dam. Existing canal channel information, past flooding information, and applicable equations for calculating discharge and tailwater depth were used to develop a relationship between flow, overtop depth, and tailwater depth. Using the flow versus probability data, and the flow versus overtop depth and tailwater depth data, a graph of probability of annual occurrence versus overtop depth and tailwater depth was developed.

Stability Analyses of Existing Dam

A computer model for determining stability of gravity dams consistent with FERC guidelines was developed at Paul C. Rizzo Associates. This model was developed in a Lotus-123 environment. With this in-house computer model: 1) uplift varies from full headwater to full tailwater over 100 percent of the base, 2) tailwater pressures are reduced during floods, 3) both static and earthquake analyses can be performed, 4) silt or sand loading on the upstream face can be added, 5) anchor forces can be included, 6) drainage galleries can be added.

Stability analyses were performed on the most critical dam section, i.e., Station 6+20 which had the highest cross section with the maximum amount of sediment behind it. Because of the questionable interconnection between the apron and buttresses and the original dam, the stability of the dam was analyzed without the apron or buttresses.

Remedial Design Concepts

Based on conversations with SCE&G personnel, conceptual enhancements were developed to 1) prevent excessive leakage through the dam, 2) correct areas of erosion at the downstream toe, and 3) improve the apron concrete. Two alternate construction procedures were presented for constructing a three-foot wide reinforced concrete wall on the upstream dam face to stop excessive leakage through the dam. Option 1 involved using a temporary sheetpile wall approximately six to eight feet upstream of the dam. Option 2 (selected alternative) involved placing a permanent sheetpile wall three feet upstream of the dam, i.e., the sheetpile wall would be the upstream face of the concrete wall. The new upstream concrete would be doweled into the existing dam and into the granite bedrock. Recommended enhancement procedures on the downstream side of the dam included placing concrete bags under the dam or apron toe where erosion had already occurred and then placing a one-foot thick reinforced concrete face on the existing apron. This concrete face would be keyed into the granite bedrock at the toe of the apron and doweled into the existing apron and buttress concrete (Figure 3). Plans, specifications, and cost estimates were prepared for the enhancement measures.

The remedial work, which was fully designed in September 1986, was not started for approximately one year because SCE&G could not obtain required construction permits. They experienced problems with the South Carolina Fish and Wildlife Commission who did

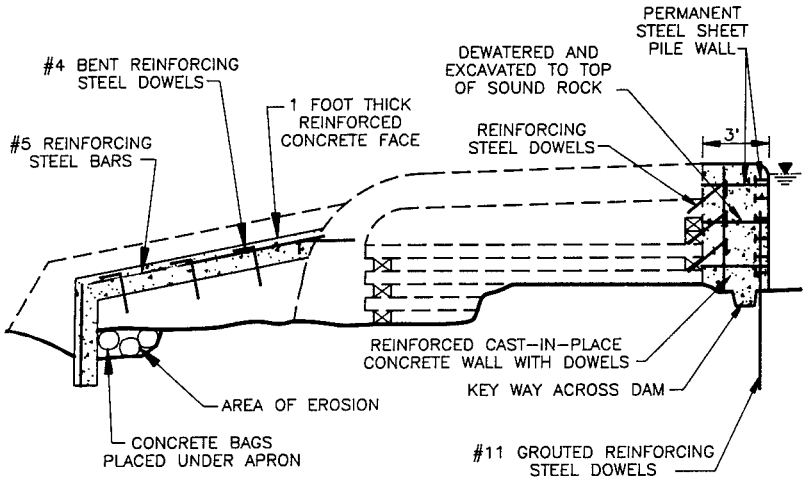

NTS

Upstream and Downstream Remedial Enhancements
Columbia Dam
Figure 3

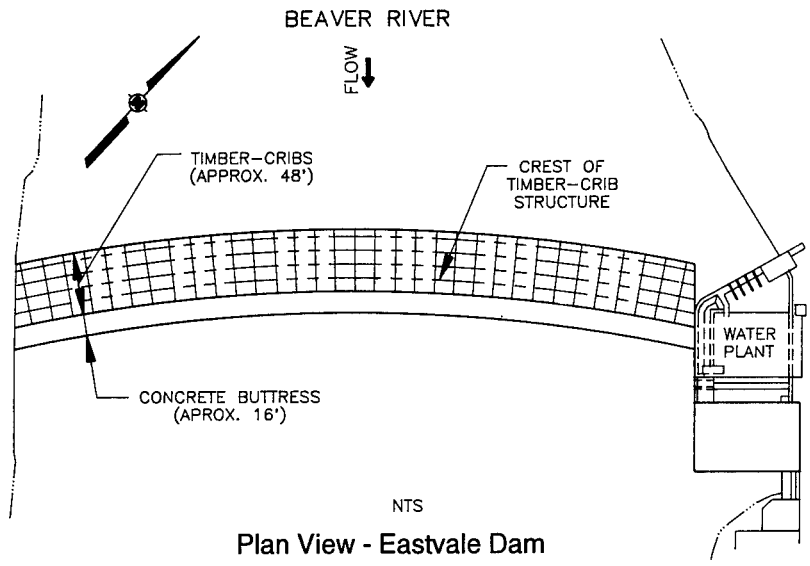

NTS

Plan View - Eastvale Dam
Figure 4

not want the excessive leakage to stop because the fishing downstream of the dam would be harmed. SCE&G also had problems with the South Carolina Historical Commission who did not want the rock-crib dam to be totally encased in concrete.

In September 1987, SCE&G became concerned about the safety of the dam. They believed that the leakage on the east side of the dam had increased substantially. Paul C. Rizzo Associates was asked to make an emergency inspection of the dam. At this time, the required permits for construction were still not issued. SCE&G also notified FERC of the leakage problem who informed them that they could proceed with emergency repairs under the FERC license regardless of the status of the state permits.

Although, the water level was low during the emergency inspection, it was noted that east of Station 2+50 flows had increased dramatically in previously recorded leak locations and also new leaks were observed. It was recommended that, as a minimum, the leaks between Stations 0+00 and 0+50 be repaired as soon as possible. In addition, it was also recommended that, if possible, repair work should extend to the first bend (about Station 2+50). FERC concurred with the recommendation to proceed with the repair work immediately.

As of the end of March 1988, the first 100 feet of the upstream repair work had been completed and work on the downstream area commenced. Staged construction phases continued across the dam in this manner up to Station 2+50. Once the permitting issues were resolved work began on the remaining length. Remedial work was successfully and effectively completed by February 1989.

EASTVALE DAM

Project History

The Eastvale Dam is located on the Beaver River between Beaver Falls (right bank) and Eastvale (left bank), in Beaver County, Pennsylvania (Figure 4), approximately 5.3 miles upstream from the confluence of the Beaver and Ohio Rivers. The dam, first called Hartman Dam, was originally constructed in 1891 using rock-filled timber-cribs. It replaced an older structure, the Adams Dam, which at one time existed immediately downstream. Hartman Dam and its appurtenant facilities were constructed to provide for a guaranteed and continuing source of potable water to the growing communities and industries along the Beaver River.

The dam is approximately 500 feet long and has a maximum height of approximately 17 feet. The dam is a fixed-crest weir structure and operates in a passive, run-of-the-river mode. When originally constructed, the crest of the dam was at Elevation 731.5 feet above mean sea level (MSL). Continued deterioration of the dam has resulted in a current average elevation of 730.7 feet MSL.

The original dam has required general repairs and replacement of structural members (normal maintenance) throughout its history, and on several occasions major repair efforts have also been undertaken to insure its integrity, most notably in 1922 and 1923, a 15-inch-thick reinforced concrete slab was placed on the top of the downstream side of the dam. A concrete slab 30 inches wide and averaging 4 inches thick was also placed along the crest of the dam. At the same time, a solid concrete buttress section, 16 feet wide, 11-1/2 feet high at the crib and 7 feet high at the downstream face, was poured against the downstream side of the timber-crib structure to key the old structure in-place (Figure 5).

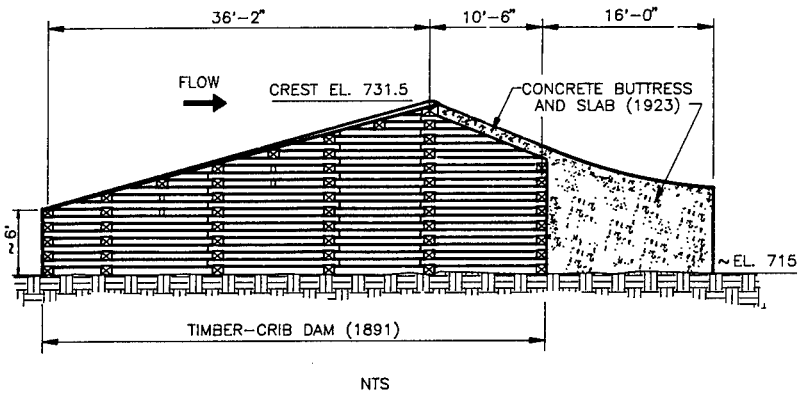

Typical Cross Section - Eastvale Dam
Figure 5

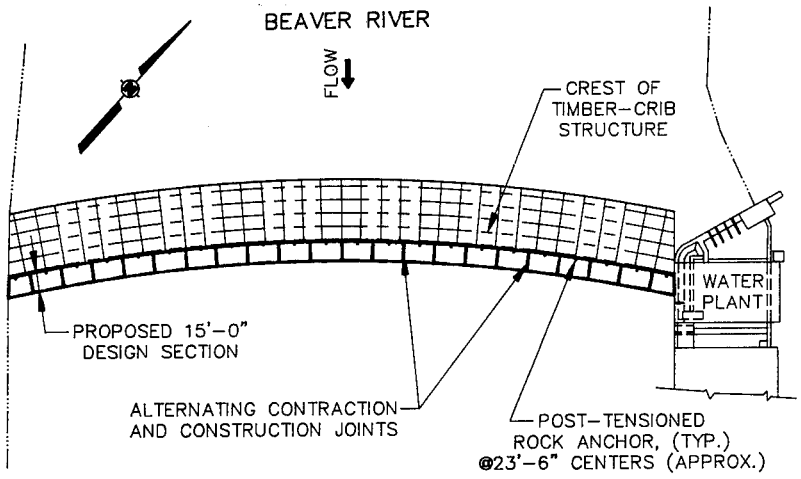

Plan View - Eastvale Dam
Downstream Buttress Stabilization
Figure 6

The impoundment created by Eastvale Dam is the Beaver Falls Municipal Authority's (BFMA) principal source of supply of potable water and flow for fire protection purposes to about 85 percent of twenty-one municipalities within Beaver County (approximately 60,000 persons). It is therefore imperative that the integrity of the dam be maintained; a loss of the established headwater pool created by the Eastvale Dam impoundment (i.e. dam breach failure) would greatly jeopardize public health and safety.

Existing Conditions

The overall condition of Eastvale Dam is poor. Significant deterioration of the dam is evident, including: spalling and cracking of the protective concrete overlay for the dam; erosion of the timber-cribbing and rock-fill; and occurrence of significant voids in the downstream concrete buttress. It is noted that the abutment masonry walls appear in good condition, and that the dam is founded on competent bedrock.

The deterioration of Eastvale Dam has resulted in significant seepage through and under the dam. Seepage beneath the dam is especially pronounced along the eastern side of the dam (i.e. water-intake side); seepage through the dam is especially pronounced throughout the central half of the dam; and minor leaks through the left abutment wall have been observed. Overall, based upon our interpretation of stream gage data, seepage is expected to be on the order of 600 to 800 cfs.

Rehabilitation Concept

Preliminary evaluation of the dam indicated that two potential rehabilitation schemes were apparent -- Downstream Buttress Stabilization and Timber-Crib Stabilization. Downstream Buttress Stabilization involves modifications to the downstream buttress of the dam to achieve stand-alone dam stability and control; this scheme includes an ogee-type concrete structure retrofitted to the existing buttress and anchored to bedrock. Timber-Crib Stabilization could involve placement of a concrete cap on the existing upstream wooden-plank face, repair of existing concrete, and complete grouting of the rock-filled crib structure. Due to efforts related to grouting the rock-filled crib structure, the uncertainty of the condition of the timbers themselves, our experience with other timber-crib dams, and the specific economics of this particular situation, rehabilitation by Downstream Buttress Stabilization was the more attractive alternative.

Based upon results of the site investigation, the viability of the Downstream Buttress Stabilization alternative was confirmed, and this approach was carried through the final design phase. Stability analyses of this alternative confirmed the feasibility of this concept. The conceptual design of this rehabilitation principally involves the following:

- Downstream buttress grouting to fill voids in the concrete of the existing buttress and to develop a suitable concrete/rock interface.

- Reinforced concrete ogee-type structure keyed and doweled into the existing downstream buttress. The crest height of the ogee surface would be to the same height as the design height of the existing structure; the upper part of the existing timber crest would be removed.

- Rock anchors tying the ogee-type structure into the bedrock foundation of the dam. Anchors would be placed two feet from the upstream face of the existing buttress; final analysis indicates that 22 anchors with a design load of 316.4 kips each would satisfy the stability criteria.

Stability Analysis

Eastvale Dam is under the jurisdiction of the Pennsylvania Department of Environmental Resources (PADER). In accordance with its low height and minimal hazard potential to downstream habitation, the dam has been classified "C-3" by PADER's Division of Dam Safety. As such, the recommended design flood for Eastvale is the flood having a 100-year recurrence frequency. The allowable factors of safety for sliding failure recommended by the FERC were used to evaluate sliding stability of the dam.

As requested by the BFMA, related to the possible future addition of a hydroelectric facility to the dam, the addition of a three-foot-high rubber dam extension to the ogee-type structure was evaluated. To facilitate the possible future addition of the rubber dam, the rock anchor loads necessary for dam stability were determined based on the loading criteria of an additional three feet of head in the upstream pool.

Weir Crest Profile Analysis

The shape of the ogee crest profile to be implemented for the rehabilitation of Eastvale Dam (i.e., buttress stabilization) was determined using the hydraulic design criteria presented in the U.S. Department of the Interior, Bureau of Reclamation publication, "Design of Small Dams," Second Edition (USBR, 1973). The "ideal" crest profile based upon our hydraulic analysis would be formed with a combination of parabolic and radial curves. Our final design effort was therefore directed towards developing a profile that, while still providing for maximum resistance to cavitation and still maintaining the required discharge capacity, would be more easily constructable.

Construction Sequence

The construction sequence for the rehabilitation project will begin with the placement of a temporary HDPE liner on the upstream face of the timber-crib structure. The temporary liner material will impede continuous seepage of water through the timber-crib structure and existing voids within the concrete buttress of the dam. Once the liner has been installed, the contractor will form and install a temporary cofferdam in front of the working area along the dam. The cofferdam will impede water from entering the construction area during the grouting of existing voids within the concrete buttress. After the grouting has been completed, a boring and testing program will be performed so that the quality of the grouting program, as well as the concrete/rock interface strength, may be verified.

Upon completion of the grouting phase, work will proceed with the construction of the ogee-type concrete addition. The surface of the existing buttress will be cleaned and roughened to sound concrete prior to overlay concrete placement. Before placing the ogee-type concrete addition, the drilling for the proposed post-tensioned rock anchors and steel dowels must be completed within the designated work area. The placement of concrete formwork and steel reinforcement will be secured prior to pouring of the ogee-type concrete addition. Once the concrete has reached its required strength, the post-tensioned

rock anchors will be installed, grouted, stressed, and tested according to design and technical specifications. The rock anchor details have been developed to permit future lift-off testing capability (Figures 6 and 7).

The top three to five feet of the existing concrete and timber-crib crest will be removed. This will afford for a better flow regime over the new downstream crest and increase the public safety by eliminating a point of access onto the river. The ogee-type concrete addition will become the new crest of the Eastvale Dam.

On behalf of the BFMA, Paul C. Rizzo Associates prepared the application documents for construction loan assistance from the Pennsylvania Infrastructure Investment Authority (PENNVEST), which provides low interest construction loans to owners and operators of water and sewer systems for infrastructure improvements. PENNVEST awarded the BFMA a loan in the amount of 1/2 of the total construction cost. Construction will commence in the spring of 1993 and is expected to be completed by the end of 1993.

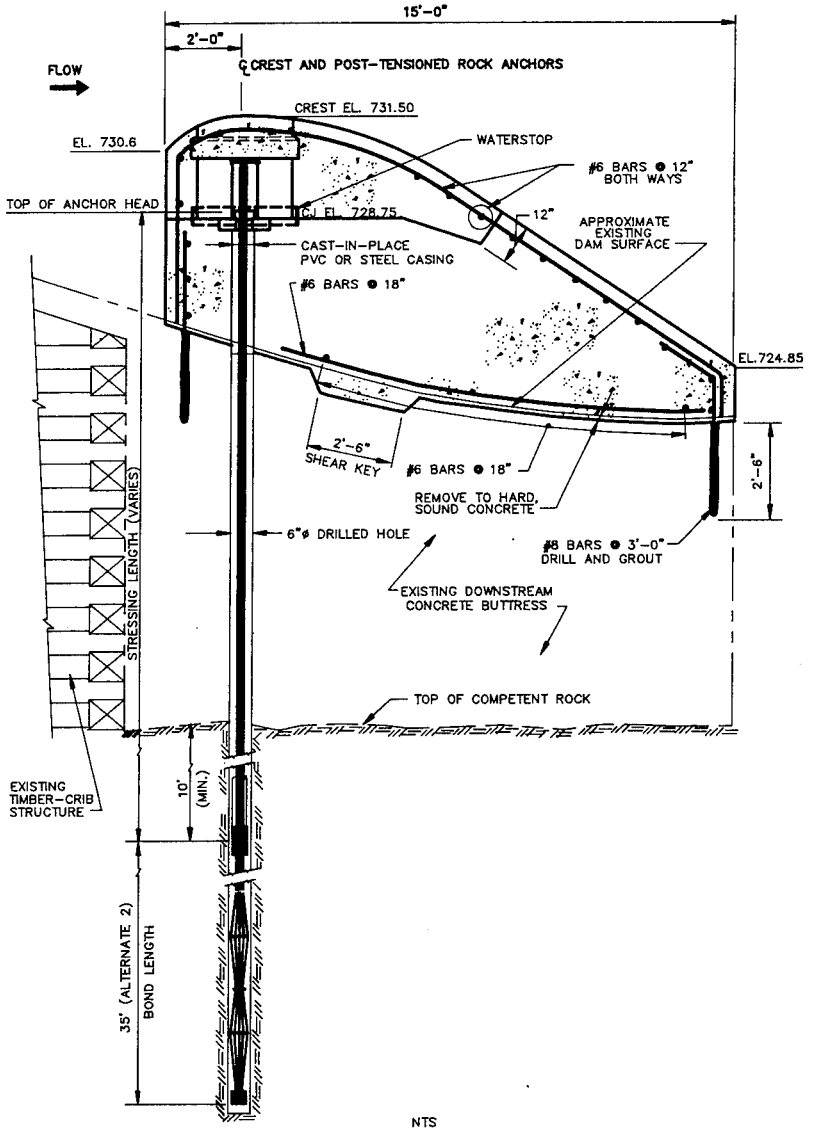

Typical Cross Section - Eastvale Dam
Downstream Buttress Stabilization
Figure 7

Replacement of Deerfield No. 5 Dam

Michael E. Rook[1]
William S. Rothgeb[2]

Abstract

This paper describes the design and construction of the replacement of No. 5 Dam and power station intake on the Deerfield River in western Massachusetts by the project owner, New England Power Company. The project consisted of removal of a timber crib dam and construction of a mass concrete dam with crest gates and modified power canal intake.

Introduction

Deerfield No. 5 Dam in northwestern Massachusetts on the Deerfield River, owned by New England Power Company (NEP), provides impoundment and water through a tunnel, canal, and penstock system for a 16 MW hydroelectric station located five kilometers downstream. In 1989, NEP determined that the existing timber crib dam was approaching the end of its service life and decided to remove and replace the dam and rehabilitate the adjoining intake for the power station.

The reconstruction of the dam presented several challenges in the design and construction:

- The project site has been developed since 1887 with numerous reconstructions and modifications. Few drawings of the present or previous structures were available.

---

[1]New England Power Company, 25 Research Drive, Westborough, Massachusetts 01582.

[2]Black & Veatch, P.O. Box 8405, Kansas City, Missouri 64114.

- The primary site consisted of an area of about 4,000 square meters (one acre).

- The only access to the dam was a public road with a bridge which crossed the river downstream of the dam at the project site. The crossing was one of the few bridges that span the river in the area.

- The river is located in a narrow channel approximately 45 meters (148 feet) wide with high banks that restricted diversion capacity during construction.

- The excavation required a 20 meter (65 foot) vertical cut at the base of a 230 meter (750 foot) high hill, with slopes of up to 45 degrees. Evidence of past slides was found by stereoscopic viewing of aerial photos.

- The foundation consisted of massive rock at the right abutment and as much as 25 meters (80 feet) of overburden at the left abutment, which was only 35 meters (115 feet) away. The overburden included spoil material from past construction and slide material from several earlier washouts of dams at the site.

Site Background

Construction on the original timber crib dam started in 1886 and was completed in 1887 for the purpose of supplying process water to a paper company. In 1901, this dam was destroyed by a storm and later reconstructed by the paper company in 1902. In 1913, NEP purchased the dam, adjacent buildings, and water and flowage rights, and started construction of the No. 5 Hydroelectric Development in 1914, which was completed and placed in commercial operation in 1915.

The Deerfield No. 5 development is located in western Massachusetts on the Deerfield River. The run-of-the-river powerhouse has a single vertical Francis unit with a rated capacity of 16 MW, generating an average of 67,400 MWh annually. The design head is 48.2 meters (158 feet), and water diverted by the timber crib dam travels through a series of three canals, two conduits, and two tunnels for approximately 5.2 kilometers (3.2 miles) before reaching the powerhouse. The No. 5 dam impounds 187,500 cubic meters (152 acre-feet), has a surface area of 153,600 square meters (38 acres), and a drainage area of 614 square kilometers (237 square miles).

Timber Crib Dam Evaluation

The original dam was constructed by the timber crib method because of the difficulty of transportation to the site, good availability of timber, and the variability of the foundation material, which ranges from rock to deep layers of soil.

Timber crib dams are constructed of round or square timbers, drift-pinned together to form square bins which are filled with rock fragments or boulders, and topped by a plank deck. The timbers are usually spaced at 2.4 meter (8 foot) centers in both directions. Typically, leakage is very great and accelerates with time; however, saturation is necessary for preservation of the crib timbers. Timber crib dams can generally tolerate slight settlements because of their composition.

The life of a well-built timber crib dam has been estimated at 20 to 30 years. Proper maintenance plays a large part in its service life, which has allowed some dams to remain in service for 80 to 100 years. A timber crib dam is largely supported by the fill and will stand for some time after the timbers have become materially decayed. Repair of timber crib dams is very difficult since timbers are buried in the fill.

The crest of No. 5 dam experienced significant settlement totaling 3.1 feet since 1901. The rates of settlement progressively increased, and in April 1984, a downstream deflection (bowing) of the crest was first observed. In an effort to maintain a consistent reservoir elevation, the crest was rebuilt three times during the second timber crib dam's lifetime. The source of crest settlement was most likely a combination of decaying timbers, cribbing compaction, and foundation movement.

Economic Replacement Assessment

An economic replacement assessment initiated in 1986 utilized a cost/risk analysis to determine the most timely and economically viable dam replacement alternative. On the basis of the station's average annual generation, installed capacity, book value, and a remaining expected development book life of 63 years, station retirement was not considered a viable solution.

The analysis reviewed the economics of several dam type alternatives under planned and unplanned replacement conditions over a five-year study period. A planned replacement option allowed for the orderly selection and design of a replacement which could be scheduled for construction in a timely and efficient manner, but also assessed the risk of dam failure before construction completion.

The unplanned replacement option assumed that the replacement would not have the advantage of organized planning and timely implementation. Unplanned replacement cost projections were comprised of dam failure related costs such as lost capacity, energy and plant availability, property damage, and a noncompetitive bidding process, followed by planned replacement costs. The study included the cost of continued station operation until dam failure, which impacted both options and consisted of penalties associated with reduced energy, capacity, and availability due to continued settlement of the timber crib dam.

To quantify the costs of a planned versus unplanned replacement, a dam failure probability was assigned to each of the following five years. These probabilities provided a formal, consistent approach to evaluate the likelihood of a failure event. Failure probabilities, which are an assessment at a particular point in time, collectively predicted probabilities of dam failure or of successful operation through time.

Study economics included the costs associated with pursuing a planned replacement in each of the five years of the study (1987-1991) versus the expenses incurred with the risk of delaying replacement throughout the same time frame. This approach optimized the planned replacement timing and expense while minimizing exposure to dam failure, station generation interruption, and downstream property damage. Cash flows for both planned and unplanned replacements were developed and adjusted by failure probabilities.

The alternative to a planned replacement option risked delaying replacement until dam failure (unplanned). The cost components of an unplanned and planned replacement were identical. Differences were in the timing of the cofferdam construction, lost generation, and property damage costs, and in the application of the annual dam failure probabilities. Costs were developed based on a dam failure occurring in the beginning of each of the five study years, which subsequently triggered a 36-month planned replacement. Costs were then accumulated in the calendar year incurred.

Study results showed that the accumulated present worth cost/risk associated with an unplanned replacement was less expensive than the 1987 (first evaluated year) and 1988 planned replacements and more expensive thereafter. Based on the analysis, NEP scheduled replacement of the dam starting in 1989.

FERC Approvals

The Deerfield No. 5 Development is one of seven hydroelectric stations within the Federal Energy Regulatory Commission's (FERC) Licensed Project No. 2323. Before dam replacement and intake rehabilitation were initiated, NEP sought from FERC a decision on how the work would be handled within the license guidelines. Upon review of the work scope, FERC determined that it could be completed under a maintenance work order, avoiding a lengthy and detailed license amendment preparation. Although the work scope was extensive, FERC's decision was based on the fact that there was to be no change in operating conditions (such as reservoir and tailwater elevations and unit flow rates).

Arrangement

Because of the narrow river channel at the project site, the primary criterion for the arrangement of the replacement dam was the size of the inflow design flood (IDF). The minimum acceptable IDF, established by NEP and FERC, was the 100 year flood, which was calculated to be 1,014 cubic meters per second (35,800 cfs). The project flood of record (since 1927) occurred in 1938 when a hurricane moved up the eastern coast and created flood flow of 674 cubic meters per second (23,800 cfs). To determine the acceptability of the 100 year flood flow for the project IDF, Black & Veatch (B&V) modeled the 9 kilometers of the Deerfield River upstream and downstream of No. 5 dam with the National Weather Service program DAMBRK. Breach analyses conducted in accordance with the FERC guidelines indicated that no significant incremental hazards occurred due to a breach of the dam at flows equal to or higher than the 100 year flood. Consequently, a project IDF of 1,014 cubic meters per second (35,800 cfs) was proposed and accepted by FERC.

The primary criteria for establishment of the project arrangement consisted of the following:

- Project spilling capacity of 1,014 cubic meters per second (35,800 cfs).
- Close control of headwater level to avoid fluctuation in the water level in the canal between the intake at the project site and the generating plant.
- Significantly reduced maintenance from what was experienced with the existing timber crib dam.
- Passage of the minimum flow.

- Passage of the project flood without impact on the existing public highway bridge located immediately downstream of the dam.

- Modified intake structure to improve hydraulic conditions and handling of river debris.

The project arrangement is indicated in Figure 1.

A concrete dam with two 2.44 m by 14.63 m (8 feet by 48 feet) hydraulically operated, single arm crest gates was selected for the spillway. The crest gates permitted passage of the IDF, and allowed control of headwater elevation and passage of river debris. The supporting concrete dam with flip bucket stilling basin was sized to meet the FERC stability criteria. High strength silica fume concrete was proposed for the flow surface to minimize erosion.

To improve the hydraulic intake, removal of the upstream portion of the existing intake was selected. The remainder of the concrete intake was judged to be in adequate condition for rehabilitation rather than replacement. The reconstructed trash racks were oriented such that river debris could be carried past the racks to the crest gates by river flow. The rehabilitation included replacement of the 3.81 m by 3.96 m (12.5 feet by 13 feet) intake sluice gate at the mouth of the tunnel leading to the power canal; replacement of two 2.44 m by 2.44 m (8 feet by 8 feet) flood sluice gates which divert water around the dam; and installation of a 1.52 m (5 foot) diameter minimum flow bypass pipe and valve arranged for the potential installation of a future generating unit. A new control building was arranged that would be directly over the new sluice gates for control of all five gates. The backup power system, supplied by a diesel-powered emergency generator, was located in a nearby building.

The protection of the highway bridge, 30 m (100 feet) downstream of the dam center line, was a major concern. To evaluate the proposed arrangement, NEP contracted with Alden Research Laboratory (ARL) of Holden, Massachusetts, to construct a physical model and conduct hydraulic studies, including the following:

- Confirmation of spilling capacity.

- Evaluation of the stilling basin and flow stability for flows up to the IDF.

- Evaluation of protection of the highway bridge.

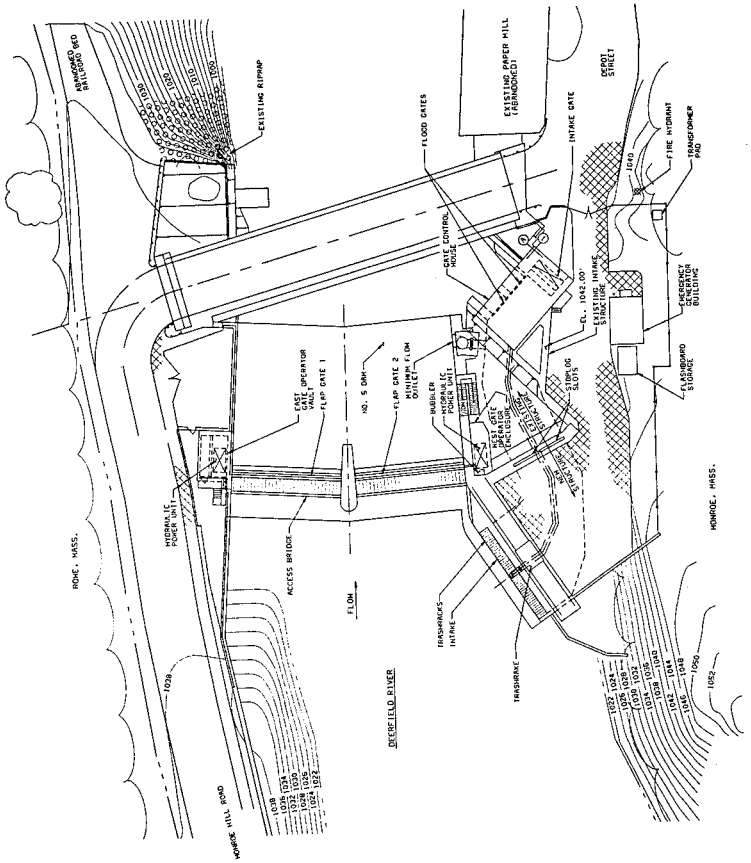

Figure 1. Project Arrangement

- Study of flow during construction and confirmation of calculated diversion capacity.
- Evaluation of the proposed intake orientation modification.
- Erosion study of proposed riprap design.

Initial tests showed that flow from the proposed flip bucket was not stable near and at the IDF, and that the existing highway bridge would be intermittently struck by the water discharge from the flip bucket. To provide more stable flow conditions, ARL tested and recommended shortened conventional stilling basin arrangements with concrete energy dissipators. A revised stilling basin to minimize excavation depth was adopted. To ensure that the flow would not impact the bridge and to improve construction accessibility, NEP entered into an agreement with the Commonwealth of Massachusetts to replace the bridge with a new prefabricated steel truss bridge with a higher elevation. The remainder of the proposed arrangement was confirmed by the hydraulic studies.

Spillway Crest Gates

The existing timber crib dam crest (El. 1,021.7), with 1.8 meter (6 foot) high flashboards, was not designed to safely pass the new IDF. The spillway dimensions necessary to pass the IDF within the site space limitations required two gate openings that were each 14.6 meters (48 feet) wide, with the spillway crest lowered to 1,019.7, and the dam crest raised to 1,042.0. These dimensions, coupled with the reservoir's historic operating elevation of 1,027.66, fixed each crest gate size at 2.44 meters (8 feet) high by 14.6 meters (48 feet) wide.

The crest gate design considered specific environmental, operation, and maintenance parameters. Environmental considerations did not allow hydraulic gate hoist placement within the waterway to avoid the potential environmental problem of oil leaking into the river. To accommodate this environmental design aspect, a torque tube flap gate was adopted. This type of gate rotates around a tube at the bottom of the leaf section.The tube extends through a wall bearing into a vault where the hydraulic operating cylinders are located.

As far as the operation and maintenance design aspects were concerned, the design further specified that the gates were to have "Zero Leakage," primarily to minimize downstream ice buildup during the severe winter months. Adherence to this specification will be determined by a performance test conducted upon project completion. The gates were also required to withstand ice loadings, adjust to accommodate reservoir fluctuations, and be capable of raising against 2.44 meters (8 feet) of flow depth over the spillway crest.

Construction Staging and River Diversion

To maintain the generating station on-line to the extent possible and permit diversion of the river, construction was divided into two phases. Phase I included removal and replacement of the existing timber crib dam and installation of the crest gates while maintaining operation of the intake. Phase II included the modification of the intake after the new dam was in place.

Staging of the cofferdams was required. Phase I required both upstream and downstream cofferdams. Cellular sheet pile cofferdams were chosen for both cofferdams to enhance construction access and minimize environmental effects. A cell common to both Phases I and II could also be constructed on the upstream side. Phase II required only an upstream cofferdam because the flood gates were above frequent tailwater elevations.

Diversion of the river during Phase I was a major concern. The intake and flood gates had the capacity to pass less than the 2-year recurrent flood. To enhance the capacity, concrete on the downstream side of the intake was removed and replaced with temporary flashboards. Additionally, a sheet pile wall was constructed between the dam and intake to permit flow over the top of the intake tunnel without spilling into the excavation. To minimize the potential flow, NEP drew down Harriman Reservoir, located 8 kilometers (5 miles) upstream of the site to allow for storage of a 10.2 cm (4 in.) rainfall over a 6 hour duration. This type of storm has a 50 year recurrence interval.

Provisions were also made for potential flooding of the excavation. The tops of the upstream cofferdams were set at an elevation which would pass the 10 year flood without breach along the road at the left abutment. Flashboards were added to prevent frequent overtopping. The tops of the cells and the excavation immediately downstream of the cells were hardened with concrete slabs. A portion of the downstream cofferdam was lowered to permit flooding of the excavation from tailwater before overtopping of the upstream cofferdams. Because NEP monitors and controls the projects upstream of the site, a minimum of 24 hours advance notice of a flow that would overtop the Phase I cofferdam could be provided.

The Phase I construction was completed without overtopping. The most serious condition occurred in August 1991 when Hurricane Bob dumped heavy rain on New England similar to the 1938 hurricane that caused the historical maximum flow at the site. Enough rain was absorbed by the drawdown in Harriman Reservoir, however, to prevent flooding at No. 5 Dam.

The agreement to replace the old highway bridge was well received by the nearby towns and also allowed the contractor to shut off public access to the site. Even with this advantage and the access provided by the cofferdams, the confined and remote site required adjustments. Laydown and staging areas in the immediate site area were restricted. Crane use had to be carefully planned. A batch plant was set up nearby because the travel time from a ready-mix plant was too long.

Excavation and Foundation Treatment

Excavation for the new spillway required a 20 meter (65 foot) vertical cut at the base of Skeeter Hill, a steep incline which had evidence of past slides and active surface movements. The vertical cut was supported by a secant wall consisting of encased steel pipe and tied back by eight rows of soil anchors drilled into the hill. The bottom of the wall was extended to depths adequate to prevent deep slope stability failures and prevent undermining by scour in case of flooding the excavation. The water table behind the wall was also drawn down to improve stability. During construction, water levels were monitored in a series of piezometers, and movements were monitored by survey points on the wall and inclinometers within the hill. The wall was abandoned in place.

Following excavation, the foundation for the new spillway was treated to improve bearing capacity and reduce potential settlements and seepage. A portion of the intended foundation contained as much as 4 meters (13 feet) of loose soil, rock, and debris from earlier constructions. To avoid further excavation depth, a grid of jet grout was injected at 250 points on 1.5 meter (5 foot) centers. Depending on soil conditions, the jet grout application effectively consolidated the foundation by either constructing columns of approximately 1.2 meters (4 feet) in diameter or by filling voids to produce a grouted mass.

Project Status

Phase I construction was completed during the summer of 1992. The gates were installed and mechanically tested without the hydraulic operators because the new control building was not to be constructed until Phase II.

As of January 1993, the intake modification was approximately 60 percent complete. Remaining construction was scheduled for completion in March 1993.

SOME PROBLEMS ENCOUNTERED IN THE DESIGN AND CONSTRUCTION OF HYDROELECTRIC PROJECTS

Edgar T. Moore[1], P.E., S.E., M. ASCE

Abstract

A discussion is first presented of some potential problems related to specific geologic and topographic conditions, concerning: pressure tunnels in permeable, low modulus rock, unfavorable dip and strike of rock strata, high in-situ rock stresses, detection of shear zones and faults, volcanic deposits, weathering in tropical zones, expansive and dispersive clays, ancient buried river channels, glacial effects and degradation in transportable materials. An additional discussion is presented concerning some potential problems related to omissions in the analysis and design of structures concerning: cavitation, vortex formation, uneven settlement and rotation of structures, vibration and resonance, inadequate provision of joints in concrete structures and deleterious chemical reactions with cement in concrete.

Introduction

A discussion is presented of some potentially significant problems related to specific geologic and topographic conditions which the author has encountered during his work in some 25 countries. The purpose of this presentation is to make designers familiar with these conditions so that they will be prepared to address their possible existence during reconnaissance and field investigations. When these conditions are not detected before construction begins, they can require significant design changes and result in serious overruns in construction time and cost. An awareness of these conditions and the consequences of overlooking them, should encourage design engineers to adopt an appropriate program of investigations.

---

[1]Consulting Civil Engineer, Hydroelectric and Water Resources Projects 1448 Sugar Creek Ct., Naperville, IL 60563. TEL: (708)778-0906

An additional discussion is presented on some omissions in the analysis and design of structures which can impair their performance or useful life. An awareness of the potentially undesirable consequences of such omissions should encourage an appropriate evaluation during design.

I. Problems Relating to Project Geology and Topography

- Pressure tunnels located along ridges and topographical noses may offer a serious potential for leakage. This is particularly true where the bordering valley sides are steep and progressive gravitational relief has resulted in well developed vertical, or near vertical, jointing in the rock mass. Weathering can be advanced and deep under such circumstances, and existing groundwater levels can be as low or lower than the proposed level of the tunnel. Because a potential for serious leakage may exist, it is imperative that exploratory drilling extend to, and some distance below, tunnel depth. Drilling must be oriented to intercept the principal joint sets recognized to exist along the tunnel alignment. The permeability of a rock mass is essentially a consequence of the discontinuities within the rock mass, such as joints and shear zones. Drilling vertically in a rock mass where the principal joints are near vertical, for example, cannot disclose much about a potential for leakage. Water pressure test must be performed at the expected tunnel operating pressure to determine the potential for leakage and necessity for installing an impermeable lining to contain leakage (Reference 1). In addition, the modulus of rock deformation, which includes both the elastic compression of the in-situ, intact portions of the rock and the inelastic closing of open joints, may be quite low. As a result, the rock mass may not share much of the internal pressure load with a reinforced concrete liner. The steel reinforcing may then be too highly stressed and strained to limit the crack width such that leakage is controlled (Reference 1). In some cases the rock modulii along the tunnel can be estimated with some accuracy prior to excavation based on an evaluation of the exploratory drill hole core and an inspection of exposed rock outcroppings in road cuts and deeply eroded water courses. The modulii of deformation should always be confirmed once the tunnel is completed. A careful evaluation may require the adoption of a steel tunnel liner in some reaches of the tunnel. A badly leaking concrete lined tunnel with inadequate reinforcing, can require an extensive and expensive grouting program to reduce leakage to acceptable limits. A reinforced concrete lining should not be considered for a tunnel in a jointed or poorly cemented, permeable rock mass with a low modulus of deformation when the tunnel is to be subjected to high internal operating pressures.

If an evaluation of conditions indicates that a steel liner should be adopted, the steel liner must also be carefully analyzed for possible support or even

lack of support from the contiguous in-situ surrounding rock when subjected to its internal pressure loading. Additionally, an evaluation must be made to assure that the steel liner can safely resist, without buckling, any possible external water pressure that can develop when the tunnel is dewatered for any reason (Reference 2).

- An unfavorable attitude (dip and strike) of major joint sets in rock strata can seriously affect the disposition and stability of major structures and excavation side slopes. This is of special importance when the joint contact surfaces are planar and are smooth or slickensided. When structures subject to lateral forces are founded on rock where the dip is downward and away from the direction of the forces and the joint surfaces daylight out of the rock mass, serious instability can occur requiring expensive anchorage and drainage considerations. This applies to the setting of gravity dams, large retaining walls, tunnel portals, access road cuts and deep side hill cuts on abutments for spillways and intake structures. Opening and establishing safe, stable portals for power tunnels and their temporary access adits to obtain additional work headings can be an extremely difficult and expensive proposition when the rock attitude is unfavorable. Figure 1 shows the required excavation slopes in steeply dipping soft shales and sandstones encountered on a project where a spillway chute was to be excavated into a dam abutment. The excavation slopes follow along the principal joint sets consisting of the bedding planes on the left side and along well developed jointing oriented approximately normal to the bedding planes on the right side. When a rock mass has been subjected to some folding, one of the principal joint sets is usually coincidental with the bedding planes, i.e. the contact surfaces between successive strata. Alternative excavation lines which would be inherently unstable are indicated for comparison by out of function dashed lines.

- The orientation and magnitude of in-situ rock stresses should be determined before locating underground structures such as large tunnels and powerhouse caverns. Across most of the U.S.A., plate tectonic movements have produced a maximum principal horizontal stress in the North American Plate in the approximate direction East Northeast by East that in some places is several times larger than the vertical stress. The trajectory of high, horizontal, in-situ rock stresses passing around a circular excavation created by a tunnel, for example produces a tangential, tensile stress at the horizontal spring line that can exceed the tensile strength of the rock. In addition, it produces a tangential compression stress at the crown and bottom invert that approaches a value 3 times greater than the average horizontal in-situ stress (Reference 3). This localized stress can sometimes be high enough to exceed the compressive strength of the rock. To prevent undesirable rockburst, rock

slabbing and severe horizontal cracking near the spring line in excavated walls, it is advantageous to orient large diameter tunnels and caverns parallel to the direction of the maximum principal horizontal stress. This author has been associated with a project where the principal horizontal rock stress was determined to be several times greater than the vertical rock stress at the level of the underground powerstation. The principal horizontal in-situ rock stress exceeded 50 percent of the rocks' average measured compressive strength. Needless to say, cavern and tunnel orientation was a very important consideration.

- The detection of the location and orientation of major discontinuities in the rock mass, such as shear zones and faults, is important to locating and constructing tunnels and underground caverns. Much can be learned from studying the orientation of existing dominant joint sets, from examining stereographic photos for recognizable surface lineaments of significant extension and, from examining topographic maps to discover surface erosion features that show a very recognizable repeating pattern. Surface erosion features can sometimes be correlated with the general direction of one or more of the dominant joint sets. Surface erosion features can be expected to develop along intensely shattered shear zones where weathering will be accelerated. Tunnels should be located and oriented to avoid major faults and wide shear zones as much as possible, to minimize stability and support problems. Obviously, crossing a wide fault or a shear zone on a heading that is almost parallel to the strike of the fault or shear zone should be avoided if at all possible. When shear zones and faults can be located reasonably well, the contractor can core drill ahead from the tunnel heading to determine the exact location, condition and width of the fault or shear zone prior to advancing his excavation into it. Appropriate precautions can then be adopted to minimize potential water inflow, roof instability and support problems.

- Volcanic deposits can present several significant problems. When considerable geologic time has passed between successive lava flows, it is possible to encounter sedimentary deposits interbedded between lava flows. When the material consists of soft, plastic clay of significant thickness, it could result in undesirable differential settlement in heavy structures, if not detected. Figure 2 depicts a cross section though a powerhouse and its foundation. An exposed escarpment at the site showed successive lava flows in contact without any apparent interruption. As a result, the powerhouse was initially thought to be founded on successive, contiguous lava flows. One of the initial exploratory drill holes indicated a clay strata at depth between lava flows. Additional drilling was then executed which disclosed a strata of soft, plastic clay of variable thickness to extend under much of the powerhouse. It was not practical or feasible to relocate the powerhouse, so in order to avoid undesirable

differential settlement, caissons had to be adopted for support as shown.

Scoriaceous zones of loose, uncemented material between successive lava flows that are in direct contact can be very permeable, and result in excessive seepage and water loss through the abutments around a dam, if not adequately treated. To emphasize the permeability of such zones, this author has seen a stream in Washington which disappears downwards into a scoriaceous zone at the bottom of an underlying lava flow to reappear some distance downstream.

Deposits of pyroclastic materials that include ash and rock particles in a loose, uncemented matrix can have a very low modulus of deformation. Pressure tunnels constructed with an unreinforced concrete liner or a lightly reinforced concrete liner through this material, can have disastrous results when they are first filled, as witnessed on a hydroelectric project in Peru. Water pressure burst through the concrete lining and caused failure of the tunnel. A similar disaster occurred in a pressure tunnel in Guatemala, constructed through a zone of relatively soft evaporites. The tunnel lining cracked badly during filling. Water then dissolved the surrounding evaporites and carried them away, creating a huge void and the subsequent complete failure of the tunnel lining within this material.

Hydrothermal activity and alteration within volcanic deposits can produce soft, collapsible materials and intolerable working conditions due to the extreme heat and humidity. As a result, tunneling becomes so difficult and costly that alternative routes must be selected. The presence of such conditions can sometimes be detected by the fact that surface rock is hot to touch, by the presence of one or more steam vents with visible coloration due to mineral deposition and in some cases by the presence of hot water seeping from a few, or many joints in the face of rock outcroppings in the river channel walls. A casual drive by or fly over will not usually disclose the presence of hydrothermal activity. The tunnel route should be examined on foot. If the project is to be located in a zone of suspected hydrothermal activity, some exploratory drilling is imperative.

- Weathering of rock abutments in tropical zones can be very advanced and deep. Where there is abundant rainfall and jointing has been well developed within the rock mass, due to regional uplift or folding, water with oxygen can penetrate to significant depths and weathering is rapid. It is not unusual to find that groundwater for some distance, well back within the abutments, is only slightly above river level. A significant problem is that very large remnants of intact rock can remain above the general, overall depth of weathering, giving a false impression of the depth to sound bedrock level, where large hydraulic structures should be founded for adequate support and stability. Exploratory drill hole depth

must consider that first sound rock contact may be in "float" rock and therefore some drill holes should extend down to river level.

- Expansive clays and colloidal dispersive clays present unique problems. Natural deposits of bentonitic clays, for example, can exhibit a very low coefficient of friction. When excavations are executed that remove the lateral support of material with bentonite clay strata that dip down into the excavation, devastating slides involving large earth masses can occur. In addition, high swelling pressures can develop within this material when confined. Unless colloidal dispersive clays are recognized and treated, they can contribute to serious piping problems. Both expansive and dispersive clays can usually be recognized in the field. Figure 3 depicts an extensive outcropping of bentonitic clay encountered in Colorado along a slope where large surface penstocks were to be located. Note the popcorn appearance of the material on the surface which has been subjected to repeated wetting and drying. Material from this same formation was being commercially quarried nearby for use in lining cattle ponds to make them water tight. Because of stability problems associated with the bentonitic material along the slope, it was decided to go underground, utilizing shafts and tunnels. Figure 4 depicts the surface of an expansive clay encountered in a borrow area. This clay exhibits typical characteristics of a colloidal dispersive clay. Note the continuous tubification development within the clay strata. Colloidal clay soils recognized to be dispersive have been used in the construction of the impermeable core of an embankment dam when no other suitable material was available (Reference 4). The material, where used to blanket the core contact at the foundation and on the abutments, had to have its properties modified by treatment with lime to protect against dispersion related piping. Specially designed sand filters had to be provided between the dispersive clay core and the dam shells.

- Under certain topographic conditions, deep ancient buried channels can be encountered. This is possible where a river has eroded deeply into the surrounding terrain to form a narrow gorge and has had a relatively steep profile. Rockslides may have occurred in ancient times creating a natural dam that raised the river level permanently in one or more places. A deposition of continuous and lenticular beds of sands, gravels, silts and boulders ranging up to house size, usually accumulate in the narrow basins created. This matrix can be very permeable. Construction of cofferdams and dewatering at these locations can be extremely difficult and costly in such circumstances. The presence of the extremely large boulders precludes the construction of a seepage cut-off using sheet piling or a slurry trench. A very long diversion tunnel may be required. Foundation cleanup and preparation will also be time consuming and very costly. The presence of a deep ancient buried channel can

seriously affect site selection and a project's arrangement. Exploration must be designed to disclose the possible presence of a deep buried channel at sites of this nature.

- When deep, thick glaciers have overlain a project in the past, where the bedrock is crystalline rock (igneous and metamorphic rock), they can produce problems for locating surface structures that must be recognized. The rebound effect as the glacier disappears, produces well developed jointing parallel to the surface of the slope, which can have a steep downhill dip. This jointing can extend some 10 to 15 meters into the rock slope, as shown in Figure 5. Secondary jointing occurs across the slope, oriented normal to the slope, together with vertical jointing oriented in the down slope direction. These 3 principal joint sets can produce unstable rock blocks up to very large size, moving down slope. This is prejudicial to the construction of surface penstocks along the slope or to the construction of surface powerhouses and switchyards at the bottom of the slope. Additionally, any hidden valleys, which may have been carved out by the glaciers in ancient times, must be detected during exploration to assure that structures are located where a suitable foundation is available.

- Tailrace degradation can be serious in erodible materials. This must be properly evaluated during the design of spillways and powerhouses and appropriate design measures adopted. A significant and permanent drop in the tailwater due to channel degradation can result in undesirable, continuous and progressive cavitation damage to turbines. A significant drop in tailwater can also prevent a hydraulic jump from occurring in the spillway resulting in sweepout and severe downstream scour. This had happened in a case in which the author served as an expert witness. The consequences were serious, leading to costly litigation. The potential for severe tailrace channel degradation should be carefully examined when the streambed is composed of transportable material that extends down to considerable depth at the dam site (Reference 5). If it is determined that tailrace degradation could be severe, a critical depth, reinforced concrete sill can be provided at the end of the spillway stilling basin to force a hydraulic jump for the full range of expected spillway discharges. Properly designed riprap erosion protection will be needed beyond the sill. Similarly a protective sill can be provided at the powerhouse to provide sufficient tailwater depth to protect the turbines against cavitation damage.

II. Problems Related to Some Omissions in the Analysis and Design of Structures

- All hydraulic structures which will convey water at high velocity require a check during design to determine cavitation index numbers at

critical points. The cavitation index numbers can be used to determine if and where aeration maybe needed. The analysis and design for aeration has been well defined (Reference 6). Provision of aeration facilities during initial construction is usually not an expensive consideration. After the project commences operation and cavitation damage develops, due to lack of aeration,it may be very difficult to schedule and perform any repairs due to a necessity to be able to make spillway releases and/or low level outlet releases at any time during the high flow flood season to prevent overtopping of dams and dikes. Continuing and progressive cavitation during this period could produce erosion of such magnitude that the structure's stability might become impaired. In any case, the cost of repairs could be extremely expensive.

- Intakes to power conduits should be arranged and configured to prevent undesirable air entraining vortex formation when operating at any expected discharge or reservoir level. Intakes must be set for adequate submergence at the minimum reservoir operating level. In addition, the intake geometry provided should produce a smooth almost linear acceleration of flow from the trashrack to the beginning of the penstock (or the turbine intake in the case of an integral intake powerhouse). Abrupt changes in direction, within the intake in both plan and profile, should be avoided. The resulting flow separation created can produce circulation that could become an air entraining vortex (Reference 7). The normal maximum operating velocity through the net area at the trashrack should preferably not exceed 1.5 m/sec., which equates to a velocity of about 1.0 m/sec. through the gross area. When the entrance velocity through the trashrack exceeds this velocity, there is a possibility that circulation will be created along the sides of the trashracks that could result in standing air entraining vortices. If a higher velocity is to be used, a hydraulic model should be considered. A strong air entraining vortex that reaches the turbine will cause rough operation and vibration and will decrease turbine efficiency.

- The design of powerhouses, large guide walls and large retaining walls to be constructed on a relatively compressible foundation should carefully examine the long term effects of allowing unbalanced foundation design pressures across the base of a large wall or monolithic structure. Differential settlement across the base can produce undesirable rotation of walls around their base and the tilting of monolithic structures. Unbalanced and differential deformations can have a damaging effect on the interaction between structures and waterstop integrity. It can also make operation of rotating electro-mechanical equipment destructive, requiring expensive and difficult rehabilitation. Design priority should be given to achieving an almost uniform pressure across the foundation for normal operating conditions and loadings, so that any long term rotation

or tilting will be within tolerable limits.

- The natural frequency of powerhouse floors and decks should be determined during design. They can then be compared with the frequency of pressure pulsations created within the hydraulic water conduit system (Reference 8). Resonance should be avoided by design modifications. Vibrations of floors in some powerhouses have been severe enough to activate circuit breakers and to cause the general loosening of connectors and fasteners, such that maintenance frequency had to be accelerated to prevent undesirable plant malfunctions.

- It is not uncommon to see projects in which designers have made inadequate provision and spacing for contraction joints in canal linings, spillway chutes and head works to account for volumetric changes in the structure due to shrinkage and temperature changes. As a result, large cracks have developed across the structures, which impair the structures' performance and require frequent maintenance. High velocity water impinging on one side of a crack can force water under the slab and create undesirable uplift if not corrected. The proper placement of joints must take into consideration the maximum temperature reached by the concrete upon hardening, the lowest ambient air and water temperatures to which the structure will be subjected, restraint developed along the foundation, the dimensions of structural elements and the amount of reinforcement placed within the concrete for structural reasons. In general, however, inspection of many structures has indicated that in areas with winter temperatures low enough to freeze water, the spacing of contraction joints in thin, lightly reinforced structures, should be about 10 meters or less, and the spacing in thick, more heavily reinforced structures should be about 20 meters or less. When these spacings are exceeded, the structures have a tendency to develop large cracks at about these spacings to relieve axial tension. The cracks produced are too large to control leakage.

- Engineers require a working knowledge of deleterious chemical reactions with cement in concrete. In an alkali-aggregate reaction, the alkaline hydroxides derived from the alkalis in the cement attack the siliceous minerals in the aggregate. An alkali-silicate gel is formed around the surface of the aggregate particles. This gel absorbs water as it becomes available, increasing in volume. This causes a volumetric change within the concrete structure leading to its deterioration. Rehabilitation of older, existing structures requires the removal and replacement of all deteriorated concrete. In addition, the potential for a continuing, progressive and destructive alkali-aggregate reaction in the remaining original concrete must be minimized by limiting access of water to this material. Proper testing of mix water, aggregate materials and the use of

low alkali cement has essentially eliminated this problem in new structures.

Sulfate attack is apparently less understood. Reactions have been seen by this author in some expensive, new structures. When clays and shales containing alkali, magnesium and calcium sulfates are encountered in the foundations and backfill for hydraulic structures, the ground water in such materials can become a sulfate solution. The sulfate solution attacks the cement in the structure to form gypsum and other products. The reactions with the sulfates leads to expansion and eventual disintegration of the structure. The attack by magnesium sulfate is more severe than by other sulfates. Concrete attacked by sulphate has a characteristic white appearance. Figure 6 shows a spillway wall in an advanced state of disintegration from sulphate attack. When tests show the foundation materials and groundwater contain sulphates special precautions can be adopted. Sulphate resistant cements should be used and a partial replacement of some cement with pozzolans can be considered. In addition, a hard, dense, impermeable concrete, with a low water/cement ratio, should be specified to reduce the structure's susceptibility to sulfate attack. The use of a lean, porous concrete bedding or working layer placed over the foundation, should be avoided, since it can make the structure more vulnerable to attack.

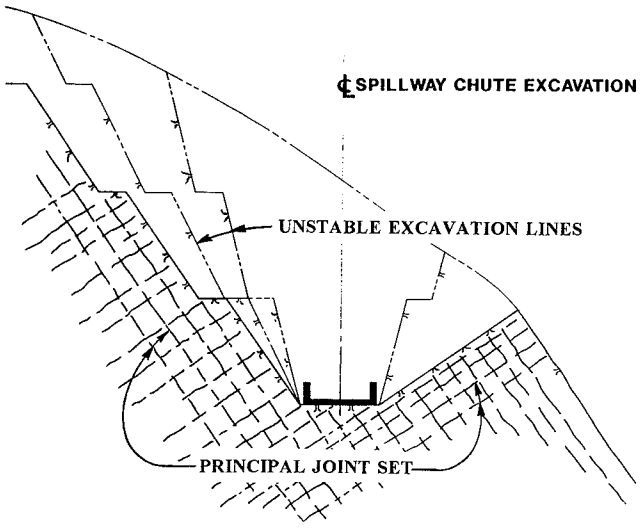

FIGURE 1
A SPILLWAY CHUTE EXCAVATION IN ROCK WITH WELL DEVELOPED JOINTING

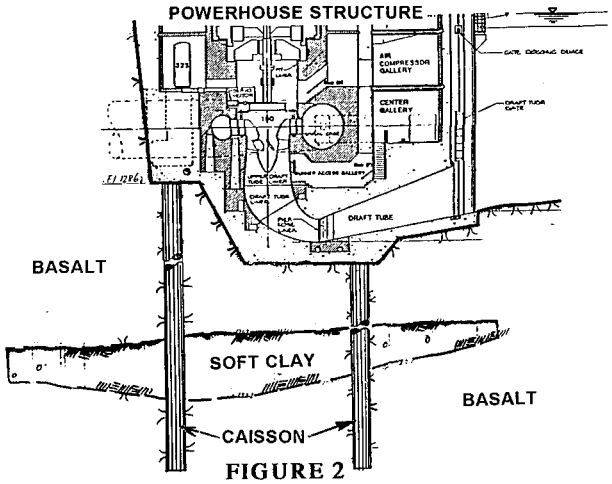

FIGURE 2
SOFT CLAY BETWEEN BASALT FLOWS REQUIRES CAISSONS

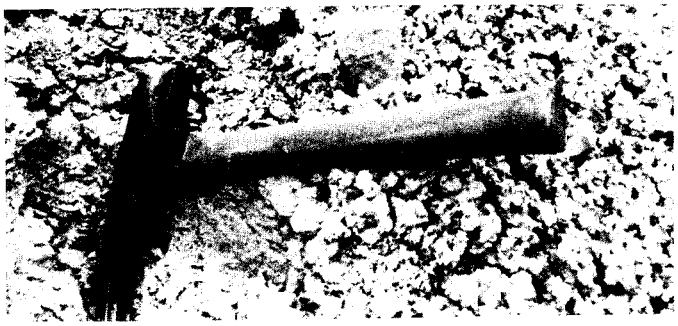

FIGURE 3
OUTCROPPING OF BENTONITIC CLAY

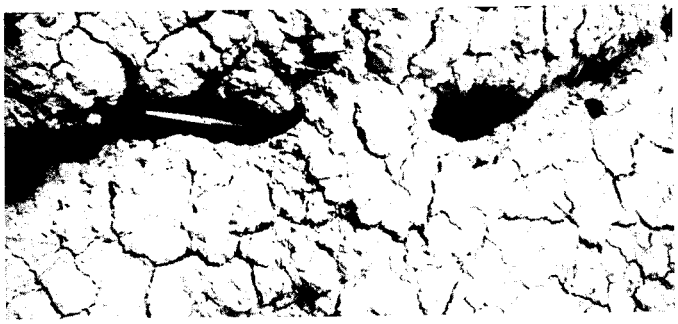

FIGURE 4
EXPANSIVE CLAY WITH DISPERSIVE CHARACTERISTICS

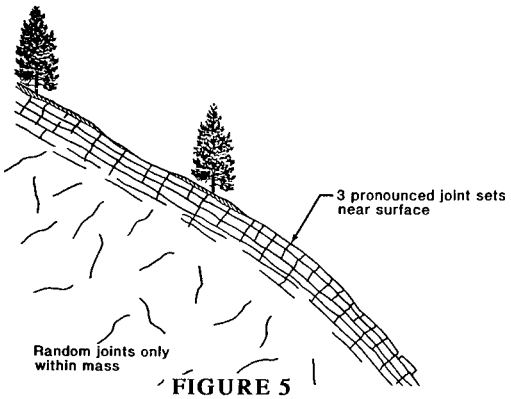

FIGURE 5
JOINTS IN ROCK MASS DUE TO REBOUND

FIGURE 6
WALL IN ADVANCED STATE OF DISINTEGRATION FROM SULPHATE ATTACK

References:

1. Moore, E.T., "Tunnels and Shafts", Vol. 2, Civil Engineering Guidelines for Planning and Designing Hydroelectric Developments. ASCE/EPRI, 1989

2. Moore, E.T., "Designing Steel Tunnel Liners for Hydro Plants:, Hydro Review, October 1990

3. Obert, L., et al, "Design of Underground Openings in Competent Rock", Bulletin 587, Bureau of Mines

4. Logani, K.L., "Dispersive Soils Chosen for Ullum Core", World Water, August 1979

5. Section H-4, "Channel Degradation", Appendix H, Design of Small Dams, Second Edition, U.S.B.R., U.S. Dept. of Interior 1973

6. Falvey, H. T., "Cavitation in Chutes and Spillways", Engineering Monograph No.s 42, U.S.B.R., U.S. Dept. of Interior 1990

7. Moore, E.T., "T.L.C. For Small Hydro: Good Design Means Fewer Headaches", Hydro Review, April 1988

8. Moore, E.T., "Avoiding Vibration in Penstocks", Volume 3, Proceedings, Waterpower 1991; Denver, Colorado

GEOTECHNICAL ENGINEERING AT THE COWLITZ FALLS PROJECT

John P. Sollo[1] & Agerico A. Cadiz[2]

Abstract

The Cowlitz Falls Project is located 10 miles southeast of Morton, Washington on the Cowlitz River and 16 miles upstream from Mossyrock Dam. The concrete-gravity dam is 145-foot high and 700 feet long, with a crest elevation of 885 feet. The two-unit powerhouse contains two Kaplan turbines operating under 87.5 feet of head and a discharge of 10,500 cubic feet per second.

The foundation rock consists of andesite lava flows, agglomeratic flow breccia, and tuffaceous layers. The tuffaceous layers consist of weakly cemented ash, and thinly bedded claystone. Numerous direct shear and unconfined compressive strength tests were performed on tuffaceous samples during construction.

Due to the location and orientation of the tuffaceous layers, the rock rib separating the diversion channel from the powerhouse excavation was reinforced with full-length, cement-grouted vertical dowels. Following excavation, a portion of the rib, where potential wedge block failure could occur, was supported with tensioned rock bolts and shotcrete.

A single-line grout curtain will extend across the length of the dam. Grout holes were drilled on ten-foot centers at the upstream face. The holes were inclined upstream at 1H:2V and ranged in depth from 30 to 150 feet.

Seismic blast monitoring was performed during excavation of the diversion channel, dam, and powerhouse. The blast monitoring data, including the site specific relationships between peak particle velocity, scaled distance, and blast design were used to control vibration along the narrow rock rib.

[1]Project Geologist, [2]Field Geologist, Bechtel Corp, San Francisco, CA.

INTRODUCTION

The project includes four spillway bays, an emergency spillway bay, a two-unit, 70-megawatt powerhouse, and tailrace channel improvement. The reservoir has a normal maximum pool elevation of 862 feet, a surface area of approximately 610 acres, and a volume of 10,800 acre-feet.

The owner is the Public Utility District No. 1 of Lewis County, Washington. Bechtel Corporation, Inc. is the project design engineer and construction manager. The notice to proceed with construction was issued to Torno America, Inc. on June 12, 1991, and construction began on June 19. The project is expected to be completed in April, 1994.

GEOLOGIC CONDITIONS

OVERBURDEN. Overburden at the project site includes colluvium and outwash terrace deposits up to 70 feet thick. On the steep slope of the right abutment the bedrock is mantled with colluvium consisting of silt and angular volcanic rock fragments. Overburden on the left abutment consists of a thick section of silt, sand, gravel, and boulders which occur as outwash deposits. An alluvial terrace with a surface elevation of about 855 feet is developed on the left bank. These deposits are blanketed with yellow brown pumice and traces of other ash which represent post-glaciation eruptions that occurred about 3,200 to 4,000 years ago.

BEDROCK. The bedrock units in the project area are assigned to the Keechelus Volcanic Group of late Eocene to early Oligocene age, about 30 to 50 million years old. The sequence includes predominantly andesitic lava flows, and flow breccia, with layers of pyroclastics and sedimentary beds referred to as "tuffaceous materials". The pyroclastic layers (tuffaceous) range from ash to lithic tuffs and tuff breccia, and laharic (mud flow) deposits.

Andesite. The andesite occurs as flow rock, and as dike rock that ranges in color from greenish-gray to dark gray to black. It is hard to very hard, unweathered, fine to medium-grained, and closely to widely jointed. It is vesicular in part, with vesicles filled with calcite or quartz and sometimes zeolite mineralization. Some intervals of andesite porphyry occur in the upper part of the right abutment. The unconfined compressive strength of the andesite is about 17,600 psi.

Agglomerate/Flow Breccia. The agglomeratic or volcanic flow breccia are typically mottled greenish-gray to dark reddish-brown, moderately soft to hard, fine to coarse grained, and are generally moderately jointed to massive. The matrix of agglomerate influences the hardness of the specific rock unit. The zones with quartz mineralization can be as hard as the andesitic flow rock while those with ash as an infilling tend to be softer

and more subject to weathering. The rock fragments within the breccia range from angular to rounded. The unconfined compressive strength of the agglomerate is about 3,000 psi.

Dike Rock. The andesitic dike rock occurs as thin, tabular bodies that range in thickness from a few inches to about four feet. The dikes are typically dark gray to black, hard to very hard, fine grained, and closely jointed. They have distinct, sharply defined contacts with the surrounding country rock. The dikes are generally more resistant to weathering than the flow rock and form elevated ridges along bedrock outcrops. The andesite dikes typically strike N 40^0-60^0 E, and are vertical.

Tuffaceous Layers. The tuffaceous rocks are generally reddish-brown to greenish-gray to brownish-gray, and soft to moderately hard. They are usually very soft where they have been altered to clay. Where unweathered, the tuffaceous rocks are generally competent, though softer than the surrounding andesite or agglomerate. They consist of a variety of materials including ash, lapilli tuff, lithic tuffs containing angular fragments of vent rock, pyroclastic flow rocks, tuffaceous breccia, and tuffaceous agglomerates. Many of the tuffaceous layers have been baked by the overlying andesite flows into a reddish-brown claystone. The unconfined compressive strength of the material is about 800 psi.

The tuffaceous layers vary in thickness from less than a foot to about 14 feet. Thickness variations occur rapidly over short distances. This is evident in the powerhouse and dam excavations, and is probably the result of having been deposited on an irregular surface, and deformed by movement and loading by subsequent lava flows.

The contact between the tuffaceous layers and the harder andesite or agglomerate is typically distinct within a few inches. It is generally rough, irregular, and undulating. Where the tuff beds are greater than about five feet thick, the contact is marked by a thick basal layer of greenish-gray agglomerate that has the appearance of "puddingstone". The tuffaceous layer/bedrock contact was considered the weak plane within the dam foundation where failure could occur.

The tuffaceous rocks tend to disintegrate rapidly when subjected to drying and rewetting. They readily slake in air as they dry and are more susceptible to weathering than the more competent andesite and agglomerate. For this reason, many of the tuffaceous layers that were exposed during excavation, were covered with a two-inch thick coating of shotcrete as a protection against weathering.

During the site investigations, seven tuffaceous layers were identified and

assigned the letter designations "A" through "G". Additional tuff layers ("H", "I" and "J") were encountered during construction.

STRUCTURE

Tuffaceous Layers. In general, the tuffaceous layers dip upstream and into the right abutment. The layers typically strike between N 30° W and N 55° W and dip 15° to 20° to the northeast.

Shear Seams. Several prominent shear seams occurred along the rock excavation walls striking N 15°-35° W, and dipping 20°-40° SW. They were typically a few inches thick, and filled with crushed and weathered rock fragments. A very prominent vertical shear seam was encountered in the excavation for the upper left abutment. The seam was approximately six inches thick, and contained tuffaceous material that was sheared, crushed, and slickensided. Three shear seams, encountered on the upper right abutment, striking N 65° W were up to four inches wide and contained crushed rock fragments with some slickensided surfaces.

Jointing. Joints and fractures were limited in vertical extent and did not extend through individual layers. The andesitic lava flows usually displayed more blocky fracturing than the agglomerate and flow breccia. Most fracturing is tight, though some open fractures with a thin clay filling occur,usually in association with near-surface weathering. The most prominent joint set was sub-horizontal with no preferred dip direction.

GROUND WATER

Ground water levels were measured during the site investigation program, in holes during drilling and in eight observation wells. Water pressure tests were made in drill holes at the dam site using single and double packer methods. The volcanic rocks are dense, and their ability to transmit ground water is controlled by the fracturing or jointing. The range of calculated permeabilities is from 1.2×10^{-2} cm/sec to less than 10^{-6} cm/sec.

The representative permeability for intervals of undifferentiated foundation rock with minor to moderate jointing ranges from 10^{-4} to 10^{-5} cm/sec. Because of their high clay content, the tuffaceous zones are one to two orders of magnitude less permeable than the andesite or agglomerate.

ROCK EXCAVATION

Rock excavation for the Cowlitz Falls Project began on the left side of the river on July 9, 1991. A total of 119 drill and blast operations were carried out, and on October 1, 1992 the rock excavation was essentially

complete. Approximately 220,200 cubic yards of rock were excavated with an average blast size of 1,645 cubic yards, and an average powder factor for the major blasts of 1.13 lbs/cy.

Production Blasting. Production blast holes had an average depth of 20 feet, on a 6 ft. x 7 ft. or 7 ft. x 8 ft. drill pattern. Blastrite 5, at 2.25 lbs/stick (16,100 fps) or ANFO prills, at 2.48 lbs/ft (13,000 fps) were the blasting agents used for production blasting. Occasionally, Minerite 2, at 1.14 lbs/stick was used. Subdrilling on the final bench blasts ranged from one to two feet.

Controlled Blasting. The perimeter holes were either smooth-blasted or pre-split, depending upon the location and depth of the excavation. Perimeter holes were spaced on three and four-foot centers along a rock surface that was not faced with concrete. Where concrete was placed against the rock surface, perimeter holes were drilled on two-foot centers. The blasting agents used in the perimeter holes were either T-1 cord, at 0.25 lbs/ft, or 200 and 400 grain cord at 0.0286 lbs/ft and 0.057 lbs/ft, respectively. In addition, one stick of Blastrite 5 was used as the bottom charge in each hole. The typical powder factor along the perimeter wall ranged from 0.10 to 0.20 lbs/sq ft. Perimeter holes were subdrilled from one to two feet.

BLAST MONITORING. A seismic blast monitoring program was conducted during rock excavation. The program was designed to monitor and evaluate blast vibration limits which were established to protect existing concrete and minimize excessive ground vibration damage.

Data Collection. The Contractor provided an Instantel DS 477 seismograph to collect the blast vibration information. The machine monitored three seismic channels, (longitudinal, transverse, and vertical) and one air pressure channel.

Strip chart readouts of particle velocity were obtained following each monitored blast. The required input data including date, distance, PPV, and maximum charge weight per delay were tabulated on the blast monitoring database. From these data the Scaled Distance values for each blast were calculated and added to the database.

Monitoring Results. Contract requirements did not allow the vector-sum velocity to exceed two inches per second at the nearest concrete structure or rock area subject to vibration damage. Of the 119 major blasts performed, 103 were monitored with the seismograph. Peak particle velocities ranged from 0.045 to 7.344 in/sec., with 19 blasts exceeding the 2 in/sec limit measured at the geophone. Except for rock

overbreak on the lower left abutment, and some cracking on the rock rib, there was no noticeable damage to rock or concrete structures due to blast vibration.

ROCK REINFORCEMENT. Rock reinforcement was used to maintain the integrity of the rock cuts and preserve the neat line limits along the excavation boundaries. Rock reinforcement along the excavation walls was provided by tensioned rock bolts, vertical rock dowels, shotcrete, and chain-link fabric.

Rock Bolting. The rock bolts were Dywidag Threadbar (ASTM A 615), Grade 60, one-inch diameter, reinforcing steel. They were typically 15 feet long, tensioned to 300 ft-lbs, and fully-encapsulated with Celtite epoxy resin. Rock bolting was installed 'as directed' along the diversion channel excavation and on a predetermined pattern in the powerhouse excavation and on the upper right abutment slope. The pattern rock bolts were installed on 8 foot centers.

Rock Rib Bolting. Tensioned, vertical rock bolts were installed on the rock rib to provide additional support against sliding on tuffaceous layers. These tensioned rock bolts were installed through tuff layer C and D upstream and through tuff layer F downstream. In the upstream area, 21 rock bolts were installed ranging in depth from 25 to 60 ft. These were 1-3/8-inch diameter, 150 KSI steel bolts, that were tensioned to 144 KIPS.

Nine rock bolts were installed through tuffaceous layer F in the downstream area. These bolts were 1-inch diameter, and ranged in depth from 20 to 40 ft. They were tensioned to 76 KIPS. The location of these rock bolts is shown on the dam and powerhouse geologic map.

Crown Bolting. Crown bolts were installed along the top of some of the rock slopes prior to blasting. These were installed about two feet behind the excavation line and spaced on about 3-foot centers along the rock cut. The bolts were resin-grouted and tensioned to 300 ft-lbs. The purpose of these rock bolts was to maintain the top shoulder of the excavation along the neat line. However, most of the crown bolts were not effective in preserving the top of the excavated slope as the rock was lifted along subhorizontal joints. The slabs of loose rock and many of the crown rock bolts were removed during foundation preparation and cleanup.

Vertical Rock Dowels. Vertical rock dowels were installed along the rock rib that separates the diversion channel from the powerhouse. They were designed and installed as pre-excavation support to maintain the integrity of the rib during construction. The dowels were one-inch diameter, grade

60, Dywidag Threadbar, reinforcing steel. They were installed on 18-inch centers along the excavation, and 12 inches behind the excavation neat line. The dowels were fully-encapsulated using cement grout. By specification, the Contractor could not blast within 50 feet of the grouted dowels for seven days following installation.

Shotcrete. Shotcrete was placed along the rock excavations for rock protection and support. As designed, a six-inch thick layer with welded-wire mesh was used along the upstream diversion channel walls and along the left wall of the intake area. Other, 'as directed' shotcrete consisted of a two-inch thick layer that protected the tuffaceous layers from air-slaking and deterioration.

ROCK TESTING

Tuffaceous Material Testing. During the site investigations, it was recognized that the tuffaceous layers were the weakest foundation rocks and they would control the stability of the dam structure. The stability of the dam and abutments against sliding along these planes was analyzed assuming that the tuff layers were continuous. The strength parameters used in the stability analysis were: 10 psi cohesion and a friction angle of 15°.

During construction, a sampling and testing program was established to verify the engineering characteristics of the tuffaceous materials. In addition to the shear strength evaluation, tests for unconfined compressive strength, unit weight, and moisture content were performed. The unconfined compression tests were performed on rock cores obtained from drilling while the other tests were performed on bulk rock samples.

Compressive Strength Testing. Eight rock core samples were collected from exploratory holes drilled on the upper right abutment and cored exploratory grout holes. The average compressive strength value for the tuffaceous material from the eight samples was 1575 psi and a unit weight of 150 pcf.

Direct Shear Testing. Direct shear tests were performed on samples of tuffaceous material that were both saw-cut and artificially fractured surfaces. Because of the uneven surfaces along the tuffaceous layers, it was difficult to obtain a smooth, slickensided plane amenable for laboratory testing. The surfaces were artificially fractured, and the resulting surfaces were generally rough and irregular. Other tests were conducted on remolded tuffaceous materials to obtain the lower bound of shear strength parameters. The samples were tested at normal stresses of 25, 50, 75, 100, 125, 150, and 175 psi. The linear regression analyses

for the data points resulted in an average cohesion (residual) value of 34 psi and an average friction angle (residual) of 23 degrees.

CURTAIN GROUTING

During the first phase of the curtain grouting program, 36 holes were drilled and grouted along the upstream face of the dam. Grout holes were 2-1/4 inch diameter (AX size) and ranged in depth from 30 to 150 ft. They were grouted by the split-spacing method with a 10-ft maximum distance between holes. A Longyear 65 drill mounted on a ECM-350 Crawlair was used to drill the grout holes. In the service bay area, the Longyear 65 was mounted on the LM-100A Crawlair or post-mounted. To ensure adequate separation between the grout curtain and the drain holes, the grout holes were inclined upstream at 1H:2V, and were drilled from an eight-foot wide plinth at the upstream base of the dam. This permitted the drain holes to be drilled from the upstream side of the drain gallery. The five-foot thick plinth was secured to the foundation rock by grouted anchor bars.

Because of the upstream inclination of both the grout holes and the tuffaceous layers, the grout curtain is deeper than is normal for a 145 ft high dam. Some of the grout holes were drilled at least 10 ft below tuffaceous layer "I" under the powerhouse, spillway no. 4 and the higher portion of the left gravity section. Grout pressures were typically two psi per foot of inclined hole depth.

Grout length intervals were typically 10 feet in length. Some variation occurred near the top of the holes where adjustments were made to grout the rock/concrete plinth interface. Because of very low grout takes, intermediate holes were not required. Some surface leakage occurred from the upper stages of grout holes located adjacent to the diversion channel. When surface leakage occurred, the grout mix was thickened until the grout loss stopped.

The initial stage of each hole was grouted with a 4:1 water to cement ratio. These mixes were thickened to 1:1 if necessary to achieve grout refusal. Refusal was defined as a grout take of less than one cubic-foot for ten minutes at pressures less than 100 psi, and for five minutes at pressures greater than 100 psi.

ACKNOWLEDGEMENTS

The authors are grateful to the Public Utility District No. 1 of Lewis County, Washington for permission to publish this paper. We would like to acknowledge the support of Mr. Robert S. Sato, who reviewed this paper.

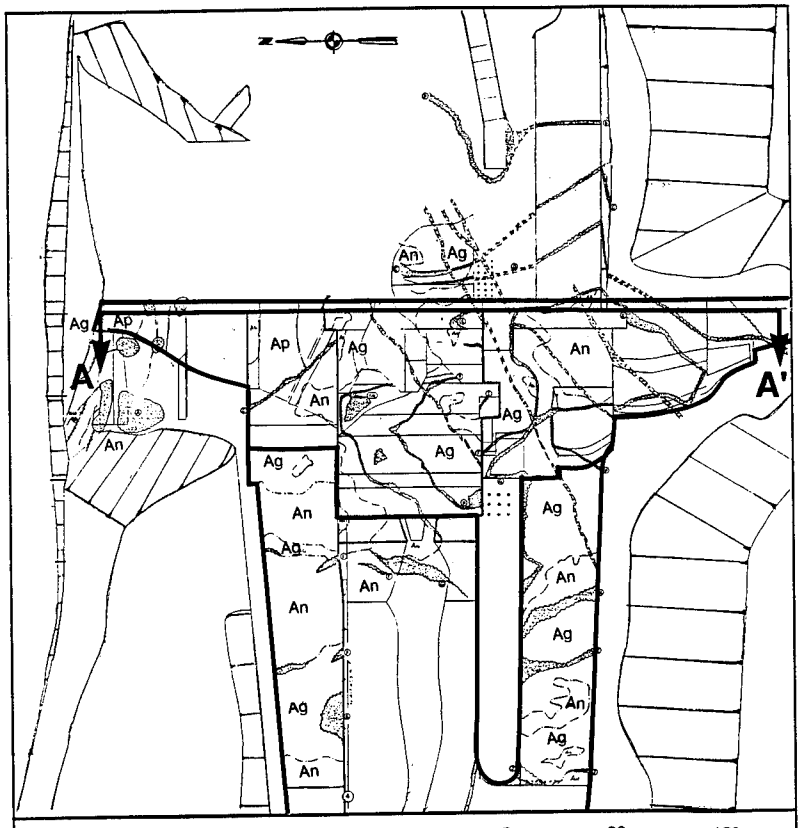

Figure 1. Geologic Plan

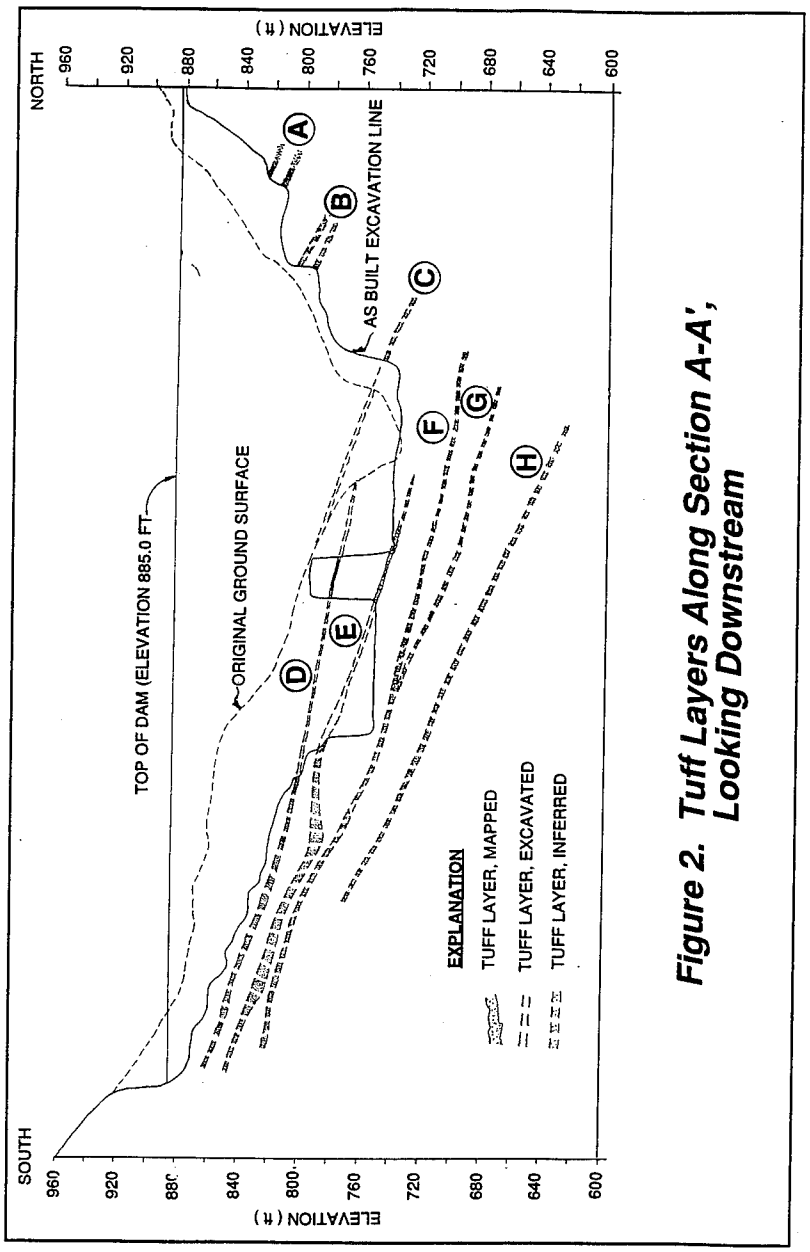

Figure 2. Tuff Layers Along Section A-A', Looking Downstream

SEISMIC HAZARD ANALYSIS FOR DAMS IN THE SOUTHEASTERN UNITED STATES

by William J. Johnson[1] and John P. Osterle A.M. ASCE[2]

ABSTRACT

The seismic hazard of the southeastern U.S. is dominated by the 1886 Charleston earthquake, with the possibility that a smaller, but locally damaging earthquake could occur essentially anywhere in the region. This paper presents an assessment of ground motion for a theoretical dam on a rock foundation with a seismic hazard defined in terms of the site being located at a distance of 150 km from a Charleston-type event (m_b ~ 6.9) and in the near-field of a smaller earthquake (m_b ~ 5.5).

The near-field ground motion is relatively easy to simulate in that strong motion recordings from similar conditions are available. The far-field motion from a Charleston-type event is more problematic. Several theoretical studies are available from which far-field response spectra can be derived, but if they are considered to be a reasonably valid representation of ground motion, they should be consistent with real earthquake records with similar conditions.

Taking into account differences in attenuation characteristics between the southeastern and western U.S., few records from rock sites are available to simulate the far-field ground motion from a Charleston-type earthquake. Even fewer are available if the recording station is required to have experienced a Modified Mercalli Intensity of VIII, similar to what the 1886 Charleston earthquake produced in much of the Piedmont. Nevertheless, some appropriate recordings are available. Our review of real records has led to the following conclusions: 1) theoretical attenuation relationships may underpredict ground motion; 2) artificial time histories derived to match theoretical response spectra may be similarly inappropriate; 3) for dams founded on rock, it is important to evaluate ground motion from rock recordings; 4) peak ground acceleration should not be the controlling criterion for defining ground motion; and 5) appropriate ground motion can be defined from real recordings.

[1] Vice President - Technology, Paul C. Rizzo Associates, Monroeville, PA 15146.
[2] Senior Project Engineer, Paul C. Rizzo Associates, Monroeville, PA 15146.

INTRODUCTION

The seismic hazard of the southeastern U.S. is dominated by the potential recurrence of the 1886 Charleston, South Carolina earthquake (m_b ~ 6.9). Recent evidence from paleoliquefaction studies (Amick et al., 1990) suggests that a second source for a large earthquake may be present between 50 and 150 kilometers north of Charleston. Further research is required, but large earthquakes may be a hazard in other areas of the southeastern U.S. than Charleston, South Carolina. In addition to the potential of a large earthquake near the coast, small, but locally damaging earthquakes have occurred throughout the southeastern U.S.

With the exception of a few dams, such as those associated with the Santee Cooper impoundments, most large dams in the southeast are located in the Piedmont, in the far-field of a Charleston-type event and they are founded on rock. For purposes of discussion, this paper derives the seismic hazard associated with the occurrence of a nearby earthquake of m_b = 5.5 and a Charleston-type earthquake occurring at a distance of 150 kilometers, assuming rock foundations.

Near-field ground motion is relatively easy to simulate, as a fairly large number of strong motion recordings are available from which to select an appropriate design input. Attenuation is not an issue, as the ground motion is by definition near the source. Estimating far-field motion is much more difficult as regional variations of ground motion attenuation must be accounted for.

Based on studies funded by the Nuclear Regulatory Commission, several researchers have developed theoretical attenuation relationships considered to be potentially appropriate for defining the variation of ground motion with a Charleston-type event. This study reviews these theoretical relationships and compares them to real earthquake recordings as a "reality check." The selection of appropriate real records is itself problematic, as most potentially applicable recordings are from the western U.S., which has attenuation characteristics substantially different from the eastern U.S. Furthermore, very few far-field rock recordings from large earthquakes are available. An additional factor to be considered is Modified Mercalli Intensity (MMI). An MMI of VIII was observed throughout much of the South Carolina Piedmont from the 1886 Charleston earthquake. If a recording station MMI of VIII is added as an additional criterion for defining a suitable strong motion record, then it is necessary to conduct a search for strong motion recordings on a world-wide basis.

This paper reviews the seismic hazard at a theoretical site in the southeastern U.S.. An attempt has been made to identify some of the pitfalls that can be encountered in defining seismic hazard and to present some possible solutions.

THEORETICAL DERIVATION OF GROUND MOTION

Two important characteristics of input ground motion for civil engineering purposes are intensity and frequency content. In general, these characteristics at a given

location depend on the magnitude of the earthquake, the hypocentral distance, and attenuation properties of the ground along the wave paths. Usually, these properties are accounted for in seismic analysis by specifying a spectral shape anchored to the peak ground acceleration (PGA). The spectral shape reflects the frequency content while the PGA measures the design intensity.

Most current building codes prescribe design ground motion by providing rules to determine PGA and prescribing spectral shapes for various soil conditions. An example is the Uniform Building Code (UBC, 1991). For important structures, such as nuclear power plants or critical dams, it is preferable to develop site-specific spectra, which more properly represent both the expected intensity and frequency content. With this in mind, in recent years seismologists have developed ground motion relations that predict PGA, peak ground velocity (PGV) and spectral pseudo-velocities (PSV) at a variety of frequencies of interest for engineering analysis. These models are, in general, based on a stochastic random vibration theory whose parameters are determined by seismological data of earthquake sources and attenuation processes (Atkinson and Boore, 1990). In general, these ground motion relationships have the form:

$$\ln(y) = c_1 + c_2 m_b + c_3 \ln(R') + c_4 R' \quad (1)$$

where:

y = PGA, PGV or PSV,

m_b = body wave magnitude,

R'= hypocentral distance (km), and

c_1, c_2, c_3, c_4 = equation constants.

The advantage of using a relationship of this type is that ground motion can be estimated at sites where local strong-motion recordings are not available.

Five attenuation relationships intended to define response spectra from earthquakes of different magnitudes, epicentral distances and site conditions in the eastern U.S. have been identified, as follows:

- McGuire (1988),
- Toro and McGuire (1987),
- Veneziano (1986),
- Boore and Atkinson (1987), and
- Atkinson and Boore (1990).

Attenuation relationships proposed by McGuire et al. (1988), Toro and McGuire (1987), and Veneziano (1986) are described by Equation 1. The attenuation relationships developed by Boore and Atkinson (1987) and Atkinson and Boore (1990) are described by magnitude-dependent coefficients instead of constants.

Two situations have been postulated for defining seismic hazard. The most severe ground motion is taken to be the recurrence of the 1886 Charleston earthquake of m_b = 6.9 (Nuttli, 1983) at an epicentral distance of 150 kilometers (i.e., far-field event). The occurrence of a near-field event of m_b = 5.5 at an epicentral distance of 20 kilometers has also been postulated to account for an event similar to that of the January 1, 1913 Union, South Carolina earthquake. The assumption of a near-field event of m_b = 5.5 is conservative, as the Union earthquake probably had an m_b of about 4.5 based on its felt area of 43,000 square miles (Nuttli et al., 1979).

The median upper-bound spectra for all of the attenuation relationships for both near-field and far-field cases are presented on Figure 1. These response spectra were developed by enveloping the highest pseudo-acceleration values computed from the five attenuation relationships. The primary difference between the near- and far-field spectra is the higher amount of energy associated with the high-frequency component for the near-field spectrum.

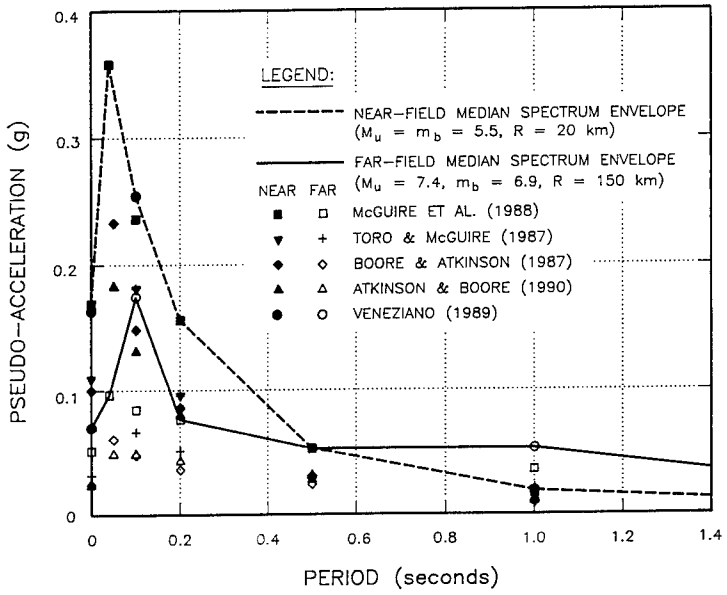

Figure 1. Theoretical Envelope Response Spectra

GROUND MOTION FROM REAL STRONG MOTION RECORDINGS

As a "reality check" for the theoretical spectra, actual strong motion recordings have been selected to compare with the theoretically-derived ground motion. Unfortunately, real recordings of large earthquakes are not available from the

southeastern U.S. and it is necessary to look to the western U.S. or elsewhere for an adequate data base. Before a western U.S. strong motion record can be selected, however, differences in ground motion attenuation between the eastern and western U.S. must be accounted for.

Comparison Of Eastern And Western United States Ground Motions

Under near-field conditions, there is little difference in ground motions between eastern and western U.S. earthquakes (Atkinson and Boore, 1990). However, significant differences occur in the far-field, because earthquakes in the eastern U.S. attenuate slower than the same sized earthquakes in the western U.S., especially the high-frequency component of ground motion.

Atkinson and Boore (1990) present attenuation relationships for both the eastern and western U.S. which have been used to compare ground motions. Although other references could have been used, it was considered preferable to use one source so that the derivation of the attenuation relationships is consistent for both the western and eastern U.S. data sets.

The results of this comparison are presented on Figure 2. As indicated, an m_b = 6.9 (moment magnitude M_u = 7.4) at an epicentral distance of 150 kilometers in the eastern U.S. is essentially equivalent to the same sized western U.S. earthquake at a distance of 85 kilometers. However, there is a substantial difference between ground motions in that eastern U.S. response spectra are enriched at high frequencies by comparison to western events. For structures with significant high-frequency modes of vibrations (above 10 hertz) the seismic hazard in the eastern U.S. might be greater than in the active areas of California (Atkinson, 1988). However, low-frequency structures, such as an earth dam, are not significantly affected by the high-frequency component of earthquake motion. This implies that the use of PGA as a sole criterion for selecting records is not appropriate.

Modified Mercalli Intensity (MMI)

MMI is a factor to be considered when selecting real strong motion records for dam design. As MMI is a description of damage, it is appropriate to know if a strong motion record was associated with an MMI similar to that postulated for the site of interest. For example if a strong motion record has all of the proper characteristics of magnitude, epicentral distance, and site conditions, but it is associated with an MMI substantially below that postulated for the site, the record may not be appropriate for design.

The MMI at a distance of 150 km from the 1886 Charleston earthquake is generally taken to be an VIII (Nuttli et al., 1984; Nuttli et al., 1986; Bollinger, 1977). Indeed, these sources indicate that an MMI of VIII was felt over much of the South Carolina Piedmont.

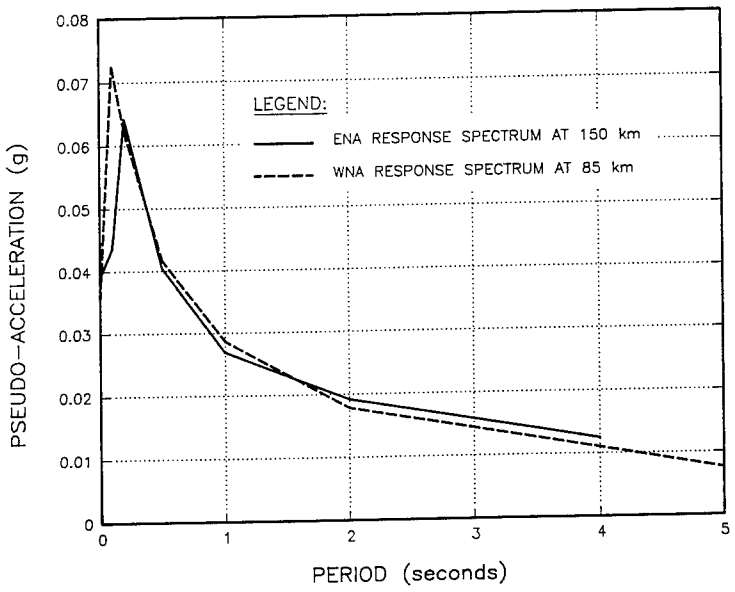

Figure 2. Equivalent far-field response spectra for eastern and western U.S.

Peak Ground Velocity (PGV)

PGV is another factor which can be used as a criterion for selecting an appropriate real earthquake record. As PGV tends to correlate with damage represented by MMI better than PGA (Wiechert et al., 1982; Street, 1982), researchers often estimate an appropriate PGV on the basis of MMI attenuation.

Two approaches for estimating ground motion parameters, including PGV, for the southeastern U.S., are presented in NUREG/CR-3755 (Nuttli et al., 1984) which was prepared for the U.S. Nuclear Regulatory Commission (USNRC). The first approach is observational as presented by Nuttli and Herrmann (Part I) and involves deriving relationships from accelerograms obtained from relatively small earthquakes recorded for the central U.S. A major disadvantage of this approach is that the relationships obtained are based on much smaller earthquakes than the 1886 Charleston earthquake. Any extrapolation beyond the range of available data may not be valid. In addition, Atkinson and Boore (1990) present data which indicate that the attenuation characteristics of the central U.S. may be different from the southeastern U.S. and this observational approach was not considered appropriate for estimating PGV.

The second, semi-theoretical approach followed by Rodriguez (Part II) incorporates a statistical analysis of MMI observations including the 1886 Charleston

earthquake to derive ground motion attenuation functions specific for the southeast U.S. For PGV, the following relationship was derived:

$$\log (PGV) = -3.43 + 0.98\, m_{bLG} - \log R' - 0.000119R$$

where:

PGV = the horizontal component of peak ground velocity in cm/sec at epicentral distance R and hypocentral distance R'

m_{bLG} = m_b for mid-plate earthquakes such as in the southeast U.S. (Nuttli and Herrmann, 1982)

For a Charleston-type earthquake of m_b ~ 6.9, the calculated PGV would be 5.3 in/sec. This estimate appears reasonable in consideration of the relationship between PGV and MMI derived by Krinitzsky and Chang (1988) for hard rock sites in the far-field which yields 6.0 in/sec. Considering that Krinitzsky and Change defined their far-field conditions as being as close as 45 kilometers from the source and they incorporated data from larger earthquakes, an estimate of site-specific PGV between 5.0 and 6.0 in/sec appears to be a reasonably conservative criterion for selecting an appropriate earthquake record.

Selection of Strong Motion Recordings

Potential strong motion records were selected with an attempt to fulfill the following criteria: rock site; $M_u > 7.0$; shallow focal depth; site MMI - VIII; PGV = 5-6 in/sec; PGA ~ 0.1 - 0.15 g. No real records were encountered which could fulfill all of these criteria. PGA was found to vary widely for otherwise similar recordings and was discarded from consideration. As few rock records are available, some consideration was made of deep alluvium records, but these were found to have overly high low frequency response when compared to rock recordings and were not considered further. Nevertheless, some representative strong motion recordings were encountered, as shown in Table 1. These records are discussed in terms of their pertaining to near- or far-field conditions.

Near - Field Records:

Three earthquake records from rock sites are proposed for simulation of near-field earthquake conditions, as follows:

- 1957 San Francisco earthquake, Golden Gate record (S80E), $M_u = 5.3$;
- 1935 Helena, Montana, Carroll College record (S90W), $M_u = 6.0$;
- 1988 Saguenay, Quebec earthquake, Chicoutimi-Nord record (transverse), $M_u = 5.8$.

TABLE 1

POTENTIALLY APPLICABLE STRONG-MOTION RECORDS[a]

Earthquake Recording Station (component)	Type	Epicentral Distance (km)	Site Geology	Moment Magnitude (M_w)	MMI[b]		PGA (g)	PGV (in/s)
					Epic.	Sta.		
1989 Loma Prieta SF, Rincon Hill (360)	Far-field	95[d]	Rock	7.1	VIII	VII	0.08[d]	2.9
1989 Loma Prieta SF, Telegraph Hill (90)	Far-field	97[d]	Rock	7.1	VIII	VI	0.09	3.8
1957 San Francisco SF, Golden Gate Park (S80E)	Near-field	11[c]	Rock	5.3	VII[c]	VII	0.10	1.8
1935 Helena, Montana Carroll College (S90W)	Near-field	6[c]	Rock	6.0	VIII	VIII	0.15	5.2
1988 Saguenay, Canada Chicoutimi-Nord, PQ (124)	Near-field	43[e]	Rock	6.0	VII[c]	< VII	0.13	1.0
1978 Miyagi-Ken-Oki, Japan Breakwater of Ofunato Harbour (E41S)	Far-Field	103[c]	Rock	7.4	N.A.	VIII	0.23	5.6

Notes: a. Data taken from Krinitzsky and Chang, 1990, except as noted.
b. Modified Mercalli Intensity Epic., Epicentral MMI. Sta., Recording Station MMI.
c. Reference: Row, 1990 (SMCAT).
d. Reference: Shakal et al., 1989.
e. Distance calculated based on station and epicentral geographic coordinates.
N.A. Not Available.

The response spectra at 5 percent damping for these three earthquakes are compared with the theoretical near-field response for $M_u = m_b = 5.5$ spectra at a distance of 20 kilometers on Figure 3. The Saguenay recording, at an epicentral distance of 43 kilometers, is not near-field, but is the nearest to the epicenter of all of the strong motion records for the 1988 Saguenay earthquake, the only earthquake of its size in eastern North America to have strong motion recordings. The response spectrum from this record closely resembles the predicted near-field spectrum. The Helena, Montana event is conservative at all but the highest frequency component of the record. This record was obtained nearly at the epicenter of an earthquake larger than the proposed near-field event. It should be noted that the intensity at the recording station was MMI VIII which is higher than the MMI VII assigned to the 1913 Union, South Carolina event. Using the Helena, Montana record as a near-field event is equivalent to postulating a recurrence of the largest earthquake to have occurred historically within the Appalachians, the 1897 Giles County, Virginia earthquake.

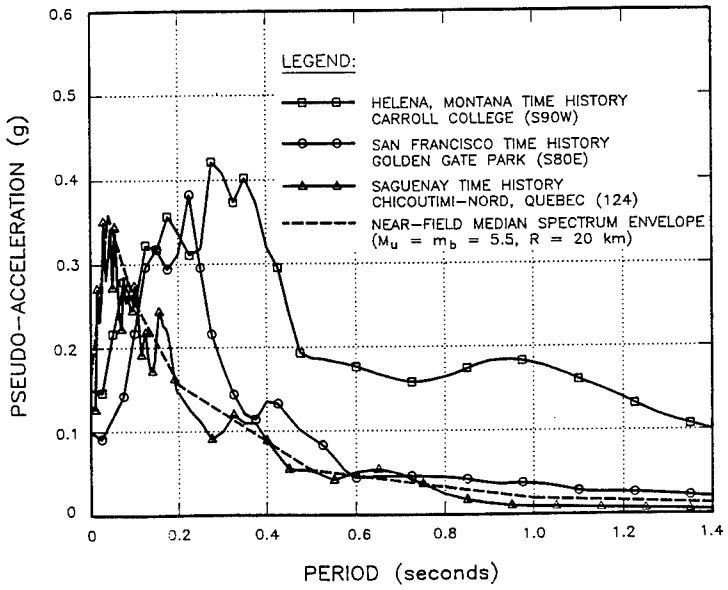

Figure 3. Near-field response spectra.

Far - Field Records:

Few far-field rock records from earthquakes larger than $M_u > 7.0$ are available from the western U.S. Two records fitting this classification, however, are the following:

- 1989 Loma Prieta earthquake, San Francisco, Rincon Hill record (N-S), $M_u = 7.1$.

- 1989 Loma Prieta earthquake, San Francisco, Telegraph Hill record (E-W), $M_u = 7.1$.

Figure 4 presents the response spectra associated with these two records along with the envelope median and median plus one standard deviation (i.e., 84th percentile for a log-normal distribution) spectra for $m_b = 6.9$ at an epicentral distance of 150 kilometers. The standard deviation of the response spectra presented on Figure 4 is equivalent to 0.5 in natural log units (McGuire, 1988) or approximately 65 percent larger than the median. Both far-field records are well outside of the range of predicted response, except at the smallest periods. A disadvantage of these two records is that they do not comply with assumptions of station MMI (VII and VI, respectively) and PGV was less than 4.0 inch/sec.

U.S. Records are not available which combine all the requirements to simulate a Charleston-type event. However, the Ofunato Harbor record of the June 12, 1978 Miyagi-Ken-Oki, Japan earthquake does match all of the criteria. This event resulted in an MMI of VIII at an epicentral distance of ~100 km. The PGA and PGV of the earthquake record are 0.27g and 5.5 in/sec, respectively. The record exceeds the expected PGA, but PGV is consistent for what would be expected from a recurrence of the 1886 Charleston event. The Miyagi-Ken-Oki record is a subduction zone earthquake as opposed to the strike-slip earthquakes typical of the western U.S. However, with a focal depth of only 30 - 40 km, the earthquake is sufficiently shallow to be representative of what could occur in the southeast U.S.

Figure 5 compares the response spectrum of the Miyagi-Ken-Oki record with the far-field theoretical spectrum envelope plus one standard deviation. This record exceeds this theoretical record at all frequencies.

SUMMARY AND CONCLUSIONS

A theoretical dam site in the southeastern U.S. has been assumed to have a seismic hazard associated with the distant occurrence of an earthquake similar to the 1886 Charleston event, as well as a smaller, local earthquake. These assumptions are considered to be typical of many dams located in the Piedmont and founded on rock. Based on a comparison of response spectra derived theoretically and from real records, the following observations have been made:

- Theoretical response spectra may underpredict the far-field ground motion from a Charleston-type event. The real records generally have a higher response than even the average plus one standard deviation theoretical spectrum. However, it is recognized that the records selected may be above average records.

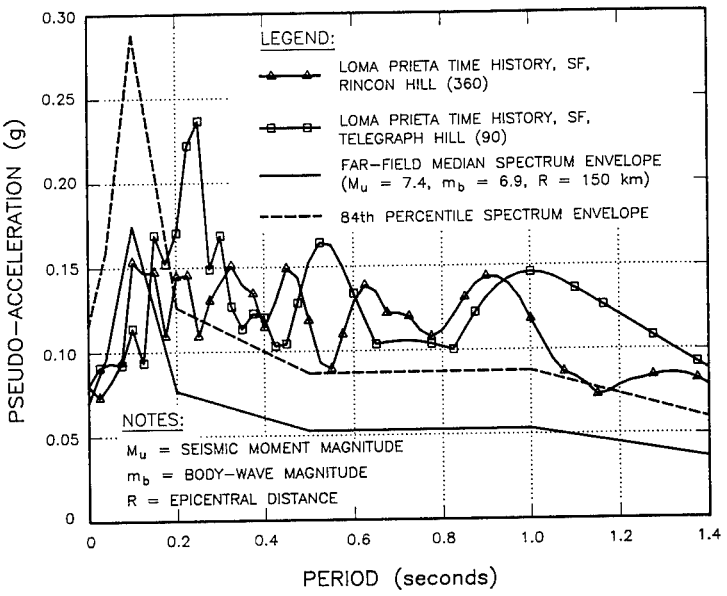

Figure 4. Far-field response spectra.

- Artificial time histories derived to match theoretical response spectra may be similarly inappropriate.

- If a dam is founded on rock, it is important to evaluate ground motion from rock recordings. Alluvial recordings frequently exhibit amplification of low frequency motion which could be overly conservative if applied to evaluating the stability of a low frequency structure, such as an earth dam.

- Peak ground acceleration (PGA) should not be the controlling criterion for defining ground motion. The real records considered to represent appropriate far-field ground motion ranged from 0.08 to 0.23 g. Significant ground motion is the spectral response at the predominant frequency of the dam, not the PGA.

Few real strong motion recordings are available to simulate the occurrence of a Charleston-type event in the far-field. Nevertheless, appropriate records are available if a world-wide data base is considered.

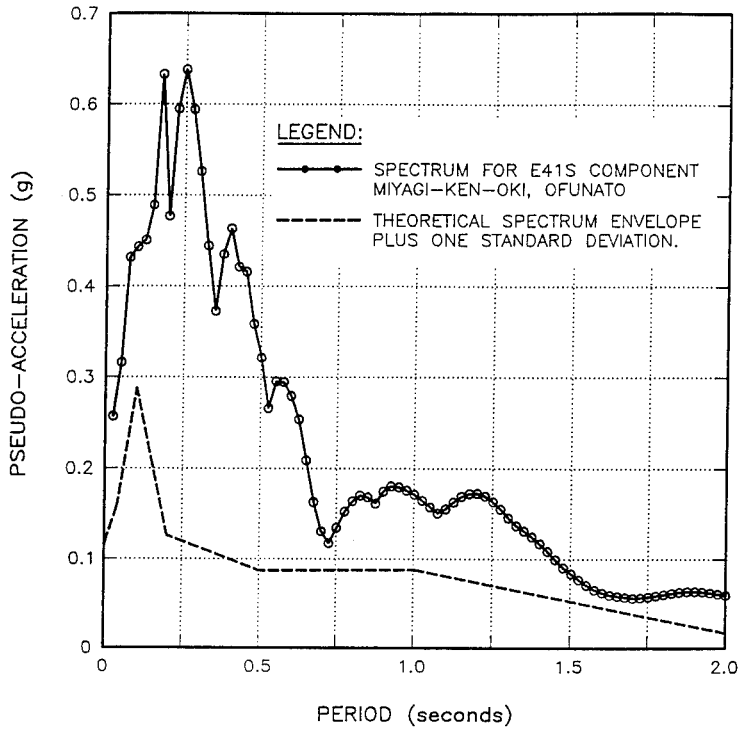

Figure 5. Miyagi-Ken-Oki, Ofunato Response Spectra

REFERENCES

Amick, D., R. Gelinas, G. Maurath, R. Cannon, E. Billington, and H. Kimppinen. (1990) "Paleoliquefaction Features along the Atlantic Seaboard," NUREG/CR-5613, 146 pp.

Atkinson, G.M. and D.M. Boore. (1990). "Recent Trends of Ground Motion and Spectral Response Relations for North America," Earthquake Spectra, Vol. 6, No. 1, pp. 15-35.

Atkinson, G.M. (1988). "Implication of Eastern Ground Motion Characteristics for Seismic Hazard Assessment in Eastern North America," Annals NYAS.

Bollinger, G.A. (1977). "Reinterpretation of the Intensity Data of the 1886 Charleston, South Carolina, Earthquake," U. S. Geological Survey Professional Paper 1028, U. S. Geological Survey, pp 17-32.

Boore, D.M. and G.M. Atkinson (1987). "Stochastic Prediction of Ground Motion and Spectral Response parameters at Hard-Rock Sites Eastern North America," Bull. Seism.Soc. Am., Vol. 77, No. 2, pp 440-467.

Krinitzsky, E.L. and F.K. Chang. (1988). "Intensity-Related Earthquake Ground Motions," Bulletin of the Association of Engineering Geologists, Vol. XXV, No. 4, pp. 425-435.

McGuire, R.K. (1988). "Engineering Model of Earthquake Ground Motion in Eastern North America," EPRI NP-6074

Mori, A.W. and C.B. Crouse. (1981). "Report SE-29, Strong Motion Data From Japanese Earthquakes," National Geophysical and Solar-Terrestrial Data Center, Environmental Data and Information Service, NOAA, Boulder, CO.

Newmark, N.M., J.A. Blume, and K.K. Kapur. (1973) "Seismic Design Spectra for Nuclear Power Plants," Journal of the Power Division, ASCE, Vol. 99, No. PO2, pp. 873-889.

Nuttli, O.W., G.A. Bollinger, and R.B. Herrmann. (1986). "The 1886 Charleston, South Carolina, Earthquake-A 1986 perspective, "U. S.. Geological Survey Circular 985, United States Government Printing Office, Washington, D.C., 52 pp.

Nuttli, O.W., G.A. Bollinger, and R.B. Herrmann. (1984). "Strong Ground Motion Studies for South Carolina Earthquakes," NUREG/CR-3755, United States Nuclear Regulatory Commission, Washington, D.C., 88 pp.

Nuttli, O.W. and R.B. Herrmann. (1984). "Motion of Mississippi Valley Earthquake," Journal of Technical Topics, ASCE, Vol. 110, No. 1, pp 54-69.

Nuttli, O.W. (1983). "Average Seismic Source Parameter Relations for Mid-Plat Earthquakes," Bull. Seism. Soc. of Am., Vol. 73, pp. 519-535.

Nuttli, O.W. and R.B. Herrmann. (1982). "Earthquake Magnitude Scales," Journal of Geotechnical Engineering Division, ASCE, Vol. 108, No. GT5, pp 783-786.

Nuttli, O.W., G.A. Bollinger, and D.W. Griffiths (1979). "On the Relation between Modified Mercalli: Intensity and Body Wave Magnitude," Bull. Seism. Soc. of Am., Vol. 69, No. 3, pp. 863-909.

Street, R.L. (1982). "Ground Motion Values obtained for the 27 July 1980 Sharpsburg, Kentucky Earthquake, Bull. Seism. Soc. Am., Vol. 72, pp 1295-1307.

Toro, G.R. and R.K. McGuire (1987). "An Investigation into Earthquake Ground Motion Characteristics in Eastern North America," Bulletin of the Seismological Society of America, Vol. 77, No. 2 pp 468-489.

Uniform Building Code (1991). International Conference of Building Officials, Whittier, California.

Veneziano, D., letter dated December 26, 1986, to D.L. Bernreuter in pp. Q123-124 of D.L. Bernreuter, J. Savy R.W. Mensing, and J.C. Chen (January 1989), "Seismic Characterization of 69 Nuclear Plant Sites East of the Rocky Mountains," Lawrence Livermore National Laboratory, NUREG/CR-5250, UCID-21517, Vol. 7.

Weichert, P.H., P.W. Pomeroy, P.S. Munro and P.N. Mork (1982). "Strong Motion Records from Miramachi, New Brunswick, 1982 Aftershocks, Earth Physicas open-file Report 82-31, Ottana, Canada.

SYNTHETIC GEOGRID REINFORCES EXISTING EARTH DAM EMBANKMENTS

Frederick Lux III[1], James R. Bakken[2], and Dean S. Steines[3]

Abstract

An inspection and analyses for the Clam River Dam in northwestern Wisconsin revealed that the embankment slopes did not meet FERC dam safety requirements. In most areas, the downstream slopes could be stabilized by grading to a flatter slope. However, flatter slopes were not possible adjacent to the powerhouse as access to the spillway and the powerhouse needed to be maintained. An engineering evaluation revealed that a synthetic geogrid reinforced slope could be constructed for approximately one third the cost of a concrete retaining wall. Slopes as steep as 1.1H:1V were designed and constructed to stabilize the embankments.

Introduction

The Clam River Dam Hydroelectric Project is situated on the Clam River near the Village of Webster in northwestern Wisconsin's Burnett County. The dam and hydroelectric facilities are owned and operated by the Northwestern Wisconsin Electric Company (NWE). The 1.2 MW run-of-river project was constructed and began generating in 1944. Normal hydraulic operating head is 35 feet. The project facilities consist of a 102-foot-long concrete spillway and powerhouse flanked on each side by earth embankments, 950-feet long on the left and 220-feet long on the right (Figure 1).

An inspection and analyses performed in 1988 and 1989 revealed that the embankment did not meet current Federal Energy Regulatory Commission (FERC) dam safety criteria with respect to slope stability. Slope stability analyses indicated that safety factors at some embankment locations were unacceptable. These areas included the upstream slopes for the sudden drawdown condition and

[1]Project Manager, Ayres Associates, 1300 W. Clairemont Avenue, Eau Claire, WI 54701
[2]Manager, Water Resources, Ayres Associates
[3]Staff Engineer, Ayres Associates

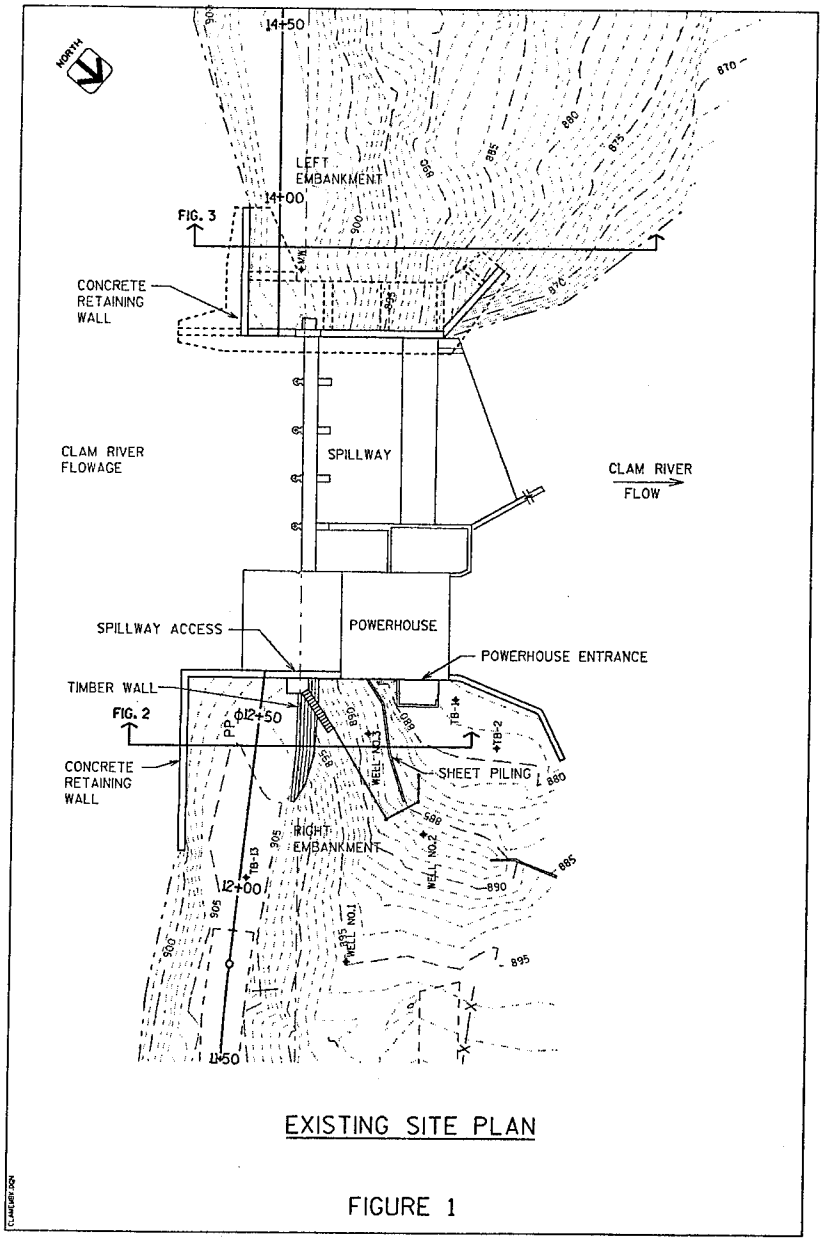

EXISTING SITE PLAN

FIGURE 1

the downstream slopes for steady seepage and earthquake conditions. Stabilization of the upstream slopes could be achieved by grading and adding riprap above and below the water surface. Most of the downstream slopes could be stabilized by grading to a flatter slope and adding a toe drain. However, flattening slopes adjacent to the powerhouse was not possible due to the location of the powerhouse entrance at the toe of the existing slope and access to the spillway at the top of the slope. Flattening the slopes adjacent to the spillway was also not possible due to the slope of the abutment and retaining walls. Therefore, another solution for stabilizing the embankments adjacent to these structures was desired.

Alternative Evaluation

The downstream slope adjacent to the spillway was about 2H:1V (horizontal:vertical), matching the slope of the abutment wall. The downstream slope adjacent to the powerhouse was about 1H:1V with a deteriorating timber crib and displaced sheet piling retaining wall. The entrance to the powerhouse is located at the toe of this slope and access to the intake and spillway gates is along the right embankment at the top of the slope . Cross sections of the right and left embankments prior to construction are shown in Figures 2A and 3A.

Several alternatives for the right embankment were evaluated for obtaining acceptable slope stability safety factors . Preliminary designs and associated costs were developed for each alternative. The alternatives evaluated include the following:

1. Concrete Retaining Wall. The concrete retaining wall has a height varying from 12 feet to 24 feet. It extended 64 feet to the right of the powerhouse.

2. Gabion Wall. Gabion wire baskets filled with rock are stacked one upon another to form a wall. The gabion wall has the same dimensions as the concret retaining wall described previously.

3. Steel Bin Wall. The steel bin wall is composed of galvanized steel bin assemblies filled with compacted earth. The bins are set into the embankment slope to form a tiered wall. The bin wall alternative consisted of two rows of bins, each about 12 feet high.

4. Synthetic Geogrid Reinforced Slope. A synthetic geogrid reinforced slope included a slope of approximately 1H:1V. with several layers of geogrids extending about 30 feet into the embankment.

5. Precast Interlocking Block Wall. A precast interlocking block wall consists of concrete blocks set in the face of the slope and anchored with geogrids. This alternative consisted of three tiers of blocks, each six feet high. This alternative did not provide the required safety factor and was eliminated from further consideration.

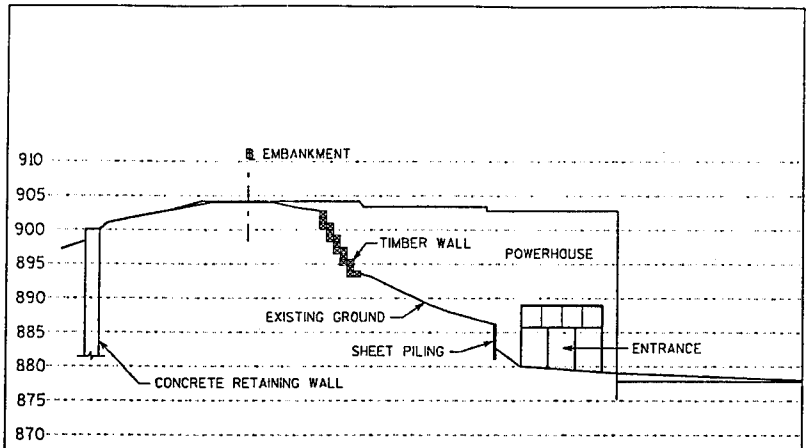

A EXISTING RIGHT EMBANKMENT

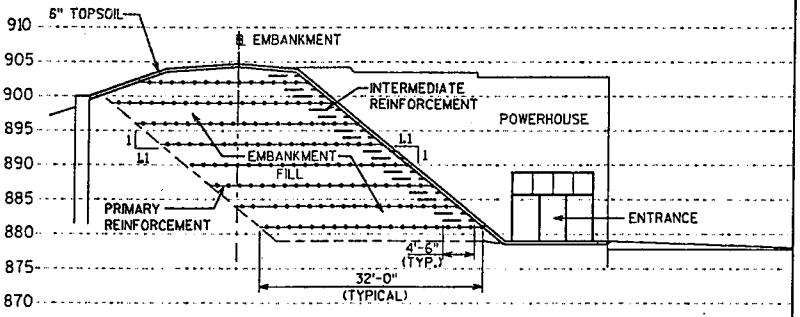

B REHABILITATED RIGHT EMBANKMENT

FIGURE 2

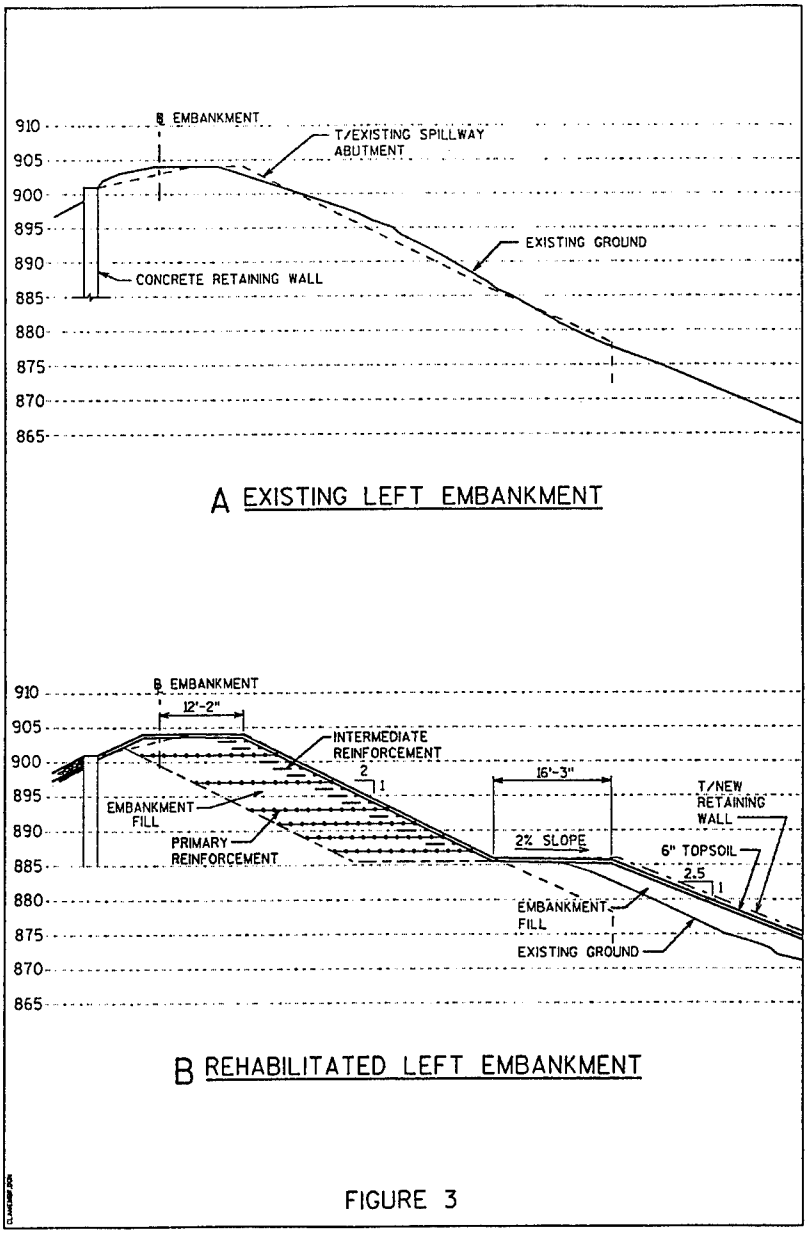
910
905
900
895
890
885
880
875
870
865
℄ EMBANKMENT
T/EXISTING SPILLWAY ABUTMENT
EXISTING GROUND
CONCRETE RETAINING WALL
A EXISTING LEFT EMBANKMENT
℄ EMBANKMENT
12'-2"
INTERMEDIATE REINFORCEMENT
2
1
16'-3"
T/NEW RETAINING WALL
EMBANKMENT FILL
PRIMARY REINFORCEMENT
2% SLOPE
6" TOPSOIL
2.5
1
EMBANKMENT FILL
EXISTING GROUND
B REHABILITATED LEFT EMBANKMENT

FIGURE 3

Conceptual costs were developed for each viable alternative. The geogrid reinforced slope was much less expensive than the remaining alternatives. Therefore, the selected alternative was the synthetic geogrid reinforced slopes. Comparative costs are listed in Table 1.

Table 1
Alternative Cost Comparisons

Alternative	Cost
Concrete Retaining Wall	$95,000
Gabion Wall	$55,000
Steel Bin Wall	$60,000
Synthetic Geogrid Reinforced Slope	$32,000

The proposed solution for stabilizing the downstream slopes in the vicinity of the powerhouse and spillway uses geogrid reinforcement in both the right and left embankments. The right embankment is designed at a 1.1H:1V slope adjacent to the powerhouse with a reinforced transition slope of 1.5H:1V. The remaining portions of the downstream right embankment is at 2.75H:1V. The left embankment is designed at a 2H:1V upper slope reinforced with geogrids, a 16-foot-wide berm, and a lower slope at 2.5H:1V. The existing deteriorated concrete wing wall at the left embankment toe was replaced and extended to accomodate the berm and lower slope. The wall is also needed to protect the embankment toe from spillway releases. A transition slope at 2.75H:1V meets the remaining slope which is also at 2.75H:1V. Figures 2B and 3B show cross sections of the rehabilitated right and left embankments, respectively, with geogrid reinforcement.

Geotechnical Investigation

Soil borings were taken and undisturbed samples were obtained for analyses to determine soil parameters for the embankment and foundation materials. Soil descriptions, water levels, and blow counts were recorded for each boring. One boring was taken on the right embankment near the powerhouse to supplement two borings that had previously been taken in 1986. Two borings were taken on the left embankment, one near the spillway abutment and one near an area of observed seepage. A fourth boring was taken near the toe of the left embankment. Piezometers were installed in each of the borings. The soils encountered in the embankment were generally sands and silty sands. Some clay was encountered in the right embankment. The foundation generally consists of dense glacial hardpan.

Two undisturbed samples were taken from the soil borings, one from each side of the embankment. Dry unit weight and natural moisture content were tested in the laboratory. Correlation between standard penetration blow counts, density, and shear strength were used to determine soil parameters required for the slope stability

analyses. Soil parameters used in the analyses are given in Table 2.

Table 2
Soil Parameters

Parameter	Embankment	Foundation
Moist Unit Weight (pcf)	121	145
Saturated Unit Weight (pcf)	128	145
Shear Friction Angle (deg)	28	46
Cohesion Intercept (psf)	0	0

Geogrid Selection

Geogrids were selected over other types of synthetic reinforcement because of their drainage capability, durability, and longevity. It was important that the reinforcement did not create a seepage path through the dam. Geogrids have large openings that allow seepage water to drain freely. Also, geogrids have been effective on other dam slope stabilization projects and have proven to be durable over time.

The initial selection of geogrids was based on design charts provided by the Tensar Corporation. Other more generic chart-based solutions are also available. The charts consider factors such as slope, slope height, soil shear friction angle, and surcharge load. The charts are based on the assumption that the soil is cohesionless and there is no pore water pressure. The total horizontal force is estimated using the Tensar design charts. The geogrid type and spacing are determined from the total horizontal force required. For example, if a total force of 15,000 lbs is required and a geogrid with an allowable tensile strength of 3,000 lbs is used, then five layers will be required. However, Tensar recommends that geogrid spacing not exceed four feet. If the initial selection results in a vertical spacing of more than four feet, then a lighter geogrid should be selected. Charts are also provided to determine the required embedment length of the geogrids.

Intermediate geogrids are placed at vertical intervals of one foot at the face of the slope to provide additional stability against shallow localized slope failures. The intermediate geogrids are lighter than the primary geogrids and extend only 4.3 feet (one roll width) into the embankment.

Slope Stability Analyses

After the initial selection of geogrids, slope stability analyses were completed to verify the design. Slope stability analyses were performed using the slope stability program PCSTABL6 developed by Purdue University. This program performs two-dimensional slope stability analyses with the capability to include reinforcement.

Slope stability analyses were performed in accordance with FERC and U.S. Army Corps of Engineers criteria. The following conditions were analyzed:

1. Steady seepage with maximum pool (downstream slopes).
2. Steady seepage with earthquake (upstream and downstream slopes).
3. Sudden drawdown (upstream slopes).

The geogrids were considered only for the downstream slopes. Required safety factors are 1.5 for steady seepage with maximum pool, 1.0 for steady seepage with earthquake, and 1.2 for sudden drawdown. A psuedo-static earthquake analysis was used for the earthquake condition with a horizontal acceleration coefficient of 0.05.

Phreatic surfaces were estimated using water levels measured in observation wells and soil borings, headwater and tailwater elevations, and observed seepage on the downstream slope. It was assumed that excavated embankment material could be used for fill with the exception of the clay found in the right embankment. The geogrids were assumed to have only a horizontal tensile contribution for reinforcement. A development length was computed based on the coefficient of interaction between the geogrids and fill material. For sandy material, a coefficient of interaction of 0.9 was used, as recommended by Tensar. The tensile strength of the geogrid was assumed to be equal to zero at the end increasing linearly to the full allowable tensile strength over a distance equal to the development length. The same length is required for overlaps of the geogrids.

Analyses used the simplified Bishop method with 100 trial failure surfaces generated. A 200 psf surcharge load was applied to the top of the embankment. The final design for the right embankment used eight layers of geogrids with an allowable tension of 2,200 lbs/ft. The vertical spacing between geogrid layers was three feet. The 1.5H:1V transition slope uses the same reinforcement. Each geogrid layer extend 32 feet into the embankment. The reinforced embankment is 26 feet in height. The left embankment required six layers of geogrids with an allowable tension of 500 lbs/ft. The vertical spacing between geogrids near the bottom of the slope was two feet while a spacing of four feet was used near the top. The height of the reinforced slope is 18 feet. The reinforced slope is situated above a berm 16 feet wide with a lower slope of 2.5H:1V.

Intermediate geogrids were placed between the primary reinforcement. These geogrids provide additional protection against shallow failures or localized sloughing. Intermediate reinforcement consists of lighter geogrids placed at the face of the slope and embedded about four feet into the embankment. Synthetic erosion mat was placed along the surface of the steep embankments to prevent topsoil erosion and to establish vegetation.

Construction

Construction of the earth embankment and installation of the geogrids were achieved using conventional techniques and equipment. A backhoe was used to excavate material from the embankment. Because of the large elevation difference, the excavation was completed by benching and creating a platform for the backhoe at various levels. Clay fill was encountered throughout the excavation at the right embankment down to the specified lower limit. Upon further evaluation, the clay was found to be unsuitable for foundation material and was subsequently removed. Additional excavation was carried out down to the hardpan foundation as much as ten feet below the specified lower limit. Silty-sand fill was used to replace the excavated clay material.

The geogrids were rolled out on a horizontal compacted soil surface and covered with the next layer of fill. The primary reinforcement was rolled out perpendicular to the downstream slope face. Intermediate reinforcement was laid parallel to the downstream slope face. Fill material was placed with front end loaders, leveled by bulldozers to a thickness of about twelve inches, and compacted with vibratory rollers. Access to the embankment was from the bottom with a ramp until fill reached approximately half way to the top of the dam at which point access was from the top of the dam. A layer of fill was placed before driving any construction equipment over the geogrids. Because compaction was critical for this dam, a compacted lift thickness of six inches was used with a minimum compaction of 92% of Modified Proctor.

Erosion control and slope protection were of great concern during and following construction. Because the slopes are very steep, significant erosion could occur with only a small amount of rainfall and runoff on the slope. Protection during construction included the construction of a berm at the top of the slope at the end of each working day to prevent runoff from the top of the dam from flowing down the slope. Plastic sheets were used to cover the slopes to provide protection of the surface.

Slope and erosion protection after construction included the placement and anchoring of erosion mat and the use of a proper seed mixture to establish a vegetative cover. Six inches of topsoil was placed over the embankment and covered with a coconut fiber erosion mat. A seed mixture using fesacues and rye to promote fast growth and trefoil and crown vetch to provide an extensive root system was used to provide long-term protection on the embankments.

Construction of the right embankment was completed in the fall of 1992. A partial drawdown of the reservoir was completed before construction began. The drawdown was required to maintain a stable slope after excavation on the right embankment. It also helped to keep the construction area free of water, resulting in better working conditions. Work on the upstream slopes was also completed during the drawdown period. Construction of the left embankment will take place in the summer of 1993. Figure 4 is a photograph showing installation of the geogrids on the right embankment.

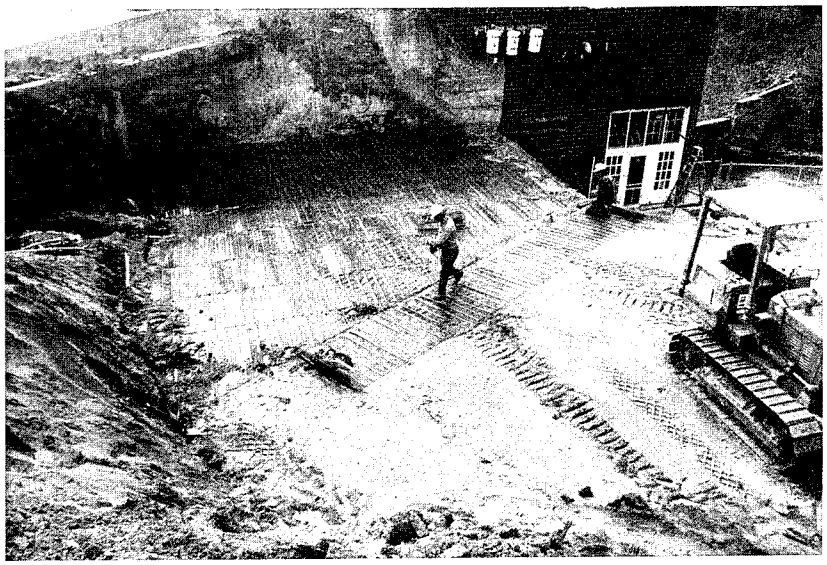

Figure 4. Installation of geogrids.

Conclusion

Synthetic geogrid reinforcement provided an economical and practical alternative for stabilizing the Clam River Dam embankments. The existing embankments did not meet current FERC dam safety requirements and required modifications. An alternative evaluation revealed that construction of geogrid reinforced slopes would result in significant savings compared to other alternatives that were evaluated. Adequate slope stability was obtained for slopes as steep as 1.1H:1V using synthetic geogrids. Construction was completed using conventional techniques and equipment.

References

Achilleos, Eftychios "User Guide for PC STABL 5M", Purdue University and Indiana Department of Highways Joint Highway Research Project, December 15, 1988.

Ayres Associates, "Inspection Report, Clam River Dam Hydroelectric Project, FERC Project No. 9185, Clam River, Burnett County, Wisconsin", December 1988.

Ayres Associates, "Clam River Dam Embankment Rehabilitation Evaluation" September 1989.

Federal Energy Regulatory Commission, "Engineering Guidelines for the Evaluation of Hydropower Projects", Office of Hydropower Licensing, July 1987.

Humphrey, D.N. and R.D. Holtz, "STABL 6 with Reinforcing Layer Option", Purdue University and Indiana Department of Highways Joint Highway Research Project, October 14, 1986.

SOCON Engineering, Inc., "Geotechnical Investigation - Clam River Dam Hydroelectric Project", May 1989.

Tensar Corporation, "Application Worksheet - Slope Reinforcement", February 1988.

U.S. Army Corps of Engineers, "Engineering and Design - Stability of Earth and Rockfill Dams, (EM 1110-2-1902)", April 1, 1970.

GEOLOGIC ASPECTS OF THE MT. HOPE PUMPED STORAGE PROJECT, DOVER, NJ

C.A. Foster[1], J.L. Rosenblad[2], R. Venkatakrishnan[3], and J.F. Wearing[4]

INTRODUCTION

The proposed Mt. Hope Waterpower Project is located at the inactive New Leonard Mine site at Mt. Hope in Rockaway Township, Morris County, New Jersey, approximately 2 miles (3.2 km) northeast of the town of Dover, New Jersey.

The concept of a pumped storage project at Mt. Hope has been studied by several private companies and public utilities over the past 20 years. Initial concepts incorporated existing underground mine workings (New Leonard Shaft) into the construction and/or operation of the lower reservoir, and increased capacity of an existing surface water body (Mt. Hope Lake) to create an upper reservoir. The most recent design reflects a closed-loop system with both the upper and lower reservoirs being excavated in rock (see Figure 1).

The upper reservoir will be contained in a basin excavated in rock, west of Mt. Hope Lake. Based on current plans, no dam will be necessary.

[1] Supervisor - Geology, Stone & Webster Engineering Corporation, 245 Summer St., Boston, MA 02210 - USA
[2] Chief Geotechnical Engineer, Stone & Webster Engineering Corporation, 245 Summer St., Boston, MA 02210 - USA
[3] Consultant
[4] Golder Associates, Inc., 305 Fellowship Road, Suite 200, Mt. Laurel, NJ 08054

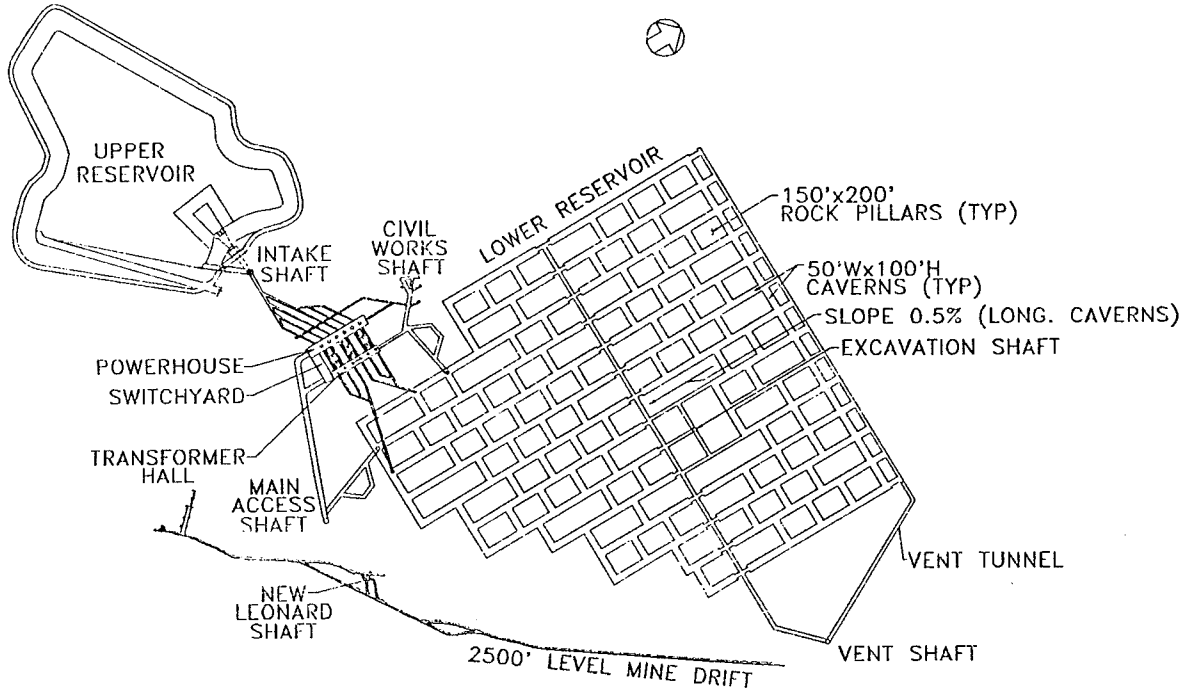

FIGURE 1 MT. HOPE WATERPOWER PROJECT - PLAN

From the upper reservoir, water will flow through a vertical intake shaft to the powerhouse located approximately 2800 feet (854 m) underground. The lower reservoir will be located approximately 2500 feet (762 m) underground. During the generating cycle, at times of peak demand, the water will be temporarily stored in the lower reservoir. It will subsequently be pumped back to the upper reservoir during off-peak periods. Several new shafts will be excavated to connect the upper works to the underground power station and lower reservoir.

A request to substitute this "Upland Alternative" for the original Mt. Hope Lake Scheme was filed with the Federal Energy Regulatory Commission (FERC) in September 1990. The Mt. Hope Waterpower Project, received a License from the Federal Energy Regulatory Commission (FERC) on August 4, 1992.

The objectives of this paper are to present the general geologic aspects of the Project and the influence that specific geologic and man made features have had on conceptual design and layout of Project facilities.

GEOLOGIC SETTING

The Mt. Hope site is located within the Reading Prong-New Jersey Highlands section of the New England Physiographic Province. The Reading Prong-New Jersey Highlands is characterized as a northeast-trending upland, underlain primarily by resistant crystalline rock. Rocks of the New Jersey Highlands have a long deformational history that has resulted in a complex over-printing of geological structures. As a result of past glaciations, younger surficial deposits of glacial and alluvia-glacial sediments directly overlie the bedrock.

The geology of the Project site is characteristic of the region, with metamorphic and igneous rocks that trend in a northeast direction. Principal rock types are alaskite, gneiss, granite, and amphibolite. The rocks are relatively hard and competent and have been extensively quarried for aggregate.

Material excavated by the Project is anticipated to be suitable for processing by the adjacent quarry operator. The existing quarry, located approximately 0.5 mile (0.8 km) north of the New Leonard Shaft, produces an estimated 5 million U.S. tons (4.5 billion kg) of crushed stone annually.

The main structural grain in rocks within the Mt. Hope Project area trends northeast-southwest. Contacts, foliation, and compositional layering within the gneisses of the Highlands generally trend northeast. A series of

major faults also trends northeast-southwest, dividing the region into a series of elongate blocks. Minor northwest-trending cross faults also occur at an oblique angle to the main structural grain, and they are steeply inclined to the southwest. The Mt. Hope Fault, which passes through the upper end of the site, is one of the larger cross faults having a mapped horizontal length of approximately 6 miles (9.7 km). The detailed U.S. Geological Survey report of the Mt. Hope Mine and other nearby mines states that the net displacement on the fault is about 300 feet (91.4 m) and the movement of the fault may have last occurred over 200 million years ago.

Two mineral resources, iron ore and bulk aggregate, are associated with the Project area. The Mt. Hope Mine is one of the oldest iron mines in the United States. The Project site includes both surface and underground mine workings. Mine workings exist throughout the southeast side of the site and extend to a depth of approximately 2500 feet (762 m). The deepest existing shaft is the New Leonard Shaft located near the central portion of the existing working. This shaft was completed to a depth of approximately 2700 feet (823 m) in 1944. There is considerable documentation available which delineates the location of the old workings. The geology confines the ore deposits to specific areas. Because the old mines are currently flooded, it is important that Project excavations are isolated from them until they are dewatered. The dewatering is scheduled to occur after completion of the upper reservoir so that the water can be pumped out of the mine into the upper reservoir for storage and later use by the Project.

Geologic constraints to Project design include the Mt. Hope Fault and the inclusion of the magnetite ore bodies within the rock strata. Current Project designs avoid these constraints by maintaining a buffer between them and the surface and underground excavations. However, the fault is intersected close to the surface by the intake shaft and the main access shaft. The location of the main access shaft is in the area of the old mines, but based on the available information, avoids penetration of the old mine workings.

A generalized geologic section of the site is shown on Figure 2.

UPPER RESERVOIR

A significant amount of quarry excavation has been carried out in the general area of the upper reservoir. Some of this excavation has been within the reservoir footprint, but above the maximum water level. Consequently, there are many rock exposures around the quarry. These exposures have been extensively mapped and there is a good understanding

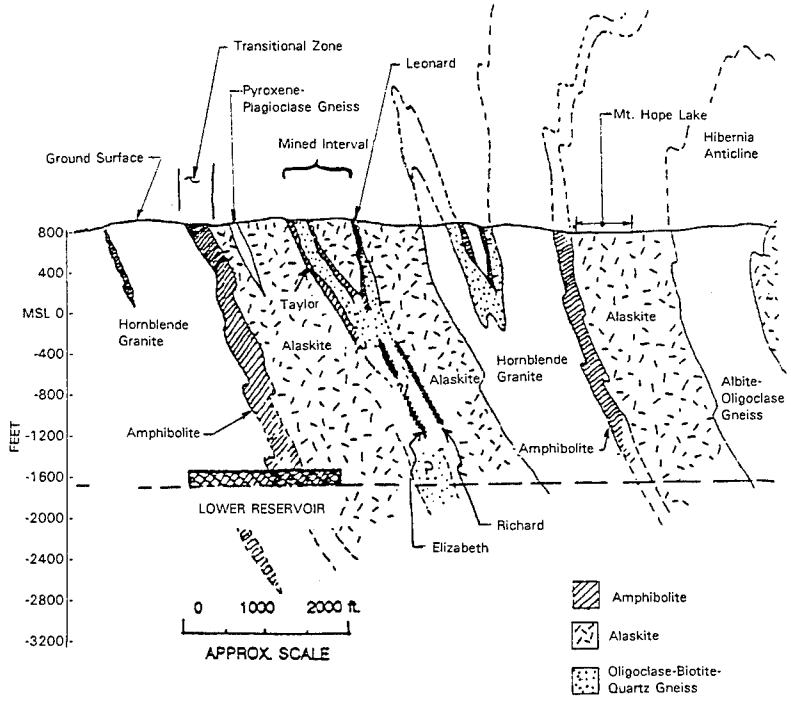

(SECTION MODIFIED FROM INFORMATION PRESENTED BY:
Sims, P.K., " Geology and Magnetite Deposits Survey",
USGS Professional Paper 287, 1958)

FIGURE 2 MT. HOPE WATERPOWER PROJECT - GENERALIZED GEOLOGIC CROSS SECTION

of the rock conditions that will be encountered in the excavation for the upper reservoir.

The southern rim of the upper reservoir is located alongside the Mt. Hope Road, and the Lake Denmark Road is to the west of the western rim of the reservoir. Along the north and eastern rim of the upper reservoir, the quarry operations have intercepted the northernmost extent of the old surface mine workings of both the Taylor and Finlay Deposits.

Eastern Rim

The eastern rim of the Upper Reservoir is a minimum of 100 feet (30.5 m) from the surface outcrop of the mine workings of the Taylor ore deposits. Historical surface workings of the deposit, near its intersection with the Mt. Hope Fault, have been previously quarried. In a small portion of the quarry workings and immediately to the southeast of the existing quarry limits, several open cuts along the ore veins still exist. In this area, and in several sections of the quarry, the footwall of the ore deposit is still visible and the rocks are generally competent. The subvertical, west (footwall) side of the open cuts exhibits a planar and smooth to undulating surface. Excavation-controlled horizontal jointing is not observed. However, longitudinal, northwest-dipping joints are evident.

Western Rim

The western rim of the upper reservoir is located within the hornblende granite. This rim follows a topographic ridge that bounds the edge of the existing quarry property. At the south end of this ridge there is a topographic hollow which drains into Mt. Hope Pond. At the north side of the ridge, beyond the excavation limits of the upper reservoir, there is a topographic low in the hornblende granite ridge which corresponds with the presumed location of the Mt. Hope Fault.

Mt. Hope Fault

The Mt. Hope Fault is known from mining operations to comprise a zone which is generally 50 feet (15.2 m) wide, and at places is up to 80 feet (24.4 m) wide. The intake shaft should intersect this fault at approximately elevation 500 feet (152 m). Here, it is anticipated that the jointing will be closely spaced and that there will be some brecciated zones with gauge and secondary minerals, including chlorite and carbonates. Based on records of prior underground mapping and extrapolation of surface conditions, the hanging wall of the Mt. Hope Fault may be more fractured than the footwall, thus more intensive efforts may be required to seal this interval to minimize leakage to and from the shaft. The footwall, by

contrast, is expected to be generally smooth and planar, with sharp contacts to the wall rock. Seams and veins of dolomite, calcite, and quartz have been noted to impinge on and penetrate into the hanging wall. Also, parallel to the Mt. Hope Fault, several small displacement sympathetic faults have been identified which exhibit chlorite gouge in filled zones up to 2 feet (0.6 m) wide. The hanging wall of the Mt. Hope Fault is expected to be beyond the northern rim of the upper reservoir. However, some of these sympathetic faults may intersect the north face of the upper reservoir, and may require additional rock support and grouting.

Weathering Effects

In general, the surface weathering below the top of rock is at less than 20 feet (6.1 m) depth. Consequently, around most of the perimeter of the upper reservoir, excavation below the maximum water level will not be affected by surface weathering as between 20 and 120 feet (6.1 and 36.6 m) of rock will have to be removed prior to the start of excavation of the reservoir itself. In local areas, particularly along the southern rim of the reservoir, the permeability may be affected by the presence of deep weathered pockets which could exist in some of the less resistant rock units adjacent to the Mt. Hope Fault and other structures. One particular band of plagioclase-biotite-quartz-schist that trends at right angles to the Mt. Hope Fault is believed to be extensively weathered to a least 65 feet (19.8 m) depth. This band of rock runs parallel to the regional foliation and trends into the northern neck of the reservoir layout. This unit, and similar sheared schistose bands, may be friable and more permeable and may require grouting. These areas will be excavated during investigations prior to construction.

Effects of Old Mine Workings

Several of the old mine workings exist adjacent to and parallel with the eastern rim of the upper reservoir. The Taylor workings currently comprise an open linear slot parallel to the eastern rim of the reservoir. The upper reservoir has been laid out so that there is a pillar of undisturbed rock, a minimum of 100 feet (30.5 m) wide, between the eastern rim of the reservoir and the footwall of the Taylor workings. The height of the exposed footwall face of the Taylor workings is about 60 feet (18.3 m). This face is standing unsupported, near vertical and the exposed rock is generally excellent. However, there are some northwest-trending, transverse joints which crosscut the face at about right angles and some steeply dipping foliation planes which strike more or less parallel to the trench alignment.

The transverse joints which have essentially the same dip and strike as the Mt. Hope Fault may be slightly open. This part of the rim areas, in consequence, will be investigated with vertical and inclined boreholes and permeability testing prior to final design. Grouting may be necessary in this area to minimize leakage.

Rock Mass Quality and Effects of Quarrying

In general, the rock quality and fracture spacing are likely to increase significantly with depth and the extent of weathering and openness of the joints are likely to decrease with depth. The most fractured, weathered and permeable rock is likely to be close to the ground surface and will be removed prior to the start of excavation of the reservoir itself, so the rock quality and watertightness are expected to be good below the water level in most of the upper reservoir.

Particular attention will be paid to the blasting close to the perimeter of the upper reservoir to minimize the required rock support and minimize the induced permeability from the blasting.

LOWER RESERVOIR

The western section of the lower reservoir will be excavated within hornblende granite, while the eastern section will be mainly in alaskite. This alaskite is variable in composition and includes several 100 to 150 feet (30.5 to 45.7 m) wide lensoid bodies of albite-oligoclase-gneiss. Some large pods of amphibolite are also likely.

Structurally, the lower reservoir is anticipated to be within a largely undeformed block of very competent rock. However, some splay faulting associated with the Taylor Thrust may be encountered at the northernmost end of the lower reservoir.

Lithology

The same broad band of rock types as described for the upper reservoir rocks will occur in the lower reservoir excavation. However, in large part, the excavations are anticipated to be located within hornblende granite and alaskite.

Currently, the main quarry workings are confined to rocks that occur to the east of the hornblende granite. Therefore, few exposures of the hornblende granite exist. In fact, the dominant rock type of the quarry is alaskite. Some oliogoclase-biotite-quartz gneiss that occupies the core and the limbs of the Mt. Hope Syncline is also being excavated by the quarry

operator. These rocks are anticipated to occur in a longitudinal band running northeast-southwest through the central section of the Lower Reservoir along with small lensoidal intercalations of pyroxene gneiss, albite-oligoclase granite and broader bands of amphibolitic migmatites.

Structure

1. Rock Mass Fabric

The fabric of the rock mass that is likely to be encountered at lower reservoir depth is considered to be similar to that described for the upper reservoir. However, overall foliation dips are expected to decrease somewhat with depth.

Rock quality is anticipated to be good except in close proximity to significant structural features. In the vicinity of longitudinal faults, such as the Taylor Thrust zone (which may be encountered at the northern end of the lower reservoir), increased jointing is anticipated such that zones of lower rock quality may occur. Lower quality rock would only be expected in the immediate vicinity of faults, such as the Taylor Thrust where a 3-foot (0.9-m) wide selvedge of chloritzied-biotite gneiss occurs paralleling the actual fault plane. Elsewhere, joint planes are anticipated to be tight and it is anticipated that the rock will generally be competent between individual discontinuities.

At depth, foliation is not likely to be open. In the underground excavation, therefore, it is anticipated that most of the rock types will be more or less "unstructured" except as evidenced by compositional and textural changes.

2. Discontinuity Characteristics

Small-scale structural features (joints, minor faults) that dominate rock conditions at surface are expected to be present at depth but may be less strongly developed. The trends of the structures are also anticipated to be similar to those measured both in the Mt. Hope Mine workings and from surface exposures in the quarry. However, much of the lower reservoir area will be excavated in rocks that are outside the lithologies that are well exposed in the surface quarry and only a few surface outcrops of the hornblende granite, for instance, occur. Joint controlled surfaces in these outcrops are widely spaced. Some evidence of foliation is present, but not as well developed discontinuity fabric.

Although locally variable, the outcrops show a predominant structural grain that strikes northeast-southwest and dips to the southeast at steep

angles. This is consistent with overall trends of the foliation within the project area and it is anticipated that the structural trend seen at surface in the hornblende granite will continue to depth.

3. Faulting

Both transverse and longitudinal faults are known to exist in relatively close proximity to the proposed cavern areas. The longitudinal faults appear to be more intimately related to the ore deposits and strongly foliated lithologies than with the alaskite or the hornblende granite.

Transverse faulting, parallel and sympathetic with the Mt. Hope Fault may also be present towards the southern end of the lower reservoir area. Such faulting, as well as the longitudinal faults, would also be expected to be characterized by zones of increased jointing and locally developed areas of brecciation and chlorite schist.

None of the faults in the immediate project area are considered active, and despite increased jointing and zones of weaker rock near the faults, they are not expected to significantly influence the integrity of the lower reservoir.

POWERHOUSE, ASSOCIATED GALLERIES, AND WATER CONDUIT SYSTEM

The powerhouse, transformer gallery, and access tunnels for the civil works will all be in hornblende granite and alaskite, except for short lengths of the access tunnels to the southeast of the powerhouse where the rock will be amphibolite or oligoclase gneiss. The rock quality of the hornblende granite and alaskite should be excellent, while the amphibolite and oligoclase gneiss may be slightly lower quality, but still good. Rock joints should be tight. All four rock types will provide good conditions for the construction of the large underground caverns and tunnels.

The old mine workings at the Project site have proved that large, stable underground openings can be excavated at the depth of the powerhouse. Analyses performed on the slopes of the old mine workings have provided data on the rock mass strength. Like the lower reservoir, the rock quality at the powerhouse, transformer gallery, and access tunnels is expected to be considerably better quality than the rock at the old mine workings, so analyses of the stability of excavations for the civil works should be conservative if rock strength parameters from the mine workings are used.

The intake tunnel, intake shaft, manifolds, and penstocks, which are all on the west side of the powerhouse, will be excavated within hornblende granite. The rock is expected to be excellent quality and the joints should be tight. It is anticipated that the rock will provide good conditions for tunneling. The minimum in-situ rock stresses are expected to be at least 2.5 times the internal pressure in the penstock manifold so there should be little risk of hydraulically fracturing the rock. The permeability of the rock is likely to be very low so leakage to the powerhouse and drainage gallery should be minimal.

The draft tubes, draft tube extensions, manifolds, and connector shaft between the powerhouse and the lower reservoir will be excavated in hornblende granite and alaskite. The rock quality in both these units is expected to be excellent. As on the upper reservoir side of the powerhouse, the rock joints should be tight and the rock should provide a good medium for tunneling. Leakage from the tunnels will be minimal.

INTAKE, ACCESS, CONSTRUCTION, AND VENTILATION SHAFTS

Intake Shaft

The proposed low pressure tunnel connecting the intake structure to the intake shaft is in the alaskite hanging wall rocks of the Mt. Hope Fault. The entire length of the tunnel is within the alaskite.

The upper part of the intake shaft will also be sunk in alaskite, and the shaft will cross the Mt. Hope Fault zone at about elevation 500 feet (152.4 m) which is at a depth of 350 to 400 feet (106.7 to 121.9 m) from the shaft collar. In this area the fault zone is expected to be 30 to 50 feet (9.1 to 15.2 m) thick. This upper part of the shaft will therefore be excavated in the good quality rock similar to the oligoclase or plagioclase-biotite-quartz gneisses that form the footwall of the Taylor ore deposit. Rock conditions in the fault zone are likely to be poorer than elsewhere in the Project and there is the potential that blocky ground and water inflows will be encountered through the fault zone. However, the old mine shafts are known to have crossed that Mt. Hope Fault without encountering significant problems.

Below the Mt. Hope Fault zone, the shaft will pass through a zone of transitional rocks that are mainly a mixture of amphibolite and biotite gneisses. Below elevation -1200 feet (-366 m), the rock will be hornblende granite and the rock quality is expected to be good to excellent.

Main Access Shaft

The collar of the proposed main access shaft is situated close to the existing New Leonard Shaft in an area where up to 30 feet (9.1 m) of mine fill exists. This material may include broken rock, sandy mine tailings, and peat. Rock, when intersected, is expected to be mostly alaskite. Once the near surface weathered zone is passed, rock quality is likely to improve as suggested by the results of several old borings drilled in the area. The borings indicate good core recovery in alaskite rock that was generally described as competent. The shaft will intercept much the same rock conditions until the Mt. Hope Fault is intersected at approximately elevation -480 feet (-146.3 m) which is at a depth of about 1300 feet (396 m) below ground surface. At this level, a zone of increased jointing and higher water inflow may be encountered similar to that expected in the area where the intake shaft crosses the Mt. Hope Fault. The fault zone is expected to be approximately 30 to 50 feet (9.1 to 15.2 m) thick in this area. Below the fault zone, the shaft will cross the entire sequence of the transitional zone rocks that are adjacent to the main ore zones. Within this group of rocks, the shaft is anticipated to encounter magnetite bearing rocks forming part of the extension to the Leonard ore body before passing into hornblende granite at the base of the excavation. Because of the depth, the transition rocks and the hornblende granite are expected to be good to excellent quality.

Lower Reservoir Excavation Shaft

The lower reservoir shaft will be collared in the eastern facies of the alaskite. Because the existing quarry operations have removed the upper weathered bedrock, the rock quality along the entire length of the shaft is expected to be good. Localized poorer rock could, however, be intercepted if pegmatitic zones are encountered during excavation. Towards the bottom of the shaft, although rock quality is still anticipated to be good, the bedrock could change into a slightly different facies of the alaskite that is intercalated with oligoclase-biotite-quartz gneisses and amphibolites.

Civil Works Shaft

The civil works shaft is located north of the Mt. Hope Fault. The shaft will be collared in alaskite, will then transverse amphibolite and finally enter hornblende granite. As in the other excavations in the footwall rocks to the Mt. Hope Fault, rock quality is anticipated to be good overall except in short lengths of the shaft.

Lower Reservoir Ventilation Shaft

The lower reservoir ventilation shaft is sited at the northeastern corner of the lower reservoir. It will be excavated between the old Elizabeth-Leonard workings and the Taylor workings, and will intercept the entire sequence of rocks that comprise the eastern limb of the Mt. Hope Syncline. The shaft is expected to also intercept several longitudinal faults such as have been commonly encountered in the mining of the northern portion of the Elizabeth and Leonard ore deposits. However, apart from these fault plane intersections, rock quality throughout the depth of the shaft is expected to be good. Although many longitudinal faults have been mapped crossing various parts of the old mine workings, they have not significantly affected overall mining excavation. Excavation of the shaft through these faults is therefore not expected to be problematic.

SUMMARY

The proposed 2000 megawatt Mt. Hope Waterpower Project is located in Rockaway Township, Morris County, New Jersey. The Project received a License from the Federal Energy Regulatory Commission (FERC) on August 4, 1992. The present design reflects a closed-loop system with both the upper and lower reservoirs being excavated in rock.

The site is located within the Reading Prong - New Jersey Highlands section of the New England physiographic Province. The geology of the site is characteristic of the region, with metamorphic and igneous rocks that trend in a northeast direction. Principal rock types are alaskite, gneiss, granite, and amphibolite. The rocks are hard and competent and have been extensively quarried for aggregate.

Geologic constraints include the Mt. Hope Fault and the inclusion of magnetic ore bodies within the rock strata. Current Project designs avoid these constraints by maintaining a buffer between them and the surface and underground excavations.

Piping Security of Glacial Till-Structure Interfaces

R. Craig Findlay[1]

Abstract

Many hydraulic structures in the northeast are founded on or constructed with glacial till. New England till is generally a suitable construction and foundation material because of its strength properties; however, with fines of low plasticity, till can be susceptible to piping. Conventional analysis of piping security includes the weighted line-of-creep method and critical gradient analysis. This paper discusses the use and limitations of these methods as they relate to structure interfaces with glacial till. Following that discussion, a new approach to analysis of piping potential is presented which, with refinement, may serve to supplement the existing methods.

Introduction

Piping, sometimes referred to as "internal erosion", is a phenomenon where soil particles forming an interface with a rigid structure erode due to seepage flow along the interface. Two conditions are necessary for piping to occur, namely, (1) seepage flow along the interface imparts sufficient force to soil particles that they will tend to move, and (2) soil particles at the seepage exit from the interface are free to move.

Design of water retaining structures to resist piping has changed little for almost six decades. Even though a few recent papers address new aspects of piping (Sherard, et al., 1976a, Sherard et al., 1976b, Koenders and Sellmeijer, 1992), current practice (FERC 1991) is to

[1]Lead Geotechnical Engineer, Northrop, Devine & Tarbell, Inc., 500 Washington Avenue, Portland, ME, 04103.

assess piping stability by critical gradient analysis (Harza, 1935) or the "weighted line-of-creep method" (Lane, 1935). Use of these methods has been described by numerous authorities (Subcommittee on Small Water Storage Projects, 1938, Creager and Justin, 1950, Terzaghi and Peck, 1967, Bureau of Reclamation, 1987, and FERC, 1991). While the methods generally provide a means of assessing the stability of an interface against piping, provided the designer understands their limitations, neither method provides an all inclusive, theoretical approach to assuring satisfactory design.

This paper will discuss the use and limitations of these methods for design of low head (less than about 10 meters) hydraulic structures in northern New England glacial till. These tills are generally low to non-plastic with typical grain size distributions as indicated on Figure 1. The author is aware of one pin hole dispersion

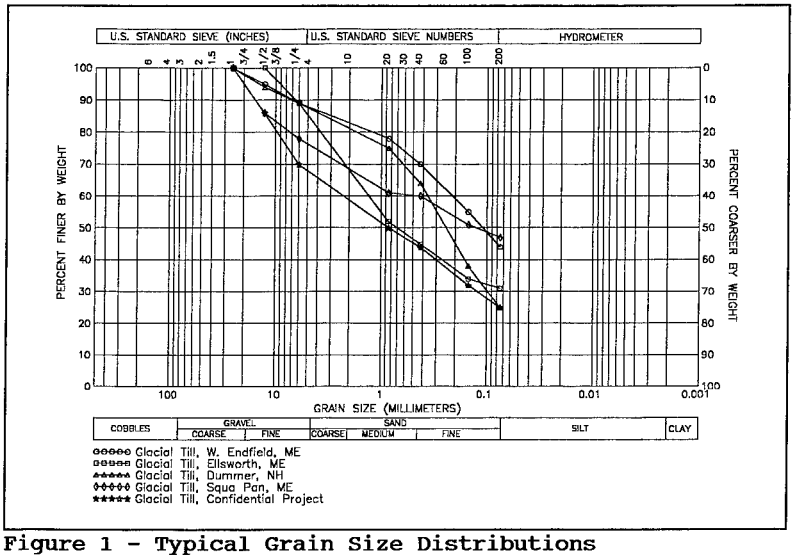

Figure 1 - Typical Grain Size Distributions

test made on a sample of glacial till from Dummer, NH, which indicated that the soil was non-dispersive. In response to the limitations of the existing methods, a preliminary theoretical approach to piping assessment, requiring further development, is presented which is based on tractive force analysis.

Weighted Line-of-Creep Method

The weighted line-of-creep method (Lane, 1935) is empirical, based on case histories. It is an extension of the theory proposed by Bligh (1910) that piping stability is dependent on percolation path length along the soil-structure interface. In development of the method, Lane analyzed 278 dams, 36 of which failed. From the analysis, Lane concluded that the resistance to piping along horizontal plane interfaces tends to be about 1/3 the resistance along vertical plane interfaces. Therefore, he defined the "weighted creep distance", l_w, as the sum of the vertical distances along an interface plus one third of the sum of horizontal distances. He designated l_w divided by the head differential (h) across the interface as the weighted creep ratio, r_w:

$$r_w = l_w/h \quad (1)$$

Lane further concluded that minimum r_w required to resist piping depends on soil type, and developed safe r_w values for 12 general soil descriptions. However, a problem with the method is that the soil descriptions are not quantified by grain size or plasticity and thus are not easily interpreted. With respect to determining safe ratios for glacial till, the designer must select an appropriate ratio from soil descriptions which include: "boulders, sand and gravel", "hardpan", and "boulders with some cobbles and gravel"; descriptions which leave much room for interpretation. In an effort to clarify this ambiguity, several cases of glacial till-structure interface performance, including both successful and unsuccessful configurations are compiled on Table 1. The following are brief project descriptions.

The Pontook Hydroelectric project offers four examples of till-structure interfaces which have not piped as well as one example where a pipe did develop. In the latter case, a pipe developed during construction along a vertical glacial till interface with a tight sheathed timber crib section. The pipe developed because a short flow path to open rockfill via an inadvertently unsheathed portion of the interface. Successful interfaces of the Pontook Project include the west dam abutment, the canal headworks, and the penstock intake.

A recent confidential project in northern New England offers an example of where a pipe developed. During excavation at the downstream side of the dam to construct a hydroelectric station, a pipe developed under the dam. The pipe was cutoff and construction was completed.

Graham Lake Dam, located in Ellsworth, Maine, offers another example of a pipe along a horizontal interface. In May of 1923, the impoundment was filling for the first time behind the newly constructed dam. The concrete gravity

PROJECT	INTERFACE DESCRIP-TION	HEAD (m)	SEEPAGE DISTANCE Vert (m)	SEEPAGE DISTANCE Horz (m)	WEIGHTED LINE OF CREEP (V+H/3) Length (m)	WEIGHTED LINE OF CREEP (V+H/3) Ratio	TRAC-TIVE RATIO To/Tc	D10 SIEVE SIZE (mm)	% PASSING 200 SIEVE	PL	PI	PERFORM-ANCE
Pontook Dummer, NH	east dam abutment	5.2	9.1	0.0	9.1	1.7	0.6	0.030	25	NP	NP	Piped
Pontook Dummer, NH	west dam abutment	5.2	37.8	0.0	37.8	7.3	2.4	0.030	25	NP	NP	OK
Pontook Dummer, NH	intake foundation	10.7	9.1	35.4	20.9	2.0	1.3	0.030	25	NP	NP	OK
Pontook Dummer, NH	intake abutment	8.8	35.4	0.0	35.4	4.0	1.3	0.030	25	NP	NP	OK
Pontook Dummer, NH	headworks abutment	9.1	34.3	0.0	34.3	3.8	1.2	0.030	25	NP	NP	OK
Confidential Project	foundation	10.7	4.9	6.1	6.9	0.6	0.3	0.023	25	NP	NP	Piped
Graham Dam* Ellsworth, ME	spillway foundation	6.7	0.0	18.6	6.2	0.9	0.9	0.008	31	NP	NP	Piped
West Enfield W. Enfield, ME	dam abutment	6.4	92.4	0.0	92.4	14.4	4.7	0.008	44	12.7	4.0	OK
Squapan Squapan, ME	dam abutment	10.2	50.3	0.0	50.3	4.9	1.6	0.001	47	14.7	14.6	OK
Woodward** Hill, NH	foundation	9.1	7.3	2.4	8.1	0.9	0.3	0.002	50	14	7	Piped
Ammonoosuc L.** Bethlehem, NH	foundation	7.0	30.5	17.1	36.3	5.2	2.2	0.010	21	NP	NP	OK
Ammonoosuc L.** Bethlehem, NH	weep hole	7.0	***	***	18.9	2.7	***	0.010	21	NP	NP	OK
Sugar River** Newport, NH	foundation	5.0	12.8	17.1	18.6	3.7	1.9	0.010	40	13	4.4	OK
Sugar River** Newport, NH	weep hole	5.0	***	***	10.5	2.1	***	0.010	40	13	4.4	OK

* Creep length estimated from photos and incomplete plans.
** From Lane, 1935, D10 based on published regional till gradations.
*** Not available

TABLE 1 - SUMMARY OF PIPING RESISTANCE ANALYSES

spillway section was founded on glacial till. During the initial filling, a pipe developed under the spillway section which resulted in a breach of the structure.

The West Enfield Project offers an example of a successful interface consisting of a retaining wall which abuts a glacial till embankment.

The Squa Pan Project offers another example of a successful glacial till-structure interface. The south spillway wall consists of a concrete gravity section which abuts a glacial till embankment.

Three additional projects are included on Table 1 which are from Lane's original work. Based on Lane's soil descriptions and the geology of the project locations, it is believed these projects are representative of glacial till interfaces.

Summarizing the case histories presented on Table 1, the four situations where pipes developed had r_w ratios ranging from 0.6 to 1.7. It is interesting to note that the case with r_w of 1.7 was for an interface with a timber crib structure rather than concrete. This may suggest timber crib interfaces could be more susceptible to piping than concrete. Without the timber crib case, the r_w range for interfaces developing pipes was 0.6 to 0.9. Interfaces where pipes did not developed had r_w of 2.0 or greater. Based on these results, it appears that interfaces with r_w of 2.0 or more have successfully resisted piping. The author currently uses r_w of 2.0 or greater for design of glacial till-structure interfaces on low head hydraulic structures.

While numerous sources reference the use of the weighted creep method, the method has not been without criticism. Because of its inherently empirical character, the method does not provide a true factor of safety. Also, the method does not consider geometry of the seepage interface. Cedergren (1989) has shown that a sheet pile cut-off is more effective at the heel of a hydraulic structure than at the toe. The weighted line-of-creep method would indicate that either configuration was equally resistant to piping, which would be incorrect. The method does not address soil confinement or use of a reverse filter, which could mitigate piping in situations of a sub-critical r_w. As a result of these and other criticisms, flow net analysis is usually a preferred approach, where applicable, because it allows definition of a factor of safety, and because it is based on theory rather than empiricism.

Critical Gradient Analysis

Coincidentally, in the same issue of ASCE Transactions that Lane presented his work, Harza (1935) published his work on seepage under dams founded on sand, forming the basis for critical gradient analysis of piping potential.

To assess piping stability, a flow net is constructed to define seepage through the soil underlying the soil-structure interface. The seepage gradient across the last flow net square or partial square as seepage exits from below the structure is compared to a "safe escape gradient", which is the "critical gradient" with an applied factor of safety (typically, 1/FS equals 1/2 to 1/4). An actual exit gradient which is less than or equal to the safe exit gradient is theoretically secure from piping. The critical gradient, i_c has a value of about 1, and is determined by:

$$i_c=(\gamma_s-\gamma_w)/\gamma_w \qquad (2)$$

where: γ_s = unit weight of soil
γ_w = unit weight of water

A drawback of the method is that it only applies to situations where seepage exits vertically upward from below an hydraulic structure. Therefore, the method is only applicable to embedded structures. In addition, the method was developed for dams founded on sand. For dams containing non-plastic fine grained material, the appropriateness of determining exit gradient by flow net analysis may be limited. This is because permeability along the soil-structure interface may be orders of magnitude greater than the inherent permeability of the foundation soil. Upon first watering of an hydraulic structure, (Findlay, 1988) observed the formation of a steady state phreatic surface along a previously unsaturated glacial till-structure interface significantly faster than the inherent permeability of the glacial till would indicate, suggesting a permeability along the soil-structure interface significantly greater than the inherent permeability of glacial till. Intuitively, increased permeability along the soil-structure interface probably becomes less significant as soil permeability increases. Interface permeability is likely near equal to soil permeability in sand, the soil type for which critical gradient analysis by flow net was originally developed. Based on the observation of higher permeability along the glacial till-structure interface, a more appropriate method may be to determine the exit gradient using the retained head divided by the flow length along the soil-structure interface, rather than flow net analysis. Where appropriate, the author has used both approaches in glacial till, basing the analysis results on that which represents the more critical case.

Proposed Tractive Force Method

As a result of the limitations of existing analysis methods, there is room for development of an additional theoretical method of piping analysis. Tractive force

analysis has been used for assessment of stream bed aggregation-deposition and design of canals (Simons, Li and Associates, 1982). The method compares the computed boundary tractive force (τ_o) imposed on the flow channel boundary to the computed critical tractive resistance (τ_c) provided by the soil particles based on their unit weight and diameter (Shields, 1936, and Gessler, 1973). Viewing piping as a velocity-of-flow/aggregation process, it follows that a similar analysis could be utilized to assess piping potential. The critical tractive resistance is that boundary tractive force imposed by water flow at which unconfined soil particles that make up the boundary will begin to move. Critical tractive force can be estimated using the Shields relation for the onset of incipient motion which is graphically presented on Figure 2. From

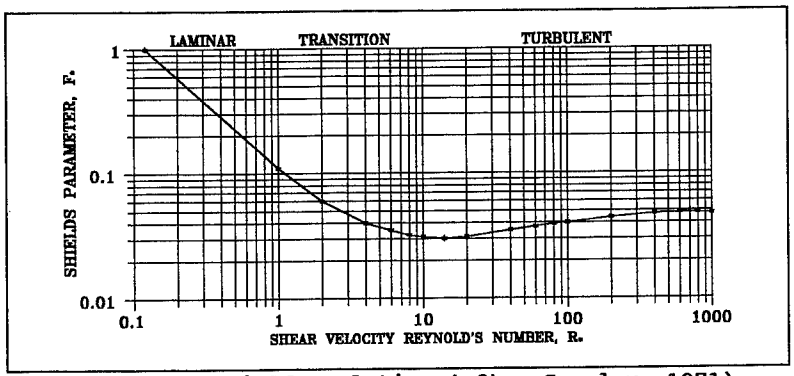

Figure 2 - The Shields Relation (after Gessler, 1971)

the figure, a value of F_*, the Shields parameter, is determined based on R_*, the shear velocity Reynold's number. R_* can be computed by:

$$R_*=(U_*D)/\nu \qquad (3)$$

where: U_* = shear velocity, approximated as 1/10 average flow velocity (L/T)
D = particle diameter (L)
ν = kinematic viscosity (L^2/T)

Incipient motion of soil particles is a function of F_*:

$$F_*=\frac{\tau_c}{(\gamma_s-\gamma_w)D} \qquad (4)$$

Solving for τ_c:

$$\tau_c = F_* (\gamma_s - \gamma_w) D \quad (5)$$

To estimate the tractive force, the following equation has been used which includes the Darcy-Weisbach friction factor, f:

$$\tau_o = 1/8 (\rho f U^2) \quad (6)$$

where: ρ = density of water (W T/L^4)
U = flow velocity (L/T)

The f term in Equation 6 is the same friction factor found in the Darcy-Weisbach formula, developed for uniform flow through pipes:

$$h_f = f \frac{L}{D_p} \frac{U^2}{2g} \quad (7)$$

where: h_f = frictional head loss (L)
L = flow length along which friction loss occurs (L)
D_p = pipe diameter (L)
g = acceleration due to gravity (L/T^2)

Solving Equations 6 and 7 for f, assuming h_f is equal to the head across the interface (h) and equating:

$$h \frac{D_p}{L} \frac{2g}{U^2} = \frac{\tau_o}{\rho} \frac{8}{U^2} \quad (8)$$

Inserting γ_w/g for ρ and solving for τ_o:

$$\tau_o = [\gamma_w h (D_p/L)]/4 \quad (9)$$

Equations 5 and 9 provide a means of assessing piping potential. However, to use the equations, several assumptions must be made. Soil piping begins by ravelling of soil particles at the downstream exit of seepage from the interface. For ravelling to progress, particularly in widely graded soils, D_p would have to be at least slightly larger than D to move smaller, unstable particles past larger, stable particles. On the verge of instability, it can be assumed that D is essentially equal to D_p. The most difficult assumption is selection of R_*, which is needed to determine an F_* value from Figure 2 for use in Equation 5. For seepage flow through soil, R_* is generally very small, and well within the laminar flow region. With increasing flow velocity, R_* increases and F_* decreases until flow becomes turbulent, in the range of R_* from about 1 to 10. Turbulent flow is associated with violent irregular flow paths, eddies and swirls. Considering the increased force

which would be imparted to soil subjected to turbulent flow, it is conceivable, for the purposes of discussion of this preliminary approach, to pose the possible association of the onset of piping with the onset of turbulent flow. If this association can be made, F_* used to determine the critical tractive resistance could be assumed to be 0.04, the approximate value at the midpoint of the turbulent threshold on Figure 2.

With these assumptions, equations 5 and 9 can be combined to form the ratio τ_c/τ_o; if τ_c/τ_o is less than 1.0, piping theoretically could occur. Table 1 includes τ_c/τ_o values for the reported case histories. The table shows reasonable agreement between projects which experienced piping and τ_c/τ_o values of less than 1.0. The good agreement between τ_c/τ_o seems to support the association of the onset of turbulence with the onset of piping in glacial till.

While the method may represent a promising approach, much additional work is admittedly necessary regarding the appropriateness of the assumptions made, the relationship between turbulence and piping, and the results of applying the method to more case histories and different soil types. Since sands require significantly longer contacts than soils such as till, use of the method with R_* equal to 0.04 would not likely result in reasonable results. As a consequence, it appears that R_* may be dependent on soil type. Another factor which needs to be addressed is that interface orientation is not accounted for by the proposed method as it is in Lane's method. The force of gravity, dependent on its direction in relation to the direction of flow, would be expected to influence resistance to piping.

Summary and Conclusions

Weighted line-of-creep ratios were tabulated for several projects that have performed successfully or unsuccessfully with regard to piping stability. Based on these cases, weighted line-of-creep ratio of 2.0 or more has been successfully used for low-head interfaces in glacial till. If appropriate, interfaces should also be analyzed using the critical gradient method in addition to weighted line-of-creep analysis. It was discussed that a potentially higher permeability exists at the interface than exists in the glacial till soil mass. As a result, critical gradient analysis should consider the retained head divided by the length along the interface in addition to the exit gradient estimated by flow net analysis, and the more critical value used.

Finally, a new preliminary method of piping analysis was presented based on tractive force analysis. Preliminary use of the method with the presented glacial till case histories yielded favorable results, but significant additional work is necessary to determine the validity of some of the necessary assumptions and appropriateness of

application to other soil types.

References

Bligh, W.G., (1910), Practical Design of Irrigation Works, Second Edition, D. Van Nostrand Co., NY, NY.

Bureau of Reclamation, (1984) Design of Small Dams, U.S. Government Printing Office, Denver, CO.

Cedergren, H.R.,(1989), Seepage, Drainage,and Flow Nets, third edition, John Wiley and Sons, NY, NY, p.27.

Creager, W.R., and Justin, J.D. (1950). Hydroelectric Handbook, John Wiley and Sons, NY, NY.

FERC (1991). Engineering Guidelines for the Evaluation of Hydropower Projects, Office of Hydropower Licensing Federal Energy Regulatory Commission, Washington, D.C.

Findlay, R.C. (1988). "Hydrostatic Pressure at a Soil Structure Interface," Proceedings of the Second International Conference on Case Histories in Geotechnical Engineering, sponsored by University of Missouri-Roll, St. Louis.

Gessler, J., (1971), "Beginning and Ceasing of Sediment Motion," River Mechanics, edited by H.W. Shen, Fort Collins, CO.

Harza, L.F., (1935). "Uplift and Seepage Under Dams on Sand," Transactions of the American Society of Civil Engineers.

Koenders, M.A., and Sellmeijer, J.B., (1992). "Mathematical Model for Piping," Journal of the Geotechnical Engineering Division, ASCE, Volume 118, No. 6, June.

Lane, E.W. (1935). "Security From Under-Seepage of Masonry Dams on Earth Foundations," Transactions of the American Society of Civil Engineers.

Sherard, J.L., Dunnigan, L.P., Decker, R.S., and Steele, E.F., (1976a), "Pinhole Test for Identifying Dispersive Soils," Journal of the Geotechnical Engineering Division, ASCE, Volume 102, No. GT1, January.

Sherard, J.L., Dunnigan, L.P., and Decker, R.S. (1976b), "Identification and Nature of Dispersive Soils", Journal of the Geotechnical Engineering Division, ASCE, Volume 102, No. GT4, April.

Simons, Li & Associates, (1982), Engineering Analysis of Fluvial Systems, Simons, Li & Associates, Fort Collins, CO.

Subcommittee on Small Water Storage Projects (1938). Low Dams, Water Resources Committee, National Resources Committee, Washington, D.C.

Terzaghi, K., and Peck, R.B., (1967). Soil Mechanics in Engineering Practice, Second Edition, John Wiley and Sons, NY, NY.

DESIGN AND PERFORMANCE OF POWER CANAL LINING

A.V.Sundaram[1], Member, ASCE

Abstract

The construction of 90 MW Summer Falls Hydro Project in State of Washington required utilizing the existing irrigation canal be used as power canal. Existing irrigation canal dikes formed essentially of dirty rockfill materials were required to be raised to contain the maximum water level in the canal. Additionally new canal was constructed extending from the existing canal. Construction materials available at the site to raise the existing canal and to construct the new canal were basically dirty rockfill with little fines obtained from the required excavation. Material such as clay for use as impervious fill to provide seepage barrier was essentially non-existent at the site. Therefore, three alternative methods of providing impervious barrier to the canal were evaluated. Finally, constructing the dike utilizing the dirty rockfill from required excavation and lining it with 4" thick Fabriform Unimat concrete was selected as a viable alternative. Since its completion in 1985, the project is operating successfully and no significant seepage is occurring and thus far no major maintenance expenditure required.

Introduction

The Summer Falls Project, consisting of power canal, diversion structure, intake structure, two 17 ft diameter and 600 ft long power tunnels, and a 90 MW (two units each of 45 MW) powerhouse, is located about 6 miles south of Coulee City, Washington on the southern end of the irrigation canal from Dry Falls Dam. Water released from the reservoir dammed by Dry Falls Dam is carried to the eastern part of the State for irrigation purposes. The reservoir, dammed by the Dry Falls Dam, serves as a collection basin midway in the Columbia Irrigation Project. Irrigation return flows and natural runoff from the northern part of the Columbia Basin are

---

1. Senior Engineer, Geotechnical Department, Harza Engineering, Chicago.

directed to the reservoir behind the Dry Falls dam, and are then released through the irrigation canal to the eastern part of the irrigation area. Approximately 6 miles south of the dam the water released from the dam through irrigation canal joins a lake over a water falls with a head difference in excess of 150 ft.

Utilizing available head between water level in the canal and that in the lake a 90 MW (two units each of 45 MW) powerhouse was constructed in the lake to augment the Bonneville Power System. This project is similar to typical run of the river project except existing storage and distribution reservoir, and irrigation canal are utilized to provide the required water and head.

Site Geology

The bedrock encountered at the Summer Falls site consists of a series of basaltic flows varying in individual thickness from 20 to 60 feet. In general, individual lava flows are characterized by 2 to 10 feet thick vesicular zones at upper surfaces, and 1 to 2 feet vesicular zones near the contact with underlying materials. Based on the cooling features, most lava flows are further subdivided into two distinct zones. The upper zone, termed the entablature, consists of vesicular basalt and displays a characteristic slabby appearance in outcrop. The underlying zone, called colonnade, consists of dense basalt with predominantly columnar cooling joint patterns. Because the individual lava flows are subjected to a number of physical and chemical processes through time, deterioration or modifications of rock within each flow unit takes place. With the rapid burial of a flow unit by another flow, the weathered rock, soil or interflow sediment is essentially preserved in place by a cap of sound durable basalt.

Power Canal Dikes

The existing irrigation canal dikes, as a part of the Grand Coulee Irrigation Project, were constructed of excavated material covered with shot rock. Material as excavated were placed at random in the dike without any emphasis for particular zoning or location within the dike. Compaction of the materials placed in the dike was accomplished essentially by the operating construction equipment used for excavation and hauling purposes. Increasing the gross head from 152 feet to 164 feet required raising 3000 ft of the existing dikes of dirty rockfill by 15 feet to contain the maximum water level in the canal. Additionally, construction of about 600 ft of new canal with about 30 feet high dikes extending from the existing irrigation canal was required. Typical cross sections of the existing, raised and new dikes are shown in Figure 1.

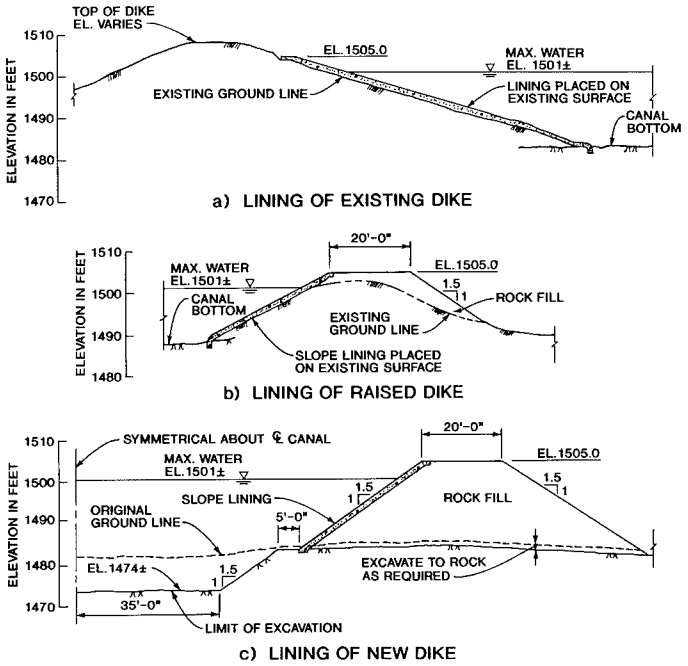

FIGURE 1. TYPICAL DIKE SECTIONS

Existing Canal Dikes

To evaluate the condition of the existing canal dikes backhoe trenches were excavated on the downstream face of the dike. The trench extended from the crest down into the foundation. Since the canal was full of water during the investigation it was not possible to excavate the trench across the entire dike width. However, the trench extended into the dike sufficiently to allow in-situ inspection and obtain samples of the materials forming the body of the dike. The inspection of the excavated trench and the results of the testing of the recovered samples revealed that the dike does not consist of sufficient fines to provide the necessary seepage barrier. Main function of the existing dikes, at the time of construction, was to serve as free board dike rather than water containment dike; therefore, it was not necessary to include properly designed zone of impervious barrier in the dike.

Available Construction Materials

The geotechnical investigations performed revealed that the only construction materials available at the site are shot rock from required excavation and silty sand from borrow within a mile of hauling distance of the project area. Shot rock from required excavation was essentially dirty rockfill with insufficient fines to provide the required impervious barrier. Silty sand from borrow did not contain enough fines to use as impervious fill.

Alternative Impervious Barrier

Due to the lack of naturally occurring impervious materials within reasonable hauling distance, lining the upstream face of the rockfill dike was considered to obtain the required impervious barrier. The lining materials considered are conventional reinforced concrete, fibrous shotcrete and fabriform. All three alternative lining methods were included in the bidding documents with the provision that the contractors can bid on only one lining alternative. With the exception of two all bidders chose fabriform lining alternative to line the canal. The total area of lining is about 30,000 sq yd and the bid price for fabriform lining was lower than for other alternatives and thus fabriform lining was selected.

Fabriform Lining

Fabriform lining consists of a double-layer fabric woven of textured nylon in a tough, multifilament warp for optimum strength, stability, adhesion, and filtering characteristics. The two fabric layers are 20x20 count per inch, 840 denier nylon, of which 50% by weight is producer bulked continuous multifilament tire cord nylon joined in a mat configuration. After being placed on the slope to be protected this fabric envelope is filled by pumping into it a highly fluid sand-cement grout mortar. The upper edge of the fabriform panel is placed in an anchor trench to prevent undercutting by ground water runoff while the bottom is anchored in a trench to keep it in place against the flowing water current. Because of its flexibility, the lining fabric can be laid on uniform slope of the new dikes as well as non-uniform slope of the existing dikes. The grout consists of a mix of portland cement, fine aggregate and water so proportioned and mixed to provide a pumpable slurry with a 28 day compressive strength of 2000 psi. Gradation of the fine aggregates is equivalent to that for ASTM C33 fine aggregates. The fabriform is usually used for erosion protection along slopes and shore lines. Depending on the application it is used in thickness varying from 4 to 24 inches with and without filter points. Varying cross section is used for erosion protection while uniform cross section is used where low permeability and low hydraulic friction is required. Uniform cross section is formed with a double layer woven fabric, joined together by spacer cords on closely

spaced centers. Relief of hydrostatic uplift pressure, if required, can be provided by inserting plastic weep tubes through the mat at specified centers. The rock fill for dike at Summer Falls with small amount of fines was not expected to cause any uplift under the lining. Therefore, a 4 inch thick uniform cross section fabriform without filter point was selected to line the dikes.

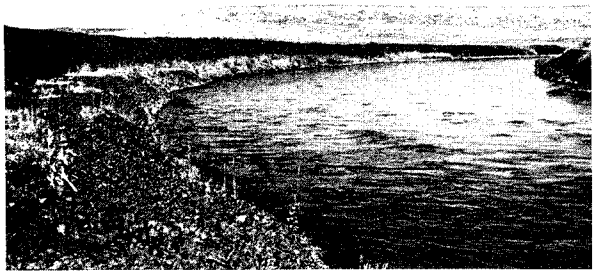

a) Existing Dike

b) Construction of New Dike

Figure 2. Photos of Existing and New Dikes

Installation of Fabriform Lining

Surface Preparation: The slope of the existing dikes varied from 1.5H:1V to 3H:1V and had vegetative growth and debris. The sloping surface and berms/benches of the existing dikes were cleared of vegetation and debris and all erratic surfaces were smoothened by excavation or placing rockfill, as required. Soft and loose rockfill was compacted adequately to provide a stable base for lining. The new dikes were constructed to neat lines and grades at a slope of 1.5H:1V on both upstream and downstream. Large boulders, rock particles with protruding sharp edges and loose rocks were removed and replaced with compacted smaller size rock particles. Photos of typical existing dike and construction of new dikes are shown in Figure 2.

Installation of Nylon Fabric Mat: After preparing the surface receiving the lining, the nylon fabric mat was spread without wrinkles and positioned at its design location. Individual mill width panels were cut to suit the required geometry and the two layers of fabric were separately joined edge to edge by heavy duty nylon thread, double stitched to obtain a minimum tensile strength of 100 psi. The fabric was securely attached to the wing walls of the intake and check structures by stainless steel strips bolted to the wall. At toe and crest of the dike a trench was excavated, the fabric was laid in the trench and anchored by concrete. Typical anchor and joint details are shown in Figure 3.

Pumping Grout: Sand, cement and water were measured and fed into the mixer to produce a grout mix having a pumpable consistency. The grout mix was introduced into the space between the layers of fabric and injected in such away that excess pressure on the fabric envelope is avoided. The mix had a water-cement ratio in the range of 0.70 to 0.75. Excess mixing water was squeezed out through the water permeable fabric causing a pronounced reduction in the water-cement ratio. The grout was pumped from the bottom up through each panel. Normally, panels were joined before grout injection; however, where this was not possible the panels were overlapped for a minimum length of two feet. In no case a butt joint of panels was allowed. Holes in the fabric left by the removal of grout hose was temporarily closed by placing a piece of burlap until the mortar set to attain a surface firm to hand pressure. No foot traffic on the grout filled fabriform was allowed for a minimum of one hour after pumping to reduce indentation on the fabriform surface. Photos of installed fabriform lining filled with grout on existing and new dikes are shown in Figure 4.

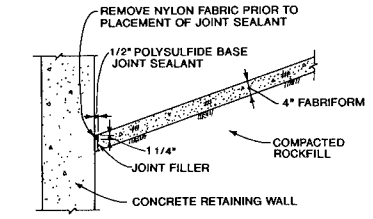

a) DETAIL AT JOINT OF LINING AND CONCRETE WALL

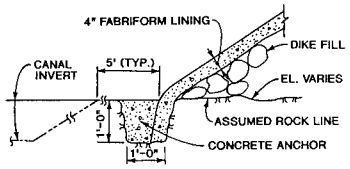

b) TOE ANCHOR DETAIL

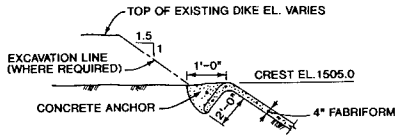

c) CREST ANCHOR DETAIL

FIGURE 3. JOINT ANCHOR DETAILS

Compressive Strength: For each batch of grout mix at least four samples of 2"x2" cubes were cast and tested for 7 day and 28 day strength, as required by the bidding documents. Seven day strength ranged from about 600 to 1400 psi with an average of about 1000 psi; 28 day strength ranged from 2000 to about 4000 psi with an average of about 3200 psi.

Performance

The installation of fabriform lining was completed in early 1984 and was tested in October, the end of the irrigation season. During this testing, some seepage was noted occurring in one concentrated area on the downstream of the left dike. After this testing the canal was shut off for the yearly non-irrigation season, the canal was practically drained and the lining

a) Existing Dike

b) New Dike

Figure 4. View of Installed Fabriform Lining

was inspected. At about middle height of the dike in the vicinity of the seepage a small depression and crack for a length of about five feet in the lining was noted. Upon further inspection and evaluation it was confirmed that the construction of lining was stopped temporarily in this area and apparently the joint treatment performed was not adequate. The crack and depression was repaired by filling the crack with mortar and covering the area with fibrous shotcrete. In 1985, the project was put into service and

since then no further seepage occurred and the performance of the lining has been excellent. An overall view of the completed project with the extent of the fabriform lining is shown in Figure 5.

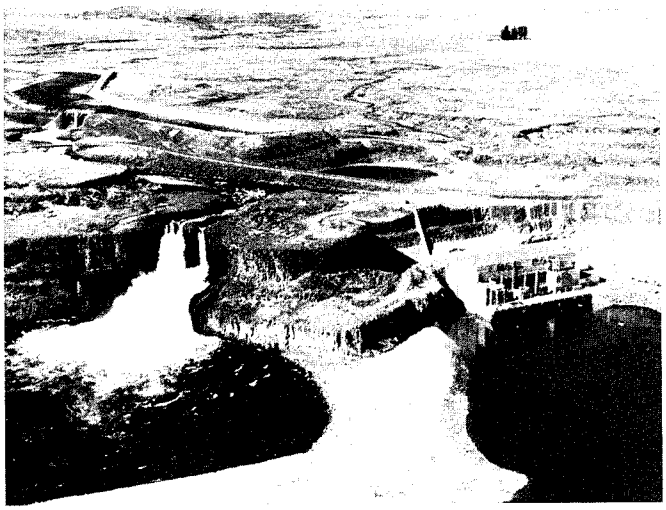

Figure 5. Photo of Project Overview

Conclusion

The Summer Falls project, completed in 1985, has been operating successfully. No significant seepage from the canal is occurring and thus far required no major maintenance expenditure. Thus, the 4" Fabriform Unimat lining has been effective in serving as seepage barrier under nominal head of about 30 ft. This successful experience has demonstrated that the Fabriform can be used to line rockfill dikes in areas, where impervious fill is lacking for use as seepage barrier. During construction careful attention must be paid to treat the construction joints to avoid undesirable seepage; if construction is interrupted, the fabriform panel joints must be properly treated prior to resuming construction.

Drawdown stability of a compacted shale rockfill

Carlos A. Jaramillo[1], David E. Kleiner[1],
Philippe P. Martin[1], Aniruddha Sengupta[1],
Archivok V. Sundaram[1]

Abstract

The unweathered Pottsville shale-sandstone-siltstone (mostly shale) from required excavation is used to construct part of the rockfill of the Upper Reservoir Dam at the Rocky Mountain Project. The following studies were recently performed to support its use.

Compactability. Field and laboratory tests showed that the shale could be placed in lifts up to 36 inches thick and compacted to a dry density of about 140 lb/ft^3 with a smooth drum vibratory compactor. The percentage of fines passing the No. 200 sieve was from 3% to 6% after compaction.

Shear strength. The angle of internal friction of the shale rockfill, based on laboratory triaxial compression tests of samples compacted to the field density, was 40 to 42°.

Analysis of piezometric response to emptying and filling the reservoir. An assessment of pore pressure retention in the shale rockfill during drawdown and filling of the upper reservoir made by a finite element study, and by comparison with instrumentation data from Bath County Project. Calculated pore pressure retention in the shale rockfill confirmed the design piezometric assumption made for the drawdown stability analyses.

Embankment stability analysis. Drawdown stability of sections located at Sta. 30+00, 90+00, and 115+00 was evaluated using shear strength and piezometric line assumptions based on results of this study.

1 Harza Engineering Company, Sears Tower, 233 South Wacker Drive, Chicago, IL 60606-6392.

The results supported the decision to place the shale rockfill in 36 inch lifts compacted by four passes of 10 ton vibratory roller. The study indicated that an average of 5% fines content would not have a detrimental effect on the stability of the rockfill.

1.0 General

The Rocky Mountain Project is a 850 Mw pumped storage development currently under construction in NW Georgia. The upper reservoir for the project will be formed by a 12,800 ft long closed dam with an average height of 80 ft. The unweathered Pottsville shale from the required upper reservoir excavation is used to construct part of the rockfill (Zone 3) of the Upper Reservoir Dam.

2.0 Field and laboratory testing

Compaction of the unweathered shale was investigated by a testfill performed during the design stage, and by a testfill carried out during the initial phases of construction. The design stage testfill evaluated the effectiveness of heavy construction equipment in breaking down the material and increasing its density. The dry densities obtained in this testfill ranged from 124 lb/ft^3 to 130 lb/ft^3 when the material was compacted in 12 in. thick lifts using 4 passes of compaction equipment. The construction stage testfill evaluated the effect of lift thickness and number of equipment passes on gradation, density and percolation.

Density, gradation, and percolation tests were performed on the initial volume of Zone 3 material placed in the embankment. The initial volume placed was constructed as a testfill, and divided in three pads. Pad 1 consisted of three 24 in. lifts each compacted by four passes of a Cat CS 533 vibratory smooth drum roller. Pad 2 consisted of two 36 in. lifts each compacted by construction traffic. Pad 3 consisted of two 30 in. lifts each compacted by two passes of a Cat CS 533 vibratory smooth drum roller.

The field tests were performed by excavating holes approximately 2 ft. deep and 3 ft. diameter within the compacted lift. The dry densities varied in the range 141 lb/ft^3 to 149 lb/ft^3, with one test showing 124 lb/ft^3. Moisture of the material varied between 1.5% to 5.4%. The gradation tests showed that the amount of fines passing the #200 sieve varied from 3% to 6%, with an average of 4.2%. The percolation tests found values ranging from 0.2×10^{-1} cm/s to 4.4×10^{-1} cm/s.

Laboratory testing included Atterberg limits, slake durability, permeability, and multistage triaxial testing of six in. diameter specimens with -¾, in. and -1 ½ in. maximum particle sizes. The liquid limit (LL) was 22, and the plasticity index (PI) was 3. Slake durability for the first cycle was 83% and

for the second cycle was 79%. The triaxial compression tests consisted of multi-stage tests at confining pressures of 1 t/ft^2 and 3 t/ft^2, and 3 t/ft^2 and 6 t/ft^2. The gradation of the material used to prepare the triaxial specimens modelled the results from field gradations, maintaining constant the percentage passing the #4 sieve. The specimens were compacted to the desired density at 7% moisture content in a 6 in. by 12 in. mold. The testing densities were selected based on field data. The first two series of specimens were compacted to a dry density of 125 lb/ft^3 according to the results available when the testing program started. Subsequent field density tests showed a higher density, which was modelled by the last specimen. The results of the triaxial test are presented in Table 1.

3.0 Evaluation of the characteristics of the unweathered shale

Petrographic and x-ray diffraction analyses of samples of upper Pottsville massive and thin to medium bedded shales indicate that the feldspar and quartz particles are silt size and, in the massive shale, are disseminated in a clay matrix, while in the bedded shales, these minerals occur as thin lenses. The results are shown in Table 2.

No montmorillonite, which could lead to swelling and/or dispersivity, or pyrite, which accelerates the weathering process, were observed (Shamburger, et al., 1975; Oakland, Lodell, 1982).

The horizontal permeability of the unweathered shale rockfill is approximated by the values measured in the field percolation tests (10^{-1} to 10^{-2} cm/s). The vertical permeability of the rockfill at the lift surface, controlled by the fines segregated from the rockfill and concentrated on top of each lift, may be in the order of 10^{-2} to 10^{-3} cm/s.

Weathering of the Pottsville shale was studied following several approaches including small scale and short term laboratory tests and large scale multi-year tests such as a testfill constructed in 1978, which was exposed to wet-dry cycles for over ten years. Slake index tests show that the shale could break down after saturation, but there was no dispersion of fines. Slake durability tests indicate that the shale is of medium durability. Accelerated weathering tests of moderately weathered shale consisting of cycles of drying and wetting of samples subjected to a constant axial load, do not indicate a loss of shear strength nor breakdown of the material into fines. Probably the most representative test is the long term exposure of the testfill constructed in 1978, which showed breakdown of the first few inches of material, but intact material deeper in its body. Generally, all the tests performed to evaluate the weathering of the Pottsville shale involved drying (oven drying for laboratory tests) and wetting of the samples, while the conditions in the embankment will involve only change in saturation, which is much less demanding of the material.

Table 1

Laboratory testing results

		Maximum particle size		
		-¾ in.	-1½ in.	
Dry unit weight (lb/ft^3)		125	125	140
Void ratio		0.348	0.348	0.203
Permeability (cm/s) Before consolidation		3.0×10^{-4}	1.8×10^{-4}	1.5×10^{-4}
After consolidation	1 t/ft^2	2.4×10^{-4}	1.2×10^{-4}	1.2×10^{-4}
	3 t/ft^2	2.0×10^{-4}	1.2×10^{-4}	
Time to 100% primary consolidation (min)				
	1 t/ft^2	2.0	2.2	3.7
	3 t/ft^2	4.0	2.2	10.8
Effective stress parameters				
	ϕ' (°)	40.1	39.9	42.6
	c' (lb/ft^2)	0	0	0

Table 2

Mineral composition of Pottsville shale

	Mineral composition (%)				
	Illite	Kaolinite	Chlorite	Quartz	Feldspar
Massive shale	45	33	10	10	2
Thin to medium bedded shale	35	26	8	25	6

4.0 Modelling of piezometric response to emptying and filling the reservoir

The study consisted of assessing piezometric response governed by both permeability (water retention) and compressibility (load transfer). The computer program GEFDYN was selected to perform the analysis: it utilizes a coupled fluid/solid non-linear soil model working in effective stresses and predicting stresses, deformations and pore pressures. The parameters of the soil model are customary engineering properties and their values were selected on the basis of experimental laboratory data when available or from

the literature. The results of the finite element analysis in terms of pore pressures were compared to the assumptions made in the limit equilibrium analyses.

The selected soil model has three components: mechanical, hydraulic and coupling through consolidation. The mechanical model selected for this analysis is the Drucker-Prager model. It is a relatively simple model, whose behavior remains linear elastic inside the yield surface. The model is defined by the following parameters: E, Young's modulus; ν, Poisson's ratio; ϕ, friction angle; c, cohesion intercept; γ_d, dry unit weight; γ_s, saturated unit weight; e_o, initial void ratio.

The hydraulic model obeys Darcy's law generalized to a volume element of soil. The hydraulic behavior of the materials during drawdown and filling of the Upper Reservoir is modeled by specifying the vertical and horizontal permeabilities for each material. Finally, coupling is implemented with the application of Biot's theory centered on the principles of conservation of mass and effective stresses.

Triaxial CU test results were used to calculate the parameters for the clay core and blanket material, and unweathered shale rockfill. The value of Young's modulus of the clay was found to vary between 2800 psi and 7000 psi, a range of values consistent with those found in the literature for hard clay and sandy clay. Poisson's ratio of the clay was assumed to be 0.3. The elastic modulus of the unweathered shale rockfill was evaluated at 9700 psi. A Poisson's ratio of 0.25 was assumed for this material. Values of Young's modulus and Poisson's ratio for the sandstone shell and the foundation material were assumed based on published data in the literature. The parameters used in the analysis are shown in Table 3.

A cross-section through Station 90+00 of the Upper Reservoir Dam was used for this analysis. The same section was used in the slope stability (limit equilibrium) analysis of the dam. Five observation points (pressure head points A, B, C, D & E) were selected to monitor the pore water pressure response in the dam. The locations of these points are shown in Figure 1.

Internal drainage provided by the downstream filter isolates the downstream shell from the hydraulic variations caused by drawdown and reservoir filling. Therefore the downstream shell was not included in the model. The downstream face of the core was assumed to be on vertical rollers in the finite element analysis.

The sandstone zone beneath the shale foundation being 100 times less pervious than the shale could be considered as an impervious zone. In the finite element model, the boundary between shale and sandstone founda-

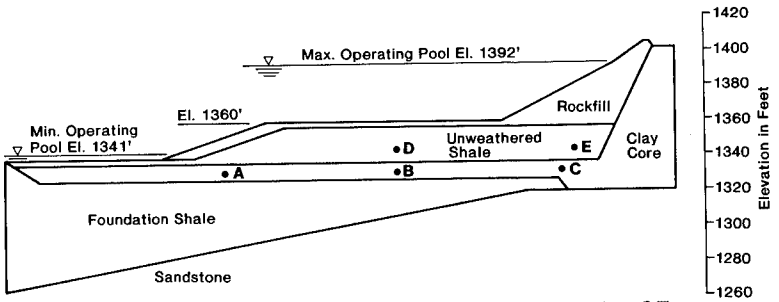

FIGURE 1. DAM CROSS SECTION AND LOCATION OF PRESSURE HEAD POINTS.

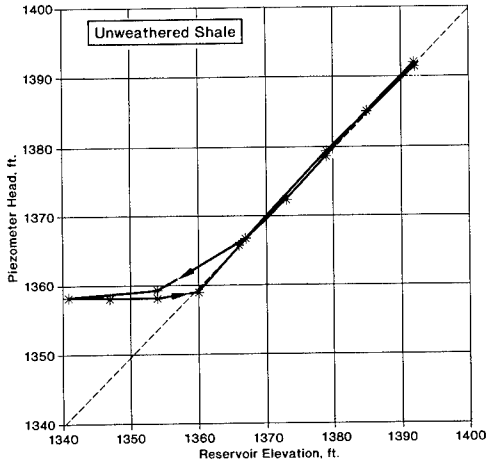

FIGURE 2. PREDICTED RESPONSE AT PRESSURE HEAD POINT D.

Table 3

Material parameters for finite element analysis

	Core and blanket	Sandstone rockfill	Shale rockfill	Shale foundation
Young's modulus, E (lb/in^2)	4200	13900	9700	208000
Poisson's ratio, ν	0.3	0.25	0.25	0.2
Effective stress parameters				
ϕ' (°)	30	40	35	45
c' (lb/ft^2)	0	0	0	0
Dry unit weight (lb/ft^3)	100	120	140	160
Saturated unit weight (lb/ft^3)	125	135	145	160
Void ratio, e_o	0.7	0.4	0.21	0.06
Horizontal permeability, k_h	$5x10^{-7}$	1	$2x10^{-3}$	$1x10^{-4}$
Vertical permeability, k_v	$5x10^{-7}$	1	$2x10^{-4}$	$1x10^{-5}$

tion was assumed as an impervious (no flow) boundary. Therefore, the sandstone foundation was not discretized.

The construction phase of the dam and the initial filling of the upper reservoir were not modeled. Instead it was assumed in the analysis that the reservoir remained at the maximum operating pool el. of 1392 until a steady state seepage condition prevailed within the dam. Drawdown of the pool started after a steady state condition was reached. It was assumed that drawdown from el. 1392 to el. 1341 would occur in 8 hours and filling from el. 1341 to el. 1392 would take 16 hours. The analysis indicated that it would take 5 cycles of drawdown and filling of the reservoir before a pseudo- steady state could be reached within the embankment.

Figures 2 and 3 show the pore pressure responses at piezometer points D and E as predicted by the numerical model during rapid drawdown and filling. The figures indicate that the unweathered shale rockfill zone within the upstream berm retained the pore water under hydrostatic condition when the pool elevation was below the top of the berm. When the reservoir level was above the top of the upstream berm, the predicted heads at points D and E followed the fluctuation of the reservoir elevation. In contrast, the pore pressure predicted at point C, close to the core, was constant for all practical purposes and thus independent of the reservoir level fluctuations; this behavior is indicative of the fact that pressure head varies with the total stress change in the core and blanket material.

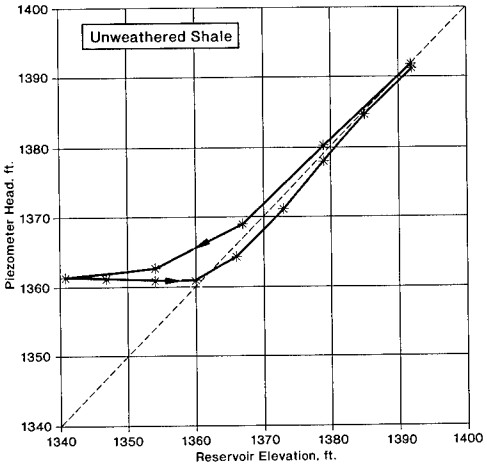

FIGURE 3. PREDICTED RESPONSE AT PRESSURE HEAD POINT E.

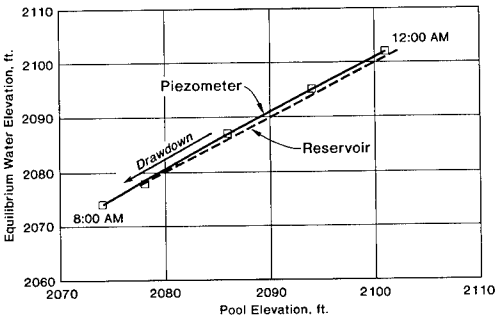

FIGURE 4. BATH COUNTY PIEZOMETER IN UNWEATHERED SANDSTONE AND SILTSTONE.

Figure 4 illustrates the pore pressure response of the rockfill zones to the fluctuating reservoirs at Bath County Project. Piezometers within Zones 2, 3, and 2-3 in the Upper Dam and within Zone 2B in the Lower Dam, constructed of materials similar to Zone 3 at Rocky Mountain and located below the minimum drawdown level, respond immediately; piezometric pressure is equal to the pressure head of the reservoir. One foot of drawdown of the reservoir results in one foot of water head decrease in the rockfill. Excess pore pressures above the level of the reservoir do not occur, confirming the calculated piezometric response.

5.0 Stability Analysis

The stability analyses were performed using Spencer's method (Spencer, 1967), as implemented in the program UTEXAS2 (Edris and Wright, 1987).

Three cross sections typical of the dam, located at approximately Sta. 30+00, 90+00 and 115+00, were selected for the analyses. The most critical loading case for a pumped storage dam is rapid drawdown, and this was the only loading case considered during the re-evaluation of the embankment stability.

The shear strength parameters used were effective stress friction angle and cohesion derived from CU triaxial compression tests. The piezometric lines used for the analyses were selected considering the compressibility of Zone 1 material and the drainage characteristics of the other materials, particularly Zone 3. Three different piezometric lines were used for Zone 3. The first piezometric line was based on the assumptions that the material maintained hydrostatic pore pressures to the top of the zone. The second piezometric line used basically assumed that the unweathered shale rockfill behaved like a soil and retained excess pore pressures to the surface of the embankment. The third piezometric line was located half way between the two other cases.

6.0 Results and Conclusions

The stability analyses confirmed the stability of the dam, as the calculated factor of safety exceeds 1.5 for the design pore pressure retention assumption, and the design shear strength parameters for Zone 3. The calculated factors of safety are also adequate for the conservative case with 50% increase in pore pressure retention in Zone 3.

The data gathered from field and laboratory testing on the unweathered Pottsville shale indicated that the assumptions used for design were conservative. The study supports the use of shale placed in 36 in. lifts compacted by four passes of a 10 ton vibratory roller in the upstream shell of the Upper Reservoir Dam, in a pad below the Zone 2 rockfill, and in the

weighting berm above the blanket. The study indicated that an average of 5% fines content would not have a detrimental effect on the stability of the rockfill.

Results of the coupled finite element study, supported by the Bath County response data, confirm the piezometric assumptions made in the design stability analyses. The pore water pressure in the unweathered shale (Zone 3) follows the reservoir level to the top of Zone 3, and then becomes hydrostatic, with the water level at the top of Zone 3.

7.0 References

Edris, E. V., Wright, S. G., 1987, "UTEXAS2 Slope Stability Package " Waterways Experiment Station, U. S. Corps of Engineers, Vicksburg

Spencer, E., 1967, "A Method of Analysis of the Stability of Embankments Assuming Parallel Interslice Forces," Géotechnique, Vol. 17, London.

Oakland, M. W., Lovell, C. W., 1982, "Classification and other Standard Tests for Shale Embankments," Purdue University, Project 84-2.

Shamburger, J. H. et al., 1975, "Design and Construction of Compacted Shale Embankments," FHWA-RD-75-61, Federal Highway Administration, Washington.

GEFDYN @ Copyright Coyne et Bellier - École Centrale Paris/LMSS - EDF/REAL "A Computer Program for **GE**omechanics **F**inite Element **DYN**amics - Two/Three-Dimensional Quasi-Static/ Dynamic Coupled Mechanical - Hydraulics Software for Non Linear Geomaterials Analysis," Version V.3, Paris, France, February 1991.

DESIGN CRITERIA FOR WATER POWER INTAKES

D. G. MURRAY

ABSTRACT

The function of the intake in a hydroelectric development is to divert the water into the penstock, conduit or turbine inlet under controlled conditions. An intake contains racks to prevent the entrance of debris and ice large enough to damage the equipment; a means of control; and a streamlined passageway to gradually accelerate the flow from the headpond to the inlet. Streamlining is required to maximize the discharge capacity while eliminating cavitation and negative pressures and minimizing loss of head.

The author has been involved with the design and construction of a number of small hydro projects. This paper reviews the hydraulic design of intake facilities including setting, alignment, inlet velocities, trashrack design and ice exclusion.

Mr. D. G. Murray is a project director at **CIMA** Engineering Consultants. He may be reached at 3400, boul. du Souvenir, Suite 600, Laval, QC, Canada, H7V 3Z2, (514) 688-4970.

Mr. Murray graduated from the University of Saskatchewan in 1970 with a degree in Civil Engineering. Since receiving his Master's degree in Hydraulic Engineering in 1973, he has worked on the hydraulics of hydropower, irrigation and water supply projects.

General

When developing small hydro installations proper design considerations are necessary in order to maximize intake efficiency from both a hydraulic and economic point-of-view[1]. The economics of small hydro and in particular, low head hydro, do not allow for inferior design. Head losses have to be minimized in order to maximize plant output.

First, the intake structure must be structurally stable under all conditions of operation. Subsequently, the intake structure must satisfy several hydraulic requirements. In meeting the requirements particular emphasis should be placed on optimizing the design of the facility to maximize the hydraulic efficiency as economically as possible.

Forebay

The forebay is the enlarged body of water just above the intake. It may be the pond formed by the diversion dam or it may be an excavated approach channel. If floating ice or debris is anticipated it is recommended to provide a deflecting device preferably at an angle of 30 to 45 degrees to the direction of flow to divert the ice and trash from the intake to the spillway or sluiceway. A typical intake and forebay arrangement are shown on Figure 1.

The alignment of the approach channel should be laid out to take advantage of any natural depressions which will decrease the channel excavation. High velocity with resultant small area and size of channel makes for low first cost but results in high friction loss, decreased head and power output. Since minimum cost can be obtained only at a sacrifice of output and since maximum output can be obtained only at an increase in cost, there is always, for every project, one size which, theoretically, will result in the greatest economy of design. Hence, the theoretical best velocity is determined by the principles of maximum economy.

Two practical considerations influence the choice of velocity. For channels in earth the velocity should not be too high to cause scour or too low to allow plant growth or deposits of silt. In cold climates, open channels should be designed to permit the development of a stable ice cover to minimize the problems associated with frazil or floating ice.

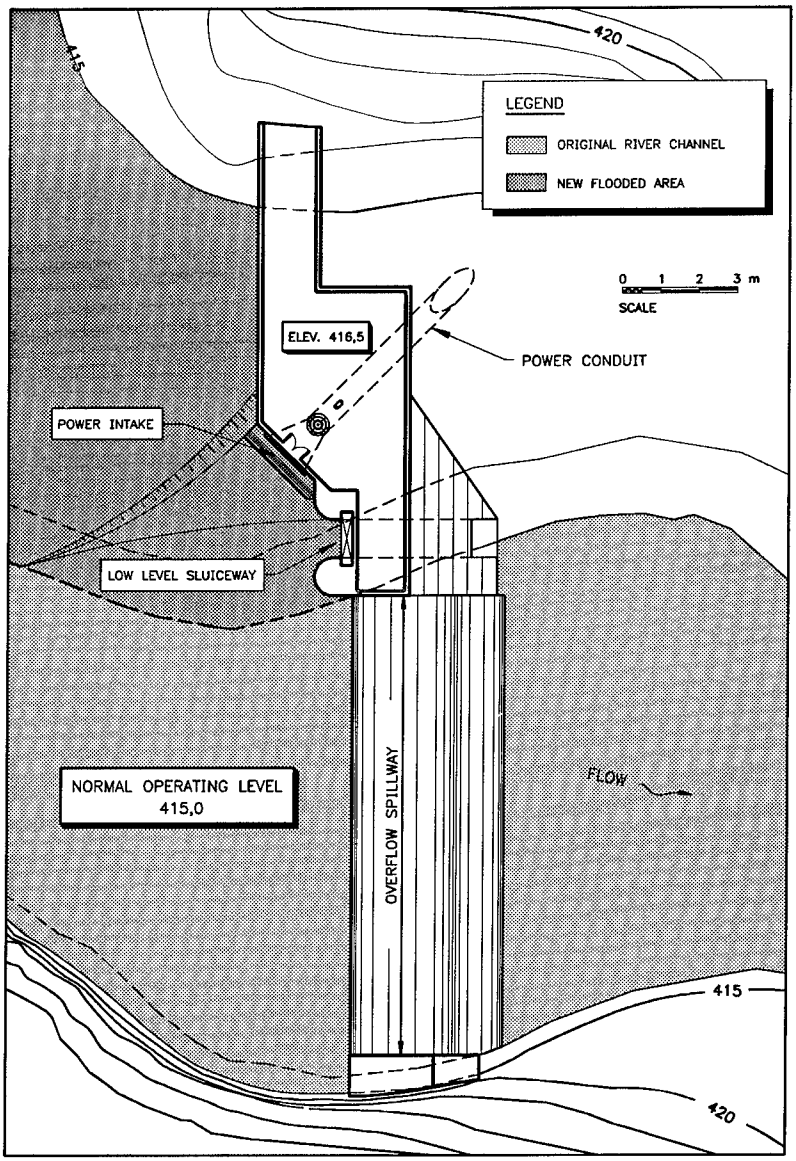

FIGURE 1 PLAN OF UPSTREAM HEADWORKS

Concrete Structure

The concrete structure should provide a smooth transition of flow from the trashracks to the penstock or to the turbine inlet. Abrupt changes in area of the water passageway should be avoided in order to minimize turbulence and consequent power loss. However, a long and gradual entrance curve will require an unnecessary amount of expensive forming. The objective is to design an entrance of minimum length in which positive pressures can be maintained at all flows.

The cost of the intake structure increases with increasing depth of gate sill below water level. For maximum economy, the gate sill should be set as high as possible. On the other hand, with gate sills at shallow depths, there is a danger of vortices forming, which may entrain air, thereby reducing the efficiency of the turbine. The concern then becomes one of establishing the gate sill as high a level as possible for economy, but below the level at which vortices are produced for hydraulic efficiency. Empirical equations[2] for submergence have been derived as a function of velocity and gate height.

A number of factors should be considered when selecting the arrangement of an intake. The intake should be aligned so that the trash and ice tend to float past and not collect at the trashracks. In rivers with considerable bed load, the intake should be arranged so that the bed deposits will not lead to a restriction or blockage of the intake. In such cases, the intake should be arranged so that a spillway or sluiceway in the dam can be operated to sluice as much of the silt deposit as possible.

Trashracks

Trashracks are designed to exclude debris from the intake water. Located upstream of the gates, trashracks should be erected in a slanting position to facilitate easier trash removal.

Spacing of the rack bars are established from a review of the requirements of the turbine equipment and the environmental constraints. From a hydraulic consideration, a wider spacing is more desirable, however, care must be exercised so that whatever debris does pass the racks would not be injurious to the wicket gates or runner blade mechanisms. Attention must be given to fish entrainment in order to minimize or eliminate the passage of fish and other marine life from being entrained through the turbine. It is essential the design of the intake be undertaken in close cooperation with the local fisheries and regulatory agents to minimize the impact on marine life.

The velocity through the net area of the trashrack should be kept within such limits so as not to cause loss of head or to call for larger intake and trashrack cross-sections. For small plants where manual cleaning is resorted to, the velocity in front of the trashrack should be limited to the order of 60-75 cm/s. In either case, velocities should be limited to approximately 90 cm/s.

Depending on the nature of the headpond, the lower range of velocities should be used for natural run-of-river plants where no ponding occurs. Accordingly, when withdrawing flow from a reservoir the higher range of velocities may be used as much of the debris such as leaves would have had a chance to settle out before reaching the intake.

The rack bars are usually 6 to 8 mm thick and approximately 50 mm wide. Bar design including the intermediate supports is a function of the unsupported bar length, the water pressure and the dynamic pressure of the floating material. An unbalanced load due to the partial or total clogging of the racks should also be considered.

In cold climates it is often necessary to adopt special precautions to prevent ice from interfering with the operation of the plant. As far as the design of trashracks are concerned, the entire rack should be set below the minimum operating level of the headpond. In this manner the rack temperature will be the same as the water temperature and will tend to minimize the problems associated with "slush" or "frazil" ice. It is desirable to permit and maintain the formation of an ice cover on the head pond. If a stable ice cover is provided, trouble from ice will be practically eliminated.

At small plants, hand raking is generally practiced. On most streams it is necessary to do very little raking during the greater part of the year. However, in the spring during the high runoff period and in the fall, when the streams carry lots of leaves, intensive raking may be required. Streams vary greatly in the amount of debris carried. Consequently, consideration should be given in the location and setting of the intake. As more submergence is provided, less raking will be required.

If a great deal of raking is required, it pays to install a mechanical raker. Such a machine can be automated to reduce labour costs. In the event a mechanical raker is necessary, a deck of sufficient width must be provided to support the raker as well as to provide space to collect and hold the debris. Whether a raker is provided initially or not it is wise to assess its potential requirement and design the intake accordingly. In that way a raker can be provided at some subsequent date with minimum alterations to the intake structure.

Gates

Gates are provided to control or regulate the flow of water through the intake. Numerous forms of control may be considered such as bulkhead gates, stoplogs, intake gates or valves. Bulkhead gates and stoplogs are required in order to dewater the downstream intake area for maintenance purposes. Intake gates and valves are required to dewater the water conduit and to serve as the second line of defense to shut off flow to the turbine.

The velocity through the gates may vary between wide limits. However, as the higher velocities result in lower gate cost but greater eddy loss and less power output, there is usually one size of gate that will make for the greatest economy of design.

Bulkhead gates and stoplogs are only installed and removed in still water whereas intake gates and valves should be designed to close against the maximum turbine flow. Types of intake gates include the sliding type that slide directly on their seats or the wheeled type where the pressure is taken by wheels attached to the gate. Should a valve be considered, it should be of the butterfly shut-off valve arrangement. Valves are generally located immediately upstream of the turbine inlet at the downstream end of the conduit whereas intake gates are located at the main intake structure at the upstream end of the conduit.

Each intake gate should be provided with a hoist or gantry crane arrangement. The gate or valve should be designed to close under its own weight or with the aid of a counterweight in the event of a loss of power.

An air vent is required downstream of the intake gate to vent the conduit or to prevent collapsing of the penstock. The size of the vent should be based on the area required to pass the full turbine flow at a maximum air velocity not exceeding 25 m/s. On large diameter penstocks the air vent may be designed to admit maintenance personnel and materials to the conduit.

Losses in Intakes

Intake losses include entrance loss, trashrack loss and head gate loss. The entrance loss is due to change in direction of flow and due to the sudden contraction of area at the inlet. On intakes with a square edged entrance or a flush headwall the entrance loss coefficient is in the order of 0.5 to 0.6. For a bevelled lip inlet, one provided with a 45° flare, the loss coefficient is reduced to approximately 0.20 to 0.25. This loss could be reduced to 0.05 by using a streamlined bellmouth inlet. However, a well designed inlet with flat surfaces approximating the streamlined shape of the bellmouth inlet as shown on Figure 2, is an excellent compromise at simplifying the complicated construction associated with the bellmouth inlet while still providing good hydraulic conditions. A loss coefficient of 0.10 is readily attainable for such a design.

Trashrack losses are a function of the cross-section, thickness and spacing of the bars and of the velocity of flow through the contracted openings. Numerous empirical formulae are available in relevant text books. As discussed previously, the velocity through the net area of the trashracks should be kept as low as practicable.

Additional losses at the intake occur at the gate slots as a result of turbulence and eddy loss as the flow passes through the gate area. Typical values of gate loss coefficient range between 0.10 and 0.15. Since gates are essential to the satisfactory operation of the intake and since gates for low head intakes are generally of a standard design little can be effected to reduce the intake loss through the gate area. The best that can be done is to provide smooth transitions through the intake area and to ensure that no surface irregularities result from the construction works.

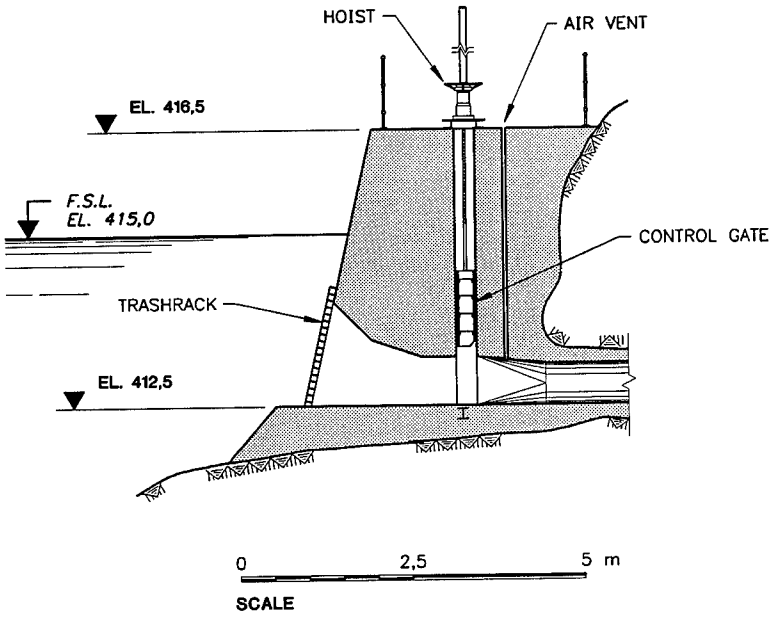

FIGURE 2

POWER INTAKE CROSS-SECTION

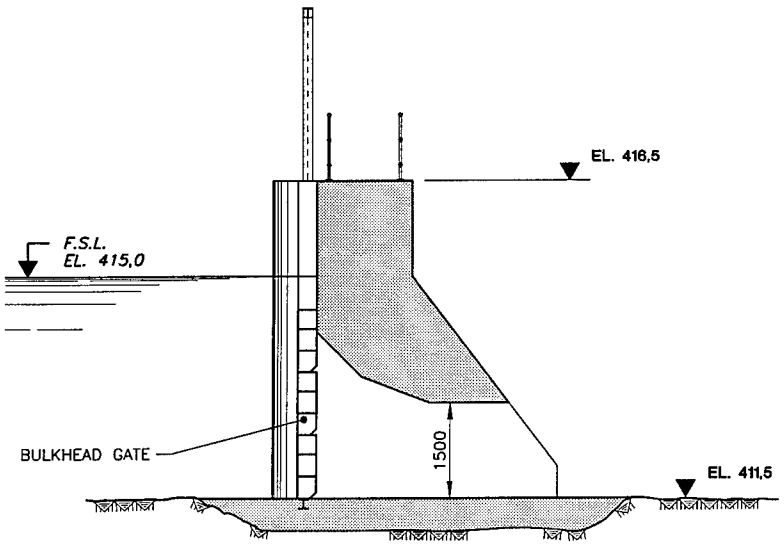

FIGURE 3

SLUICEWAY CROSS-SECTION

Silt Traps and Excluders

On heavy silt laden streams it is necessary to provide special devices such as silt traps and silt excluders to control and trap excessive silt loads in the water. During normal operations the silt will progressively build up toward the intake. Periodically it may be necessary to sluice the accumulated deposits from in front of the intake. This can be accomplished provided the sluiceway is located immediately adjacent to the power intake and that the discharge capacity of the sluiceway is at least twice the capacity of the intake. The approach and sill of the sluiceway should be set approximately one metre below the sill of the power intake to provide a dead storage area for the silt. A typical section through a sluiceway is shown on Figure 3. During flood periods the sluiceway should be operated at full capacity to maintain a clear channel in front of the intake.

Summary

A properly designed intake will continue to reap rewards for the life of the project. Particularly in the development of low head hydro, where head is at a premium, a concerted effort to design and construct an economic hydraulically efficient intake is well worth the time and effort.

References

1. D. G. Murray and J. L. Gordon, "Intake Design: Concepts to Minimize Cost and Maximize Output", Hydro Review, Spring 1985.

2. J. L. Gordon, "Vortices at Intakes", Water Power & Dam Construction, April 1970.

Energy Dissipation in stepped spillway

Hsien-Ter Chou[1]

Abstract

A well-designed stepped spillway dissipates sufficient energy of the overlying cascade flow, and consequently reduces the size of the downstream energy dissipator. Flows over stepped spillways are categorized into two types, nappe flow at small discharges and skimming flow at large discharges (Essery and Horner, 1971; Sorensen, 1985; Peyras et al, 1992). In this paper, the flow and energy dissipation over stepped spillways are investigated by employing theoretical analysis. The friction coefficients and energy dissipation are determined based on given conditions such as spillway slope, step height, step numbers and incoming discharge.

The onset of skimming flows occurs when the critical depth is about the same as the step height ($h = 1.01\ y_c$), which is close to the criteria based on experimental analysis (Rajaratnam, 1990).

Introduction

According to the experimental observations (Essery and Horner, 1971; Sorensen, 1985; Peyras et al, 1992), the flow patterns in a stepped spillway can be divided into the following two regimes: 1) nappe flow at small discharges, and 2) skimming flow at large flow rates (Figure 1). In the nappe flow, the water cascades over each step as a sequence of falling jets. The energy dissipation is mainly due to jet mixing on the step and possible hydraulic jump thereafter. In the skimming flow, the water flows downward

[1] Associate Professor, Department of civil Engineering, National Central University, Chung-Li, Taiwan 32054, R.O.C.

as a quasi-smooth stream overlying the recirculation zone between step tips. Part of the energy is substracted from the main stream to sustain the triangular cavity flow.

Although stepped spillways have been built for small and moderate dams in many countries (Sorensen 1985; Peyras et al 1992), their design rules are not available because the complex overlying flows are still not quantified. In this study, the stepped spillway is assumed to be wide, with a constant slope, and be composed of m identical steps. The energy dissipation in both nappe flow and skimming flow regimes will be explored in the following sections.

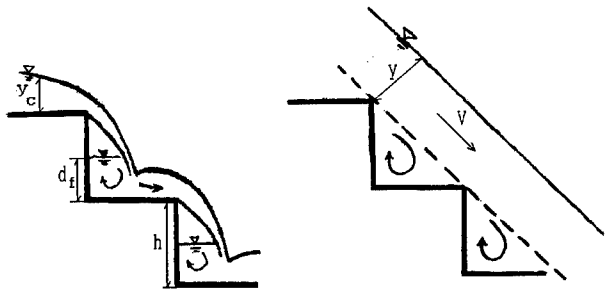

a) Nappe Flow Regime b)Skimming Flow Regime

Figure 1 Flow Patterns over Stepped Spillways

Nappe Flow Regime

In the regime of nappe flows, the flow behavior over a single step is close to that of a free overfall (Figure 1a) . The classical paper of Moore (1943) provides excellent analysis and experimental results in this aspect. After dropping down from the step edge, the water jet hits the lower step surface then flows horizontally. If the air entrainment is neglected, the flow rate per unit width, q, is noted as

$$q=V_c y_c=V_1 y_1 \qquad (1)$$

where y_c = critical water depth ahead of the step edge, V_c = critical velocity, y_1 = the water depth right after the

deflection, V_1 = average velocity at y_1 section. The specific energy at the y_1 section, E_1, can be expressed as

$$\frac{E_1}{y_c}=\frac{y_1}{y_c}+\frac{1}{2}\left(\frac{y_c}{y_1}\right)^2 \qquad (2)$$

White (1943), who in the discussion of the preceding reference (Moore, 1943), derived the velocity at the y_1 section by employing the momentum equation as follows

$$\frac{V_1}{V_c}=\frac{1.06+\sqrt{\frac{h}{y_c}+\frac{3}{2}}}{\sqrt{2}} \qquad (3)$$

From eqs. (2) and (3), the specific energy at y_1 section can be written as

$$\frac{E_1}{y_c}=\frac{\sqrt{2}}{1.06+\sqrt{\frac{h}{y_c}+\frac{3}{2}}}+\frac{\left(1.06+\sqrt{\frac{h}{y_c}+\frac{3}{2}}\right)^2}{4} \qquad (4)$$

As pointed out by Moore (1943), eqs. (3) and (4) should be valid only for uniform flows, and for neglecting the hydrostatic pressure effect on the deflection of the jet. Nevertheless, eq. (4) agrees quite well with Moore's experimental data, and is adopted in this study to evaluate the energy loss in the nappe flow regime.

The recirculating water depth behind the falling jet, d_f, can be analyzed by employing the momentum equation again (Moore, 1943),

$$\left(\frac{d_f}{y_c}\right)^2=\left(\frac{y_1}{y_c}\right)^2+2\left(\frac{y_c}{y_1}\right)-3 \qquad (5)$$

Onset Condition for Skimming Flows

The onset of skimming flow can be regarded as the condition when the recirculating zone reaches the maximum value, i.e., $d_f = h$. Combining equations (2),(4) and (5), the following equation is obtained

$$\frac{h}{y_c}=1.01 \qquad (6)$$

Equation (6) states that the flow is in the nappe flow regime if the height of a single step is greater than the critical depth for the given overflow, other wise the skimming flow occurs.

Rajaratnam (1990) analyzed previous experimental data (Sorensen,1985; Essery and Horner, 1971), and concluded that the skimming flow occurs when h/y_c is less than 1.25. It should be noted that the last two cases in Sorensen's C-series data, i.e., C9 and C10 with h/y_c = 1.21 and 1.54, respectively, violate eq. (6), and will not be used for data analysis. As noted by Rajaratnam, these cases may be just in the transition between nappe flow and skimming flow.

Skimming Flow Regime

When the overflow is large enough to keep the flow pattern in the skimming flow regime, it becomes fully developed turbulent flow after the first few steps. Thereafter, the flow pattern is very similar to that of the quasi-smooth flow in large roughness pipe flow (Morris, 1955; Knight and Macdonald,1979), or flows over large ripples in flumes and natural rivers (Vanoni and Hwang, 1967). In addition to the skin friction, some additional energy is required to maintain the recirculating flow between step tips. From the view point of hydraulics, we can divide the total bed shear stress, τ, into two parts, i.e., skin friction part ,τ' , and the form drag part, τ'', (Vanoni and Hwang 1967). The form drag is corresponding to the extra energy loss due to the recirculation flow.

$$\tau=\tau'+\tau''=\gamma R\sin\theta \qquad (7)$$

with

$$\tau' = \gamma R S' \tag{8}$$

$$\tau'' = \gamma R S'' \tag{9}$$

where γ = the specific weight of water, R = the hydraulic radius, θ = the inclined angle of the spillway, and S' and S" denote the energy slopes for τ' and τ", respectively.

The average velocity, V, relative to the shear velocity, u*, can be represented as

$$\frac{V}{u_*'} = \sqrt{\frac{8}{f'}}, \frac{V}{u_*''} = \sqrt{\frac{8}{f''}} \tag{10}$$

where f' and f" are the friction coefficients for skin friction and form drag, respectively, and

$$u_*' = \sqrt{\frac{\tau'}{\rho}}, u_*'' = \sqrt{\frac{\tau''}{\rho}} \tag{11}$$

where ρ = water density. The calculation of f' is available either from Moody diagram or from the explicit formula for pipe flows (Swamee and Jain, 1976)

$$f' = \frac{0.25}{[\log_{10}(\frac{k_s}{3.7D} + \frac{5.74}{Re^{0.9}})]^2} \tag{12}$$

and for open channels (Chow, 1959; Yen, 1992)

$$f' = \frac{8n_g^2}{R^{1/3}} = \frac{8n^2 \frac{g}{K_n^2}}{R^{1/3}} \tag{13}$$

where k_s = equivalent roughness, D = pipe diameter, Re = Reynolds number, n_g = modified Manning's coefficient (with

a dimension of $L^{1/6}$), n = the traditional Manning's coefficient, g = the gravitational acceleration, K_n = 1 for SI units and K_n = 1.486 for English units (Yen, 1992).

For a wide channel with a normal depth of y, eq. (13) can be rewritten by using the dimensionally homogeneous Manning's formula as

$$f' = \frac{8\left(\frac{n_g}{y_c^{1/6}}\right)^2}{\left(\frac{y}{y_c}\right)^{1/3}} \tag{14}$$

The form drag coefficient , f", for the triangular type of roughness in the fully two-dimensional turbulent flow can be expressed as the functional form of

$$f'' = F_1(h, y, \sin\theta) \tag{15}$$

where θ = the inclined angle of the spillway, h = the step height and y = the normal water depth. In terms of exposure ratio and steepness, the following combination is adopted (Vanoni and Hwang, 1967)

$$f'' = F_2\left(\frac{y}{h\sin\theta\cos^2\theta}\right) \tag{16}$$

Analyzing Sorensen's data (at the Section of Step 42) shows that

$$\frac{1}{\sqrt{f''}} = 1.82\log_{10}\left(\frac{y}{h\sin\theta\cos^2\theta}\right) - 0.30 \tag{17}$$

Since Sorensen's data are for $\theta = 52^\circ$ only, further data will be needed to verify eqs. (16) and (17) for different inclined angles.

For a spillway with a height of H, the upstream total head, H_o, can be assumed to be

$$\frac{H_o}{y_c}=\frac{H}{y_c}+\frac{3}{2} \qquad (18)$$

The energy loss due to both skin friction and form drag in the spillway, dE, can be calculated accordingly,

$$dE=H_o-E_1=(f'+f'')\frac{\frac{H}{\sin\theta}}{4R_h}\frac{V^2}{2g} \qquad (19)$$

or in terms of y_c,

$$\frac{dE}{y_c}=\frac{f'+f''}{8\sin\theta}\frac{H}{y_c}\left(\frac{y_c}{y}\right)^3 \qquad (20)$$

So the specific energy approaching the toe, in the skimming flow regime, can be calculated based on the combination of eqs. (2), (14), (17), (18) and (20).

Energy Dissipation Analysis

The energy loss in the spillway is one of primary concerns for hydraulic engineers. As the energy dissipation increases, the toe velocity decreases. Consequently, the downstream protection structure can be reduced. As an example, Figure 2 illustrates the energy dissipation in several types of spillways with a constant slope of 1 (vertical) on 0.78 (horizontal). Both the specific energy at the toe (horizontal axis) and the height of the spillway (vertical axis) are nondimensionalized with respect to the critical depth of overlying flow rate. Curve F, the upstream total energy (i.e., eq. 18) is plotted as a reference. Different types of spillways are presented, i.e., a smooth spillway with a Manning's n of 0.012 (Curve D) , an free overfall without considering hydraulic jump (Curve E, representing the nappe flow of one single step), and stepped spillways with overlying skimming flows(Curves A, B, C and Sorensen's data).

In the skimming flow regime, the energy dissipation decreases as the step number, m, increases, i.e., smaller recirculating zones require less energy. The smooth

spillway thus is the special case of infinite steps. Sorensen's data exhibits more energy loss than the prediction according to eq. (20), which may be attributed to the air entrainment, and the complex flow pattern near the toe. The upper limit for the skimming flow regime can be found in Figure 2 based on eq. (6) and the relationship of $H = m\ h$. For example, a stepped spillway of 10 steps will be in the skimming flow regime when H/y_c is less then 10 (see Curve A). To apply Figure 2 for the nappe flow regime without considering hydraulic jump, we just simply replace H/y_c with h/y_c in Curve E to find the corresponding E_1/y_c. In other words, the more step numbers dissipates more energy in the nappe flow. However it should be noted that the flow type becomes skimming flow as $h/y_c \leq 1$.

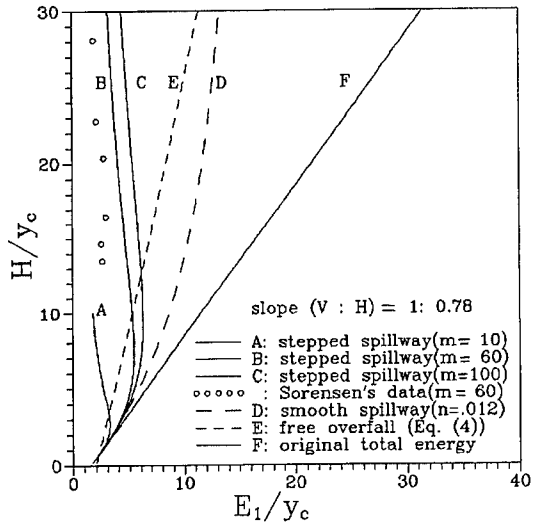

Fig. 2. Energy Loss over Different Types of Spillways

Conclusion

The energy dissipation for both nappe flow and skimming flow over a stepped spillways is analyzed in this study. For a spillway with a constant slope and identical

steps, the energy loss over the spillway decreases with increasing step numbers in skimming flow regime. However, the more step numbers dissipates more energy in the nappe flow regime. The onset of skimming flow is found when the step height is about the same as the critical depth for the overlying flow rate ($h = 1.01\ y_c$) . More data are needed to analyze the form drag coefficient for the large trianglar roughness in the skimming flow.

References

Chow, V.T. (1959). "Open channel hydraulics." McGraw-Hill Book Co. Inc., New York, 680 pp.

Essery, I.T.S., and Horner, M.W. (1971). " The hydraulic design of stepped spillways." Report 33 Constr. Industry Res. and Information Assoc., London, England.

Knight, D.W., and Macdonald, J.A. (1979). "Hydraulic Resistance of Artificial Strip Roughness." J. Hydraulic Engrg., ASCE, Vol. 105, No.6, pp.675-690.

Moore, N.L. (1943) "Energy Loss at the Base of a Free Overfall." Transcations of ASCE, Vol. 108, PP.1343-1392.

Morris, H.M. (1955). "Flow in Rough Conduits. " Transactions of ASCE, Vol. 120, pp.373-410.

Peyras, L., Royet, P., and Degoutte, G. (1992). "Flow and Energy Dissipation over Stepped Gibion Weirs." J. Hydraulic Engrg., ASCE, Vol. 118, No.5, pp.707-717.

Rajaratnam, N. (1990). "Skimming Flow in Stepped Spillways." J. Hydraulic Engrg., ASCE, Vol. 116, No. 4, pp.587-591.

Sorensen, R.M. (1985). "Stepped Spillway Hydraulic Model Investigation." J. Hydraulic Engrg., ASCE, Vol. 111, No.12, pp.1461-1472.

Swamee, P.K. and Jain, A.K. (1976). "Explicit Equations for Pipe-Flow Problems." J. of Hydraulic Engrg., ASCE, Vol. 102, No. 5.,pp 657-664.

Vanoni, V.A. and Hwang, L.S. (1967). "Relation between Bed Forms and Friction in Streams." J. of Hydraulic Engrg., ASCE, Vol. 93; No. 3, pp.121-144.

Yen, B.C. (1992). "Dimensionally Homogeneous Manning's Formula." J. Hydraulic Engrg., ASCE, Vol. 118, NO.9, pp.1326-1332.

HYDRAULIC DESIGN OF A LOW SUBMERGENCE SIPHON INTAKE

by David E. Hibbs[1], Richard L. Voigt, Jr.[2], Mark J. Sundquist[3], John S. Gulliver[4], and Norm Scott[5], Members, ASCE

ABSTRACT

A physical scale model study was conducted to assess the formation of vortices, design appropriate vortex suppression devices, establish the intake submergence depth, and measure the head loss through the intake and the approach velocities at the trash racks for a vertically inverted siphon intake. A vortex suppression device consisting of 12 inch by 2 inch prototype members at one foot on center in both directions, inserted around the intake below the water surface, was found to suppress all surface vortices for intake submergences as low as 3 feet for the design discharge of 1000 cfs.

INTRODUCTION

Physical scale models are a useful design aide for hydraulic engineers. Problematic flow regimes that can not always be predicted by mathematical or computer models can often be identified and corrected through the use of scale models. This study focussed on the formation of vortices, or rotational flow about an axis.

---

[1]Research Assistant, St. Anthony Falls Hydraulic Laboratory, University of Minnesota, Mississippi River at Third Ave. S.E., Minneapolis, MN 55414. (612) 627-4588.

[2]Research Fellow, St. Anthony Falls Hydraulic Laboratory. (612) 627-4601.

[3]President, STS Hydropower Ltd., 111 Pfingsten Road, Northbrook, IL 60062. (708)272-5741.

[4]Associate Professor, St. Anthony Falls Hydraulic Laboratory, (612) 627-4600.

[5]Principal Engineer, STS Hydropower Ltd., 3340 Ranser Road, Lansing, MI 48906.

Intake vortices tend to form near separation zones, where the path of a fluid particle is abruptly forced to change direction. Vortices are undesirable at hydropower intakes since the axial rotation of the fluid tends to decrease the efficiency of the unit. The unsteady character of intake vortices can also cause severe structural vibrations. Finally, strong vortices at the water surface can entrain significant quantities of air, reducing the water discharge capacity of the unit.

This paper discusses the use of a scale model to assess and mitigate the formation of vortices at the intake to a proposed 3 MW hydroelectric facility at the Lake Chesdin reservoir in east-central Virginia. In conjunction with the scale model study, a selective withdrawal computer model was used to estimate the dissolved oxygen concentration (DO) of the water entering the intake. This paper also discusses the results of the selective withdrawal modeling leading to the subsequent modification of the preliminary intake design.

PRELIMINARY INTAKE DESIGN

The preliminary design consisted of a 12 foot diameter vertically inverted siphon intake with a semi-circular lip, proceeding through a five segment elbow and through a contraction to a 10 foot diameter penstock, as shown in Figure 1. The intake centerline would be only 11 feet from the inside face of the dam. A horseshoe shaped floating crib would abut the dam and encompass the intake, as shown in Figure 2. Vertical trash racks suspended from the floating crib would support a solid bottom plate beneath the intake. It was originally

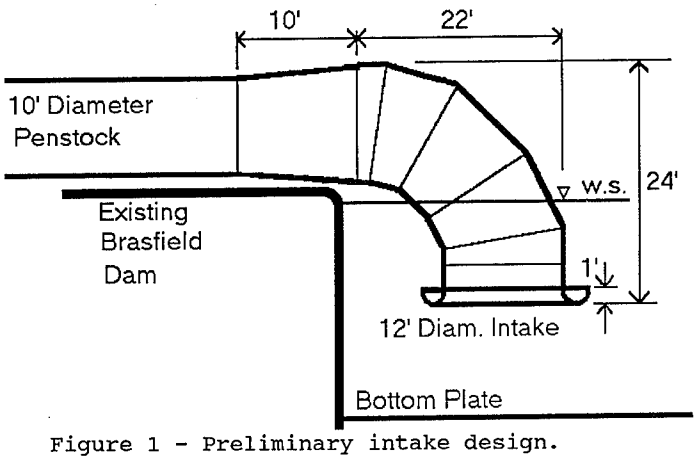

Figure 1 - Preliminary intake design.

estimated the intake should be submerged 8 to 12 feet to decrease the likelihood of surface vortices forming (Gulliver et al.,1986). Using loss coefficients taken from Miller, 1978, the headloss of the preliminary intake design was estimated to be approximately 0.6 feet at the design discharge of 1000 cfs.

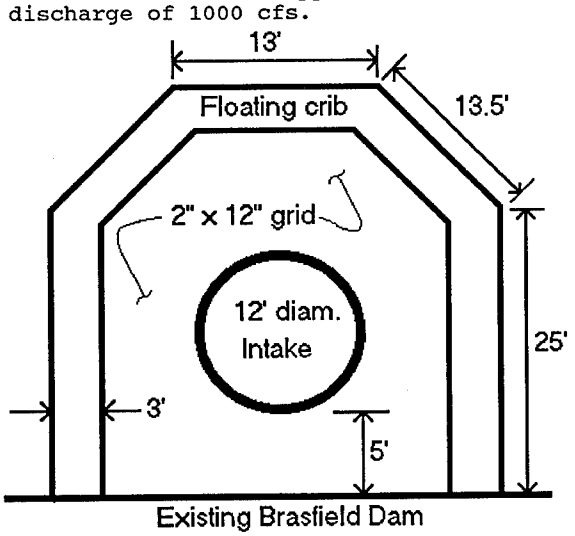

Figure 2 - Floating crib and vortex suppression grid.

MODEL DESIGN

The intake was modelled using Froude scaling:

$$Fr = \frac{V_m}{\sqrt{gL_m}} = \frac{V_p}{\sqrt{gL_p}} \quad \ldots\ldots\ldots\ldots\ldots\ldots\ldots\ldots\ldots\ldots\ldots\ldots\ldots\ldots (1)$$

in which Fr = Froude number; V_m = velocity in the model; V_p = velocity in the prototype; g = acceleration due to gravity; L_m = characteristic length in the model; and L_p = characteristic length in the prototype.

Froude scaling is based on a ratio of inertial and gravitational forces and does not account for the scale differences of other forces such as friction and surface tension. To account for the various scale effects, there are several model design criteria that should be followed. First, to avoid viscous scale effects on intake vortices, the characteristic length dimension (intake diameter) in the model must be greater than 5 inches (Cambell, 1983) and the radial Reynolds number of the model, as defined in

Equation (2), should be greater than 10^5 (Anwar, 1981).

$$Re_r = \frac{Q}{\nu S} \quad \ldots\ldots (2)$$

in which Re_r = radial Reynolds number; Q = discharge; ν = kinematic viscosity; and S = submergence of intake. The model scale was chosen to be 1:24. The 12 foot diameter prototype intake corresponds to a 6 inch diameter model intake, and a prototype submergence of 3 feet yields a model radial Reynolds number of 2.8×10^5.

Second, to avoid approach flow scale effects upon pipe flow swirl, the approach Reynolds number, as defined in Equation (3), should be greater than 2.4×10^4 (Padmanabhan and Hecker, 1984).

$$Re_a = \frac{V_a h}{\nu} \quad \ldots\ldots (3)$$

in which Re_a = approach Reyonlds number; h = depth of the reservoir; V_a = velocity of approach flow; and ν = kinematic viscosity. At a distance of 24 inches in front of the model intake, the approach Reynolds number was found to be 4×10^4 at a discharge of 1000 cfs.

Third, to avoid scale effects due to surface tension, the Weber number of the model, as defined in Equation (4) should be greater than 600 (Cambell, 1983).

$$W = \frac{\rho V_i^2 D}{\sigma} \quad \ldots\ldots (4)$$

in which W = Weber number; D = intake diameter; V_i = intake velocity; ρ = liquid density; σ = surface tension. The Weber number of the model was 630. The 1:24 scale satisfied each scaling criterion. Unless otherwise noted, all dimensions, velocities, and flow rates listed in this paper are those of the prototype.

MODEL CONSTRUCTION

The model intake was fabricated from 6 inch diameter clear acrylic pipe and mounted in a vertically adjustable harness on a 12 foot by 13 foot by 30 inch plywood basin simulating a portion of the reservoir. The walls of the basin near the intake were made of plexiglas to allow underwater viewing of the approach flow. The morphology of the reservoir was simulated by affixing polypropylene sheets to wooden forms on the floor of the test basin shaped from topographic maps of the reservoir.

The siphon discharge was controlled by a valve on the penstock tube and was measured with a V-notch weir and point gauge. For each test run, the inflow to the basin was set slightly higher than the siphon discharge. The excess flow passed over a weir on the side of the test basin, creating a stable and reproducible water surface elevation in the test basin.

DISSOLVED OXYGEN CONSIDERATIONS

Limited field data indicated that the reservoir was stratified during the summer, with a slight thermocline evident at a depth of approximately 10 feet, as shown in Figure 3. Water withdrawn from the upper levels of the reservoir would meet or exceed the local water quality standards, whereas, the water withdrawn from the lower portion of the reservoir would often need some sort of DO augmentation. To determine how shallow of an intake submergence was required to avoid this expensive DO augmentation, the SELECT computer model (Davis et al., 1987) was run for the temperature and DO profile given in Figure 3. The results of the discharge DO versus the depth of withdrawal are summarized in Figure 4 for three specific discharges.

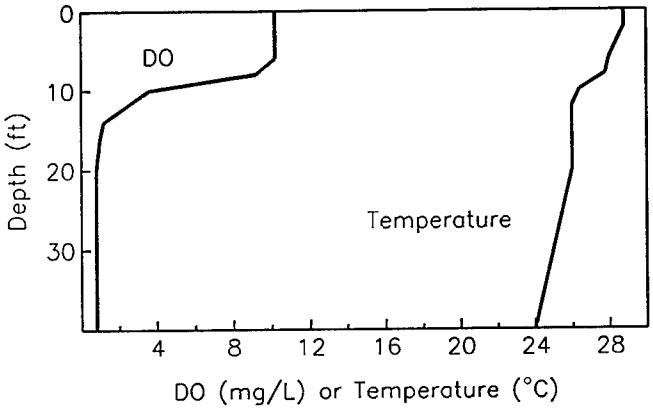

Figure 3 - Lake Chesdin DO and temperature profiles, August, 1991.

The SELECT computations are based on a point sink withdrawal. The depth of withdrawal in the prototype can be approximated as mid-depth between the intake lip and the bottom plate. Thus, if the intake lip was at a depth of 10 feet, and the bottom plate was positioned 8 feet below the intake lip, the depth of withdrawal would be at a depth of (10+18)/2=14 feet.

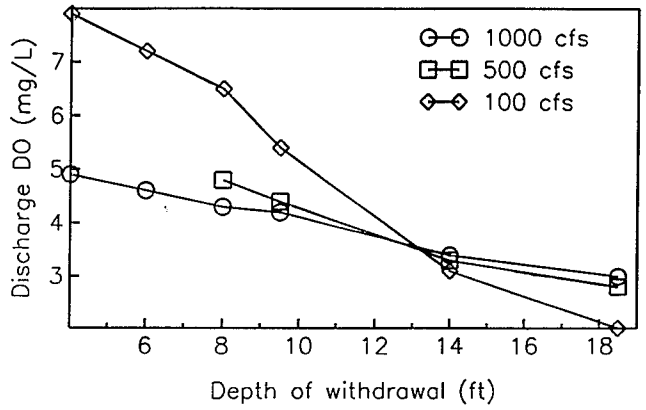

Figure 4 - Results of selective withdrawal modeling

The DO standard for the river downstream of the Lake Chesdin reservoir is 6 mg/L. Figure 4 indicates that for the reservoir conditions shown in Figure 3, this DO standard would not be met at full discharge (1000 cfs). To facilitate the withdrawal of high DO surface water, the intake should be raised to a minimum possible submergence and the vertical separation between the intake lip and the bottom plate should also be minimized.

INTAKE MODIFICATIONS

The low submergence requirement resulting from the SELECT modeling complicated the design. Not only were surface vortices more likely to occur at low intake submergences, but if the intake system was raised 5 to 10 feet, the pressure at the high point of the penstock would approach vapor pressure; it would be increasingly difficult to avoid cavitation and to maintain prime.

Scale model tests conducted with the preliminary intake design indicated that the intake submergence could be substantially reduced from the original estimates of 8 to 12 feet without creating non-mitigatable free surface vortices. To avoid the reduction of pressure in the penstock that would occur if the entire intake system was simply raised several feet, the penstock was held at its original elevation and the intake submergence was decreased by trimming the bottom 7 feet off the intake/bend, as shown in Figure 5. A new semi-circular lip was attached to the intake and the modified design was used for the duration of the study.

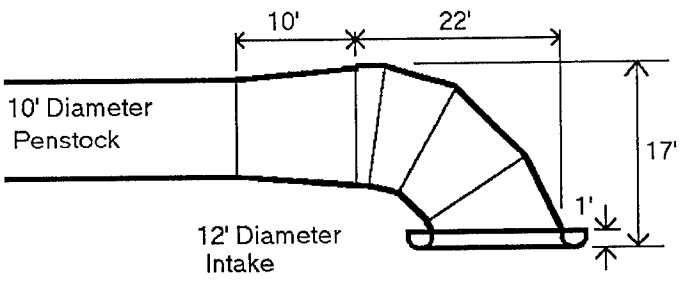

Figure 5 - Modified intake design

ASSESSMENT AND MITIGATION OF SURFACE VORTICES

At the design flow of 1000 cfs, the intake was tested for the formation of surface vortices for submergences of 3, 5, 7, and 9 feet. Powdered dye was sifted onto the water surface to aide in identifying the vortices. Surface vortices were observed at all submergences tested. At submergences of 3, 5, and 7 feet, the vortices were strong enough to entrain air bubbles (Hibbs et al., 1992).

To eliminate the surface vortices, a horizontal grid consisting of 2 inch wide by 12 inch tall members arranged at 12 inches on center in both directions was installed 6 inches below the water surface, inside of the floating crib around the intake, as shown in Figure 2. The grid was found to suppress surface vortices at all intake submergences tested. For DO considerations, an intake submergence of 3 feet was adopted, the minimum required to accommodate the vortex suppression grid and the intake lip.

MINIMIZATION OF FLOOR VORTICES

With the aide of injected dye, floor vortices on the bottom plate were readily visible. A system of trial and error was instigated to minimize the vortices' intensity. The bottom plate was adjusted to provide 7, 8, 9 and 10 feet of clearance between the intake and the bottom plate. Floor vortices were observed at each test depth. However, at clearances of 9 and 10 feet, the intensity of the vortices was diminished to an acceptable level. A clearance of 9 feet was adopted, placing the bottom plate at a depth of 12 feet.

The depth of withdrawal was now established at (3+12)/2=7.5 feet. As can be seen from Figure 4, at 1000 cfs, a depth of 7.5 feet corresponds to a discharge DO of only 4.4 mg/L. The reservoir stratification was quite weak in August 1991 due to reservoir withdrawal practices in place at that time. A stronger stratification would improve the discharge DO concentration, hopefully up to the standard of 6 mg/L.

VELOCITY MEASUREMENTS

For structural and maintenance considerations, the maximum allowable velocity at the trash rack was established at 2 fps. Velocities near the trash rack were measured at seven locations approximately 2 feet outside the crib. At each location a Marsh McBirney electromagnetic current meter was used to measure the normal and parallel components of the horizontal velocity at each of three vertical positions: 4 feet, 8 feet, and 12 feet below the water surface. The approach velocities and angles of approach are shown in Figure 6. The maximum approach velocity measured was 1.16 fps.

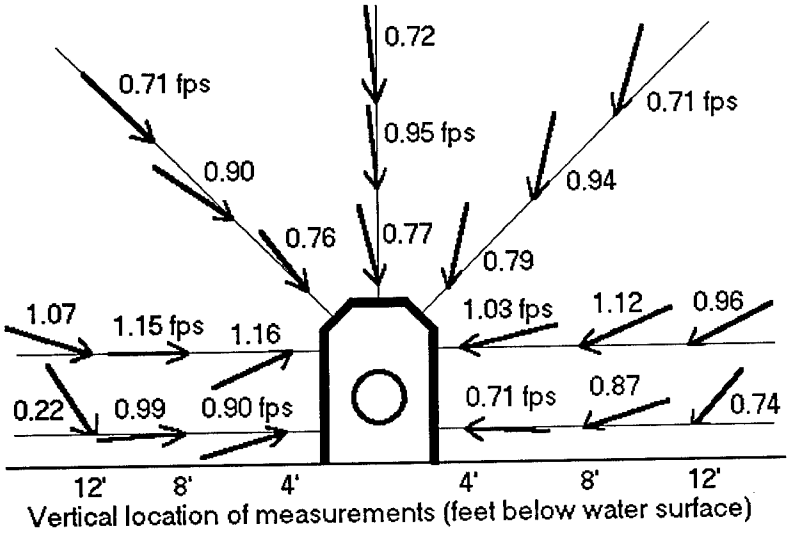

Figure 6 - Approach velocities at 1000 cfs.

HEAD LOSS MEASUREMENTS

The combined head loss through the intake, bend, and constriction was measured using a U-tube manometer filled with miriam yellow indicating fluid. One side of the manometer was connected to the water surface of the test basin away from the intake, where the velocity was negligible. The other side of the manometer was connected to pressure taps on the penstock 4 diameters downstream of the constriction. The head loss through the intake and bend was measured to be 0.7 feet of water.

The headloss across a trashrack was calculated to be 0.05 ft using minor loss coefficients by Idel'chick, 1986, and the velocities shown in Figure 6.

CONCLUSIONS

The model study provided several pieces of information that could not have been obtained from mathematical or computational modeling:

- Without a vortex suppression device in place surface vortices were present at all intake depths tested from 3 feet to 9 feet.
- With a vortex suppression grid consisting of 2 inch x 12 inch members at 12 inches on center just below the water surface inside the floating crib, intake submergence could be reduced to a depth of 3 feet with no surface vortices present.
- Intensities of floor vortices on the bottom plate were minimized with the clearance between plate and intake set at 9 feet or greater.
- The head loss through the intake and bend was measured to be 0.7 feet of water.
- The maximum velocity at the trash rack was measured to be 1.16 ft per second.

ACKNOWLEDGEMENTS

This work was supported by STS Hydropower Ltd. The authors wish to thank Ben Erickson for his help with the data collection and the Saint Anthony Falls Hydraulic Lab shop staff for their timely construction of the model.

APPENDIX I - REFERENCES

Anwar, H.O. (1981). "Measurement of Non-Dimensional Parameters Governing the Onset of Free Surface Vortices: Horizontal and Vertically Inverted Intakes," Report IT 216. Hydraulics Research Station, Wallingford, England.

Cambell, N.J. (1983). "Modeling Free Surface Vortices in

Vertical Pumping Pits," M.S. Thesis, Utah State University, Logan Utah.

Davis, J.E., J.D. Holland, M.L. Schneider, and S.C. Wilhelms (1987). "SELECT: A Numerical One Dimensional Model for Selective Withdrawal," Inst. Rep. E-87-2, Waters Experiments Station, U.S. Army Corps of Engineers, Vicksburg, MS.

Gulliver, J.S., A.J. Rindels, and K.C. Lindblom (1986). "Designing Intakes to Avoid Free-Surface Vortices," International Water Power and Dam Construction, 38(9):24-28.

Hibbs, D. E., R.L. Voigt, Jr., J.S. Gulliver, and B.G. Erickson (1992). "Hydraulic Model Study of the Siphon Intake to the Brasfield Dam Hydroelectric Facility," Project Report No. 327, St. Anthony Falls Hydraulic Laboratory, University of Minnesota, Minneapolis, MN.

Idel'chick, I.E. (1986). Handbook of Hydraulic Resistance, Hemisphere Publishing, Washington D.C.

Miller, D.S. (1978).Internal Flow Systems, British Hydromechanics Research Association, Cranfield, Beford, England.

Padmanabhan, M. and G. E. Hecker (1984). "Scale Effects in Pump Sump Models," Journal of Hydraulic Engineering, Vol. 110(11).

APPENDIX II - NOTATION

The following symbols are used in this paper:

- D = intake diameter
- Fr = Froude number
- g = gravitational acceleration
- h = reservoir depth
- L_m = characteristic length in model
- L_p = characteristic length in prototype
- Q = discharge
- Re_a = approach Reynolds number
- Re_i = intake Reynolds number
- S = intake submergence
- V_a = approach velocity
- V_i = intake velocity
- V_m = velocity in model
- V_p = velocity in prototype
- W = Weber number
- ν = kinematic viscosity
- ρ = fluid density
- σ = surface tension

DESIGN METHODOLOGIES FOR LABYRINTH WEIRS

Frederick Lux III, P.E., M. ASCE[1]

Abstract

The development and hydraulic basis of design methods for calculating the discharge capacity of labyrinth weirs are described. Hydraulic performance predictions using these design methods are compared to actual labyrinth weir test results to evaluate their effectiveness. Based on this assessment, a recommended design method is presented that allows evaluation of the suitability of the labyrinth weir. Various parameters that affect the labyrinth's performance are discussed based upon the performance of hydraulic model tests of actual labyrinth spillways.

Introduction

The labyrinth weir increases the effective crest length by varying the shape of the crest in plan, allowing larger discharges to pass at the same head. The weir is characterized by a broken axis in plan, generally with the same triangular or trapezoidal planform repeated periodically (Figure 1). Therefore, for the same total width, the labyrinth weir presents a larger crest length than a straight weir. Consequently, for the same head and crest shape, the discharge per unit width is substantially increased.

The ability of the labyrinth weir to pass large flows at comparatively low heads has led to its use for canal check and diversion structures, hydropower headwater control structures and, principally, spillways for dams. It is particularly suited for use where the overflow weir width is restricted or where the flood surcharge space is limited. For example, to address dam safety concerns, the labyrinth weir is used to increase the spillway capacity at existing dams without increasing the flood surcharge space. Its relatively low cost in comparison with gated structures

[1]Project Manager, Ayres Associates, P.O. Box 1590, Eau Claire, WI 54702-1590

has led to its use for controlling headwater supply ponds or canal levels during excessive inflows. Being an overflow structure, the labyrinth weir provides a more reliable operation and requires less maintenance than a gated structure. The accidental opening of control gates can result in the loss of valuable water or damage to downstream areas, while not opening the gates at the appropriate time may lead to dam or canal failure. The labyrinth weir has also proven to be a cost-effective solution because of its construction simplicity and inherent structural stability.

Labyrinth Flow Description

Because of its nonlinear planform, many factors affect the discharge capacity of the labyrinth. Ideally, the discharge should increase in direct proportion to an increase in total crest length. However, this is only the case for labyrinth weirs operating at low heads. The flow pattern in a labyrinth weir passes through four phases as the upstream head increases: fully-aerated, partially-aerated, transitional, and suppressed.

In the fully-aerated phase the flow falls freely over the entire length of the labyrinth crest. The upstream head is small and neither nappe convergence at the upstream apex nor the depth of tailwater have any affect on the discharge coefficient. In this phase, the weir behaves almost ideally when compared to a straight weir with the same crest shape.

As the upstream head over the crest increases, the tailwater level rises and limited space forces opposing nappes to converge at the upstream apexes. This phenomenon makes aeration of the nappes at the upstream apexes difficult. The onset of nappe interference defines the beginning of the partially-aerated phase. Because of nappe interference, the flow in the upstream apexes becomes suppressed and air is drawn under the nappe at the downstream apexes to maintain aeration. A stable air pocket is formed along each side wall and downstream apex of the labyrinth.

By further increasing the upstream head, the nappe becomes suppressed at various locations along the crest. The stable air pocket breaks up into smaller pockets that intermittently move upstream along the side walls. This is the beginning of the transitional phase. It is difficult at times to visually distinguish between the partially-aerated and transitional phases, but the transition phase can be easily identified as a discontinuity in the discharge coefficient curve.

Finally, when the flow over the weir forms a solid, non-aerated nappe, it is in the suppressed phase. As the upstream head increases further, this last flow phase leads eventually to full submergence of the labyrinth weir, severely restricting its usefulness. The labyrinth is completely submerged usually when the flow depth over the crest is greater than the height of the labyrinth (Taylor, 1968).

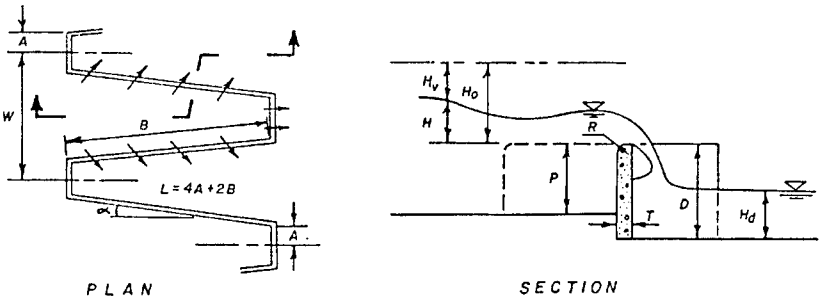

W = Cycle width
L = Cycle crest length
A = Apex half length
P = Upstream wall height
D = Downstream wall height
A = Side wall angle
B = Wall length
T = Wall thickness
R = Crest radius
H_o = Total head
H_v = Velocity head
H = Upstream head
H_d = Downstream head

Figure 1. Definition of labyrinth parameters.

Design Methodologies

Even though use of the labyrinth weir has broad applications, its complicated flow pattern and unusual layout have been a drawback to its use. Several different approaches have been tried to study the performance of labyrinth weirs to develop general design guidelines. However, most labyrinth weirs constructed to date were developed using these guidelines, but checked using site-specific hydraulic model studies to confirm the results. Significant discrepancies were found between the model test results and the predicted results using a generalized design method.

The first and most extensive investigation of labyrinth weirs was performed by Hay and Taylor (Taylor 1968, Hay & Taylor 1970). Their work presented a method to evaluate the theoretical discharge of a labyrinth weir in relation to a straight sharp crested weir. They found that the efficiency of a labyrinth crest for a particular planform may be expressed as Q_l/Q_n where: Q_l equals discharge over the labyrinth weir of length, L, under piezometric head, H; and Q_n equals discharge over a straight weir of length, W, at the same head. Many of the early labyrinth spillway designs used the Hay and Taylor method for preliminary sizing and design.

Site-specific hydraulic model tests have shown that the actual labyrinth discharge is as much as 25 percent lower than that predicted by the Hay and Taylor method, particularly at values of H/P exceeding 0.4 (Cassidy et al. 1985, Houston 1982, Mayer 1980).

The Bureau of Reclamation discovered that the Hay and Taylor design method assumed that the upstream velocity head was the same for both the straight weir and the labyrinth weir (Houston, 1982). Because the discharge per unit width of a labyrinth weir is substantially higher than that for a straight weir, this underestimation of the actual velocity head using Hay and Taylor's design method would be most pronounced at high values of H/P.

Rather than incorporate an imaginary sharp crested weir into the labyrinth design method, Darvas (1971) proposed the use of the traditional weir formula to calculate the discharge. This design approach was also used by LNEC in Portugal for the design of six labyrinth spillways (Magalhaes, 1985, Magalhaes et al., 1989). Magalhaes slightly modified Darvas approach by making the discharge coefficient nondimensional. The problem with the use of this design method for general application was that the results were restricted to the labyrinth weir parameters used to develop the discharge coefficient. If a parameter such as the crest shape or cycle width to height ratio was changed, the design charts gave erroneous results. Indeed, the discharge coefficient design charts developed by Magalhaes do not match Darvas's results for similar labyrinth planforms because they used different crest shapes.

Another approach developed by Indlekofer and Rouve (1975) was to consider the labyrinth weir as a series of straight weirs with corners. Thus, each apex of a labyrinth weir can be considered a corner of a polygonal weir. Their study determined the length of the disturbed zone along the weir crest at various upstream heads and the discharge capacity within this disturbed zone. However, their results were developed using sharp crested weirs which maintained fully aerated flow in the zone of disturbance. With the onset of nappe interference and loss of aeration in the upstream apexes at values of H/P greater than about 0.25, the use of this design method is restricted to low head situations.

Rather than comparing the hydraulic performance of labyrinth weirs to straight weirs or using a weir formula, one can examine the labyrinth weir's performance as a unique entity by using dimensional analysis. Further, as the flow over a labyrinth weir is three-dimensional, it does not lend itself readily to a mathematical description. The dimensional analysis approach is the current method used for labyrinth weir design.

Dimensional Analysis

Assuming that the hydraulic model studies conducted were of sufficient scale to neglect viscous and surface tension effects, the dimensional analysis can be reduced to a kinematic solution where the gravitational acceleration, g, is the only important remaining fluid parameter. The geometry of the flow pattern and the parameters of the labyrinth for one cycle are defined in

Equation 1. The only remaining parameter is the discharge per cycle, Q. Using these parameters, the discharge per cycle is defined by the function:

$$Q = f (L, A, W, P, D, T, S_C, H_o, H_d, g) \quad (1)$$

in which S_C is a parameter defining the labyrinth crest shape. The upstream velocity head, H_v, upstream piezometric head, H, the wall length, B, and the side wall angle are not included in Equation 1 because they are not independent variables. Each of these parameters can be calculated using some of the variables in Equation 1. Using the techniques of dimensional analysis, Equation 1 may be expressed as:

$$Q = C\ W\ H_o\sqrt{g\ H_o} \quad (2)$$

where

$$C = f \left(\frac{L}{W}, \frac{A}{W}, \frac{W}{P}, \frac{D}{P}, \frac{T}{P}, S_C, \frac{H_o}{P}, \frac{H_d}{D} \right) \quad (3)$$

Equation 2 is a general form of the overflow weir equation using the cycle width, W, as the characteristic length for the labyrinth. The crest length, L, could have been used as the characteristic length also, but the cycle width is more suitable for design purposes since the total width, W_t, is usually known. Examining Equation 3, all but the last two non-dimensional ratios describe the labyrinth geometry. The last two ratios describe the upstream and downstream flow boundaries.

Experimental Results

Most systematic hydraulic model studies of labyrinth weirs have been conducted in rectangular flumes with a level gradient and uniform entrance and exit conditions. These systematic studies differ from site-specific model studies used to evaluate a particular labyrinth configuration. In general, the systematic studies were limited to symmetrical labyrinths having trapezoidal or triangular planforms, the same upstream and downstream wall heights (D = P), a wall thickness from 0.50 to 0.75 inches, and no backwater effects. Applying these test constraints to Equation 3, the discharge coefficient function reduces to:

$$C = f \left(\frac{L}{W}, \frac{W}{P}, S_C, \frac{H_o}{P} \right) \quad (4)$$

Early systematic model studies were conducted by Taylor (1968) and the Houston (1982) using sharp-crested crest sections due to its ease of construction. More practical crest shapes using a quarter-circle, half-circle or elliptical sections have also been tested (Taylor, 1968, Mayer, 1980, Amanian, 1987 and Magalhaes, 1989). The systematic hydraulic model studies tested labyrinth weirs with

length magnification ratios, L/W, varying from 1.33 to 8 and vertical aspect ratios, W/P, varying from 2 to 6. These ranges encompass most of the labyrinth weirs that have been constructed. All test results indicated that the number of cycles used and the attachment to the side wide at the upstream or downstream end of the cycle had no effect on the discharge coefficient.

For sharp-crested labyrinths having the same length magnification ratio, L/W, the difference between the discharge coefficients at various vertical aspect ratios, W/P, was found to be a constant. Based on a least squares analysis of the data, the variation between the vertical aspect ratio and the discharge coefficient was quantified for the ranges under consideration. Using this correlation for W/P greater than 2, Equation 2 can be redefined to:

$$Q = C_W \left(\frac{W/P}{W/P + k}\right) W H_o \sqrt{g H_o} \qquad (5)$$

The parameter, k, which is a constant from the least squares analysis, has a value of 0.18 for triangular and 0.10 for trapezoidal planforms having A/W equal to 0.0765. The discharge coefficient, C_W, uses the subscript, w, since it is based on the cycle width, W, and the vertical aspect ratio correlations.

For prototype labyrinths, construction considerations make another crest shape desirable. The quarter-round and elliptical crest shapes are the most commonly used. These shapes are easy to form and concrete can be placed through a gap between the top of the arc and downstream wall forms. Design charts for quarter-round crests were prepared using the difference between discharge coefficients for sharp-crested and quarter-round-crested labyrinth weirs for the trapezoidal and triangular planforms using the systematic tests on rounded crest labyrinth weirs conducted by Mayer (1980). Use of a quarter-round crest resulted in a slightly higher discharge coefficient than that of the sharp-crested weir labyrinth, particularly at low values of Ho/P. Magalhaes (1989) paper contains design charts for the ogee crest shape.

The resulting discharge coefficients for quarter-round labyrinth weirs are presented in Figure 2 for the triangular and trapezoidal planforms. Taylor's model test results (1968) agree closely with the results in Figure 2. Figure 2 clearly shows that the discharge coefficient decreases as the head increases based upon observed flow conditions. The greatest decrease in the discharge coefficient occurs in the aerated region. This decrease is caused by nappe interference, which begins at the upstream apexes and progresses towards the downstream apexes as the head increases. In the suppressed region, the discharge coefficient curve is flatter because the labyrinth acts much like a broad-crested weir. The lack of continuity in the transition region results from the nappe losing aeration and becoming suppressed.

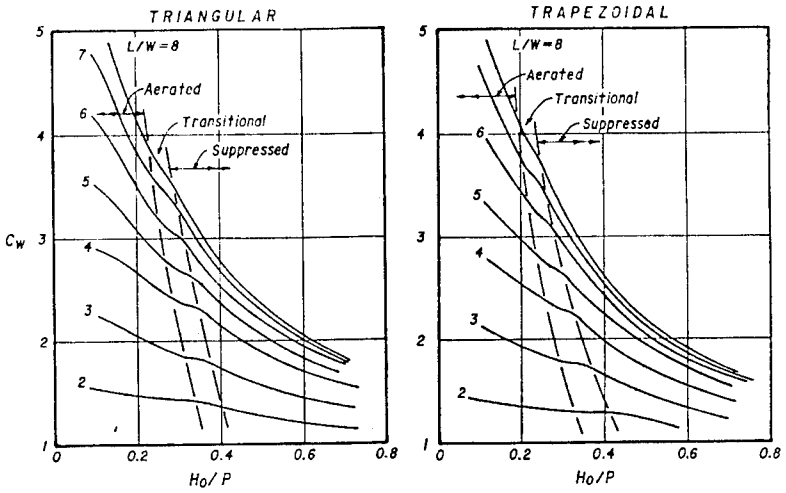

Figure 2. Discharge coefficients for quarter-round-crested labyrinths (Courtesy Bureau of Reclamation).

Figures 3 and 4 present a comparison between site-specific hydraulic model tests and predicted results. The Boardman labyrinth spillway model test results (Cassidy et al., 1985) are compared to the predicted results using Hay and Taylor's method (1970) and the author's method in Figure 3. The plotted results clearly show the discrepancy between the model test results and the results using Hay and Taylor's method at high values of H_o/P. The discharge curve using the writer's method is slightly higher than the model test results yet follows the trend of the actual results.

The site-specific labyrinth model test results for the Boardman, Ute, and Hyrum Dam spillways are shown in Figure 4 along with results using the writer's method (Cassidy et al., 1985; Houston, 1982; and Houston, 1983). For the Ute and Boardman labyrinth spillways, the author's method predicts a higher discharge coefficient by a maximum of about 8 percent. Approach and entrance losses could account for this discrepancy. Poor entrance conditions significantly affected the end cycles at Ute Dam. The predicted results compare favorably with the model test results for Hyrum Dam where approach and entrance losses were minimal.

Design Method

The following design method is based upon the use of quarter-round-crested labyrinth weirs and the recommendations contained in the previous section. Equation 5 and the two charts contained in

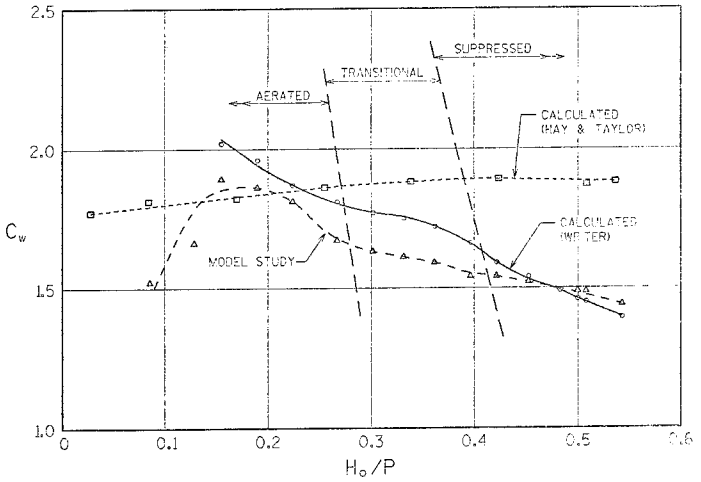

Figure 3. Boardman Spillway - Discharge Coefficients (L/W = 2.98), (Courtesy ASCE)

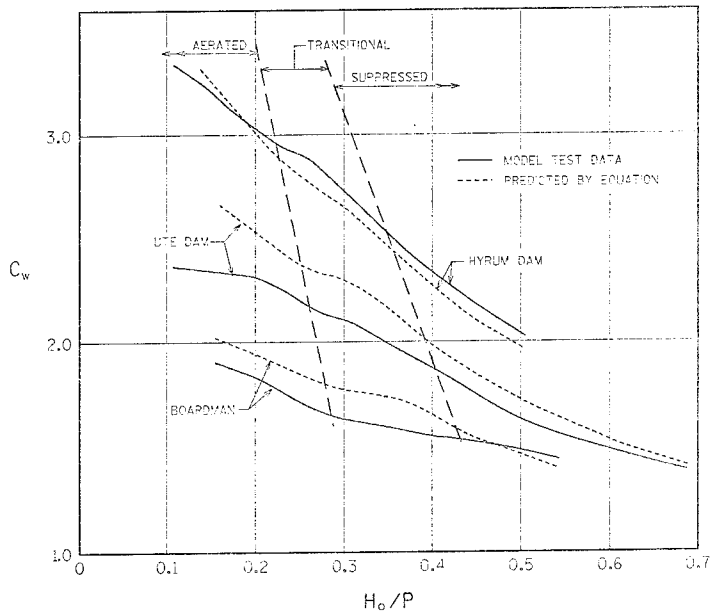

Figure 4. Predicted versus actual labyrinth discharge coefficients from selected site-specific model tests.

Figure 2 can be used for design: one for triangular planforms and the other for trapezoidal planforms with A/W equal to 0.0765. The accuracy of the predicted performance should be within about 3 percent of actual performance after consideration of approach and entrance losses.

1. Determine the labyrinth structure's location and total channel or structure width available considering site conditions.
2. Define the maximum allowable operating head on the weir, H_{max}, to satisfy the operational requirements.
3. Define the maximum discharge, Q_t, to be accommodated at the maximum operating head.
4. Select a value for the crest height, P, based on a trial value of H_{max}/P equal to 0.50. Revise the crest height or maximum operating head based on foundation or site limitations if necessary.
5. Determine the cycle width, W, and number of cycles, n, based on a trial estimate of the vertical aspect ratio equal to 2.5.
6. Revise the value of n to a whole number based on the total channel available and calculate the value of the cycle width, W, and the vertical aspect ratio, W/P.
7. Solve Equation 5 for the discharge coefficient, C_w, using the appropriate value of k for the planform utilized.
8. Enter Figure 2 using the values of H_{max}/P and C_w for the planform utilized and determine the length magnification ratio, L/W. For those planforms that have A/W between the triangular and trapezoidal planforms shown, use both charts and interpolate the value of L/W.
9. Using the major labyrinth parameters determined thus far, sketch and determine the actual dimensions of the labyrinth weir. Revise the initial computations using the final dimensions determined from the layout to check the adequacy of the design.

The following steps allow prediction of the labyrinth weir's performance over the full range of operation.

10. Select a number of values of Ho/P from 0.1 to H_{max}/P.
12. For each value of H_o/P, determine C_w by interpolation from the design charts in Figure 2 using the design value of L/W.
13. Using Equation 5, calculate the labyrinth discharge for each value of H_o/P.

For example, a labyrinth weir is to be designed to pass a maximum discharge of 2650 cfs at a head not to exceed 3.35 feet. Based on site conditions, the maximum channel width was determined to be 40 feet. Using a trapezoidal planform with a quarter-round-crest shape, a two-cycle labyrinth weir was sized for the maximum discharge using a 20.0 feet cycle width, 9.65 feet for crest height, 71.9 feet for crest length, and 1.5 feet for the apex half length. The resulting ratios are 0.347 for Ho/P, 2.07 for W/P, 3.61 for L/W and 0.075 for A/W for the selected design. The

computations for developing a discharge rating curve are illustrated in Table 1. This labyrinth design is planned for construction at the Forestport Hydropower Project in New York.

Table 1. Performance calculation of designed weir

H_o/P	H_o ft	C_w	Q_t cfs
0.10	0.97	2.51	520
0.15	1.45	2.43	920
0.20	1.93	2.31	1340
0.25	2.41	2.17	1760
0.30	2.90	2.07	2210
0.347	3.35	2.01	2670

Conclusions

The hydraulics of labyrinth weirs have been examined and the performance documented over the range of parameters likely to occur in practice. A method for calculating the hydraulic performance of labyrinth weirs has been developed and presented as a simple procedure using an overflow weir equation and design charts for the discharge coefficient. Using this method, the leading dimensions of the labyrinth structure can be determined and the discharge rating curve for the weir developed.

References

1. Amanian, N., "Performance and Design of Labyrinth Spillway," thesis presented to the Utah State University, Logan, Utah, in 1987, in partial fulfillment of the requirements of the degree of Master of Science in Civil and Environmental Engineering.
2. Cassidy, J.J., C.A. Gardner & R.T. Peacock, "Boardman Labyrinth - Crest Spillway," J. Hyd. Engr., ASCE, Vol. 111, No. HY3, March 1985.
3. Darvas, A., Discussion of "Performance and Design of Labyrinth Weirs" by Hay & Taylor, J. Hyd. Div., ASCE. Vol. 97, No. HY8, August 1971.
4. Hay, N. & G. Taylor, "Performance and Design of Labyrinth Weirs," J. Hyd. Div., ASCE, Vol. 96, No. HY11, November 1970.
5. Houston, K.L., "Hydraulic Model Study of Ute Dam Labyrinth Spillway," Report No. GR-82-7, Bureau of Reclamation, Denver, Colorado, 1982.
6. Houston, K.L., "Hydraulic Model Study of Hyrum Auxiliary Labyrinth Spillway," Report No. GR-82-13, Bureau of Reclamation, Denver, Colorado, 1983.

7. Indlekofer, H. & G. Rouve, "Discharge Over Polygonal Weirs," J. Hyd. Div., ASCE, Vol. 101, No. HY3, March 1975.
8. Lux, F. & D.L. Hinchliff, "Design and Construction of Labyrinth Spillways," Q59, R15, 15th Congress of ICOLD, Lausanne, Switzerland, 1985.
9. Magalhaes, A.P., "Labyrinth-Weir Spillways," Q59, R24, 15th Congress of ICOLD, Lausanne, Switzerland, 1985.
10. Magalhaes, A.P. & M. Lorena, "Hydraulic Design of Labyrinth Weirs," Memoria No. 736, Laboratorio Nacional De Engenharia Civil, Lisboa 1989.
11. Mayer, P.G., "Bartletts Ferry Project Labyrinth Weir Model Studies," Project No. E-20-610, Georgia Institute of Technology, Atlanta, Georgia 1980.
12. Taylor, G., "The Performance of Labyrinth Weirs," thesis presented to the University of Nottingham, Nottingham, England, in 1968, in partial fulfillment of the requirements of the degree of Doctor of Philosophy.

Modeling of River Ice Processes for Hydropower Facilities in Cold Regions

Randy D. Crissman[1], M. ASCE

Abstract

Both physical and mathematical models can be used in developing an improved understanding of the hydraulic and ice processes that may affect the design and/or operation of hydropower facilities in cold regions. Applying both to the same problem, if done properly, can aid in the interpretation and reduce the uncertainty of the results. The pros and cons of physical and mathematical modeling of river ice processes are discussed. The use of physical and mathematical modeling to study ice transport and jamming processes that adversely affect the New York Power Authority's (Authority) and Ontario Hydro's (OH) generating facilities on the upper Niagara River is discussed.

Introduction

Existing or potential future hydroelectric generating facilities located in cold regions can be affected by the formation of ice in rivers and/or reservoirs which supply water for their operation. The problems that ice creates for operating hydropower facilities are numerous and include blockage of intakes and trash racks, accelerated deterioration of concrete structures, and the exertion of forces due to expansion of ice sheets or impacts from moving ice on structures. Ice covers that form in the rivers or reservoirs upstream or downstream of most hydropower facilities need to remain stable throughout the winter to minimize these ice problems. The stability of an ice cover is primarily affected by the weather, but can also be affected by operation of the hydropower facility.

Assessing the impacts of ice on the design and operation of a hydropower generating facility or the impact of the facility on the ice regime of a river or reservoir is not straightforward in most cases. In the case of existing facilities, "operating experience" may be adequate to respond to most ice problems. However, the range

1. Senior Hydraulic Engineer, New York Power Authority, Niagara Power Project, P. O. Box 277, Niagara Falls, New York 14302-0277

of "operating experience" may not be sufficient to allow for appropriate responses to extreme conditions or combinations of events which have not been experienced. Furthermore, "operating experience" may be constrained by regulatory or operating constraints. For planned facilities, there is no direct experience to draw upon.

Physical and/or mathematical modeling of a proposed or, in some cases, existing hydropower facility is almost always needed to assess potentially significant ice impacts. Modeling is used to assess these impacts by simulating the hydraulic and ice processes, physical features, and operational characteristics of the facility. The results of the modeling may help establish design criteria for new facilities or extend the range of "operating experience" for existing facilities. However, both modeling approaches have deficiencies and the uncertainties in using only one approach may be quite significant.

This paper discusses how the use of both physical and mathematical models can be used to reduce the uncertainty in modeling hydraulic and ice processes that affect the design and/or operation of hydropower facilities. In particular, the application of the concepts to a comprehensive physical and mathematical modeling effort to assess the relationship between the occurrence of ice jams in the upper Niagara River and the operation of the existing and planned future expansions of the hydroelectric generating stations at Niagara Falls is discussed.

Modeling of River Ice Processes

Once it has been decided that modeling is needed to better understand the impacts of ice on a generating facility or the impacts of a generating facility on the ice regime, the first step is to identify the important processes that need to be modeled. This is an important step, because it may affect the geometrical scale(s) selected for a physical model or the complexity of a mathematical model. For example, in modeling ice jamming processes, it is important to know whether cohesion forces (freeze bonding) are important. If so, then they must be properly incorporated into the modeling. If not, they can be neglected and the modeling may be simplified.

The use of either a physical or mathematical model to assess the impacts of ice is affected by several factors including the size of the area to be modeled, the complexity of the boundary conditions, the complexity of the flow fields, and the level of theoretical knowledge of the important processes. Physical models are usually selected when the problem is complex and the theoretical knowledge, which is needed for mathematical modeling, is incomplete. On the other hand, mathematical models are typically selected for less complicated problems where the theoretical knowledge is adequate or for problems in which the dimensions of the area to be modeled are so large that it would make a physical model impractical.

Physical Modeling

As in more conventional physical hydraulic models, physical models of river ice processes should ideally maintain geometric, kinematic, and dynamic similitude with the prototype. However, complete similitude is practically impossible and

compromises are typically needed to design a model that will address the important issues. As in most physical models of free surface flows, the fluid properties of water are difficult to scale to meet the requirements of both Froude number and Reynolds number similitude. Therefore, Froude number similitude using water with flows that fall within the turbulent flow range of Reynolds number is required for river ice models. However, the similitude requirements for physical models of river ice processes are more complicated than those for typical free surface flow models. Phenomena that are more difficult to model include the two-phase flow characteristics of the ice transport and accumulation processes, the cohesion force effects of freezing, and the ice strength characteristics. Michel (1978), Wuebben (1993), Ettema et al (1992), and Ashton (1986) present good overviews of the similitude requirements for physical models of river ice processes.

Uncertainties in the results of physical modeling of river ice processes are the consequence of the inability to adequately maintain similitude with the prototype. Geometric similarity is only possible in undistorted (scale for horizontal and vertical dimensions is equal) models. Most physical models of large areas or long reaches of natural rivers are typically distorted, with the vertical scale being larger than the horizontal scale, to accommodate modeling space or cost constraints. In addition, vertical distortion may be required to accommodate constraints imposed by the requirement to maintain turbulent flows or the characteristics of the model ice material. An example of the latter would be the model ice strength, which is important in modeling ice forces on structures. Distorted models are best applied to situations where the flow fields are predominately two-dimensional and have hydrostatic pressure distributions. When flow fields are highly three-dimensional, like those in the vicinity of a hydropower intake, distortion can cause the vertical hydrodynamic forces in the model to be greater than the horizontal forces by a factor equal to the distortion ratio. This can introduce significant uncertainties in, for example, modeling ice jamming processes, if the distortion ratio is high.

Other factors which affect the uncertainty of physical modeling of river ice processes include the geometrical and strength characteristics of the model ice, surface tension, thermodynamic influences on cohesion (freeze bonding) and ice strength, and wind forces. The material used to simulate the ice in a physical model is largely related to the purpose of the modeling. In modeling cohesionless ice jamming processes[2], for example, the model ice may be a granular material or irregularly distributed fragments of a material with a density, size distribution, and angle of internal friction that are comparable to the prototype. In modeling the performance of a navigation ice boom, the flexural and compressive strengths of the ice are important and thus may require the use of chemically modified real ice or a synthetic material with the appropriate strength characteristics (Abdelnour et al, 1987). In any case, the availability of suitable model ice materials is limited. Even though the modeler may carefully attempt to replicate the dominant prototype ice characteristics, significant uncertainty in modeling results can occur (Kennedy et al, 1981).

2. Such conditions may occur in a spring break-up ice jam when cohesion forces (freeze bonding) are low.

Thermodynamic processes have a significant influence on the cohesion forces (freeze bonding) within ice accumulations and the strength of ice. Although refrigerated models have been used (Calkins, 1983) to study the thermodynamic effects on river ice processes, they are expensive to operate and can introduce other uncertainties depending on the type of processes being modeled. Simulation of cohesion between model ice pieces in non-refrigerated models has been attempted by coating the model ice with a binding agent. This approach is messy and yields only qualitative results that may be hard to repeat. The uncertainties related to the thermodynamic processes in physical modeling of river ice problems can be significant.

Wind stresses applied to the surface of river ice can exert forces which, in some instances, may dominate ice transport. This force component is virtually impossible to simulate and scale properly in large scale physical models of river ice processes. Reynolds number similitude is required for modeling the wind stress. However, as stated earlier, it is not possible to achieve both Froude number and Reynolds number similitude. Attempts to incorporate the effects of wind stress by flowing water beneath the ice (Calkins et al, 1981) showed some promise, but warrant further evaluation (Kennedy et al, 1981). Again, the inability to adequately simulate the wind generated forces, when they are deemed to be important, can introduce significant uncertainty in physical modeling results.

Mathematical Modeling

Several mathematical models of river ice processes have been developed in recent years to be used as tools in the analysis and design of hydraulic works in cold region rivers (Petryk et al, 1981). Most of these models link a one-dimensional (in space), steady-state flow model (backwater computation) to empirical or theoretical models of ice processes. They typically model heat transfer at the air-water, air-ice, and ice-water interfaces, ice formation and dissipation, surface and undercover (erosion) transport of ice, and ice cover stability and progression.

A recent improvement in this modeling approach has included replacing the steady-flow model with an unsteady flow model (Lal and Shen, 1991; Petryk et al, 1991). Improved models of some of the ice processes have also been developed. An example is the use of a two-layer model that separates surface ice transport from ice that remains in suspension in the flow (Lal and Shen, 1991). The application of both the steady and unsteady flow versions of these models is limited to situations whose characteristics closely match the assumptions and limitations of the models.

In all of the models mentioned, the formation of an ice cover due to bridging or lodgment is not explicitly simulated, because an adequate theory has not yet been developed for this dynamic process. Therefore, bridging at a prospective location is a required input to the model. The models can then be used to determine the consequences if bridging at the specified location were to occur.

Shen et al (1990) proposed an analytical framework for simulating the dynamic transport of river ice, which includes equations of motion and continuity for the ice that can be coupled to the equations of motion and continuity for the water

flow. The ice transport model includes a viscous-plastic constitutive relationship that incorporates a Mohr-Coulomb pressure term to model the material properties of the ice. Lal and Shen (1991) applied this concept to a one-dimensional model of ice transport to assess the potential for applying the method in two-dimensions. The one-dimensional model has limited application, since river ice transport as well as ice jamming processes are two-dimensional phenomena.

Shen and Chen (1992) developed a two-dimensional model for river ice dynamics. In this model, the hydrodynamic equations are solved using a Eulerian finite element model. The ice dynamics equations are solved using a Lagrangian particle scheme. The ice dynamics and hydrodynamics are coupled through interactions at the interface between the ice and the water.

All of these mathematical models are based on theories that are not universally accepted or proven. Many components of the models are not well understood physically, let alone mathematically. Much research is needed to refine the theory and support it with observations and experiments. On the other hand, these models have some advantages over physical modeling. For example, similitude does not limit the modeling, because the prototype is modeled at full-scale. In addition, processes which can't be simulated in a physical model, such as wind stresses and thermodynamic processes, can be replicated with proper calibration. However, as in physical modeling, uncertainties are potentially significant.

Modeling of Ice Jamming on the Upper Niagara River

The Authority is in the process of upgrading its hydroelectric generating facilities at its Niagara Power Project, located on the Niagara River, to provide additional peaking capacity. As part of this undertaking, at the request of the Federal Energy Regulatory Commission (FERC), which issued and maintains the operating license for the Niagara Power Project, the Authority is conducting studies aimed at evaluating the relationship between the project's design and operation and the formation of ice jams in the upper Niagara River. Several integrated studies are underway to determine the relationship, if any, between hydropower operations and the formation of ice jams, to evaluate possible methods for reducing the likelihood that jams will occur, and to develop strategies for limiting the negative impacts (generation losses and flooding) of ice jams (Crissman et al, 1992). The most severe ice problems occur when ice from Lake Erie, located about 35 km upstream from the Authority's intakes, enters the river during storm events.

One objective of the studies is to determine what can be done, if anything, to increase the ice transport capacity of the upper Niagara River in the reach near the water intakes for the Niagara Power Project. This reach, shown in Figure 1, is referred to as the Grass Island Pool. In light of the uncertainties in the modeling of river ice processes, both a physical model and a mathematical model are being used to study and develop a better understanding of the ice transport and ice jamming processes in this reach for the existing physical and operating conditions and will be used to assess possible mitigating measures. The models and the general approach that are being used and some preliminary results are subsequently described.

Physical and Mathematical Models of the Grass Island Pool

The boundaries of the physical model of the Grass Island Pool are shown in Figure 1. Some of the design parameters for the model are included in Table 1. The model was required to have a distortion ratio no greater than three (3) to minimize the discrepancy between the vertical and horizontal force components on the ice transport processes. The model was built and is being operated by Alden Research Laboratory, Inc. of Holden, MA. The ice island shown in Figure 1 typically forms whenever there is a high discharge of ice from Lake Erie. It is modeled as a permanent feature in the physical model.

The model ice is a crushed polypropylene with a density of 0.92, a size distribution ranging from 1 mm to 13 mm and a D_{50} of 6 mm, and an internal angle of friction (dry) of about 46°. A single layer of this model ice on the surface of the model corresponds to ice about 0.3 m thick in the prototype. The model ice is fed into the model as a slurry from a head tank. The ice inflow rate can be accurately controlled to simulate a wide range of ice concentrations (area of ice per unit area of water surface) and is collected and returned to the head tank for reuse. The model was not designed to simulate thermodynamic or wind stress influences on ice transport.

The mathematical model of the Grass Island Pool reach is based on the work of Shen and Chen (1992). The boundaries of the mathematical model of the Grass Island Pool are identical to those of the physical model, including the ice island. The mathematical model can simulate thermodynamic and/or wind stress influences on ice transport, though somewhat empirically.

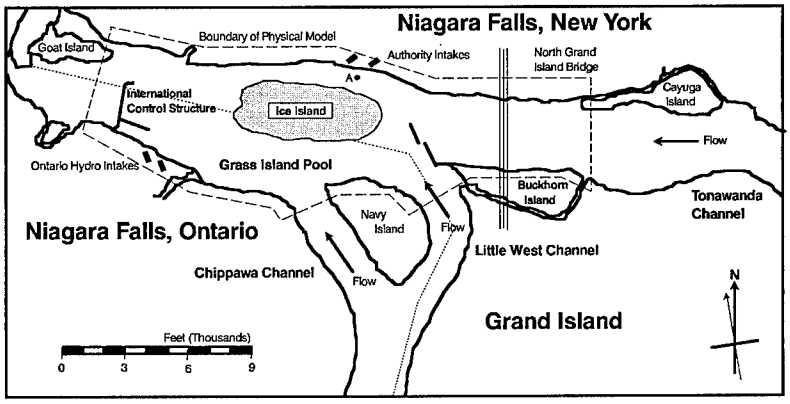

Figure 1: Grass Island Pool Reach of the Upper Niagara River (1,000 feet = 305 m).

Table 1

Design Parameters for the Grass Island Pool Physical Model

Design Parameter	Value or Range of Values
Horizontal Scale (model : prototype)	1 : 120
Vertical Scale (model : prototype)	1 : 50
Distortion Ratio	2.4
Horizontal Flow Scale (model : prototype)	1 : 42,426
Vertical Flow Scale (model : prototype)	1 : 101,823
Horizontal Time Scale (model : prototype)	1 : 16.97
Vertical Time Scale (model : prototype)	1 : 7.07
Total River Flow (prototype)	0 to 9,350 cms
Authority Diversion (prototype)	0 to 2,980 cms
Ontario Hydro Diversion (prototype)	0 to 1,960 cms
Flow Past Control Dam (prototype)	1,420 to 7,080 cms
Reach Length (model : prototype)	62 m : 7,470 m
Reach Width (model : prototype)	21 m : 2,520 m
Maximum Depth (model : prototype)	0.2 m : 12 m

Approach to Using the Physical and Mathematical Models

The use of both a physical and mathematical model to study the ice processes in the reach shown in Figure 1 was judged to be required by the Authority and an independent board of consultants (Crissman et al, 1992). The hydrodynamic and ice transport processes in the Grass Island Pool are essentially two-dimensional in the areas far afield from the intakes and are highly three-dimensional in the areas near the intakes. Therefore, it was not appropriate to use simple mathematical models or a small-scale physical model. Furthermore, the state-of-the-art of two-dimensional mathematical models of river ice processes was not advanced enough to rely on them exclusively. However, it was also deemed inappropriate to rely solely on the use of a physical model, because of the uncertainties inherent in the physical modeling of river ice processes. Therefore, it was decided that both modeling techniques should be used and that they should proceed, as closely as possible, in parallel.

The physical modeling program has three phases; baseline tests, screening tests of possible mitigating measures, and detailed testing of two to three of the most promising measures. The baseline tests are intended to establish a baseline condition for the ice jamming processes against which the performance of several mitigating measures can be compared. Both the baseline and screening tests are to be conducted for a limited range of variables. The general criterion for selecting a mitigating measure for more detailed studies, based on results of the physical modeling, was established. It merely states that the impact of the mitigating measure must be significant enough to overwhelm the uncertainties in the physical modeling.

The degree to which the uncertainties must be overwhelmed is quite subjective. Therefore, the mathematical model is to be used as a tool for reducing the

subjectiveness of this criterion. Since the characteristics of the model ice are constant and the factors that can be varied in the physical model are limited, the goal is to simulate the ice processes in the physical model with the mathematical model. This mathematical clone of the physical model will be used to assess the potential impacts of, for example, the influences of unsteady flow, wind forces, variable ice thickness distributions, and thermal processes on ice transport, factors which the physical model can't easily replicate.

The first objective is to develop a calibrated mathematical model[3] that can replicate the observations and measurements obtained from the baseline tests conducted in the physical model. This effort is currently underway. Once calibrated, the mathematical model will be used to assess the impacts of the factors which can't be modeled in the physical model on the baseline results. This same approach will be used in assessing the performance of the mitigating measures evaluated in the screening tests and in the detailed performance testing.

To illustrate, Figure 2 contains results of simulations conducted in the physical and mathematical models for a set of specified test conditions. It shows the temporal variation in ice thickness at a location near the Authority's intakes (Point A in Figure 1) as measured in the physical model (without wind) and as computed in the mathematical model (with and without wind). The results indicate that when compared to the physical model results, the mathematical model (without wind) under-predicts the thickening. Although it is not shown, the mathematical model (without wind) also over-predicts the ice velocity relative to the measurements from the physical model. This appears to be caused by the difficulty in developing a constitutive model that can accurately describe the changing material properties of the ice during its transition from a viscous-plastic material to a solid material. The mathematical model is currently being modified to better reflect this transition, which should improve the calibration results. The mathematical model's under-predictions of ice thickness may also be related to the distortion in the physical model. The ice thicknesses may be greater than would occur in an undistorted physical model.

Figure 2 also shows how the effect of wind can influence the ice thickening processes near the Authority's intakes (Point A in Figure 1). The ice was subjected to a 50 km/hr wind[4] from the southwest, which is the prevailing wind direction for ice transport periods that are susceptible to ice jamming. Although the results were obtained using the version of the mathematical model which has not been fully calibrated, the relative impact can be seen by comparing the with- and without-wind results. Note that the ice thickness has increased faster and is thicker in the with-wind case. This result indicates that the physical model may over-predict the ice transport capacity of the Grass Island Pool in conditions that are actually encountered in the prototype. Therefore, the physical modeling results need to be closely evaluated before any possible mitigating measures can be recommended.

3. The mathematical model was first calibrated, to the extent possible, against data observed in the prototype to ensure that the model was capable of producing reasonable results.

4. The wind stress coefficient is representative of that for the prototype.

Conclusion

This paper has discussed the types of uncertainties inherent in the use of physical and mathematical modeling of river ice processes. It has also presented an approach in which a mathematical model of river ice processes is being used to assess the potential magnitude of such uncertainties in a distorted physical model of river ice processes near a hydropower intake. If appropriately implemented, this approach may help develop recommendations for better design and/or operating criteria for hydropower plants or other civil works that are either affected by river ice or that have some impact on the river ice regime.

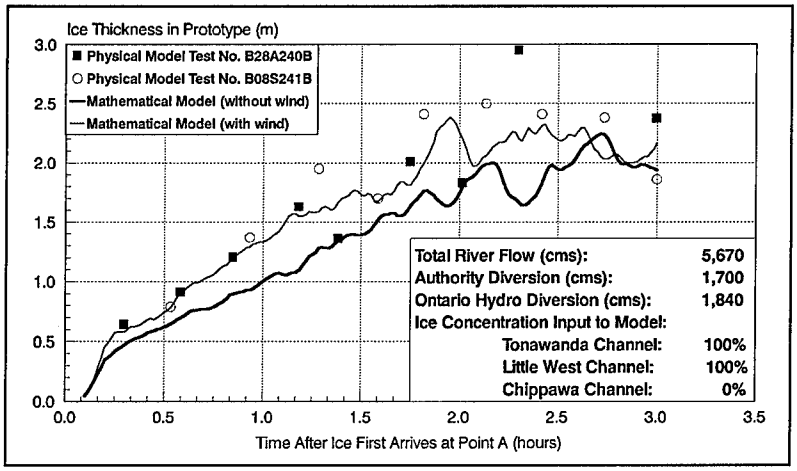

Figure 2: Ice Thickness Near Authority's Intake As Simulated in the Physical and Mathematical Models.

References

Abdelnour, R., Nawar, A., and Kotras, T., "Modeling and Experimentation: A Tool for Hydro Operation," Proceedings of EPRI/CEA Workshop/Seminar on Hydroelectric Operations and Maintenance, Winter Operations and Ice Problems, Montreal, Quebec, Canada, August 1987, 19 pp.

Ashton, G. (editor), River and Lake Ice Engineering, Water Resources Publications, Littleton, Colorado, 1986.

Calkins, D., "Modeling of Ice Discharge in River Models," Proceedings of the ASCE Conference on Frontiers in Hydraulic Engineering, Cambridge, MA, August 9-12, 1983, pp. 285-290.

References (continued)

Calkins, D., Sodhi, D., and Deck, D., "Port Huron Ice Control Model Studies," Proceedings of the 6th International Symposium on Ice, International Association for Hydraulic Research, Quebec City, Quebec, Canada, July 27-31, 1981, Vol. 1, pp. 361-377.

Crissman, R., Ettema, R., Gerard, R., and Andres, D., "A Plan for Studying Ice Jamming Processes on the Upper Niagara River," Proceedings of 11th International Symposium on Ice, International Association for Hydraulic Research, Banff, Alberta, Canada, June 15-19, 1992, Vol. 1, pp. 527-538.

Ettema, R., Crissman, R., Andres, D., and Gerard, R., "Physical Modeling of Ice Accumulation at Hydraulic Structures," Proceedings of 11th International Symposium on Ice, International Association for Hydraulic Research, Banff, Alberta, Canada, June 15-19, 1992, Vol. 1, pp. 515-526.

Kennedy, J., Lazier, S., Michel, B., Rumer, R., "Review of Ice-Hydraulic Model Studies," U. S. Army Engineer District, Detroit, Michigan, July 1981, 86 pp.

Lal, A. M. W. and Shen, H. T., "Mathematical Model for River Ice Processes," Journal of Hydraulic Engineering, American Society of Civil Engineers, Vol. 117, No. 7, 1991(a), pp. 851-867.

Lal, A. M. W. and Shen, H. T., "A Numerical Method for Simulating Dynamic River Ice Transport," Report No. 91-12, Dept. CEE, Clarkson University, Potsdam, NY, 1991(b), 95 pp.

Michel, B., Ice Mechanics, Les Presses De L'Université Laval, Quebec, Canada, 1978, 499 pp.

Petryk, S., Panu, U., Kartha, V., and Clément, F., "Numerical Modeling and Predictability of Ice Regimes in Rivers," Proceedings of the 6th International Symposium on Ice, International Association for Hydraulic Research, Quebec City, Quebec, Canada, July 27-31, 1981, Vol. 1, pp. 426-435.

Petryk, S., Carson, R., Hodgings, D., Parkinson, F., and Beltaos, S., "Development of a Comprehensive Numerical River Ice Model," Monograph on Cold Regions Hydrology and Hydraulics, American Society of Civil Engineers, New York, New York, 1991, pp. 739-760.

Shen, H. T. and Chen, Y. C., "Lagrangian Discrete Parcel Simulation of Two-Dimensional River Ice Dynamics," Report No. 92-9, Dept. CEE, Clarkson University, Potsdam, NY, July 1992, 137 pp.

Shen, H. T., Shen, H., and Tsai, S., "Dynamic Transport of River Ice," Journal of Hydraulic Research, International Association for Hydraulic Research, Vol. 28, No. 6, 1990, pp. 659-671.

Wuebben, J., "Physical Modeling," Monograph on Ice Jams (Chapter 6), National Research Council of Canada (to be published in 1993).

Pulsation Problems in Hydroelectric Powerplants
Some Case Studies

Anders Wedmark[1]

Introduction

Francis turbines have an inherent tendency to produce pulsation problems when operating at non-optimum load. This is due to the fact that the water still has a rotational component as it leaves the runner and enters the draft tube. The rotation of the water will in turn induce a pressure pulsation. The frequency of the pressure pulsation will be relatively low, approximately of 0.5 - 5 Hz (Rheingans, 1940). This pressure pulsation can in turn interact with the water conduit and may reach amplitudes that are detrimental to the equipment or intolerable from an operating standpoint.

The situation is fundamentally different in a kaplan turbine. Here the blades are continually adjusted to eliminate the water rotation after the runner. Consequently, this type of pulsation problems are very rare in kaplan turbines.

Kvaerner has developed a method to minimize the problems of pressure pulsations. The basic concept is to let the turbine draw air from the top of the generator, through the shaft and discharge the air in the draft tube, below the runner hub (see fig. 1).

However, during recent years Kvaerner has encountered a number of installations where this approach has not been possible. This paper describes the methods that were used, and experiences gained, in some of these cases.

[1] Senior Project Engineer, Kvaerner Hydro Power, Inc, 100 First Stamford Place, Stamford, CT 06902.

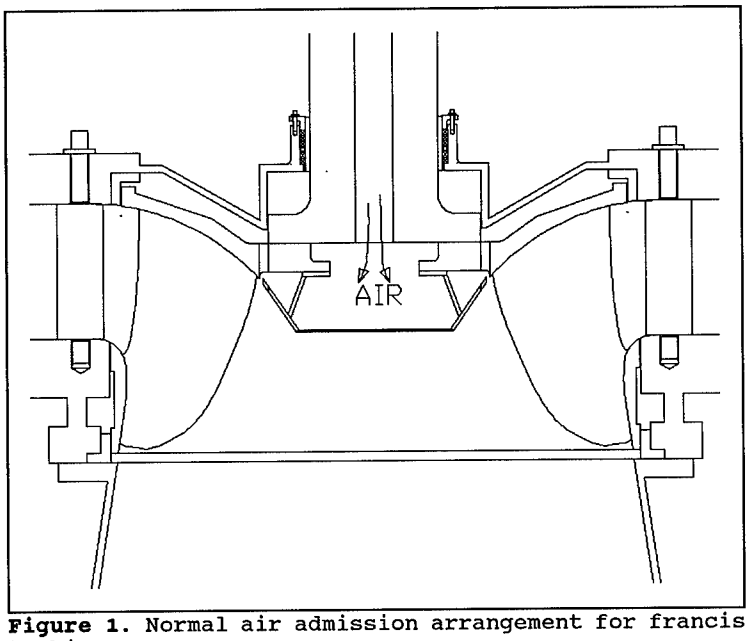

Figure 1. Normal air admission arrangement for francis turbine.

Case 1.

This powerplant contains two horizontal francis turbines rated at 3,000 kW and operating under a head of 70 m and at a speed of 720 rpm. It is connected to a penstock, approximately 3 km long.

These units experienced pulsations with a frequency of 2.6 Hz, when operated at part load. Although the units are identical, the magnitude of the pulsations differed substantially. In unit 1 the pressure pulsations measured in the draft tube were as high as 17 % of the head at some loads. In unit 2 they were only approximately 3 % of the head. However, the frequency of the pulsations was the same in both units.

These units had a pressure tap connection in the draft tube cone. In an attempt to alleviate the pulsation problem the pressure tap was opened to the atmosphere and the machine was allowed to draw air through the hole. This had some positive effect, but did not completely remedy the problem.

Encouraged by the positive effect of opening the pressure tap to air it was decided to enlarge the hole and also to drill more holes around the draft tube circumference. After this work was performed it was discovered that only the top hole drew air. The others discharged water instead.

This situation led to the conclusion that the pressure in the draft tube was too high for enough air to enter. It was also anticipated that addition of more air would solve the problem.

One way of getting more air into the draft tube is of course to hook up a compressor. However, this can be quite costly and the compressor would require a constant supply of power to operate.

The solution finally decided on was to locally lower the pressure around the aeration holes. This was accomplished by constructing conical shapes around the holes (see fig. 2). The cones were manufactured from stainless steel and welded to the draft tube wall. One cone was made for each of the four holes and they were connected to a manifold outside the draft tube. The manifold was then connected to a valve so the total amount of air could be regulated.

The cone works in much the same way as an airplane wing. When the water is forced to speed up when passing the cone, the static pressure will decrease. The lower static pressure will then allow air to be drawn into the draft tube.

The addition of the cones in the draft tube had a dramatic effect on the pulsations. When opening the air valve the pulsations completely disappeared.

Conclusions: Admission of air can be very effective, even if the air is not admitted at the runner center. Air admission through the draft tube wall is very simple to install, but care must be taken that the pressure situation inside the draft tube is suitable. It may be more difficult to arrange if the turbine runner is submerged below the tailwater elevation.

CASE 2.

This powerplant contains one horizontal francis turbine rated 5000 kW and operating under a head of 85 m and at a speed of 514 rpm. During commissioning pulsations were noted at wicket gate openings below 50 % and in a narrow band around 85 - 90 %. The maximum pressure pulsation amplitude was approximately +/- 7 % of total head. It was

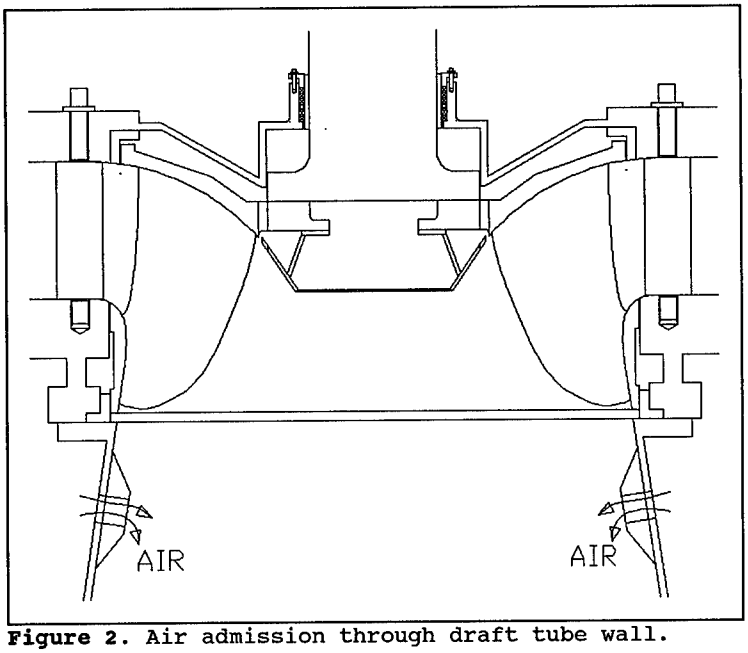

Figure 2. Air admission through draft tube wall.

interesting to note that the pulsations disappeared at 100 % gate opening.

The frequency of the pulsation corresponded very well with the natural frequency of the penstock. After a load rejection the penstock pressure would oscillate with the same frequency as the pulsation.

This powerplant employs a penstock that was built a long time ago and the current strength was not known in detail. Even though the pulsation amplitude was not considered detrimental to turbine or generator equipment, a solution was sought to the problem due to the uncertainties about the penstock.

First attempt: In a first attempt to reduce the pulsation, air was admitted through the head cover and the runner unloading holes to the draft tube (see fig. 3). As mentioned in the introduction this is not the optimum place to discharge the air in the draft tube, but good results had been obtained with this method at other sites. Unfortunately, very little improvement was noted at this site.

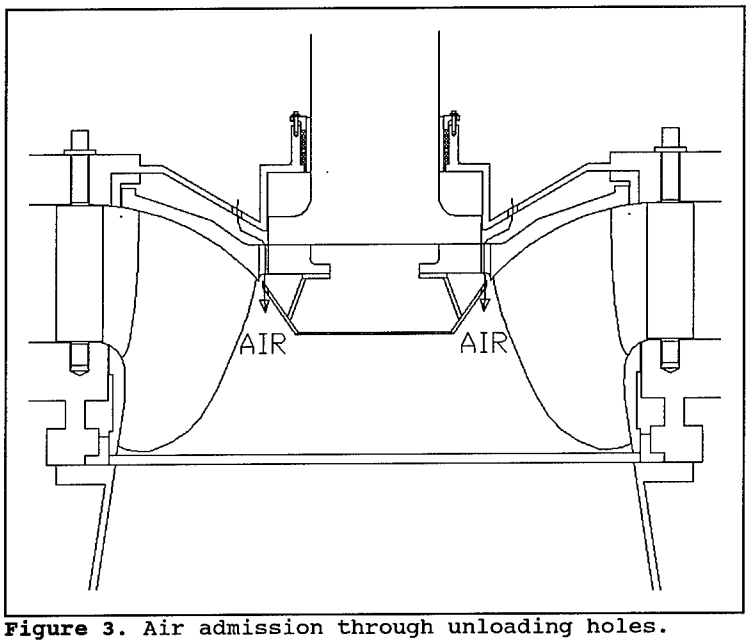

Figure 3. Air admission through unloading holes.

Second attempt: Next step was to connect an air compressor to the air inlet manifold. This allowed a larger amount of air to be injected into the draft tube. A reduction of the pulsation amplitude with up to 40 % was noted. However, this method did not completely eliminate the problem. As the air compressor was costly and would require a continuous supply of power to operate, it was decided not to make this installation permanent.

Third attempt: After the air admission approach had been investigated, attention was shifted to mechanical means. A special winged nosecone (see fig. 4) had been investigated in the Kvaerner laboratory and also applied on prototype turbines with great success. Model tests had even shown an increase in efficiency at part load and overload. Such a nosecone was designed and installed in the turbine. After installation the range of gate openings at which pulsations occurred become narrower, but the maximum pulsation amplitude was essentially unchanged.

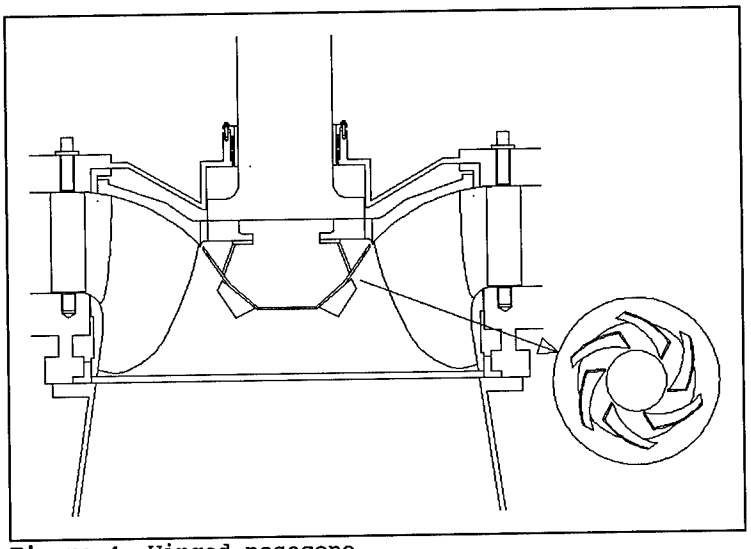

Figure 4. Winged nosecone.

Fourth attempt: In a final effort to alleviate the problem four straightening fins were installed in the draft tube (see fig. 5). This approach had been reported to be quite successful in several cases. Again, the effort was met with only a partial success. Pulsation amplitude was decreased in the low gate range, but maximum pulsation amplitude in the high gate range was still essentially unchanged.

The final outcome of the exercise was to avoid operation in the now fairly narrow range where pulsations occurred.

Conclusions: It is interesting to note how techniques that had been well proven in the laboratory and at other installations failed to give the desired results at this particular site. This case illustrates well the fact that pulsation problems are very difficult to predict and model.

Case 3.

This powerplant contains two horizontal francis turbines rated at 2,000 kW and 1,000 kW respectively. They operate under a head of 119 m and at a speed of 1200 and 1800 rpm respectively. The powerplant is connected to a long penstock.

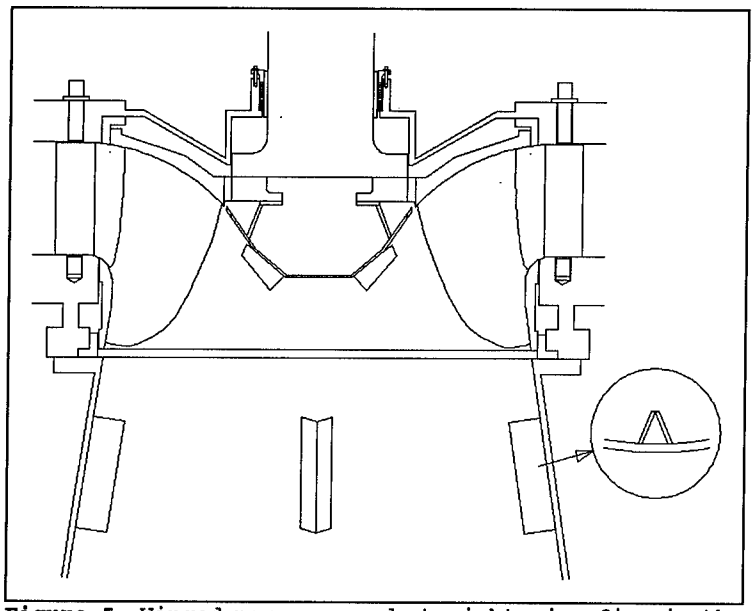

Figure 5. Winged nosecone and straightening fins in the draft tube.

During commissioning this plant showed pulsation problems in the part load range. To introduce air into the area below the turbine runner a structure was installed in the draft tube. This structure basically consisted of a pipe through the draft tube that ended just below the runner. The pipe was secured to the wall of the draft tube by four vanes. Outside the draft tube was a valve so the air flow could be regulated. See fig 6.

This arrangement permits air to be introduced at the most effective way below the runner. When the air valve was opened the pulsations disappeared as expected.

However, one disadvantage with the draft tube structure is that it disturbs the flow in the draft tube and lowers the overall efficiency of the units. Theoretical estimates pointed towards approximately one percent decrease in efficiency. Tests made on other turbines with similar structures point towards losses of the same magnitude. It should also be emphasized that care must be taken in the design of the structure inside the draft tube. It is subject to cavitation and large fluctuating hydraulic forces.

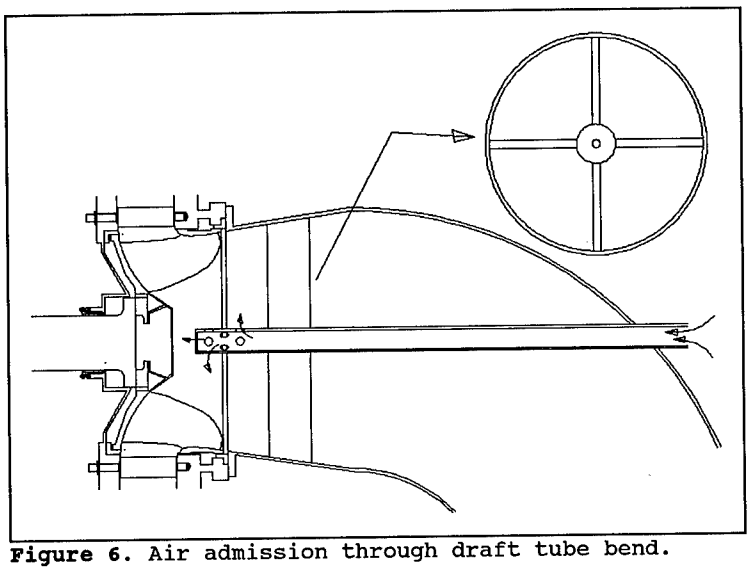

Figure 6. Air admission through draft tube bend.

During testing of the units complete efficiency measurements were made. To determine the effect of the introduction of air, measurements were taken both with the air valve closed and the air valve open. The measured efficiency varied between a 0.2% decrease to a 0.2% increase. This was well within the accuracy of the test. It was concluded that the introduction of small amounts of air does not have a measurable effect on turbine efficiency.

In this context it may be mentioned that accurate tests by Vattenfall Utvecking AB at a 100,000 kW unit showed a small increase in efficiency at medium load (0 - 0.3 %) and a small decrease in efficiency at high load (0.3 - 0.5 %).

Conclusions: To solve the pulsation problem it is possible to introduce air to the area below the runner by means of a structure in the draft tube. However, this structure itself may decrease turbine efficiency. The introduction of small amounts of air has very little impact on turbine efficiency.

Case 4.

This powerplant contains one vertical francis turbine rated at 72,200 kW and operating under a head of 89 m and at a speed of 200 rpm.

During commissioning of the turbine power swings were noted in the high load range. It was determined that the power swings were unacceptable to the grid. The wicket gate opening was therefore limited. When the units were tested it was discovered that they did not meet the output guarantee with the gate limitation in place. Air was then admitted to the turbine, but this had only marginal effect on the pulsations.

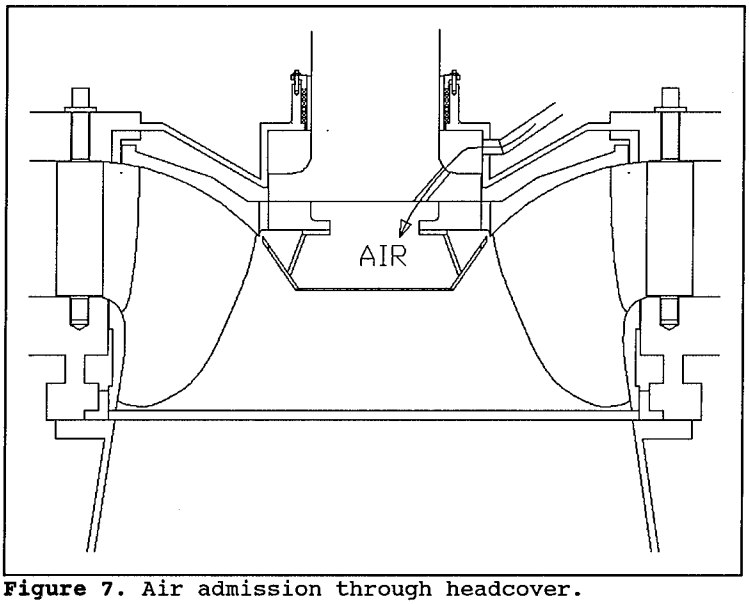

Figure 7. Air admission through headcover.

The turbine had an air admission system consisting of pipes from the head cover to an area just below the stuffing box. The air was then conducted through holes in the shaft flange to the area below the runner hub (see fig. 7). A non-return valve in the pipes secured that no water leakage occurred into the power station.

This system appears to be very similar to the normal air admission system shown in fig 1. However, some notable differences exist. During one phase of the pulsation

cycle water flows back through the piping. When the runner rotates, the water in the shaft and the area below the seal will rotate with it. This rotation will cause an increase in pressure due to centrifugal forces. In addition, the flow path from the headcover to the runner center is quite complicated. The water flow may experience significant resistance on its way back and fourth during a pulsation cycle. Both these effects may decrease the amount of air that can be drawn to the runner.

Fortunately, this turbine was prepared for air admission in the normal way. When the hole through the shaft was opened the pulsation amplitude decreased and it was now possible to remove the limitation on wicket gate opening. After these modifications the turbine met the guarantees.

Conclusions: This case shows that even minor deviations from the proven air admission design may give unsatisfactory results. The system with air admission through the head cover may have certain advantages (like being more compact and not necessitating a hole through the shaft) but in the end it did not have the desired effect.

References:

Rheingans, W.J., Power Swings in Hydroelectric Power Plants, Published in Transactions of the ASME, April 1940, pp 171 - 177.

AN IMPROVED FISH SAMPLER AT CABOT STATION

John R. Whitfield[1], George E. Hecker[2], and Thang D. Nguyen[2]

ABSTRACT

Fish mortality encountered with a preliminary sampling screen at the Cabot Station log sluice led to a detailed hydraulic model study and the development of a new fish sampler. Results of the model study and the positive experience with implementing and operating the new sampler in the fall of 1992 are described.

INTRODUCTION

The Turners Falls Hydroelectric project, located on the Connecticut River in northeastern Massachusetts, was constructed between 1905 and 1915. The project is operated by the Western Massachusetts Electric Company, a subsidiary of Northeast Utilities, and consists of the Turners Falls Dam, an adjacent canal gatehouse structure, a 2.1 mile long power canal, and two hydroelectric plants on the canal (Figure 1). Cabot Station is located at the downstream end of the power canal and contains six vertical shaft Francis units with a total nameplate rating of 51 MW at a flow of 12,500 cfs.

For upstream fish migration, fish ladders were constructed in 1980 adjacent to Cabot Station and the Turners Falls dam. More recently, efforts have concentrated on providing downstream fish passage around the turbines. At Cabot Station, the existing log sluice, a curved 180 ft long concrete structure and flow control gate located at the south (downstream) end of the plant, needed to be tested as a potential powerhouse bypass. The goal of the bypass facility at Cabot Station is to pass downstream migrating fish around the turbines without inducing fish mortality. Anadromous species of concern include Atlantic Salmon, American Shad, and Blueback Herring. To determine the efficiency of the log sluice as a bypass, a first attempt at a sampling and counting facility was made in the summer of 1991.

---

[1] Northeast Utilities Service Company, Hartford, Connecticut
[2] Alden Research Laboratory, Inc., Holden, Massachusetts

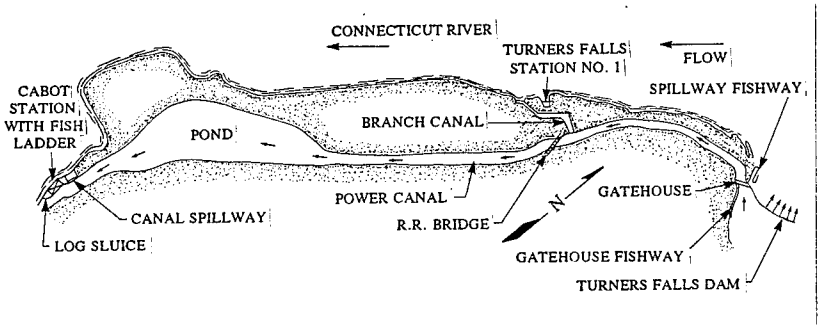

FIGURE 1 TURNERS FALLS PROJECT AND CABOT STATION (PLAN)

For fish sampling, an inclined woven, metal wire screen (referred to as the preliminary sampler) was installed in the upstream end of the log sluice. The preliminary sampler was tested in the fall of 1991 and was found to cause excessive mortality of juvenile clupeids. The problem appeared to be related to adverse hydraulic conditions on the log sluice sampler during sampler operation, as evidenced by very turbulent, impinging flow patterns (Figure 2). To improve flow conditions and to address sampling needs, the Alden Research Laboratory, Inc. (ARL) conducted a detailed physical model study of the log sluice and sampler. The goal of this study was to determine if hydraulic improvements to the sampler could be made so as to significantly reduce sampling mortality while maintaining the ability to individually sample at the log sluice and the adjacent trash trough. The model study lead to a new fish sampler design, which was installed and operated in 1992. This paper describes results of the model study and the positive experience with the new sampler during the fall of 1992.

MODEL STUDY

General Description: A hydraulic 1:7 scale model of the Cabot Station log sluice and the existing fish sampling facilities was constructed and tested based on Froude similitude at ARL. Due to super critical flow in the inclined log sluice, only the upstream third of the log sluice containing the sampling structure needed to be modeled. A sufficient upstream area (about 100 x 80 feet) of the canal forebay and the adjacent powerhouse intake structure was included to ensure similar approach flow conditions near the log sluice entrance. Most testing was performed with the model upstream pool kept constant at "normal canal" condition.

Since flow through the powerhouse units would have no practical effect on flow conditions within the log sluice sampler, no flow through the units was simulated. However, a portion of the powerhouse trash trough, including the outlet onto the log sluice, was modeled. Efforts were made to reproduce flow conditions within the trash

trough and the pattern of discharge into the log sluice sampling flow. The typical log sluice sampling flow during the 1991 sampling condition was about 200 cfs. This flow was controlled by a 16 ft wide log sluice gate lowered 2.5 ft below the canal water surface, followed by a bulkhead gate with a 5 ft wide vertical slot (see Figure 2). Field velocity measurements performed by plant personnel indicated an average flow of about 80 cfs through the fully open trash trough.

Modeling of flow conditions at and through a porous screen requires that the model and prototype screens have the same head loss coefficients. This will be true if the screens have the same geometry, percent open area, and relative effect of viscous versus inertial forces. The latter factor was considered by selecting a large model scale ratio to achieve a sufficiently high Reynolds number based on the screen bar (wire) dimension. The first two factors were considered by using the actual prototype screens, the wire or bar members still being small enough compared to other geometrically scaled members. Structural support members below the screen were modeled to cause the same percent area blockage. In this way, the relative magnitude of flow remaining on the screen versus that passing through the screen was properly simulated.

The preliminary sampler consisted of a metal grating topped by a 1/4" square mesh wire screen. For the new sampler, preference was given to a wedge-wire type screen based on favorable experience with other fish guidance projects (Ref. 1, 2,). Advantages of the wedge-wire screen include a smooth screen surface, less clogging with debris, and commercial availability at different porosities. Three screen porosities (18, 30, and 57% open area) were tested to develop the final design, all with a bar width of 2.4 mm and spacings of 0.5, 1.0, and 3.2 mm, respectively. A detailed description of the model and testing procedure is given in Ref. 3.

Testing of Preliminary Sampler: The model was first tested with the preliminary sampler installed under the same conditions as during the 1991 fall sampling. The original sampler, consisting of a 32 ft long screen section preceded by a 6 ft long solid plate fitting inside the 16 ft wide log sluice, was hinged about a downstream axis so that its upstream end could be lowered onto the log sluice bottom when in use (Figure 2). A fish collection trough, one half of a 2.5 ft diameter pipe, was attached to the downstream end of the screen to provide a flow connection to the fish counting station. Flow was set by lowering the main sluice gate 2 to 2.5 ft below the normal canal water surface. To restrict the sampling flow to the middle, a bulkhead gate with a 5 ft wide vertical slot was added upstream of the sampler, but downstream from the main sluice gate.

Comparison of model flow patterns with a video taken at the prototype of the original sampler indicated that the model satisfactorily reproduced the major prototype flow features. Figure 3 shows a photograph of the model with sampling flow through both the log sluice bulkhead gate and the adjacent trash trough entering from the side. Sampling flow from the vertical slot of the bulkhead gate splashed at steep angles onto the concrete log sluice floor, creating very turbulent flow conditions near the upstream end of the fish sampler including a boil upstream from the nappe impact zone. The flow situation was aggravated with simultaneous trash trough flow. Due to the lateral impact

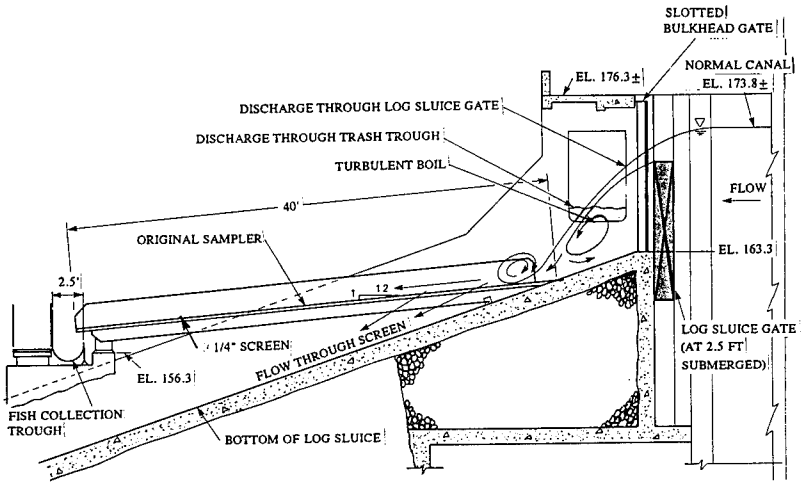

FIGURE 2 SCHEMATIC OF PRELIMINARY SAMPLER IN OPERATION

FIGURE 3 MODEL FLOW CONDITION AT PRELIMINARY SAMPLER

of the trash trough discharge, the main sampling flow was deflected and splashed intermittently over the left side wall of the sampler. In general, water did not reach the downstream portion of the sampler, leaving fish to move along the dry, inclined screen. Clearly, these flow conditions were unfavorable for fish passage and may have contributed to the fish mortality experienced in the field.

Development of New Sampler: It was clear that sampling flow conditions at the log sluice could only be substantially improved by reducing the water fall height from the canal to the log sluice entrance, and by minimizing the impact of the lateral trash trough discharge on the log sluice flow. Since it was desired not to use an excessive amount of flow for fish sampling (as this flow would then be lost for power production), the reduction in fall height was best achieved by raising the sampler instead of lowering the sluice gate and using the slot in the downstream bulkhead gate to restrict the sampling flow. The latter option would have required a very narrow vertical slot. As a result, the sluice gate was completely depressed in all subsequent testing, and efforts were devoted to optimizing the geometry of the (downstream) bulkhead opening and the attached screen sampler. Tests were performed with different bulkhead slot openings (width and depth) and raised positions of the sampling screen, using different screen porosity combinations and lateral sampler widths to produce a smooth flow transition over the screen surface to the downstream fish collection device. The testing program was enhanced by input from engineers and fish biologists from NUSCO, Harza Engineering, and from state and federal fishery agencies.

The final design is shown in Figures 4 and 5. It consisted of a horizontal sampler made of a 9 ft long solid plated upstream section followed by a 17.5 ft long porous section made of wedge-wire screen with a 30% open area (bar spacings of 1 mm and top bar width of 2.4 mm). The screen surface was 4 feet below the normal canal water level, and the upstream end of the sampler was level with the bottom of the 11 ft wide and 4 ft deep bulkhead slot. The width of the sampler (between side walls) was contracted in the flow direction to maintain just enough flow at the downstream end of the screen to allow a smooth flow transition into the fish collection trough, in turn leading to the fish counting facility. The collection trough consisted of three fourths of a 1.75 ft radius pipe, and it was considered that various degrees of porosity may be constructed into the pipe to control the water depth.

To allow separate sampling through the trash trough, an inclined wedge-wire screen of 57% porosity was installed in the trough outlet at an angle of 20 degrees to the horizontal, connecting the invert of the trough with the solid plated portion of the log sluice sampler. The bulk of the trash trough flow passed through the screen underneath the main sampler, while the fish and some water flowed over the top of the screen and could be conducted separately from the log sluice sampling flow to the fish counting station.

As illustrated in Figures 4 and 5, model testing of the final design indicated reasonably smooth, and unidirectional flow over the entire sampler and screen surface, conditions which were considered favorable for fish passage and sampling. The water

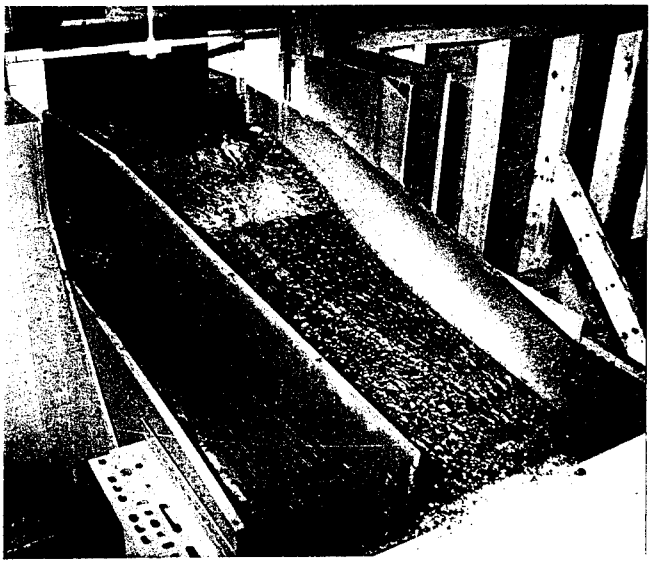

FIGURE 4 MODEL FLOW CONDITION AT NEW SAMPLER

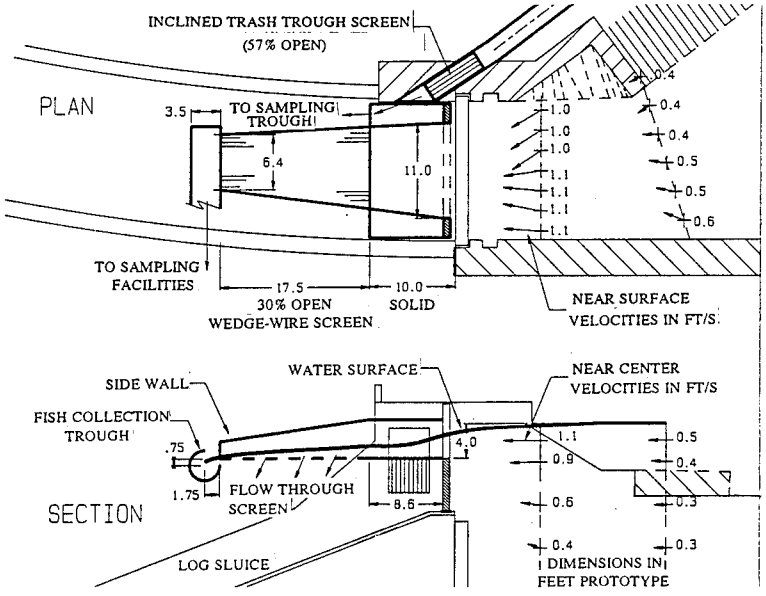

FIGURE 5 DETAILS OF THE NEW SAMPLER (FROM MODEL STUDY)

depth above the sampler typically dropped from 2.5 to 3 feet near the log sluice entrance to about an inch at the downstream end of the screen, resulting in a steady discharge of about 5 cfs into the fish collection trough out of a total sample inflow of 210 cfs through the log sluice opening. A comparable view of the prototype is shown in Figures 6 and 7. With the screened trash trough in operation, a sampling flow of 2 cfs over the top of the inclined screen was indicated, out of a total trash trough flow of about 60 cfs.

To obtain information on flow velocities in the forebay and near the log sluice entrance, relative to fish attraction, velocity measurements were made in the model in the approach region of the log sluice and over the sampler. Results of typical approach velocities measured near the water surface (averaged over a depth of 4 ft) are indicated as vectors in Figure 5. For normal canal conditions, near surface velocities upstream of the log sluice entrance were about 0.4 to 1 ft/s, while velocities over the upstream end of the sampler ranged from 3 to 10 ft/s (prototype).

FIELD INSTALLATION

The final proposed fish sampler design that was developed at the Alden Research Laboratory was immediately forwarded to the Harza Engineering Company in the spring of 1992 for development of engineering/construction drawings. In order to install and test the new facility prior to the fall 1992 migration of juvenile clupeids, engineering and construction had to be expedited. As a result, NUSCO opted to receive engineering drawings in partial shipments and started the steel fabrication process without detailed shop drawings. This approach was successful due to the close working relationship NUSCO maintained with the fabrication/construction contractor and the outstanding fabrication expertise which this contractor demonstrated. Efforts were made to reutilize the main structural members of the preliminary sampler in the construction of the new sampler.

Construction of the new sampling facility began in mid June 1992 and was completed by early September of the same year. The most challenging aspects of the construction included foundation installations on a 45 degree angle slope with various encounters with buried water mains and electrical conduits. In addition several outages of overhead 13,000 volt electrical distribution lines were required to accommodate the installation of major structural members.

FIELD TESTING

The sampling facility was initially field tested in early September 1992 and overall, testing proceeded nearly flawlessly. Some impingement was experienced on the wedge-wire screen in the trash trough, possibly because the angle of the screen was too steep. Field adjustments were made to minimize impingement in the trash trough and further improvements to the design of that lateral screen are planned.

It should also be noted that initial observations of the flow entering the flume at the end of the sampler caused concern to the project biologist. Due to variations in the forebay pond elevation caused by load changes at Cabot Station, the flow exiting the

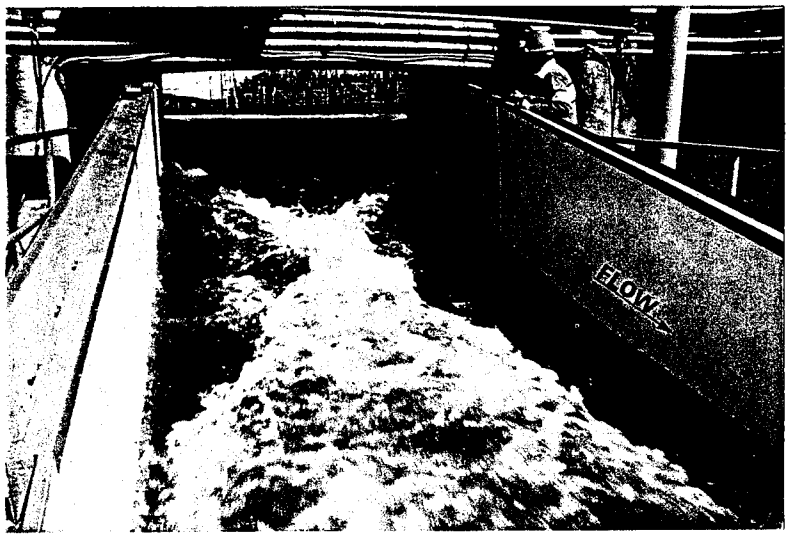

FIGURE 6 NEW SAMPLER IN OPERATION (VIEW LOOKING UPSTREAM)

FIGURE 7 NEW SAMPLER IN OPERATION (VIEW OF DOWNSTREAM END)

sampler screen produced turbulence in the flume. This turbulent flow, however, did not prove to cause any mortality upon close examination of juvenile clupeids that reached the sampling table. In fact, the log sluice sampler was operated from September 15, 1992 through November 3, 1992 with no visible impact to any fish that were counted.

The primary objective of the 1992 juvenile clupeid study was to determine the proportion of juvenile clupeids migrating through the log sluice and the optimum trash trough opening rather than passing through Cabot Station turbines. The data indicated that 88% of the American shad and 94% of the blueback herring emigrating through project works did so by way of the log sluice and trash trough. Most passage was through the sluice; the contribution from the trash trough was small.

An estimated total of 855,200 juvenile clupeids were collected on the sampler during the course of the season. As noted above, incidences of fish mortality or injury on the log sluice sampler were rare. Some fish collected on the sampler were held for use in other studies. Mortality among these fish, which were sometimes held for several days, was about 0.5%.

CONCLUSION

Fish mortality experienced in the fall of 1991 at the preliminary Cabot Station log sluice sampler was attributable to poor flow conditions at the sampler, and prompted a hydraulic model study to allow a rapid assessment of the hydraulic problem and development of a new sampler design. The new sampler, including facilities for separate sampling from the adjacent trash trough and a downstream fish collection and counting station was engineered, designed, constructed, and operationally tested in time for the fall 1992 juvenile shad migration season. The new bypass and sampling system functioned well as is documented in 1992 study results. Within two weeks of operation, over 100,000 fish (mainly juvenile shad) were physically counted passing the new log sluice sampler with no signs of injury or mortality. In comparison, the amount of fish using the adjacent trash trough bypass was insignificant. Based on estimates of the total turbine entrainment rate at Cabot Station from net catches at selected intake bays, the fish count from the new sampling facility yielded a log sluice/trash trough bypass efficiency of over 88 percent. Further sampling is planned for the Spring of 1993 to determine the bypass efficiency of the new sampler with Atlantic Salmon smolts.

ACKNOWLEDGEMENT

The authors would like to thank C.P. Ruggles (Fishery Consultant) for his input during various stages of the study.

REFERENCES

1. F.C. Winchell, and C.W. Sullivan, "Evaluation of an Eicher Fish Diversion Screen at Elwha Dam", Proceedings of the Waterpower 91 International Conference, Vol.1, pp. 93-102, Denver, Colorado, July 24-26, 1991.

2. Harza Engineering Company and RMC Environmental Services, "Turners Falls Downstream Fish Passage Studies / Downstream Passage of Juvenile Clupeids, 1992", 2/3 Draft report , pp. 35-38.

3. T.D. Nguyen, and G.E. Hecker, "Hydraulic Model Study of the Cabot Station Log Sluice Fish Sampler", Report 154-92/M295F, Alden Research Laboratory, Holden, Massachusetts, September 1992.

DEBRIS REMOVAL FROM A LOW-VELOCITY, INCLINED FISH SCREEN

By F. A. Locher[1] M. ASCE, P. J. Ryan[2] M. ASCE, V. C. Bird[3], and P. Steiner[4]

Abstract
An air backwash system for the Potter Valley Intake Inclining Horizontal Fish Screen Facility was developed through testing of a prototype section of the screen in a test flume located at the project site. Effects of sparger pipe spacing, sparger hole configuration, duration of air burst, and type of debris were investigated. The test program and development of the final configuration of the sparger system are described in this paper.

1. 0 Introduction

The Potter Valley Hydroelectric Project, located near Potter Valley in Mendocino County, California, is owned and operated by Pacific Gas and Electric Company (PG&E). This 9.2-megawatt project was completed in 1928 and provides both irrigation water and power to Potter Valley. In order to comply with regulatory requirements for screening fish at the intake, a state-of-the-art Inclining Horizontal Fish Screen Facility has been developed. Cleaning these large screens was of particular concern because the site is unattended, and a reliable, automatic cleaning system was required to handle significant quantities of floating debris. The experimental testing of a full-scale section of the screen to develop a

1 Chief Hydraulic Engineer, Geotechnical and Hydraulic Engineering Services, Bechtel Corp., P. O. Box 193965, San Francisco, CA 94119
2 Chief Hydrologic Engineer, Geotechnical and Hydraulic Engineering Services, Bechtel Corp., P. O. Box 193965, San Francisco, CA 94119
3 Civil Engineer, Hydro Engineering & Construction, Pacific Gas & Electric Company, One California St., San Francisco, 94106
4 Principal, Steiner Environmental Consulting, P. O. Box 250, Potter Valley, CA 95469

satisfactory air-backwash system for the Potter Valley Inclined Horizontal Fish Screen Facility is presented herein.

2.0 System Description

Cape Horn Dam, located on the Eel River in North-Central California, forms Van Arsdale Reservoir. The reservoir is small and the project operates as a run-of-the river project with flows regulated by an upstream dam and reservoir. The Potter Valley Hydroelectric Project diverts up to 310 cfs through the intake in Van Arsdale Reservoir passes the flow through a tunnel and penstock and delivers the flow to the Potter Valley Powerhouse. Releases from the power house are used for irrigation in Potter Valley; excess flow is returned to the Russian River at Lake Mendocino.

As part of the relicensing requirements, PG&E modified the original intake in 1972 and installed a vertical "Bates" traveling screen. Heavy debris loading during flood periods and accumulation of bed-load material at the intake resulted in continuous malfunctions and extensive maintenance. Because of the poor performance in screening fish and excessive operating cost, the "Bates" screen was taken out of service in 1976.

In order to comply with the regulatory requirements for an operating fish screen at the site, PG&E began a major program for design of a new fish screen facility. Figure 1 depicts an isometric view of the Inclined Horizontal Fish Screen Facility for the Potter Valley Intake. This facility was developed by PG&E in close cooperation with the California Department of Fish and Game (CDF&G), the U.S. Fish and Wildlife Services (USFWS), and the National Marine Fishery Services (NMFS). The basic criteria governing the design of the screen itself were:

1. **Velocity**. CDF&G criteria require that the maximum discharge through the screen shall not exceed 0.33 cfs per square foot of screen opening. This is equivalent to an average approach flow velocity normal to the screen of 0.33 ft/sec.

2. **Screen**. The screen shall be wedgewire screen with 3 mm (1/8") openings between wires, and the wedgewires shall be oriented perpendicular to the flow. CDF&G criteria state that the "screens shall have a minimum open area of 1.5 square feet per cubic foot/second." When combined with the approach flow velocity criterion, this implies that the screen porosity should be 50%. A range of 40 to 60% was deemed acceptable.

The approach flow velocity criterion requires that the minimum screen

area be 87 m^2 (310 cfs/0.33 ft/sec = 940 ft^2.). The need for such a large screen area, the restricted space available, the necessity to handle significant debris, and the requirements for minimum operating costs led to the design shown in Figure 1. This new intake structure will be located directly over the existing tunnel to Potter Valley Powerhouse.

As indicated on Figure 1, the structure consists of two bays aligned at approximately 135° to the direction of flow in Van Arsdale Reservoir. A hydraulic model study was used to develop a guidewall to provide a uniform approach flow to the screens for the full range of operating conditions. The fish screens are designed to operate when the flow in the Eel River is less than 212 m^3/s (7500 cfs). In the fish screening mode, flow passes over a gravel trap, through a set of bar screens and into the fish screening bays as illustrated in Figure 1. A maximum flow of 8.78 m^3/s (310 cfs), or 4.39 m^3/s (155 cfs) per bay, will be screened. Approximately 0.23 m^3/s (8 cfs) per bay will be used to bypass fish and debris. When flows in the Eel River exceed 212 m^3/s (7500 cfs), the flow will be bypassed through the gravel trap and directly into the power tunnel.

The fish screens will be mounted on an 24 m (80 ft) long steel frame which will be adjustable between approximately 7° and 11° to maintain a constant depth of flow at the outlet into the fish pump chamber. Adjusting the angle of the screen allows for a 1.2 m (4 ft) variation in the water level in Van Arsdale Reservoir.

The fish screens will be constructed of Hendricks B9 wedgewire screens with the bars oriented perpendicular to the flow as required by CDF&G and USFWS. The screens will be mounted 229 mm (9 ") above a series of perforated plates whose porosity is varied to maintain a uniform flow through the screens. The variation in porosity of the perforated plates was determined using a hydraulic model of the intake structure and fish screen facility (Locher et. al., 1993).

3.0 Debris Removal

Debris loads at the existing intake in Van Arsdale Reservoir vary significantly in composition and quantity throughout the year. Deposition of debris could lead to non-uniform distribution of flow through the screen, or hot spots where the through-screen velocity could exceed the CDF&G velocity criteria. Operation and maintenance costs for cleaning the large screen area of approximately 112 m^2 (1200 ft^2) were also of particular concern. Since the intake is at a relatively remote location, it was concluded that a reliable, automatic method of cleaning the screen was necessary, particularly in view of the fact that spring or summer freshets could bring significant quantities of debris to the structure day or night.

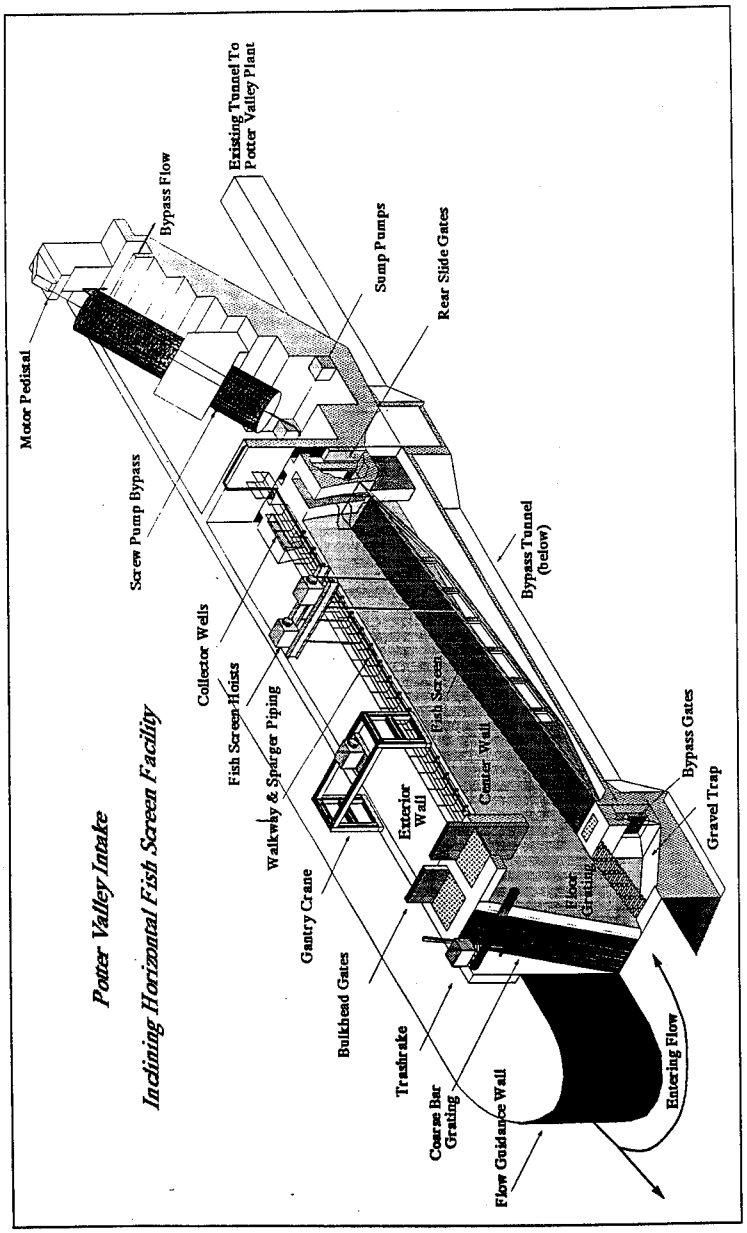
Potter Valley Intake
Inclining Horizontal Fish Screen Facility
Motor Pedistal
Screw Pump Bypass
Bypass Flow
Existing Tunnel To Potter Valley Plant
Sump Pumps
Rear Slide Gates
Collector Wells
Fish Screen Hoists
Walkway & Spargar Piping
Gantry Crane
Bulkhead Gates
Trashrake
Coarse Bar Grating
Flow Guidance Wall
Fish Screen
Center Wall
Exterior Wall
Floor Grating
Bypass Tunnel (below)
Bypass Gates
Gravel Trap
Entering Flow

In late spring and summer, the principal debris problem is caused by filamentaceous algae, moss, and aquatic grasses which grow profusely during this period. The existing trashracks at the present intake are especially difficult to clear of the filamentaceous algae. Debris in the fall consists of leaves, long pine needles, twigs, branches, some remnants of filamentaceous algae and aquatic grasses.

Several mechanical means of cleaning the screen were considered, including various arrangements of scrapers, brushes, and modified rakes. None of these alternatives met criteria for simplicity in construction, ease of operation, and overall reliability. It was concluded that an air backwash system would be the most satisfactory method of cleaning the screens. The principal advantages of the air-backwash system were the following:

1. There was a minimum of moving parts. The basic system is a passive set of pipes with solenoid-operated valves. All of the valves would be above the water surface and easily accessible.

2. There was no mechanical system that could harm the fish during the cleaning cycle.

3. A programmable controller would allow for complete flexibility in operating and changing the system to meet varying debris loads.

4. All operating equipment such as compressors, valves, and control equipment would be above the water surface and easily accessible for maintenance.

Although there was a precedent for using an air-backwash system at Twin Falls, located on the South fork of the Snoqualmie River in the State of Washington (Ott and Jarrett, 1992), there were several major differences between the two sites:

1. The Twin Falls screen operates at a fixed angle of 4° from the horizontal, whereas the Potter Valley screen angle varies between 7° and 11°.

2. The through-flow velocity at Twin Falls is 0.15 m/s (0.5 ft/sec) compared to the 0.1 m/s (0.33 ft/sec) at Potter Valley.

3. The sweeping component, or flow parallel to the screen is 1.2 m/s (4 ft/sec) at Twin Falls compared to 0.3 m/s (1.0 ft/sec) at Potter Valley.

4. The screen wedgewires are oriented parallel to the flow at Twin Falls, but are perpendicular at the Potter Valley facility.

5. The characteristics of the debris differ with the debris at Twin Falls consisting primarily of leaves and organic material in the fall.

In view of the uncertainties associated with design of an air backwash system, it was concluded that a series of tests should be conducted on a full-scale section of the prototype screen. The principal objectives of the tests were the following:

1. To establish the spacing of the sparger pipes.

2. To determine the size and configuration of the holes in the sparger piping.

3. To investigate the effects of the duration of the air burst and the operating pressure on cleaning the screen.

4. To study the effect of screen angle on the performance of the backwash system.

5. To evaluate the relative performance of various configurations using debris from the Eel River for test material, thus providing some confidence in the expected performance under actual debris conditions.

4.0 Test Facility

4.1 Flume The test facility was constructed at the existing intake in Van Arsdale Reservoir by Steiner Environmental Consulting of Potter Valley. The intake location was selected because of the readily available supply of water, but especially because of the ease with which debris from the Eel River could be obtained.

The test facility consisted of a flume 781 mm (2.56 ft) wide, 14.63 m (48 ft) long and walls 1.82 m (6 ft) high. A viewing section 4.88 m (16 ft) long was constructed with lexan panels in the wall of the flume. Water was pumped from the Potter Valley intake structure, passed through the flume and discharged back to Potter Valley Reservoir. A once through system was chosen because of the extensive tests with large quantities of debris.

4.2 Screen

The test screen was a section of Hendricks B9 wedgewire screen with 3 mm (1/8") openings between the wedgewires, and the wedgewires oriented perpendicular to the flow. The screen was 6.4 m (21 ft) long, 762 mm (2.5 ft) wide, and could be raised and lowered to change the angle of the screen with the horizontal. The screen was mounted on the top of a

truss 229 mm (9") deep. Plywood panels were mounted on the lower chords of the truss; holes were drilled in the plywood to provide a variable porosity.

Four sections, each 1.2 m (4 ft) long were used to test the air-backwash systems. Interior baffles were installed to divide the screen into compartments. Division of the prototype screen into compartments is necessary because of the varying porosity of the perforated plates under the screen required to maintain uniform flow through the screen. Without the subdivided into compartments, short-circuiting would occur. A sketch of the test screen is shown on Figure 2.

4.3 Air Supply

Tests of the screens for the Twin Falls Project indicated that a volume of air equal to the volume between the screen and the perforated plate was required for an effective backwash system. On this basis, four air tanks with a volume of 0.57 m^3 (20 ft^3) each were fabricated. Each tank supplied one 1.2 m (4 ft) test compartment. The valves and piping were arranged so that more than one tank could be connected to one test section if required. The tanks were pressurized with a portable air compressor prior to testing. Test pressures up to 758 KPa (110 psig) were used.

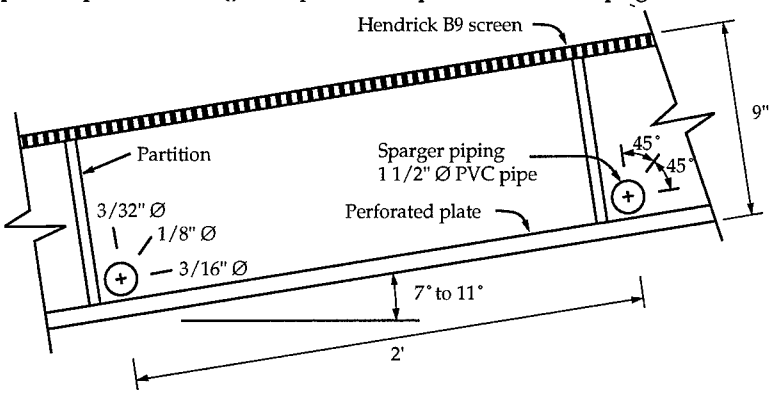

Figure 2. Final Configuration of Sparger Piping

5.0 Development of System

5.1 Preliminary Tests

The initial size and spacing of the sparger holes was 4.8 mm (3/16") diameter on 51 mm (2") centers, based on the configuration of the Twin Falls system (Ott and Jarrett, 1992), with the sparger pipes spaced on 610 mm (2 ft) centers. The principal objectives of the tests were to study the effects of the duration of the air blast, the influence of porosity of the perforated plates, the size, number, and orientation of the sparger holes,

the effect of the screen angle, and the type of debris on the performance of the backwash system.

Virtually all of the testing was qualitative. The flow rate and approach-flow velocity distribution were determined with a Marsh-McBirney electromagnetic current meter to establish prototype velocities in the test facility. A video camera was used to record each test. Upon completion of a test series, the video was viewed frame by frame on site with a monitor. Comparisons with previous tests were made and modifications made to the test apparatus. It would have been virtually impossible to make rapid judgements on the relative merits of the various configurations without the slow-motion, frame by frame analysis using the video.

Tests were conducted with and without debris. Tests without debris were run to determine whether the air blast would satisfactorily cover the panel and to quickly eliminate unsatisfactory arrangements.

The initial tests were run with an arrangement similar to the Twin Falls air backwash system. The results were not satisfactory primarily because of the orientation of the wedgewire screens. With the wedgewires oriented perpendicular to the flow, the wedgewires acted like a series of turning vanes. Thus, when the jet from the air sparger hit the screen, it was immediately turned through almost 90° and exited normal to the screen. With the wedgewires parallel to the flow at Twin Falls, there was apparently considerable carry-over of the backwash effects from one sparger pipe to another due to the fact that the jet was not turned normal to the screen. Debris tests at Potter Valley showed that there were dead areas between the sparger pipes where debris was not removed from the screen. Consequently, a different configuration had to be developed.

5.2 Developmental Tests

A series of different configurations with different orientation and size of sparger holes and sparger pipe spacing were run. The following results were obtained:

1. Jetting action is essential to removal of debris. Several configurations based on the idea that filling the space between the screen and perforated plate and letting buoyancy lift the debris off the screens was unsuccessful. The jets must act over the entire screen area.

2. A hole size of 4.8 mm (3/16") provided the best performance for one row of holes. Three rows of holes of different sizes were required to cover the screen with a jetting action.

3. The removal of the debris is accomplished primarily in the first few seconds. A one second burst is too short, two seconds is not entirely satisfactory, and three seconds appeared optimum. A longer burst often resulted in recirculation through the screen which brought debris back to the screen, and running the system to steady-state definitely gave poor results. The initial entrainment of water and air, followed by a violent bursting action through the screen was most effective.

4. An initial air pressure greater than 690 KPa (100 psig) gave significantly better debris removal than pressures less than 690 KPa (100 psig).

5. The effect of changing the angle of the screen had a significant effect on the trajectory of the air-water jet. Consequently, what was the optimum alignment of the sparger holes at 7° often left a dead area at 11°.

6. A 1.2 m (4 ft)long compartment appeared marginally satisfactory, but compartments 610 mm (2 ft) long with one sparger pipe per compartment were a significant improvement. A divider wall was necessary for each sparger pipe to prevent interference between one section and the next, so that using 1.2 m (4 ft) long compartments and reducing the number of sparger pipes and interior baffles was unsuccessful.

7. The porosity of the perforated plate did not have a significant effect on the performance of the system because it is only the initial transient burst, entraining the volume of water between the screen and perforated plate, that is effective in removing debris.

5.3 Final Configuration and Tests

The final layout consists of 38 mm (1-1/2") diameter PVC pipe spaced on 610 mm (2 ft) centers as shown on Figure 2. There are three rows of sparger holes, the first row aligned with the perforated plate, the second at 45°, and the third at 90°. The hole sizes are 4.8 mm (3/16") in the first row, 3 mm (1/8") at 45°, and 2.4 mm (3/32") in the row at 90°. Each sparger pipe is located within a 610 mm (2 ft) long compartment. The additional baffles are actually desirable from a hydraulic point of view because they further reduce any problems of short-circuiting the perforated plate.

Final tests were run with a layer of debris 38 to 51 mm (1-1/2 to 2") thick deposited on the screen. The debris consisted of long pine needles, filamentaceous algae, aquatic grasses and leaves. The pine needles seemed to interlock the mass and provide the most tenacious mix of debris. A pressure difference of about 50 to 100 mm (2 to 4 inches) of water was created by this mat of debris. Cleaning was satisfactory; end effects due to the supporting truss were eliminated by making all three holes at the

end of the sparger pipe 4.8 mm (3/16") diameter to provide a better cleaning action. Successive operation of the chambers in sequence from upstream to downstream with a pause of 10 seconds or greater between successive panels moved debris through and out of the screen bay.

Some tests were run with a coat of latex paint on the wedgewires dried tacky to the touch to simulate algal growth. The scrubbing action of the air-water jets successfully removed 90% of the latex paint. We believe that periodic air blasts in the summer months will thus control any algal growth on the screens. Tests were also run with gravel; gravel sizes up to 38 mm (1-1/2 ") were moved up the screen by the backwash system.

6.0 Conclusions

1. An air backwash system will satisfactorily remove debris from the Inclined Fish Screen Facility proposed for the Potter Valley Intake.

2. The orientation of the wedgewires had a significant effect on the design of the sparger system. Three rows of holes oriented as shown on Figure 2 were required to provide the jetting action necessary to clean the screen.

3. Most of the debris removal takes place in the first few seconds. A three-second burst of air was found to be the most effective.

4. An initial pressure of 690 KPa (100 psig) or greater provided the most satisfactory cleaning action.

5. Successive operation of the screen panels from upstream to downstream effectively removal the debris from the screen and screen chamber.

Acknowledgements: Detailed design of the test flume was carried out by Mr. David Menasian of Steiner Environmental Consultants, who also assisted with the test program. Mr. Gene Geary, Fisheries Biologist, Pacific Gas and Electric and Dr. Scott Tu, Civil Engineer, Pacific Gas and Electric also assisted with the testing and evaluation of results.

Appendix - References

Locher, F. A., Bird, V. C., and Ryan, P. J., "Hydraulic Aspects of a Low-Velocity, Inclined Fish Screen", Proceedings ASCE National Hydraulic Engineering Conf., San Francisco, California, July 1993 (to be published)

Ott, R. F. and Jarrett, D. P. , "Air Burst Fish Screen Cleaning System for the Twin Falls Hydroelectric Project", Proceedings Northwest Hydroelectric Association, Portland, Oregon, January 1992

OPERATIONAL LOAD TESTING OF TRAVELING FISH SCREENS

RICHARD VAUGHN[1]

SUMMARY

New longer fish screens are being developed to improve passage of fish at some hydropower projects in the Northwest. The first prototypes were used at McNary Dam in 1991. Testing was performed on the prototypes by Teledyne Engineering Services. The data will be used in the design of 42 permanent screens which will be used at this project. Additional testing will be performed at The Dalles and Little Goose Dams, where more screens will be installed, because differences in turbine flow and turbine intake geometry can lead to large differences in loading.

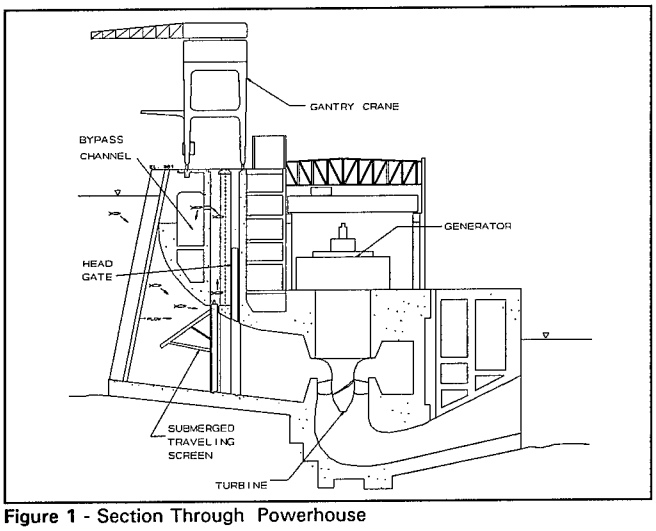

Figure 1 - Section Through Powerhouse

[1]Mechanical Engineer, US Army Corps of Engineers, Hydroelectric Design Center

INTRODUCTION

Background

Screening of turbines at hydropower plants on the Columbia and Snake Rivers has been utilized for the past fifteen years to help rebuild diminished stocks of salmon and steelhead. Juvenile fish originate in fresh water and migrate downstream toward the ocean. Before the screens were installed, these young fish would pass through the turbines where some would be injured or killed due to the pressure differential and water shear forces. The cumulative fish loss when there is a series of dams on the river is large. The screens are used to divert the young fish before they enter the turbine. See Figure 1. The fish are guided by the screens into a bypass channel. From there, they are either released downstream of the dam or loaded onto barges and transported downstream to miss the other dams.

Early investigations into screening of these turbines revealed that most of the juvenile fish traveled in the upper 1/3 of the turbine intake. This led to the design of screens which were 20' long.

There has been an extensive amount of biological testing to measure the screens' ability to guide fish. This testing revealed that at some of the hydropower plants,

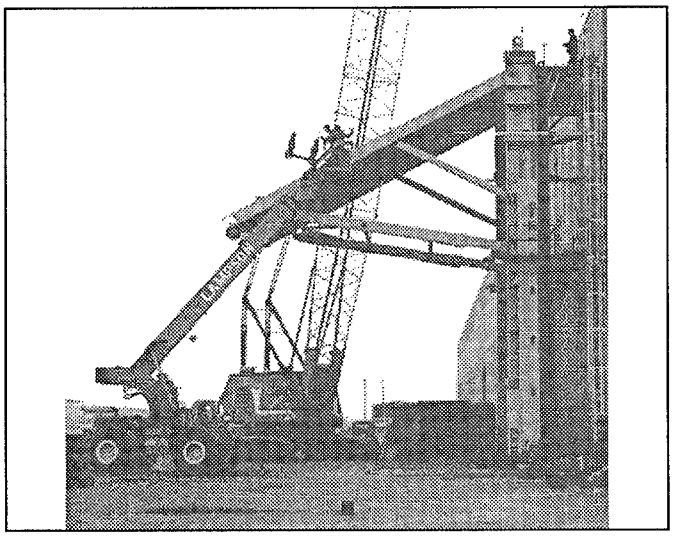

Figure 2 - Submerged Bar Screen

the performance was inadequate. The need arose for screens which were longer than the present ones so that they would guide a greater percentage of the fish. New prototype screens which were twice as long as the old ones were designed and fabricated. These prototype long screens were 40 feet long. See Figure 2.

Two different types of prototype long screens were made for McNary Dam, screens with a stationary stainless steel bar screen (Submerged Bar Screen, Figures 4 and 5) and screens with a rotating polyester mesh (Submerged Traveling Screen, Figure 3). The rotation of mesh on the submerged traveling screen removes debris by backflushing it off as the mesh travels to the back side of the screen. The bar screen uses a mechanical trash sweep to remove debris. A selection of one type of screen will be made based upon the ability to guide fish and keep them free of injuries. Additional prototype screens are being made for Little Goose and The Dalles dams. Based upon the results of the prototype screens and subsequent fine tuning of the designs, it is expected that 144 long screens will be built for The Dalles, McNary, Little Goose and Lower Granite dams by 1998.

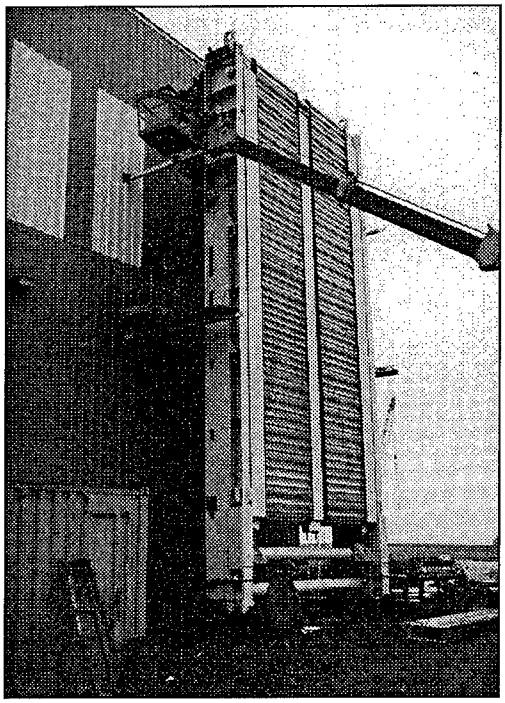

Figure 3 - Submerged Traveling Screen

The loading on the old screens had been previously measured with manometers. This method was inaccurate because the load was dynamic. For this reason, the design loading used, 180 lbs./ft^2, was conservative.

This resulted in a very robust structural design for the original short screens.

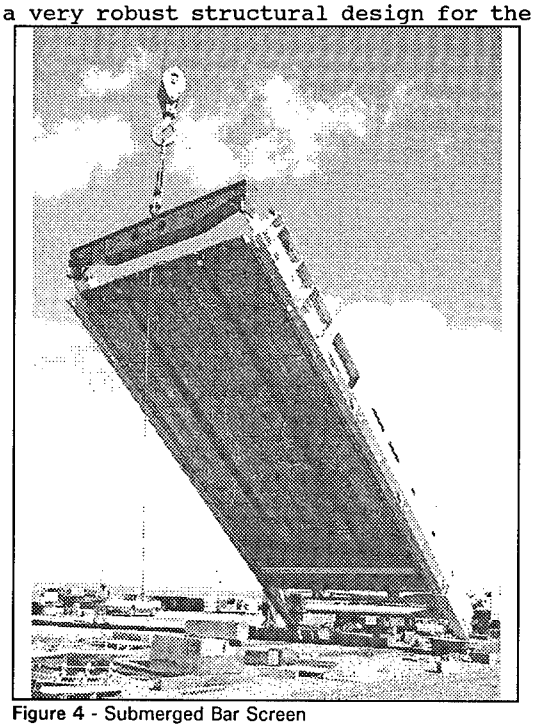

Figure 4 - Submerged Bar Screen

Because the long screens would now block a much larger portion of the turbine intake, the head loss at the screens and thus the structural loading would increase significantly. It was also suspected that vibration would be a major factor. It was imperative that a better way to measure loads be employed. Determination of the loads on the long screens could be done by three methods, 1) numerical modeling, 2) physical modeling, 3) measuring loads on the prototype. Measuring loads on the prototype was the chosen method. The bar screen and polyester mesh are open so most of the water hitting these surfaces passes through. If these surfaces get plugged with debris, the loading will increase. Therefore the screens were tested in both conditions, unplugged and plugged.

Objective

The objective of the testing was to a) measure the reactions where the inner frame of the screen is supported b) measure the torque in the drive shafts of the traveling screen and bar screen c) determine how the load varies over the surface of the screen d) measure vibration of the screen e) determine the natural frequency of the inner frame. This data would be used to make any necessary changes to the design prior to large scale fabrication.

METHOD OF APPROACH

The existing short traveling screens and drawings of the prototype long screens were evaluated for optimum sensor selection and placement to accomplish these objectives. A major factor in the selection process was sensor survivability in the high water flow rates and high turbulence in the turbine intakes. Reliable data transmission from the sensor locations on the screens to the data acquisition station, housed in a trailer on the deck of the powerhouse, was another consideration.

TEST PLAN

Instrumentation was installed on one traveling screen and on one bar screen. The original plan was to install the instrumentation while the screens were fabricated so that they would be ready for testing when they were delivered to McNary Dam. Because fabrication time was very tight, this plan had to be changed. The revised plan called for installation of the instrumentation on-site at McNary Dam after all of the tests for fish guidance were complete.

Each screen was tested in 8 different load cases. The load cases included plugged and unplugged conditions at four different turbine-generator loads ranging from 0 MW to 80 MW.

TEST EQUIPMENT

Sensors

Objective (a): Determine Screen Loads

Determination of the total loading of the inner frame and screen assembly, shown in the deployed position in Figure 2, was a prime objective of the test. This was accomplished by replacing the two main pivot pins and one of the pins in each of the four supporting struts with pins instrumented to measure the shear loads in each pinned joint. The main pivot pins were each instrumented and calibrated in two axes, to provide complete load information regardless of the orientation of the screen. Each of the strut pins was instrumented to measure load in one axis; that axis was maintained parallel to the supporting strut by a keeper plate, so that all loads through the pin and strut to the outer frame was monitored. Based on the final deployed position of the screen, the final strut angles, and the load data provided by the bonded resistance strain gage instrumented shear pins, the total screen loads and distribution could be ascertained with accuracy. The instrumented shear pins were each fabricated and

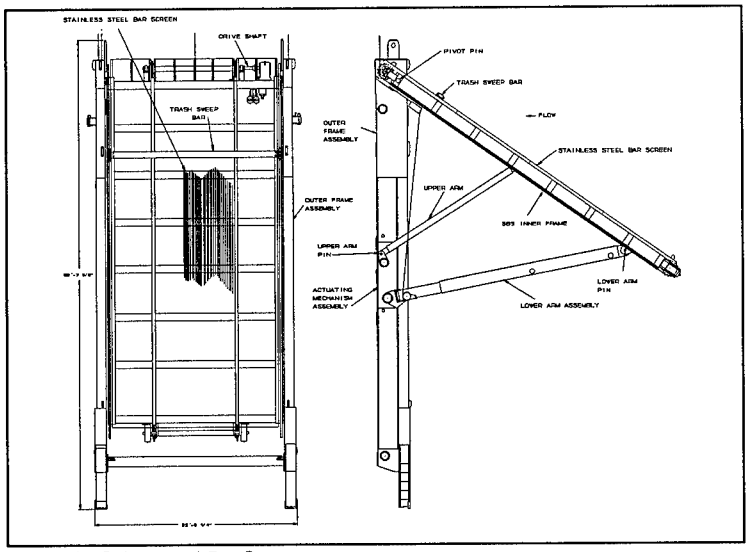

Figure 5 - Submerged Bar Screen

calibrated in a laboratory environment before installation on the prototype screen assembly.

Objective (b): Determine Screen Drive Requirements

A bonded resistance strain gage full torque bridge was installed on a drive shaft on each of the prototype screens. Each installation was waterproofed, and the excitation and signal cable routed through the hollow shaft to a submersible slip ring assembly recessed in the end of the shaft. A stationary cable was routed from the slip-ring assembly to join one of the main cable bundles, located at the main screen pivot pins in the upper corners of the inner frame. All sensor cables were continuous from sensor to instrumentation; no underwater splices were used, to ensure maximum reliability.

Objective (c): Determine Load Variation Over the Screen

The instrumented shear pins provided much of this information. In addition, on the submerged traveling screen several of the transverse link bars supporting the mesh between the two drive chains were instrumented to measure the shear near one end. One bar, initially near the top upstream position, and another at the bottom downstream position, were selected, and provided with sufficient excess cable to move the length of the screen.

This arrangement would work for 1/2 revolution of the belt assembly. After that, the cable would break. During the test, the screen drive was activated, and the shear loads on the transverse link bars recorded during traverse of the link bars up the upstream face and down the downstream face simultaneously. Three of the perforated plate supports - one near the top, one near the bottom, and one near the center - were instrumented with bonded resistance strain gage full shear bridges at each end. These latter bridges were given a pseudo-calibration using a hydraulic jack and 10 kip load cell, applied near the center of the plate and centered over each support in turn.

Objective (d): Quantify Screen Vibrations

Overall screen vibrations could be determined from the shear pin data. Additionally, accelerometers were installed at the lower center and lower left corner of the inner frame, looking downstream. Two accelerometers, one sensing acceleration normal to the screen plane and the other sensing transverse acceleration, were installed at each location.

Objective (e): Determine the natural frequency of the deployed inner frame

This was accomplished in water by recording the accelerometer data as the deployed screen assembly was lowered to the bottom and impacted at the limit of travel.

Additional components of the submerged traveling screen were instrumented to quantify operational loads for design purposes. The four inner frame diagonal braces were each instrumented with a bonded resistance strain gage full tension bridge to sense tension and compression loads resulting from wracking of the inner frame.

All sensor cables were waterblocked twisted shielded pair cables, continuous from sensor to surface, and attached to the inner frame by cable ties.

Signal Conditioning and Recording

All bonded resistance strain gage sensor data was signal conditioned by strain gage amplifiers. All sensor data was recorded using FM analog tape recorders. Oscillographs were used to provide on-site visual data for data quality checks and for preliminary data reduction. An FFT analyzer provided frequency and phase information, helping to determine whether opposite corners of the lower end of the inner frame were moving

in the same direction simultaneously, for example.

TEST PROGRAM

The testing was performed the week of September 16, 1991. The submerged traveling screen was tested first in turbine unit 5. Each turbine has three intake slots, designated "A", "B", and "C". Each of these slots has a screen installed in it. The instrumented screen was installed in the "C" slot and was plugged with plywood. All structural loads plus the vibration were measured. The next day, the screen was removed so the plywood material could be taken off. It was put back down and tested in the unplugged condition. Again, all structural loads and vibration were measured. In addition, the drive shaft torque and loading on the link bars was measured.

The following day, the plugged submerged bar screen was tested in turbine unit 6. This screen was placed in the "B" slot. We knew the distribution of flow in the "A", "B" and "C" slots (37%, 35% and 28% respectively) so we felt that we could comfortably predict how loadings would change from one slot to another.

On the last day of testing, the submerged bar screen was unplugged and tested in the "B" slot, obtaining results on loadings, vibration and drive loads.

TEST RESULTS

A summary of the traveling screen operational test results in tabulated in Tables I through IV. As so often happens in testing, one of the most interesting results occurred as a result of a change in plans. The original plan was to test both screens in the same slot, as it was felt that current velocity surveys of the three intake slots of each turbine were sufficient to predict slot-to-slot differences in the hydrodynamic loading. For operational reasons, this proved to be impractical, and so two screens were tested in adjacent slots. there were addition test differences: the STS was tested with the head gate in the standard position while the SBS was tested with no head gate. This situation is judged to be acceptable, since the two screen types are identical in the plugged condition; i.e., they have the same flow restriction.

A comparison of the 80 MW columns in tables I and III shows that this was not the case. The inner screen main pivot pin resultant loads were on average 24% higher, the lower support loads 11% higher, and the upper support loads are twice as high in slot 5B as in slot 5C.

Granted, some of the load increase in the upper supports could be a result of the adjustment of the redundant supports, but lowering the upper support contribution will raise the remaining support loads. The overall increase in loading from the "C" slot to the "B" slot was as expected, but the change in load distribution on the screen was unanticipated.

Two plots of accelerometer data follow Tables I-IV. The first plot is of the double-integrated acceleration data for the left and center accelerometers for the SBS 80 MW case. Displacement at the accelerometer location is less than 40 mils. the second plot is a cross spectrum of the two signals, showing that the phase shift is nearly zero and so the two points are moving essentially in unison.

CONCLUSIONS

After reviewing the test results, it was clear that the new long screens would have to be redesigned for higher loading prior to using them on a permanent basis. We found that the plugged screen in "B" slot had an average load over the surface of the screen of 270 lbs./ft^2. Extrapolating this data using the information we had on flow distribution, the load in the "A" slot would be 300 lbs./ft^2. The design criteria was 180 lbs./ft^2. Even though the screens were overloaded during the test, they were not in danger of failing at these loads during a short term test.

The drive loads on the Submerged Bar Screen were very high when the trash sweep hits the stops at its ends of travel. The Submerged Bar Screen control uses an electronic load sensing device which should stop the motor with a minimal increase in motor amps when end of travel is reached. This load sensing device was not performing as expected. The torque which was measured in the drive shaft indicated that the motor was near the stall condition. This problem will be addressed and we will use the same test method to evaluate whether the changes are acceptable.

We concluded that the vibration of the screen is minimal and will cause no operational problems.

HYDRAULIC VS. MECHANICAL DRIVES FOR STEEL STRUCTURES

Parveen Gupta[1]

ABSTRACT:

Traditionally, electrical or electromechanical drives have been used to operate steel structures like locks, gates, large valves, or bridges etc. These drives, though reliable, are custom built and need constant maintenance. Also, transmission over large distances, stringent safety regulations and high demands on controls make Hydraulic drive and controls the obvious choice.

Properly designed electro-hydraulic systems provide an economical solution to complex needs. Advent of microprocessor has increased the scope of these drives tremendously.

This paper deals with comparison of hydraulic drives with commonly used mechanical drives.

HISTORY:

Most of us gathered here today have been involved with Civil construction projects like hydro-electric power plants, irrigation and navigational systems, flood control systems and movable bridges etc.

Most of these projects involve operation and control of gates, valves and bridges.

[1]Manager, Civil Engineering, The Rexroth Corporation,
2315 City Line Road, Bethlehem, PA. 18017

Following are the requirements of a drive system:

A) Drive should be simple and reliable.
B) Low maintenance / easy to repair.
C) In case of power failure, still possible to operate (via emergency power or manually).
D) Compact.
E) Cost effective (considering the initial & maintenance costs).

These requirements can be achieved in any of the following ways:

1) Electrical drive.
2) Electro-mechanical drive.
3) Electro-hydraulic drive.

ELECTRICAL DRIVE:

Use of pure electrical drive for opening and closing, and control of gates, although it sounds simple, is not practical due to the required force (torque), location, controllability, physical size, and reliabilty, etc.

ELECTRO-MECHANICAL DRIVE:

Typical electro-mechanical drive has electrical motor, reduction gear, chain / belt drive, gear box, and the crank system, etc.
See figure 1 & 2 for typical mitre gate drive and sluce drives.

ELECTRO-HYDRAULIC DRIVE:

In these types of drives, electrical motor will typically be connected to a hydraulic pump. Oil is pumped through the control valves and via oil pipes to the hydraulic cylinder (or motor) which in turn operates the gates.
See Figure 3 for typical mitre gate and sluce drive.

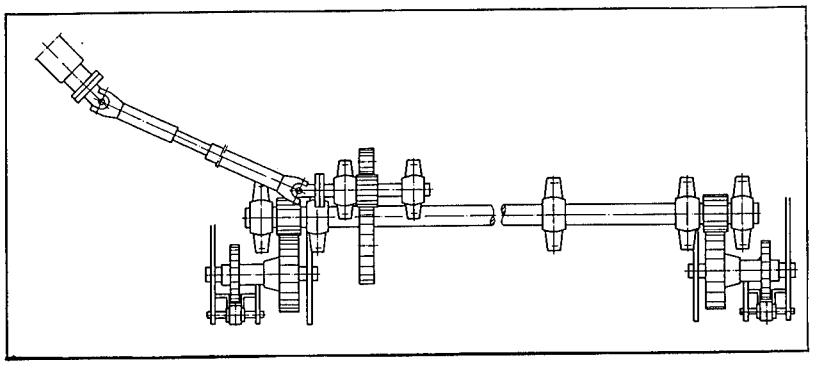

Figure 1: Mitre Gate Drive

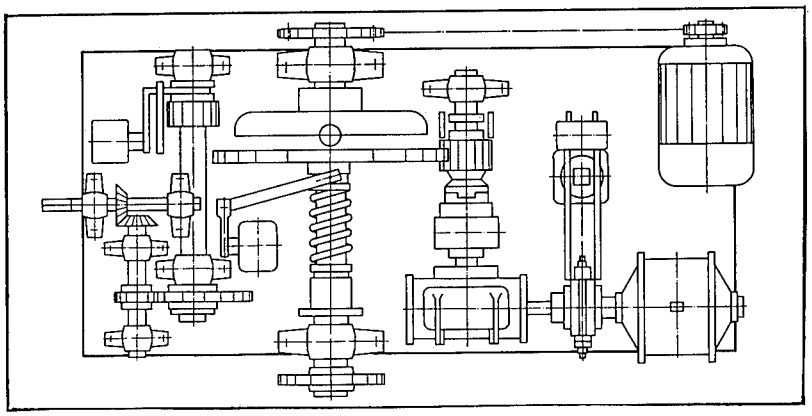

Figure 2: Sluice Drive

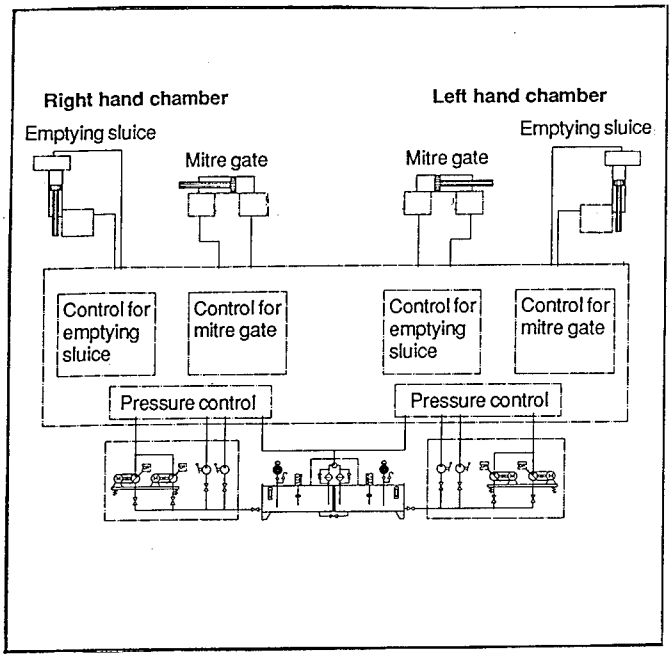

Figure 3
Mitre Gate & Sluice Drive

COMPARISON OF MECHANICAL AND HYDRAULIC DRIVES

MECHANICAL	HYDRAULIC
I. Power Transmission	
• Articulated chains, gear racks, joined racks, worm gears or leaf segments, used as lifting elements, are driven by an electrical motor.	• Hydraulic cylinder (or motors) used as a lifting element and are driven by pressurized oil, which is supplied by a hydraulic power unit.
• Transmission element is a multistage gearbox working on a pinion – or rope drum	• Transmission element is hydraulic oil, which, in comparison to the mechanical transmission element is not subject to wear.
II. Components	
• Major structural components such as lifting elements, gearboxes, frames, etc. are custom designed and specially built.	• Hydraulic drives consist of components, which are produced in large quantities. Spare parts are therefore available as an off the shelf product.
• Spare parts are therefore difficult to obtain, have long delivery times and because of their uniqueness, are extremely expensive.	• Only some parts of a hydraulic cylinder which are related to the stroke are custom made. All other parts of cylinder and system are standard industrial components.

MECHANICAL	HYDRAULIC
III. Physical Layout	
• Lifting components and drive elements have to be close.	• Because the power transmission is achieved by pressurized oil, there is almost no limitation in distance between the lifting and drive element.
No flexibility in the position of the mechanical elements.	
Deviations in the line of force and power transmission over great distance is difficult to achieve and extremely expensive.	This allows for possible savings in underground structures.
IV. Maintenance	
• The lifting components require constant maintenance and lubrication.	• In the hydraulic drive system the energy carrier, oil, acts as a lubricant/corrosion protector.
• These lubricants may cause environmental pollution.	• Maintenance normally would be limited to inspection.
• Wear on the lifting components influences the safety factors.	• It is common to use environmental friendly hydraulic fluids.

MECHANICAL	HYDRAULIC
V. Operating Features	
• Smooth starting and deceleration is difficult to achieve, is inaccurate and can only be achieved at great costs.	• Speed control as well as smooth starting and deceleration is easy to obtain because of the the very simple, standard components (Proportional valves, variable pumps).
• Overload protection is not accurate (slipping clutch).	• In contradiction to mechanical drives, overload protection/ safety valves can be adjusted easily and accurately.
VI. Special Features	
a) Synchronization:	
• Synchronization can be done but is more involved and due to more external parts is susceptible to damage, etc.	• Can be achieved rather easily by proportional hydraulic system and cylinder position feedback (CIMS).
b) Underwater	
• Typical mechanical system cannot be used under water.	• Cylinders can be partially or completely under water and even the drive station can be submerged. The system, however, must be designed accordingly. This has been done in the past.

Finally, following are the major components of the two drive systems:

MECHANICAL	HYDRAULIC
Electrical motor	Hydraulic power unit
Coupling	Inter-connecting piping
Gear box	Hydraulic cylinder
Winch	
Cable/Chain	

Above mentioned features have been known and used for decades in deciding whether to use an electro-mechanical or an electro-hydraulic drive.

Following recent developments have opened an altogether new horizon of opportunities for electro-hydraulic drives:

- Electronic Controls: Advent of micro processor, PLC, PC and their integration into the electro-hydraulic drives have made electro-hydraulic drives much more attractive.

  One can conveniently program the acceleration / deceleration rates, dwell times, store the data for recordkeeping and maintenance etc. changes if required, can be made in field and rather quickly.

- Environmentally Safe Fluids: Over the years, most commonly used hydraulic fluids were petroleum based oils. If these oils leak in the environment, it would create major problems. In the last decade or so, use of environmentally safe fluids have become more common. With more testing and development of safer fluids, we are sure they will be used more and more in the years to come.

- High Pressure: In the past, typical system pressure for civil engineering applications were approximately 1,000 to 1,500 psi. These days 2,000 to 3,000 psi is very common and can be achieved using standard components and normal design practices. Higher pressures reduce the size of cylinders and other components without compromising on safety.

Thus, we at Mannesmann Rexroth believe electro-hydraulic drives would become almost standard for the future. Mechanical drives may only be used for very small loads.

KEY TECHNICAL FEATURES OF HYDRAULIC CYLINDERS

By J.A.C. Wels
Director

CONTENTS

1. Introduction

2. Comparison hydraulics - mechanics

3. Examples of use of hydraulic actuators in movable bridges and gates operation.

4. New features in design:
   * Sealing
   * Hydraulic medium
   * Corrosion protection

5. Integration hydraulics / electronics for synchronisation purposes.

6. CIMS functioning principle

1. INTRODUCTION

Hydraulic cylinders and hydraulic systems have, although wrong, the image of not being able to function free of leakage and as such are not accepted as an adequate alternative for electric-mechanic solutions.
Based on a long standing european experience in this field completed with the most recent developments in the hydraulic cylinder design, it is evident that a hydraulic solution in many cases offers advantages against the electric/mechanic alternative.

2. COMPARISON HYDRAULICS - MECHANICS

To start a summary of the advantages of a hydraulic system (see encl. 1).
Comparing both system on cost point of view, we have to distinguish initial costs and maintenance costs.

A summary of initial costs can be found in encl. 2. In this case it shows an indication regarding hydraulic systems for the movement of radial gates. The table is part of a report from ASME, author Chander K. Sehgal, Harza Engineering Company, Chicago, IL60606-4288.

3. EXAMPLES OF USE OF HYDRAULIC ACTUATORS IN MOVABLE BRIDGES AND GATES OPERATION

Niantic River Bridge

The Niantic River Bridge operated by the Department of Transport and is located near East Lime, Waterford Connecticut.
The bridge halves are actuated by:
4 Pieces heavy duty double acting hydraulic cylinders

Bore	320 mm
Rod diamater	180 mm
Stroke	2640 mm
Working pressure	200 bar
Test pressure	250 bar

including bottom and top pivots of one-piece forgings according ASTM A668 Class K.

Harry S. Truman Dam

Harry S. Truman Dam, in operation since October 1979, is located on the Osage River about 1½ miles northwest of Warsaw, Missouri.

With a length of 1800 m and a height of 38 m. the 6 generating units produce hydroelectric power with a total capacity of 160.000 kW.
In case of an emergency with the turbine the draft tube will be closed by lowering the inlet and outlet gate to prevent flooding of the power house. In the original situation the inlet gates could be lowered hydraulically, the outlet gates are lowered by gravity using a gantry crane. Because of the flow the outlet gate will be pushed against its guides. In that case the gate will not go down by gravity because of friction.

The 12 telescopic cylinders will replace the gantry crane, see encl. 3a. and 3b. The cylinder (working partly under water) can push down the gate (6100 mm wide) with a max. force of 500 kN over a stroke of 12 meters.
The encl. 3c. shows the buckling calculation.
The piston rods are protected against corrosion by Ceramax 1000.

Scope of supply:
12 Pieces 5 stage telescopic cylinders:

	Bore (mm)	Rod diameter (mm)
Stage 1	254	125
Stage 2	360	280
Stage 3	460	400
Stage 4	550	500
Stage 5	640	600

Total stroke	12.195 mm
Working pressure	140 bar
Test pressure	210 bar

The Zandvliet bridge

The Zandvliet bridge, located in the harbour of Antwerp, Belgium, is similar to the Berendrecht bridge, on which a presentation was given at the "Movable Bridge Conference" in 1990 by Mr. Dr.Ing. L. Cypers of the Belgium Ministry of Public Works. To refresh the memory we will recapitulate in short the main features of this bridge.

One important difference to the Berendrecht bridge, however, is that the piston rods of the hydraulic drive cylinders have been provided with the unique Ceramax 1000 piston rod coating.

Recapitulation

The main function of the Zandvliet bridge, in operation since 1966, is to allow road and rail traffic to cross the Zandvliet lock. After the Frederik-Hendrik bridge, the Oudendijk brdige and the Berendrecht bridge had been refurbished, the Zandvliet bridge was next. The Zandvliet bridge, a bascule type, is provided with a counter weight to balance the flap. The bridge structure is supported by two bascule axes built-in in a torsional tube, connecting both main girders. Each bascule axis has one two-row roller bearing. The Deck of the bridge has a length of 62.9 meters and a width of 10.2 meters.

Two almost vertical mounted hydraulic cylinders, generate the bascule movement. The bridge rotates 89 degrees. Each cylinder is mounted in a support, allowing rotations in two mutually perpendicular axes. The bridge can be locked in open as well as in closed position. The locking is also achieved hydraulically. A hydraulic cylinder pushes a steel cylindrical pin into a ring shaped element in the bridge.

The main characteristics of the hydraulic equipment can be found in encl. 4. Its design is based on standards specified by the Belgium Ministry of Public Works and based on thirty years of experience. Some of the most significant specifications are:

1. The hydraulic jacket is designed for a pressure of 1,5 times the maximum working pressure. Lame's formula is used and the safety factor agains rupture is 4.
2. Euler's formula is used to design the cylinder rod. The safety factor against buckling is 1.5.
3. Oil flow is limited to 3 meter/sec.
4. All important bearings are two-row, self alligning spherical bearings.
5. Cylinder rod material is carbon steel of the type St52.3N according DIN 17100 provided with the unique Ceramax 1000 piston rod coating.
6. Pipe connections are achieved by using flange couplings with O-rings.

Ceramax 1000

It was common use, that for cylinders built under contract of the Belgium Ministry of Public Works the piston rod had to be made out of stainless steel, type AISI 431, which would be plated with a chromium layer of at least 35 microns.

As in all industrial areas in the world however, the environment becomes more and more poluted with accids. The accids are in combination with the salty environment an excellent athosphere for pitting corrosion.

The advantages of Ceramax convinced the Belgium Ministry of Public Works to use Ceramax as the standard for the future.

4. NEW FEATURES IN DESIGN

Sealing

Sealing a hydraulic cylinder is some kind of a paradox. Sealing in a static situation is not that much of a problem, a V-shape multi-lip seal can deal with.
A hydraulic cylinder, however, is designed to move a load and then the paradox becomes clear. For smooth operation, the seal needs an oil film for proper functioning. Apart from that for long life reasons oil film is also needed for protecting the seal from wearing out too quick.
It is the task of the engineer to design the whole sealing concept in such a way that oil is prevented from dripping out and still having a smooth and long service life operation. We have for that reason four basic concepts (see encl. 5).
Also the sealing principles of the installated pipe works expecially where this pipe work is connected to the hydraulic actuator is important (see encl. 6-8).

Hydraulic medium

New hydraulic oil are developed such as biodegradable oil. These types of hydraulic oil probably do not create problems for the hydraulic actuator engineers but more for the pump and valve manufacturers. Tests are already going on for years.

Corrosion protection
Because of environmental circumstances, we have to take more care of the corrosion protection of the piston rod and the cylinder body.
This corrosion resistance increase is achieved for the piston rod by using the new ceramic piston rod coating, called CERAMAX. In the meantime this coating is as from 31-12-1991 patented in the USA under nr. 5.077.139.

5. INTEGRATION HYDRAULICS / ELECTRONICS FOR SYNCHRONISATION PURPOSES

There is a growing need for either a read-out possibility of the position of the piston rod or to synchronize two or more cylinders.

For this reason we developed a positioning measuring system, called Ceramax Integrated Measuring System (CIMS).
Existing position indicators in hydraulic cylinders, horizontal or under an angle operation are not advisable with strokes over 5 meters.
See encl. 9.

6. THE PRINCIPLES OF CIMS

The Ceramax Integrated Measuring System (CIMS) is developed for position measurement on hydraulic CERAMAX cylinders. The system is integrated in the cylinder and contains no moving mechanical parts. It can be used on cylinders of any length. Because of the operating principle the system can only be used on CERAMAX coated cylinders.

The system consists of a small sensor which is mounted in the cylinder head. This sensor is connected to an electronic box. This box contains the electronics which convert the sensor signal to a standard output signal. The electronic box is normally mounted close to the sensor on the cylinder.

The system is also able to generate an additional velocity signal. Several output formats for displacement and velocity are available to ease integration into a user system.
See encl. 10.

ENCLOSURE 1

HYDRAULICS COMPARED TO MECHANICS

- Higher degree of operational reliability
- More practical to have higher capacity
- Ultimate speed control possibilities
- Positive closing
- Higher degree of automation (synchronisation)
- Less space / weight
- Reduced vibration
- Simple installation at site
- Minimum of maintenance
- Economic operation

COMPARATIVE ESTIMATED INSTALLED COSTS OF HYDRAULIC HOISTS VERSUS WIRE ROPE/CHAIN HOISTS FOR TAINTER GATES

TAINTER GATE SIZE	HYDRAULIC HOIST		WIRE ROPE/CHAIN HOIST			
	HOIST CONNECTED ON D/S SIDE		HOIST CONNECTED ON U/S SIDE		HOIST CONNECTED ON D/S SIDE	
	ESTIMATED* HOISTING CAPACITY	ESTIMATED COST	ESTIMATED** HOISTING CAPACITY	ESTIMATED COST	ESTIMATED*** HOISTING CAPACITY	ESTIMATED COST
20' X 20'	70t	$ 45,000	16t	$ 25,000	20t	$ 35,000
30' X 30'	110t	$ 80,000	32t	$ 55,000	45t	$ 70,000
40' x 40'	180t	$140,000	65t	$115,000	90t	$140,000
50' x 50'	280t	$200,000	110t	$200,000	150t	$240,000
60' xx 60'	400t	$300,000	170t	$300,000	250t	$360,000
80' x 20'	200t	$100,000	80t	$120,000	100t	$125,000
100' x 20'	250t	$120,000	100t	$150,000	125t	$165,000

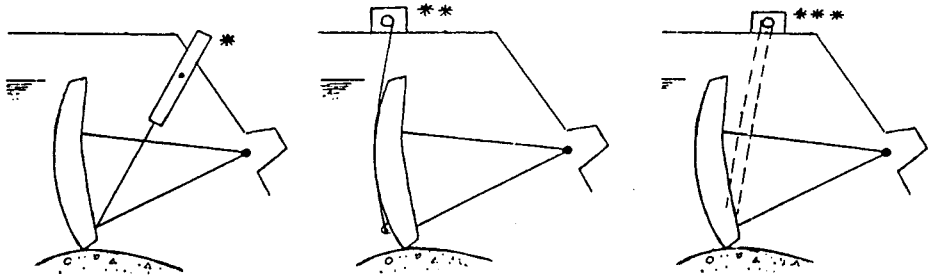

ENCLOSURE 3a.

ENCLOSURE 3b.

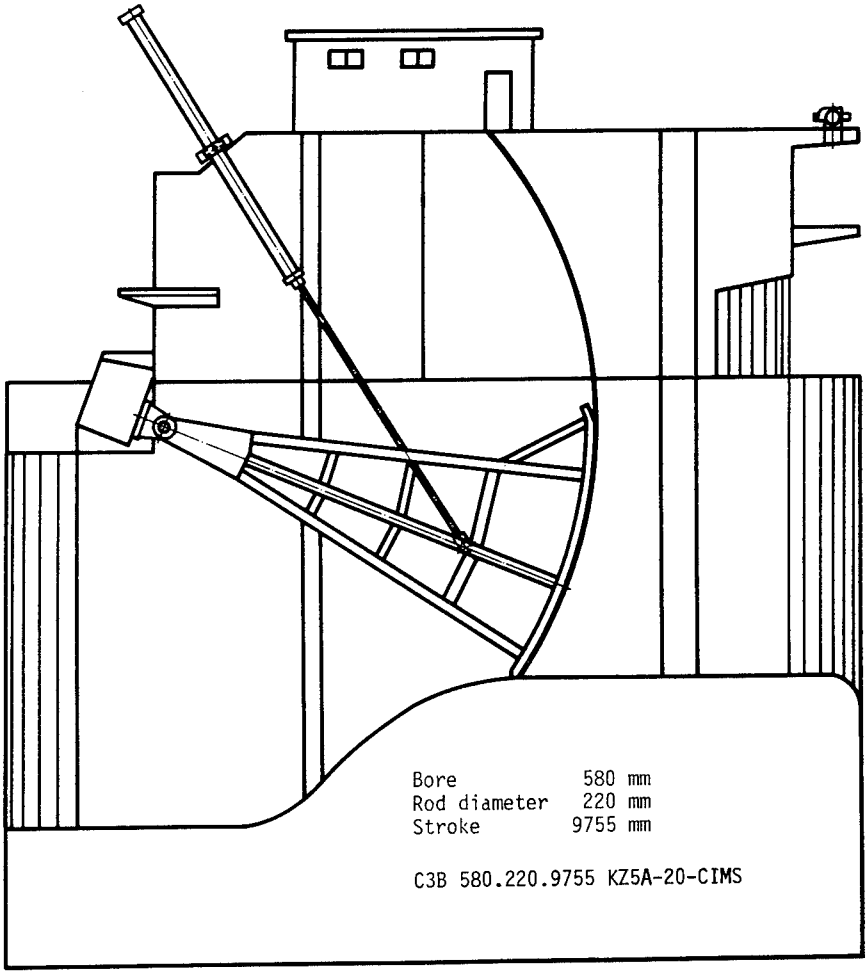

ENCLOSURE 3c.

```
**********************************************************************************
                HYDRAUDYNE CYLINDERS B.V. TECHNICAL CALCULATIONS
**********************************************************************************


Calculation of pure buckling                                        311


Assumptions:

The cylinder is located vertical
There are no sideloads, working on the extended pistonrod
The factor of safety is calculated in fully extended position

Formulas:

Buckling is influenced not only by the distance from mounting to mounting
but also by the mounting style.

See also appendix FIG 311.

Buckling is calculated with the Euler formula

Euler formula:

      π² x E x Istng
FE = ----------------
           lk'²


           π
Istng  = ---- x (Ds^4 - ds^4)
           64
E = 210000 N/mm² = 30457926 PSI

lgrens = π x √( E / Y.P.)

If lambda ≥ lgrens than Euler is valid

Slenderness
            4 x lk'
lambda = -------------
         √(Ds² + ds²)

Because these hydraulic cylinders consist out of more pieces with different momen
Inertia, the influence of the moments of inertia is calculated into a reduction o
the bucklinglength, for all cases B in appendix FIG 311.
The calculation are done acc. Falk: Die Knickformeln fÜr den Stab mit n
teilstÜcken konstanter Biegesteifigkeit Ingenieursarchiv XXIV 1956
```

ENCLOSURE 4

MAIN CHARACTERISTICS OF THE ZANDVLIET BRIDGE

1. Bascule mechanism

a. **Cylinder**

Number	2
Bore	630 mm
Rod	315 mm
Stroke	3.800 mm
Working pressure	245 bar
Disposition	vertical

b. **Hydraulic pump group**

Number	4
Type of pump	variable flow axial piston pump
Driving electro motor power	75 kW

2. Bolting mechanism open position

a. **Cylinder**

Number	2 x 2
Bore	125 mm
Rod	70 mm
Stroke	230 mm
Working pressure	204 bar
Disposition	horizontal

b. **Hydraulic pump group**

Number	2 x 2
Type of pump	fixed flow axial piston pump
Driving electro motor power	7,5 kW

3. Bolting mechanism closed position

a. **Cylinder**

Number	2
Bore	50 mm
Rod	28 mm
Stroke	200 mm
Working pressure	100 bar
Disposition	horizontal

b. **Hydraulic pump group**

Number	2
Type of pump	gear pump
Driving electro motor power	1,1 kW

ENCLOSURE 5

MANNESMANN REXROTH
Hydraudyne Cylinders

CERAMAX 1000

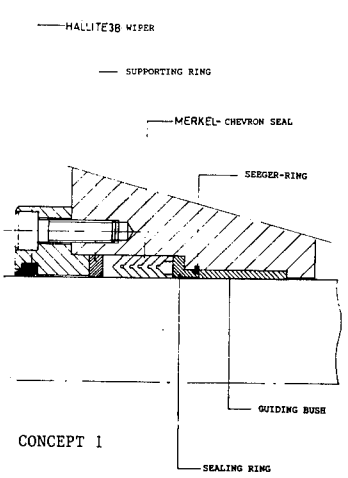

CONCEPT 1

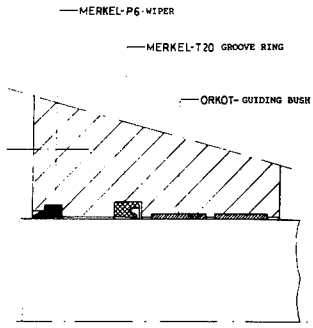

CONCEPT 2

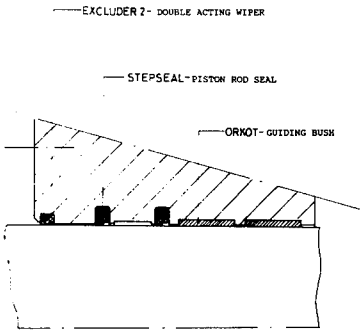

CONCEPT 3

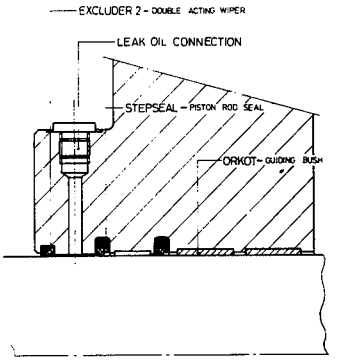

CONCEPT 4

ENCLOSURE 6

MANNESMANN REXROTH
Hydraudyne Cylinders

Welding Connections with O-ring seal

LOW pressure welding flange
(ND 16 - NW80)

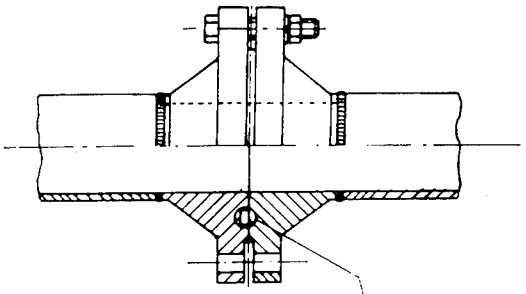

HIGH pressure welding flange
(ND 250-NW80)

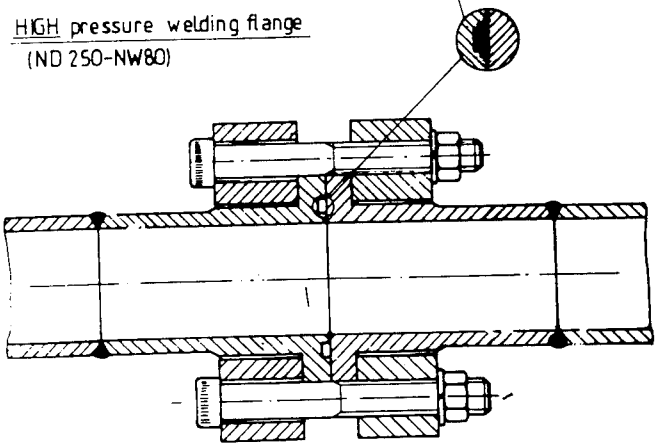

ENCLSOURE 7

MANNESMANN REXROTH
Hydraudyne Cylinders

Welding Connections with O-ring seal

SAE WELDING FLANGE WITH O-RING SEAL

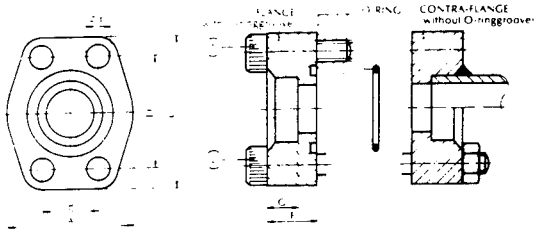

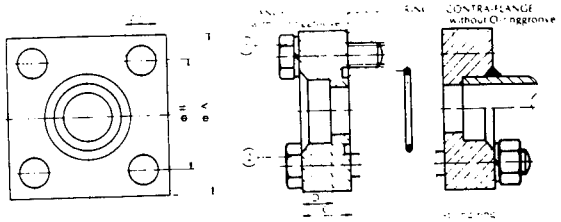

WELDING-NIPPLES WITH O-RING SEAL

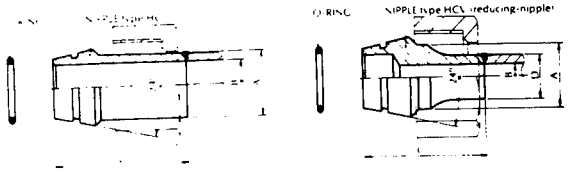

ENCLOSURE 8

MANNESMANN REXROTH
Hydraudyne Cylinders

WELDING CONNECTION COUPLING

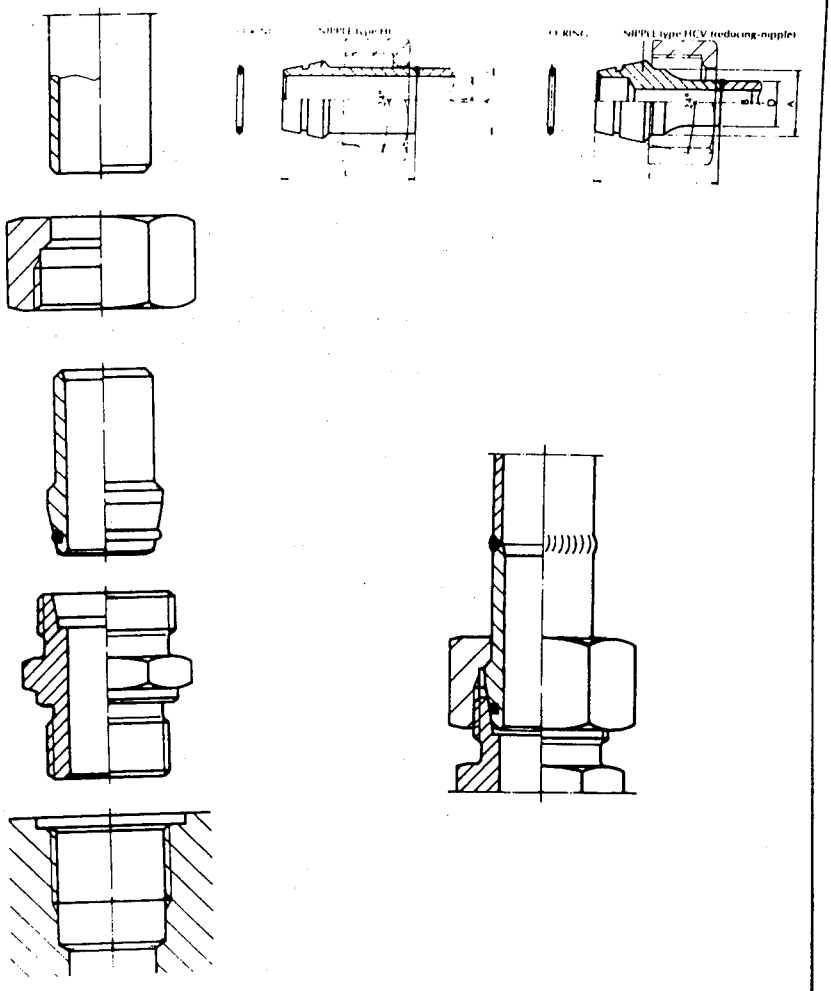

ENCLOSURE 9

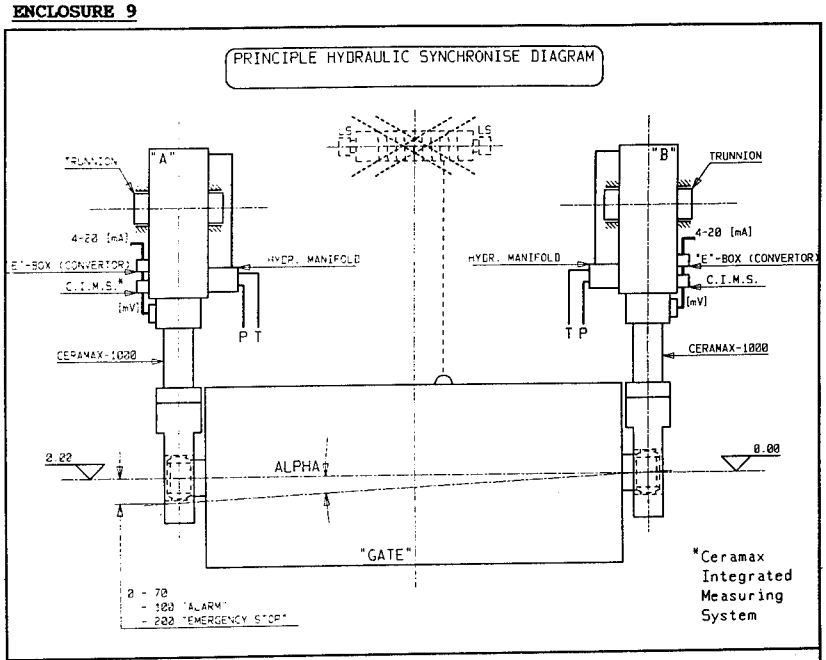
PRINCIPLE HYDRAULIC SYNCHRONISE DIAGRAM
"A"
"B"
TRUNNION
TRUNNION
4-20 [mA]
"E"-BOX (CONVERTOR)
C.I.M.S.
[mV]
HYDR. MANIFOLD
HYDR. MANIFOLD
4-20 [mA]
"E"-BOX (CONVERTOR)
C.I.M.S.
[mV]
P T
T P
CERAMAX-1000
CERAMAX-1000
2.22
ALPHA
0.00
"GATE"
0 - 70
- 100 "ALARM"
- 200 "EMERGENCY STOP"
*Ceramax
Integrated
Measuring
System

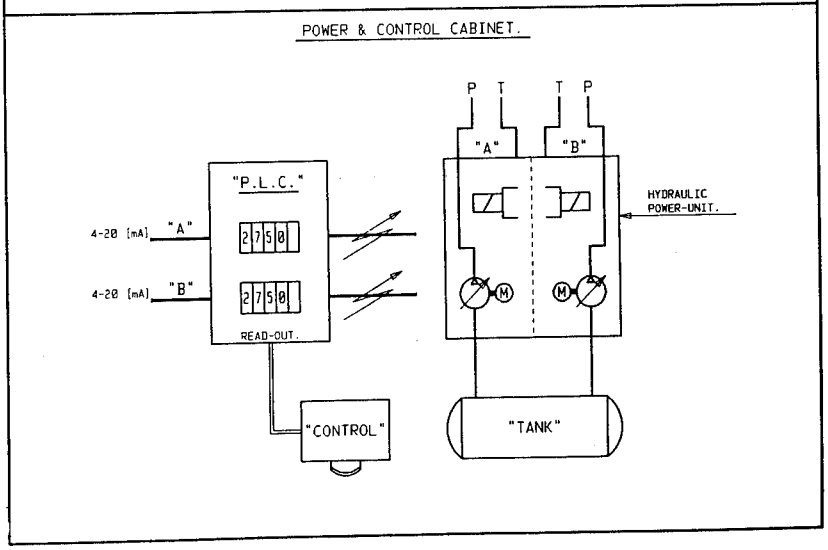
POWER & CONTROL CABINET.
P T T P
"A"
"B"
"P.L.C."
4-20 [mA] "A"
4-20 [mA] "B"
2750
2750
READ-OUT.
HYDRAULIC
POWER-UNIT.
M
M
"CONTROL"
"TANK"

ENCLOSURE 10

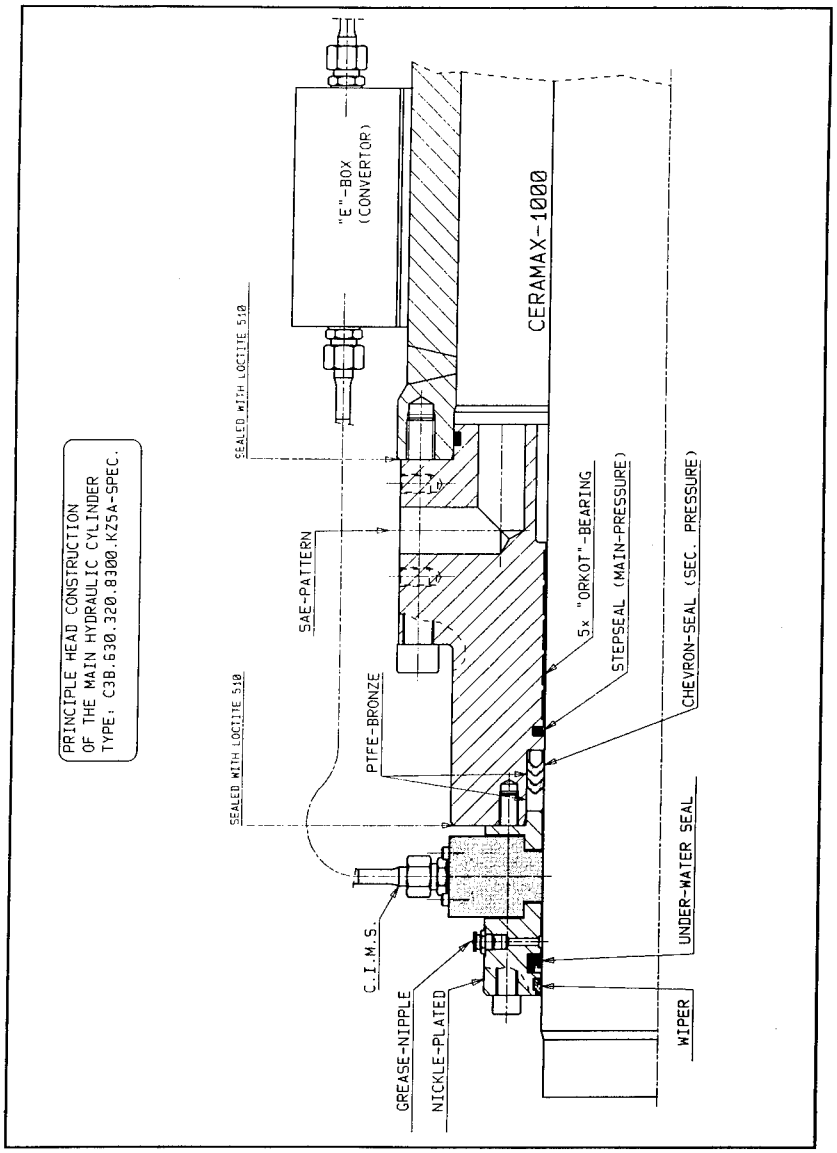

LUBRICATION SYSTEMS FOR SPEED INCREASERS USED IN HYDROGENERATING APPLICATIONS

R. S. Pelczar[1]

ABSTRACT

In today's marketplace, owners and developers are scrutinizing equipment selections more than ever before. The ultimate goal in their effort is to maximize their return on investment. This is achieved by maximizing reliability, availability and efficiency while minimizing the equipment procurement, installation, and operating costs. In applications which incorporate speed increasers, there is an ever-growing awareness of the critical aspects of equipment selection and a more thorough evaluation of offerings. One of the key aspects affecting the longevity of a speed increaser is lubrication.

The lubrication system is the life line of the speed increaser and must support the drive under all modes of operation. Proper equipment selection, lubricant type and viscosity, along with continuous attention to quality/condition will play a major role in determining the life of the system.

This paper will review different aspects of lubrication and lubrication system equipment selections with comments relative to their limitations or impact on the operation of the turbine system. Key optional features will be presented along with an explanation of their usefulness. A discussion of the importance of oil sampling and system maintenance will be presented in order to heighten awareness to their impact.

[1]Product Specialist - Speed increasers for hydrogenerating applications, Philadelphia Gear Corporation, 181 S. Gulph Road, King of Prussia, PA., 19406.

INTRODUCTION

Lubrication is critical to the modern hydro-turbine/geared/generator system. New technology, materials, and manufacturing methods have brought about the development of equipment which is more compact, efficient, capable of higher performance, and yielding greater life. Along with these developments, there has evolved a need for optimum lubrication to the equipment, in order to ensure it will yield the service life intended.

The continued successful operation and long life of the equipment is dependent upon the continuous supply of lubrication oil of proper quantity, quality and condition. Additionally, the lubrication system must support the equipment under all modes of operation.

The lubrication system has five functions to perform:

a) Reduce Friction
b) Transfer Heat
c) Minimize Wear
d) Transfer/Remove Wear Particles
e) Reduce Rust and Corrosion

Failure of the lubrication system to perform any one or more of these functions may result in premature failure of the equipment.

ELASTOHYDRODYNAMIC LUBRICATION

Lubrication can be defined as the control of friction and wear between adjacent surfaces by the development of a lubricant film between them, called an elastohydrodynamic (EHD) oil film.

The EHD oil film thickness between adjacent surfaces depends on the elastic deformation of these surfaces and the hydrodynamic properties of the lubricant itself.

Consider the contact between two surfaces such as gear teeth or bearing rollers. As load is applied, the surfaces elastically deform and contact over a finite area. The contact force between the two surfaces, known as Hertzian Contact, gives rise to a pressure distribution over the region of contact with the maximum hertzian pressure at the center. Hydrodynamic fluid pressures from the lubricant oil film are generated at the entry region just before the hertzian deformation area.
(See Figure _____)

FIGURE 1

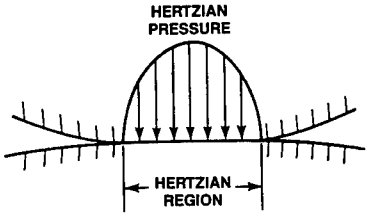

Pressure distribution over contact region.

The hydrodynamic fluid pressure is trying to separate the two surfaces while the load is trying to force them together.

FIGURE 2

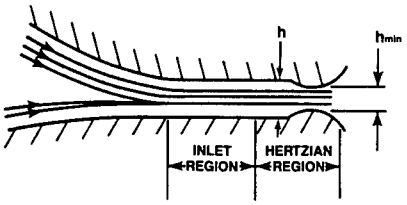

Hydrodynamic fluid pressure separates surfaces.

The high contact pressure in the inlet area produces a rapid rise in viscosity which results in sufficiently high hydrodynamic film pressures to separate the two surfaces.

The generated EHD film thickness is quite small, usually less than 1.25 micrometer, these thin EHD films are often not much larger than the height of the individual asperities caused by the surfaces in contact.

EHD oil film thickness is significant. If the two surfaces are not fully separated, the EHD film leaves local area of asperity contact which become vulnerable to the initiation of surface fatigue.

The fatigue life of line contact bodies such as gear teeth and bearing rollers is determined by a complex combination of speed, load, lubricant temperature, setting and alignment. The lubricant's role in this interaction is determined primarily by speed, viscosity, and temperature. The effect of these factors on the fatigue life of elements can be dramatically altered at higher temperatures with lower viscosity, and thinner resultant oil films. Therefore, the selection of the correct lubricant for any application requires a careful study of expected operational and environmental conditions.

LUBRICANTS

When choosing a lubricant, conditions such as operating speeds, normal and exceptional load conditions, methods of sealing, temperature range, moisture condition, bearing design, and quantity of lubricant all affect the final choice.

A suitable lubricant will have successful previous experience in the continuous lubrication of similar equipment in the same service, particularly with regard to foaming, rusting, sludging, and separation from water and other impurities.

The selection of one oil to lubricate a system with several components such as generator bearings, speed increaser, and turbine guide bearing frequently results in a compromise. Even though the system appears to operate satisfactory, the life or performance of one of the components may be reduced. It is usually desirable to use an oil of higher viscosity to lubricate a speed increaser than that required for the generator and guidebearings, therefore, it may be desirable to use a higher viscosity for the system.

The dominant property in the selection of any oil is **viscosity** - a measure of a fluids' flow characteristics. Viscosity is usually expressed in terms of the time required for a standard quantity of a fluid at a given temperature to flow through a standard orfice. Horsepower losses, bearing exit temperatures, and oil-film thickness decrease with lower viscosity values and increase with higher viscosity values.

According to ISO standards, viscosity of petroleum oil is expressed in mm^2/second (centistokes, cst) at 40^oC and/or 100^oC.

The measure of the rate of change of viscosity with temperature is called the **viscosity index** or VI. The higher the VI, the less change in viscosity with temperature. When cold starting is an important aspect of the rotating equipment operation, a lubricant with a high viscosity index is used.

LUBRICANT TYPES

There are two basic types of lubricants used to lubricate gear drives:

1) Petroleum Based Mineral oils
2) Synthetic Lubricants

MINERAL OILS

Petroleum based mineral oils are a complex mixture of hydrocarbon molecules derived from the refining of crude oil. For almost every situation, petroleum products have been found to excel as lubricants. Mineral oils are usually compounded with different chemical additives to improve specific properties. These additives, when properly formulated into a lubricant, can increase lubricant life, provide greater resistance to corrosion, increase load-carrying capacity, and enhance other properties.

SYNTHETIC LUBRICANTS

Synthetic lubricants are products that consist of base fluids manufactured by chemical synthesis or molecular restructuring to meet predetermined physical and chemical qualities desired for certain operating parameters. They must be optimized for each particular application relative to compatibility with previous lubricants, or with components of the mechanical system such as elastomeric materials and textile filter materials.

Synthetic lubricants can be up to 4 times more costly than petroleum based oils, therefore, they are conventionally reserved for problem applications such as extremely high or low temperatures, equipment subjected to frequent overloads, and equipment with a marginal lubrication system.

EXTREME PRESSURE ADDITIVES

When severe operating conditions are anticipated, the use of a lubricant with an extreme pressure (EP) additive may help prevent surface scoring damage in the contact areas.

EP additives are chemically complex materials which, when activated by localized area high temperatures, form a low shear strength film at the contact area, thus preventing scoring.

LUBRICATION SYSTEMS/OIL DELIVERY

Most gear driven hydro-generator systems utilize a forced feed lubrication system whereby lubricant of the proper quantity, viscosity and cleanliness is positively introduced to the gears and bearings. The major differences among the types of systems employed are in the method for delivery and cooling of the oil.

DIRECT DRIVEN OIL DELIVERY

The most common delivery method is through the use of a direct driven, positive displacement lube oil pump as a primary pump. This approach has a distinct advantage in that the delivery of the oil is ensured whenever the turbine shaft rotates. A positive displacement pumps' output is directly proportional to its' operating speed. A direct driven pumps' selection is influenced by its ability to operate safely and adequately at runaway speed conditions. This generally leads to the selection of a large pump because the speed increaser's rated power oil flow demands must be satisfied at rated operating speeds that are considerably lower than the runaway conditions. Additionally, the pumps' net minimum inlet pressure, which governs its ability to pump, must be adequate to achieve delivery of the heavier oil viscosity at start up conditions. This requirement dictates that the oil reservoir should be located near the direct driven pump.

Special system design consideration must be taken to supplement the direct driven pumps' delivery at start up and at subsynchronous rotational speeds, where oil output is less than the operating requirements of the system. Conversely, other provisions within the system must address the excessive direct driven pump output at overspeed, which will require oil sump capacity considerations and sump baffling for the elimination of entrained air.

MOTOR DRIVEN OIL PUMP DELIVERY

A.C. motor driven pumps offer an economical means of oil delivery. Since motor driven pump operation occurs at a constant speed, the pump selection can be optimized for their most efficient oil flows. These flows are based on the oil demands at the overspeed condition. The motor driven pumps' power demands are governed by the horsepower required to drive the pump to achieve the heavier oil viscosity delivery at start-up. As the operating equipment temperature rises and the oil viscosity lessens, the power demand drops off. Motor driven pumps offer the advantage of lube system location and pump configuration flexibility, provided the pumps' net minimum inlet pressure, which governs its' ability to pump, is adequate.

Where electric motor driven pumps are exclusively utilized to provide oil supply, special considerations must ensure that a continuous power supply is maintainable. This will ensure against oil flow interruption which could potentially damage the geardrive. A typical example of a motor driven lube pump schematic is shown on Figure A.

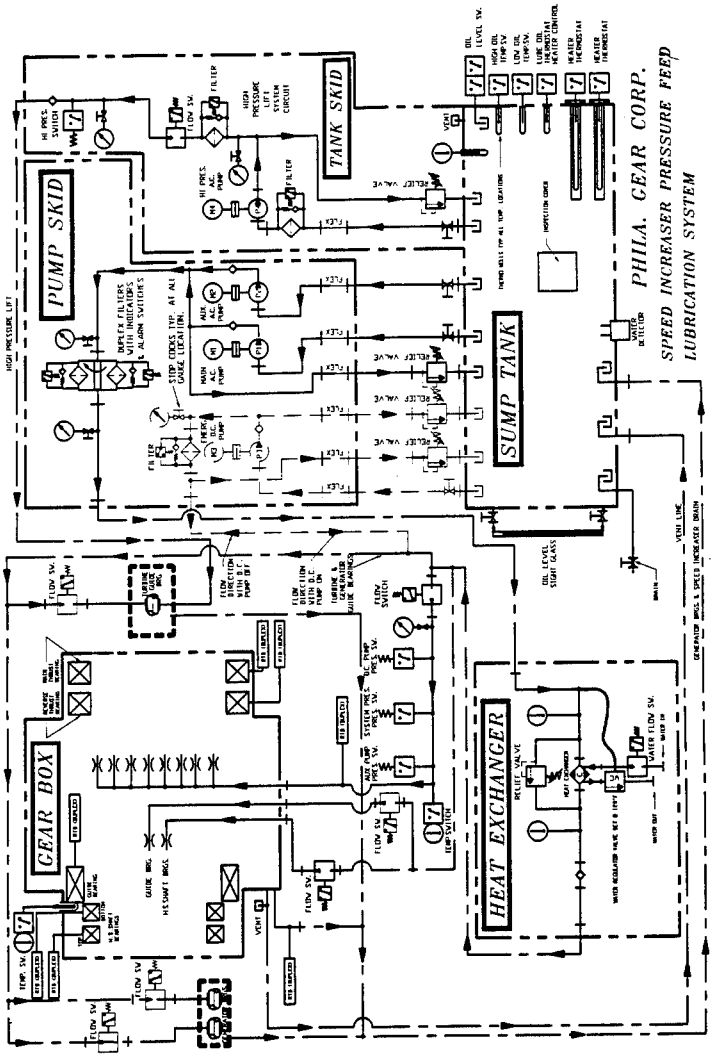

FIGURE A - PRESSURE FEED LUBRICATION SYSTEM

GRAVITY FEED OIL DELIVERY

Another type of oil delivery system is the gravity feed system. Motor driven pumps are the essential motive force for delivery of oil in this type of system, which utilizes the head obtained as a consequence of plant layout to obtain the necessary speed increaser oil inlet pressure. Approximately 55 feet of height difference is the minimum necessary to generate the oil pressure required for a hydroturbine-generator application. This is necessary to overcome the centrifugal pressure created by epicyclic speed increasers in the runway condition.

A schematic arrangement of a typical lubrication system employing gravity distribution is shown on figure B. The distinguishing feature of this system is the delivery of the oil to the header from the overhead gravity tank. This ensures that if a service pump stops, lubrication is maintained for a short while due to the reserve in the gravity tanks, thus allowing time for shutdown of the rotating equipment.

The gravity feed system requires a substantial oil volume in the headtank to effect a safe system shutdown, as well as a volume of oil in the oil sump reservoir to supply normal operation of the motor driven pumps. Additionally, oil sump heaters must be adequately selected to heat the combined system oil capacity while system is shutdown.

LUBRICATION SYSTEMS/TEMPERATURE CONTROL

The second important function of the lubrication system is to provide heat removal. Adequate cooling is necessary to maintain oil viscosity control and oil quality. Although in general, gears may be exposed to an ambient temperature of up to 55^{O}C (131^{O}F), high temperatures influence the operation of a geardrive by increasing the oxidation rate of the lubricant and decreasing lubricant viscosity. Based on (155^{O}F), every 25^{O}F increase in a typical mineral oil temperature halves the lubricant life.

The typical hydro turbine generating system will employ an external cooling method to dissipate all of the losses from the drive system. The type of cooling system employed will usually be a water cooled heat exchanger, although air-oil heat exchangers are feasible for up to 6mw systems.

WATER COOLED HEAT EXCHANGER

Water cooled heat exchangers are the most effective, compact and economical heat removal methods to install. The cooling medium may be a closed loop system, municipal water supply or river water. The cooling medium cleanliness is an important factor as it affects cooler performance and system operating temperature. A thermostatic valve with sensor in the lubrication system can regulate the supply of coolant to the heat exchanger and ensure that the proper lubricant temperatures are maintained. Coolant filtration of at least 100 mesh is necessary to maintain cooler effectiveness and prevent fouling.

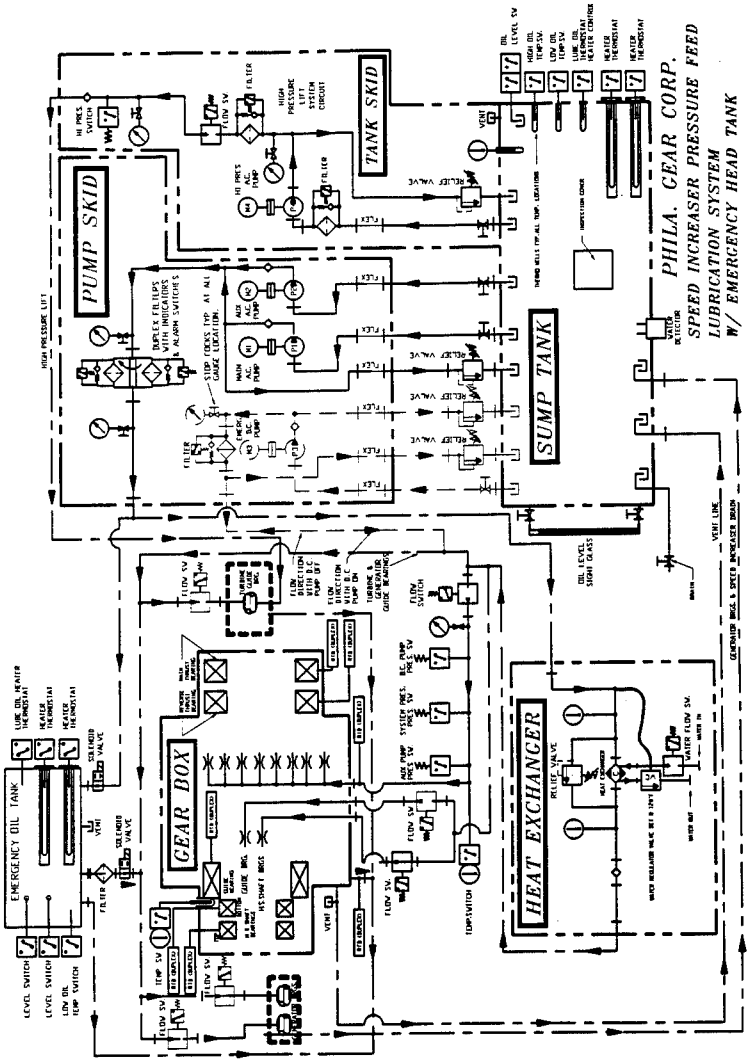

FIGURE B - GRAVITY FEED LUBRICATION SYSTEM

There are two types of water cooled heat exchangers typically employed, they are the shell and tube type where oil in the shell of the cooler is cooled by the passage of tubes with circulated coolant, and the plate and frame type which alternates plate chambers of lube and coolant. The plate and frame type is available in an air gap version which isolates any potential chance of intermixing the lubricant with the coolant.

AIR - OIL HEAT EXCHANGER

Air-oil heat exchangers utilize ambient air as a cooling medium. The main advantage to utilizing this approach for system heat removal is that the water cooling system and its associated maintenance is completely eliminated. Other advantages are that air movement through the cooler can be used to move air in damp areas, and heat discharged from the cooler can either be vented from the powerhouse in the summer or recovered to heat the powerhouse in the winter.

Air-oil coolers are limited in their practical application to systems of approximately 6MW or less. Beyond this capacity the air oil coolers become prohibitively large, moving large volumes of air in the powerhouse. A typical, high efficiency air-oil cooler for a 5MW system will move approximately 20,000 to 25,000 SCFM air. An air-oil cooler should be equipped with a thermostatic by pass valve for cold oil viscosity operation, and a temperature switch to regulate the motor driven fan to prevent excessive oil cool down.

When selecting an air-oil heat exchanger for a given installation, careful consideration must be given to the potential maximum ambient temperature as well as the maximum potential power at the site. Failure to adequately address these areas will serve to limit energy capture or risk equipment damage from over temperature operation.

OIL RESERVOIR HEATERS

Geared systems, which are used in powerplants located in cold climates, must incorporate provisions which will enable oil to circulate freely and not cause high torques at start-up. An acceptable low temperature gear oil should have a pour point at least $5^{o}C$ ($9^{o}F$) lower than the expected powerhouse ambient start-up temperature.

If a suitable low temperature gear oil is not available, the gear drive must be provided with a sump heater to bring the oil up to a temperature at which it will circulate freely for starting. The heater should be designed so as to avoid excessive localized heating, which could result in rapid degradation of the lubricant. Designs which isolate the heating rods from direct contact with the oil are ideal, as they serve to avoid oil coking around the rods and enable heater removal without draining the oil sump.

LUBRICATION SYSTEMS/FILTRATION

Lubricant cleanliness is a major concern relative to maximizing the service life of rotating equipment. The filters play a key role in ensuring that abrasive particles are removed from the system. In addition to the filtration of fluids, the filter may incorporate a bypass for clogged element conditions, a magnetic drain plug to collect metallic particles, and visual and electrical cleanliness indicator.

In force feed lubrication systems, the oil must be supplied through a filter media which is compatible with the lubricant, meets the viscosity requirements without excessive pressure drop, and removes particulate matter consistent with the design of the rotating equipment. For gear drives with rolling element bearings, the filter media should be no coarser than 40 Microns. Where hydrodynamic oil film bearings are used, extreme load conditions may yield and oil film thickness which is less than .001 inch, consequently, the oil filtration should be 25 Micron or finer. The filtering area should be sized so the clean filter pressure drop at normal operating temperature is approximately 7psi or less using the proper micron filtration.

Finally, because of the continuous operating nature of a hydroelectric system serious consideration to the incorporation of duplex filters will enable filter change over without shutting down the system.

LUBRICATION SYSTEMS/OIL RESERVOIRS

OIL RESERVOIRS-INTEGRAL OR SEPARATE

The ideal location for an oil reservoir is integral with the speed increaser. This is not always possible with some speed increaser configurations and oil volumes. Where sumps are integrated, the oil sump heaters will also serve to heat the gearbox internals and minimize high starting torques. Pumps which are direct driven by the speed increaser shafts also benefit by the close proximity of the oil sump, because of the limited pump suction capacity.

Where separate oil sumps are used with motor driven pumps, they offer flexibility in system configuration and location.

The minimum sump capacity should be at least 150 percent of the motor driven pump capacity in GPM, or three times the shaft driven pump capacity at rated speed. Additionally, allowance should be made for any lubricant runback from return piping. Motor and shaft driven pump suction piping should be located and baffled to prevent direct flow from return piping. Suction ports for each pump must be separate in order to prevent cavitation at the pump. Return piping from pressurized relief valves should be discharged at the bottom of the sump below the oil level. The sump should be designed so that it can be practically cleaned and include a suitable access opening for clean out. Finally, the oil sump bottom should be sloped with a low point to accommodate complete drainage and possible interface with a water detection device.

LUBRICATION SYSTEMS/ACCESSORIES

In order to provide reliable service, the lubrication system must incorporate sufficient sensors to allow continuous and complete monitoring of system condition. Some useful sensors are listed as follows:

RESISTANCE TEMPERATURE DETECTORS (RTD) - Allow continuous monitoring of temperatures at key locations such as oil supply and drain temperatures as well as sump temperature. RTD's should be duplex type to obtain redundant readings for accuracy.

TEMPERATURE SWITCHES - Used as a trigger to shutdown at overtemperature, and a permissive for cold temperature start-up. Typically located in the main oil reservoir and lube oil supply lines.

PRESSURE SWITCHES - Used as a mechanism to trigger operation of auxiliary back up pumps, or to initiate a signal for system shutdown when pressure is lost at the main oil inlet.

FLOW SWITCHES - Used as a trigger to signal loss of flow below the minimum oil demand requirements of the system.

WATER DETECTOR - Used as means to detect the presence of water in the system.

LUBRICATION SYSTEMS/PIPING

The lubrication system piping is intended to distribute the lubrication oil in accordance with the system design requirements, and be as simple and direct as practical. Braces and supports must be provided to prevent damage from misuse or vibration. Equipment interfaces should have flanged connection points to facilitate dismantling. Interconnecting piping to major assemblies must be installed in such a way as to ensure that no abnormal forces or moments are applied to the assembly. A flexible joint of suitable pressure and misalignment capacity should be considered for major assembly connection in order to isolate equipment vibrations and accommodate component growth. Suction piping must be arranged and installed to prevent entrapment of air. Drain piping should always slope in the direction of flow. Pipe joints should be located to facilitate component removal/disassembly, and located so that leakage will not impinge on potentially dangerous components. When made up, the pipe should be thoroughly cleaned to prevent debris from entering the rotating equipment. Special considerations to internal pipe preservation and system flushing must be taken in areas of high humidity.

LUBRICATION SYSTEMS/MAINTENANCE

The lubrication system is a key element in the longevity of the rotating equipment. It must be continually maintained so that it is functioning at its' peak performance. A systematic method of inspection, condition verification, and documentation is important to avoid any unexpected system shutdowns and equipment damage. Areas of concern in the maintenance activities include:

CLEANLINESS - Dust, dirt, grit, and wear particles in the lubricant supply must be kept to a minimum. Filter and strainer elements should be serviced regularly to avoid circulating contaminants with the oil and to avoid excessive pressure drops that can reduce the quantity of oil supplied to the gear drive.

LUBRICANT CONDITION - The service life of a lubricant is adversely affected by high temperatures, water, and/or emulsions, solid contaminants, and operating environment. An oil sample should be drawn from the oil sump at scheduled intervals and analyzed by the lubricant supplier or a reputable laboratory. The lubricant supplier should be consulted for typical oil condemning limits for the particle oil used.

SENSOR/SWITCH SETTING - An annual check of all switches solenoids, and sensors to verify operation as per lubrication system schematic specified settings. System vibrations and environmental conditions can alter settings, thereby affecting critical timing of sensor functions.

AUXILIARY PUMP FUNCTIONAL CHECK - Motor driven pumps and other motorized accessories should be checked at scheduled intervals to verify operability, proper oil delivery, pressures, and motor power draw. Relief valve settings should be checked to ensure that the required oil delivery is supplied to the gear drive.

FLOW AND PRESSURE CHECK - Flows and pressure drops at the cooler, filters, and inlet to the rotating equipment, should be routinely monitored, and recorded to identify any trends that are developing.

COOLER CONDITION - An annual check of cooler condition is important to maintain cooler efficiency. Water cooled heat exchanger coolant ports should be checked for any fouling or blockage. All sacrificial anodes should be replaced. Air-oil cooler core fins should be checked and cleaned of any dirt build up that would affect heat transfer efficiency.

BREATHERS - Oil breathers should be checked frequently as they will be dirty. Any blockage in the breather could potentially lead to a leakage elsewhere in the drive in order to relieve pressure.

VISUAL COMPONENT CHECK - The entire lubrication system should be checked daily for all indicator guage reading, pipe connections, vibrations, bolted connections, oil leaks or seepage, loose accessories, and wiring connections

SOUND LEVELS - The operating sound level of the pumps should be routinely noted. An increase in sound level could indicate the presence of air in the lube system, blockage at the pump intake, air leaks in the pump shaft seal, worn or loose parts in the pump, filter blockage, or high oil viscosity from the fluid being too cold.

GREASED POINTS - Some motors and pumps are equipped with greased bearings which must lubricated at intervals recommended by the manufacturer.

SUMMARY

The lubrication system plays a vital role in the success of the mechanical rotating system. Continued success is dependent upon the uninterrupted supply of the proper quantity, quality, and condition of lubrication oil. A systematic method of inspection, condition verification, and documentation is essential to avoid any unexpected system shutdowns and equipment damage. Attention to these details will help maximize an owners' return on investment

REFERENCES

Mobil Oil Corp., Mobil **EHL** Guidebook, Mobil Oil Corp., Fairfax, Virginia 1979,1981,1992.

American Gear Manufacturers Association AGMA 250.04 Industrial Gear Lubrication AGMA 427.01 systems considerations for critical service gear drives.

American Gear Manufacturer's Association, Alexandria, Virginia

The Timken Company, Lubrication, The Timken Company, Canton, Ohio, 1991.

SUBJECT INDEX

Page number refers to first page of paper.

Accuracy, 1564, 2177
Acoustic detection, 219
Acoustic measurement, 308, 2187
Adjustment, 2120
Admixtures, 1349
Aeration, 354, 371, 381, 2075, 2080
Aeration tanks, 229
Aging, 1584, 1659, 1694
Alloys, 1951
Aquatic environment, 1040
Aquatic habitats, 2089
ASCE Committees, 870
Assessments, 29
Audits, 504
Automation, 923, 1180, 1189, 1218, 1438, 1537, 1564, 1594, 1841, 2006

Balancing, 1959, 2030
Bank erosion, 410
Bearing capacity, 2160
Bearing design, 1879
Bearings, 1795
Benefit cost analysis, 139
Benefits, 494, 1160, 1189
Biological properties, 328
Boating, 2114
Brazil, 2151
Bridges, 1465

Calibration, 766A
Canada, 1208, 1746
Canal linings, 1349
Capital costs, 1941
Case reports, 229, 239, 556, 1418, 1554
Cavitation control, 994, 1713, 2120
Cavitation corrosion, 1713, 1822
Cavitation resistance, 738
Clogging, 1741
Coating, 1822
Cofferdams, 698, 1681
Cold regions, 1408
Columbia River, 767
Comparative studies, 308, 1639, 2012
Compliance, 504, 698, 728, 805, 930, 1554
Composite materials, 1907
Compressive strength, 1291
Computation, 571, 1091, 1247
Computer aided manufacturing, 581
Computer analysis, 269
Computer applications, 363, 913, 2030
Computer hardware, 1130
Computer models, 494, 633, 796, 1025, 1079, 1120, 1198
Computer programs, 777, 796, 975, 984, 1189
Computer software, 1130
Computerized control systems, 1160, 1180, 1457, 1841, 2006
Computerized design, 581, 671, 831, 940, 2040
Concrete deterioration, 860, 1497, 1822
Concrete, reinforced, 2167
Configuration, 1889
Construction, 688, 1218, 1228, 1238, 1279, 1368, 1517
Construction costs, 120
Construction materials, 1358
Construction methods, 633
Construction planning, 186
Consultants, 428
Consulting services, 437
Contract administration, 1681, 1733
Control, 1951
Control equipment, 1031
Control systems, 571, 603, 1130, 1160, 1170, 1537, 1564, 1671, 1870
Corrosion control, 642, 1465, 1507, 1831
Corrosion resistance, 1951
Cost analysis, 129, 139, 2006
Cost control, 710, 1659, 2124
Cost effectiveness, 120, 354, 464, 787, 878, 1457, 1527, 1545, 1812, 1841, 2065, 2089
Cost estimates, 591
Cost savings, 603, 688, 811, 1180, 1831

Costs, 1574
Cracking, 860, 1723, 2167
Crossflow, 2012

Dam construction, 1257, 1269
Dam design, 1269
Dam failure, 930
Dam foundations, 1291, 1301
Dam safety, 946, 1091, 1208, 1315
Dam stability, 975, 1301
Damage prevention, 1850
Dams, 11, 29, 219, 249, 344, 363, 534, 612, 747, 796, 831, 841, 860, 885, 894, 923, 1120, 1228, 1554, 1777, 2075, 2114, 2187, 2197
Dams, arch, 728
Dams, buttress, 688, 698
Dams, concrete, 688, 805, 811, 821, 903, 975, 1269, 1291
Dams, earth, 1208, 1315, 2160
Dams, gravity, 1291
Dams, rockfill, 1257, 1301, 1358, 2124
Data analysis, 239, 354
Data collection systems, 923, 940
Database management systems, 1025
Databases, 410, 955
Debris, 1438, 1741, 1746, 1777
Decision making, 1703
Deflection, 612, 860
Demolition, 2160
Design, 328, 571, 581, 642, 688, 747, 930, 1004, 1228, 1238, 1279, 1408, 1517, 1574, 1629, 1671, 1931, 1941, 1966, 1996, 2114
Design criteria, 110, 149, 591, 710, 787, 1014, 1218, 1247, 1368
Design improvements, 120, 698, 1339, 1649
Deterioration, 2160
Developing countries, 29, 99
Development, 80, 1448, 1907
Dewatering, 1812
Diagnostic routines, 1786
Diesel engines, 661
Digital techniques, 269, 1180
Discharge measurement, 1397
Disturbances, 1150
Diversion structures, 747
Drainage systems, 831
Drawdown, 249, 1358
Ductility, 1951
Dynamic response, 1150
Dynamic tests, 1959

Earthquake loads, 975
Earthquake resistant structures, 841
Economic analysis, 57, 562, 1198, 1607, 1639, 1923, 2065
Economic growth, 24
Economic justification, 57
Economic models, 70
Efficiency, 1584, 1629, 1913, 2012, 2022, 2060, 2120
Effluents, 642
Electric power transmission, 661
Electrical equipment, 1594, 1664, 1850, 1907
Electronic equipment, 1465, 1889
Embankments, 1315
Endangered species, 249, 420, 454, 767
Energy conservation, 2060
Energy development, 766A
Energy dissipation, 1378
Environmental audits, 239
Environmental effects, 29
Environmental factors, 129
Environmental impacts, 99, 110, 258, 437, 464, 486, 504, 652, 1659
Environmental issues, 11, 89, 371, 391, 545, 562, 1031, 1040, 1238, 1681
Environmental quality, 1527
Environmental quality regulations, 296
Environmental research, 208
Equipment, 110, 603, 1584
Equipment costs, 1483
Erosion control, 400
Estimates, 169, 1746, 2144
Evaluation, 1, 24, 219, 344, 1664, 2131
Evolution, development, 534, 2151
Experience, 381, 720, 1428
Exploration, 2134

Fabrication, 1574, 2050
Failures, investigations, 603, 1850, 1976, 2080
Fatigue life, 1014

Feasibility studies, 89, 197, 1923
Federal laws, 179
Federal project policy, 486, 821
Federal-state relationships, 179, 464
Field tests, 1619, 1639, 1649, 1822, 1996
Financing, 524
Finite element method, 612, 728, 831
Fish habitats, 338, 381, 420, 2095
Fish management, 159
Fish protection, 110, 120, 129, 139, 149, 159, 169, 249, 258, 308, 338, 454, 767, 1428, 2114, 2187
Fish reproduction, 186, 197
Fish screens, 219, 318, 328, 344, 1438, 1448
Fisheries, 208
Flood control, 885, 1756
Flood frequency, 1100
Flood routing, 1120
Flow, 1079
Flow characteristics, 1083, 1140, 2124, 2144
Flow coefficient, 1378
Flow control, 1941
Flow duration curves, 296
Flow measurement, 2095, 2105, 2187
Flow patterns, 11, 1060
Flow rates, 2167
Fluid dynamics, 2105
Forecasting, 1060, 1079, 1083
Fouling, 1031
Frequency analysis, 1100
Frequency distribution, 1795
Friction coefficient, hydraulic, 1378
Funding allocations, 47, 57

Gates, 1457, 1465, 1812
Geology, 1279
Geometry, 1966
Geotechnical engineering, 1291
Glacial till, 1339
Global warming, 1070
Government agencies, 129, 514
Government policies, 766F
Gravity, 821
Gravity loads, 851
Great Lakes, 258, 965
Grinding, 994
Guidelines, 545, 870, 930, 946, 1694

Harbor structures, 642
Hazards, 1703
Headwaters, 80, 286, 494
History, 80, 534, 766F, 2134, 2151, 2197
Hydraulic design, 1368, 1387, 1397, 1537, 2040
Hydraulic engineering, 1465, 1986
Hydraulic models, 1150, 1428, 1986, 2095, 2177
Hydraulic performance, 2022
Hydraulic properties, 1408
Hydraulic structures, 269, 1100, 1339, 1457, 1703, 1713, 1822, 1959, 1966, 2167
Hydraulics, 318
Hydrodynamic configurations, 1060
Hydroelectric power, 80, 2197
Hydroelectric power generation, 120, 129, 229, 249, 363, 371, 410, 486, 1170, 1483, 1545, 1564, 1767, 1786, 1860, 1889, 1899, 1931, 1941, 1976, 1996, 2105, 2134, 2151
Hydroelectric powerplants, 1, 11, 47, 57, 70, 99, 110, 139, 149, 159, 169, 179, 197, 208, 229, 239, 258, 286, 318, 338, 354, 381, 391, 400, 420, 428, 437, 443, 454, 464, 476, 494, 504, 514, 524, 545, 556, 562, 571, 581, 633, 642, 652, 661, 671, 710, 720, 757, 766A, 766F, 777, 796, 870, 878, 894, 940, 984, 1031, 1040, 1050, 1083, 1110, 1150, 1189, 1198, 1218, 1238, 1279, 1349, 1368, 1408, 1418, 1428, 1448, 1497, 1537, 1584, 1594, 1607, 1659, 1664, 1671, 1681, 1694, 1733, 1741, 1812, 1841, 1850, 1870, 1879, 1913, 2006, 2060, 2075, 2095, 2108, 2131
Hydroelectric resources, 39, 767
Hydrologic data, 766A, 1025, 1079
Hydrologic models, 766A
Hydrostatic pressure, 851

Ice mechanics, 1408

Incentives, 1733
Indexing, 1607
India, 99
Inflatable structures, 1208
Inflow, 946
Innovation, 1986, 2065, 2108
Inspection, 894, 1694
Installation, 1418, 1931
Instream flow, 286, 296, 2089
Instrumentation, 622, 913, 923
Insulation, 1607, 1907
Intakes, 328, 1269, 1368, 1387, 1438, 1741, 1777
Irrigation, 661, 2060
Irrigation dams, 420

Jet diffusion, 1527
Joint ventures, 524

Kansas, 2197

Laboratory tests, 328
Lakes, 89
Leakage, 1497, 2167
Legislation, 420, 454, 486, 494
Licensing, 179, 229, 239, 258, 296, 338, 400, 410, 428, 437, 443, 454, 476, 486, 504, 514, 545, 766F, 777, 1040, 1664, 2089
Linearity, 2012
Linings, 1831
Load criteria, 1247
Load distribution, 1189
Load tests, 1448
Load transfer, 1913
Local governments, 878
Low head, 710

Machinery, 391, 885, 984, 2177
Maintenance, 661, 1694, 1703
Maintenance costs, 984
Management, 1746, 2108
Management methods, 428, 1733
Manufacturing, 1931, 1951
Mapping, 1777
Materials failure, 1014
Mathematical models, 186, 1408
Maximum probable flood, 841, 940, 946, 965, 975, 1091, 1100, 1110, 1120, 1208
Measurement, 1767
Measuring instruments, 1966
Mechanical engineering, 2050
Mechanical properties, 1959
Methodology, 955, 1397
Mines, 1326
Mississippi River, 1756
Missouri River, 1507
Model tests, 2040, 2105
Modeling, 1110
Models, 179, 747, 1100, 2187
Monitoring, 159, 805, 913, 930, 984, 1025, 1756, 1767, 1786, 1879
Monte Carlo method, 1083
Mountains, 1070
Municipal water, 1923, 2060

Navier-Stokes equations, 2105
Navigation, 766F
Networks, 1120, 1160
New York, State of, 534
Niagara River, 1060
Nondestructive tests, 1723
Numerical analysis, 1140
Numerical calculations, 1004, 1040
Numerical models, 612, 903

Oils, 1483
Operation, 1228
Optimization, 354, 1004, 1170, 1986, 1996, 2006, 2040, 2050
Overtopping, 1507
Oxygen transfer, 1050
Ozone, 1767

Peaking capacities, 410, 720, 757
Penstocks, 622, 870, 1150, 1247, 1497, 1507, 1574, 1723, 1831
Performance evaluation, 622, 1198, 1397, 1545
Permits, 476
Physical properties, 1387
Pipe flow, 1140
Piping, erosion, 1339

Planning, 428, 787
Pollution control, 2131
Pools, 269
Power output, 1584, 1619, 1941, 2120
Power plant location, 2144
Powerplants, 1130
Precipitation, 965
Predictions, 186
Pressure reduction, 1418, 1527
Pressure responses, 738
Probabilistic methods, 955
Production planning, 1083
Productivity, 671, 994, 2177
Programs, 149, 186, 1554
Project evaluation, 29, 39, 47, 70, 80
Project feasibility, 363, 1170
Project planning, 89, 99, 208, 286, 381, 524, 556, 562, 591, 633, 652, 757, 777, 1238, 1517, 1629, 1733
Prototype tests, 1448, 2177
Prototypes, 1907
Public benefits, 545
Public land, 556
Public safety, 878
Pump turbines, 1004, 1619, 1629, 1639, 1649, 2022, 2030, 2040, 2050
Pumped storage, 24, 89, 400, 591, 622, 757, 787, 913, 1140, 1160, 1326, 1870, 1976, 2030, 2065
Pumping, 1860

Quality control, 671, 1014, 1786, 2050
Quantitative analysis, 1703, 1756

Rainfall duration, 955, 965
Rainfall frequency, 955
Rainfall-runoff relationships, 1091
Ramps, 1
Real-time programming, 1060, 1079
Recreation, 11
Recreational facilities, 2114
Redundancy, 1870
Regional analysis, 476, 965, 1070, 1301
Regulation, 514
Regulations, 443, 652, 805
Rehabilitation, 39, 47, 57, 70, 197, 688, 698, 720, 811, 1257, 1497, 1507, 1545, 1584, 1594, 1607, 1619, 1629, 1639, 1649, 1659, 1671, 1681, 1703, 1850, 1976
Reliability, 1554, 2022
Reliability analysis, 47, 70
Remote control, 1594
Renewable resources, 24
Repairing, 1723
Research, 738
Research and development, 994, 1031
Reservoir design, 757, 1326
Reservoir operation, 767, 903, 1070
Reservoir system regulation, 1, 249, 787, 796, 2080
Reservoirs, 208, 1746, 2022, 2060
Retrofitting, 464, 671, 1527
Risk analysis, 39, 2108
River systems, 2134
Rivers, 197, 363
Rock excavation, 1326
Rockfill structures, 1349
Runoff, 1110

Safety, 1812, 1841
Safety analysis, 851, 870
Safety education, 878
Safety factors, 1247
Safety programs, 841, 885, 894, 913, 923
Samplers, 1428
Sampling, 2089
Scale, ratio, 1050
Scheduling, 556
Sediment control, 400
Sediment transport, 1756
Sedimentation, 747, 1025
Seepage control, 633, 841, 903, 1339, 1349
Seismic analysis, 1301
Sensitivity analysis, 1070, 1091
Shale, 1358
Shellfish, 391, 2131
Silts, 903
Similitude, 1050
Simulation models, 1, 24, 777
Slope stability, 1315
Specifications, 1257, 1899
Speed changes, 1860

Speed control, 1483
Spillway capacity, 851
Spillways, 603, 885, 1218, 1228, 1378, 2124
Springs, mechanical, 1879
Stability, 571
Stability analysis, 728, 805, 811, 821, 831, 1315, 1358
Stability criteria, 2124
Standardization, 296, 2065
State agencies, 443, 476
State laws, 179
Static tests, 1959
Statistical analysis, 738, 2144
Statistics, 443
Stress, 860
Stress analysis, 612, 728
Structural analysis, 851, 1649
Submerged discharge, 1387
Subsurface investigations, 1326
Surface finishing, 1831
Surge, 1517
Surveys, 1860
System reliability, 1870

Tanks, 1517
Testing, 344, 1438, 1517, 1574
Tests, 169, 318, 1741, 1899, 2030
Thailand, 894
Theories, 1378
Thermal analysis, 1899
Three-dimensional analysis, 811, 821, 1140
Timber construction, 1269
Topographic surveys, 1279
Transducers, 308
Transient flow, 2080
Trends, 437, 514, 524, 1130, 2108, 2134, 2151
Tunnels, 622
Turbine discharges, 1198, 1899, 1913
Turbines, 149, 159, 169, 219, 308, 318, 338, 371, 581, 710, 720, 738, 994, 1004, 1014, 1050, 1170, 1180, 1418, 1483, 1527, 1537, 1545, 1564, 1607, 1659, 1664, 1713, 1723, 1767, 1777, 1795, 1879, 1889, 1913, 1923, 1931, 1966, 1976, 1986, 1996, 2006, 2012, 2075, 2105

Underground structures, 591, 1671
Unit hydrographs, 940, 946

Valves, 1457
Variability, 1860
Velocity, 344
Velocity distribution, 269
Velocity profile, 2095
Vibration analysis, 1795
Vibration control, 1291, 1619, 1959, 2120
Vibration measurement, 1786, 1795
Vortices, 1387

Washington, 286
Water chemistry, 2080
Water flow, 2197
Water quality, 139, 371, 381, 2131
Water resources, 39
Water resources development, 534
Water resources management, 2144
Water supply systems, 1923
Water treatment, 391
Water treatment plants, 652
Watersheds, 1110
Waterways, 766F
Weirs, 1397, 2075
Welding, 1713
Wetlands, 562, 1040
Wildlife, 454
Wind energy, 24, 1889
Wooden structures, 1257, 2160

AUTHOR INDEX

Page number refers to first page of paper.

Abelin, Stefan M., 1659
Adams, J. Stephens, 381
Afrateos, H., 1070
Ahlgren, Charles S., 870
Alam, Sultan, 1756
Alevras, R. A., 258
Allegretti, Daniel W., 179
Amadei, Bernard, 831
Amaral, Steve, 328
Anderson, Roger B., 1664
Andresen, Øistein, 1870
Ardis, Colby V., 2144
Aronoff, Miriam S., 486
Aziz, N. M., 2012

Babb, Al, 747
Bachman, Gary D., 239, 454
Bahn, K. David, 1959
Bai, Jia Cong, 738
Bakken, James R., 1315
Barbosa, Paulo Sergio Franco, 2151
Barbour, Edmund, 11
Barker, Thomas J., 930
Barksdale, Bob, 1733
Barnes, Marla, 437
Barrett, Peter R., 975
Barton, Daniel J., 229, 1257
Barton, James D., 767
Battige, David S., 410
Bauer, Martin, 2060
Belmona, Issam M., 269
Benson, Steve, 728
Bergquist, R. Joseph, 1923
Bernhardt, Paul A., 1607
Bevivino, J. Perry, 1180
Bhat, Param D., 1497
Birch, Rick, 2187
Bird, V. C., 1438
Bishop, N. A, 1238
Bishop, Norman A., 671
Bivens, Tony, 391
Blair, William H., 652
Blanchette, Michael, 747
Bley, Wendy C., 777
Bockerman, Ronald W., 1507
Boggs, Howard, 811, 903
Bohac, Charles E., 354
Bohr, Joseph R., 308
Bollmeier, Warren S., II, 24
Bondarenko, Alan, 1257
Boomhower, Deborah D., 777
Bove, L. Greg, 777
Brand, Bruce, 821
Bratsberg, K., 581
Brekke, Hermod, 1014
Brighton, Dick, 1822
Brock, W. Gary, 381
Brosowski, Ralf, 1160
Brown, Peter W., 179
Browne, M., 1189
Bruggink, David J., 354
Brundage, Harold M., III, 208
Busse, E. June, 1923
Buttorff, Leslie, 11

Căda, Glenn F., 139
Campbell, Edward D., 661
Caploon, A., 2050
Cassidy, John J., 946
Chacour, S., 2040
Chapman, Craig L., 39, 2108
Chapman, Wayne, 562
Chen, De Xin, 738
Chen, K., 2131
Chen, Xiang Ying, 1140, 2105
Chinnaswamy, C., 831
Chou, Hsien-Ter, 1378
Choudhry, Mohammed I., 1594
Christensen, Peter J., 120
Clemen, David M., 1694
Coates, Michael E., 1879
Colwill, W., 2040
Conners, M. Elizabeth, 2089
Cook, James, 1170
Cook, T. C., 318
Cook, Tom, 344
Corbit, R. B, 2050
Corbu, Ion, 1060

Corwin, Allen G., 642
Coulson, Stuart T., 1966
Courage, Lloyd, 1208
Coutu, André, 1966
Cover, Charles K., 494
Crissman, Randy D., 1060, 1408
Cross, Gerald L., 2160
Cross, John P., 1083
Curtis, Max O., 688
Cybularz, Joseph M., 371

Daley, Dave, 903
Dardeau, Elba A., Jr., 391
DeAngelis, D. L., 2095
Degnan, J. R., 1649
Deitz, Ronald E., 1639
DelloRusso, Steven J., 2167
Desai, V. R., 2012
DeWitt, Tom, 437
Dillis, Matthew P., 777
Domermuth, Robert B., 197
Donalek, Peter, 2120
Dool, Robert E., 1659
Downing, John, 338
Dulin, Richard V., 603
Dumont, Michael F., 186, 197
Durrans, S. Rocky, 1100
Dusenberry, Donald O., 2167
Duxbury, Steve L., 1841

Eberlein, Douglas T., 940
Ecton, Henry G., 766A
Edwards, F. W., 1777
Eichenberger, M., 1004
Eichert, Bill S., 777
Ellis, Raymond O., 603
Elver, Steven A., 363, 1228
Emery, Lee, 443
Eng, P., 1497
Englert, Thomas L., 410

Fan, Shou-shan, 1025
Fargo, James M., 545
Faulkner, Ellen B., 1110
Feik, Cheryl M., 454
Ferguson, John W., 149
Ferguson, Robert W., 1841
Findlay, R. Craig, 1339
Finis, Mario, 710
Finn, Michael J., 1681
Fisher, Frank S., 591
Foadian, H., 975
Fonnesbeck, Kenneth C., 556
Foote, Peter S., 186, 197, 208
Foster, C. A., 1326
Franc, Gary M., 296
Francfort, J. E., 129
Franklin, D. E., 984, 1767
Frithiof, Richard K., 1120
Froehlich, Donald R., 1545
Fuller, Mark, 562

Garga, V. K., 2124
Getter, Robert D., 642
Geuther, J., 2040
Geuther, J. J., 1649
Gibbard, Michael, 1150
Gibson, John, 1554
Gibson, John Z., 805
Gill, Harbinder S., 1247
Goede, E., 1004
Gotzmer, Jerrold W., 946
Graham, Mary Jane, 239
Greely, Gail Ann, 504
Greenplate, Brian S., 371
Gulliver, John S., 1050, 1387
Gupta, Parveen, 1457
Gusberti, Gary, 994

Haag, Thomas, 1554
Hadjissavva, P. S., 1070
Hall, W. W., 1238
Hamill, John, 1554
Hansen, D., 2124
Harlow, James H., 1564
Harper, George A., 955
Harty, F., 2040
Harty, Fred, 1517
Harty, Fred R., Jr., 787
Hauser, Gary E., 2075
Hawthorne, Ken S., 1713
Hayes, Stanley J., 1694
Haynes, Michael J., 1671
He, Jianming, 1140, 2105

Hecht, Jack H., 159
Hecker, G. E., 318
Hecker, George E., 1428
Hegseth, D. G., 1777
Hegseth, David, 885
Heisey, Paul G., 169
Helwig, P. C., 796
Henry, Laurence F., 2030
Henry, P., 2177
Henwood, Mark I., 1
Hibbs, David E., 1387
Hildebrand, Lisa, 878
Hoffman, David K., 1
Hokenson, Reynold A., 1584
Holder, Karl-Ludwig, 1160
Holmberg, Mark, 1545
Homa, John, Jr., 2089
Howe, Jack C., 1996
Howell, William C., 428
Huang, Ning, 24
Hughes, Brian, 1746
Hughes, Robert J., 1130
Hui, Samuel L., 946
Husebø, Rein, 1786

Illangasekare, Tissa H., 831

Jablonski, Timothy A., 1537
Jager, H. I., 2095
Jaramillo, Carlos A., 1358
Jennings, Aaron A., 2144
Jensen, Tore, 1870
Johnson, Van A., 1941
Johnson, William J., 1301
Johnston, Samuel V., 308
Jones, Donald W., 139
Jones, Malcolm S., Jr., 757
Joyet, Robert A., 688

Kahl, Thomas L., 1218
Kalen, Sam, 420
Kaltsouni, M., 851
Kanakis, George, Jr., 1079
Katherman, Russell L., 1976
Kepler, James L., 1639
Kepler, Jeffery L., 1959
King, Robert, 747
Kissel, Peter C., 524
Kleiner, D. E., 622
Kleiner, David E., 1358
Knarr, C. Michael, 930
Kneitz, Paul R., 652
Knowlton, Robert J., 1996
Koebbe, Rick S., 2065
Koseatac, A. Sinan, 710
Kouvopoulos, Y. S., 1070
Krecké, Mathias, 1160
Kries, John R., 1812
Kurrus, Joseph A., 1584
Kwan, Francis, 1060

Laakso, J., 984, 1767
Lacivita, Ken, 1060
Lagassa, George K., 29
Lambert, Thomas R., 1040
Lange, C., 2131
Lange, Cameron L., 1031
Larson, John R., 1664
Lauchlan, I., 1238
Laukhuff, Ralph L., 1756
Laura, Robert A., 1079
Lemon, David, 2187
Levy, Dan, 1889
Lewis, Mark, 1733
Li, Shen Cai, 738
Linnebur, Mark, 811
Lispi, Daniel R., 208
Livingstone, Alan B., 777
Locher, F. A., 1438
Luck, Bob, 1850
Ludewig, Peter W., 1996
Lund, Guy S., 612, 811, 903
Luraas, Halvard, 571
Luttrell, Edwin C., 913
Lux, Frederick, III, 1315, 1397
Lynch, Timothy, 1517
Lyons, Rodney, 831

Magauer, Peter F., 1986
Mahasandana, Taweesak, 894
Malm, C. F., 1795
Malone, Kevin, 249
Manson, Harry A., 841
Martin, Philippe P., 1358

Martinchich, Paul, 1257
Massey, Kristina, 1517
Mathur, Dilip, 169
Matousek, John A., 159
Mattice, Jack, 338
Mattingly, Stan B., 923
Maurer, Bryan R., 229
May, Chris W., 1247
Maynard, William A., 1574
McEntyre, Tommy, 885
McGraw, David S., 1110
McGregor, F. Robert, 562
McKay, Hugh G., 661
McKenery, Stephen F., 930
McLaren, D. G., 1899
McLaughlin, Richard E., 2114
McPheat, John, 1150
Medley, David F., 1951
Metzger, Susan G., 159, 2089
Meyer, Hans, 1941
Miller, Donald F., 1507
Miller, Lawrence M., 208
Mimikou, M. A., 1070
Mittelstadt, Richard L., 57
Mombelli, H.-P., 2177
Moore, Edgar T., 1279
Morris, D. I., 975
Morris, Doug, 831, 965
Morris, Douglas I., 946, 955
Murray, D. G., 1368
Musick, John, 562

Nash, Michael F., 1594
Nelson, Guy, 2060
Nesvadba, J., 1913
Newell, Vann A., 841, 860
Newman, W., 1899
Nguyen, Thang D., 1428
Nielsen, Niels, 1746
Niziol, Jacob S., 698
Niznik, J., 851
Nolt, J. R., Jr., 2050
Norlin, James A., 47
Nylund, R., 1189

Obradovich, Patricia, 70
O'Hara, Thomas F., 955
Onken, Steven C., 2006
Oriole, Kenneth A., 710
Osterle, John P., 1301
Ozment, Kathryn M., 1120

Padula, Stephen D., 777
Pansic, Nicholas, 940
Paolini, Edward M., 698
Papaioannou, Peter E., 1629
Parker, Darle, 885
Pavone, Mike, 728
Payne, Thomas R., 208
Pei, Zhe Yi, 738
Pelczar, R. S, 1483
Pelz, Brian, 1208
Phillips, John H., 1996
Pizzimenti, John J., 249
Pollock, B. C., 984, 1767
Powell, Rex C., 1247
Price, Bradford S., 80, 534
Proctor, William D., 2075
Purdy, Clayton C., 1619
Putnam, Matthew J., 777
Pytko, Russ, 1733

Quist, John E., 633, 1664

Raeburn, Roger L., 1
Raffel, David N., 269
Railsback, Steven F., 1040
Ransom, Bruce H., 219, 308
Rao, Avaral S., 1713
Rashid, Y. R., 975
Readio, David, 2197
Reed, Katherine E., 504
Regan, Patrick J., 1723
Rehder, R. H., 1899
Reynolds, Robert D., 688
Riddle, Hal, 1517
Rinck, Charles, 1907
Rinck, Chuck, 1850
Rinehart, B. N., 129
Rinehart, Stephen D., 1629
Rizk, Tony A., 2075
Rizzo, Paul C., 229, 1257
Robert, D., 1913
Rohlf, John, 720

Roluti, Michael, 11
Rood, Ken, 1746
Rook, Michael E., 1269
Rosenblad, J. L., 1326
Rothenberger, Von, 2197
Rothfuss, Blake D., 110
Rothgeb, William S., 1269
Roudnev, Aleksander S., 1941
Royer, Douglas D., 169
Ruane, Richard J., 354, 2080
Rudolph, Richard M., 633, 1664, 1812
Ruell, Stephen T., 1218
Rutherford, Jim H., 1584
Rutledge, John Lee, 1120
Ryan, P. J, 1438

Sabo, M. J., 2095
Sadden, Brian, 249
Sadler, James F., 1741
Sale, M. J., 2095
Sale, Michael J., 286
Schäfer, R., 1860
Schimek, Gary M., 1110
Schlect, Ed, 1554
Schlect, Edward, 1584
Schmoyer, D. D., 2095
Scott, Jeff A., 787
Scott, Norm, 1387
Sebestyen, A., 1004
Seifarth, Randy V., 1931
Sengupta, Aniruddha, 1358
Severin, Mark A., 1198
Sheaffer, John R., 562
Sherman, Kathleen, 400
Shiers, Paul F., 591
Short, T., 2131
Shveyd, Difa, 1527
Silkworth, Steven G., 1681
Silva, Louis G., 1527
Simpson, Angus, 1150
Singleton, Jim, 1545
Slattery, Patrick E., 757
Slopek, Richard, 1208
Smith, Ian M., 286
Smythe, A. Garry, 1031
Soileau, Cecil W., 1756
Sollo, John P., 1291
Sommers, G. L., 129
Song, Charles C. S., 1140, 2105
Steele, Robert D., 2022
Steig, Tracey W., 219
Steiner, P., 1438
Steines, Dean S., 1315
Stoiber, William, 1594
Stutsman, Richard D., 1831
Su, S. T., 89
Sullivan, C. W., 318
Sullivan, Charles, 328, 338, 344
Sullivan, Thomas J., 777
Sumner, Andrew C., 1594
Sundaram, A. V., 1349
Sundaram, Archivok V., 1358
Sundquist, Mark J., 363, 464, 1387
Swearingen, F. R., 1777
Swiger, Michael A., 486, 514

Taft, E. P., 318
Taft, Ned, 328, 338, 344
Tanner, David T., 860
Tappel, Paul, 249
Terens, L., 1860
Thompson, Eric J., 1050
Tomlinson, Edward M., 965
Toms, Ed A., 612, 1091
Trenka, Andrew R., 24
Tung, T. P., 796, 2124
Twitchell, Jeffrey E., 476, 766F

Van Patten, Marc, 728
Van Winkle, W., 2095
Vaughn, Richard, 1448
Vecchio, Michael J., 410
Veitch, Jamie, 1170
Venkatakrishnan, R., 1326
Verma, Rameshwar D., 99
Voigt, Richard L., Jr., 1387

Wagner, C., 851
Wagner, Charles D., 841, 860
Waldow, George, 720
Wallace, Jim, 1795
Wallman, Randy, 994
Walsh, James, 1170
Wamser, Mark J., 777

Wang, Cheng Xi, 738
Wang, Lee L., 1198
Wangensten, O., 1189
Ward, Patrick, 1517
Waters, Curtis D., 1619
Waugh, Jerry, 1923
Wearing, J. F., 1326
Webber, David F., 1671
Wedmark, Anders, 1418
Wells, Alan W., 159, 410, 2089
Wels, J. A. C., 1465
Whalen, K. G., 258
Whalen, Kevin G., 159
Whitfield, John R., 1428
Whittaker, M. Curtis, 464
Whittle, Daniel J., 514
Winchell, Fred, 328, 338, 344
Wong, Joe, 1822
Wong, K. L., 622
Wood, A. M., 622
Wood, Robert D., 428
Woodbury, Mark S., 940
Wright, William D., 661
Wunderlich, Walter O., 1703

Yale, John B., 1671
Yeh, C. H., 851
Yeoman, Ellen H., 1040
Yin, Au-Yeung, 894
Young, K., 2131

Zawacki, Bill, 1545
Zemke, William E., 110
Zhang, Boting, 2134
Zhang, L., 975
Zilar, Rick, 1584
Zipparro, V. J., 851

WATERPOWER '93

W. David Hall, Editor

Proceedings of the International Conference on Hydropower, Nashville, TN, August 10- 13, 1993

The perceived simplicity of production of hydropower gives it a less dramatic public image than that of some other sources of energy. While hydropower is the most efficient energy technology, opportunities exist to improve its performance and its existence with the environment. This three-volume set surveys up-to-the-minute information and contemporary issues concerning hydroelectric power. Contributors discuss topics ranging from economics and finance to licensing and legal concerns, from dam safety to computer applications. Papers address water quality, diversion screens, and instream flows; turbine impacts on fish and fish protection; the design, manufacturing, and testing of turbines; and the rehabilitation and modernization of various hydroelectric plants, among many other subjects.

ISBN 0-87262-924-4